

Total Synthesis and Semi-Synthesis of Secondary
Metabolites Isolated from the Fermentation of
Amycolatopsis DEM30355

by

Stephanie Morton

A thesis submitted in partial fulfilment of the requirements for
the degree of

Doctor of Philosophy



July 2016

Acknowledgements

Acknowledgements

First and foremost, I thank my supervisor, Dr Michael Hall, for his direction, support and patience throughout the past four years. Thanks to all the members of Team MJH, past and present, who have made the research lab and office such a wonderful place to work. A special thanks to Dr Joseph Cowell for his help (in everything but grammar) and entertainment.

In addition, I thank Dr Nick Allenby and Dr Bernhard Kepplinger, without whom this research would not have been realised, as well as other members of Demuris Ltd. Thanks also to Professor William McFarlane, Dr Paul Waddell and Dr Joe Gray for their assistance and advice in NMR spectroscopy, X-ray crystallography and mass spectrometry respectively. I especially thank Dr Corinne Wills for all of her help and support throughout my PhD.

Finally, thanks to my family and friends for their unending encouragement. A special thanks to Chris (and his endless supply of tea and biscuits), for putting up with me and for giving me the motivation to complete this work.

Abstract

Part 1

The novel antibacterial DEM30355/A **1** was isolated from the fermentation broth of *Amycolatopsis DEM30355*. We aimed to synthesise DEM30355/A **1** to determine the absolute stereochemistry and access DEM30355/A analogues. Using a Baylis-Hillman reaction between tricarbonyl **2** and ketone **3**, we constructed the oxygenated quaternary centre at C^{4a} of DEM30355/A **1** in adducts **4** and **5** (Figure 1).

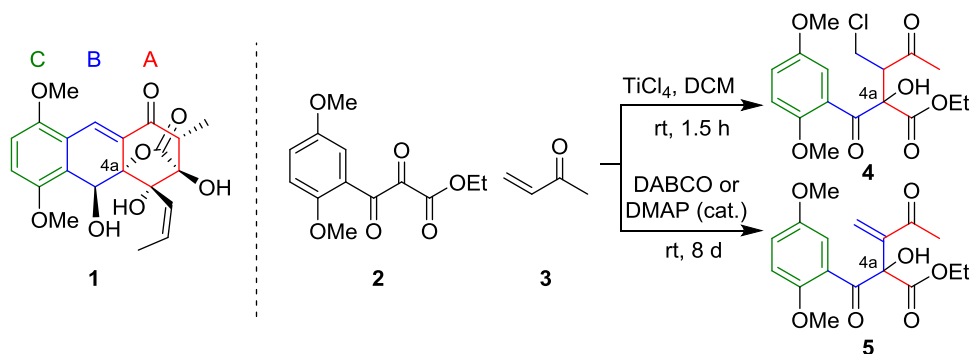


Figure 1: Left – structure of DEM30355/A **1**. Right - Baylis-Hillman reactions to synthesise adducts **4** and **5**

In an alternate route, a Diels-Alder reaction between diene **6** and dienophile **7** was used to generate cycloadducts **8** – **11**, containing the A, B, C ring core of DEM30355/A **1** (Figure 2).

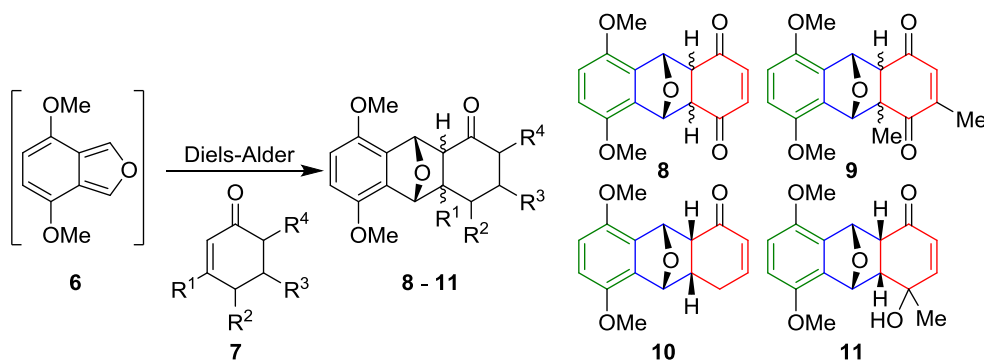


Figure 2: Synthesis of cycloadducts **8** – **11** via a Diels-Alder reaction from isobenzofuran **6**

Alongside this Diels-Alder route, we aimed to synthesise dienophile **12** from shikimic acid **13**, to generate DEM30355/A **1** as a single enantiomer (Figure 3).

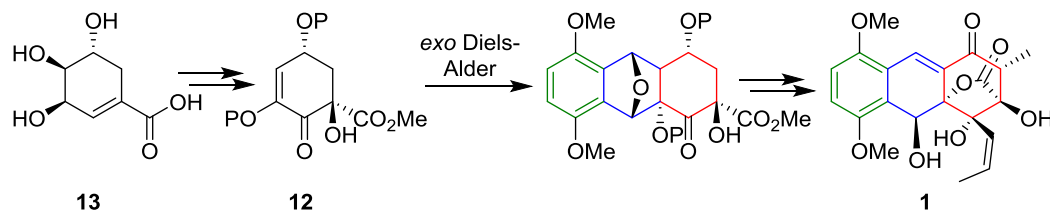


Figure 3: Planned route to DEM30355/A **1** as a single enantiomer from shikimic acid **13**

Following the synthesis of alkene **14**, a key sterically directed dihydroxylation reaction gave diol **15**, which was oxidised to ketone **16**. Base-catalysed conversion of ketone **16** to dienophile **12** was attempted, however the product of this reaction is compound **17** (Figure 4).

Abstract

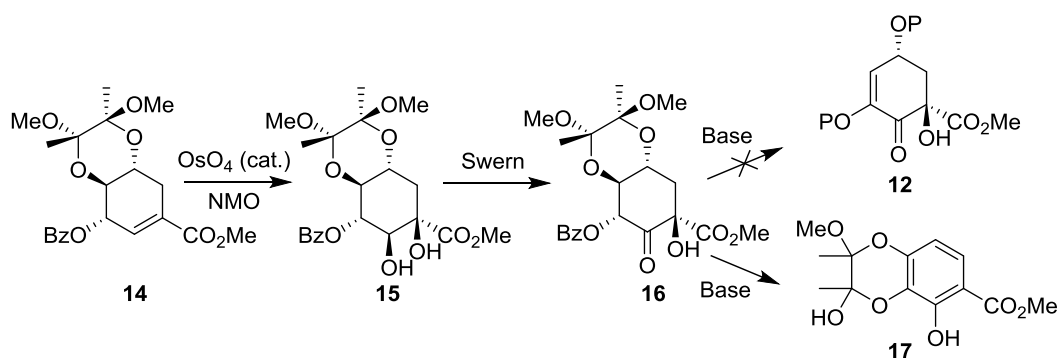


Figure 4: Two-step synthesis of ketone **16** from alkene **14** and the subsequent reaction with base generating aromatic compound **17**

Part 2

Antibacterial DEM30355/B2 **18** was identified in the fermentation broth of *A. DEM30355* (Figure 5). We targeted new drug leads via semi-synthetic modification of DEM30355/B2 **18**.

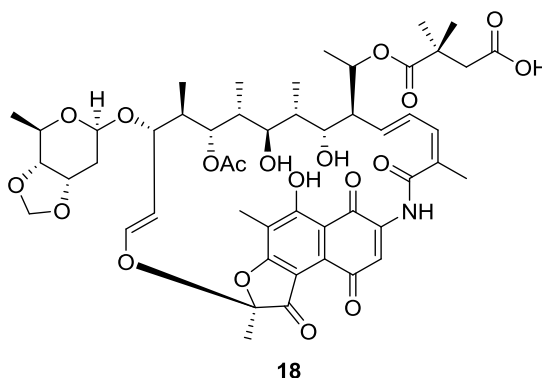


Figure 5: Structure of DEM30355/B2 **18**

Following isolation of DEM30355/B2 **18** via a key acid-base extraction, we successfully generated semi-synthetic DEM30355/B2 derivatives **19** and **20** (Figure 6). These compounds are undergoing investigation to assess their inhibition activity against drug-resistant bacterial dependent RNA polymerase.

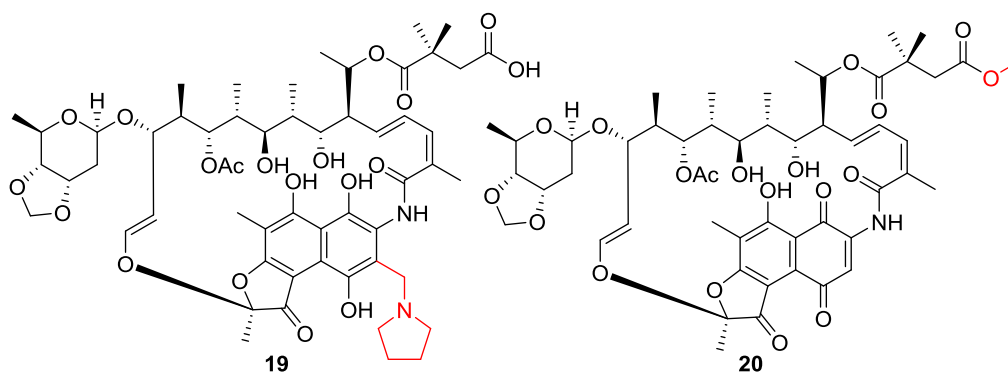


Figure 6: Structures of DEM30355/B2 derivatives **19** and **20**

List of Abbreviations

E _a	Activation energy
Ar	Aromatic
AIBN	Azobisisobutyronitrile
B	Base
Bz	Benzoyl
Bn	Benzyl
dppf	1,1'-Bis(diphenylphosphino)ferrocene
Boc	<i>Tert</i> -butyloxycarbonyl
br	Broad
calcd	Calculated
CAN	Ceric ammonium nitrate
CDMT	2-Chloro-4,6-dimethoxy-1,3,5-triazine
COSY	Correlated spectroscopy
CSA	Camphorsulfonic acid
d	Days
6deb	6-Deoxyerythronolide B
DEBS	6-Deoxyerythronolide B synthase
DMP	Dess-Martin periodinane
DBU	1,8-Diazabicyclo[5.4.0]undec-7-ene
DABCO	1,4-Diazabicyclo[2.2.2]octane
DDQ	2,3-Dichloro-5,6-dicyano-1,4-benzoquinone
DCM	Dichloromethane
D-A	Diels-Alder
DMDO	Dimethyldioxirane
DMAC	Dimethylaluminium chloride
DMAP	4-(Dimethylamino)pyridine
DMSO	Dimethyl sulfoxide
eq.	Equivalents
FDA	Food and Drug Administration
g	Grams
GI ₅₀	Half maximal cell proliferation concentration
IC ₅₀	Half maximal inhibitory concentration
HMBC	Heteronuclear Multiple Bond Connectivity
HSQC	Heteronuclear Single Quantum Coherence
HOMO	Highest occupied molecular orbital
HOBT	Hydroxybenzotriazole

Abbreviations

HRMS	High resolution mass spectrometry
h	hours
IR	Infrared
lit.	Literature
LUMO	Lowest unoccupied molecular orbital
Mp	Melting point
<i>m</i> CPBA	<i>Meta</i> chloroperoxybenzoic acid
MeOH	Methanol
MRSA	Methicillin-resistant <i>Staphylococcus aureus</i>
Me	Methyl
mg	Milligram
mL	Millilitre
MIC	Minimum inhibitory concentration
min	Minutes
M	Molar
^{<i>n</i>} BuLi	<i>n</i> -Butyl lithium
NBS	<i>N</i> -bromosuccinimide
NMO	<i>N</i> -Methylmorpholine <i>N</i> -oxide
NMR	Nuclear magnetic resonance
<i>p</i> TSA	<i>Para</i> -toluene sulfonic acid
PBS	Phosphate-buffered saline
Ph	Phenyl
PTAD	4-Phenyl-1,2,4-triazoline-3,5-dione
PCC	Pyridinium chlorochromate
R _f	Retention factor
RNAP	Ribonucleic acid polymerase
Rif ^r	Rifampicin resistant
rt	Room temperature
NaHMDS	Sodium bis(trimethylsilyl)amide
TBDMS	<i>Tert</i> -butyldimethylsilyl
TBSOTf	<i>Tert</i> -butyldimethylsilyl trifluoromethanesulfonate
THF	Tetrahydrofuran
TMEDA	Tetramethylethylenediamine
TLC	Thin layer chromatography
TFA	Trifluoroacetic acid
TSE	2-(Trimethylsilyl) ethyl
TASF	Tris(dimethylamino)sulfonium difluorotrimethylsilicate
TB	Tuberculosis

Table of Contents

CHAPTER 1. INTRODUCTION.....	1
1.1 Natural Products as Drug Sources	1
1.2 Clinically Used Unmodified Natural Products.....	4
1.2.1 Natural Products as Anticancer Drugs	4
1.2.2 Natural Products as Antibacterial Drugs	5
1.3 Clinically Used Modified Natural Products.....	6
1.3.1 Modified Natural Products as Anticancer Drugs.....	6
1.3.2 Modified Natural Products as Antibacterial Drugs	6
1.4 Increasing Isolated Yield of Natural Products.....	8
1.4.1 Penicillin: Darwinian Selective Breeding ('Bio'-Synthesis).....	8
1.4.2 Taxol: Plant Cell Cultures ('Bio'-Synthesis)	9
1.4.3 6-Deoxyerythronolide B: Heterologous Host Expression.....	9
1.4.4 Discodermolide: Total Synthesis of Natural Products ('Chem'-Synthesis).....	10
1.5 Generation of New Natural Product Inspired Drug Leads	12
1.5.1 Total Synthesis of Natural Products as a Route to Natural Product Analogues	13
1.5.2 Precursor-Directed Biosynthesis of Natural Product Analogues ('Chem-Bio'- Synthesis).....	14
1.5.3 Mutasynthesis ('Chem-Bio' Synthesis).....	16
1.5.4 Recombinant DNA Technology.....	17
1.6 The Hidden Potential of Wild-Type Microorganisms	18
1.6.1 Genome Mining	18
1.6.2 Extremophiles and "Unculturables"	19
1.7 Project Focus: Actinomycete Bacteria	19
1.7.1 Project Aims	19
CHAPTER 2. ISOLATION AND SEMI-SYNTHESIS OF DEM30355/B2	21
2.1 Introduction	21
2.1.1 Global Impact of Tuberculosis.....	21
2.1.2 Treatment of Tuberculosis	21
2.1.3 Development of Rifampicin 65	22
2.2 Project Background	24

Table of Contents

2.2.1	Introduction to DEM30355/B2.....	24
2.2.2	Mode of Action of Rifampicin 65	25
2.2.3	Comparison of DEM30355/B2 73 and Rifampicin 65	26
2.2.4	Project Aims	26
2.3	Results and Discussion	28
2.3.1	Structural Assignment of DEM30355/B2 73	28
2.3.2	Isolation of DEM30355/B2 73 from the Crude Isolate of <i>Amycolatopsis DEM30355</i>	36
2.3.3	Structure Activity Relationship Studies of the Rifamycins.....	38
2.3.4	Planned Semi-Synthetic Modifications of DEM30355/B2 73	39
2.3.5	Semi-Synthesis of Rifamycin S 68	40
2.3.6	Semi-Synthetic Investigations of DEM30355/B2 73	43
2.4	Conclusions and Future Work	57
CHAPTER 3. TOTAL SYNTHESIS OF THE C AND B RINGS OF DEM30355/A		59
3.1	Introduction to Total Synthesis	59
3.1.1	Project Aims	59
3.1.2	Total Synthesis of Rishirilide B 96	60
3.1.3	Comparison of Rishirilide A 95 and DEM30355/A 94	64
3.2	Results and Discussion	66
3.2.1	Barbier Coupling Route to DM-DEM30355/A 115	66
3.2.2	Enolate Coupling Route to DM-DEM30355/A 115	71
3.2.3	Synthesis of DM-DEM30355/A 115 via a Michael Addition/ Enolate Trapping Multi- Component Reaction	80
3.2.4	Baylis-Hillman Synthesis of DM-DEM30355/A 115	87
3.3	Conclusions and Future Work	99
CHAPTER 4. DIELS-ALDER SYNTHESIS OF DEM30355/A		101
4.1	Introduction	101
4.1.1	Mechanism of the Diels-Alder Reaction	101
4.1.2	The Diels-Alder Reaction in Total Synthesis	102
4.2	Project Aims	105
4.3	Results and Discussion	107

Table of Contents

4.3.2	Diels-Alder Reactions with <i>in situ</i> Generation of 4,7-Dimethoxyisobenzofuran 199	109
4.3.3	Diels-Alder Reaction with 4-Hydroxy-4-methylcyclohexa-2,5-dien-1-one 237 as the Dienophile.....	120
4.3.4	Examination of the Reaction of Diels-Alder Cycloadduct 233-b with Base	122
4.3.5	Single Enantiomer Synthesis of DEM30355/A 94	124
4.3.6	Synthesis of Ketone 262	133
4.4	Conclusions and Future Work	144
CHAPTER 5. EXPERIMENTAL		147
5.1	General Experimental Information	147
5.1.1	Analysis	147
5.1.2	Procedures	147
5.1.3	Isolation of DEM30355/B2 73	148
5.1.4	NMR Assignment of DEM30355/B2 73	150
5.1.5	Synthesis of DEM30355/B2 Methyl Ester 88	153
5.1.6	Synthesis of Pyrrolidino DEM30355/B2 89 and 90	155
5.1.7	Exemplar Procedures in the Semi-Synthesis of DEM30355/B2 73	158
5.1.8	3-Iodo-6,6-dimethylcyclohex-2-en-1-one 119	159
5.1.9	Ethyl 2-hydroxy-3-(2-methyl-1,3-dioxolan-2-yl)propanoate 132	160
5.1.10	Ethyl 2-benzyl-2-hydroxy-3-(2-methyl-1,3-dioxolan-2-yl)propanoate 138	161
5.1.11	Ethyl 2-hydroxy-4-oxopentanoate 140	162
5.1.12	3-Hydroxy-5-methyldihydrofuran-2(3 <i>H</i>)-one 143	163
5.1.13	3-(Benzyloxy)dihydrofuran-2(3 <i>H</i>)-one 145	164
5.1.14	(<i>E</i>)-4-(2,5-Dimethoxyphenyl)but-3-en-2-one 147	165
5.1.15	4-(2,5-Dimethoxyphenyl)-4-(phenylthio)butan-2-one 158 and Diethyl (<i>E</i>)-2-(4-(2,5- dimethoxyphenyl)-2-oxobut-3-en-1-yl)-2-hydroxymalonate 159	166
5.1.16	Ethyl 3-(2,5-dimethoxyphenyl)-3-oxopropanoate 171 and 1,5-Bis(2,5- dimethoxyphenyl)-3-methylpentane-1,5-dione 175	168
5.1.17	Ethyl 3-(2,5-dimethoxyphenyl)-2,3-dioxopropanoate 167	170
5.1.18	Ethyl 2-(2,5-dimethoxybenzoyl)-2-hydroxy-3-methylene-4-oxopentanoate 168	171
5.1.19	Ethyl 3-(chloromethyl)-2-(2,5-dimethoxybenzoyl)-2-hydroxy-4-oxopentanoate 180	172
5.1.20	5,8-Dimethoxy-1,4-dihydro-1,4-epoxynaphthalene 205	173
5.1.21	5,8-Dimethoxy-3,4,4a,9,9a,10-hexahydro-9,10-epoxyanthracen-1(2 <i>H</i>)-one 226 ..	174
5.1.22	5,8-Dimethoxy-4a,9,9a,10-tetrahydro-9,10-epoxyanthracene-1,4-dione 227 and 228	175

Table of Contents

5.1.23	5,8-Dimethoxy-2,9a-dimethyl-4a,9,9a,10-tetrahydro-9,10-epoxyanthracene-1,4-dione 233-a and 233-b	177
5.1.24	5,8-Dimethoxy-3a,4,9,9a-tetrahydro-1 <i>H</i> -4,9-epoxybenzo[<i>f</i>]isoindole-1,3(2 <i>H</i>)-dione 235	179
5.1.25	5,8-dimethoxy-3a,4,9,9a-tetrahydro-4,9-epoxynaphtho[2,3- <i>c</i>]furan-1,3-dione	180
5.1.26	4-Hydroxy-4-methylcyclohexa-2,5-dien-1-one 237	181
5.1.27	4-Hydroxy-5,8-dimethoxy-4-methyl-4a,9,9a,10-tetrahydro-9,10-epoxyanthracen-1(4 <i>H</i>)-one 238	182
5.1.28	Methyl (3 <i>R</i> ,4 <i>S</i> ,5 <i>R</i>)-3,4,5-trihydroxycyclohex-1-ene-1-carboxylate 242	183
5.1.29	Methyl (2 <i>S</i> ,3 <i>S</i> ,4a <i>R</i> ,8 <i>R</i> ,8a <i>R</i>)-8-hydroxy-2,3-dimethoxy-2,3-dimethyl-2,3,4a,5,8,8a-hexahydrobenzo[<i>b</i>][1,4]dioxine-6-carboxylate 243	184
5.1.30	Methyl (2 <i>S</i> ,3 <i>S</i> ,4a <i>R</i> ,8a <i>S</i>)-2,3-dimethoxy-2,3-dimethyl-8-oxo-2,3,4a,5,8,8a-hexahydrobenzo[<i>b</i>][1,4]dioxine-6-carboxylate 247	185
5.1.31	Methyl (2 <i>S</i> ,3 <i>S</i> ,4a <i>R</i> ,8 <i>R</i> ,8a <i>S</i>)-8-((<i>tert</i> -butyldimethylsilyl)oxy)-2,3-dimethoxy-2,3-dimethyl-2,3,4a,5,8,8a-hexahydrobenzo[<i>b</i>][1,4]dioxine-6-carboxylate 250	186
5.1.32	Methyl (2 <i>S</i> ,3 <i>S</i> ,4a <i>R</i> ,8 <i>S</i> ,8a <i>S</i>)-8-(benzoyloxy)-2,3-dimethoxy-2,3-dimethyl-2,3,4a,5,8,8a-hexahydrobenzo[<i>b</i>][1,4]dioxine-6-carboxylate 254	187
5.1.33	Methyl (2 <i>S</i> ,3 <i>S</i> ,4a <i>R</i> ,8 <i>S</i> ,8a <i>S</i>)-8-((4-bromobenzoyl)oxy)-2,3-dimethoxy-2,3-dimethyl-2,3,4a,5,8,8a-hexahydrobenzo[<i>b</i>][1,4]dioxine-6-carboxylate 255	188
5.1.34	Methyl (2 <i>S</i> ,3 <i>S</i> ,4a <i>R</i> ,8 <i>S</i> ,8a <i>S</i>)-8-((2-iodobenzoyl)oxy)-2,3-dimethoxy-2,3-dimethyl-2,3,4a,5,8,8a-hexahydrobenzo[<i>b</i>][1,4]dioxine-6-carboxylate 256	189
5.1.35	Methyl (2 <i>S</i> ,3 <i>S</i> ,4a <i>R</i> ,8 <i>S</i> ,8a <i>S</i>)-8-((4-iodobenzoyl)oxy)-2,3-dimethoxy-2,3-dimethyl-2,3,4a,5,8,8a-hexahydrobenzo[<i>b</i>][1,4]dioxine-6-carboxylate 257	190
5.1.36	Methyl (2 <i>S</i> ,3 <i>S</i> ,4a <i>R</i> ,8 <i>S</i> ,8a <i>S</i>)-2,3-dimethoxy-2,3-dimethyl-8-((4-nitrobenzoyl)oxy)-2,3,4a,5,8,8a-hexahydrobenzo[<i>b</i>][1,4]dioxine-6-carboxylate 258	191
5.1.37	Methyl (2 <i>S</i> ,3 <i>S</i> ,4a <i>R</i> ,6 <i>R</i> ,7 <i>S</i> ,8 <i>S</i> ,8a <i>S</i>)-8-(benzoyloxy)-6,7-dihydroxy-2,3-dimethoxy-2,3-dimethyloctahydrobenzo[<i>b</i>][1,4]dioxine-6-carboxylate 259	192
5.1.38	Methyl (2 <i>S</i> ,3 <i>S</i> ,4a <i>R</i> ,6 <i>R</i> ,8 <i>R</i> ,8a <i>S</i>)-8-(benzoyloxy)-2,3-dimethoxy-2,3-dimethyl-6-((methylthio)methoxy)-7-oxooctahydrobenzo[<i>b</i>][1,4]dioxine-6-carboxylate 263	193
5.1.39	Methyl (2 <i>S</i> ,3 <i>S</i> ,4a <i>R</i> ,6 <i>R</i> ,8 <i>R</i> ,8a <i>S</i>)-8-(benzoyloxy)-6-hydroxy-2,3-dimethoxy-2,3-dimethyl-7-oxooctahydrobenzo[<i>b</i>][1,4]dioxine-6-carboxylate 262	195
5.1.40	Methyl 3,5-dihydroxy-2-methoxy-2,3-dimethyl-2,3-dihydrobenzo[<i>b</i>][1,4]dioxine-6-carboxylate 267	196
References		197
Appendix		203

Chapter 1. Introduction

The use of natural products in medicine is recorded as far back as 2600 BC, where clay tablets from Mesopotamia reference hundreds of bioactive substances derived from plants.¹ These medicines were mostly limited to the use of simple plant extracts. Thousands of years later, advancements in chemical science allowed small molecule natural products to be manipulated, to improve their ability to act as drugs. For example, in the 19th century, pioneering chemists synthesised acetylsalicylic acid (Aspirin) from the plant natural product, salicylic acid.² Later in 1928, Alexander Fleming paved the way for drug development from microbial sources, with the discovery of penicillin from a *Penicillium* mould.^{2,3} There is a constant need to develop new therapeutic agents, for example to tackle the emergence of drug-resistant bacteria. Now, modern advances in genetics have demonstrated the hidden potential of microorganisms to generate new drug leads, with genome sequencing identifying cryptic biosynthetic gene clusters (BGCs), as in the genome of *Streptomyces coelicolor*. Some BGCs are believed to encode novel compounds which, by developing new cultivation methods and utilising recombinant DNA technology, may lead to new therapeutic agents in the future.⁴

1.1 Natural Products as Drug Sources

The importance of natural products in the development of new therapeutic agents can be deduced by examining the sources of new drugs approved for clinical use (Figure 1).⁵

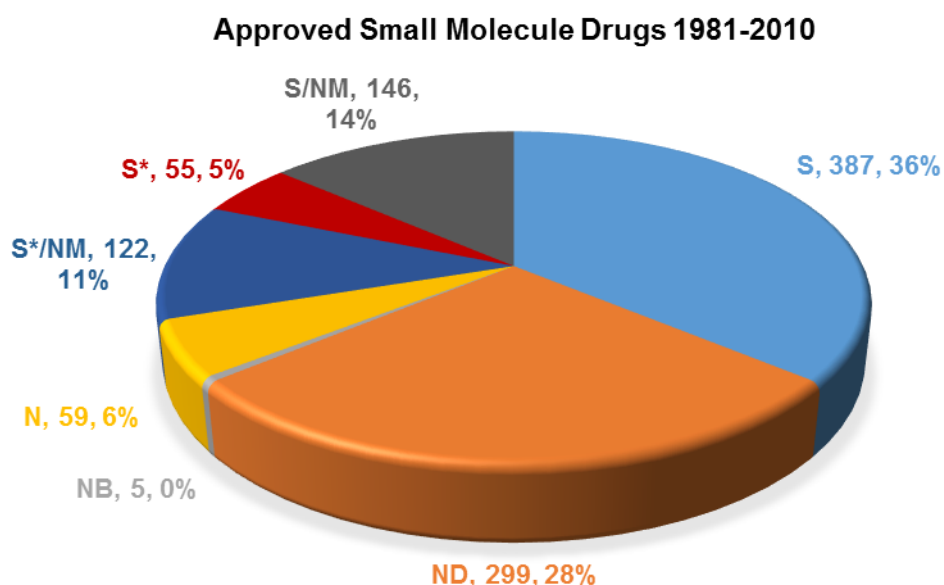


Figure 1: Graphical representation of the origins of small molecule drugs introduced for use in the period 1981 - 2010⁵

According to a survey of the literature by Newman and Cragg⁵, the new small molecule drugs were defined and categorised as follows:

Chapter 1. Introduction

- Synthetic (S) – a totally synthetic drug, not influenced by natural products. Such drugs usually originate from random library screening. For example the anticancer compound sorafenib, was developed using combinatorial chemistry.⁵
- Synthetic natural product mimic (S/NM) – a totally synthetic drug that mimics a natural product. An example is the synthetic anticancer drug Gleevec, an inhibitor of BCR-ABL tyrosine kinase which binds to the adenosine triphosphate binding site.^{5,6}
- Synthetic* (S*) – a totally synthetic drug, with a pharmacophore from a natural product. For example, the antiviral drug famciclovir is a synthetic analogue of the natural product, guanosine.⁷
- Synthetic* natural product mimic (S*/NM) – a totally synthetic drug with a pharmacophore from a natural product. The drug mimics a natural product. An example is tamibarotene (anticancer), a synthetic retinoid compound that binds to retinoic acid receptors.⁸
- Natural (N) – an unmodified natural product used as a drug, such as penicillin G.
- Natural product 'botanical' (NB) – natural mixtures of bioactive compounds. For example, the anticancer topical treatment Curaderm contains a naturally occurring mixture of solasodine glycosides.⁹
- Natural derivative (ND) – a drug derived from a natural product, often by semi-synthetic means. An example is roxithromycin, a semi-synthetic derivative of the natural product, erythromycin A.¹⁰

In the period 1981 – 2010, 50% of the 1073 new small molecule drugs approved by the Food and Drug Administration (FDA) were S*, S*/NM, N, NB, or ND and thus influenced by natural products (Figure 1).⁵ The ratio of totally synthetic drugs to drugs inspired by natural products varies between disease categories. For example, of the 99 small molecule anticancer drugs introduced in 1981-2010, 64% were of natural product origin. On the other hand, of the 104 small molecule antibacterial compounds introduced in the same period, an impressive 75% were of natural product origin (Figure 2).⁵

Approved Small Molecule Anticancer and Antibacterial Drugs 1981-2010

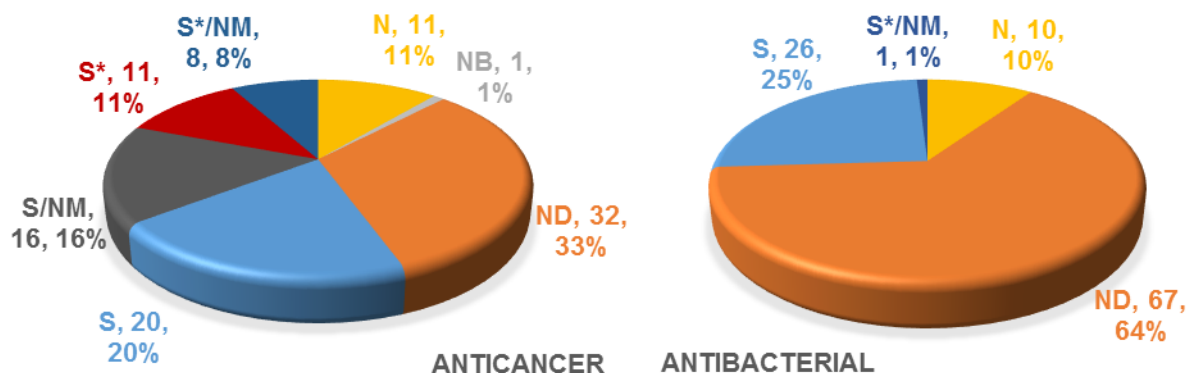


Figure 2: Comparison of the origin of anticancer and antibacterial drugs introduced in 1981-2010⁵

Bioactive small molecules are isolated from a wide range of sources. These include terrestrial and marine animals, plants, fungi and bacteria. During the years 1970-2006, 24 structurally unique natural products from 10 compound classes were discovered, each of which resulted in the approval of a new drug entity.¹¹ Of these discovered natural products, 62% were from bacterial sources, 21% from plants and 17% from fungi (Figure 3).¹¹

Source of New Natural Products Discovered Between 1970-2006 Leading to an Approved Drug Between 1981-2006

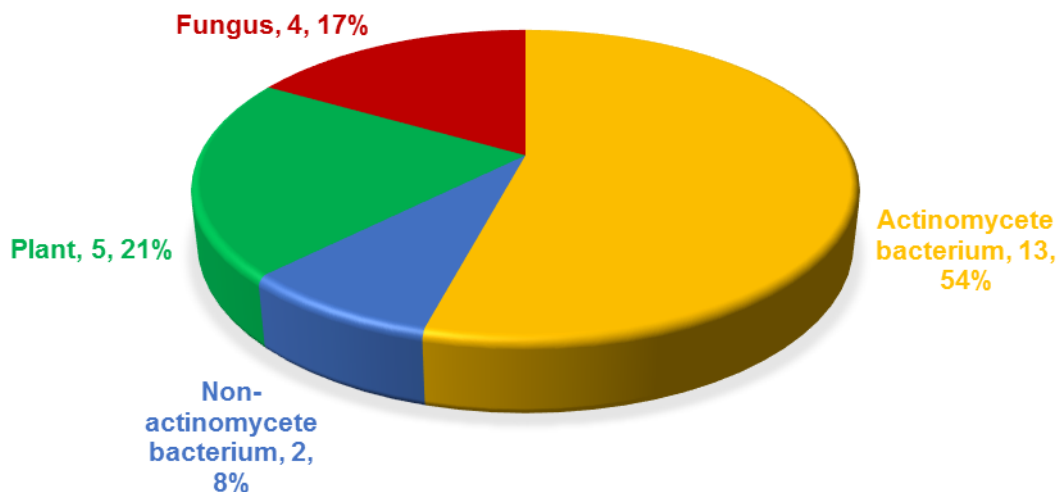


Figure 3: Graphical representation of the source of the new natural products discovered between 1970-2006 that led to an approved drug in the period 1981-2006¹¹

From herein we will focus on drugs based on natural products which pertain to the treatment of cancer and bacterial infections.

1.2 Clinically Used Unmodified Natural Products

1.2.1 Natural Products as Anticancer Drugs

Taxol **1** (paclitaxel) is a diterpene, originally isolated from the bark of *Taxus brevifolia* (*T. brevifolia*), following a screening programme to identify anticancer compounds (Figure 4).¹² It was approved for clinical use by the FDA in 1992, for the treatment of ovarian cancer.^{12,13} In cancerous cells, Taxol **1** interferes with microtubule formation, preventing cell mitosis and thus cell division.¹⁴

Trabectedin **2** is an alkaloid which was isolated from the sea squirt, *Ecteinascidia turbinata* (Figure 4).¹⁵ It was approved for use in 2007 by the European Medicines Agency (EMA) for the treatment of soft tissue sarcoma, and in 2009 for the treatment of ovarian cancer.¹⁵ In cancerous cells, trabectedin **2** binds to the minor groove of DNA, thus interfering with transcription and leading to cell death through double strand DNA breaks.¹⁶

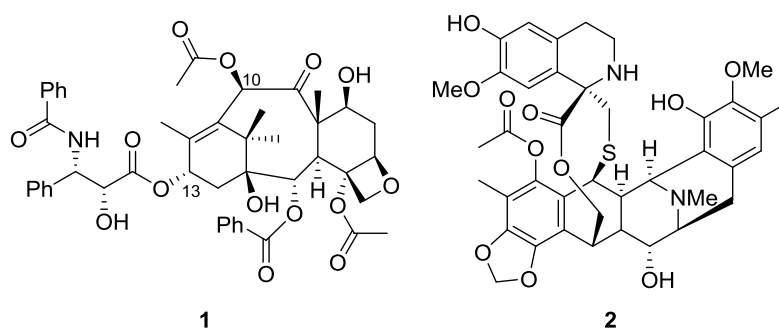


Figure 4: Structures of Taxol **1** and trabectedin **2**

Both Taxol **1** and trabectedin **2** are examples of unmodified natural products used as drugs, although both are now made industrially using chemical synthesis. Due to the problems associated with isolating the compound from bark, Taxol **1** is currently obtained through semi-synthesis of the natural product 10-deacetylbaccatin III **3**, by introduction of the ester functionality at C¹³ and the acetyl group at C¹⁰ (Figure 5).¹² 10-Deacetylbaccatin III **3** is isolated from needle extracts of *T. baccata*, which are more easily harvested and re-grow.¹⁷ Due to the difficulties in farming marine creatures and the limited supply of the natural product from this source, trabectedin **2** is also obtained through semi-synthesis. Optimisation of the fermentation of *Pseudomonas fluorescens* bacteria provided access to kilogram quantities of cyanosafraicin B **4**, a related natural product, which is converted in 21 synthetic steps to trabectedin **2** (Figure 5).¹⁸

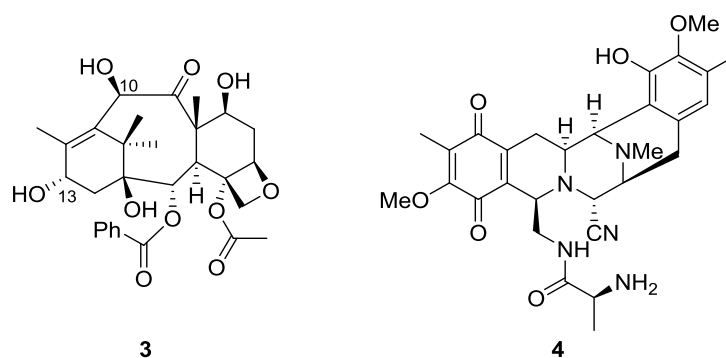


Figure 5: Structures of 10-deacetylbaccatin **3** and cyanosafracin B **4**

1.2.2 Natural Products as Antibacterial Drugs

Penicillin G **5** is a famous example of an unmodified natural product derived from a fungal source, first used clinically in 1941 for the treatment of Gram-positive bacterial infections, like *Staphylococcus aureus* (*S. aureus*) (Figure 6).¹⁹ Penicillin G **5** was originally isolated from the mould, *Penicillium rubens* (*P. rubens*), after the microbe was observed to have antibiotic activity against *Staphylococcus* bacteria.^{3,20} Penicillin G **5** is a member of the β -lactam family of antibacterial agents, the bactericidal properties of which arise from their ability to inhibit penicillin-binding protein, a transpeptidase vital for bacterial cell wall synthesis.²¹

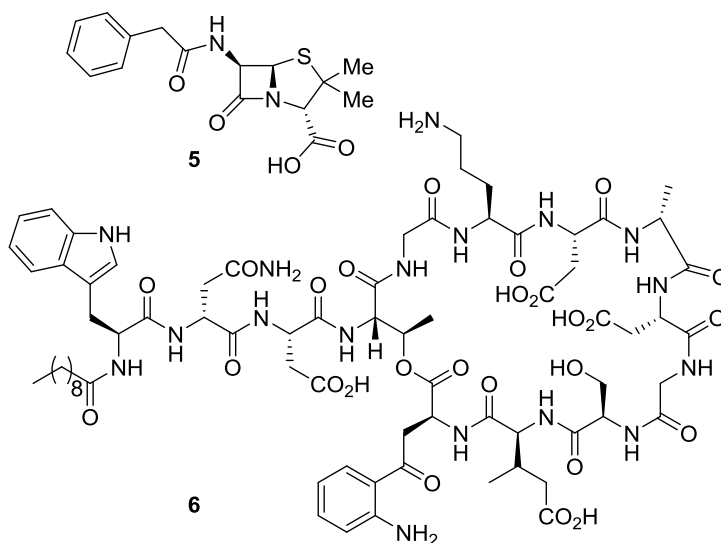


Figure 6: Structures of penicillin G **5** and daptomycin **6**

The cyclic lipopeptide, daptomycin **6** was isolated from *Streptomyces roseosporus*, following screening of the bacterial fermentation extract for antibiotic activity (Figure 6).²² It was introduced for clinical use in 2003, for the treatment of complicated skin infections caused by Gram-positive bacteria.^{23,24} Daptomycin **6** interferes with bacterial cell wall synthesis, by inducing oligomerisation within the cytoplasmic membrane, leading to cell death.²⁵

1.3 Clinically Used Modified Natural Products

As shown in the examples above, the use of unmodified secondary metabolites from a range of sources is commonplace in the treatment of cancer and bacterial infection. However, it is often necessary to chemically modify a natural product to improve its pharmacological properties, to make it a clinically usable compound.

1.3.1 Modified Natural Products as Anticancer Drugs

In 1966, following screening of plant extracts for biological activity, camptothecin **7** was isolated from the tree, *Camptotheca acuminata* (Figure 7).^{26,27} Camptothecin **7** showed promising anticancer properties, but was too toxic for clinical use. Topotecan **8** is an analogue of camptothecin **7**, which contains a solubilising tertiary amine group at C⁹ (Figure 7). Topotecan **8** is made through semi-synthesis of camptothecin **7**, through a one-pot, sequential hydrogenation then oxidation reaction to generate **9**, followed by condensation of compound **9** with formaldehyde and dimethylamine (Figure 7).²⁸ The hydrochloride salt of topotecan **8** was approved by the FDA in 1996 for the treatment of ovarian cancer.²⁷ The anticancer properties of both topotecan **8** and camptothecin **7** arise from their ability to inhibit topoisomerase I, thus disrupting DNA replication, leading to cell death.²⁶

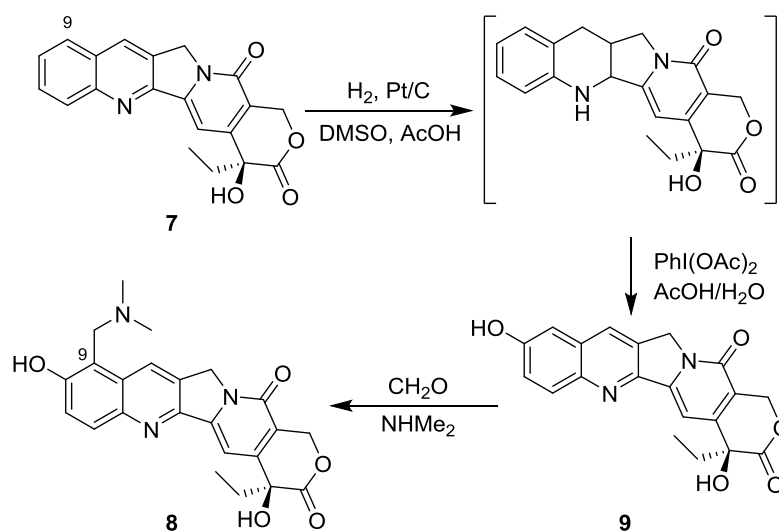


Figure 7: Synthesis of topotecan **8** from camptothecin **7**

1.3.2 Modified Natural Products as Antibacterial Drugs

Erythromycin A **10**, isolated from *Saccharopolyspora erythraea* (*S. erythraea*), was first introduced for clinical use in 1952 for the treatment of bacterial infections, such as *Legionella pneumophila*.^{29,30} It is an orally administered antibiotic, but is degraded in the acidic environment of the stomach to inactive compounds **11** and **12** (Figure 8).³¹ This results in variable gastrointestinal absorption that must be compensated for with high drug dosage.¹⁰

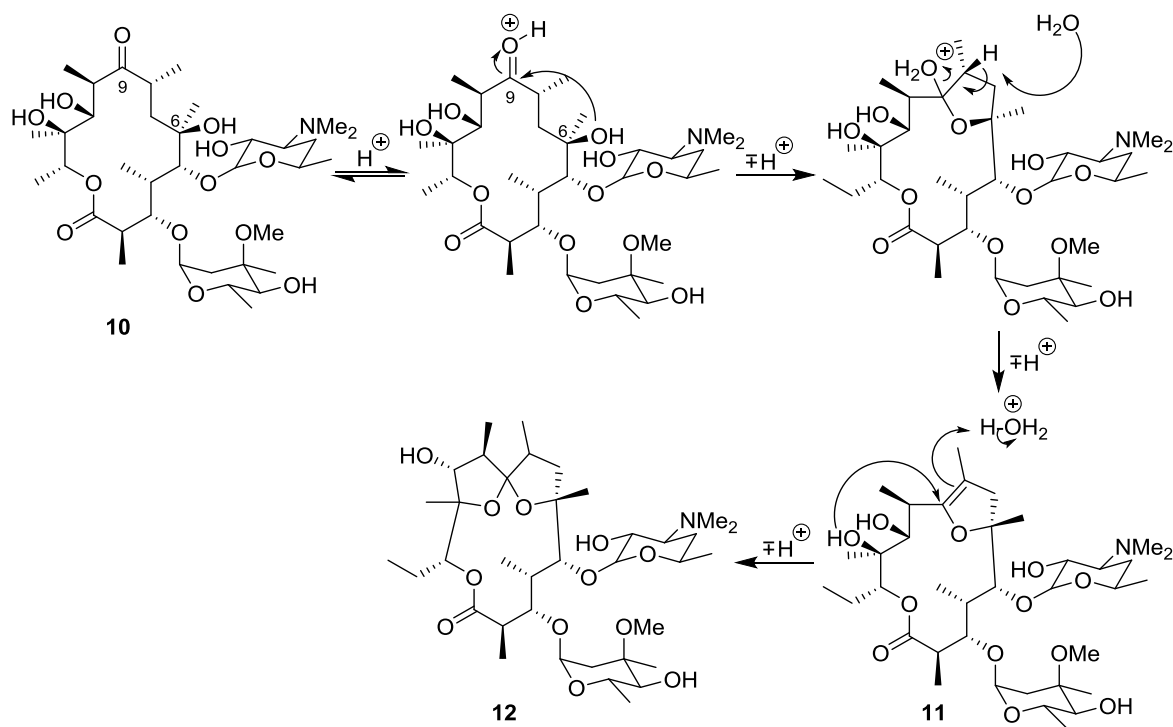


Figure 8: Acid catalysed degradation of erythromycin A **10** to compounds **11** and **12**

To solve this issue, the semi-synthetic drug roxithromycin **13** was developed. Roxithromycin **13** is synthesised from erythromycin A **10**, by conversion of the ketone at C⁹ to an oxime **14**, followed by O-alkylation to give roxithromycin **13** in a 60% overall yield (Figure 9).³² This modification prevents acid catalysed degradation of the antibiotic, leading to the introduction of roxithromycin **13** for clinical use in 1987.⁵ Roxithromycin **13** and erythromycin A **10** are bacteriostatic drugs that inhibit protein synthesis within bacteria, though disruption of ribosome functioning.³⁰

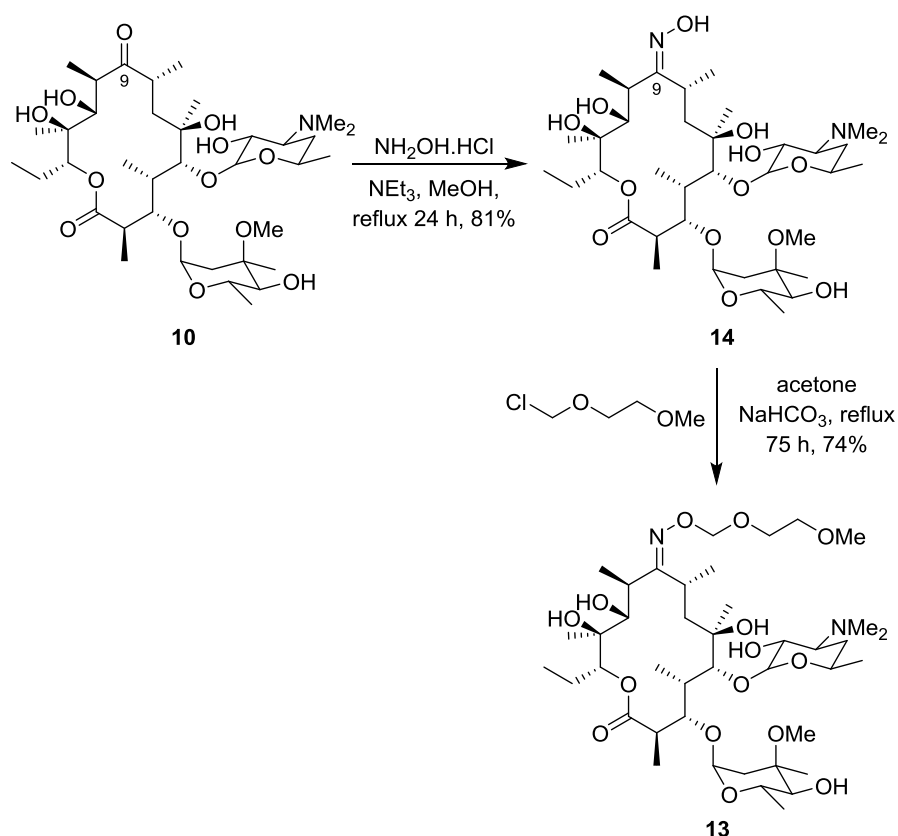


Figure 9: Synthesis of roxithromycin **13** from erythromycin A **10**

The precursors to roxithromycin **13** and topotecan **8**, erythromycin A **10** and camptothecin **7** respectively, were made biosynthetically in a living organism and then altered using synthetic chemistry to give the target molecules. This method of biosynthesis followed by chemical modification will be herein defined as ‘Bio-Chem’-synthesis.³³

1.4 Increasing Isolated Yield of Natural Products

1.4.1 Penicillin G: Darwinian Selective Breeding (‘Bio’-Synthesis)

For a natural product or natural product derivative to advance to new approved drug status, a sustainable, high-yielding source of the natural product must be developed. In some cases, this problem can be overcome by combining the use of an alternative natural source with synthetic chemistry, as discussed previously. However, an alternative approach is to selectively breed the natural product producer, to obtain higher isolated yields of the desired natural product. We will define this traditional, biology-only approach as ‘Bio’-synthesis.

This Darwinian selective breeding method is illustrated with the antibacterial agent, penicillin G **5**. Penicillin G **5** was originally isolated from a strain of *P. rubens*.^{3,20} The titre of penicillin G **5** from this microbe was approximately $1.2 \mu\text{g mL}^{-1}$.³⁴ Early screening of other strains identified a higher producer, *Penicillium chrysogenum* (*P. chrysogenum*), which generated 100 times more penicillin G **5** than the original.³⁵ This strain was subsequently subjected to cycles

of mutation and selection of the highest producing organisms, to give strains of *P. chrysogenum* used industrially today, which produce titres of 42 - 60 mg mL⁻¹.³⁴

This Darwinian method of applying selection and mutation cycles is very effective in developing overproducers and has the advantage that it does not require an in depth understanding of the producing organism to affect results. However the process is very time consuming, with industrial strains of *P. chrysogenum* taking decades to develop, therefore more rapid methods are being examined.³⁵

1.4.2 Taxol: Plant Cell Cultures ('Bio'-Synthesis)

As discussed previously, due to the difficulties in harvesting the natural product directly, Taxol **1** is produced industrially through chemical modification of the plant natural product, 10-deacetylbaccatin III **3**.¹² An alternative method, which avoids the issues associated with cultivating and harvesting whole plants, is to produce Taxol **1** using plant cell cultures.^{17,36,37}

Taxol-producing plant cell cultures are typically established in suspension. The cultures are developed from *Taxus* calluses, collections of undifferentiated cells growing on a solid medium, obtained by harvesting Taxol-producing tissues, such as needle tissue.^{17,36} A cell suspension culture is established by introducing small clusters of these undifferentiated cells into a liquid medium. These suspension cultures can be maintained through regular subculture. Extensive research has been conducted to optimise the yield of Taxol **1** from plant cell cultures.^{17,36,37} Like with penicillin-producing microorganisms, the first stage involved screening plant cell cultures and selecting the higher producing cells, which were then cloned. Subsequently, it has been found that feeding the cell cultures with precursors like sugars and phenylalanine, increased Taxol **1** production compared to the controls.¹⁷ The highest yield of Taxol **1** from plant cell cultures, 0.5%, was obtained by feeding a culture of *Taxus media* with methyl jasmonate.^{17,38} Methyl jasmonate is an elicitor, believed to have a role in the regulation of plant defence genes.³⁸

Following optimisation of the culture conditions to generate higher isolated yields of Taxol **1**, plant cell culture is likely to develop as a dominant source of the drug in the future.

1.4.3 6-Deoxyerythronolide B: Heterologous Host Expression

In some cases, it is not practical to source a natural product from its native producing organism. For example, 99% of bacteria are uncultivable under laboratory conditions.³⁹ Even if an organism can be cultivated, some species like many actinomycete bacteria, grow too slowly for economical industrial production.³⁵ An alternative method is to use recombinant DNA technology, to enable the production of a desired secondary metabolite in a heterologous host.³⁵

Chapter 1. Introduction

The use of recombinant DNA technology has been applied to the biosynthesis of the erythromycin A **10** precursor, 6-deoxyerythronolide B (6deb) **15**, in the common, fast-growing heterologous host, *Escherichia coli* (*E. coli*) (Figure 10).⁴⁰ In the native producer of erythromycin A **10** (*S. erythraea*), 6deb **15** is synthesised by deoxyerythronolide B synthase (DEBS), an enzyme which consists of 3 modules; DEBS 1, 2 and 3.⁴⁰

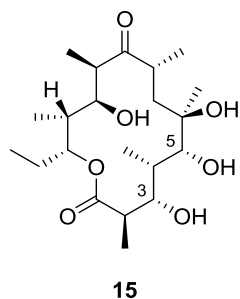


Figure 10: Structure of 6-deoxyerythronolide B **15**

A strain of *E. coli* was engineered to synthesise 6deb **15**, by insertion of the *eryAI*-III genes encoding for DEBS 1 – 3 and insertion of the genes, *pccA* and *pccB*, which enable the synthesis of the DEBS precursor (2*S*)-methylmalonyl-coenzyme A, into the genome of *E. coli*. From this mutant *E. coli* strain, 0.1 mmol of 6deb **15** per gram of cellular protein per day was produced.⁴⁰ Industrial strains of *S. erythraea* produce 0.2 mmol of erythromycin per gram of cellular protein per day, the result of many years of Darwinian selective breeding.⁴⁰ This highlights an advantage of heterologous host expression over selective breeding; it can rapidly generate overproducers in a much shorter time period.

1.4.4 Discodermolide: Total Synthesis of Natural Products ('Chem'-Synthesis)

The success of methods that use living organisms to source a desired natural product is evident in the examples discussed, however in some cases this is not possible. For example, the anticancer compound discodermolide **16**, was originally isolated from the marine sponge, *Discodermia dissoluta* (*D. dissoluta*), following screening of marine extracts for biological activity (Figure 11).⁴¹ In a similar way to Taxol **1**, discodermolide **16** stabilises microtubule formation, disrupting the replication of cancerous cells. The isolation of discodermolide **16** from *D. dissoluta*, which resides in deep sea waters and gives a 0.002% wet mass yield of discodermolide **16**, was not feasible to supply sufficient quantities for clinical trials. In addition, attempts to identify the biosynthetic gene cluster of discodermolide **16** for use in heterologous expression, have so far failed.⁴² Therefore the only option was to carry out the total synthesis of discodermolide **16**, a task undertaken by researchers at Novartis.⁴³

Chapter 1. Introduction

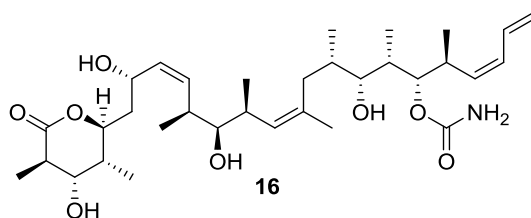


Figure 11: Structure of discodermolide **16**

In the total synthesis of discodermolide **16**, an Evans aldol reaction between aldehyde **17** and the enolate of compound **18**, was used to generate oxazolidinone **19** (Figure 12).⁴³ The oxazolidinone of **19** was cleaved using hydrogen peroxide and lithium hydroxide. This yielded a carboxylic acid which was coupled with 2-chloro-4,6-dimethoxy-1,3,5-triazine (CDMT) **20** to form a triazine ester, followed by reaction with *N,O*-dimethylhydroxylamine, to give Weinreb amide **21**.⁴³

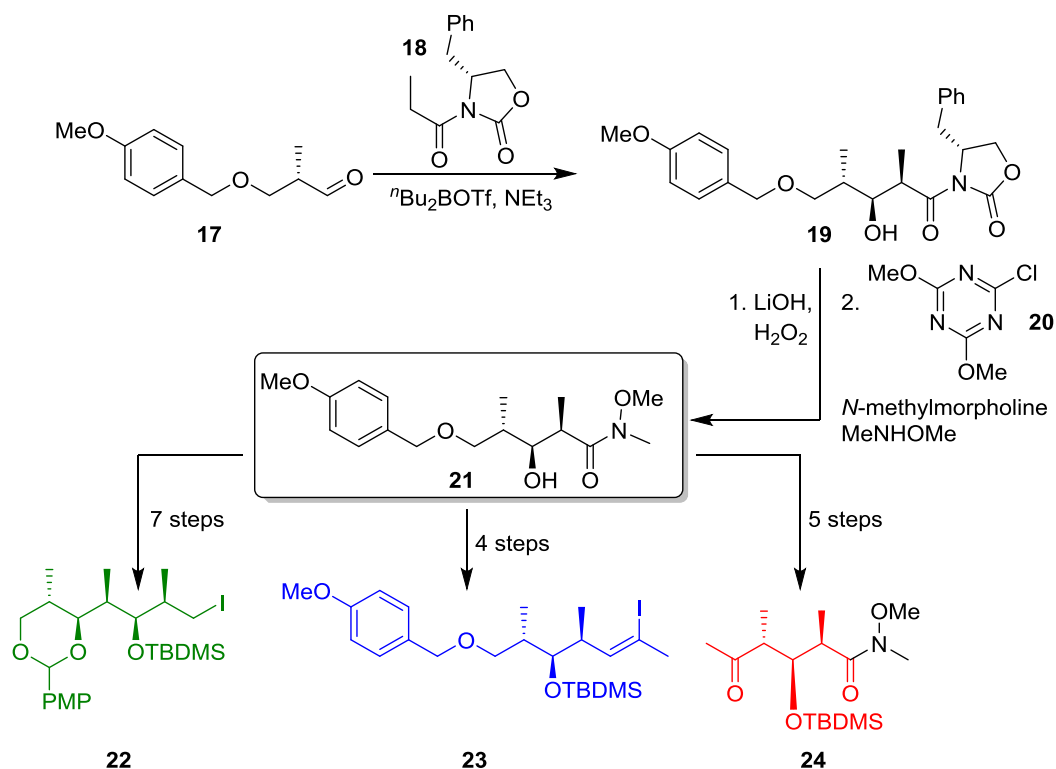


Figure 12: Novartis synthesis of discodermolide **16** - generation of Weinreb amide **21** from aldehyde **17**⁴³

From Weinreb amide **21**, the intermediate compounds **22**, **23**, and **24** were synthesised in four, seven and five steps respectively (Figure 12). A Suzuki coupling of intermediates **22** and **23** was used to give compound **25**, which was subsequently converted to α - β -unsaturated aldehyde **26** (Figure 13). A key mismatched aldol reaction was used to synthesise alcohol **27**; ketone **24** was reacted with (+)-*B*-chlorodiisopinocampheylborane and triethylamine to generate the corresponding boron enolate, which was reacted with α - β -unsaturated aldehyde **26** to give alcohol **27**. Reduction of the ketone of **27**, followed by alcohol deprotection and

intramolecular cyclisation gave discodermolide **16**, in an overall yield of 0.65% over 39 steps. Using this method, 60 g of discodermolide **16** was obtained.^{43,44}

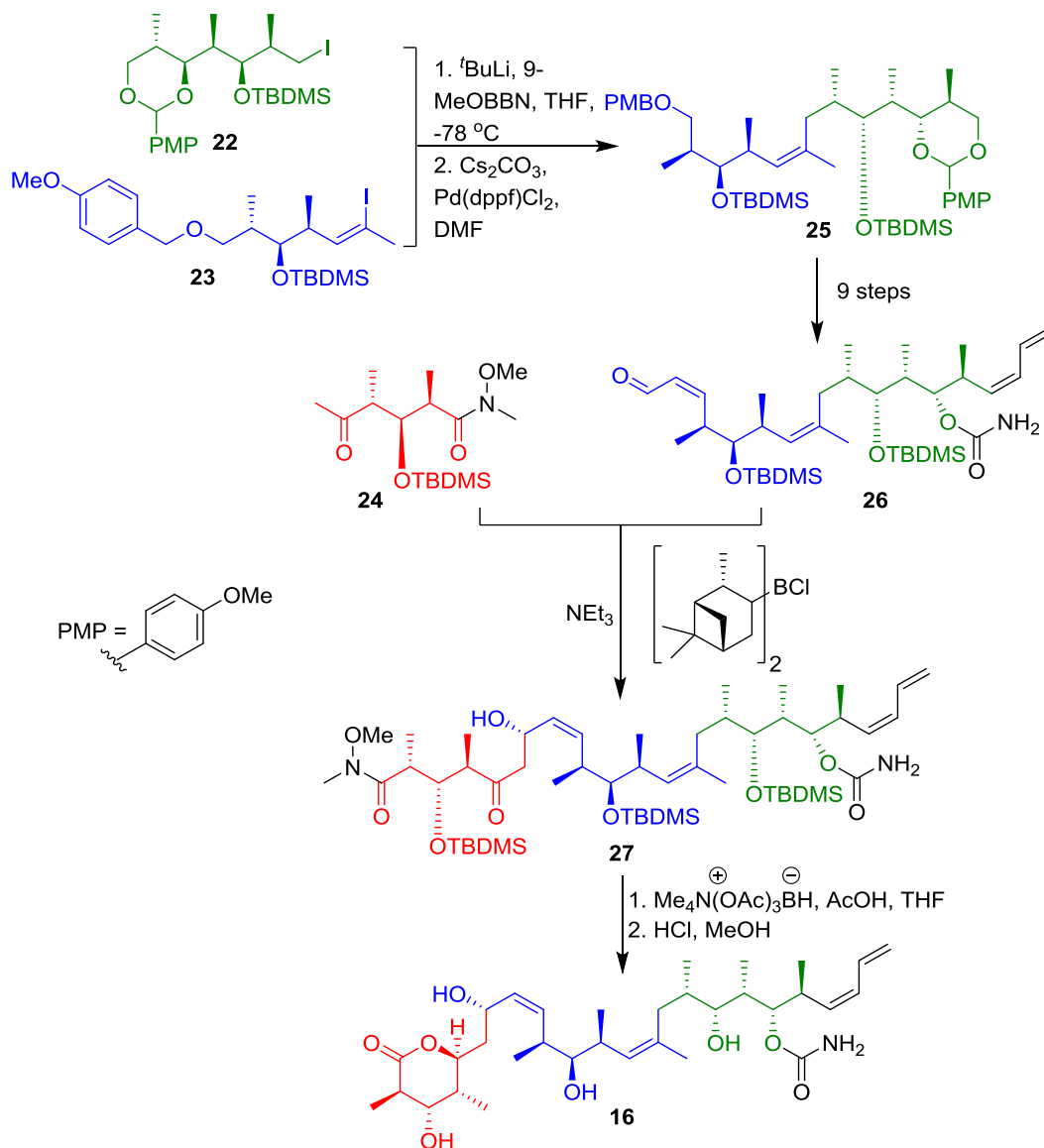


Figure 13: Novartis synthesis of discodermolide **16** from intermediates **22**, **23**, and **24**

In this case, total synthesis was vital for the progression of discodermolide **16** into clinical trials. Although not ideal, with lengthy synthetic sequences and low yields, the total synthesis of discodermolide **16** shows that it is possible to source natural products from chemical synthesis.

1.5 Generation of New Natural Product Inspired Drug Leads

So far we have focussed on clinically used natural products, which were originally isolated following traditional bioassay guided techniques. In this method, extracts from natural sources including plant, microbial and marine isolates, are screened for activity against, for example, bacterial or cancerous cells. This technique remains invaluable in the development of natural product inspired drugs. However, the continual need for new compounds to identify drug leads

has encouraged the development of alternative methods, which are not reliant on the discovery of novel compounds naturally biosynthesised by an organism.

1.5.1 Total Synthesis of Natural Products as a Route to Natural Product Analogues

Spirotryprostatins A and B were isolated from fermentation of the fungal species, *Aspergillus fumigatus* in 1996.⁴⁵ They are inhibitors of mammalian tsFT210 cell cycle progression at the G2/M phase, with IC₅₀ values of 197 μM for spirotryprostatin A and 14 μM for spirotryprostatin B.⁴⁵ In 1998, Danishefsky and Edmonson published their total synthesis of spirotryprostatin A **28** (Figure 14). The synthesis involves a key *N*-bromosuccinimide (NBS) mediated rearrangement of indole **29**, believed to proceed via brominated intermediate **30**, followed by Boc removal to give spirooxindole **31**. Spirooxindole **31** is converted to diketopiperazine **33** through reaction with acyl chloride **32**, followed by Troc removal and subsequent intramolecular cyclisation. Diketopiperazine **33** is then converted to spirotryprostatin A **28** in 3 steps, in a 10% overall yield.⁴⁶

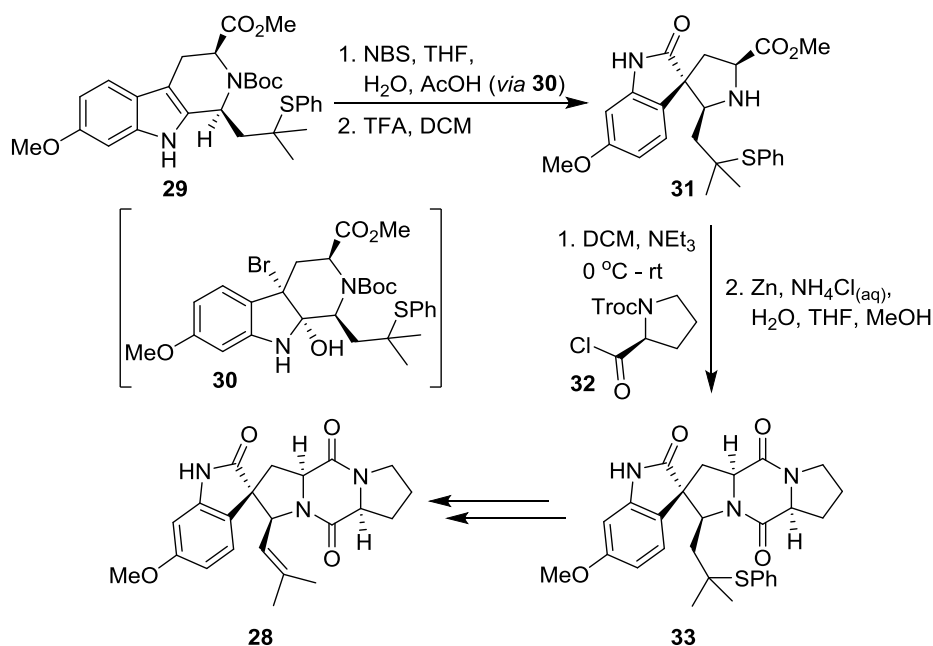


Figure 14: Total synthesis of spirotryprostatin A **28**⁴⁶

Through development of this totally synthetic route to spirotryprostatin A **28**, a range of analogues **34** - **38** of the natural product was accessed (Figure 15). The inhibitory activity of spirotryprostatin A **28** and analogues **34** - **38** was assessed against two human breast cancer cell lines, MCF-7 and MDA-MB-468. Spirotryprostatin A **28**, analogues **34** and **35** showed similar activities, with no inhibition of MCF-7 observed (IC₅₀ > 300 μM), but inhibition of MDA-MB-468 was observed at IC₅₀ concentrations of 85 - 110 μM. Analogues **36**, **37** and **38** showed inhibitory activity against both cell lines, with inhibition of MDA-MB-468 observed at IC₅₀ concentrations of 2.0 x 10⁻² - 2.5 x 10⁻² μM (Figure 15).⁴⁷

Chapter 1. Introduction

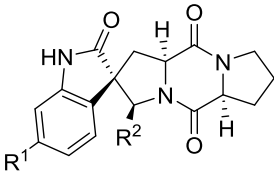
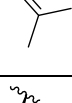
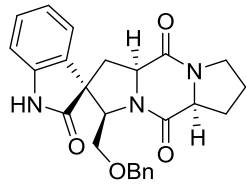
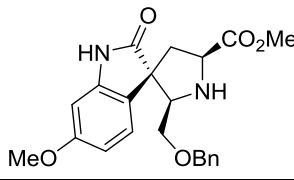
	Compound	R ¹	R ²	IC ₅₀ (μM)	
				MDA-MB-468	MCF7
	28	OMe		110	> 300
	34	H		100	> 300
	35	OMe		85	> 300
	36	OMe		2.5 x 10 ⁻²	100
	37			2.0 x 10 ⁻²	80
	38			2.0 x 10 ⁻²	40

Figure 15: Anticancer activity of spirotryprostatin A **28** and analogues **34 - 38**

Thus, total synthesis is a valuable tool in the generation of bioactive natural product analogues as new drug leads, particularly those which cannot be accessed through chemical modification of the natural product.

1.5.2 Precursor-Directed Biosynthesis of Natural Product Analogues ('Chem-Bio'-Synthesis)

An alternative to totally synthetic methods to generate new drug leads is precursor-directed biosynthesis ('Chem-Bio'-synthesis). Synthetic precursors are fed to wild-type microorganisms and incorporated into a biosynthetic pathway, to generate 'unnatural' natural products.

This method has been applied to synthesise analogues of manumycin **39**, a bacterial secondary metabolite which shows antineoplastic activity via inhibition of farnesyl protein transferase (FTPase) (Figure 16).⁴⁸ Manumycin **39** consists of a cyclohexenone core with two unsaturated side chains, **A** and **B**. The manumycin producer, *Streptomyces parvulus* (*S. parvulus*) was fed with 36 precursors (both aromatic and non-aromatic) in separate fermentations. The fermentations were harvested, extracted and analysed by TLC. Feeding *S. parvulus* with 9 of the aromatic precursors led to the isolation of 8 manumycin analogues **40 - 47**, which were categorised into 3 classes: Class 1 analogues contained side chain **A** (analogues **40 - 44**), Class 2 analogues contained side chain **B** (analogues **45** and **46**) and the Class 3 analogue contained both chains **A** and **B** (analogue **47**) (Figure 16).^{49,50}

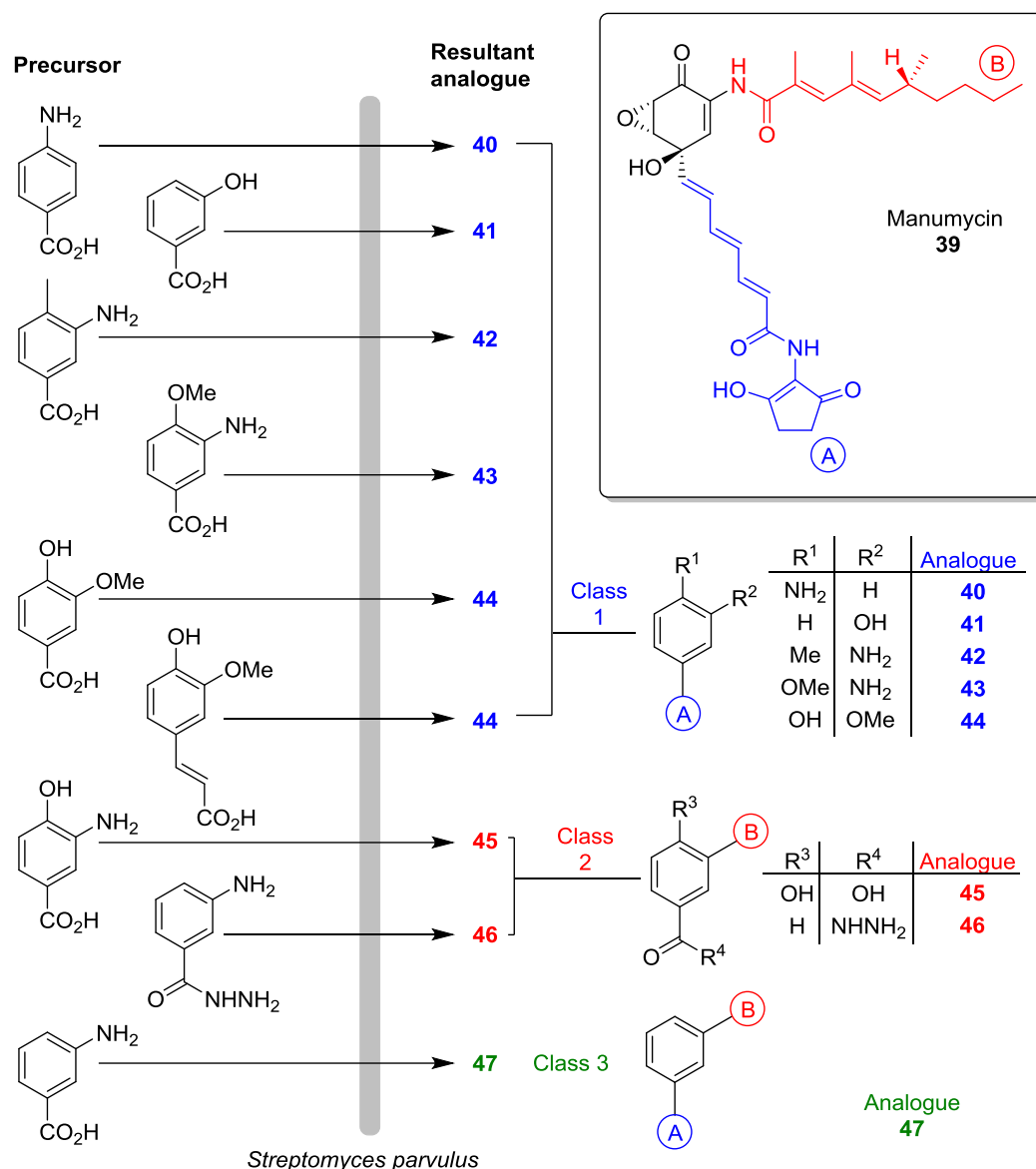


Figure 16: Precursor - directed biosynthesis of manumycin analogues **40** – **47**^{49,50}

A disadvantage of feeding wild-type strains to produce analogues is that the synthetic precursors are in competition with the natural precursors biosynthesised by the organism. To compensate, high concentrations of synthetic precursors (55 mmol dm⁻³ in the *S. parvulus* study) must be added to the fermentation. This is a problem if the synthetic precursors are not readily available. Another disadvantage of using wild-type strains is that the availability of both synthetic and natural precursors can lead to the biosynthesis of multiple products, thus complicating the purification procedure.⁴⁴ In the experiment where *S. parvulus* was fed with 3-hydroxybenzoic acid, manumycin **39** was isolated in addition to analogue **41** (Figure 16).⁴⁹

Precursor-directed biosynthesis ('Chem-Bio'-synthesis) is a simple method which has allowed access to natural product analogues and thus to new drug leads, however the method is limited by the natural-product producing organism in both the range and quantity of these compounds

it can produce. Such issues can be overcome through genetic manipulation of the producing organism, or through heterologous host expression.

1.5.3 Mutasynthesis ('Chem-Bio' Synthesis)

An alternative method to target new compounds, which avoids the precursor competition problem associated with feeding wild-type organisms, is mutasynthesis. Mutasynthesis is an extension of precursor-directed biosynthesis, where genetic modification is used to develop mutant organisms that cannot biosynthesise a particular natural product precursor. Such mutant organisms are dependent on precursor feeding to synthesise a particular secondary metabolite.⁴⁴

Mutasynthesis has been used to generate novel erythromycin analogues. A mutant strain of *S. erythraea*, unable to biosynthesise erythromycins A **10** and B without supplementation with erythronolides A and B, was selected for fermentation. The fermentation broth of this strain was supplemented with (8*S*)-8-fluoroerythronolide A **48**, leading to the isolation of two novel erythromycin A analogues, **50** and **51** (Figure 17). Feeding the same strain with (8*S*)-8-fluoroerythronolide B **49** also generated two new compounds, **52** and **53**.⁵¹

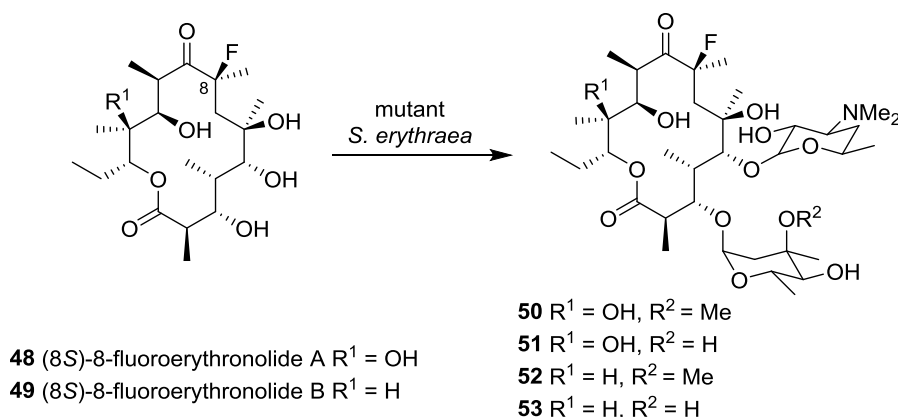


Figure 17: Structures of erythromycin analogues **50** - **53** generated through mutasynthesis

The antibiotic activity of the fluorinated analogues **50** and **52** were comparable to the natural erythromycins A and B. For example, the minimum inhibitory concentration (MIC) values of **50** and **52** against *S. aureus* were $0.195 \mu\text{g mL}^{-1}$ and $0.097 \mu\text{g mL}^{-1}$ respectively, compared to $0.097 \mu\text{g mL}^{-1}$ and $0.195 \mu\text{g mL}^{-1}$ for erythromycin A **10** and B respectively.⁵¹

A limitation of both mutasynthesis and also precursor-directed biosynthesis, is the substrate specificity of the enzymes involved in the biosynthetic pathway. For example, in the precursor-directed synthesis of manumycin analogues **40** - **47** discussed previously, only 9 out of 36 synthetic precursors tested led to the isolation of a new manumycin analogue.⁴⁹ In spite of this limitation, feeding experiments with both wild-type (precursor-directed biosynthesis) and mutant organisms (mutasynthesis), continue to allow access to novel compounds, which would

be difficult if not impossible to generate through other means, such as semi-synthetic modification of related natural products.³³

1.5.4 Recombinant DNA Technology

Recombinant DNA technology, in addition to increasing isolated yields of a natural product, is a valuable technique in the generation of novel natural product analogues. For example, manipulation of the *eryA* genes encoding the polyketide synthase (PKS) that generates erythromycin A **10**, has given access to novel tylactone derivatives.⁵²

In wild-type *S. erythraea*, 6deb **15** is hydroxylated to erythronolide B **54**. Following this, mycarose is added to the C³ hydroxyl group and desoamine to the C⁵ hydroxyl group, by the mycarosyltransferases, EryBV and EryCIII respectively, generating erythromycin A **10** (Figure 18).

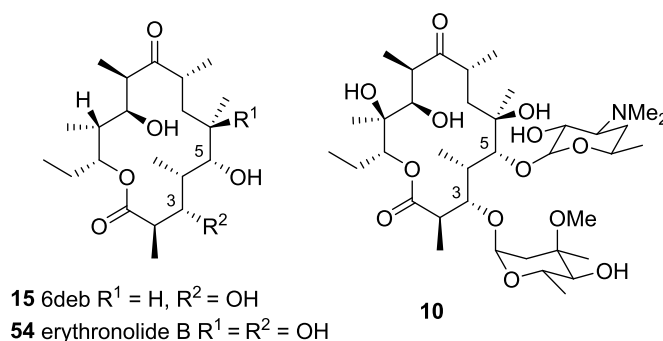


Figure 18: Structures of 6-deoxyerythronolide B **15**, erythronolide B **54** and erythromycin A **10**

Leadlay *et al.* synthesised a hybrid strain of *S. erythraea* through deletion of *eryBV*, *eryCIII* and *eryA I-III* and expression of the mycaminosyltransferase gene, *tylm2*, from *Streptomyces fradiae* (*S. fradiae*).⁵² To test the ability of this new system to synthesise hybrid glycosides, the researchers fed tylactone **55** to a fermentation of the novel *S. erythraea* strain. The group were able to identify two 'unnatural' macrolide compounds, 5-*o*-desosaminyl-tylactone **56** and 5-*o*-glucosyl-tylactone **57**, from the fermentation broth (Figure 19).⁵²

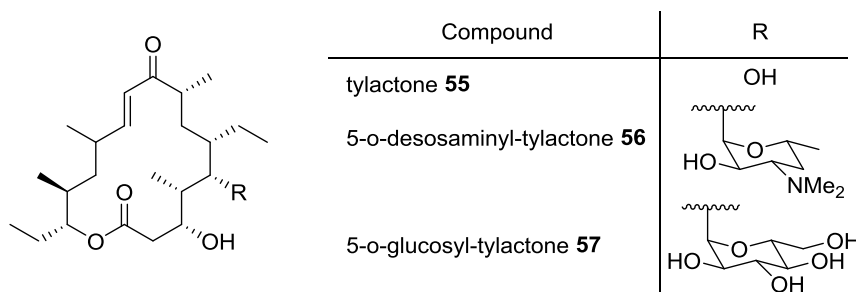


Figure 19: Structures of tylactone **55**, 5-*o*-desoaminyl-tylactone **56** and 5-*o*-glucosyl-tylactone **57**

Thus, recombinant DNA technology allows the design and manipulation of biosynthetic pathways, to access novel 'unnatural' natural products. Through the continued development

of this technology, the potential of such hybrid biosynthetic systems to generate high yields of novel compounds as new drug leads, will be realised.^{33,35,53}

1.6 The Hidden Potential of Wild-Type Microorganisms

1.6.1 Genome Mining

As evidenced by the metabolic engineering of the erythromycin A **10** producer, *S. erythraea*, mutant microbial strains have the potential to uncover new drug leads in the future. Genetic sequencing has also revealed the potential of well-studied, wild-type microbes to potentiate the generation of novel metabolites. For example, *S. coelicolor* contains 16 cryptic biosynthetic gene clusters (BGCs), some of which are believed to encode novel compounds.⁴ It is probable that such cryptic BGCs are 'silent' under the constraints of laboratory cultivation. Hence, the development of new cultivation techniques may activate cryptic BGCs, leading to the isolation of new secondary metabolites. For example, examination of the genome of *Aspergillus nidulans* (*A. nidulans*) revealed the presence of multiple copies of genes encoding for anthranilate synthases, the function of which was previously unknown within *A. nidulans*.⁵⁴ *A. nidulans* was cultured under 40 different conditions and the extracts analysed, which revealed the presence of new compounds in the extract where *A. nidulans* was grown by solid state fermentation on rice medium. A scale-up of this fermentation led to the isolation of 4 novel compounds, including alkaloid **58** (Figure 20).⁵⁴

Alternatively, 'silent' BGCs may be activated through expression in mutant organisms using genomics.⁴ For example, genetic sequencing of *Streptomyces avermitilis* revealed *sav76*, a gene encoding a terpene synthase, the function of which was previously unknown. Cane and co-workers developed a synthetic *sav76* gene which was incorporated into the heterologous host, *E. coli*, for over-expression of the recombinant SAV_76 protein. Subsequent incubation of the purified SAV_76 protein led to the isolation of a novel compound, avermitilol **59** (Figure 20).⁵⁵

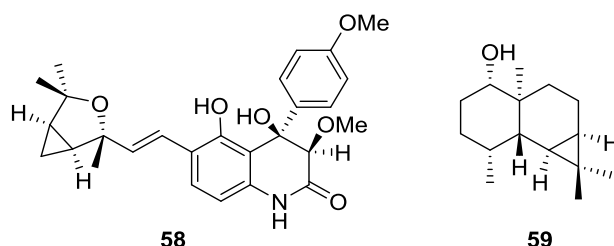


Figure 20: Structures of alkaloid **58** and avermitilol **59**

Genome mining has led to the isolation of novel natural products via activation of previously silent BGCs, and advancements in recombinant DNA technology and cultivation methods to activate silent BGCs are likely to reveal new drug leads in the future.^{4,56}

1.6.2 Extremophiles and “Unculturables”

To date, it is estimated that less than 1% of bacterial species and 5% of fungal species have been discovered.³⁹ The identification of new species, such as microorganisms that grow in extreme environments (extremophiles), enables the isolation of new drug leads. For example, the novel anticancer compound, berkelic acid **60**, was isolated from a fungus obtained from an acidic (pH 2.5), metal-contaminated lake (Figure 21).⁵⁷ Berkelic acid **60** was shown to be active against the human ovarian cancer cell line, OVCAR-3, with a GI₅₀ of 91 nM.⁵⁷

Berkelic acid **60** was isolated following laboratory cultivation of the natural product producing fungus. However, many microorganisms cannot be grown under laboratory conditions, for example it is estimated that 99% of bacteria are uncultivable, therefore efforts are underway to generate new cultivation techniques. This is exemplified by the development of a method by Ling and co-workers, to grow otherwise uncultivable soil bacteria in their natural habitat, in a diffusion chamber device known as the iChip.⁵⁸ From a new bacterial species, *Eleftheria terrae*, Ling and co-workers isolated teixobactin **61**, a novel compound which was active against Gram-positive bacteria, with an MIC of 0.25 µg mL⁻¹ against MRSA (Figure 21).⁵⁸

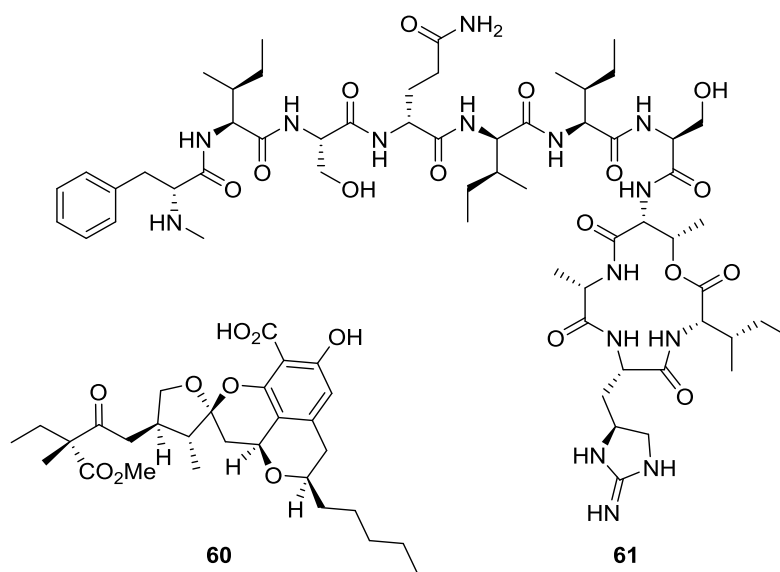


Figure 21: Structures of berkelic acid **60** and teixobactin **61**

Thus, the discovery of new microbial species in combination with advancements in cultivation techniques, will potentially unearth new natural products for use as drugs.

1.7 Project Focus: Actinomycete Bacteria

1.7.1 Project Aims

This project aims to investigate new antibacterial compounds from a novel actinomycete bacterium, *Amycolatopsis DEM30355* (*A. DEM30355*), which was discovered in an extreme desert environment.⁵⁹ We will focus on two secondary metabolites identified from the fermentation broth of *A. DEM30355* - an ansamycin and a novel polyketide. We will examine

Chapter 1. Introduction

the semi-synthesis of the ansamycin and the total synthesis of the polyketide, to develop new antibacterial drug leads.

Chapter 2. Isolation and Semi-Synthesis of DEM30355/B2

2.1 Introduction

2.1.1 Global Impact of Tuberculosis

Tuberculosis (TB) is a global disease, affecting approximately one third of the population. In most cases the infection is latent and asymptomatic, however an estimated 1 in 10 develop the active infection.⁶⁰ In 2014, 9.6 million people were actively infected with TB and there were an estimated 500,000 cases of multi-drug resistant TB (MDR-TB).⁶⁰ 1.5 million people died from the disease in 2014 alone.⁶⁰ Of these deaths, 190,000 were attributed to MDR-TB.⁶⁰

2.1.2 Treatment of Tuberculosis

The nature of *Mycobacterium tuberculosis* (*M. tuberculosis*), the pathogen responsible for most human TB infections, makes the disease difficult to treat.⁶¹ After the initial infection, the bacteria are transported to the pulmonary tissue, where they develop into granuloma.⁶² The granuloma prevent the bacterial infection from spreading, however they also protect the bacteria, allowing them to persist for an extended period of time.⁶² The ability of *M. tuberculosis* to enter a dormant state and evade antibacterial treatment leads to recurring infection and drug resistance.⁶³

The treatment of TB involves a combination of drugs that target bacteria in differing states of metabolic activity, over a period of months. The standard treatment for non-resistant TB is a daily dose of ethambutol **62**, pyrazinamide **63**, isoniazid **64** and rifampicin **65** for the first two months, followed by daily doses of isoniazid **64** and rifampicin **65** alone for a further four months (Figure 22). The lengthy treatment regime for TB is often not completed and has contributed to the emergence of resistant strains.⁶⁴

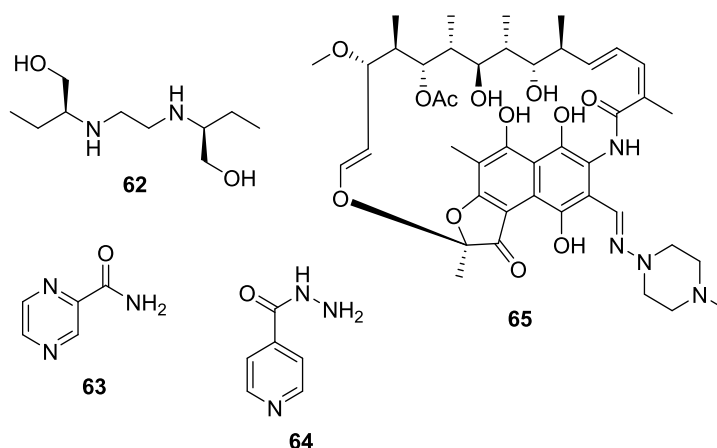


Figure 22: Structures of the anti-TB drugs ethambutol **62**, pyrazinamide **63**, isoniazid **64** and rifampicin **65**

2.1.2.1 Isoniazid **64** and Ethambutol **62** in the Treatment of Tuberculosis

M. tuberculosis has a complex cell wall, which is highly hydrophobic and thus difficult to permeate.⁶⁵ The two synthetic drugs, isoniazid **64** and ethambutol **62**, target cell wall synthesis

in active *M. tuberculosis* bacteria (Figure 22). Isoniazid **64** was discovered in 1952 and is a pro-drug which, upon activation, inhibits the biosynthesis of mycolic acid, a major component of the bacterial cell wall, leading to cell death.⁶⁴⁻⁶⁶ In 42 – 58% of clinically isolated isoniazid-resistant strains of *M. tuberculosis*, there is a mutation of the *katG* gene which encodes primary mycobacterial catalyse-peroxidase, the enzyme believed to be responsible for activating isoniazid **64** in non-resistant organisms.⁶⁵

Ethambutol **62** (Figure 22), introduced for the treatment of TB in 1966, prevents bacterial cell replication by interfering with arabinosyl transferases, which are responsible for the biosynthesis of arabinogalactan, another major component of the cell wall.⁶⁶ In 65% of clinically isolated ethambutol-resistant bacteria, there is a mutant *embB* gene which encodes arabinosyl transferase.⁶⁷

2.1.2.2 Pyrazinamide 63 and Rifampicin 65 in the Treatment of Tuberculosis

The ability of *M. tuberculosis* to enter a dormant state whereby the bacterium has low metabolic activity and does not replicate, contributes to the difficulties encountered in eradicating the disease.⁶¹ Most antibiotic compounds only target pathways that are active in replicating bacteria, such as cell wall synthesis or DNA replication. Pyrazinamide **63** (Figure 22), first reported in clinical use in 1952, is a synthetic pro-drug which specifically targets partially-dormant bacteria residing within inflamed tissue.^{68,69} The bactericidal properties of pyrazinamide **63** are believed to arise from disruption of the bacterial cell membrane potential.⁶⁹ Pyrazinamide **63** is converted to its active form, pyrazinoic acid, by pyrazinamidase within the bacterium and mutation of the *pncA* gene which encodes pyrazinamidase, gives rise to resistant strains.⁶⁹

Rifampicin **65** (Figure 22) is a bactericidal drug against active and semi-dormant bacteria and, in addition to pyrazinamide **63**, significantly reduced the length of TB treatment from 12 -18 months to 6 - 9 months.⁶⁴ Rifampicin **65** is a semi-synthetic derivative of the bacterial natural product, rifamycin B. In this project we aim to identify new drug leads to target rifampicin-resistant (Rif^r) strains of bacteria, therefore we will discuss the mode of action of this drug in more detail later.

2.1.3 Development of Rifampicin 65

In 1957, Sensi and co-workers isolated rifamycin B **66** from the fermentation broth of *Nocardia mediterranei*, a species later reclassified as *Amycolatopsis rifamycinica* (Figure 23).^{70,71} Rifamycin B **66** itself is not active against bacteria, but in aqueous oxygenated solutions, rifamycin B **66** undergoes oxidation to give rifamycin O **67**, followed by hydrolysis to rifamycin S **68** (Figure 23).⁷⁰ Rifamycin S **68** in turn can be reduced to give rifamycin SV **69** (Figure 23). The rifamycins S **68** and SV **69** were found to be excellent antibiotics, particularly against

Gram-positive bacteria, as well as *M. tuberculosis*.⁷⁰ It is worth noting that, in biological systems, rifamycin S **68** and SV **69** are likely to exist in equilibrium with each other.

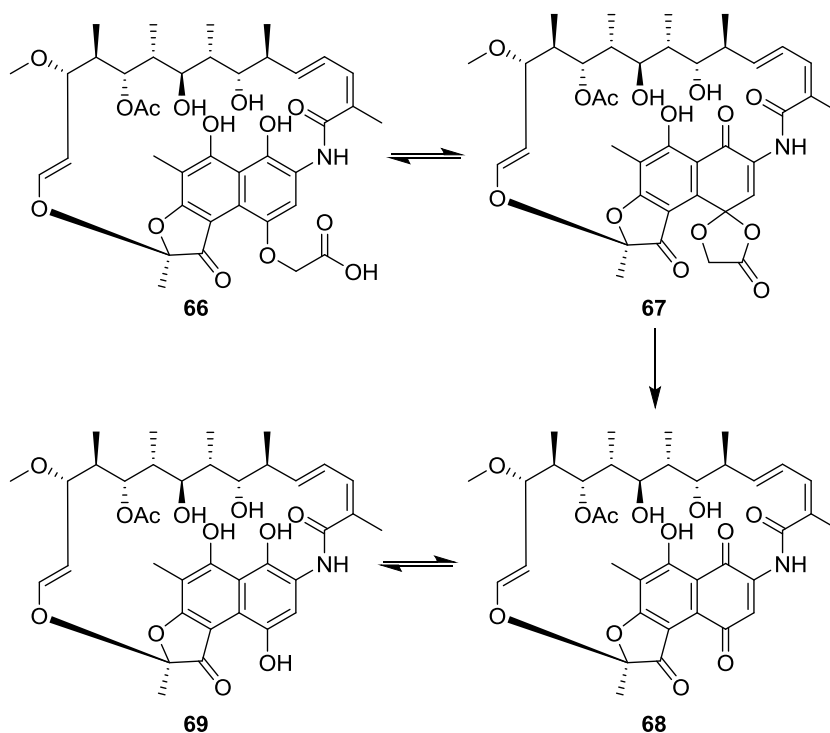


Figure 23: Conversion of rifamycin B **66** to rifamycin SV **69** via rifamycin O **67** and rifamycin S **68**

The hydrochloride salt of rifamycin SV **69** was introduced for clinical use for the treatment of Gram-positive infections, but the drug was not orally active due to poor absorption in the gastrointestinal tract, and it was readily excreted from the body following parenteral administration.⁷⁰ To improve the pharmacokinetic properties, an intensive programme of screening rifamycin derivatives for antibiotic activity ensued, which identified rifampicin **65** as a promising drug lead. Rifampicin **65**, a semi-synthetic analogue of rifamycin B **66**, had significantly improved pharmacokinetics; it was active by oral administration and was not rapidly excreted from the body, leading to the approval of rifampicin **65** for clinical use by the FDA in 1971 (Figure 24).⁷⁰ Rifampicin **65** and related rifamycin drugs, such as rifabutin **70**, rifapentine **71** and rifalazil **72**, are non-competitive inhibitors of bacterial RNA polymerase (RNAP), an enzyme responsible for RNA synthesis (Figure 24).⁷²

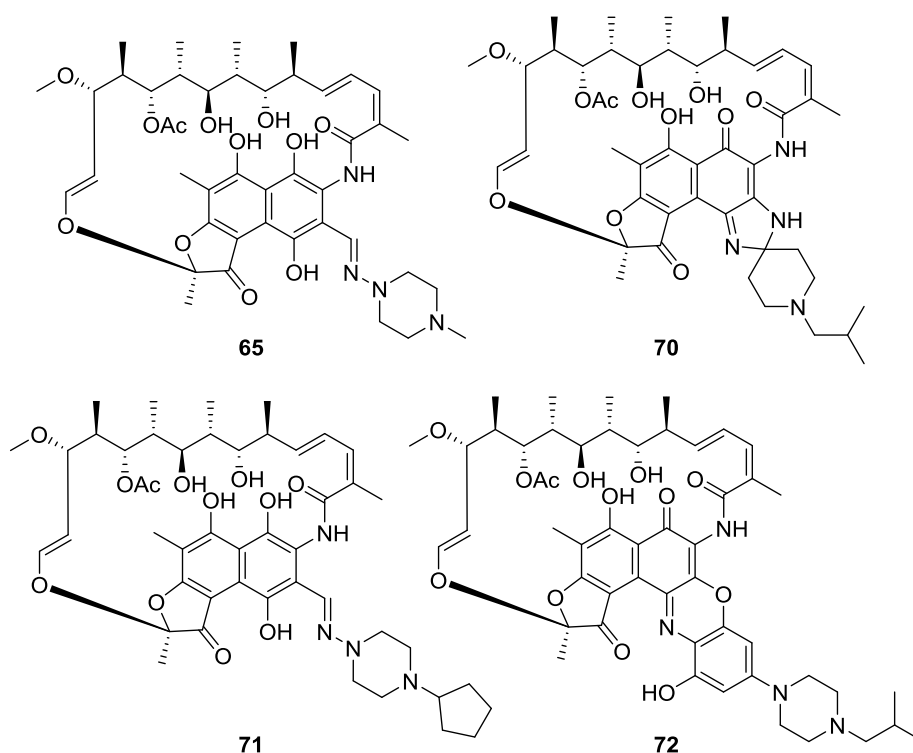


Figure 24: Structures of the rifamycin antibiotics rifampicin **65**, rifabutin **70**, rifapentine **71** and rifalazil **72**

2.2 Project Background

2.2.1 Introduction to DEM30355/B2

Our group collaborates with Demuris Ltd., a biology-based company which focuses on the identification of new antibiotic compounds from bacterial strains. From the fermentation of a novel strain, *Amycolatopsis DEM30355* (*A. DEM30355*), Demuris identified a new antibiotic compound, DEM30355/B1, which appeared to react in the presence of oxygen to give the related compound, DEM30355/B2.⁵⁹ DEM30355/B2 was active against a range of Gram-positive bacteria (Dr B. Kepplinger). An X-ray crystal structure was obtained which suggested DEM30355/B2 was the previously isolated compound, kanglemycin A **73**, a structural relative of rifampicin **65** (Figure 25).^{59,73}

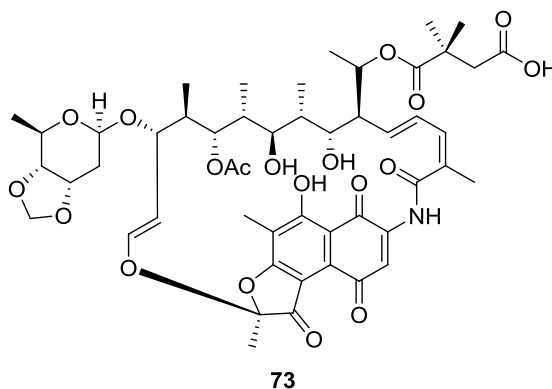


Figure 25: Structure of DEM30355/B2 **73** (kanglemycin A)

An *in vitro* enzyme inhibition assay was carried out (L. Ceccaroni), which compared the activity of DEM30355/B2 **73** and rifampicin **65** against wild type and mutant rifampicin-resistant (Mut Rif^r) RNAP derived from *E. Coli* (Figure 26).

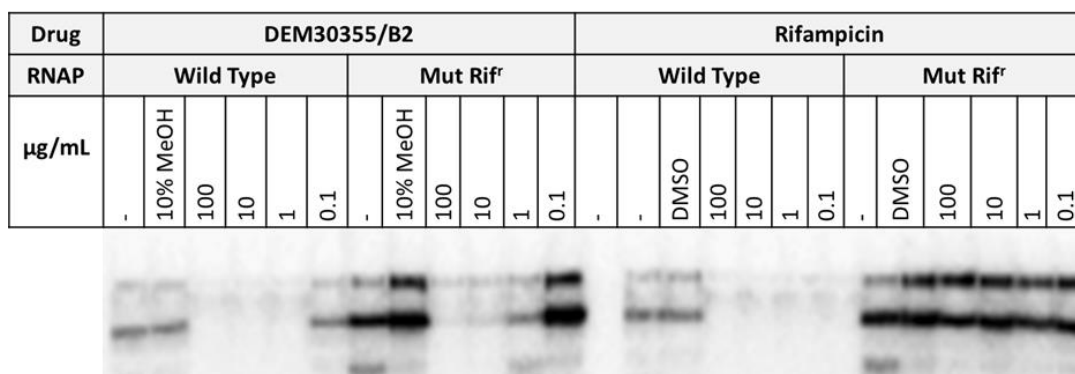


Figure 26: Results of an *in vitro* enzyme inhibition assay comparing the inhibition activities of DEM30355/B2 **73** and rifampicin **65** against wild type and mutant rifampicin-resistant RNAP, derived from *E. coli*. Gel electrophoresis was used to monitor the production of RNA and thus the activity of RNAP. The black bands correspond to RNA, indicative of no inhibition of RNAP

Interestingly, DEM30355/B2 **73** showed much better activity against Mut Rif^r RNAP (inhibition observed at 10 µg/mL) than rifampicin **65** (Figure 26).

2.2.2 Mode of Action of Rifampicin 65

Studies have shown that rifampicin **65** binds to the β -subunit region of RNAP, the core of which is highly conserved within bacterial species.^{74,75} Campbell *et al.* solved the crystal structure of rifampicin **65** bound in *Thermus aquaticus* RNAP, illustrating the regions of rifampicin **65** important for binding in the β -subunit (Figure 27).^{74,76} Structure activity relationship (SAR) studies have shown that the hydroxyl groups at C⁸, C²¹ and C²³ are important for activity.^{77,78}

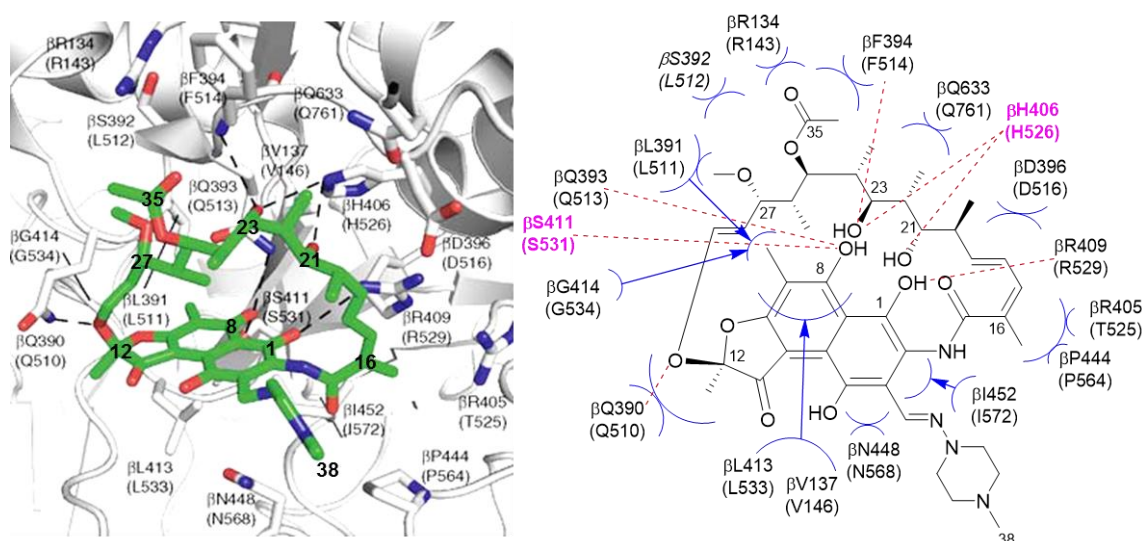


Figure 27: Left - crystal structure of rifampicin **65** bound to the RNAP β -subunit.⁷⁶ Right – schematic drawing of the interactions of rifampicin **65** with residues in the RNAP β -subunit: red = hydrogen bonding; blue = van der Waals interactions. RNAP residues are reported as in *T. aquaticus* RNAP. The parenthesis report the corresponding RNAP residues as in *E. coli* RNAP. The most common mutations leading to Rif^r *M. tuberculosis* occur in the residues shown in pink⁷⁶

Genetic mutations are more likely to persist if the result of the mutation does not affect the normal functioning of the organism. The β -subunit of bacterial-dependent RNAP is an allosteric site, therefore mutations in this region are well tolerated by the bacterium. Rifampicin-resistance commonly arises from single-point mutations in the *rpoB* gene which encodes the RNAP β -subunit; 96% of clinically isolated Rif^r strains of *M. tuberculosis* contain a mutated *rpoB*, with the most common mutations (shown in pink Figure 27) being missense mutations at serine 531 (43% of cases) and histidine 526 (36% of cases).⁷⁹

Assuming that DEM30355/B2 **73** also binds to the β -subunit of bacterial-dependent RNAP, we must question why DEM30355/B2 **73** shows improved activity compared to rifampicin **65** against Mut Rif^r RNAP.

2.2.3 Comparison of DEM30355/B2 **73** and Rifampicin **65**

If we compare the structures of DEM30355/B2 **73** and rifampicin **65** (not including the imine group at C³ of rifampicin **65** that is introduced through semi-synthetic modification of rifamycin S **68**), we can see that the two molecules share the same ansamycin core (Figure 28). DEM30355/B2 **73** has three additional groups: a deoxy-sugar moiety at C²⁷, an ester group at C³¹ and a methyl group at C³¹ in place of an O-methoxy group and two protons respectively in rifampicin **65**.

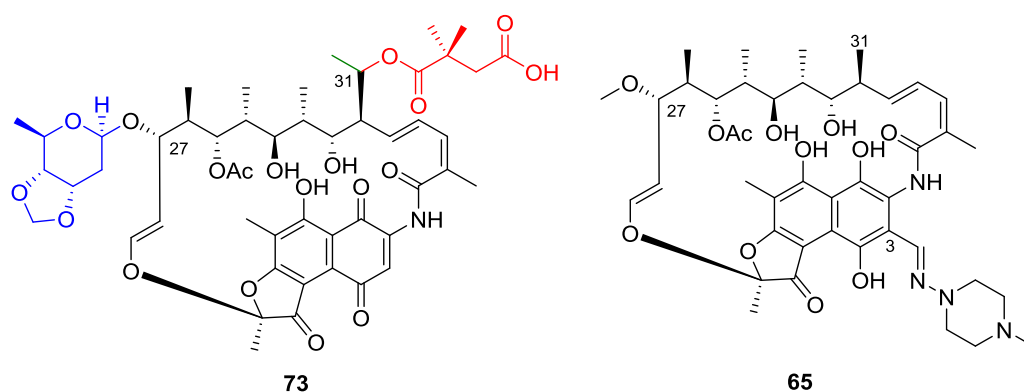


Figure 28: Comparison of the structure of DEM30355/B2 **73** with rifampicin **65**

Consequently, we postulate that the deoxy-sugar and ester group may offer additional binding points in the RNAP β -subunit, through H-bonding and/or van der Waals interactions with the groups in this region, leading to the observed activity of DEM30355/B2 **73** against Rif^r RNAP derived from *E. coli* in the *in vitro* enzyme inhibition assay (Figure 26).

2.2.4 Project Aims

Due to this observed activity of DEM30355/B2 **73** against Rif^r RNAP and the importance of identifying new treatments against Rif^r strains of *M. tuberculosis*, we will target new drug leads via semi-synthetic modification of DEM30355/B2 **73**.

Chapter 2. Isolation and Semi-Synthesis of DEM30355/B2

In this project we aim to:

- Confirm the proposed structure of DEM30355/B2 **73** through assignment of the NMR data.
- Develop an efficient isolation protocol to access pure DEM30355/B2 **73** from the crude fermentation isolate of *A. DEM30355*.
- Synthesise new analogues of DEM30355/B2 **73** for SAR studies and to identify new antibacterial drug leads.

2.3 Results and Discussion

2.3.1 Structural Assignment of DEM30355/B2 **73**

A large scale fermentation of *A. DEM30355* was carried out at the Centre for Process Innovation (CPI). The fermentation was harvested and subjected to downstream processing by Dr B. Kepplinger. In preliminary work on the isolation of DEM30355/B2 by Dr B. Kepplinger, a crystal structure was obtained, which suggested DEM30355/B2 was the previously isolated compound, kanglemycin A **73** (Figure 29).⁷³

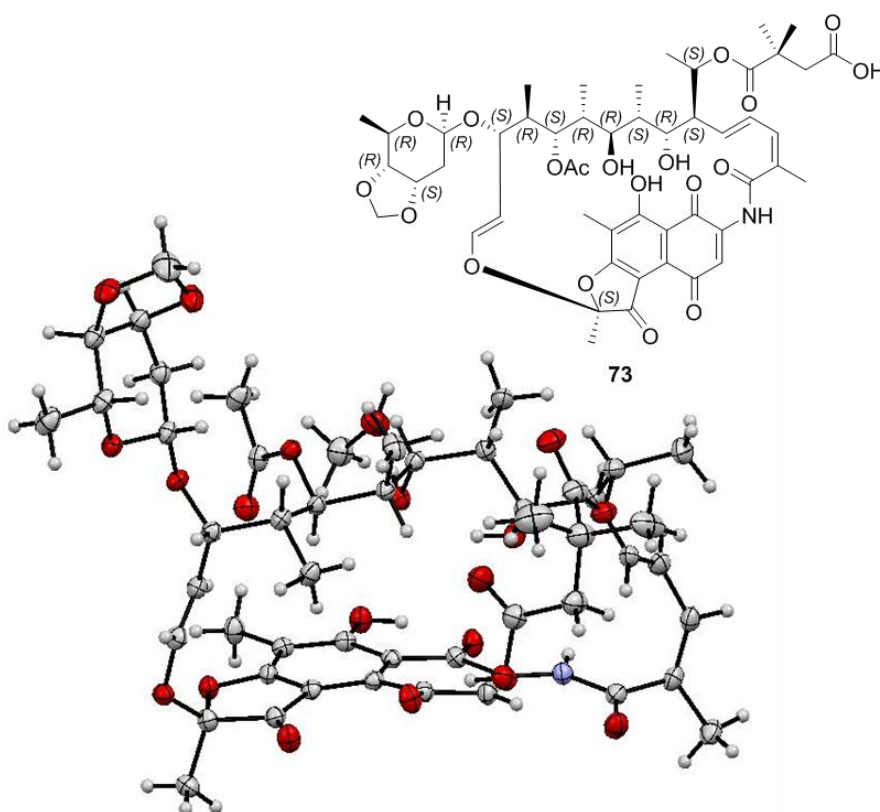


Figure 29: Crystal structure of DEM30355/B2 **73** and R/S assignment of the stereocentres⁵⁹

Due to the structural similarities between our proposed structure of DEM30355/B2 **73** with the rifamycins, it is likely the two share a similar biosynthetic pathway. It is known that a mixture of rifamycins is isolated from fermentation of the producing bacteria, *A. rifamycinica*, therefore we had reason to suspect that isolated DEM30355/B2 may also contain a mixture of related compounds.⁸⁰ We planned to use NMR analysis to determine whether the bulk DEM30355/B2 sample was consistent with the X-ray-determined structure **73** (Figure 29).

DEM30355/B2 **73** was provided by Dr B. Kepplinger and a ¹H NMR spectrum of the sample in deuterated DCM was collected (Figure 30).

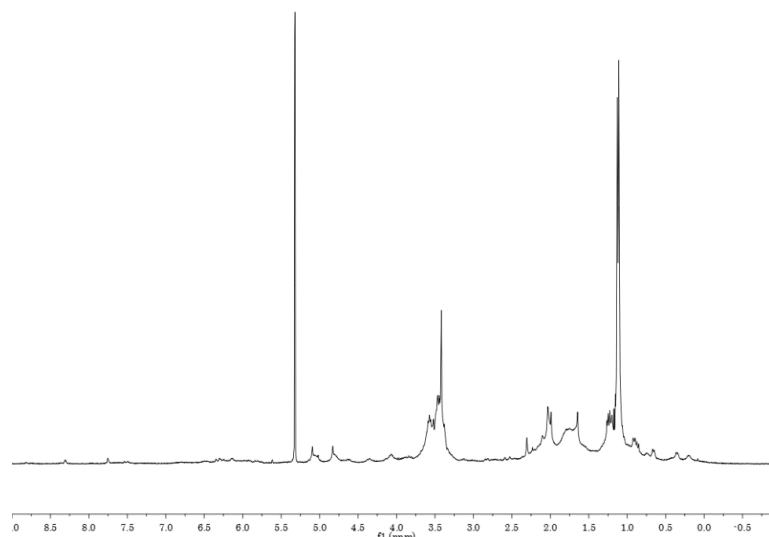


Figure 30: ^1H NMR spectrum of DEM30355/B2 **73** prior to size-exclusion chromatography

The ^1H NMR spectrum showed the sample was contaminated with a number of molecules. Complex peaks were observed at ~ 3.5 ppm, indicating the presence of other metabolites, such as polypeptides (Figure 30).

To remove these impurities, the sample was subjected to size-exclusion column chromatography (LH20 in methanol) and the resultant material analysed by ^1H NMR in deuterated DCM (Figure 31).

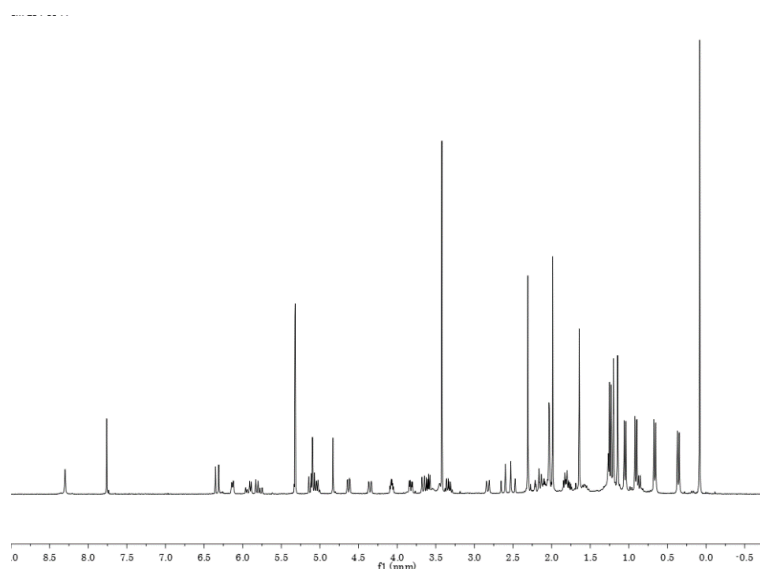


Figure 31: ^1H NMR spectrum of pure DEM30355/B2 **73** following size-exclusion chromatography

At this stage, analysis showed the sample was sufficiently pure to collect additional NMR data for structure confirmation. Therefore we conducted further NMR experiments on DEM30355/B2 and attempted to map the observed data onto the X-ray-derived structure **73**, to determine if the two were consistent.

2.3.1.1 ^1H and ^{13}C NMR Assignment of DEM30355/B2 **73**

Herein we will present the key NMR data of DEM30355/B2 **73** which were important for our structural assignment. Upon examination of the ^1H NMR spectrum, two distinctive signals were apparent at 2.66 ppm (1H, d, $J = 16.8$ Hz) and 2.54 ppm (1H, d, $J = 16.8$ Hz), which implied a geminally coupled methylene group, assigned as C^{35}H_2 . The HMBC spectrum showed correlations (shown in red, Figure 32) from the proton signals at 2.66 and 2.54 ppm, to two carbonyl carbon signals at 172.0 ppm (C^{33}) and 176.0 ppm (C^{36}), and a geminal dimethyl group (C^{34}). In conjunction with a key HMBC correlation (shown in blue, Figure 32) which was observed from a proton signal at 5.07 ppm (1H, app q, $J = 6.4$ Hz), corresponding to C^{31}H , to the carbon signal at 176.0 ppm (C^{33}), we were able to assign the $\text{C}^{31} - \text{C}^{36}$ fragment of DEM30355/B2 **73** shown below.

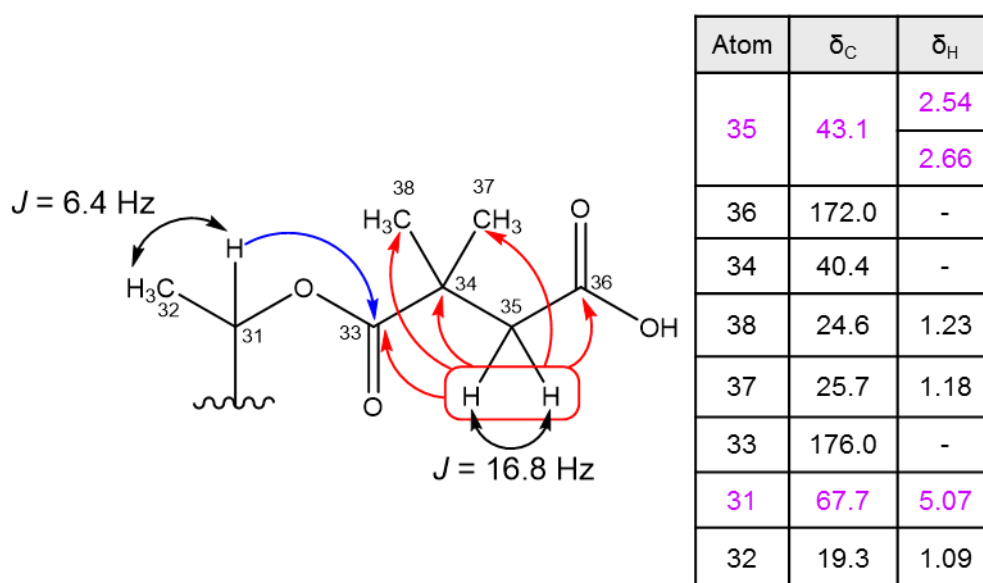


Figure 32: ^1H and ^{13}C NMR assignment of the $\text{C}^{31} - \text{C}^{36}$ fragment of DEM30355/B2 **73**. Selected HMBC and COSY interactions are shown

An important HMBC correlation (shown in blue, Figure 33 (a)) was observed from the proton signal at 5.07 ppm (C^{31}H) to a carbon signal at 52.4 ppm (C^{20}). A COSY interaction (shown in blue, Figure 33 (b)) was observed between a proton signal at 2.17 ppm (1H, app t, $J = 9.7$ Hz), corresponding to C^{20}H , and a signal at 5.83 ppm (1H, dd, $J = 9.7$ Hz), corresponding to C^{19}H . Further COSY interactions (shown in green and pink, Figure 33 (b)) enabled us to deduce C^{19}H was part of a butadiene moiety. We observed HMBC correlations (shown in green, Figure 33 (a)) between a signal at 5.97 ppm (1H, dd, $J = 15.9, 6.2$ Hz), corresponding to C^{18}H of the butadiene group, and a carbon signal at 171.0 ppm (C^{15}). Furthermore, a HMBC correlation (shown in red, Figure 33 (a)) was observed between the carbonyl signal at 171.0 ppm (C^{15}) and a broad, singlet proton signal at 8.35 ppm, suggesting an amide group. Based on these data, we assigned the $\text{C}^{15} - \text{C}^{20}$ fragment of DEM30355/B2 **73** shown below.

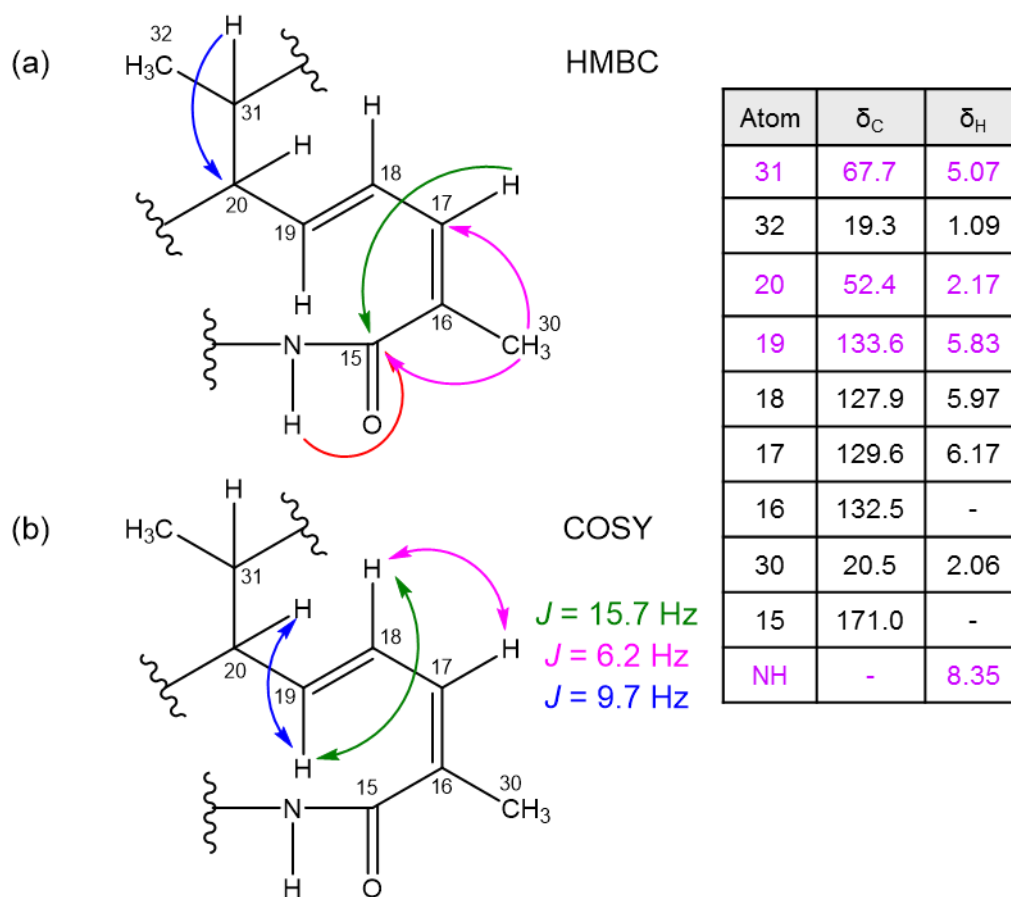


Figure 33: ^1H and ^{13}C NMR assignment of the $\text{C}^{15} - \text{C}^{20}$ fragment of DEM30355/B2 **73**. Key HMBC (a) and COSY (b) interactions are shown

In the HMBC spectrum, there were correlations (shown in red, Figure 34) from the proton signal at 8.35 ppm (amide NH) to two carbonyl carbon signals at 184.3 ppm (C^1) and 185.3 ppm (C^4). Further HMBC correlations (shown in blue, Figure 34) were observed from a proton signal at 7.80 ppm (1H, s) corresponding to aromatic C^3H , to the carbon signals at 184.3 ppm (C^1) and 185.3 ppm (C^4). In addition, HMBC correlations (shown in green, Figure 34) were detected from a proton signal at 2.34 ppm (3H, s), associated with C^{14}H_3 , to six carbon signals in the aromatic region. One of these aromatic carbon signals at 131.5 ppm, assigned to the quaternary carbon signal at C^{10} , was HMBC correlated (shown in blue, Figure 34) with the proton signal at 7.80 ppm (C^3H). This suggested a 1,4-naphthoquinone moiety. Using the observed data, we assigned the $\text{C}^1 - \text{C}^{10}$ fragment of DEM30355/B2 **73** shown below.

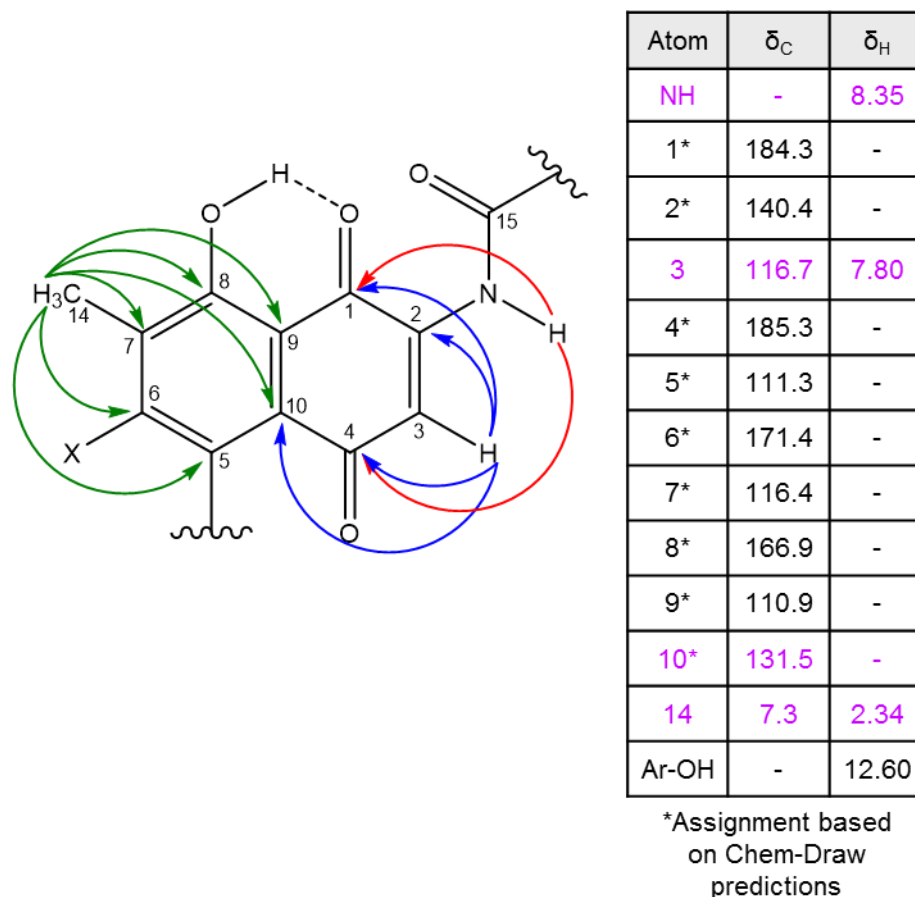


Figure 34: ^1H and ^{13}C NMR assignment of the $\text{C}^1 - \text{C}^{10}$ fragment of DEM30355/B2 **73**. Selected HMBC correlations are shown

If we return to the proton signal at 2.17 ppm (C^{20}H), we observed a COSY interaction (shown in orange, Figure 35 (b)) between this signal and a proton signal at 3.70 ppm (1H, d, $J = 10.1$ Hz), corresponding to C^{21}H . We observed HMBC correlations (shown in brown, Figure 35 (a)) from the signal at 3.70 ppm (C^{21}H) in the ^1H spectrum to signals corresponding to the carbon atoms in a branched hydrocarbon chain. The significant HMBC correlations were as follows;

- A HMBC correlation (shown in orange, Figure 35 (a)) from a proton signal at 3.86 ppm (1H, dd, $J = 9.1, 3.0$ Hz), corresponding to C^{27}H , to a carbon signal at 96.8 ppm, associated with C^{44} .
- A HMBC correlation (shown in green, Figure 35 (a)) from a proton signal at 4.39 ppm (1H, d, $J = 9.9$ Hz) corresponding to C^{25}H , to a quaternary carbon signal at 173.6 ppm (C^{41}), corresponding to the carbonyl carbon atom of an acetoxyl group.

In addition, the ^1H NMR spectrum contained signals at 5.14 ppm (1H, d, $J = 12.8$ ppm) and 6.37 ppm (1H, d, $J = 12.8$ ppm), corresponding to two vicinally coupled alkene protons (C^{28}H and C^{29}H). An important HMBC correlation (shown in blue, Figure 35 (a)) was detected from the proton signal 6.37 ppm (C^{29}H) to a carbon signal at 23.1 ppm (C^{13}). In combination with key HMBC correlations (shown in red, Figure 35 (a)) from a proton signal at 1.68 ppm (3H, s),

associated with $C^{13}H_3$, to two quaternary carbon signals at 193.5 ppm (C^{11}) and 109.3 ppm (C^{12}), we assigned the $C^{11} - C^{13}$ and $C^{20} - C^{29}$ fragments of DEM30355/B2 **73** shown below.

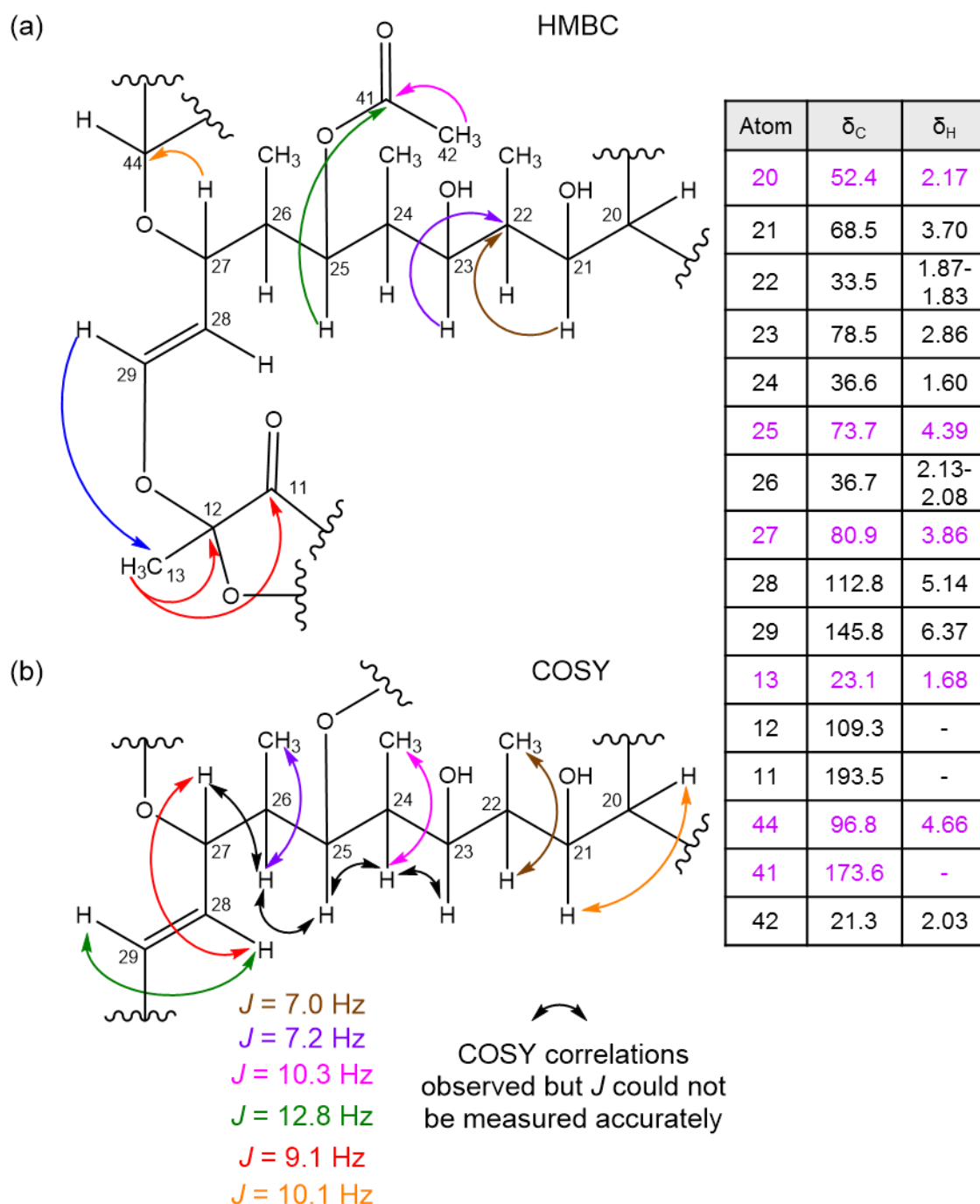


Figure 35: 1H and ^{13}C NMR assignment of the $C^{11} - C^{13}$ and $C^{20} - C^{29}$ fragments of DEM30355/B2 **73**. Key HMBC (a) and COSY (b) interactions are shown

In the COSY spectrum of DEM30355/B2 **73**, starting from a proton signal at 4.66 ppm ($C^{44}H$), we observed COSY interactions (shown in black, Figure 36 (b)) that were characteristic of a cyclic structure. In addition, we observed HMBC correlations (shown in green, Figure 36 (a)) from two proton signals at 5.13 ppm (1H, s) and 4.87 ppm (1H, s), corresponding to $C^{47}H_2$, and carbon signals at 75.5 ppm (C^{48}) and 74.3 ppm (C^{46}). Thus we were able to assign the deoxy-sugar fragment from $C^{44} - C^{50}$ of DEM30355/B2 **73** shown below.

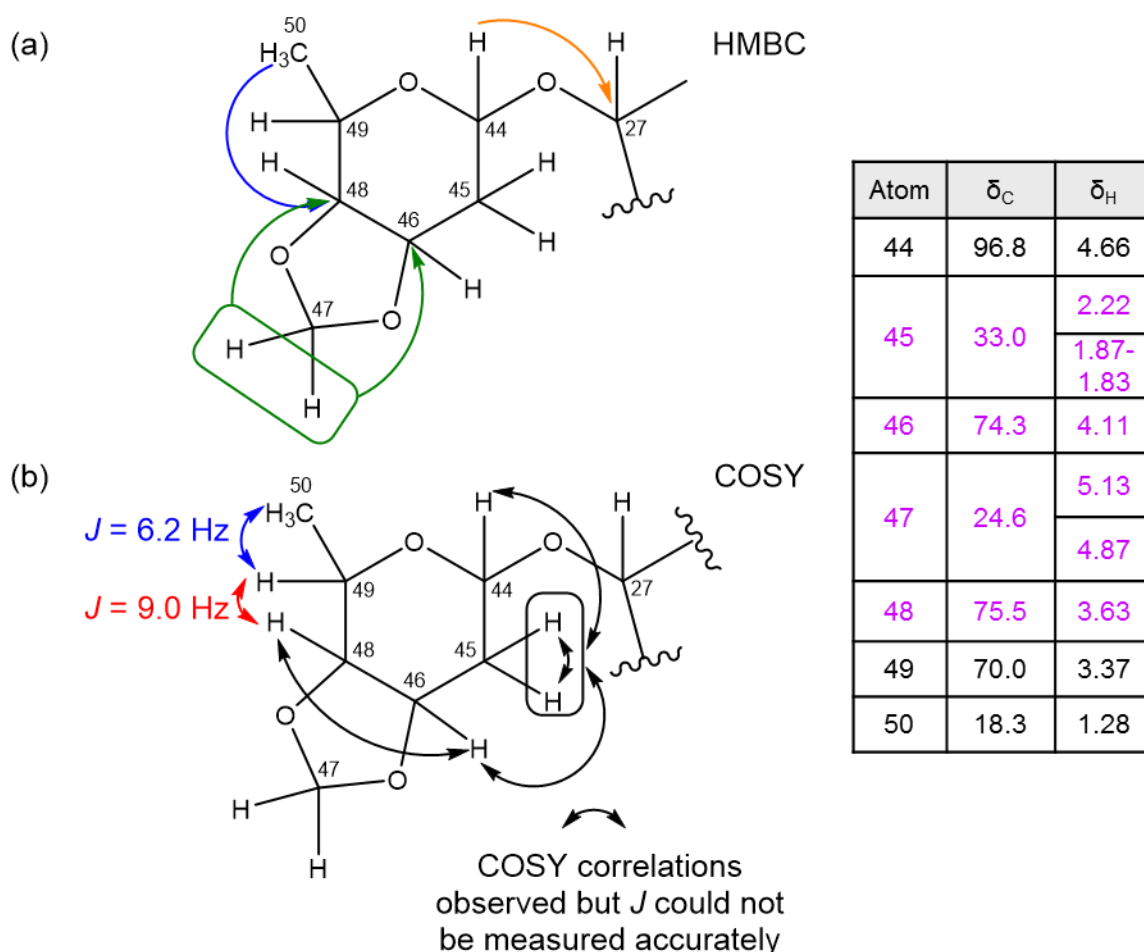


Figure 36: ^1H and ^{13}C NMR assignment of the $\text{C}^{44} - \text{C}^{50}$ fragment of DEM30355/B2 **73**. Key HMBC (a) and COSY (b) interactions are shown

The NMR analysis of DEM30355/B2 was consistent with our proposed structure as determined by X-ray analysis, confirming that the bulk material isolated was kanglemycin A **73** (Figure 37).

Thus we chose to continue to investigate this system as a starting point for semi-synthesis, to develop new anti-tuberculosis compounds for medical application in the future. To adhere to this aim, we needed to isolate more DEM30355/B2 **73** from the crude isolate of *A. DEM30355*.

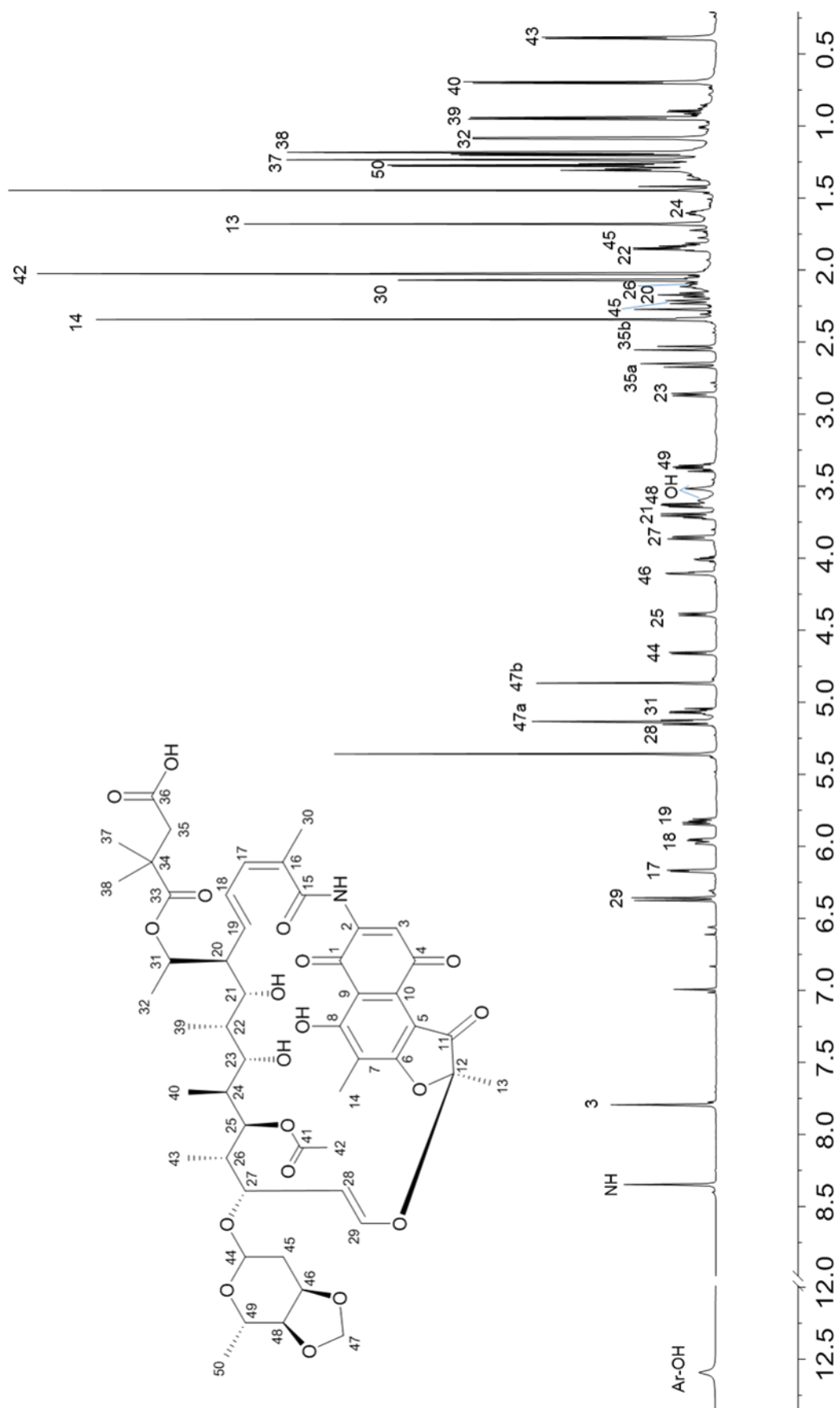


Figure 37: ¹H NMR spectrum of DEM30355/B2 **73**

2.3.2 Isolation of DEM30355/B2 73 from the Crude Isolate of *Amycolatopsis DEM30355*

The next step was to develop an efficient isolation protocol to access DEM30355/B2 73 in a high purity for use in our semi-synthetic approach to new bioactive variants. We were supplied with crude isolate from the fermentation of *A. DEM30355*, which had been pre-processed by Dr B. Kepplinger following the procedure below, to concentrate the bioactive material in preparation for isolation (Figure 38).

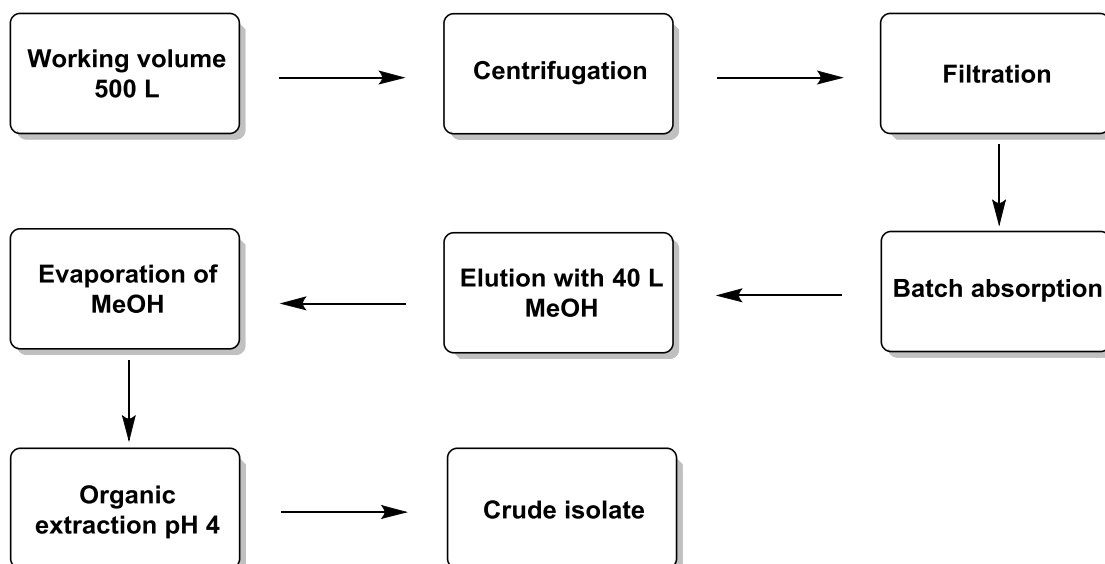


Figure 38: Pre-processing procedure carried out by Dr B. Kepplinger on the crude isolate of *A. DEM30355*

This crude isolate contained a mixture of DEM30355/A (see Chapter 3) and DEM30355/B2 73 along with a number of other secondary metabolites. Several isolation protocols were developed in conjunction with Dr B. Kepplinger and Dr J. Cowell, focussing on the purity of the isolated DEM30355/B2 73, the isolation of associated natural products and the efficiency of the isolation procedure. During our purifications, a mixture of ¹H NMR, TLC, HPLC and bioassay were used as appropriate to monitor the presence and purity of the bioactives of interest. Here we will present a representative isolation protocol, focussed on the efficient production of DEM30355/B2 73, which was developed independently (for further information on isolation protocols see Chapter 5).

A sample of crude isolate (4.420 g) was subjected to normal phase column chromatography (eluent: gradient 100% ethyl acetate to 100% methanol, buffered with 0.1% formic acid), to remove lipid residues (Figure 40). From here, a second normal phase chromatography step (eluent: gradient 100% diethyl ether to 100% ethyl acetate then 100% methanol) was used to separate the two main bioactive compounds present, DEM30355/A and DEM30355/B2 73. At this point it was necessary to carry out an additional procedure to further purify the sample containing DEM30355/B2 73. We envisaged that the carboxylic acid group at C³⁶ could be used to aid the purification procedure, through use of an acid/base extraction (Figure 39).

Chapter 2. Isolation and Semi-Synthesis of DEM30355/B2

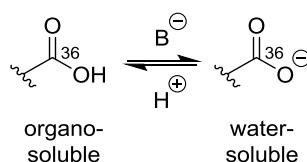


Figure 39: Reversible formation of water-soluble carboxylate anion from organo-soluble carboxylic acid of DEM30355/B2 **73**

Thus the sample was dissolved in toluene and DEM30355/B2 **73** was extracted into aqueous 5% NaHCO₃ solution, with the non-polar impurities remaining in the organic layer. Following acidification of the aqueous layer, DEM30355/B2 **73** was recovered through extraction with ethyl acetate (Figure 40).

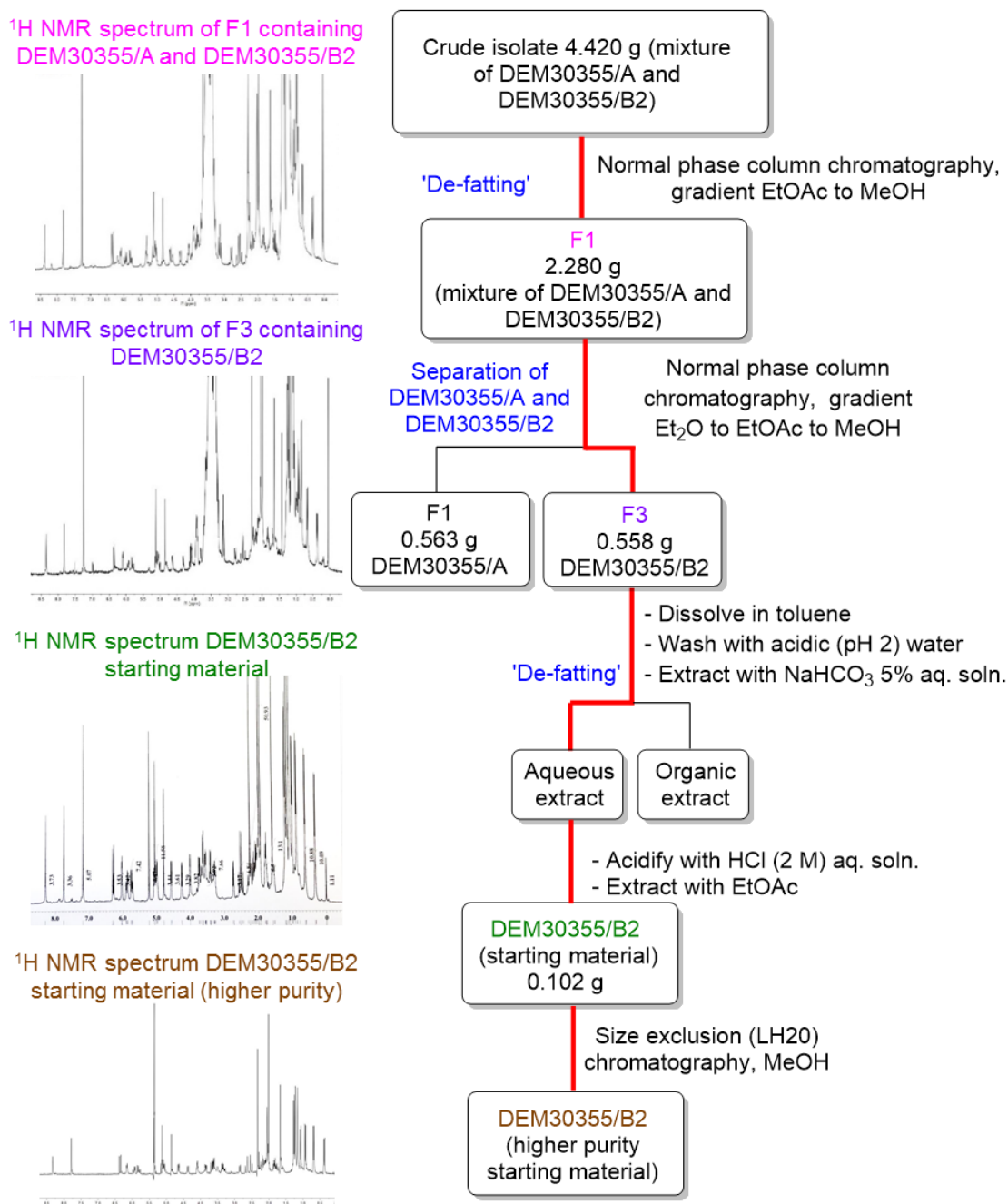


Figure 40: Isolation of pure DEM30355/B2 **73** from the crude fermentation isolate of *A. DEM30355*

Following this protocol, DEM30355/B2 **73** (0.102 g) was isolated in a 3% overall yield with respect to the mass of the crude isolate. At this stage DEM30355/B2 **73** was suitably pure for use in our planned semi-synthesis work, however if required, a late stage size exclusion column chromatography step could be used to further improve the purity of DEM30355/B2 **73** (Figure 40).

With a successful large scale isolation protocol developed and a sufficient quantity of purified DEM30355/B2 **73** in hand (~150 mg), we began the examination of semi-synthetic approaches to the modification of DEM30355/B2 **73**, for the development of a SAR model against Rif^r RNAP. We ultimately aimed to synthesise derivatives of DEM30355/B2 **73** to identify new drug leads for the treatment of Rif^r *M. tuberculosis* infection.

2.3.3 Structure Activity Relationship Studies of the Rifamycins

An extensive SAR study of the rifamycins was conducted by Wehrli and Staehelin.^{77,78} Prior to this study, it was found that rifamycin B **66** did not possess antibacterial activity.⁷⁰ However antibacterial activity was observed if the free carboxylic acid of rifamycin B was 'blocked', for example through conversion to an amide **74** (Figure 41).⁸¹

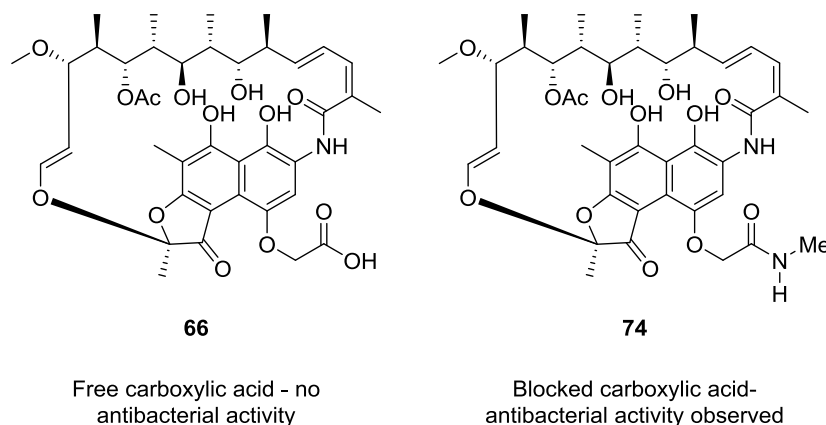


Figure 41: Structures of rifamycin B **66** and antibacterial rifamycin B derivative **74**

Interestingly in Wehrli and Staehelin's study, it was found that rifamycin B **66** inhibited bacterial σ -dependent RNAP (*E. coli*) in an *in vitro* enzyme inhibition assay.⁷⁷ They suggested that the polar carboxylic acid group of rifamycin B **66** prevents permeation of the molecule through bacterial membranes, thus preventing the compound from reaching RNAP *in vivo*.⁷⁷

In general, Wehrli and Staehelin found that any modification to the ansamycin chain of the rifamycins (reduction and epoxidation of the C=C bonds, acetylation of the hydroxyl groups and cleavage of the chain) resulted in reduced inhibition activity against RNAP (*E. coli*) (Figure 42). For example, with rifamycin SV **69** the percentage inhibition activity of RNAP was > 90% at 0.6 $\mu\text{g/mL}$. This was reduced to 50% at the same concentration, in the rifamycin derivative where all three C=C bonds were saturated. No inhibition activity was observed in the derivative whereby the ansamycin chain had been cleaved at C¹².^{77,78}

In addition, it was found that functionalisation at C³ and substitution of the OH at C⁴ were well tolerated, and led to improved RNAP inhibition (Figure 42). The exception was that introduction of a bulky 3-barbiturate group at C³ caused low RNAP inhibition activity (30% at 0.6 µg/mL), likely the result of a change in conformation of the ansamycin chain. Furthermore, the study showed that rifamycin S **68** (quinone form) and rifamycin SV **69** (hydroquinone form) were equally active, with >90% inhibition of RNAP observed at 0.6 µg/mL. Wehrli and Staehelin also found that the OH groups at C⁸, C²¹ and C²³ were important for RNAP inhibition, as acetylation of these hydroxyl groups led to diminished activity (Figure 42).^{77,78}

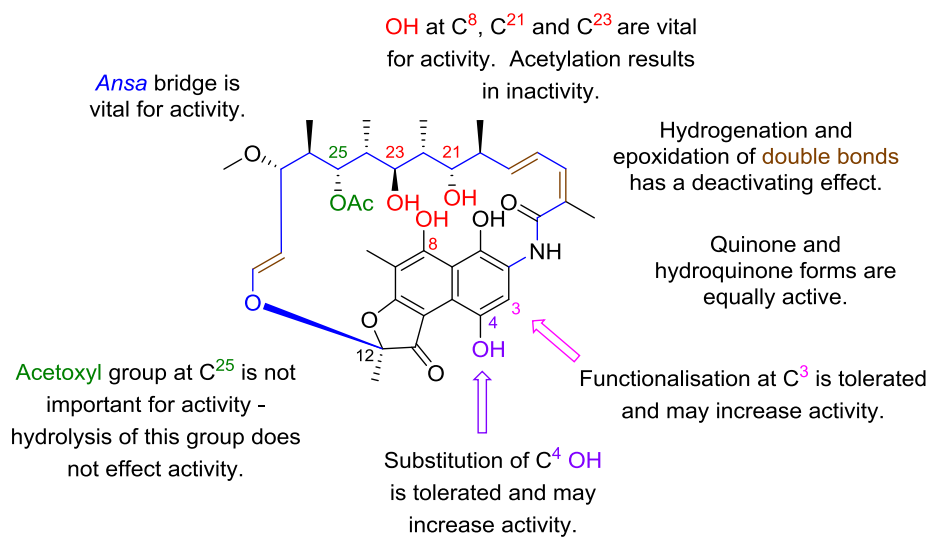


Figure 42: SAR study of the rifamycins⁷⁷

2.3.4 Planned Semi-Synthetic Modifications of DEM30355/B2 **73**

We were interested in the synthesis of bioactive DEM30355/B2 derivatives therefore, with consideration of the results from the SAR study on the rifamycins, we planned to conduct semi-synthetic modifications of DEM30355/B2 **73** which would not alter the ansamycin chain.^{77,78} Instead we would focus on modifications which had enhanced the activity of the rifamycins, namely functionalisation at C³ and substitution of the oxygen at C⁴ of DEM30355/B2 **73** (Figure 43).

As discussed previously (see section 2.2.3), DEM30355/B2 **73** contains additional groups in comparison to the rifamycins, namely a deoxy-sugar moiety at C²⁷ as well as a methyl and an ester group at C³¹. We postulated that these additional groups may have been responsible for the observed activity of DEM30355/B2 **73** against Rif^r RNAP. To test this theory, we planned to examine removal of the deoxy-sugar moiety at C²⁷ and the C³³-C³⁶ fragment of DEM30355/B2 **73** via acetal hydrolysis and ester hydrolysis respectively (Figure 43).

In addition, we would investigate methods to “block” the free carboxylic acid group at C³⁶ of DEM30355/B2 **73**, to examine the effect on RNAP inhibition and *in vivo* bioassay studies against pathogenic bacteria (Figure 43). We postulated that removal of the free carboxylic

acid at C³⁶ may improve the pharmacokinetic properties of the DEM30355/B2 derivatives, for the same reasons as described previously (see section 2.3.3) with regards to rifamycin B **66**.

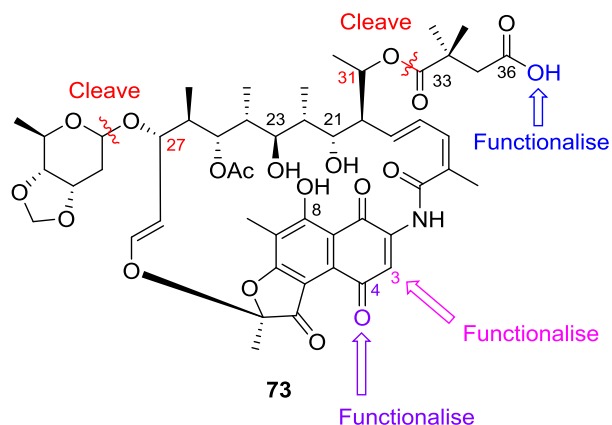


Figure 43: Planned semi-synthetic modifications of DEM30355/B2 **73**

2.3.5 Semi-Synthesis of Rifamycin S **68**

Given the limited availability of the starting material, DEM30355/B2 **73**, we would first test our planned semi-synthetic modifications on the structurally related ansamycin, rifamycin S **68**, which was readily available through oxidation of commercially available rifamycin SV Na salt **75**.

2.3.5.1 Conversion of Rifamycin SV Na Salt **75** to Rifamycin S **68**

Thus rifamycin SV Na salt **75** was dissolved in water and the solution was acidified with hydrochloric acid (2 M). The resultant red precipitate, rifamycin SV **69**, was isolated by filtration. In a second step, potassium hexacyanoferrate (III) was used to oxidise rifamycin SV **69** to rifamycin S **68** (Figure 44).⁷⁰

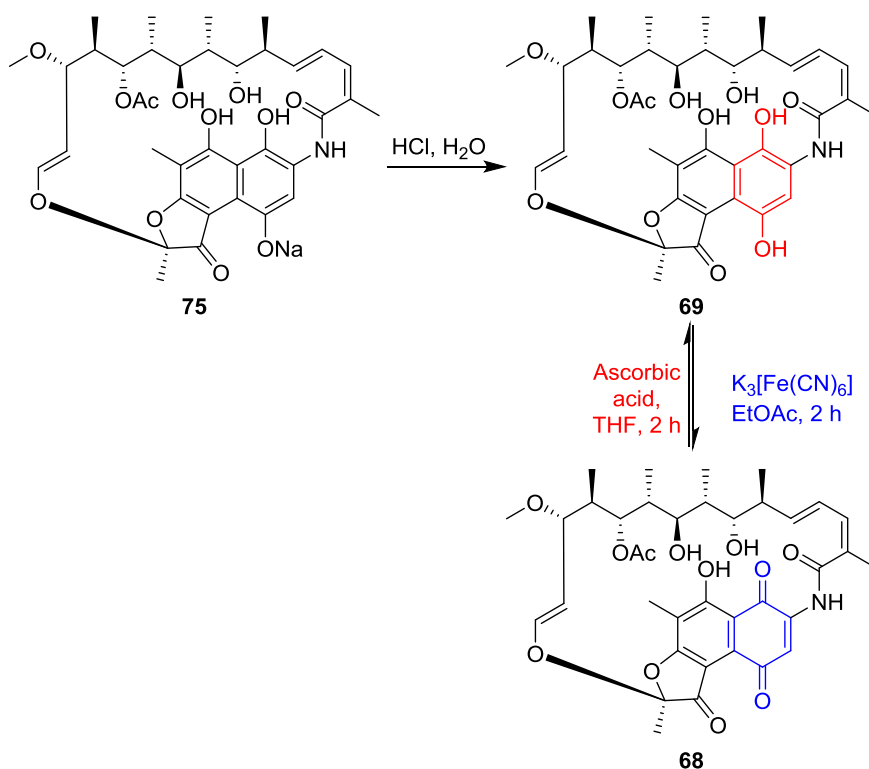


Figure 44: Conversion of rifamycin SV Na salt **75** to rifamycin SV **69** then rifamycin S **68**

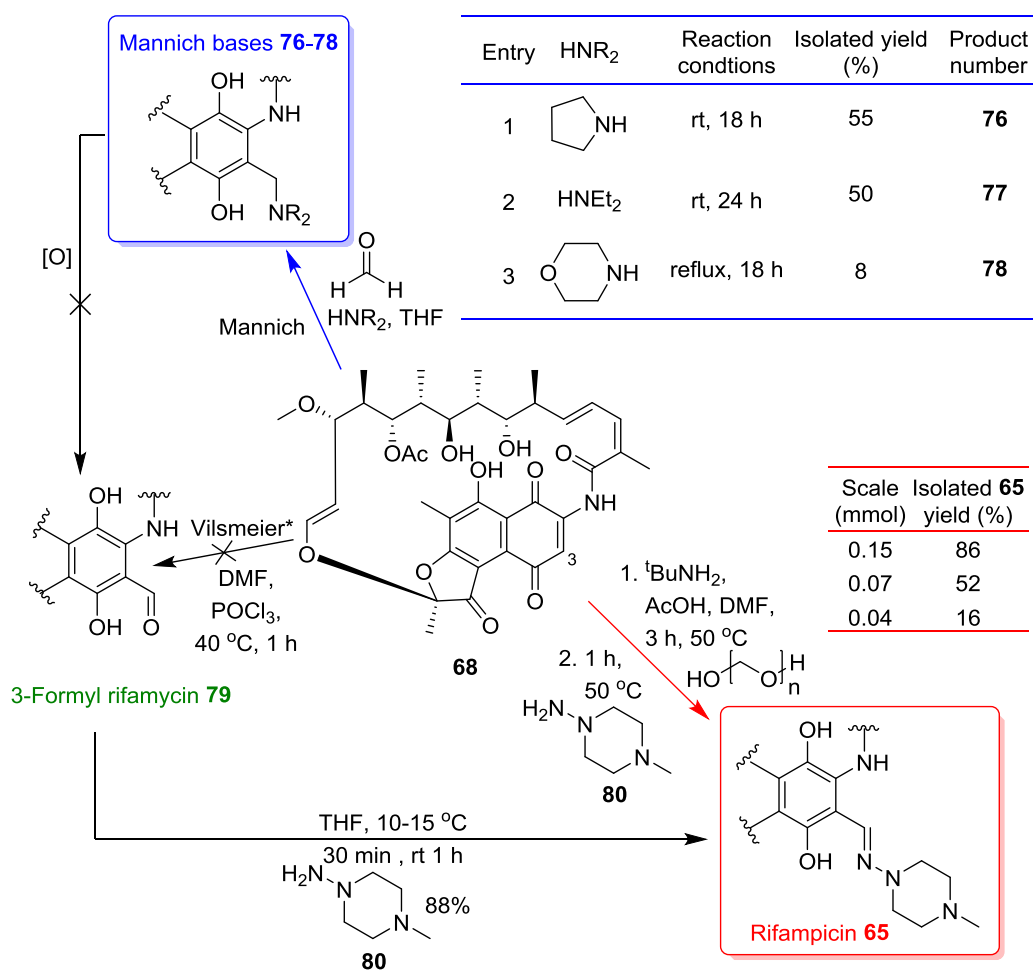
Following solvent extraction, rifamycin S **68** was obtained in a 97% yield over the two steps (Note: if desired, rifamycin S **68** can be reduced to rifamycin SV **69** with ascorbic acid).⁷⁰

With a sufficient quantity of rifamycin S **68** in hand, we moved on to investigate semi-synthetic modification of the compound. The aim was to optimise the chemistry to aid in the future semi-synthetic modification of DEM30355/B2 **73**, of which we had a very limited supply.

2.3.5.2 Functionalisation at C³ of Rifamycin S **68**

The SAR study by Wehrli and Staehelin indicated that functionalisation of position C³ in the rifamycins led to improved activity against RNAP derived from *E. coli*.^{77,78} Thus functionalisation of the analogous position in DEM30355/B2 **73** was a key objective in our planned semi-synthetic modifications to target bioactive DEM30355/B2 derivatives. There have been many reported procedures for the functionalisation of C³ in rifamycins S **68** and SV **69**, however the experiments were conducted on gram scales.⁸²⁻⁸⁴ We needed to optimise the chemistry for use on the milligram scale, as suitable for our future reactions with DEM30355/B2 **73**.

A range of reaction conditions was screened in order to examine functionalisation of rifamycin S **68** at the C³ position of the naphthoquinone ring. In each case, TLC was used to monitor the reaction, with ¹H NMR and/or mass spectrometry used to identify any new products formed (Figure 45).



*Vilsmeier reaction was conducted on rifamycin SV **69**

Figure 45: Reactions examined to generate rifampicin **65** via semi-synthetic modification of rifamycin S **68**

We also examined halogenation of the C³ position through the reaction of rifamycin S **68** or SV **69** with iodine in pyridine, tetrabutylammonium bromide and NBS, however only starting material **68** or **69** was recovered in each case.⁸⁵

2.3.5.3 Synthesis of Rifampicin Mannich Bases **76 - 78**

In our reactions we focused on the synthesis of rifampicin **65**, as in future we wanted to apply the same chemistry to generate the rifampicin analogue of DEM30355/B2 **73**, for a direct comparison of the biological activity. There was literature precedent to suggest that Mannich bases **76 - 78** (blue box, Figure 45) could be converted in two steps to rifampicin **65**, via oxidation to 3-formyl rifamycin **79** (green, Figure 45) then condensation with 1-amino-4-methylpiperazine **80**.⁸³

To synthesise Mannich bases **76 - 78**, rifamycin S **68** (1 eq.) was reacted with formaldehyde (3 eq.) and a chosen secondary amine (2 eq.) in THF (blue arrow, Figure 45).⁸² In each case the crude material was purified by column chromatography and analysed by mass spectrometry. The mass spectra showed peaks corresponding to desired products **76 - 78**, therefore we deduced the reactions were successful. The best yield of the Mannich product

was obtained from the reactions using pyrrolidine and diethylamine as the nucleophile (blue Table, entries 1 and 2, Figure 45). The poor yield of morpholino derivative **78** (blue Table, entry 3, Figure 45) was the result of the compound's instability towards silica gel chromatography.

With a successful route to Mannich bases **76** – **78** developed, we moved on to examine oxidation reactions to generate 3-formyl rifamycin **79**.

2.3.5.4 Synthesis of 3-Formyl Rifamycin SV **79**

To synthesise 3-formyl rifamycin **79** (green, Figure 45), Mannich bases **76** – **78** (blue, Figure 45) were screened under a range oxidising conditions using potassium hexacyanoferrate (III), manganese dioxide, ceric ammonium nitrate (CAN), *n*-amyl nitrite and lead(IV) acetate (Figure 45).⁸³ However in each case the starting material was recovered. As an alternative method, we examined a Vilsmeier acylation of rifamycin SV **69**, however no product **79** was formed and starting material **69** decomposed (Figure 45). At this stage we chose to examine a different route to the synthesis of rifampicin **65**.

2.3.5.5 One-Pot Synthesis of Rifampicin **65** from Rifamycin S **68**

There was literature precedent to suggest that rifampicin **65** could be prepared in a one-pot procedure from rifamycin S **68**.⁸⁶

Rifamycin S **68** (1 eq.) was reacted with *tert*-butylamine (1.4 eq.) and an excess of paraformaldehyde in DMF, in the presence of acetic acid (3.7 eq.) (red arrow, Figure 45). After 3 hours at 50 °C, 1-amino-4-methylpiperazine **80** was added, and the reaction continued for a further hour at 50 °C.⁸⁶

The ¹H NMR spectrum of the crude material showed disappearance of the signal at 7.58 ppm corresponding to C³H in rifamycin S **68**, and new signals were apparent at 3.24 - 3.04 ppm (4H, m) and 2.57 ppm (4H, m) which suggested four CH₂ groups. Therefore we could deduce that desired rifampicin **65** had been generated in the reaction. This was subsequently isolated following column chromatography in a 52% yield (70 μmol scale). It was found that the isolated yield of rifampicin **65** was dependent on the scale of the reaction (red Table, Figure 45).

After successfully generating Mannich bases **76** – **78** and rifampicin **65** from semi-synthetic modification of rifamycin S **68**, we moved on to apply the same chemistry to synthesise derivatives of DEM30355/B2 **73**.

2.3.6 Semi-Synthetic Investigations of DEM30355/B2 **73**

Our aim was to generate semi-synthetic derivatives of DEM30355/B2 **73**, a structural relative of rifamycin S **68**, to target new drug leads against rifampicin-resistant (Rif^r) strains of bacteria. One of our targeted derivatives was the DEM30355/B2 rifampicin analogue, to allow

comparison of the antibacterial activity of rifampicin **65** and the DEM30355B2 analogue against both rifampicin susceptible and Rif^r bacteria.

2.3.6.1 Synthesis of the DEM30355/B2 Rifampicin Analogue **81**

To synthesise rifampicin DEM30355/B2 analogue **81**, we planned to use the same synthetic procedure we had developed for the small scale synthesis of rifampicin **65** from rifamycin S **68** (Figure 46).⁸⁶

DEM30355/B2 **73** was reacted with *tert*-butylamine and an excess of paraformaldehyde in DMF, followed by addition of 1-amino-4-methylpiperazine **80** (Table 1).

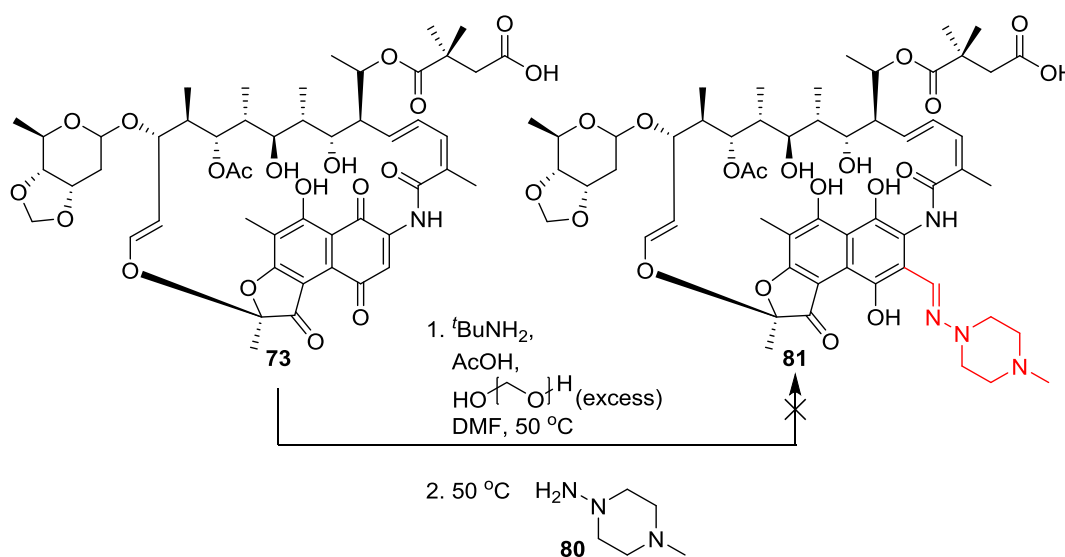


Figure 46: Reaction scheme to synthesise DEM30355/B2 rifampicin analogue **81** from DEM30355/B2 **73**

Table 1: Reaction conditions examined to synthesise DEM30355/B2 rifampicin analogue **81** from DEM30355/B2 **73**

Entry	$t\text{BuNH}_2$ eq.	Acetic acid eq.	1-Amino-4- methyl piperazine eq.	Reaction time
1	1.4	3.6	2.6	1. 3 h 2. 1 h
2 ^[a]	1.4	3.9	2.6	1. 3 h 2. 1 h
3	1.4	4.5	2.6	1. 5 h 2. 18 h
4	2.4	8.7	4.5	1. 3 h 2. 1 h

^[a]5 x larger scale and 2.5 x more concentrated than entry 1

In the first experiment, we employed the same reaction conditions that were previously used to synthesise rifampicin **65** from rifamycin S **68**. Analysis of the crude reaction material by mass spectrometry showed no peaks corresponding to desired product **81** and DEM30355/B2

73 was recovered (Table 1, entry 1). We hypothesised this may be a concentration issue as a result of the small reaction scale, therefore the concentration was increased 2.5 fold compared to the initial experiment (Table 1, entry 2). Once again unreacted starting material **73** was recovered. Increasing the reaction time (Table 1, entry 3) and increasing the equivalencies of the reactants (including paraformaldehyde) (Table 1, entry 4) also did not result in product **81** as shown by mass spectrometry and ^1H NMR analysis of the crude material.

There are several explanations as to why DEM30355/B2 rifampicin analogue **81** was not isolated in the reactions we tested. DEM30355/B2 **73** is more polar than rifamycin S **68** for which this chemistry was optimised, due to the presence of the carboxylic acid. With access to more DEM30355/B2 **73**, in future we would examine using a more polar aprotic solvent like DMSO, which may be required to sufficiently solvate DEM30355/B2 **73**, to allow the desired reaction to occur. However, given our limited supply of DEM30355/B2 **73** and the time constraints, optimisation of this route to generate desired analogue **81** was not feasible, therefore we decided to investigate alternative semi-synthetic modifications.

2.3.6.2 Synthesis of DEM30355/B2 Rifalazil Analogue **82**

Rifalazil **72** is an alternative semi-synthetic rifamycin antibiotic, which has been shown to be up to 64 times more active against TB infections than rifampicin **65** (Figure 22).⁸⁷ In addition, rifalazil **72** is active against certain strains of Rif^r *M. tuberculosis*, although a large proportion of Rif^r bacterial strains remain resistant to all the rifamycin antibiotics.⁸⁸

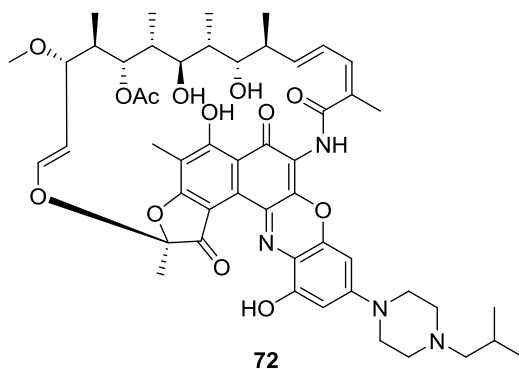


Figure 47: Structure of rifalazil **72**

We aimed to synthesise rifalazil DEM30355/B2 analogue **82**, for comparative bioassay studies against pathogenic bacteria (Figure 48). DEM30355/B2 **73** was reacted with aminophenols **83** and **84**, followed by an oxidative work-up (Table 2).⁸⁹ The reactions were monitored by TLC and the crude material was analysed using mass spectrometry.

Chapter 2. Isolation and Semi-Synthesis of DEM30355/B2

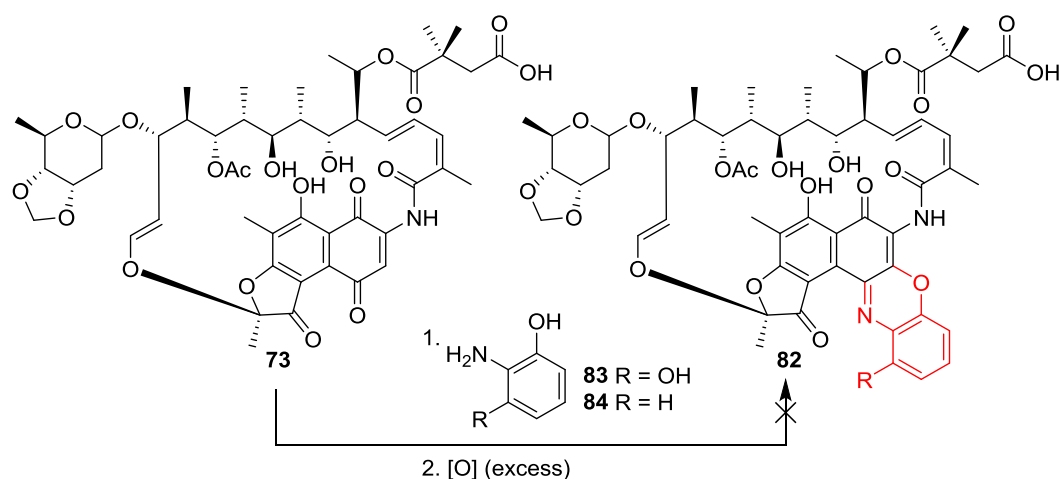


Figure 48: Reaction scheme to synthesise DEM30355/B2 rifalazil analogue **82** from DEM30355/B2 **73**

Table 2: Reaction conditions examined to synthesise DEM30355/B2 rifalazil analogue **82** from DEM30355/B2 **73**

Entry		R	Eq.	Reaction conditions
1	OH	OH	1	1. THF: Toluene (1:1), rt, 12 d 2. EtOAc, $\text{K}_3[\text{Fe}(\text{CN})_6]$, rt, 18 h
2	OH	OH	10	1. THF: Toluene (1:1), rt, 13 d 2. EtOH, MnO_2
3	H	H	1	1. THF, rt, 18 h 2. EtOH, MnO_2

In the first reaction we tested using 2-amino resorcinol hydrochloride **83** (R = OH), no reaction was observed by TLC after a lengthy reaction time (Table 2, entry 1). Increasing the equivalencies of 2-amino resorcinol **83** also did not result in an observed reaction by TLC, and starting material **73** was recovered (Table 2, entry 2). There was literature precedent to suggest that the presence of two hydroxyl units in the nucleophile **83** may result in a redox reaction generating hydroquinone DEM30355/B2.⁹⁰ Therefore we changed the nucleophile to 2-amino phenol **84**, however once again no product **82** was observed by TLC or through mass spectrometry analysis, and starting material **73** was recovered (Table 2, entry 3).

In future, we would examine alternative nucleophiles to generate rifalazil analogue **82**, however given the time constraints and limited starting material **73** supply, we decided to investigate different modifications.

2.3.6.3 Acidic and Basic Hydrolysis of DEM30355/B2 **73**

We hypothesised that the observed inhibitory activity of DEM30355/B2 **73** against Rif^r RNAP (taken from *E. coli*) may be the result of additional stability induced by H-bonding and/or van

der Waals interactions with the deoxy-sugar moiety of DEM30355/B2 **73** at C²⁷ (Figure 49). To test this theory, we wanted to generate derivatives of DEM30355/B2 **73** without the deoxy-sugar group in place for SAR studies.

To remove the deoxy-sugar group at C²⁷, we planned to cleave the acetal unit that connected the sugar to DEM30355/B2 **73**. DEM30355/B2 **73** was reacted under acidic and basic hydrolysis conditions and the crude material analysed by mass spectrometry for new product peaks (Table 3). We anticipated that hydrolysis may affect other groups of DEM30355/B2 **73**, so we included these masses in our search (Figure 49). In each case an excess of the acid or base was used.

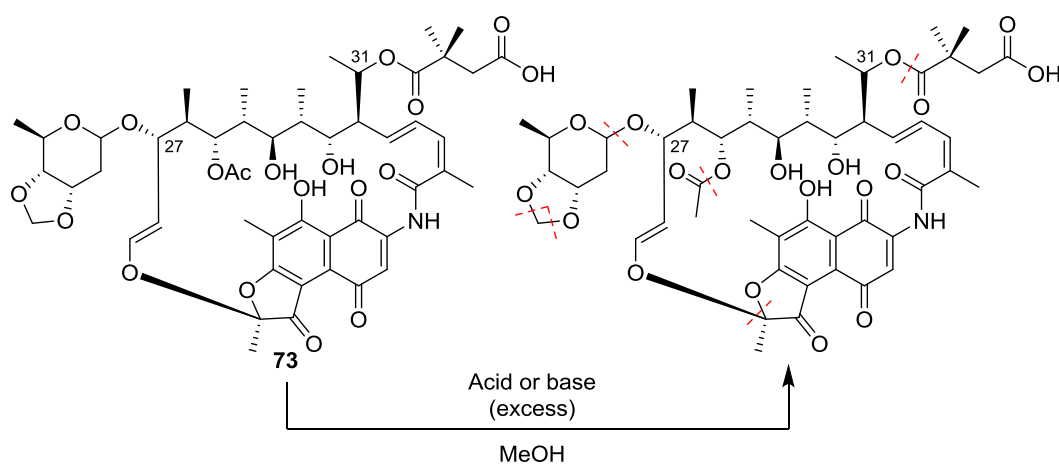


Figure 49: Reaction scheme showing the possible areas of DEM30355/B2 affected by the reaction of DEM30355/B2 **73** with acid or base

Table 3: Reaction conditions examined in the hydrolysis of DEM30355/B2 **73**

Entry	Reaction conditions
1	NaOH, 6 h
2	<i>p</i> TSA, 18 h
3	<i>p</i> TSA, 4 h

The mass spectra of the crude material from the initial reactions using NaOH and *p*TSA showed no peaks corresponding to starting material **73** (Table 3, entries 1 and 2). Peaks with a lower mass than DEM30355/B2 **73** were evident, however these did not correspond to our targeted product(s). We repeated the reaction with *p*TSA using a shorter reaction time (Table 3, entry 3). In this case we observed peaks corresponding to starting material **73** and hydrolysis product **85**, where the sugar group of DEM30355/B2 **73** had been cleaved (Figure 50).

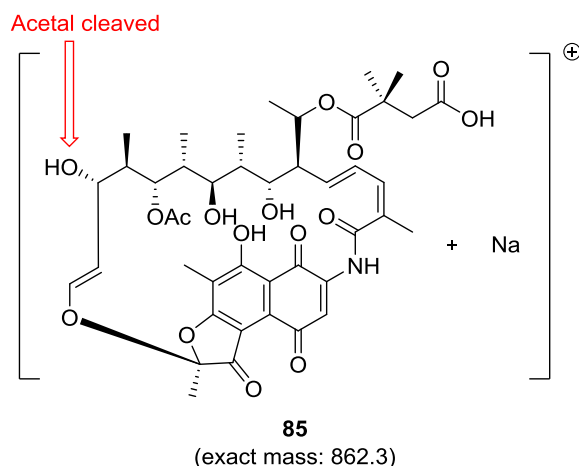


Figure 50: Structure of DEM30355/B2 derivative **85** associated with a peak at m/z 862.3 $[M+Na]^+$ in the mass spectrum

In future, with access to more DEM30355/B2 **73**, we would optimise this reaction and isolate derivative **85**, to allow further characterisation to be carried out.

2.3.6.4 Synthesis of DEM30355/B2 Derivative **86** via EDCI Coupling

We aimed to block the free carboxylic acid group of DEM30355/B2 **73**, to determine the effect on the antibacterial activity of the compound. We anticipated this may be achieved through EDCI coupling of DEM30355/B2 **73** to generate amide **86** (Figure 51).

DEM30355/B2 **73** (1 eq.) was reacted with EDCI (1.5 eq.) and 4-methoxybenzylamine (1.5 eq.) in the presence of nucleophilic catalysts (Table 4).

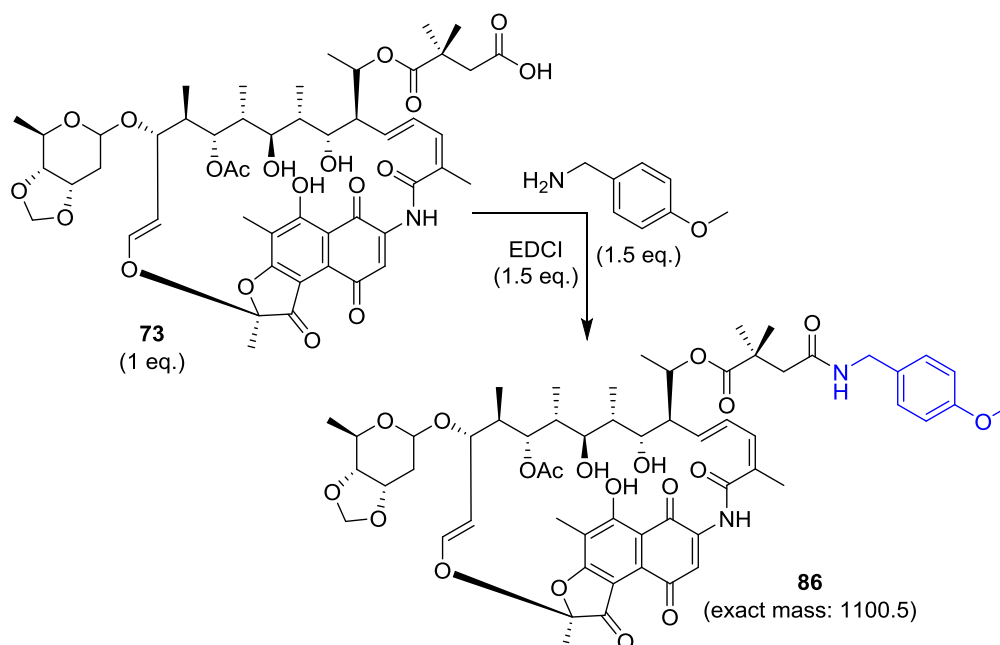


Figure 51: Reaction scheme for the synthesis of amide **86** from an EDCI coupling reaction of DEM30355/B2 **73** with 4-methoxybenzylamine

Chapter 2. Isolation and Semi-Synthesis of DEM30355/B2

Table 4: Reaction conditions examined in the EDCI coupling reaction of DEM30355/B2 **73** with 4-methoxybenzylamine

Entry	Reaction conditions	Observed ions ^[a]
1	DCM- <i>d</i> ₂ , DMAP (0.1 eq), rt, 27 h	73 ^[b]
2	DCM, HOBT (0.1 eq), rt, 27 h	73 ^[b] and [86 +H] ⁺ and [86 +Na] ⁺
3	DCM- <i>d</i> ₂ , DMAP (0.1 eq), rt, 24 h ^[c]	73 ^[b]
4	DCM, HOBT (0.1 eq), rt, 24 h ^[c]	73 ^[b]

^[a]Through analysis of the mass spectrum of the crude material

^[b]Peaks corresponding to [**73**+H]⁺, [**73**+Na]⁺ and [**73**-H+2Na]⁺ were observed

^[c]DEM30355/B2 **73**, EDCI and HOBT or DMAP were reacted for 1 h prior to the addition of 4-methoxybenzylamine

The crude reaction material from each experiment was analysed by mass spectrometry. In each case, peaks corresponding to unreacted starting material **73** were observed. However, in one experiment using hydroxybenzotriazole (HOBT), we also observed *m/z* peaks at 1101.3* and 1123.4* corresponding to desired product **86** (Table 4, entry 2) (*Note: the masses stated have been corrected by -0.7 mass units, using the cluster of ions at [M+H]⁺, [M+Na]⁺ and [M-H+2Na]⁺ of DEM30355/B2 **73** as a standard).

With this promising result, we opted to scale up this reaction, to isolate a sufficient quantity of amide **86** for further analysis and bioassay, therefore the reaction was repeated using the same conditions, on a 5 fold larger scale.

The ¹H NMR spectrum of the crude material appeared to show signals corresponding to unreacted starting material **73** and a new product(s) (Figure 52).

Chapter 2. Isolation and Semi-Synthesis of DEM30355/B2

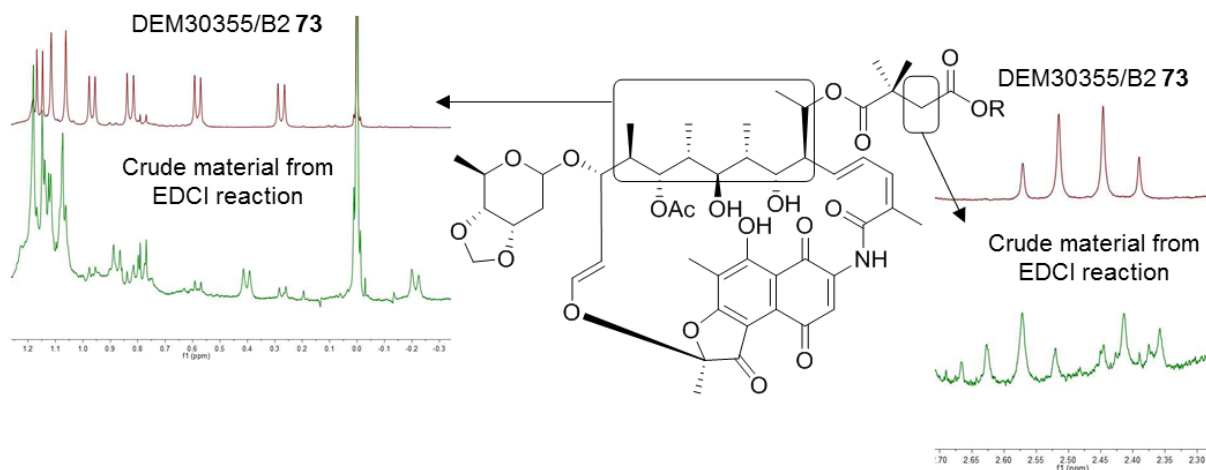


Figure 52: Expansion of the ^1H NMR spectra of DEM30355/B2 **73** and the crude material from the EDCI reaction. Left – signals corresponding to the methyl groups of the ansa chain. Right – signals corresponding to the CH_2 group next to the carboxylic acid

The crude material was subjected to size exclusion chromatography (LH20 in methanol), followed by semi-preparative HPLC. The HPLC spectrum showed a peak at 30 minutes corresponding to unreacted DEM30355/B2 **73**, and three new peaks at 18 minutes, 22 minutes and 28 minutes corresponding to unidentified products (Figure 53).

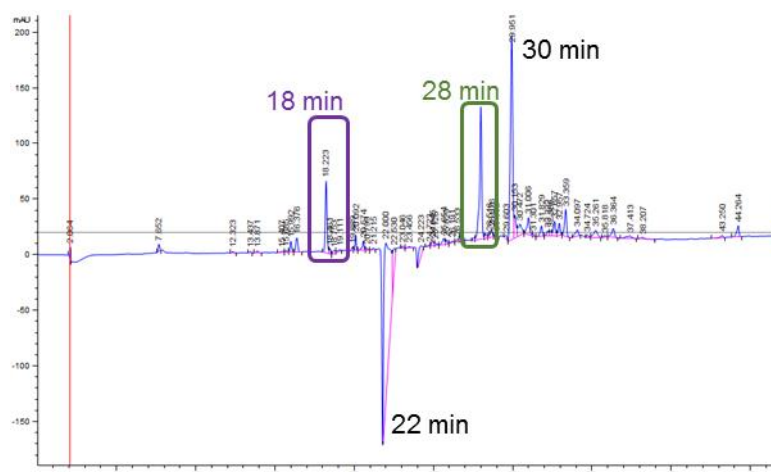


Figure 53: HPLC trace of sample from EDCI reaction of DEM30355/B2

Unfortunately the negative peak at 22 minutes was not recognised by the automated collection system, however the new peaks at 18 minutes and 28 minutes were collected and analysed by mass spectrometry (Figure 54).

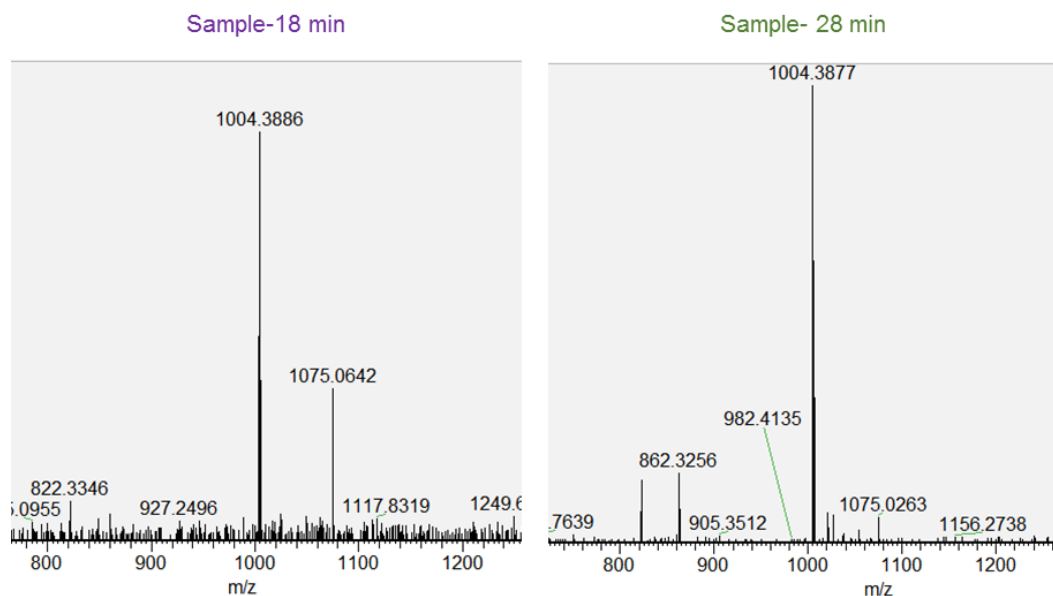


Figure 54: Expansion of the mass spectra of sample-18 min and sample-28 min isolated by semi-preparative HPLC of the EDCI reaction material

To our surprise, the mass spectra of both samples did not contain any peaks corresponding to desired product **86**, only a peak at $m/z = 1004.4$, corresponding to $[M+Na]^+$ of starting material **73** (Figure 54). This suggested that the signals in HPLC spectrum corresponded to DEM30355/B2 **73** in a different oxidation state to the quinone form which appeared at 30 minutes (Figure 53).

This prompted us to consider that the apparently new signals we had observed in the ^1H NMR spectrum of the crude material (Figure 52) may correspond to the hydroquinone form of DEM30355/B2.

2.3.6.5 Reduction of Quinone DEM30355/B2 **73** to Hydroquinone DEM30355/B2 **87**

To test this theory, DEM30355/B2 **73** was reacted with an excess of the reductant, ascorbic acid, at room temperature to generate hydroquinone DEM30355/B2 **87** (Figure 55).

Chapter 2. Isolation and Semi-Synthesis of DEM30355/B2

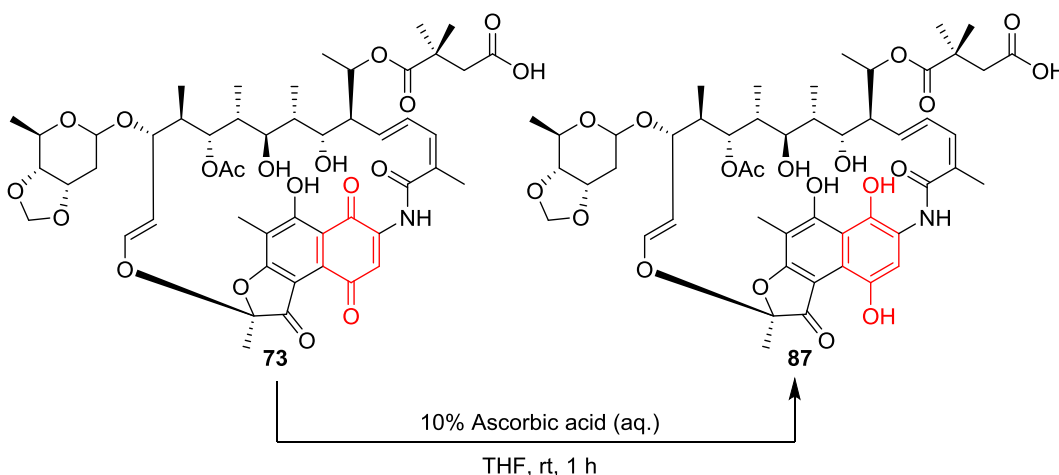


Figure 55: Reduction of quinone DEM30355/B2 **73** to hydroquinone DEM30355/B2 **87**

After 1 hour, when TLC indicated the reaction was complete, the reaction mixture was extracted with ethyl acetate and the crude material analysed by ^1H NMR.

We compared the ^1H NMR of the spectrum of DEM30355/B2 **73** (quinone form), hydroquinone DEM30355/B2 **87** and the crude material of the EDCI reaction (Figure 56). Analysis of the spectra indicated the EDCI crude sample contained both hydroquinone DEM30355/B2 **87** and quinone DEM30355/B2 **73**, which was consistent with our hypothesis. However, a doublet peak at 0.4 ppm was observed, which did not correspond to either quinone DEM30355/B2 **73** or hydroquinone DEM30355/B2 **87**, suggesting the presence of a new product arising from the EDCI reaction.

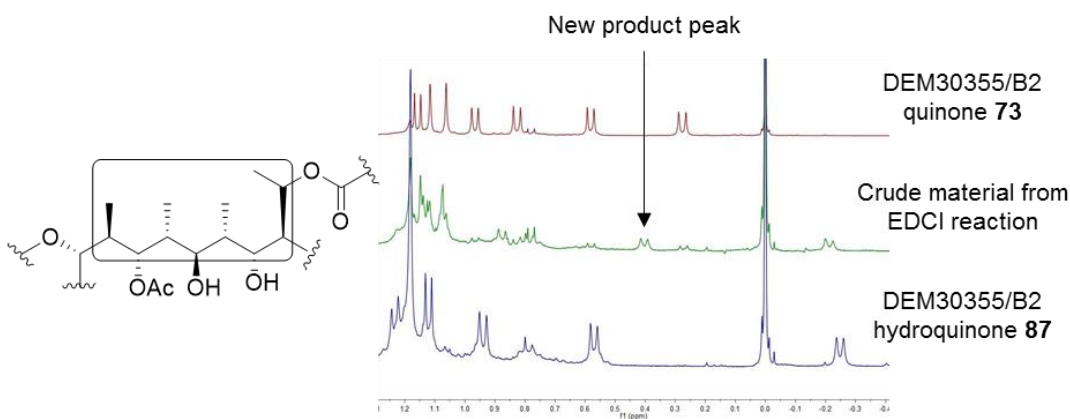


Figure 56: Expansion of the ^1H NMR spectra of quinone DEM30355/B2 **73**, the crude material from the EDCI reaction and hydroquinone DEM30355/B2 **87**, in the region showing signals corresponding to the methyl groups of the ansa chain

We postulate that redox chemistry of the naphthalene group of DEM30355/B2 **73** may interfere with the EDCI reaction. Therefore in future we would try conducting the reaction both in the presence of a reductant and an oxidant to render the naphthalene in one oxidation state, to try and push the EDCI reaction to completion. Following optimisation of the reaction and isolation of amide **86**, the sample would be subjected to bioassay, to identify any interesting biological activity.

2.3.6.6 Synthesis of DEM30355/B2 Methyl Ester **88**

As an alternative to EDCI coupling to “block” the free carboxylic acid of DEM30355/B2 **73**, we investigated methylation of the carboxylic acid OH to give methyl ester **88** (Figure 57). We reacted DEM30355/B2 **73** (1 eq.) with TMS-diazomethane (4 eq.) in methanol.

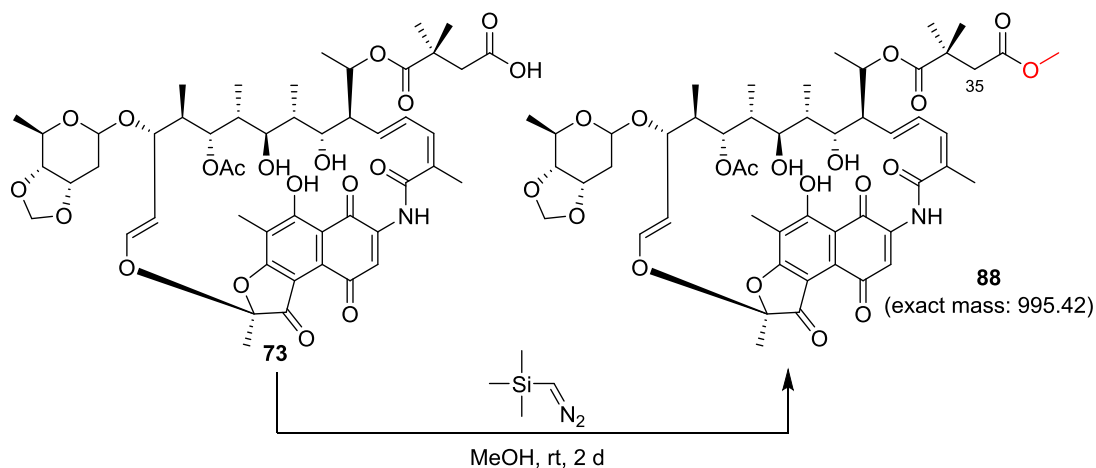


Figure 57: Methylation of DEM30355/B2 **73** to synthesise methyl ester **88**

After a reaction time of 2 days, TLC showed DEM30355/B2 **73** remained in the reaction mixture therefore a further 4 eq. of TMS-diazomethane were added. After 4 days, TLC showed loss of starting material **73** and the reaction was quenched. Following purification by column chromatography, the sample was analysed by NMR, which indicated a new product had been generated. Through analysis of the HSQC spectrum, we were able to identify signals at 2.65 ppm and 2.43 ppm corresponding to C³⁵H₂ in the new derivative of DEM30355/B2 (Figure 58).

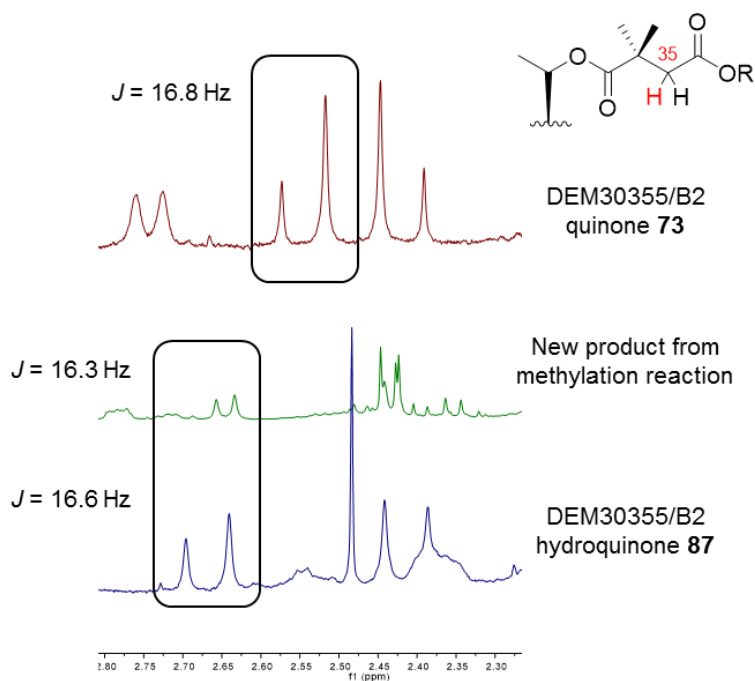


Figure 58: Expansion of the ¹H NMR spectra of quinone DEM30355/B2 **73**, the new product from the methylation reaction and hydroquinone DEM30355/B2 **87**. The highlighted signals correspond to C³⁵-H, with $J_{H35-H35}$ reported

The geminal coupling constant of the C³⁵ proton at 2.65 ppm in the sample ($J = 16.3$ Hz) did not correspond to the analogous proton at C³⁵ in either quinone DEM30355/B2 **73** ($J = 16.8$ Hz) or hydroquinone DEM30355/B2 **87** ($J = 16.6$ Hz), suggesting a new DEM30355/B2 derivative (Figure 58).

The sample was analysed by High Resolution Mass Spectrometry (HRMS). We were able to observe m/z peaks at 996.4 and 1018.4 corresponding to the $[M+H]^+$ and $[M+Na]^+$ ions respectively of singly-methylated product **88** (Figure 59).

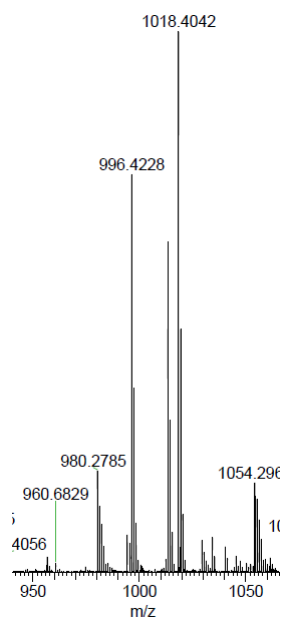


Figure 59: Expansion of the mass spectrum of methyl ester **88** showing m/z peaks corresponding to $[M+H]^+$ and $[M+Na]^+$ ions

In future, we hope to scale up this reaction to obtain more methyl ester **88** for further analysis using NMR, to confirm our proposed structure.

With this positive result, we examined other semi-synthetic modifications of DEM30355/B2 **73**.

2.3.6.7 Synthesis of Pyrrolidino DEM30355/B2 **89**

In our preliminary work on the semi-synthesis of rifamycin S **68**, we successfully synthesised Mannich bases **76** - **78** (see section 2.3.5). The best reaction generated pyrrolidino rifamycin **76**, in terms of yield and product stability. Therefore we applied the same synthetic procedure to synthesise the analogous pyrrolidino DEM30355/B2 derivative **89** (Figure 60).⁸²

Chapter 2. Isolation and Semi-Synthesis of DEM30355/B2

DEM30355/B2 **73** (1 eq.) was reacted with pyrrolidine (2 eq.) and formaldehyde (3 eq.) in THF.

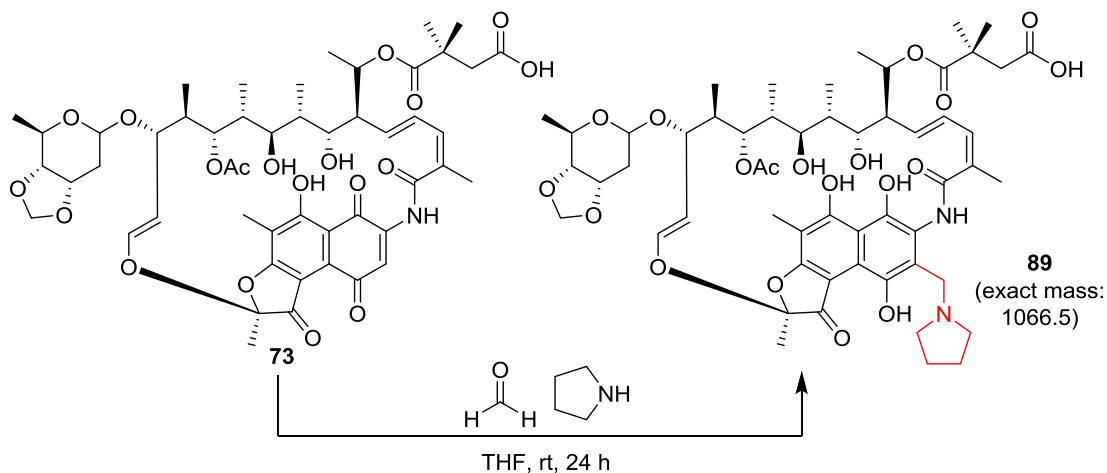


Figure 60: Mannich reaction of DEM30355/B2 **73** to generate pyrrolidino DEM30355/B2 **89**

After 24 hours at room temperature, TLC showed new spots in addition to starting material **73**, and the reaction was stopped. The crude material was initially purified by column chromatography; unreacted **73** was recovered and a new product was isolated. Mass spectrometry analysis of the purified sample showed ions corresponding to desired product **89**, with a m/z peak at 1065.48 ($[M-H]^-$), in addition to starting material **73**. To separate desired product **89** from DEM30355/B2 **73**, the sample was subjected to size-exclusion chromatography (LH20, methanol) and the resultant sample analysed by HPLC. The HPLC spectrum contained three peaks at 24.7 minutes, 26.6 minutes and 27.0 minutes, suggesting a mixture of products (Figure 61).

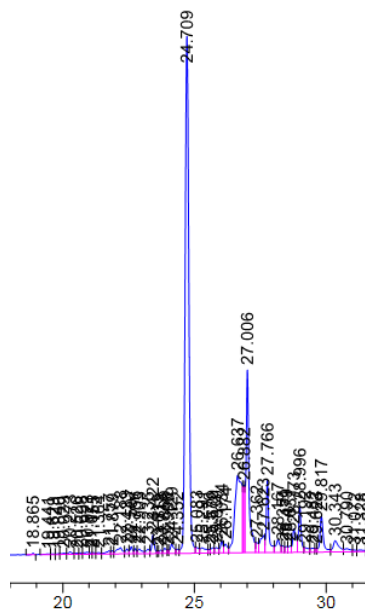


Figure 61: HPLC trace of the sample from the Mannich reaction of DEM30355/B2 following size-exclusion chromatography

Chapter 2. Isolation and Semi-Synthesis of DEM30355/B2

We attempted to separate the mixture using semi-preparative HPLC. The compound corresponding to the well resolved peak at 24.7 minutes was collected in one fraction, however the peaks at 26.6 and 27.0 minutes could not be separated and were collected together.

The two fractions collected, sample-24.7 min and sample-26.6+27.0 min, were analysed by HRMS (Figure 62).

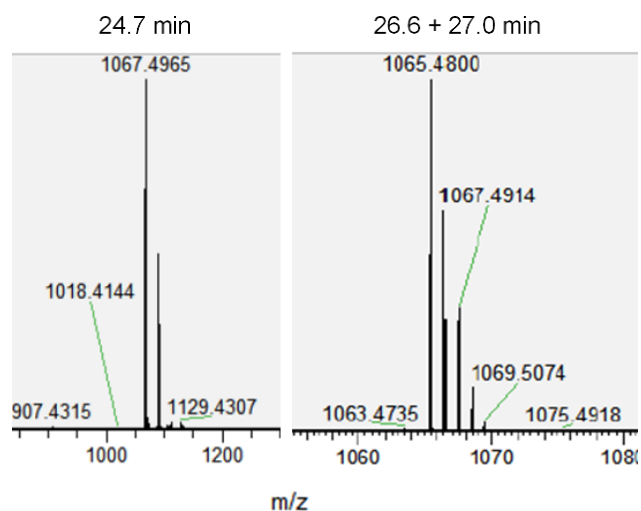


Figure 62: Expansion of the mass spectra of sample-24.7 min and sample-26.6+27.0 min isolated following semi-preparative HPLC

The mass spectrum of sample-24.7 min showed a peak at 1067.5 m/z, corresponding to hydroquinone pyrrolidino product **89** (Figure 60). The spectrum of sample-26.6+27.0 min, showed peaks at 1067.5 and 1065.5, consistent with pyrrolidino product in a mixture of the hydroquinone **89** and quinone **90** forms (Figure 63).

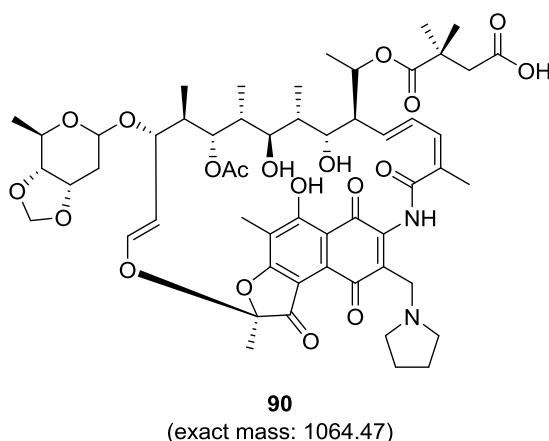


Figure 63: Structure of hydroquinone pyrrolidino-DEM30355/B2 **90**

Thus we could conclude we had isolated hydroquinone pyrrolidino-DEM30355/B2 **89** (2.7 mg, 2.5 μ mol, 17% yield) and a mixed sample of quinone and hydroquinone pyrrolidino-DEM30355/B2 **89** and **90** (2.0 mg).

2.4 Conclusions and Future Work

Through analysis of extensive NMR data in combination with an X-ray structure (Dr B. Kepplinger), we have assigned DEM30355/B2 as kanglemycin A **73**, which had previously been isolated.⁷³ An *in vitro* enzyme inhibition assay indicated that DEM30355/B2 **73** inhibited rifampicin-resistant (Rif^r) RNAP derived from a mutant *E. coli* strain (L. Ceccaroni), therefore we aimed to generate analogues of this compound through semi-synthesis to identify new antibiotic drug leads. We have developed an efficient isolation protocol to access pure DEM30355/B2 **73** in sufficient quantities (~150 mg) for semi-synthesis, through use of a key acid-base extraction

The most successful procedure we examined to functionalise the C³ position of DEM30355/B2 **73** was a Mannich reaction using formaldehyde and pyrrolidine, to give Mannich bases **89** and **90** (blue, Figure 64). In addition, the most successful method to functionalise the free carboxylic acid group of DEM30355/B2 **73** was to methylate using TMS-diazomethane, generating methyl-ester **88** (red, Figure 64). Derivatives **88**, **89**, and **90** are currently undergoing investigation to assess their inhibition activity against Rif^r RNAP (H. M. Sejzi).

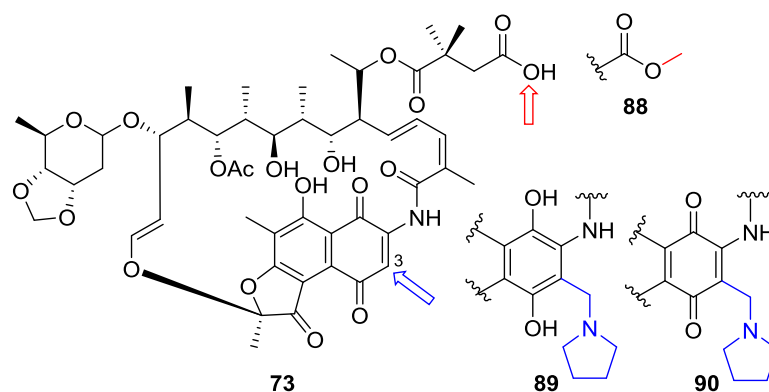


Figure 64: Structures of DEM30355/B2 **73** and the semi-synthetic derivatives methyl ester **88**, hydroquinone Mannich base **89** and quinone Mannich base **90**

In the future, we would resume our efforts to synthesise rifampicin and rifalazil analogues of DEM30355/B2. We anticipate that our previous attempts to functionalise the C³ position of DEM30355/B2 **73** to synthesise these derivatives may have been hindered by unwanted side reactions involving the carboxylic acid. Therefore we would protect the carboxylic acid of DEM30355/B2 as the methyl ester **88**, then repeat the chemistry we have examined before, to generate analogues **91** and **92** (Figure 65).

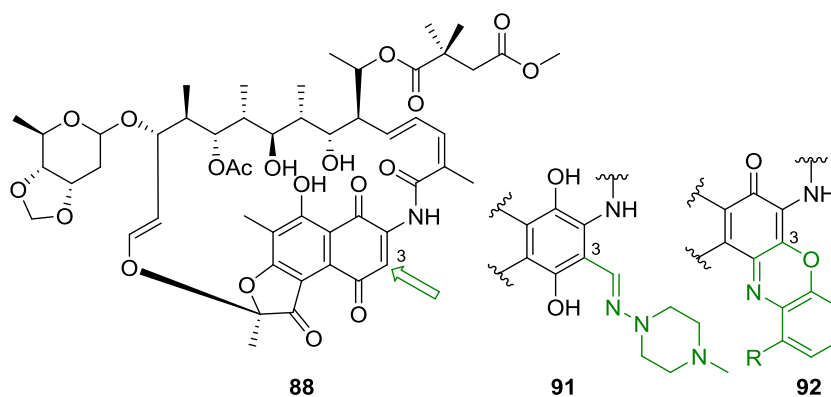


Figure 65: Structures of future DEM30355/B2 **73** semi-synthetic targets, methyl ester rifampicin analogue **91** and methyl ester rifalazil analogue **92**

We also considered that redox reactions of the naphthalene ring of DEM30355/B2 **73** may have hindered the synthesis of rifampicin and rifalazil analogues **81** and **82** respectively, as well as amide **86** from the EDCI reaction (Figure 66). Therefore in future, to target these derivatives, we would examine redox buffered reactions using a mild reductant or oxidant. If this redox buffering approach was successful, we would apply the same method to synthesise halogenated derivatives **93**, which may be used to generate other compounds through Pd cross-coupling.

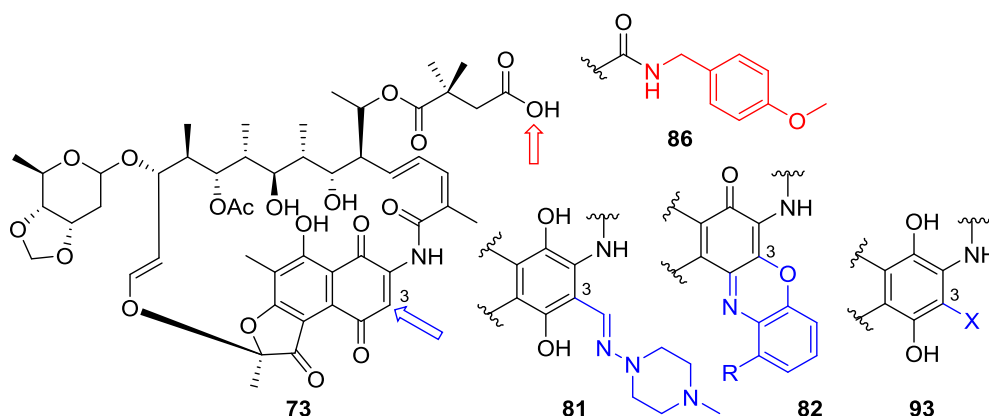


Figure 66: Structures of future DEM30355/B2 **73** semi-synthetic targets, amide **86**, rifampicin analogue **81**, rifalazil analogue **82** and halogenated derivative **93**

Chapter 3. Total Synthesis of the C and B Rings of DEM30355/A

3.1 Introduction to Total Synthesis

Total synthesis (“Chem”-synthesis) is the construction of a natural product using chemical reactions, from commercially available starting materials. In Chapter 1 we discussed the importance of total synthesis as a source of the natural product, discodermolide **16**, a compound which could not be economically obtained through typical “Bio”-synthetic approaches, such as cultivating the natural-product producing organism (Figure 67).^{42,43} We also discussed the use of total synthesis to generate new drug leads, using analogues of spirotryprostatin A **28** which were made by total synthesis and showed inhibitory activity against two human cancer cell lines, as an example (Figure 67).^{46,47}

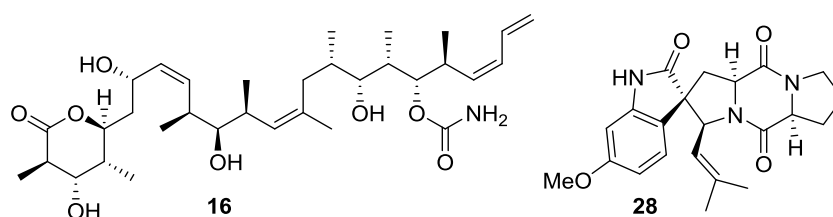


Figure 67: Structures of discodermolide **16** and spirotryprostatin A **28**

From a non-therapeutic point of view, the total synthesis of complex natural products, which often contain multiple stereocentres, is a worthwhile challenge to synthetic chemists. Through the practice of total synthesis, many important synthetic techniques and theories have emerged, such as the Barton reaction, developed in the total synthesis of aldosterone, and the Woodward-Hoffman rules, sparked by observations in Woodward’s synthesis of vitamin B12.⁹¹⁻⁹⁴ In addition, total synthesis is a useful tool to elucidate the absolute stereochemistry of a compound. For example, early total syntheses of both enantiomers of discodermolide **16** revealed the absolute stereochemistry of the molecule, an important consideration for both target investigation and for subsequent manufacture of the compound for use in drug trials.⁹⁵

3.1.1 Project Aims

In this chapter we will discuss work towards the total synthesis DEM30355/A **94**, a novel compound isolated from the fermentation broth of *Amycolatopsis DEM30355* (Chapter 2) (Figure 68). The relative stereochemistry of DEM30355/A **94** is shown, as determined through X-ray crystallography analysis (Dr M. J. Hall) however the absolute stereochemistry has not been determined.

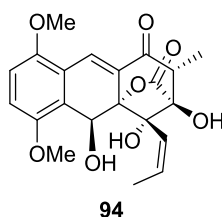


Figure 68: Structure of DEM30355/A **94** (relative stereochemistry shown)

DEM30355/A **94**, which has a highly oxygenated polyketide structure, is active against Gram-positive bacteria (Dr B. Kepplinger). By developing a synthetic route to DEM30355/A **94**, we aim to:

- Determine the absolute stereochemistry of the natural product
- Synthesise DEM30355/A analogues for SAR studies and to probe the mode of action
- Synthesise DEM30355/A analogues to identify new antibiotic drug leads

DEM30355/A **94** is structurally related to rishirilides A **95** and B **96**, isolated from *Streptomyces rishiriensis* in the 1980s (Figure 69). The rishirilides are α 2-macroglobulin inhibitors, with IC_{50} values of 100 μ g/mL and 35 μ g/mL for rishirilides A **95** and B **96** respectively.⁹⁶ α 2-Macroglobulin is a glycoprotein that inhibits fibrinolysis, the breakdown of blood clots. Therefore α 2-macroglobulin inhibitors are useful in the treatment of thrombosis and related conditions. Furthermore, rishirilide B **96** is an inhibitor of glutathione *S*-transferase, with an IC_{50} value of 26.9 μ M.⁹⁷ Glutathione *S*-transferase is an enzyme implicated in promoting resistance to particular anticancer agents. Combining an inhibitor of this enzyme with other anticancer therapeutic agents, has the potential to overcome this resistance, improving the efficacy of treatment.⁹⁸

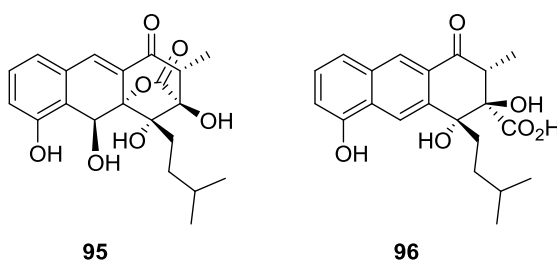


Figure 69: Structures of rishirilide A **95** and rishirilide B **96**

3.1.2 Total Synthesis of Rishirilide B **96**

3.1.2.1 Danishefsky's Total Synthesis of (-)-Rishirilide B

The interesting bioactivity of rishirilide B **96** has prompted several research groups to pursue the total synthesis of the molecule. Danishefsky *et al.* devised a convergent synthesis of racemic and *ent*-rishirilide B **97**, based upon a key regioselective Diels-Alder (D-A) reaction (Figure 70).⁹⁹ The total synthesis of *ent*-rishirilide B **97** starts with the synthesis of dienophile **98** (Figure 70). Cyclohexenone **99**, synthesised from enantiopure (*R*)-3-methylcyclohexan-1-one, is subjected to Rubottom oxidation conditions, by first reacting compound **99** with NaH and *tert*-butyl dimethylsilyl trifluoromethanesulfonate (TBSOTf) to generate the silyl enol ether, followed by oxidation with dimethyldioxirane (DMDO). The Me group at C² sterically directs epoxidation to the opposite face, generating product **100** with an anti-arrangement with respect to the C³ alcohol, as seen in the natural product. The allylic position of compound **100** is then oxidised in two steps, through a Wohl-Ziegler reaction with azobisisobutyronitrile (AIBN) and *N*-bromosuccinimide (NBS) to generate a brominated intermediate, followed by solvolysis to

give diol **101**. The secondary alcohol of diol **101** is subsequently oxidised using Dess-Martin periodinane (DMP), to give dienophile **98**, corresponding to the A ring of *ent*-rishirilide B **97**.⁹⁹

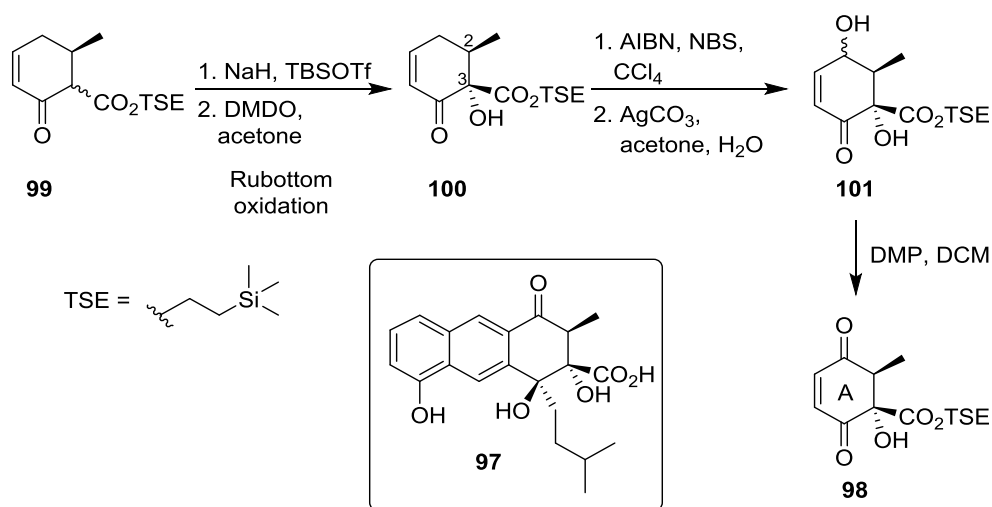


Figure 70: Synthesis of Danishefky's dienophile **98** in the total synthesis of *ent*-rishirilide B **97**

The next stage was to build the B ring of *ent*-rishirilide B **97**. Danishefsky uses benzocyclobutene **102** to generate a reactive dimethide diene *in situ*, which undergoes a regioselective and *exo* selective D-A reaction with dienophile **98**, to give D-A cycloadduct **103** (Figure 71).⁹⁹

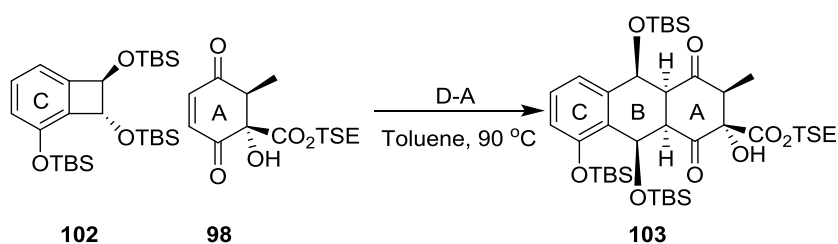


Figure 71: Key Diels-Alder reaction to generate adduct **103** in Danishefsky's synthesis of *ent*-rishirilide B **97**

Following the D-A reaction, two TBS protected alcohol groups are removed from D-A adduct **103** with camphorsulfonic acid in refluxing methanol (Figure 72). This is followed by a directed Grignard addition of *iso*-pentylmagnesium bromide to resultant naphthalene **104** to give diol **105**. The tertiary alcohol of naphthalene **104** directs addition of the isopentyl group to the same face, by chelating with the organomagnesium reagent, resulting in an *anti*-arrangement of the adjacent hydroxyl groups at C³ and C⁴ as seen in *ent*-rishirilide B **97**. Finally, deprotection of diol **105** using tris(dimethylamino)sulfur(trimethylsilyl)difluoride (TASF) gives (-)-rishirilide B **97**, in an overall yield of 0.4% over 10 steps from (*R*)-3-methylcyclohexan-1-one.^{99,100}

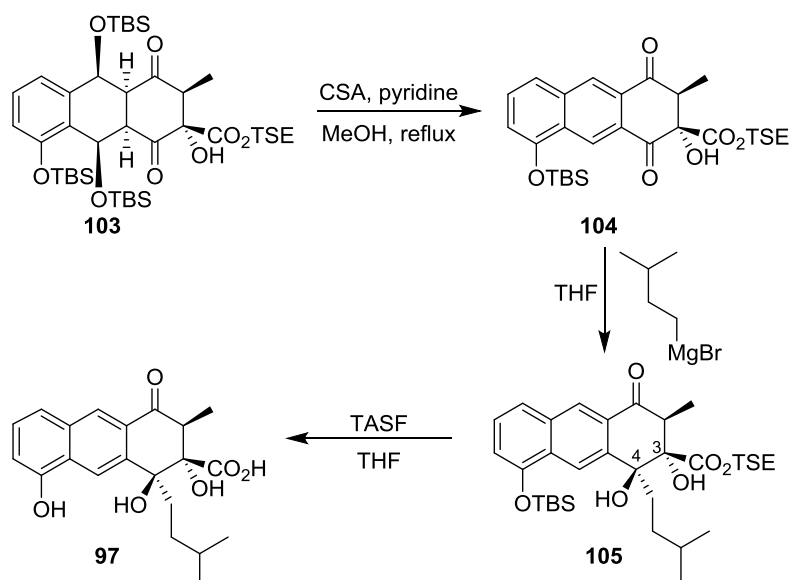


Figure 72: Conversion of Diels-Alder cycloadduct **103** to ent-rishirilide **B 97** in Danishefsky's total synthesis

Through the total synthesis of (-)-rishirilide **B 97** and subsequent specific rotation measurements, Danishefsky *et al.* were able to establish the absolute stereochemistry of the naturally occurring product as (+)-rishirilide **B 96**.⁹⁹ The use of total synthesis to determine the absolute stereochemistry of natural products is widespread. It is one of the options available if the absolute stereochemistry of a natural product cannot be determined through other methods, such as using X-ray crystallography (often via synthetic modification to include a heavy atom), or via comparison of experimental and calculated electronic circular dichroism (ECD) and vibrational circular dichroism (VCD) spectra.

3.1.2.2 Pettus' Total Synthesis of Rishirilide B 96

The Pettus group were the first to synthesise (+)-rishirilide **B 96** as found in nature.¹⁰⁰ Following the synthesis of protected aromatic diol **106**, the total synthesis then proceeds with a Mitsunobu reaction with chiral *N*-alkoxyamide **107**, followed by removal of the Boc protecting group to give aryl-ether **108** (Figure 73).¹⁰⁰ Oxidative dearomatisation by the reaction of aryl-ether **108** with iodosylbenzene-trimethylsilyl triflate, followed by intramolecular cyclisation is used to synthesise lactone **109**, corresponding to the A ring of rishirilide **B 96**.¹⁰⁰

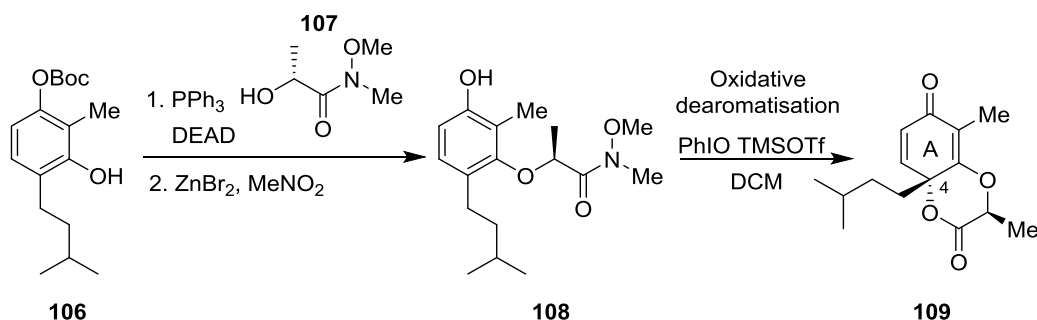


Figure 73: Synthesis of Pettus' dienophile **109** via a key oxidative dearomatisation of aryl-ether **108**¹⁰⁰

The enantioselectivity of the cyclisation results from the effect of the chiral auxiliary on the transition state which, to minimise the dipole, adopts a boat conformation over a chair conformation (Figure 74). Thus lactone **109** is generated as the major product, which has the correct stereochemistry at C⁴ as seen in (+)-rishirilide B **96**.¹⁰⁰

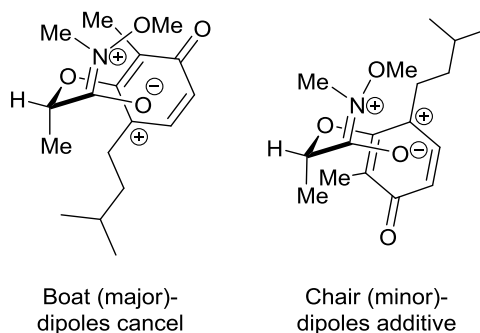


Figure 74: Origin of the enantioselectivity in the conversion of aryl-ether **108** to dienophile **109**

Compound **109** is then employed as a dienophile in a regioselective D-A reaction with a dimethide diene, generated *in situ* by heating sulfone precursor **110** (Figure 75). At the high temperatures used in this reaction, the D-A cycloadduct undergoes spontaneous β -elimination of the methoxy group, to generate an intermediate which is subsequently oxidised with DDQ to give naphthalene **111**. *N*-(dimethylaluminium)-*N'*-*N'*-dimethylhydrazide is used as a Lewis acid to ring open the lactone of **111**, followed by the addition of Hünig's base to form an enolate which is trapped with dimethylcarbonyl chloride, to give compound **112**. In a similar way to the OH directed addition of *iso*-pentylmagnesium bromide to diol **105** in Danishefsky's synthesis, the carbonyl of compound **112** undergoes a directed addition with lithiated vinyl ether, ultimately setting up the *anti* arrangement of the adjacent hydroxyl units at C³ and C⁴ as seen in rishirilide B **96**, followed by oxidation with DMDO to give triol **113**. Triol **113** undergoes four subsequent steps, leading to the isolation of (+)-rishirilide B **96** in an overall yield of 12.5% over 18 steps.¹⁰⁰

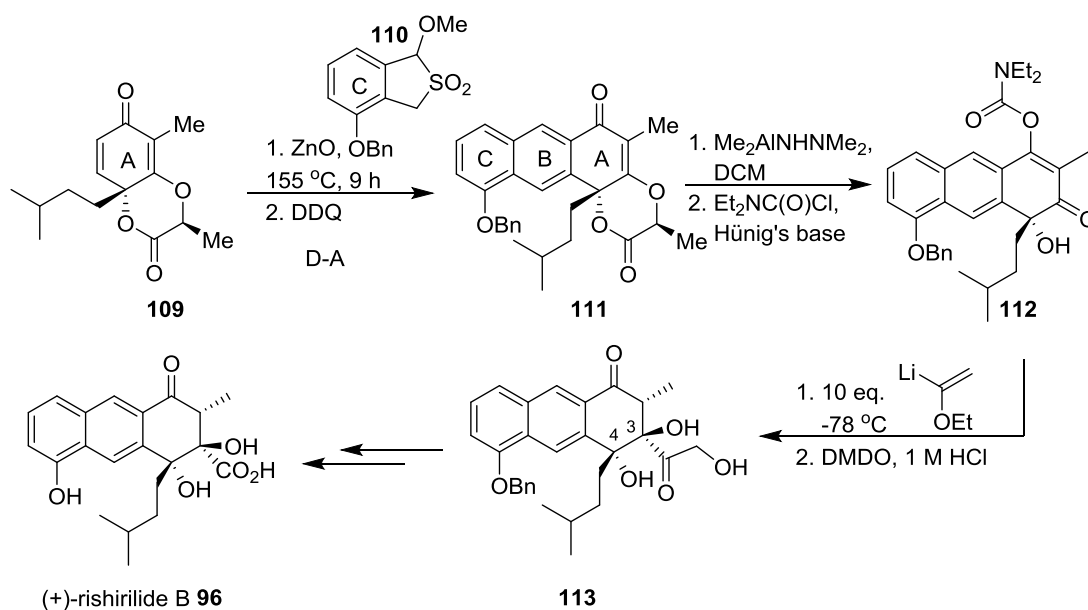


Figure 75: Key Diels-Alder reaction to generate cycloadduct **111** and its subsequent conversion to rishirilide B **96** in Pettus' total synthesis¹⁰⁰

Through the total synthesis of (+)-rishirilide B **96**, Pettus *et al.* developed an innovative method towards the enantioselective oxidative-dearomatisation of 2-alkyl substituted resorcinol **108** to give an oxygenated, cyclic product **109** with a stereogenic centre (Figure 73).¹⁰⁰ Such highly functionalised compounds have application as precursors to a variety of other natural products, such as (+)-bisorbicillinol **114** (Figure 76).¹⁰¹

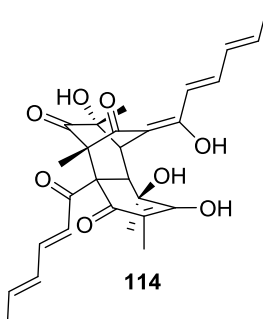


Figure 76: Structure of (+)-bisorbicillinol **114**

3.1.3 Comparison of Rishirilide A **95** and DEM30355/A **94**

In spite of the progress made in the synthesis of rishirilide B **96**, there have been no published total syntheses of rishirilide A **95** (Figure 77). Presumably, this is due to the difficulty in constructing the quaternary centre at C^{4a}, whilst avoiding competing aromatisation of the B ring, leading to rishirilide B-like structures.

Chapter 3. Total Synthesis of the C and B Rings of DEM30355/A

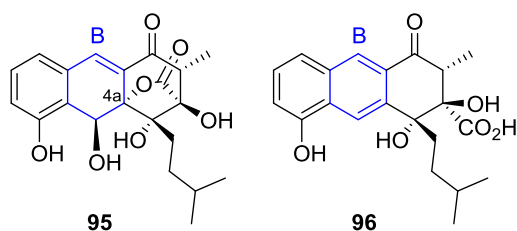


Figure 77: Structure of rishirilide A **95** and rishirilide B **96**

This quaternary centre at C^{4a} is present in our target, DEM30355/A **94**, and construction of this site will be carefully considered in our planned routes. By devising a working synthetic route to DEM30355/A **94**, we could also apply this method to the synthesis of rishirilide A **95**.

Due to the acidity of the proton at C², DEM30355/A **94** exists as an epimeric mixture at this position (Figure 78).

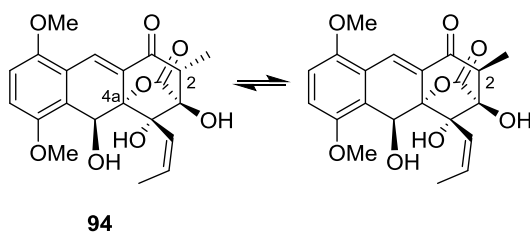


Figure 78: DEM30355/A **94** exists as an epimeric mixture due to the acidity of the proton at C²

Therefore to simplify our synthetic approach, we will target C² de-methyl DEM30355/A **115** (DM-DEM30355/A **115**) (Figure 79). DEM30355/A **94** may still be reached, if desired, through a late stage methylation.

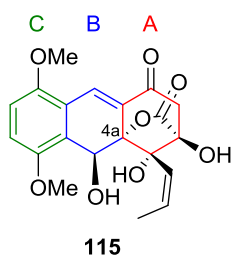


Figure 79: Structure of C² de-methyl DEM30355/A **115**

3.2 Results and Discussion

We examined a multitude of synthetic routes to C² de-methyl DEM30355/A **115** (DM-DEM30355/A **115**) (Figure 80). In Chapter 4, we discuss our work towards the construction of the A, B and C ring core framework of DEM30355/A **94** using Diels-Alder (D-A) chemistry. In this chapter, we focus on the construction of the C and B rings of DM-DEM30355/A **115**, including the synthesis of the key oxygenated centre at C^{4a}.

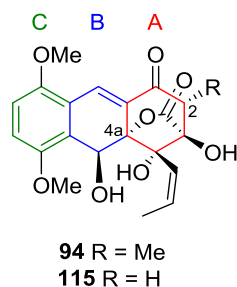


Figure 80: Structures of DEM30355/A **94** and C² de-methyl DEM30355/A **115**

3.2.1 Barbier Coupling Route to DM-DEM30355/A **115**

The first route we will discuss, examines disconnections of bonds C¹⁰-C^{10a} and C^{4a}-O of DM-DEM30355/A **115** (Figure 81). In this route, we planned to use a Barbier coupling reaction between 3,6-dimethoxyphthalaldehyde **116** and compound **117**, followed by ring closure of the resultant adduct **118** to generate the target, DM-DEM30355/A **115**.¹⁰²

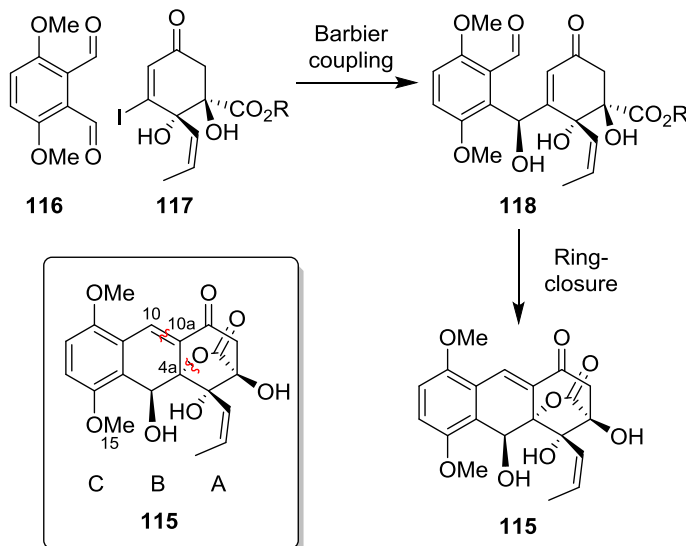
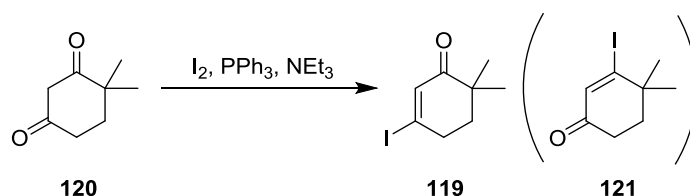


Figure 81: Planned synthetic route to DM-DEM30355/A **115** using Barbier coupling chemistry

3.2.1.1 Synthesis of 3-Iodo-6,6-dimethylcyclohex-2-en-1-one **119**

We planned to synthesise 3-iodo-6,6-dimethylcyclohex-2-en-1-one **119** as a test system for our proposed route, via a modified Appel reaction (Figure 82).¹⁰³ 4,4-Dimethylcyclohexenone **120** (1.0 eq.) was added to a stirred suspension of iodine (1.1 eq.), triphenylphosphine (1.1 eq.) and triethylamine (1.1 eq.) in solvent and heated at reflux (Table 5). In each case, the crude material was analysed by ¹H NMR and purified through column chromatography.

Figure 82: Synthesis of 3-iodo-6,6-dimethylcyclohex-2-en-1-one **119**Table 5: Reactions conditions examined in the synthesis of 3-iodo-6,6-dimethylcyclohex-2-en-1-one **119**

Entry	Reaction conditions	119 Isolated yield (%)
1	THF, reflux, 5 d	3
2	Toluene, reflux, 5 d	10 ^[a]
3	MeCN, reflux 4 d	33
4	MeCN, reflux, 3 d	40
5	MeCN, reflux, 3 d	49
6	MeCN, reflux, 3 d	86
7	MeCN, reflux, 3 d	72
8	MeCN, reflux, 3 d	54

^[a]Isolated as a mixture of regioisomers **119**: **121** in a 1.0: 0.7 ratio

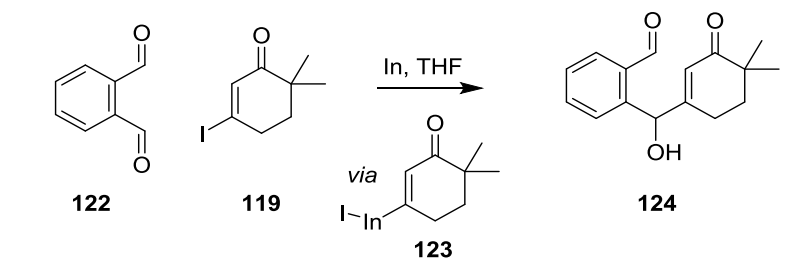
In our initial reactions which tested the reaction solvents THF, toluene and MeCN, the best yield of iodo-compound **119** was obtained from the reaction in MeCN (Table 5, entry 3).¹⁰³ An interesting observation was that in refluxing toluene, a second minor compound was isolated alongside expected product **119** (Table 5, entry 2). Based on ¹H NMR analysis, we have assigned this compound to be isomer **121** (Figure 82). Presumably this more sterically encumbered isomer is generated as a result of the higher reaction temperature in this experiment. Repetition of the modified Appel reaction in MeCN gave variable yields, which may be due to the practical difficulties of reacting a relatively volatile starting material, 4,4-dimethylcyclohexenone **120**, at high temperatures for long periods of time. However, with careful optimisation of the reaction set up and isolation protocols, 3-iodo-6,6-dimethylcyclohex-2-en-1-one **119** could be obtained in a yield of 86% (Table 5, entry 6).

3.2.1.2 Barbier Coupling Reactions Using 3-Iodo-6,6-dimethylcyclohex-2-en-1-one **119**

With 3-iodo-6,6-dimethylcyclohexenone **119** in hand, we moved on to test the Barbier coupling with indium metal, which was selected as 'RIn' type reagents are known to be functional group and moisture tolerant.¹⁰² The equivalencies of phthalaldehyde **122** (0.5 mmol, 1 eq.) and the reaction concentration (THF, 5 mL) were kept constant throughout all the reactions (Table 6).

Chapter 3. Total Synthesis of the C and B Rings of DEM30355/A

Table 6: Reaction conditions examined in the attempted synthesis of product **124** via Barbier coupling



Entry	Indium	Indium eq.	119 eq.	Additive	Reaction conditions
1	shot	1.1	1.0	-	rt, 18 h sonication
2	shot	5.0	1.0	-	rt 3 d, 40 °C 5 d ^[a] , rt 24 h, 45 °C 24 h
3	powder	1.2	1.2	-	3 d rt ^[b] , 18 h rt, 24 h 40 °C, 11 d rt ^[c] , 18 h 45 °C
4	shot	2.0	1.0	LiCl (2.0 eq.)	40 °C, 4 d

^[a]LiCl (5 eq.) was added after this point

^[b]In(III)Cl₃ (1.2 eq) was added after this point

^[c]1,2-dibromoethane (0.2 eq) was added after this point

In the initial reaction (Table 6, entry 1), the ¹H NMR spectrum of the crude material after 18 hours showed that no reaction had occurred as the starting materials, 3-iodo-6,6-dimethylcyclohexenone **119** and phthalaldehyde **122** remained unchanged. We anticipated this may be due to the low reactive surface area of indium shot, slowing the formation of desired organoindium species **123**. Therefore we increased the equivalencies of indium shot from 1.1 eq. to 5.0 eq. (Table 6, entry 2) and tried using indium powder (Table 6, entry 3) to increase the available surface area, but once again no desired product **124** could be observed using ¹H NMR analysis. Due to the low reactivity of indium alone, we investigated additives and indium metal activating agents, namely lithium chloride to facilitate the insertion of indium into the C-I bond and to generate mixed metal organoindium/ lithium species (Table 6, entries 2 and 4), the Lewis acid catalyst indium (III) chloride, to increase the electrophilicity of aldehyde **122** (Table 6, entry 3) and the entrainment agent, 1,2-dibromoethane (Table 6, entry 3) (Note: In our experiments (Table 6, entries 2 – 4), the reaction conditions were altered when no reaction was observed by TLC).¹⁰⁴

A new product was observed by TLC using lithium chloride and the higher reaction temperature of 40 °C (Table 6, entry 4). Analysis of the crude material by ¹H NMR showed unreacted

starting materials 3-iodo-6,6-dimethylcyclohexenone **119** and phthalaldehyde **122** and a new compound, with peaks at δ_{H} 6.80 (1H, dt, $J = 10.1, 4.0$ Hz), 5.84 (1H, dt, $J = 10.1, 2.0$ Hz), and 2.30 (2H, tdd, $J = 6.0, 4.0, 2.0$ Hz). This new compound was, however, shown to be 6,6-dimethyl-2-cyclohexen-1-one **125**, likely resulting from the formation of desired organoindium **123** followed by protonation rather than reaction with aldehyde **122** (Figure 83).¹⁰⁵

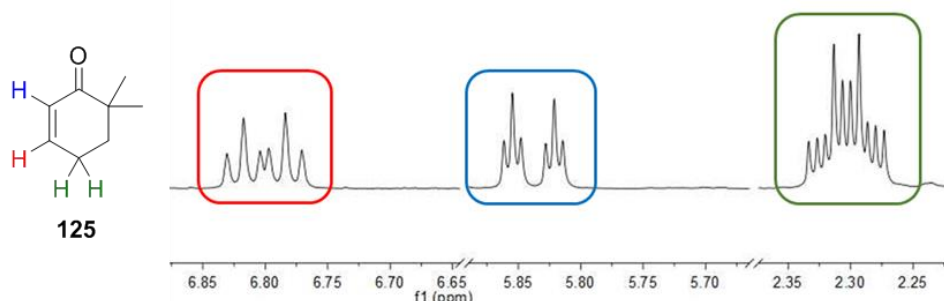
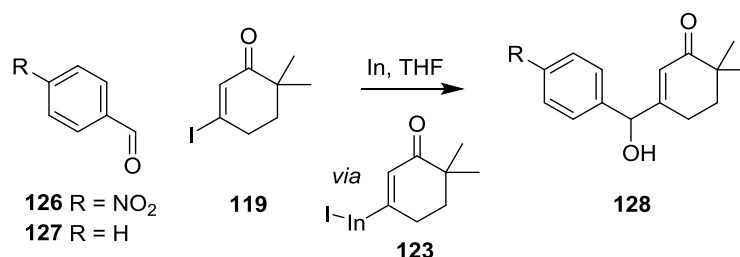


Figure 83: Expansion of the ^1H NMR spectrum leading to the assignment of 6,6-dimethyl-2-cyclohexen-1-one **125**

This suggested that the desired reaction had not occurred due to the poor reactivity of aldehyde **122**. Therefore we tested the reactivity of electron rich and electron poor aromatic aldehydes, namely benzaldehyde **126** and 4-nitrobenzaldehyde **127** respectively (Table 7).

Table 7: Reaction conditions examined in the synthesis of product **128** via Barbier Coupling



Entry	Aldehyde	Indium	Indium eq.	119 eq.	Additive	Reaction conditions	Reaction outcome
1	 126	powder	3.0	1.0	LiCl (3.0 eq.)	50 °C 10 d ^[a] , rt 11 d	starting materials recovered
2	 127	powder	3.0	1.0	LiCl (3.0 eq.)	50 °C 10 d ^[a] , rt 17 d	starting materials recovered

^[a]1,2-dibromoethane (0.3 eq.) added at this point

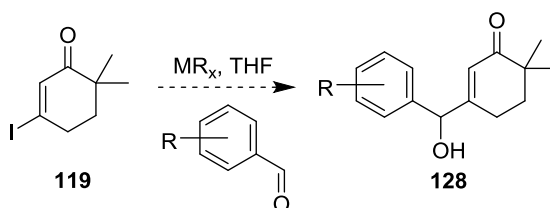
In both cases, unreacted 3-iodo-6,6-dimethylcyclohex-2-en-1-one **119** and the aromatic aldehyde were recovered (Table 7). With failure of the organoindium reactions to generate

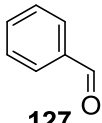
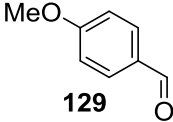
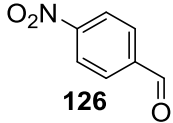
desired product, we moved on to examine different organometallic reagents, specifically organomagnesium and organolithium, which we expected to be more nucleophilic.

3.2.1.3 Examination of Organomagnesium and Organolithium Species Derived from 3-Iodo-6,6-dimethylcyclohex-2-en-1-one **119**

We decided to investigate an alternative method to convert iodo-compound **119** to the corresponding organometallic, namely a halogen-metal exchange reaction with *iso*-propylmagnesium chloride or *n*-butyl lithium, followed by reaction with arylaldehydes (Table 8).¹⁰⁶

Table 8: Reaction conditions examined in the synthesis of product **128**



Entry	Aldehyde	Aldehyde eq.	119 eq.	Reagent	Reagent eq.	Reaction conditions
1		1	1.2	<i>i</i> PrMgCl.LiCl	1.2	[a]0 °C, 1 h, THF
2	127	1.5	1.0	<i>n</i> BuLi	1.1	-78 °C, 4 h, THF
3		1.6	1.0	<i>n</i> BuLi	1.1	-78 °C, 4.5 h, THF
4		1.5	1.0	<i>n</i> BuLi	1.1	-78 °C, 2 h, THF

[a]*i*PrMgCl.LiCl was added to solution of **119** at -78 °C. The resultant solution was stirred at 0 °C for 30 min then cooled to -78 °C before the addition of aldehyde **127**

In each reaction, no signals corresponding to desired product **128** could be observed in the ¹H NMR spectra of the crude material, although 6,6-dimethyl-2-cyclohexen-1-one **125** was generated in the reaction with *iso*-propylmagnesium chloride (Table 8, entry 1).

As it was apparent from our experiments that coupling aromatic aldehydes **122**, **126**, **127** and **129** to 6,6-dimethyl-2-cyclohexen-1-one **119** via a Barbier type reaction looked unfeasible, we

moved on to investigate a different synthetic route to DM-DEM30355/A **115** which would rely on an alternative disconnection approach.

3.2.2 Enolate Coupling Route to DM-DEM30355/A **115**

Next we examined disconnections of bonds C¹⁰-C^{10a} and C⁵-C^{5a} of DM-DEM30355/A **115** (Figure 84). Following this retrosynthetic analysis, we envisaged DM-DEM30355/A **115** could be synthesised by initially constructing the C³-C⁴ bond using an enolate reaction between alkyne **130** and ester **131**.

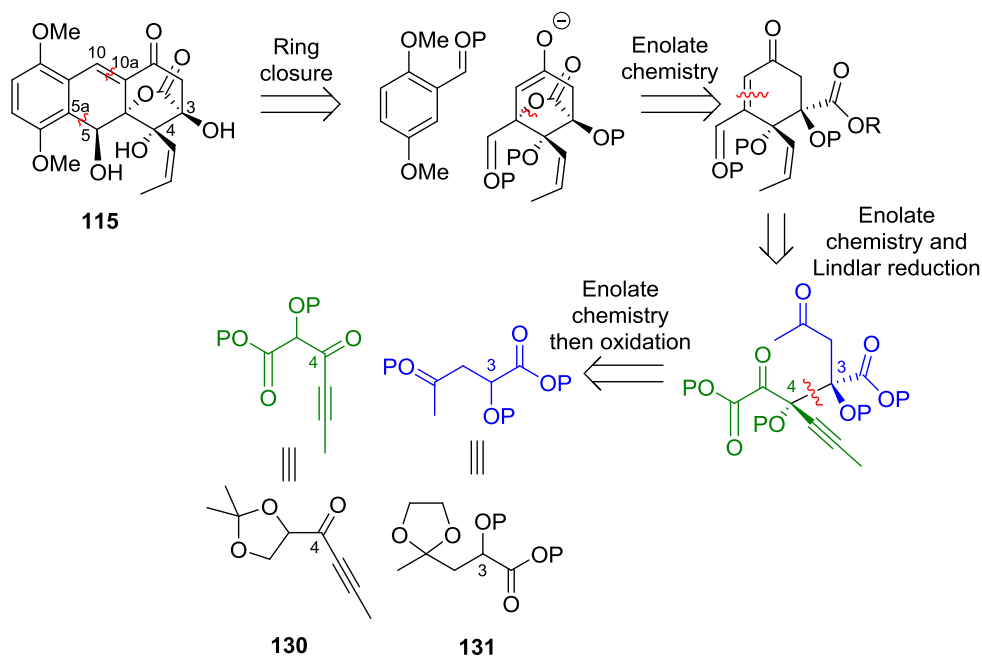


Figure 84: Planned synthetic route to DM-DEM30355/A **115** using enolate coupling

Alkyne **130** had already been synthesised within our group (A. Bayazeed), therefore the first step was to synthesise ester **131**, which we envisaged achieving by first synthesising ethyl 2-hydroxy-3-(2-methyl-1,3-dioxolan-2-yl)propanoate **132** and subsequently protecting the alcohol (Figure 85).

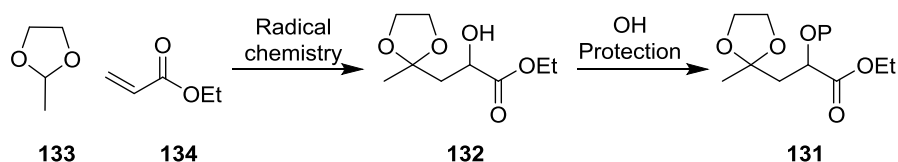


Figure 85: Planned synthesis of ester **131** via radical chemistry to synthesise alcohol **132** followed by OH protection

3.2.2.1 Synthesis of Ethyl 2-hydroxy-3-(2-methyl-1,3-dioxolan-2-yl)propanoate **132**

Ishii *et al.* reported that methyl 2-hydroxy-3-(2-methyl-1,3-dioxolan-2-yl)propanoate **136** could be synthesised in a good yield (81%) in the reaction between 2-methyl-1,3-dioxolane **133** and methyl acrylate **135** (Figure 86).¹⁰⁷ The reaction was conducted under an atmosphere of

oxygen, in the presence of catalytic quantities of *N*-hydroxyphthalimide (NHPI) and cobalt (II) acetate.

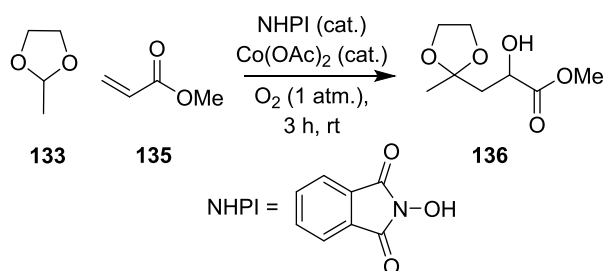
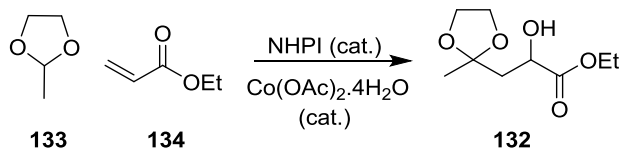


Figure 86: Ishii's synthesis of methyl 2-hydroxy-3-(2-methyl-1,3-dioxolan-2-yl)propanoate **136** via the reaction between 2-methyl-1,3-dioxolane **133** and methyl acrylate **135**¹⁰⁷

We adapted this approach to synthesise ethyl 2-hydroxy-3-(2-methyl-1,3-dioxolan-2-yl)propanoate **132**. Ethyl acrylate **134** was added to a stirred solution of 2-methyl-1,3-dioxolane **133**, NHPI, and cobalt (II) acetate tetrahydrate at room temperature (Table 9).

Table 9: Reaction conditions examined in the synthesis of ethyl 2-hydroxy-3-(2-methyl-1,3-dioxolan-2-yl)propanoate **132** from 2-methyl-1,3-dioxolane **133**



Entry			NHPI	Co(OAc) ₂ ·4H ₂ O	Reaction conditions	132 Isolated yield (%)
	eq.	eq.	eq.	eq.		
1	5	1	0.05	[a]	rt, 3 h, open system	14
2	5	1	0.05	5 x 10 ⁻⁴	rt, 18 h, open system	10
3	5	1	0.05	5 x 10 ⁻⁴	22 °C, 3 h open system	0
4	4	1	0.05	5 x 10 ⁻⁴	25 °C, 3 h, air balloon	5
5	5	1	0.05	5 x 10 ⁻⁴	25 °C, 3 h, air balloon	9
6	2	1	0.01	1 x 10 ⁻²	rt, 18 h, air balloon	trace
7	5	1	0.05	5 x 10 ⁻⁴	rt, 18 h, air balloon	9
8	5	1	0.05	5 x 10 ⁻⁴	rt, 18 h, air balloon	13
9	5	1	0.05	5 x 10 ⁻⁴	rt, 3 h, O ₂ balloon	0

[a] One crystal of reagent used

The reaction was initially carried out at room temperature for 3 hours as described in the

literature, albeit in an open system as opposed to an atmosphere of oxygen.¹⁰⁷ After this time, 2-methyl-1,3-dioxolane **133** was removed under reduced pressure and the crude material was purified using column chromatography, to give ethyl 2-hydroxy-3-(2-methyl-1,3-dioxolan-2-yl)propanoate **132** in a 14% yield (Table 9, entry 1). Attempts to improve the yield of the reaction through increasing the reaction time or employing a more constant reaction temperature (22-25 °C in an oil bath) and moving to a closed system (to reduce reagent evaporation), proved inconclusive (Table 9, entries 2-9). It was noticeable that the reaction yields suffered significantly when the equivalencies of reagents used differed to those described in the literature (Table 9, entries 4 and 6).¹⁰⁷ Oxygen is a key reagent in the reaction, thus we postulated that under air, the partial pressure of oxygen in the reaction may be too low and that an atmosphere of oxygen may be necessary to increase the reaction yields. Therefore the reaction was repeated under 1 atmosphere of oxygen, using literature equivalencies of reagents.¹⁰⁷ TLC analysis of the reaction after 2 hours showed that product **132** had been formed, however no **132** was isolated, potentially due to its volatility during work up (Table 9, entry 9).

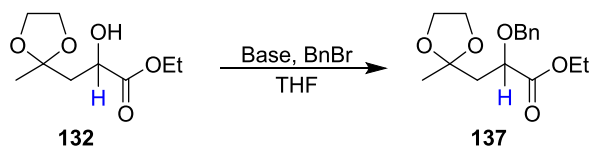
Given the problems associated with using volatile reagents (2-methyl-1,3-dioxolane **133** and ethyl acrylate **134**) under an atmosphere of oxygen and in isolating a volatile product **132**, we decided to test the next stage in the synthesis. Despite the low yields in these reactions, we were able to isolate sufficient quantities of product **132** to continue and attempt the OH protection. Should the following planned synthetic route to DM-DEM30355/A **115** prove successful, more time would be invested in optimising the synthesis of precursor **132**.

3.2.2.2 OH-Protection of Ethyl 2-hydroxy-3-(2-methyl-1,3-dioxolan-2-yl)propanoate 132

The next step was to protect the hydroxyl group of ethyl 2-hydroxy-3-(2-methyl-1,3-dioxolan-2-yl)propanoate **132** (Table 10). Alcohol protection is required at this stage to both allow orthogonal deprotection of different hydroxyl groups later in the synthesis and to reduce the volatility of **132**. A benzyl protecting group was selected as, when necessary, we anticipated the group would readily be removed under orthogonal hydrogenation conditions.

Ethyl 2-hydroxy-3-(2-methyl-1,3-dioxolan-2-yl) propanoate **132** was reacted with benzyl bromide in the presence of a suitable base (Table 10).

Chapter 3. Total Synthesis of the C and B Rings of DEM30355/A

 Table 10: OH Protection reaction conditions examined in the synthesis of benzyl-protected compound **137**


Entry	132 eq.	Base	Base eq.	BnBr eq.	Reaction conditions	Isolated yield (%)
1	1	NaH	2.0	3.0	THF, ^[a] 0 °C - rt, 30 mins	unreacted 132 ^[b]
2	1	NaH	1.1	4.0	THF, ^[c] rt, 18 h	unidentified decomposition products
3	1	LDA	1.2	3.0	THF, ^[d] 0 °C, 1 h	unreacted 132 (19%), unidentified decomposition products
4	1	NaHMDS	2.0	2.0	THF, ^[e] 0 °C, 2 h	product 137 (~5% ^[f]) and by-product 138 (10%)
5	1	NaHMDS	2.2	2.2	THF, ^[e] 0 °C, 18 h	unreacted 132 , product 137 (~5% ^[f]), by-product 138 (19%)

^[a]Solution of NaH and **132** in THF was stirred for 30 min at 0 °C before BnBr was added

^[b]As shown in the crude ¹H NMR spectrum

^[c]Solution of NaH and **132** was stirred for 1 h at rt then cooled to 0 °C before BnBr was added

^[d]Solution of LDA and **132** was stirred at 0 °C for 1 h then cooled to -78°C before BnBr was added

^[e]Solution of NaHMDS and **132** was stirred for 30 min at 0 °C before BnBr was added

^[f]Isolated yield is approximate as sample was contaminated with unidentified decomposition product(s)

In the first attempt at the protection reaction with benzyl bromide, NaH was used as the base. After a reaction time of 30 minutes, only starting material **132** was seen in the ¹H NMR spectrum of the crude reaction mixture (Table 10, entry 1). Increasing the reaction time and temperature led to the isolation of unidentified decomposition products (Table 10, entry 2). Reactions employing benzyl bromide and the more organosoluble base, lithium diisopropylamide (LDA), also showed no formation of desired product **132** (Table 10, entry 3). We then examined the replacement of LDA with the sterically bulky base, sodium bis(trimethylsilyl)amide (NaHMDS). After a reaction time of 2 hours, two compounds - a major by-product **138** and a minor product - could be isolated by column chromatography, in addition to unreacted starting material **132** (Table 10, entry 4).

¹H NMR analysis of the minor product showed two, one proton doublets at 4.49 ppm and 4.30 ppm, which were coupled to each other with $J = 11.3$ Hz, characteristic of a benzylic O-CH₂ in close proximity to a chiral centre. Therefore based on the ¹H NMR data, we have assigned the minor compound to be desired product **137** (~5% isolated yield) (Figure 87).

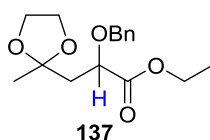


Figure 87: Structure of benzyl-protected compound **137**, isolated as a minor product in the reaction of alcohol **132** with benzyl bromide

With desired product **137** identified, we attempted to improve the yield of **137**. The reaction time was increased from 2 to 18 hours (Table 10, entry 5), however the yield of **137** remained low and the yield of by-product **138** increased. Consequently we decided to investigate the structure of by-product **138** to gain a better understanding of the reaction.

The ^1H NMR spectrum of by-product **138** contained two, one proton doublets at 2.95 and 2.84 ppm, coupled to each other with $J = 13.3$ Hz, again suggesting a geminally coupled CH_2 group. HMBC data showed this proton spin system was in close proximity to a quaternary aromatic carbon centre at 135.7 ppm, suggesting that these protons were part of a benzylic CH_2 group attached to carbon, not oxygen as expected. Thus we have determined that compound **138** is in fact a structural isomer of **137** (10% isolated yield), the result of deprotonation of the proton α to the carbonyl of **132**, followed by enolate attack on benzyl bromide (Figure 88).

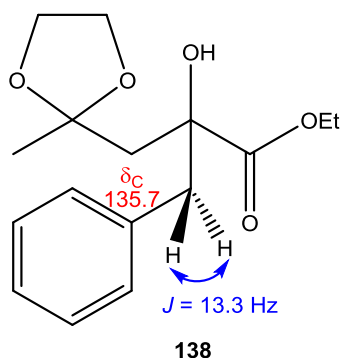


Figure 88: Structure of compound **138**, the major product generated in the reaction of alcohol **132** with benzyl bromide. Key NMR data which aided the structural assignment is shown

The unexpected product **138** appears to be formed preferentially in this reaction over desired benzyl-protected compound **137**. This may be due to an intramolecular hydrogen bond helping to stabilise the OH group and making the proton α - to the carbonyl more acidic, resulting in deprotonation and benzylation at the α -position (Figure 89).

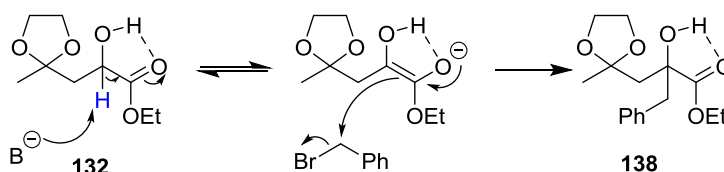


Figure 89: Intramolecular hydrogen bonding may favour the formation of compound **138** over OH protected compound **137** in the reaction of alcohol **132** with benzyl bromide

As the major product of the reaction between alcohol **132** and benzyl bromide was undesired isomer **138**, we believed this method would not be a feasible route to sufficient quantities of OH-protected compound **137**, required to proceed in our planned synthetic route. Therefore we moved on to examine an alternative synthetic route to OH-protected compound **137**.

3.2.2.3 Synthesis of Ethyl 2-hydroxy-4-oxopentanoate **140** via Selective Reduction of Ethyl 2,4-dioxopentanoate **139**

We envisaged that OH-protected compound **137** may alternatively be synthesised using a selective reduction of the α -keto ester of ethyl 2,4-dioxopentanoate **139** to generate ethyl 2-hydroxy-4-oxopentanoate **140**, followed sequentially by OH and ketone protection (Figure 90).

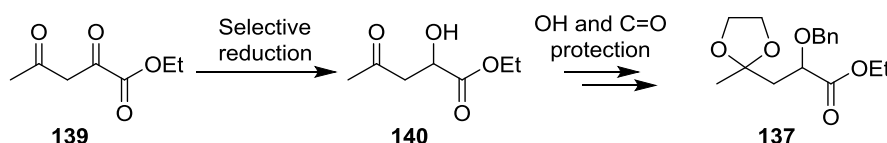
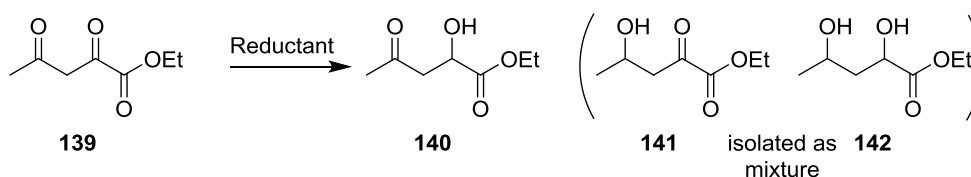


Figure 90: Planned synthesis of OH-protected compound **137** via selective reduction of ethyl 2,4-dioxopentanoate **139** then alcohol and ketone protection

The first step was to investigate the reduction of ethyl 2,4-dioxopentanoate **139** with hydride reducing agents, namely sodium tetraborohydride and DIBALH (Table 11).

Table 11: Reaction conditions examined in the synthesis of ethyl 2-hydroxy-4-oxopentanoate **140**



Entry	139 eq.	Reducing agent	Reducing agent eq.	Hydride eq.	Reaction conditions	Isolated product yield
1	1	NaBH ₄	0.5	2.0	THF, 0 °C, 1 h 50 min	140 (14%), 141 + 142 (~29%)
2	1	NaBH ₄	0.3	1.2	THF, 0 °C, 2 h	[a]
3	1	NaBH ₄	0.4	1.5	MeOH, 0 °C, 30 mins	140 (29%) ^[b] , 141 + 142 (~6%)
4	1	NaBH ₄	0.3	1.0	MeOH, 0 °C, 20 mins	140 (20%) ^[b]
5	1	DIBALH	1.1	1.1	THF, -78 °C, 45 min	[b]
6	1	DIBALH	2.0	2.0	THF, -78 °C, 1 h	[b]

^[a]Product **140**: unreacted **139** in 1: 2 ratio, estimated from analysis of the ¹H NMR spectrum of the crude reaction material

^[b]Starting material **139** recovered

In the first reaction we tested, we obtained two fractions following column chromatography (Table 11, entry 1). ^1H NMR analysis of the minor fraction showed that the spectrum contained two signals at 2.96 ppm (1H, dd, $J = 17.4, 4.1$ Hz) and 2.88 ppm (1H, dd, $J = 17.4, 6.2$ Hz). Through coupling constant analysis, we could deduce that these two protons were geminally coupled to each other ($J = 17.4$ Hz). The two protons at 2.96 and 2.88 ppm were coupled to another proton at 4.46 ppm (1H, dd, $J = 6.2, 4.1$ Hz), which suggested the presence of an ABC spin system, corresponding to a CH_2CH moiety. Through interpretation of these data, we have assigned this compound as desired alcohol **140** (14% isolated yield) (Figure 91).

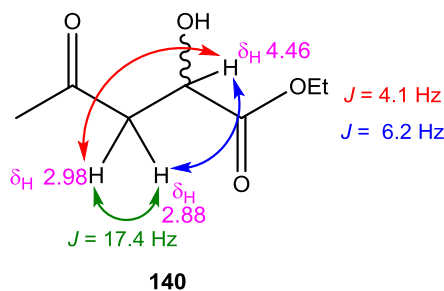


Figure 91: Key NMR data in the assignment of ethyl 2-hydroxy-4-oxopentanoate **140**

^1H NMR analysis of the major fraction indicated a complex mixture of products. The spectrum contained a doublet Me group signal at 1.39 ppm and a doublet Me group signal at 1.33 ppm, which is consistent with each Me group being adjacent to a CH moiety. Based on these ^1H NMR data we proposed the major fraction contained the singly and doubly reduced products, **141** and **142** respectively (Figure 92).

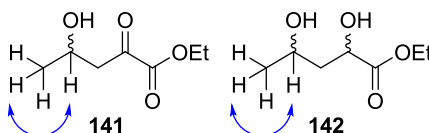


Figure 92: Structure of additional products **141** and **142** generated by reduction of ethyl 2,4-dioxopentanoate **139**, identified through the appearance of doublet Me signals in the ^1H NMR spectrum

Reducing the equivalents of sodium borohydride (Table 11, entry 2) and the reaction time (Table 11, entries 3 and 4) did not result in significant improvements to the isolated yield of desired product **140**, whilst attempting the reduction at a low temperature in the presence of DIBALH resulted in the recovery of starting material **139** only (Table 11, entries 5 and 6).

Given the difficulties associated with the reduction reactions tested, we decided to examine a different route to ethyl 2-hydroxy-4-oxopentanoate **140**.

3.2.2.4 Synthesis of Ethyl 2-hydroxy-4-oxopentanoate **140** via Reduction of Ethyl 2,4-dioxopentanoate **139** then Selective Oxidation

As an alternative route to ethyl 2-hydroxy-4-oxopentanoate **140**, we hypothesised that we could reduce both of the ketones of ethyl 2,4-dioxopentanoate **139** to give ethyl 2,4-

dihydroxypentanoate **142**, then selectively oxidise the least hindered alcohol to generate the target compound **140** (Figure 93).

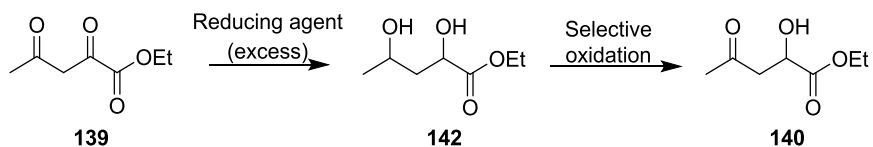
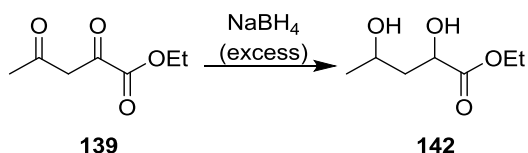


Figure 93: Proposed synthesis of ethyl 2-hydroxy-4-oxopentanoate **140** via the reduction of ethyl 2,4-dioxopentanoate **139** to compound **142** followed by selective oxidation

Therefore ethyl 2,4-dioxopentanoate **139** was reacted with an excess of sodium borohydride at room temperature, followed by purification of the crude reaction material by column chromatography (Table 12).

Table 12: Reaction conditions examined in the reduction of ethyl 2,4-dioxopentanoate **139**



Entry	139 eq.	NaBH_4 eq.	Hydride eq.	Reaction conditions	143 Isolated yield (%)
1	1	1	4	MeOH, rt, 18 h	30 ^[a]
2	1	1	4	MeOH, rt, 4 d	58

^[a]Yield is approximate as the ^1H NMR spectrum of the sample showed impurities

From the first reaction we tested, a new product **143** was isolated in addition to a mixture of unidentified reduction products (Table 12, entry 1). The ^1H NMR spectrum of the new product **143** contained two overlapping one proton signals at 4.64 – 4.45 ppm. One of these signals could be distinguished at 4.57 ppm (1H, dd, $J = 8.3, 11.2$ Hz). The spectrum also contained two signals at 2.73 ppm (1H, dd, $J = 12.5, 8.3$ Hz) and 1.86 ppm (1H, dd, $J = 12.5, 11.2$ Hz), suggestive of a geminally coupled CH_2 group ($J = 12.5$ Hz), adjacent to the CH at 4.57 ppm. The chemical shift of this CH group suggested it was in close proximity to an electronegative moiety, which considering the starting materials, was likely to be an oxygen atom and/or carbonyl group. In addition, the presence of a signal at 1.47 ppm (3H, d, $J = 6.2$ Hz) suggested a CH_3CH moiety. Therefore, based on these ^1H NMR data, we have assigned the new compound as hydroxy-lactone **143** (30% isolated yield) (Figure 94). Lactone **143** likely results from the reduction of ethyl 2,4-dioxopentanoate **139** to ethyl 2,4-dihydroxypentanoate **141**, followed by intramolecular cyclisation (Figure 95).

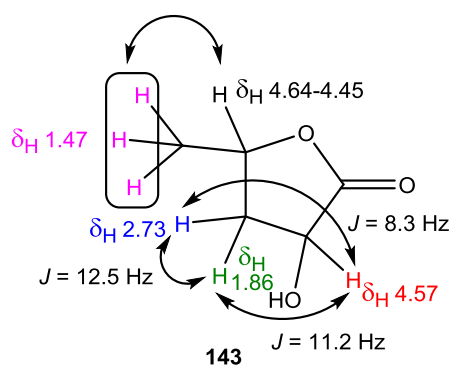


Figure 94: Structure of lactone **143** and the key NMR data which aided in structural assignment

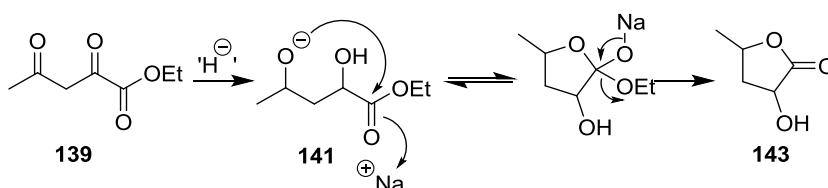


Figure 95: Mechanism showing the formation of lactone **143** from the reduction of **139** to alcohol **141** followed by intramolecular cyclisation

We envisaged OH-protected hydroxy-lactone **143** could be used as an alternative to our initial target **140**. Consequently, to increase the yield of compound **143** for subsequent use in OH-protection reactions, we increased the reaction time from 18 hours to 4 days, which resulted in the isolation of hydroxy-lactone **143** as the sole product, in a much improved yield of 58% (Table 12, entry 2).

With a working route to hydroxy-lactone **143** developed, we then examined the OH-protection chemistry.

3.2.2.5. Synthesis of 3-(Benzyloxy)dihydrofuran-2(3H)-one **145**

As a test system, we decided to investigate OH-protection of a compound structurally related to hydroxyl-lactone **143** synthesised previously, namely α -hydroxy- γ -butyro lactone **144** (Figure 96). We planned to react α -hydroxy- γ -butyro lactone **144** with benzyl bromide to generate benzyl-protected hydroxy-lactone **145**, for use in our proposed enolate coupling reactions with alkyne **130** (Figure 96).

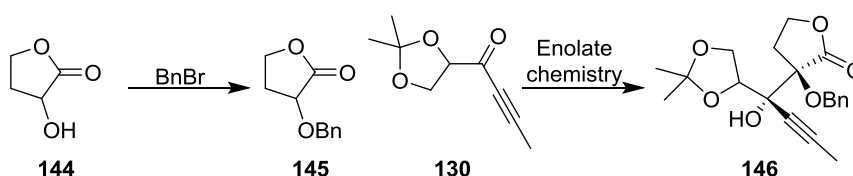


Figure 96: Planned synthesis of adduct **146** via an enolate coupling reaction between alkyne **130** and OH-protected lactone **145**

α -Hydroxy- γ -butyro lactone **144** was reacted with benzyl bromide and the base, NaHMDS at room temperature (Figure 97).

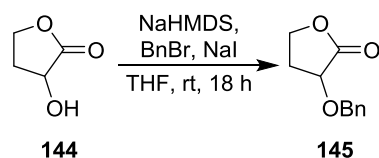


Figure 97: OH protection of α -hydroxy- γ -butyrolactone **144** to give benzyl compound **145**

Following purification of the crude material by column chromatography, a new compound was isolated. The ^1H NMR spectrum of the product contained two signals at 4.91 ppm (1H, d, $J = 11.8$ Hz) and 4.71 ppm (1H, d, $J = 11.8$ Hz). These signals are characteristic of a benzylic $\text{O}-\text{CH}_2$ in close proximity to a stereogenic centre. Therefore, based on the ^1H NMR data, we have assigned the isolated product as desired OH-protected compound **145** (39% yield).

With a sufficient quantity of OH-protected lactone **145** in hand, we could proceed to the next step.

3.2.2.6 Enolate Reaction Between 3-(Benzyloxy)dihydrofuran-2(3H)-one **145** and 1-(2-Methyl-1,3-dioxolan-4-yl)but-2-yn-1-one **130**

The next stage was to test the enolate reaction between OH-protected lactone **145** and 1-(2-methyl-1,3-dioxolan-4-yl)but-2-yn-1-one **130**, which had previously been synthesised (A. Bayazeed), to generate adduct **146**. Alkyne **130** was added to a pre-mixed solution of lactone **145** and NaHMDS (Figure 98).

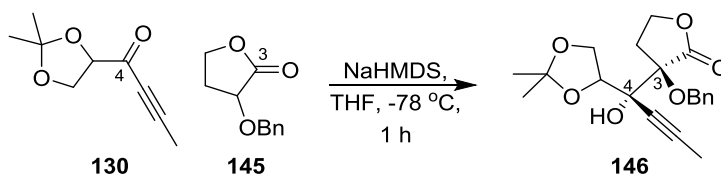


Figure 98: Reaction conditions examined in the attempted synthesis of adduct **146**

After a reaction time of 1 hour, analysis of crude reaction material by ^1H NMR showed unreacted **145**, and no peaks corresponding to our desired product **146** could be observed.

Given the time constraints, we decided at this point to focus on alternative synthetic routes to DM-DEM30355/A **115**. In future we would screen different reaction conditions, including the use of alternative bases such as NaH or LDA, to encourage the desired enolate reaction between **145** and **130** to proceed.

3.2.3 Synthesis of DM-DEM30355/A **115** via a Michael Addition/ Enolate Trapping Multi-Component Reaction

The third synthetic route to DM-DEM30355/A **115** we will discuss, examines disconnections of the $\text{C}^{10\text{a}} - \text{C}^{4\text{a}}$ and $\text{C}^5 - \text{C}^{5\text{a}}$ bonds (Figure 99). We envisaged using a multi-component reaction, consisting of Michael addition to (*E*)-4-(2,5-dimethoxyphenyl)but-3-en-2-one **147** followed by trapping of the resultant enolate with a reactive carbonyl compound, to generate alcohol **148**.

Chapter 3. Total Synthesis of the C and B Rings of DEM30355/A

This would construct the oxygenated quaternary centre at C^{4a}, a key component in the synthesis of the target, DM-DEM30355/A **115**. From here, β -elimination of **148** to give **149**, followed by ring closure would give diol **150**, with the B ring of DM-DEM30355/A **115** in place.

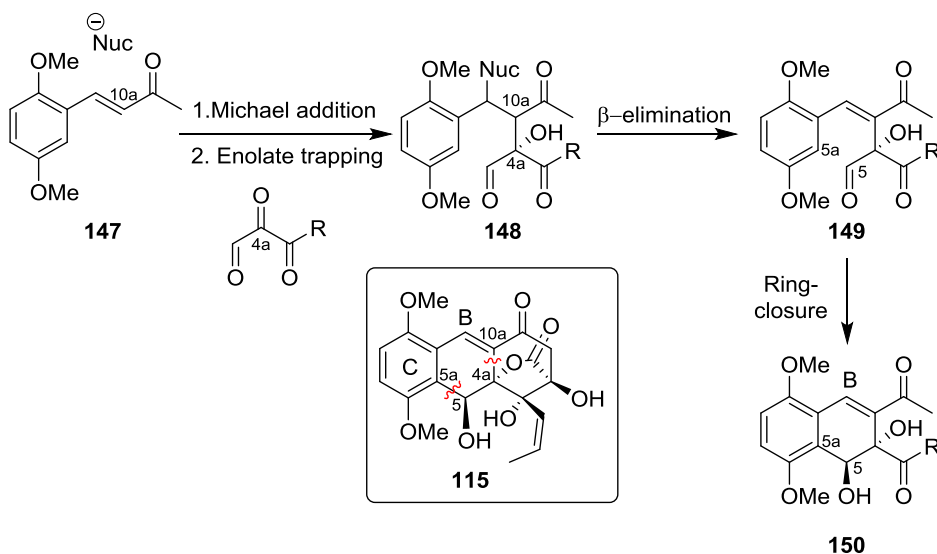


Figure 99: Proposed synthetic route to alcohol **150** containing the C and B rings of DM-DEM30355/A **115** via a key Michael addition/enolate trapping multi-component reaction

The first step was to synthesise the starting material, ketone **147**.

3.2.3.1 Synthesis of (E)-4-(2,5-Dimethoxyphenyl)but-3-en-2-one **147**

We anticipated that (E)-4-(2,5-dimethoxyphenyl)but-3-en-2-one **147** could be synthesised using a Wittig reaction between 2,5-dimethoxybenzaldehyde **151** and (acetylmethylene)triphenylphosphorane **152** (Figure 100).

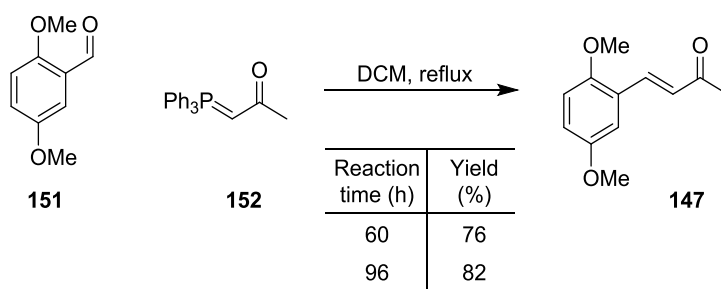


Figure 100: Wittig synthesis of (E)-4-(2,5-dimethoxyphenyl)but-3-en-2-one **147**

After 60 hours at reflux, (E)-4-(2,5-dimethoxyphenyl)but-3-en-2-one **147** was isolated by column chromatography in a 76% yield, which was improved to 82% by increasing the reaction time to 96 hours (Figure 100).

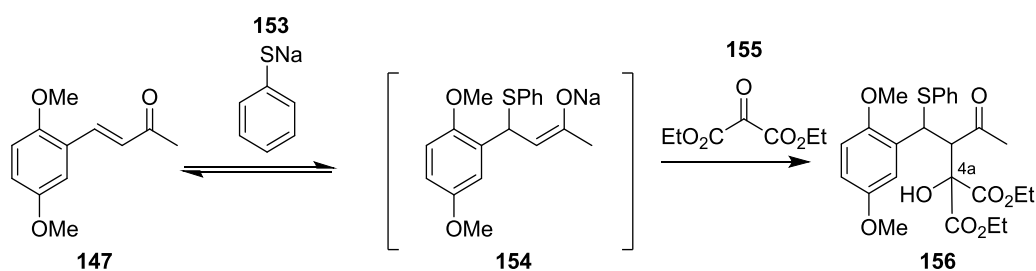
With gram quantities of compound **147** in hand, we proceeded to the following stage in the synthetic route.

3.2.3.2 Investigations into a Michael Addition/ Enolate Trapping Reaction from (*E*)-4-(2,5-Dimethoxyphenyl)but-3-en-2-one **147**

The next step in our planned route was to react compound **147** with a nucleophile and trap the resultant enolate **154** with a reactive carbonyl species to generate adduct **156**, thereby constructing the oxygenated quaternary centre at C^{4a}. We envisaged that small aromatic thiols would be suitable soft nucleophiles to undergo Michael addition with compound **147**.

(*E*)-4-(2,5-Dimethoxyphenyl)but-3-en-2-one **147** (1 eq.) was reacted with sodium thiophenolate **153** (1 eq.), followed by the addition of diethyl ketomalonate **155** (1 eq.) as a reactive carbonyl species, to trap enolate **154** and generate adduct **156** (Table 13).

Table 13: Reaction conditions examined in the synthesis of adduct **156** from ketone **147**



Entry	Reaction conditions	Reaction outcome
1	DCM, rt, 9 d	starting material recovered
2	MgCl ₂ (1 eq.), THF, rt 2 d, 55 °C 1 d	starting material recovered

In the reactions tested, a long reaction time (Table 13, entry 1), the addition of a Lewis acid catalyst and increasing the reaction temperature (Table 13, entry 2), failed to generate any desired adduct **156** as shown by analysis of the ¹H NMR spectrum of the crude reaction material. Therefore we moved on to examine the alternative reagent, thiophenol **157**, which we anticipated would be more reactive.

Initially (*E*)-4-(2,5-dimethoxyphenyl)but-3-en-2-one **147** was reacted with thiophenol **157** under basic conditions, followed by addition of diethyl ketomalonate **155** (Figure 101).

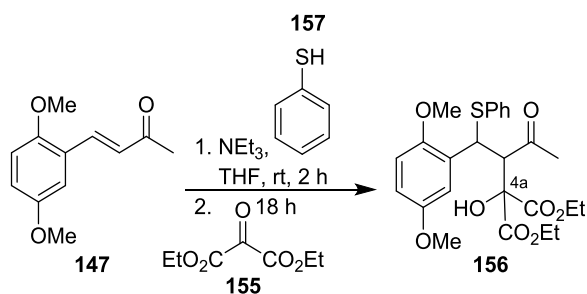


Figure 101: Initial reaction tested using thiophenol **157**, in the attempted synthesis of adduct **156**

Following column chromatography of the crude material, two new compounds were isolated, in addition to unreacted starting material **147**. The ^1H NMR spectrum of the less polar product contained two signals at 5.11 ppm (1H, t, $J = 7.4$ Hz) and 3.02 ppm (2H, d, $J = 7.4$ Hz), suggesting an AB_2 spin system, which we assigned as a CHCH_2 moiety. The HMBC spectrum showed correlations between the signal at 5.11 ppm and signals at 134.7 ppm and 130.4 ppm, which correspond to two quaternary aromatic carbon atoms. This suggested that the CH corresponding to the signal at 5.11 ppm, was connected to two different benzene-like ring systems. In addition, the HMBC spectrum showed correlations between the signals at 5.11 ppm and 3.02 ppm, with a carbon signal at 205.9 ppm. This suggested the CHCH_2 group (associated with signals at 5.11 ppm and 3.02 ppm) was connected to a ketone carbonyl group. Thus, we have determined that the isolated compound was not desired product **156**, rather sulfide **158**, isolated in a 15% yield, generated by Michael addition of thiophenol **157** to (*E*)-4-(2,5-dimethoxyphenyl)but-3-en-2-one **147** (Figure 102) (Note: sulfide **158** was the major product as shown by the ^1H NMR spectrum of the crude reaction material, however the isolated yield of sulfide **158** following column chromatography was low due to the similar R_f values of sulfide **158** and starting material **147**).

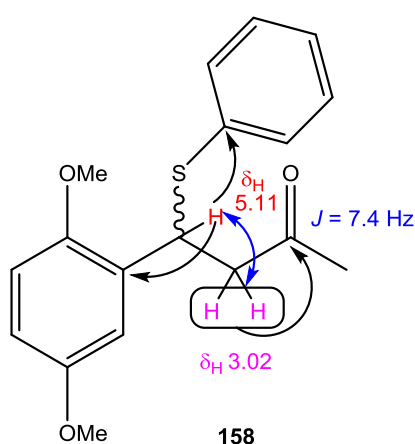


Figure 102: Structure of sulfide **158** and key NMR data which aided in the structural assignment

The ^1H NMR spectrum of the more polar isolated product showed two signals at 7.90 ppm (1H, d, $J = 16.4$ Hz) and 6.73 ppm (1H, d, $J = 16.4$ Hz), suggesting a $\text{HC}=\text{CH}$ alkene group with a *trans* arrangement of the protons. The HMBC spectrum showed correlations between the

signals at 7.90 ppm and 6.73 ppm, with carbon signals at 123.6 ppm and 153.2 ppm, suggesting the alkene was in close proximity to an aromatic group. In addition, the alkene CH signal at 6.73 ppm was correlated to a carbon signal at 197.0 ppm, suggesting the alkene was part of an α - β unsaturated ketone. In addition, this C=O signal at 197.0 ppm was correlated to a signal at 3.55 ppm corresponding to a CH₂, suggesting a HC=CH-(C=O)-CH₂ unit. Further HMBC correlations were observed between the signals at 3.55 ppm (CH₂) and a carbon signal 77.3 ppm, corresponding to a quaternary carbon bonded to several electron withdrawing groups, and a carbonyl carbon at 169.7 ppm, characteristic of an ester carbonyl group. HMBC correlations were also observed between the C=O at 169.7 ppm and a four proton signal at 4.28 ppm (q, $J = 7.1$ Hz), suggesting the presence of two equivalent ethyl ester groups. Therefore we were able to deduce that this new compound was not desired product **156** but alcohol **159**, isolated in a 15% yield (Figure 103).

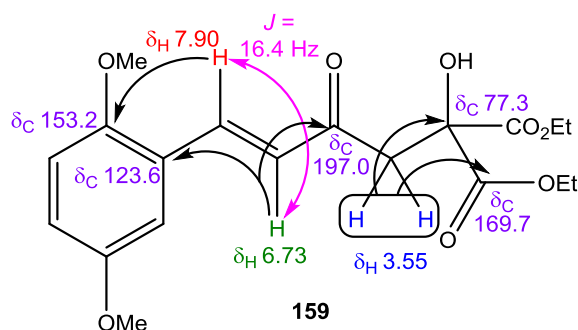


Figure 103: Structure of alcohol **159** with key NMR data important in the structural assignment shown

Alcohol **159** is likely generated from deprotonation of the alkyl proton α to the α - β unsaturated ketone **147**, followed by attack of the resultant enolate **160** on diethyl ketomalonate **155** (Figure 104).

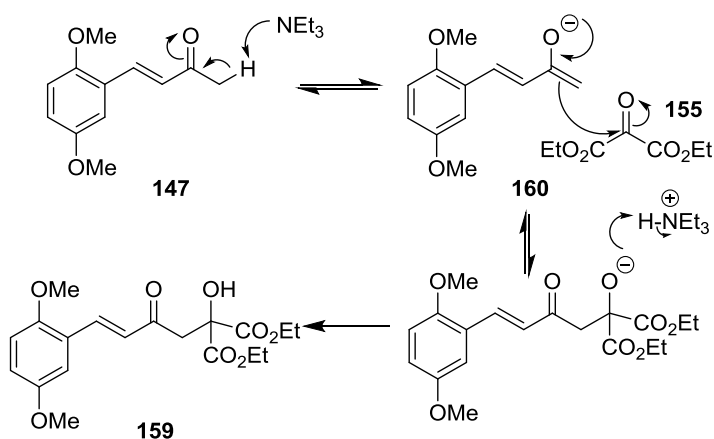


Figure 104: Mechanism of the formation of alcohol **159** from ketone **147**

Crystals of sulfide **158** and alcohol **159** were grown by slow evaporation from DCM and X-ray crystal structures were obtained, which support our proposed assignments (Figure 105).

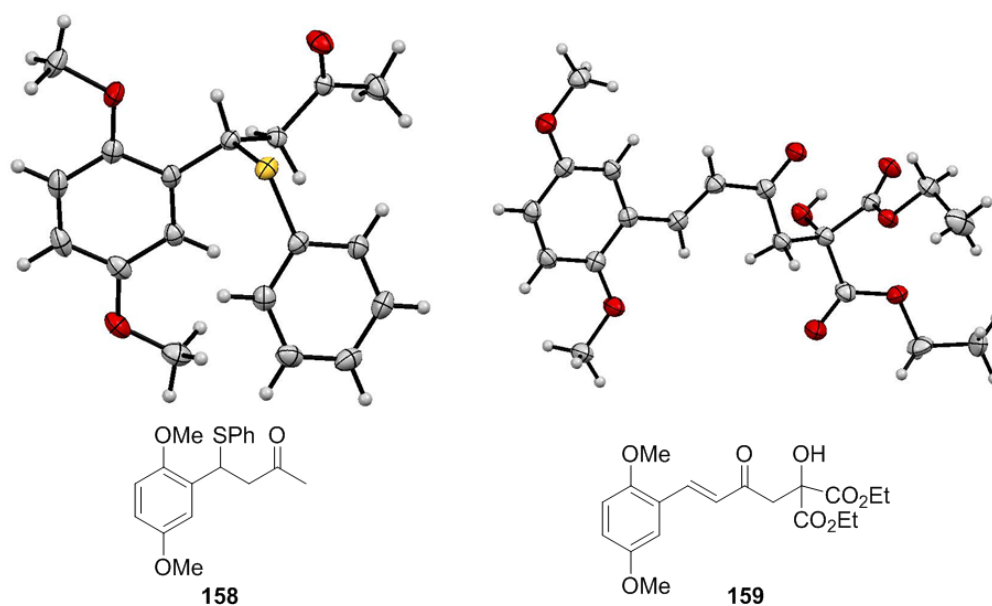
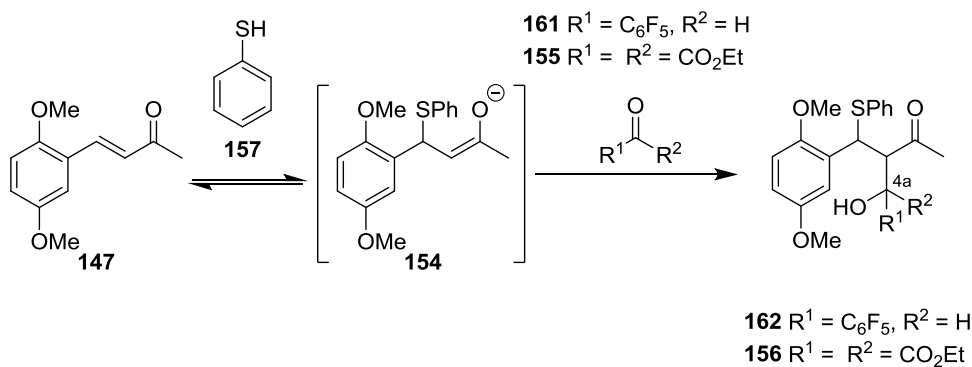


Figure 105: X-ray crystal structures of sulfide **158** (left) and alcohol **159** (right)

Sulfide **158** and alcohol **159** crystallise in the monoclinic space groups, $P2_1/c$ and $C2/c$ respectively.

After determining that both isolated products, sulfide **158** and alcohol **159**, from our initial reaction did not correspond to the targeted adduct **156** (Table 14, entry 1), we moved on to examine alternative reaction conditions (Table 14, entries 2 – 5) such as using a Lewis acid to activate both the α - β unsaturated ketone towards Michael addition, and diethyl ketomalonate **155** towards condensation with the resultant enolate **154**.

Chapter 3. Total Synthesis of the C and B Rings of DEM30355/A

 Table 14: Reaction conditions examined in the attempted synthesis of adducts **156** and **162**


Entry	147 eq.	157 eq.	$R^1-C(=O)-R^2$ eq.	$R^1-C(=O)-R^2$ eq.	Reaction conditions	Starting material 147 : sulfide 158 ratio ^[a] 147 : 158
1	1.0	1		2.0	NEt ₃ (1.4 eq.), THF, rt, 18 h ^[b]	1.0: 1.3 ^[b]
2	1.2	1	155	1.2	NEt ₃ (1 eq.), THF, rt, 18 h	2.0: 1.0
3	1.0	1		1.4	DMAC (2 eq.), DCM, -78 °C, 2 h ^[d]	1.0: 1.3
4	1.0	3	161	2.0	NEt ₃ (1.1 eq.), THF, rt, 9 d	1.0: 0.0
5	1.0	3		2.0	NEt ₃ (0.1 eq.), THF, rt, 9 d	1.0: 0.0 ^[e]

^[a]Determined through analysis of the ¹H NMR spectrum of the crude material

^[b]Other reagents stirred for 2 hours prior to the addition of **155**

^[c]Products **158** and **159** isolated, both in 15% yields, following column chromatography. A mixed fraction contained starting material **147** and **158**, therefore isolated yield of **158** is significantly lower than the reaction yield

^[d]Other reagents stirred for 4 h prior to the addition of **155**

^[e]Trace quantity of **159** observed

In the subsequent Michael addition/ enolate trapping reactions of compound **147**, the addition of diethyl ketomalonate **155** earlier in the reaction and reducing the equivalencies of both diethyl ketomalonate **155** and triethylamine (Table 14, entry 2), as well as addition of the Lewis acid catalyst, dimethylaluminium chloride (DMAC) (Table 14, entry 3), did not result in the formation of desired adduct **156** according to the ¹H NMR spectrum of the crude material, only sulfide **158**. The use of the more electrophilic carbonyl compound, pentafluorobenzaldehyde **161**, as the enolate trapping agent, also failed to generate desired adduct **162** (Table 14, entries 4 and 5).

Thiophenol **157** is a very powerful nucleophile, therefore it was surprising that a significant quantity of (*E*)-4-(2,5-dimethoxyphenyl)but-3-en-2-one **147** remained unreacted in the reactions. The observation suggested that the α - β unsaturated system of (*E*)-4-(2,5-dimethoxyphenyl)but-3-en-2-one **147** was a poor Michael acceptor, which may be explained by 'push-pull' stabilisation from the conjugated electron rich aromatic ring. If we consider (*E*)-4-(2,5-dimethoxyphenyl)but-3-en-2-one **147** as a model for the α - β -unsaturated system in the DEM30355/A **94**, our results suggest that the observed antibacterial activity of this compound against Gram-positive bacteria (Dr B. Kepplinger) is unlikely to arise from Michael addition, for example of cysteine residues, to the α - β -unsaturated system.

As the reaction conditions tested did not generate desired Michael addition/ enolate trapping adducts **156** and **162**, we moved on to examine alternative synthetic routes to DM-DEM30355/A **115**.

3.2.4 Baylis-Hillman Synthesis of DM-DEM30355/A **115**

As an alternative synthetic route to DM-DEM30355/A **115**, we envisaged using a key Baylis-Hillman reaction between tricarbonyl **163** and methyl vinyl ketone **164** to synthesise alcohol **165**, with construction of the oxygenated quaternary centre at C^{4a} (Figure 106). Following the synthesis of alcohol **165**, we imagined using two synthetic strategies to generate DM-DEM30355/A **115** and saturated analogues of DEM30355/A **166**.

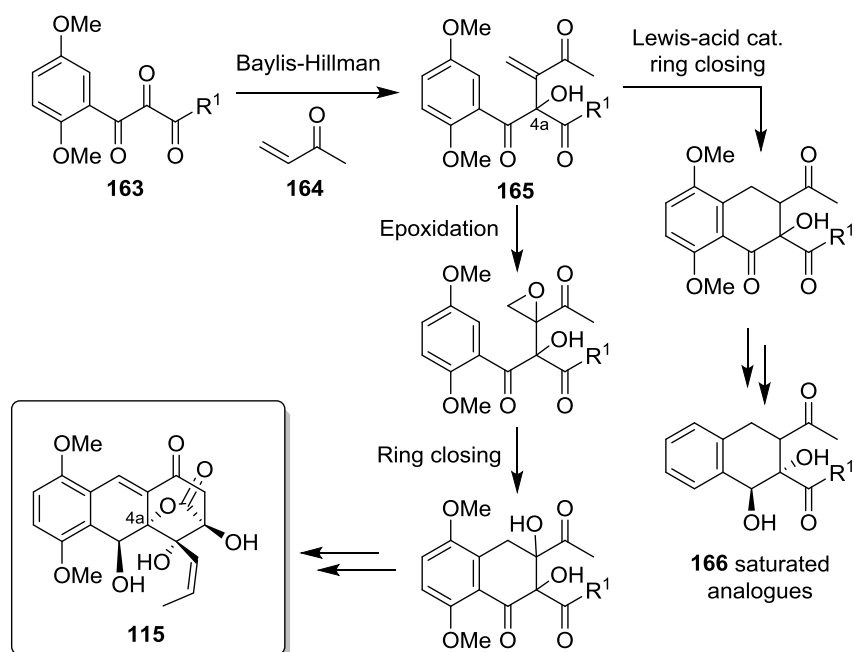


Figure 106: Proposed Baylis-Hillman route to DM-DEM30355/A **115** and DEM30355/A saturated analogues **166**

To begin with, we planned to synthesise ethyl 3-(2,5-dimethoxyphenyl)-2,3-dioxopropanoate **167** as a test system to examine our proposed Baylis-Hillman route (Figure 107). We anticipated that the central carbonyl group of compound **167** would be the most reactive towards nucleophilic attack, as it is activated by two electron withdrawing C=O groups. In

addition, we expected both the benzylic carbonyl and ester carbonyl groups to be less electrophilic and therefore less reactive, due to resonance stabilisation from the aromatic group and OEt group respectively.

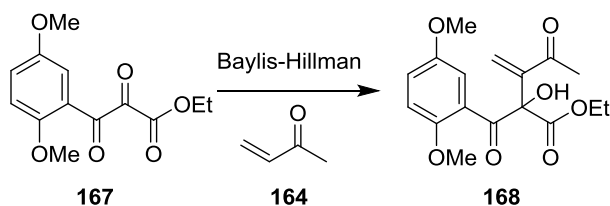


Figure 107: Planned synthesis of Baylis-Hillman product **168** from tricarbonyl **167**

The first step was to synthesise ethyl 3-(2,5-dimethoxyphenyl)-2,3-dioxopropanoate **167**.

3.2.4.1 Friedel-Crafts Synthesis of Ethyl 3-(2,5-Dimethoxyphenyl)-3-oxopropanoate **171**

We anticipated ethyl 3-(2,5-dimethoxyphenyl)-2,3-dioxopropanoate **167** could be synthesised via a Friedel-Crafts reaction between 1,4-dimethoxybenzene **169** and ethyl 3-chloro-3-oxopropionate **170** to give ethyl 3-(2,5-dimethoxyphenyl)-3-oxopropanoate **171**, followed by oxidation (Figure 108).

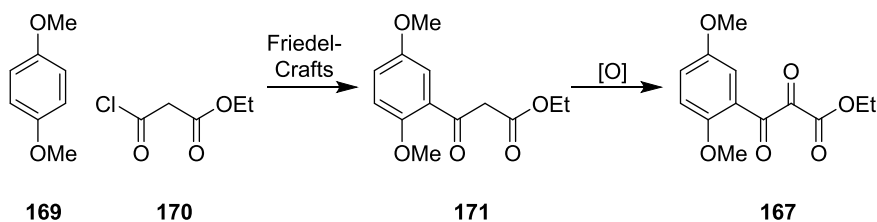
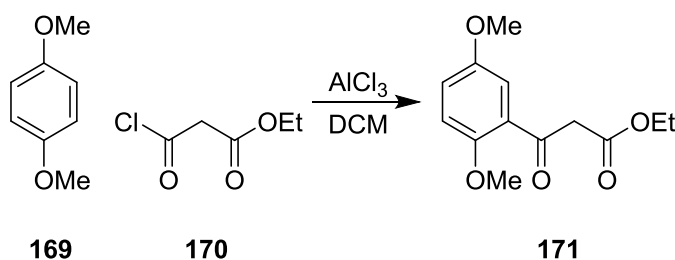


Figure 108: Planned synthesis of tricarbonyl **167**

The first step was to synthesise ethyl 3-(2,5-dimethoxyphenyl)-3-oxopropanoate **171**. 1,4-Dimethoxybenzene **169** and ethyl 3-chloro-3-oxopropionate **170** were reacted in DCM in the presence of a Lewis acid (Table 15).

Table 15: Reaction conditions examined in the Friedel-Crafts synthesis of ethyl 3-(2,5-dimethoxyphenyl)-3-oxopropanoate **171**

Entry	169 eq.	170 eq.	AlCl ₃ eq.	Reaction conditions	171 Isolated yield (%)
1	1.0	1.1	1.2	DCM, rt, 3 d	0 ^[a]
2	1.0	1.2	1.5 ^[b]	DCM, rt, 10 d	0 ^[a]
3	1.0	1.2	3.6	DCM, rt, 18 h	19%
4	1.0	1.8	3.6	DCM, rt 1h, 40 °C 18 h ^[c] , rt 2 d	12%

^[a]Starting material only observed in the ¹H NMR spectrum of the crude material

^[b]Different batch of AlCl₃ used

^[c]1.2 eq. **170** added initially, followed by 0.6 eq. after this point

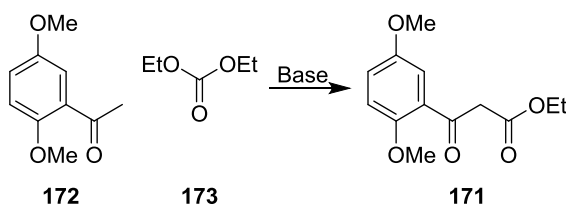
In the first Friedel-Crafts reactions we tested, no product **171** was observed in the ¹H NMR spectra of the crude material (Table 15, entries 1 and 2). We postulated that in our reactions, aluminium coordinated to the two carbonyl oxygens of ethyl 3-chloro-3-oxopropanoate **170**, preventing the formation of the reactive acylium ion species and, as a result, the formation of desired product **171**. To overcome this problem, we increased the equivalencies of AlCl₃, which resulted in the isolation of our targeted dicarbonyl product **171**, although in a poor yield of 19%, with starting material **169** recovered (Table 15, entry 3). Increasing the reaction temperature did not improve the isolated yield of product **171**, possibly due to the volatility of ethyl 3-chloro-3-oxopropanoate **170**. We contemplated that the yield of product **171** from the Friedel-Crafts reaction may be improved by increasing the equivalencies of AlCl₃ and through syringe-pump mediated addition of acyl chloride **170**.

However, given the time constraints, we decided to examine a different synthetic route to ethyl 3-(2,5-dimethoxyphenyl)-3-oxopropanoate **171**.

3.2.4.2 Synthesis of Ethyl 3-(2,5-dimethoxyphenyl)-3-oxopropanoate **171** Using Enolate Chemistry

As an alternative route to synthesise ethyl 3-(2,5-dimethoxyphenyl)-3-oxopropanoate **171**, we examined enolate chemistry between 2,5-dimethoxyacetophenone **172** and diethyl carbonate **173**, under basic conditions (Table 16).¹⁰⁸

Chapter 3. Total Synthesis of the C and B Rings of DEM30355/A

 Table 16: Reaction conditions examined in the enolate synthesis of ethyl 3-(2,5-dimethoxyphenyl)-3-oxopropanoate **171**


Entry	172 eq.	173 eq.	Base	Base eq.	Reaction conditions	Product ratio ^[a]	Isolated yield (%) ^[b]
1	1.0	2.0	NaH	3.0	Toluene, reflux, 30 min	171 : 174 1.5: 1.0	171 (16%), 174 (3%) ^[c]
2	1.0	2.0	NaH	2.0	Toluene, rt, 3 d	unreacted 172	-
3	1.0	1.5	NaHMDS	1.5	THF, rt, 18 h ^[d]	171 : 174 : 175 9.0: 1.0: 1.2	171 (24%), 175 (2%)
4	1.0	1.5	NaHMDS	1.5	THF, rt, 20 h ^[d]	171 : 174 : 175 2.8: 1.0: 1.0	171 (38%), 175 (14%)
5	1.0	2.0	NaHMDS	2.0	THF, rt, 3 d ^[e]	171 : 174 : 175 2.4: 1.0: 0.8	-

^[a]Determined using the ¹H NMR spectrum of the crude reaction material

^[b]Isolated by column chromatography

^[c]Low yield as **171** and **174** had similar R_f values. Most isolated as a mixed fraction

^[d]Base and **172** stirred at -78 °C for 1 h prior to the addition of **173**

^[e]Base and **172** stirred at -78 °C for 30 min prior to the addition of **173**

In the first reaction using NaH, two new compounds were isolated following purification of the crude material by column chromatography (Table 16, entry 1).¹⁰⁸ By comparison of the ¹H NMR data with those of ethyl 3-(2,5-dimethoxyphenyl)-3-oxopropanoate **171** previously synthesised, we could conclude one of the compounds was indeed desired product **171**, isolated in a 16% yield.

The ¹H NMR spectrum of the second isolated compound showed two signals at 5.08 ppm (1H, q, $J = 6.5$ Hz) and 1.50 ppm (3H, d, $J = 6.5$ Hz), suggesting an AB₃ spin system, corresponding to a CHCH₃ moiety. The chemical shift of the signal at 5.08 ppm, corresponding to the CH group, suggested that the CH was bonded to an electron withdrawing group. In addition, the ¹H NMR spectrum showed three signals at 6.97 ppm (1H, d, $J = 2.9$ Hz), 6.81 ppm (1H, d, $J = 8.8$ Hz) and 6.76 ppm (1H, dd, $J = 8.8, 2.9$ Hz) corresponding to a 1,2,4-trisubstituted aromatic system and two, three proton singlets at 3.82 and 3.78 ppm, corresponding to two methoxy groups. Thus, based on the ¹H NMR data, we were able to deduce that the compound was alcohol **174** (~3% isolated yield) (Figure 109).

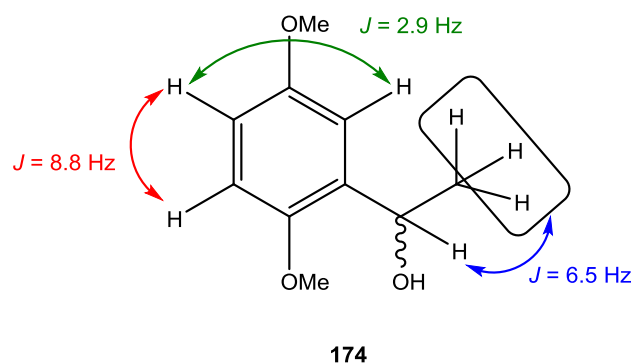


Figure 109: Structure of alcohol **174** and the key NMR data which aided structural assignment

Unusually, this alcohol **174** appeared to be the product of the keto-reduction of 2,5-dimethoxyacetophenone **172**, possibly from the NaH at high temperatures. Using a lower reaction temperature did not result in a reaction (Table 16, entry 2), therefore we examined an alternative base, NaHMDS (Table 16, entries 3 – 5). These reactions successfully generated desired product **171**, however reduction product **174** was still observed in the ^1H NMR spectra of the crude reaction material, albeit in a much lower concentration than observed in the reaction with NaH (Table 16, entry 1). Purification of the crude material by column chromatography led to the isolation of desired product **171**, as well as a new compound **175**.

The ^1H NMR spectrum of new compound **175** contained two signals at 1.00 ppm (3H, d, $J = 6.6$ Hz) and 2.65 ppm (1H, app dt, $J = 13.4, 6.6$ Hz), indicating a CH_3 group adjacent to a CH unit, coupled to each other with $J = 6.6$ Hz. The COSY NMR spectrum showed coupling between this CH signal at 2.65 ppm and signals at 3.06 ppm (2H, dd, $J = 16.1, 6.0$ Hz) and 2.89 ppm (2H, dd, $J = 16.1, 7.5$ Hz), consistent with two equivalent sets of geminally coupled ($J = 16.1$ Hz) CH_2 groups, thus we could deduce the molecule was symmetrical about the carbon of the CH group. In addition, the HMBC spectrum showed a correlation between the signals at 3.06 ppm and 2.89 ppm, corresponding to the geminally coupled CH_2 , with a signal at 201.9 ppm, consistent with a ketone carbon atom. The HMBC spectrum also showed a correlation between this signal at 201.9 ppm and two signals at 7.19 ppm (2H, d, $J = 3.2$ Hz) and 6.87 ppm (d, $J = 9.0$ Hz), corresponding to two equivalent aromatic rings. Based on this data, we proposed the new product was diketone **175** (2% isolated yield) (Figure 110).

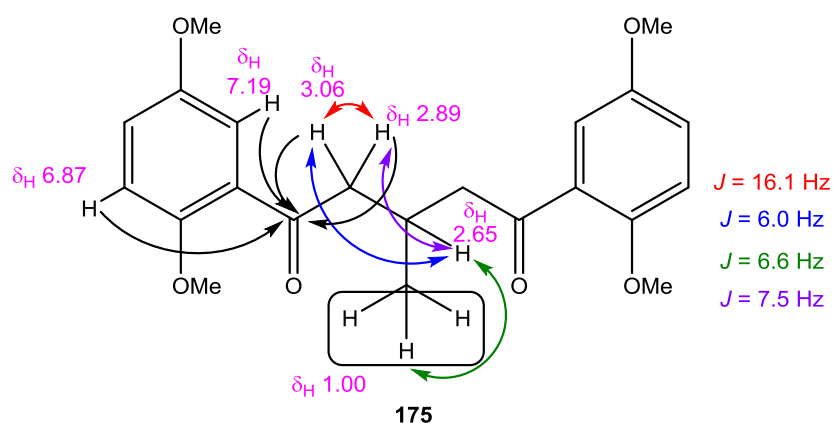


Figure 110: Structure of diketone **175** with the key NMR data for structural assignment shown

In the previous reaction between 2,5-dimethoxyacetophenone **172** and diethyl carbonate **173** where NaH had been used as the base (Table 16, entry 1) we had postulated that the generation of alcohol **174** may be the result of an unusual hydride addition to 2,5-dimethoxyacetophenone **172**. However, alcohol **174** was also generated in our reactions using NaHMDS and since this reagent does not contain hydride, we were prompted to consider an alternative explanation. We propose that under our reaction conditions, a Meerwein Ponnendorf Verley reaction occurs between 2,5-dimethoxyacetophenone **172** and ethoxide **176**, generated from the decomposition of diethyl carbonate **173**, to give alcohol **174** and ethanol (Figure 111).

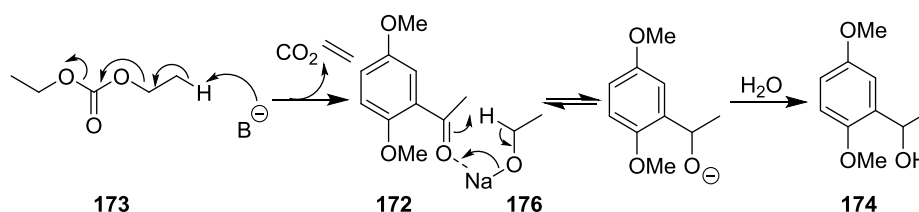


Figure 111: Proposed mechanism of the formation of alcohol **174** via a Meerwein Ponnendorf Verley reaction

This mechanism also can be used to explain the generation of diketone **175**. Initially an aldol reaction between the enolate of 2,5-dimethoxyacetophenone **177** and ethanal occurs, followed by an E1cB reaction to give α - β -unsaturated ketone **178** (Figure 112). This compound **178** then undergoes a Michael addition reaction with the enolate **177** of a second molecule of 2,5-dimethoxyacetophenone, followed by tautomerisation to give diketone **175**.

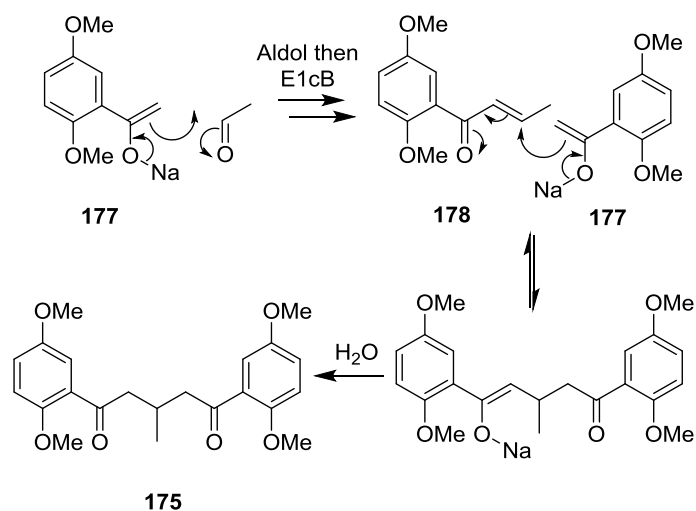


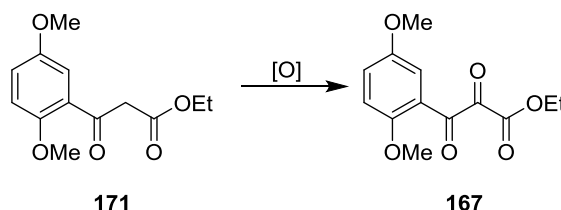
Figure 112: Proposed mechanism for the formation of diketone **175**

Despite the formation of unwanted side products **174** and **175**, we were able to obtain sufficient quantities of the target product from the enolate reactions, ethyl 3-(2,5-dimethoxyphenyl)-3-oxopropanoate **171**, to proceed to the next step.

3.2.4.3 Synthesis of Ethyl 3-(2,5-dimethoxyphenyl)-2,3-dioxopropanoate **167**

We then moved on to examine oxidation of ethyl 3-(2,5-dimethoxyphenyl)-3-oxopropanoate **171** to generate the tricarbonyl compound, ethyl 3-(2,5-dimethoxyphenyl)-2,3-dioxopropanoate **167**, which would act as a key intermediate in the synthesis of DM-DEM30355/A **115** and saturated analogues of DEM30355/A (Table 17).

Chapter 3. Total Synthesis of the C and B Rings of DEM30355/A

 Table 17: Reaction conditions examined in the oxidation of compound **171** to tricarbonyl **167**


Entry	171 eq.	[O]	[O] eq.	Reaction conditions	Isolated yield 167
1	1.0	CAN	0.2	DCM, rt, 4 h	171 recovered
2	1.0	CAN	0.1	MeCN, rt, 7 h	171 recovered
3	1.0	CAN	0.1	MeCN, rt, 24 h	171 recovered
4	1.0	CAN	0.1	MeCN, rt, 7 d	29%
5	1.0	DMP	1.2	DCM, pyridine (3 eq.), rt, 18 h	40% ^{[a][b]}
6	1.0	DMP	1.2	DCM, pyridine (3 eq.), rt, 18 h	32% ^[b]
7	1.0	NBS DMSO	1.0 excess ^[c]	50 °C, 2 d	53% ^[b]
8	1.0	NBS DMSO	1.0 excess ^[c]	50 °C, 3 d	49% ^[b]
9	1.0	NBS DMSO	1.0 excess ^[c]	50 °C, 3 d	74%

^[a]Unreacted **171** isolated (~24%).

^[b]Yield of **167** compromised by formation and isolation of hydrate

^[c]Oxidant is DMSO which is used as the reaction solvent

In the initial reactions using ceric ammonium nitrate (CAN) (Table 17, entries 1 – 4), the reactions were very slow, with new product **167** only observed after 7 days (Table 17, entry 4). Following purification of the crude material by column chromatography, product **167** was isolated and analysed. The ¹³C NMR spectrum showed a new carbonyl carbon signal at 192.7 ppm and the two proton singlet at 3.94 ppm in the ¹H NMR spectrum of starting material **171**, had disappeared. Thus, in combination with HRMS data, we concluded that the new compound was desired tricarbonyl **167**, isolated in a 29% yield. As oxidation of compound **171** using CAN was very slow, we decided to examine alternative oxidising conditions.

We anticipated that the hypervalent iodine compound, Dess-Martin periodinane (DMP) would be more reactive than CAN towards the oxidation of ethyl 3-(2,5-dimethoxyphenyl)-3-

oxopropanoate **171**. This proved to be the case, as after 18 hours at room temperature, the ^1H NMR spectrum of the crude reaction material indicated product **167** had been generated. The formation of hydrates **179** of the product **167** made purification by column chromatography difficult (Figure 113), resulting in the isolation of desired compound **167** in poor yields of 32 and 40% (Table 17, entries 5 and 6), although these were much improved when compared to the oxidations using CAN.

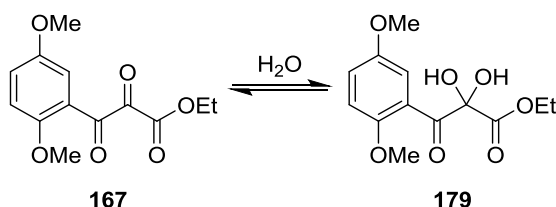


Figure 113: Formation of hydrate **179**

Next we examined radical oxidation of ethyl 3-(2,5-dimethoxyphenyl)-3-oxopropanoate **171**, mediated by *N*-bromosuccinimide in DMSO (Table 17, entries 7 – 9).¹⁰⁹ Although the yields of product **167** generated from these reactions were variable, the proportion of product hydrates **179** generated was much lower than in the DMP reactions and, following optimisation of the column chromatography conditions, desired 3-(2,5-dimethoxyphenyl)-2,3-dioxopropanoate **167** could be isolated in yields as high as 74% (Table 17, entry 9).

With a working synthetic route to tricarbonyl **167** developed, we could then move on to examine Baylis-Hillman reactions.

3.2.4.4 Baylis-Hillman Reaction Between Ethyl 3-(2,5-dimethoxyphenyl)-2,3-dioxopropanoate **167** and Methyl Vinyl Ketone **164**

The next stage in the synthesis was to use Baylis-Hillman chemistry between 3-(2,5-dimethoxyphenyl)-2,3-dioxopropanoate **167** and methyl vinyl ketone **164**, to synthesise compound **168** (Figure 114). The reaction would allow construction of the quaternary oxygenated centre at C^{4a}, a key site in our planned route to DM-DEM30355/A **115**.¹¹⁰

3-(2,5-Dimethoxyphenyl)-2,3-dioxopropanoate **167** was reacted with methyl vinyl ketone **164** in the presence of a nucleophilic catalyst (Table 18, entries 1-4).

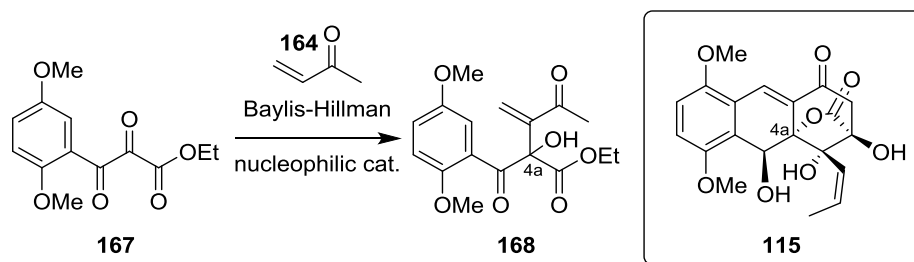


Figure 114: Planned Baylis-Hillman reaction between tricarbonyl **167** and methyl vinyl ketone **164** to generate adduct **168**

Table 18: Baylis-Hillman reaction conditions examined to synthesise adduct **168**

Entry	167 eq.	164 eq.	Catalyst	Catalyst eq.	Reaction conditions	Isolated yield ^[a]
1	1.0	2.0	DABCO	0.1	THF, rt, 4 d	unreacted 167 (85%) ^[b]
2	1.0	4.0	DABCO	0.1	THF, rt, 8 d	unreacted 167 (38%) ^[b]
3	1.0	4.0	DABCO	1.0	THF, rt, 8 d	unreacted 167 (16%) and product 168 (30%)
4	1.0	2.0	DMAP	0.1	THF, rt, 8 d	product 168 (17%)

^[a]Isolated using column chromatography

^[b]¹H NMR of the crude material showed product **168**, but following chromatography **168** appeared to decompose

In the first reactions using DABCO, the ¹H NMR spectrum of the crude material showed unreacted starting material **167** in addition to a new product, with signals at 6.28 ppm and 6.02 ppm, however we found that the new compound degraded under column chromatography conditions (Table 18, entries 1 and 2). Increasing the equivalencies of DABCO 10 fold (Table 18, entry 3) and changing the nucleophilic catalyst to DMAP (Table 18, entry 4), improved the ratio of new product to starting material **167** as shown by analysis of the ¹H NMR spectrum of the crude material. After purification of the crude material by column chromatography, we were able to isolate the new compound. Following analysis of the ¹H NMR spectrum of this new product, which contained a signal at 4.35 ppm (2H, app qd, $J = 7.1, 2.4$ Hz) characteristic of a diastereotopic CH₂ group and two, one proton doublets at 6.28 ppm and 6.02 ppm, characteristic of geminally coupled ($J = 1.3$ Hz) alkene protons, we could deduce that the product was target alcohol **168** (30% and 17% isolated yield, following reaction with DABCO and DMAP respectively) (Figure 115).

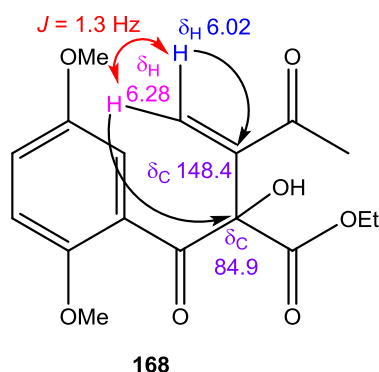


Figure 115: Structure of Baylis-Hillman adduct **168** with the NMR data key for structure elucidation shown

Given the poor yields and long reaction times of the reactions tested, we then examined the use of a Lewis acid, titanium tetrachloride, in our Baylis-Hillman reactions to generate alcohol **168** (Figure 116).

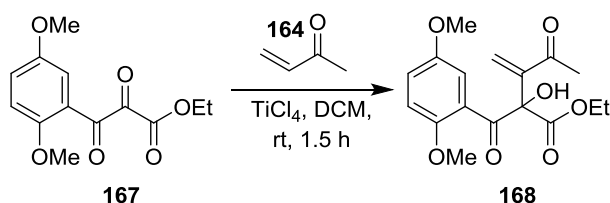


Figure 116: Baylis-Hillman reaction examined using titanium chloride

A new compound was isolated following purification of the crude material by column chromatography, however analysis of the ^1H NMR spectrum showed that it was not Baylis-Hillman product **168**.

The ^1H NMR spectrum of the new product **180** showed a signal at 4.00 ppm (1H, dd, $J = 9.0, 4.4$ Hz), and two signals at 3.88 ppm (1H, dd, $J = 11.6, 4.4$ Hz) and 3.77 ppm (1H, dd, $J = 11.6, 9.0$ Hz), characteristic of an ABC spin system, which corresponded to a CH group bonded to a CH_2 group. The chemical shift associated with the carbon atom of this CH_2 group was 40.9 ppm, suggesting a $\text{CH}_2\text{-X}$ group. In addition, the HMBC spectrum showed correlations between the CH_2 proton signals and a peak at 209.7 ppm, characteristic of a ketone carbon atom. Furthermore, a broad, one proton singlet at 4.71 ppm showed HMBC correlations to a carbon signal at 168.3 ppm, suggesting an OH group in close proximity to an ester carbonyl carbon atom. From these data, in combination with the mass spectrum which showed an isotopic pattern characteristic of one chlorine atom, we deduced that the new compound was chlorinated Baylis-Hillman adduct **180** (31% yield) (Figure 117).¹¹¹

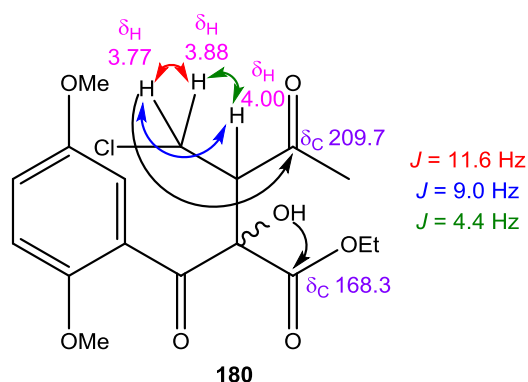


Figure 117: Structure of chlorinated Baylis-Hillman product **180**, with the NMR data important for structure elucidation shown

Chapter 3. Total Synthesis of the C and B Rings of DEM30355/A

Even though chlorinated compound **180** was not the intended target, we anticipated the chlorine atom would be an advantage in later stages of the synthesis, as it would allow ring closure using Friedel-Crafts alkylation.

3.3 Conclusions and Future Work

In this project we aimed to develop a synthetic route to DEM30355/A **94**, a novel polyketide isolated from fermentation of *A. DEM30355*, which was shown to be active against Gram-positive bacteria (Dr. B. Kepplinger) (Figure 118). In this chapter we focused on the construction of the C and B rings of DM-DEM30355/A **115**, as well as the quaternary oxygenated centre at C^{4a} (Figure 118).

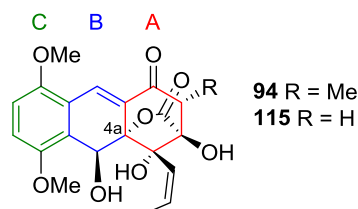


Figure 118: Structures of DEM30355/A **94** and DM-DEM30355/A **115**

The most successful method we examined to synthesise the left hand portion of DM-DEM30355/A **115** including C^{4a} was a Baylis-Hillman reaction between methyl vinyl ketone **164** and 3-(2,5-dimethoxyphenyl)-2,3-dioxopropanoate **167**. In the presence of the nucleophilic catalysts, DABCO and DMAP, the product of this reaction is alkene Baylis-Hillman adduct **168**, however in the presence of titanium tetrachloride, the product is chlorinated compound **180** (Figure 119).

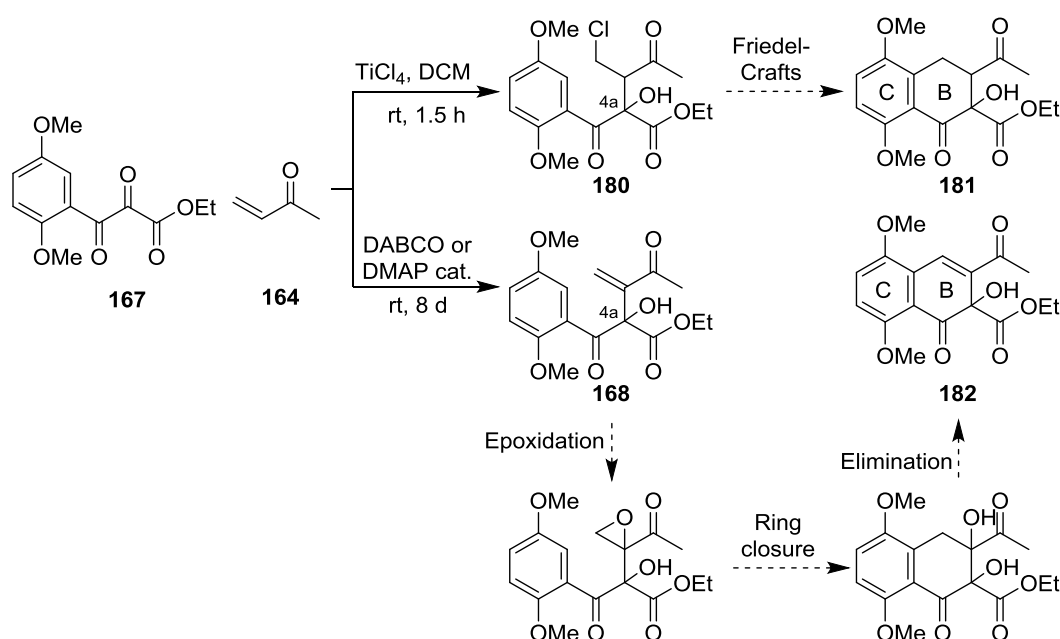


Figure 119: Synthesis of Baylis-Hillman adducts **168** and **180** and proposed route to close the B ring of both compounds

To continue this route, the next step would be to carry out ring closure and generate the B ring of DM-DEM30355/A **115**. An advantage of continuing the synthesis from chlorinated adduct **180** is that we could use Friedel-Crafts alkylation to carry out ring closure, allowing access to a new class of saturated DEM30355/A analogues **181** (Figure 119). On the other hand,

continuing from alkene Baylis-Hillman product **168** would allow us to construct the α - β unsaturated system as found in the natural product, via epoxidation of alkene **168** followed by ring closure and elimination to give **182** (Figure 119).

Following ring closure to generate the B ring, OH-directed reduction of the C⁵ ketone of naphthalene **182** would generate diol **183**, with an *anti*-arrangement of the two OH groups at C^{4a} and C⁵ as seen in DM-DEM30355/A **115** (Figure 120).¹¹² After the synthesis of ester **185** via nucleophilic attack of C^{4a} – OH of compound **183** on acyl chloride **184**, an intramolecular aldol reaction may be used to generate lactone **186**. Subsequently, a key pinacol coupling reaction would simultaneously close the A and D rings of DM-DEM30355/A **115** (Figure 120) (Note: protection and deprotection steps are omitted from our discussion of our planned future work for clarity).¹¹³

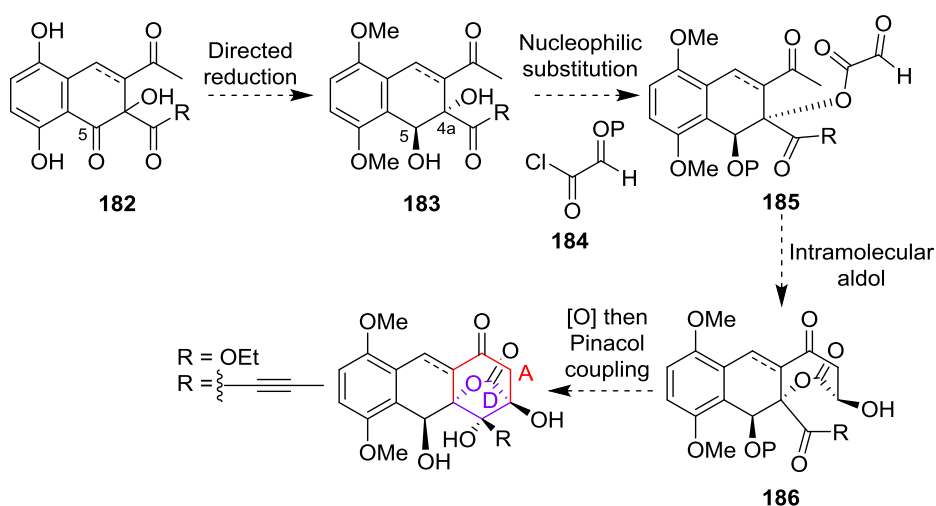


Figure 120: Proposed synthetic route to form the A and D rings of DM-DEM30355/A **115** via a key pinacol reaction

When R is a propyne group, a final stage Lindlar reduction may be used to give DM-DEM30355/A **115**. The highly oxygenated small molecules synthesised in each step would be subjected to bioassay, to identify any interesting biological activity.

We will now discuss an alternative synthesis of DEM30355/A **94**, which examines the synthesis of the A, B, C ring core structure, using Diels-Alder chemistry.

Chapter 4. Diels-Alder Synthesis of DEM30355/A

4.1 Introduction

In this chapter we continue our investigations towards the total synthesis of DEM30355/A **94** and analogues to develop new bioactive drug leads, for SAR studies and to determine the absolute stereochemistry of the natural product. Previously we focused on the synthesis of the C and B rings of DEM30355/A **94** (Chapter 3). In this chapter, we discuss our work towards the synthesis of the A, B and C rings of DEM30355/A **94** through Diels-Alder chemistry (Figure 121).

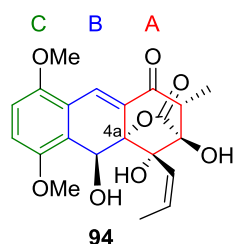


Figure 121: Structure of DEM30355/A **94**

4.1.1 Mechanism of the Diels-Alder Reaction

One of the most important developments in the total synthesis of natural products came in 1928, when Otto Diels and Kurt Alder published their findings on the [4+2] cycloaddition reaction that bears their names.¹¹⁴ The Diels-Alder (D-A) reaction is a pericyclic reaction between a diene **187** and a molecule possessing a multiple bond **188** (the dienophile), allowing the formation of two new C-C bonds and new stereocentres in a simultaneous, 100% atom efficient reaction (Figure 122).

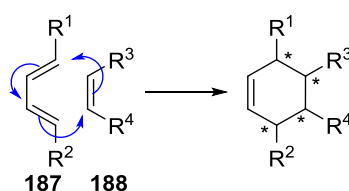


Figure 122: Reaction mechanism of the Diels-Alder reaction, with the construction of 4 new stereocentres

In general, the D-A reaction is stereoselective in favour of the *endo* product, due to stabilising secondary orbital interactions between the HOMO and LUMO of the reactants (Figure 123).¹¹⁵

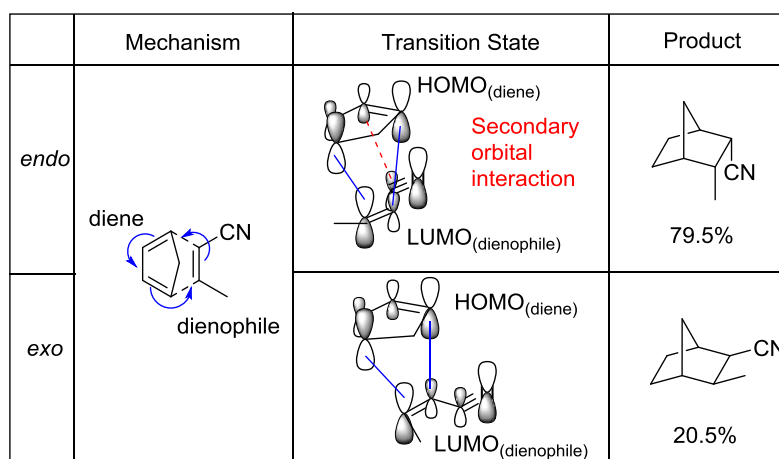


Figure 123: Origin of *endo* selectivity in the Diels-Alder reaction between cyclopentadiene and *cis*-crotononitrile at 25 °C¹¹⁵

The ability of the D-A reaction to construct 6-membered rings and new stereocentres, has been exploited in the total synthesis of many natural products.¹¹⁴

4.1.2 The Diels-Alder Reaction in Total Synthesis

4.1.2.1 The Total Synthesis of Reserpine 189

Reserpine **189** was isolated from the plant, *Rauwolfia Serpentina*, in 1952 by Schlittler *et al.*, and possesses antihypertensive and antipsychotic properties (Figure 124).^{116,117} Woodward *et al.* reported their total synthesis of reserpine **189** in 1956.¹¹⁸ The first step in Woodward's synthesis is an *endo* D-A reaction between vinylacrylic acid **190** and quinone **191**, giving cycloadduct **192** (Figure 124).^{116,118}

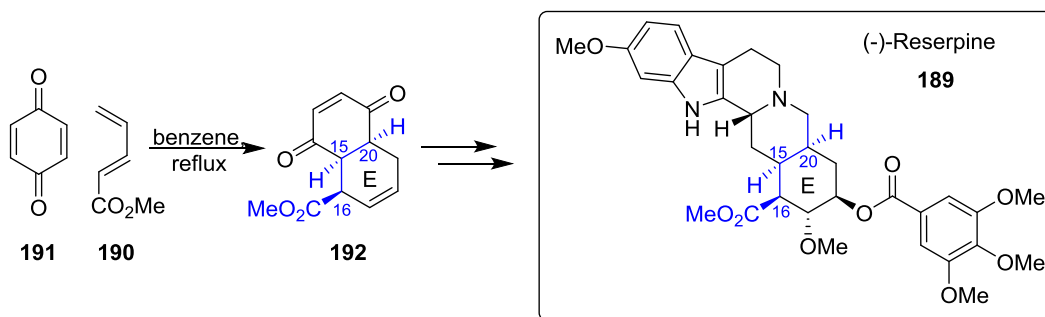


Figure 124: Right - structure of reserpine **189**. Left - key Diels-Alder synthesis of the *E* ring of reserpine **189**

This initial D-A step successfully constructed the 6-membered *E* ring of reserpine **189** and introduced three contiguous stereogenic centres at C¹⁵, C¹⁶ and C²⁰ as seen in the natural product (Figure 124).^{116,117}

4.1.2.2 The Total Synthesis of Halenaquinone 193

Another example of the D-A reaction in total synthesis is described in Rodrigo and co-workers' synthesis of the antibiotic, halenaquinone **193**, which was isolated from the marine sponge, *Xestospongia exigua*, in 1983 (Figure 125).^{119,120} The synthesis of (\pm)-halenaquinone **193** involves an oxidative ketalisation reaction between 2-methoxy-4-methylphenol **194** and dienol

195 in the presence of (bis(trifluoroacetoxy)iodo)benzene (BTIB), succeeded by an intramolecular D-A reaction of the resultant ketone **196** to generate compound **197**. Compound **197** then undergoes a Cope rearrangement to generate tricyclic ketone **198**, which is subsequently employed as a dienophile in another key D-A reaction with isobenzofuran **199** as the diene, to give D-A adduct **200**.¹²⁰

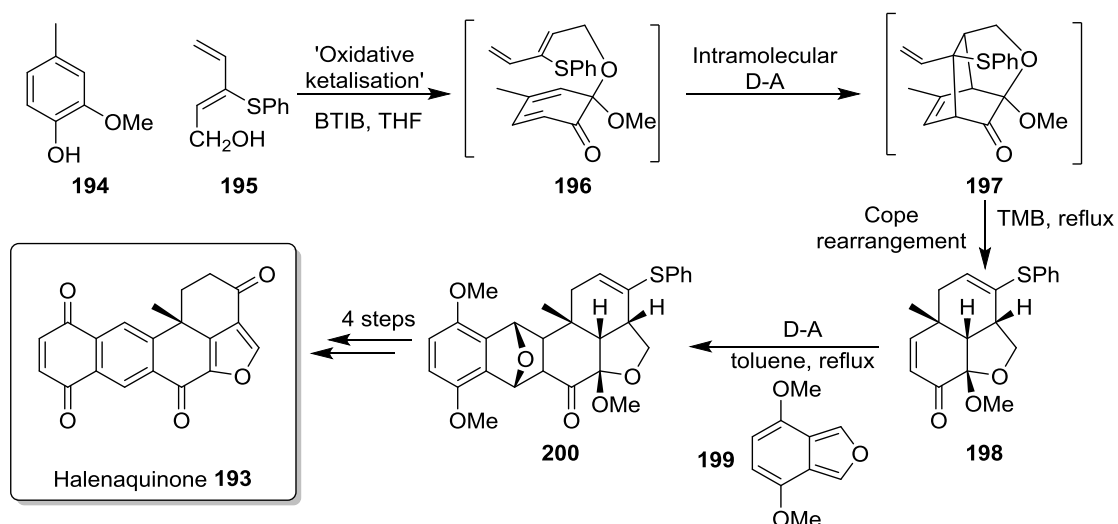


Figure 125: Rodrigo's total synthesis of halenaquinone **193**¹²⁰

Using this method, Rodrigo *et al.* were able to synthesise racemic halenaquinone **193** in a 4% yield over 8 steps (Figure 125).¹²⁰

4.1.2.3 The Partial Synthesis of Dynemicin A **202**

Magnus *et al.* also describe the use of this isobenzofuran diene **199** in their synthesis of the anthraquinone moiety **201** of dynemicin A **202** (Figure 126). Dynemicin A **202**, an antitumour compound, was isolated from the soil bacterium, *Micromonospora chersina* in 1989.¹²¹ The synthetic procedure involves a D-A reaction between isobenzofuran **199** and alkyne **203** as the dienophile, to generate D-A cycloadduct **204**.¹²²

Chapter 4. Diels-Alder Synthesis of DEM30355/A

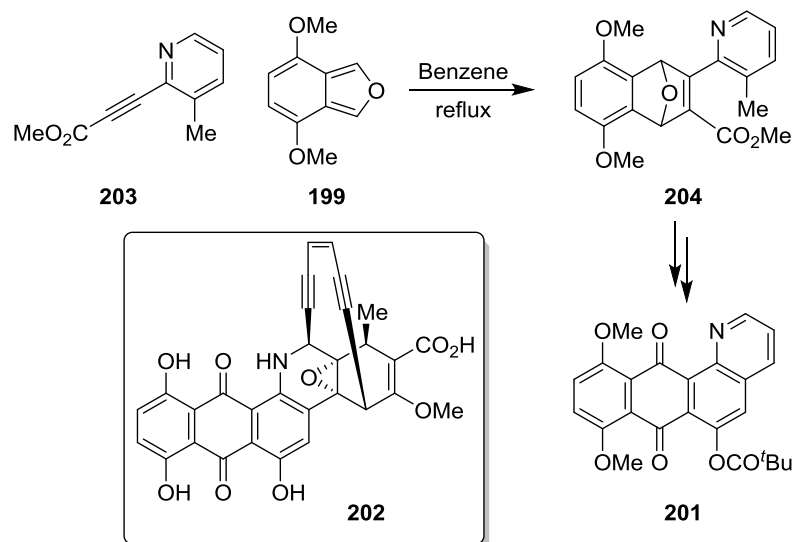


Figure 126: Structure of dynemicin A **202** and the key Diels-Alder reaction in the synthesis of the anthraquinone moiety **201**

The starting material, diene **199**, was itself synthesised via a cascade series of pericyclic reactions from 5,8-dimethoxy-1,4-dihydro-1,4-epoxynaphthalene **205** (Figure 127). Epoxynaphthalene **205** was subjected to an inverse electron demand D-A reaction with 3,6-di-2-pyridyl-1,2,4,5-tetrazine **206** to give D-A cycloadduct **207**, which rapidly undergoes a retro D-A reaction to give tricyclic compound **208**, with the concurrent release of N₂. Compound **208** then undergoes a second retro D-A reaction to generate the desired isobenzofuran **199** and pyridazine **209**.¹²²

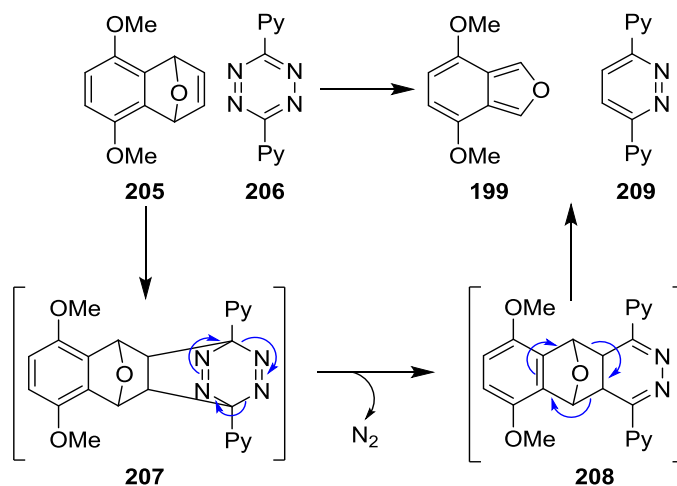


Figure 127: Reaction mechanism to synthesise isobenzofuran diene **199**

Despite the apparent instability of isobenzofuran **199**, Magnus *et al.* were able to isolate the compound through column chromatography for use in their D-A reactions.¹²²

4.2 Project Aims

In this chapter we aim to synthesise the three ring carbon skeleton of DEM30355/A **94**, via a key D-A step. Through disconnections of bonds C¹⁰-C^{10a} and C^{4a}-C⁵, we plan to construct the A, B, C ring core structure of DEM30355/A **94**, using a D-A reaction between isobenzofuran diene **199** and a cyclic dienophile **210**, to generate D-A adducts **211** (Figure 128). This approach will allow construction of the key quaternary centre at C^{4a}. Following the synthesis of D-A adducts **211**, we aim to introduce the benzylic alcohol and α - β -unsaturated ketone as in DEM30355/A **94** via base catalysed ring opening to generate compound **212** (Figure 128).

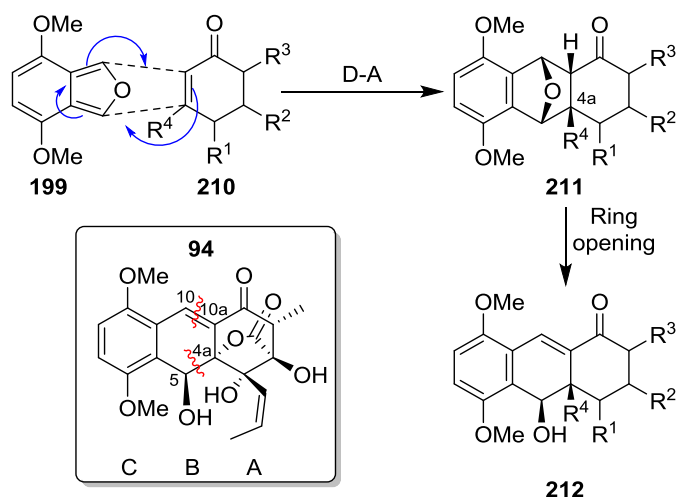


Figure 128: Planned synthetic route to DEM30355/A analogues **212**

In concurrence with our D-A investigations, we aim to synthesise DEM30355/A **94** as a single enantiomer. We will target the enantiomer of DEM30355/A **94** which is analogous to the proposed absolute configuration of rishirilide A **95** (Figure 129).⁹⁹

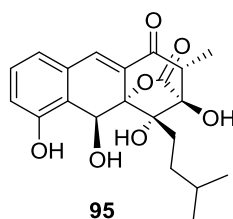


Figure 129: Proposed absolute stereochemistry of rishirilide A **95**

Starting from shikimic acid **213**, we will examine the diastereoselective synthesis of dienophile **214**, with the aim of constructing the chiral centre at C³ (Figure 130). Following the synthesis of dienophile **214**, we will investigate a D-A reaction to give D-A cycloadduct **215**, which may be subsequently converted to DEM30355/A **94**. With consideration of the Danishefsky and Pettus syntheses of rishirilide B **96** (Chapter 3), we predict such a bulky dienophile will undergo an *exo* selective D-A reaction.^{99,100}

Chapter 4. Diels-Alder Synthesis of DEM30355/A

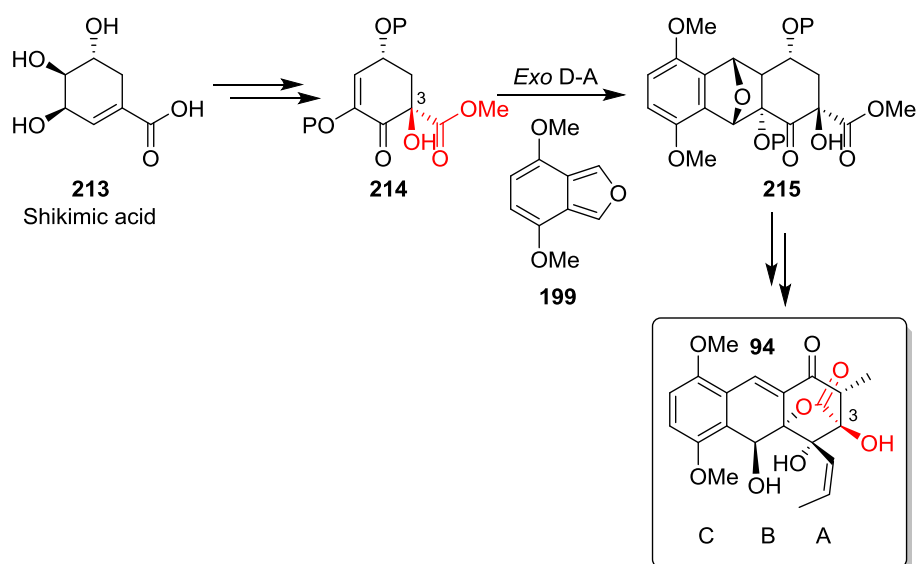


Figure 130: Planned synthetic route to DEM30355/A **94** as a single enantiomer

Following the synthesis of DEM30355/A **94**, we aim to determine the absolute stereochemistry of the molecule through optical rotation measurements. As in Chapter 3, through our investigations we aim to synthesise a range of DEM30355/A analogues for SAR studies and target elucidation, as well as to identify new antibacterial drug leads.

4.3 Results and Discussion

We planned to synthesise analogues of DEM30355/A **94** via a D-A reaction between isobenzofuran **199** and cyclic dienophiles **210**, followed by base catalysed ring opening to give compounds **212** (Figure 131). This would act as a test system for subsequent investigations into the D-A synthesis of DEM30355/A **94** as a single enantiomer, as well as provide a range of analogues **212** for bioassay and SAR studies. Such compounds would contain much of the functionality as in DEM30355/A **94**, including the A, B, C ring framework, a benzylic alcohol and an α - β unsaturated ketone. In addition, the D-A reaction would allow introduction of the quaternary centre at C^{4a}.

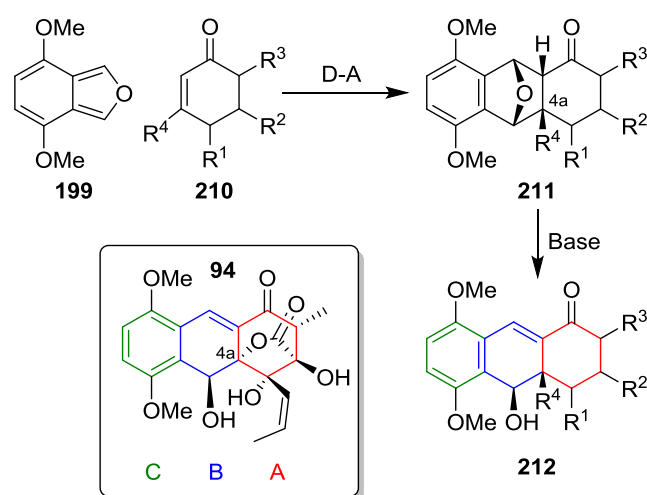


Figure 131: Planned Diels-Alder synthesis of DEM30355/A analogues **212**

The first step was to synthesise diene **199**. We planned to synthesise 4,7-dimethoxyisobenzofuran **199** following the method described by Magnus *et al.* in their partial synthesis of dynemycin A **202**, from the reaction between 5,8-dimethoxy-1,4-dihydro-1,4-epoxynaphthalene **205** and 3,6-di-2-pyridyl-1,2,4,5-tetrazine **206** (Figure 132).¹²²

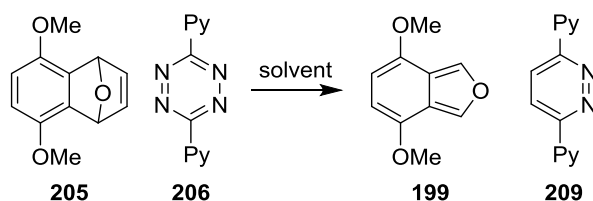


Figure 132: Planned synthesis of diene **199** from epoxynaphthalene **205**

Tetrazine **206** was commercially available and so the first step was to synthesise epoxynaphthalene **205**.

4.3.1.1 Synthesis of 5,8-Dimethoxy-1,4-dihydro-1,4-epoxynaphthalene 205

5,8-Dimethoxy-1,4-dihydro-1,4-epoxynaphthalene **205** was synthesised via a D-A reaction between furan and benzyne **217**, generated *in situ* from the reaction between LDA and 2-bromo-1,4-dimethoxybenzene **216** (Figure 133).¹²³

In each reaction, LDA (1.1 eq.) was reacted with 2-bromo-1,4-dimethoxybenzene **216** (1.0 eq.) in THF at -78 °C, followed by the immediate addition of furan (20 eq.).

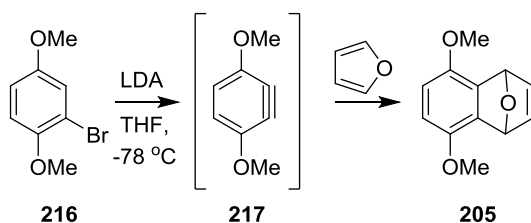


Figure 133: Synthesis of 5,8-dimethoxy-1,4-dihydro-1,4-epoxynaphthalene **205**

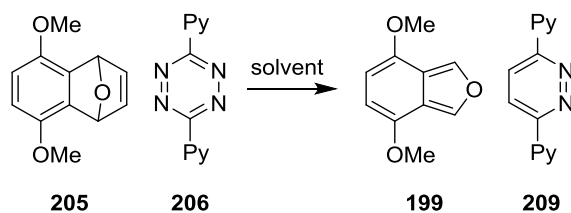
Following purification of the crude material by column chromatography, desired epoxynaphthalene **205** was isolated in an excellent yield (87%).

With sufficient quantities of epoxynaphthalene **205** in hand, we moved on to the next step.

4.3.1.2 Synthesis of 4,7-Dimethoxyisobenzofuran 199

The next step was to synthesise 4,7-dimethoxyisobenzofuran **199**, using the cascade reaction between 5,8-dimethoxy-1,4-dihydro-1,4-epoxynaphthalene **205** and 3,6-di-2-pyridyl-1,2,4,5-tetrazine **206** (Figure 132). In their partial synthesis of dynemycin A **202**, Magnus *et al.* reported that 4,7-dimethoxyisobenzofuran **199** was isolated following column chromatography as a moderately stable solid and an X-ray structure of the compound **199** was published, however no isolation procedures have been reported.^{122,124}

Following the method reported by Magnus *et al.* for the synthesis of isobenzofuran **199**, epoxynaphthalene **205** and tetrazine **206** were reacted together under ambient conditions, with the reactions monitored by TLC for the loss of starting material **205** (Table 19).¹²²

Table 19: Reaction conditions and isolation procedures examined to generate diene **199**

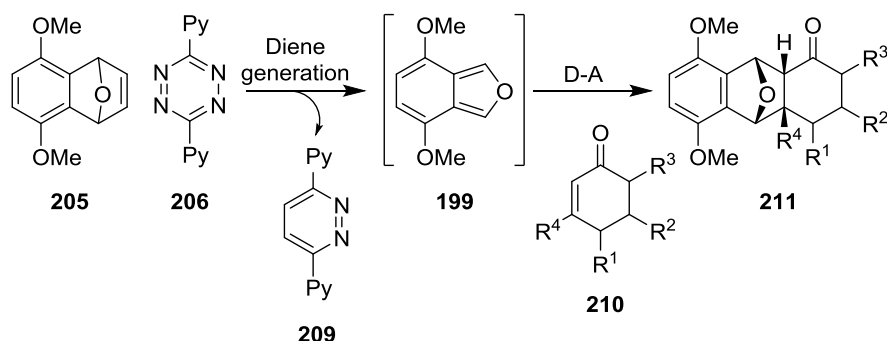
Entry	205 eq.	206 eq.	Reaction conditions	Purification
1	1	1.1	THF, rt, 1 h	silica gel chromatography
2	1	1.0	DCM, rt, 1 h	acid wash

In the first reaction we examined, the ^1H NMR spectrum of the reaction mixture after 1 hour showed signals at 7.90 ppm (1H, s), 5.85 ppm (1H, s) and 3.77 ppm (3H, s) corresponding to desired 4,7-dimethoxyisobenzofuran **199**, however the compound decomposed following column chromatography (Table 19, entry 1). We repeated the reaction with the inclusion of an acid wash step to remove pyridazine **209**, however once again decomposition of 4,7-dimethoxyisobenzofuran **199** was observed (Table 19, entry 2).

Given the difficulties associated with isolating isobenzofuran **199**, we considered generating the compound *in situ* in our D-A reactions.

4.3.2 Diels-Alder Reactions with *in situ* Generation of 4,7-Dimethoxyisobenzofuran **199**

As a modification to our original planned D-A reactions, we envisaged a one-pot reaction between epoxynaphthalene **205** and tetrazine **206** to generate 4,7-dimethoxyisobenzofuran **199**, followed by addition of dienophile **210** to synthesise desired D-A cycloadduct **211** (Figure 134). We anticipated that product **211** would result from an *endo* selective D-A reaction.

Figure 134: Planned one-pot synthesis of Diels-Alder cycloadduct **211**

We then tested the D-A reactions between 4,7-dimethoxyisobenzofuran **199** and a range of dienophiles **210**.

4.3.2.1 Diels-Alder Reaction with 3-Ethoxycyclohex-2-en-1-one **218** as the Dienophile

Initially we chose to examine 3-ethoxycyclohex-2-en-1-one **218** as the dienophile, to allow construction of the quaternary oxygenated centre at C^{4a}, which is present in DEM30355/A **94** (Figure 135).

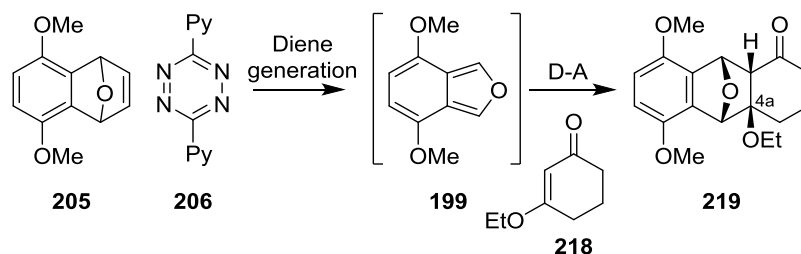
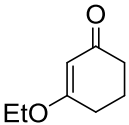


Figure 135: Proposed synthesis of cycloadduct **219** via a Diels-Alder reaction between diene **199** and 3-ethoxycyclohex-2-en-1-one **218**

5,8-Dimethoxy-1,4-dihydro-1,4-epoxynaphthalene **205** was reacted with 3,6-di-2-pyridyl-1,2,4,5-tetrazine **206**, with the reactions monitored by TLC for the loss of epoxynaphthalene **205**. At this point, 3-ethoxycyclohex-2-en-1-one **218** was added to the reaction mixture (Table 20).

Table 20: Diels-Alder reaction conditions examined using 3-ethoxycyclohex-2-en-1-one **218** as the dienophile

Entry	205 eq.	206 eq.	 218 eq.	Reaction conditions
1	1	1	7.0	DCM, rt, 18 h ^[a]
2	1	1	1.0	THF, 3 d, rt
3	1	1	1.5	Toluene, reflux, 28 h

^[a]Dienophile **218** added at the beginning of the reaction

In our reactions using ethoxycyclohex-2-en-1-one **218** as the dienophile, no product **219** signals were observed in the ¹H NMR spectrum of the crude reaction material, despite varying the solvent, increasing the reaction temperature and time, and increasing the equivalencies of dienophile **218** (Table 20, entries 1-3). We postulated that dienophile **218**, which contains an electron donating OEt group, was too electron rich to undergo a normal electron demand D-A reaction with diene **199**, therefore we decided to examine organo-catalysed D-A reactions using Schreiner's bistiourea catalyst **220** and proline **221** (Figure 136).^{125,126} We postulated that bistiourea catalyst **220** and proline **221** would lower the LUMO of ethoxycyclohex-2-en-

1-one **218** via the formation of a hydrogen bonded adduct and enamine **222** respectively, thus decreasing the E_a for the D-A reaction.

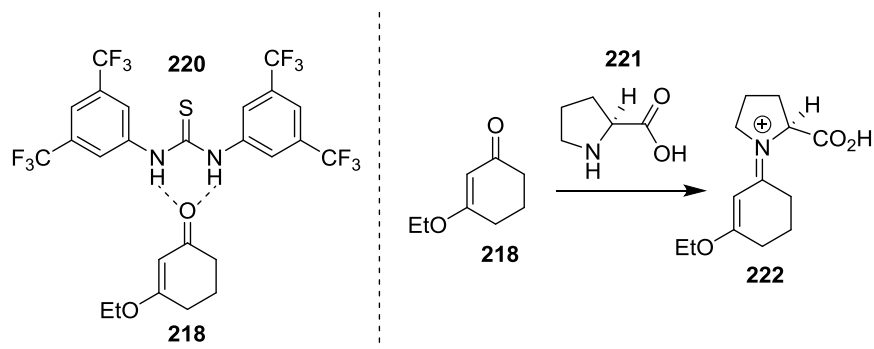
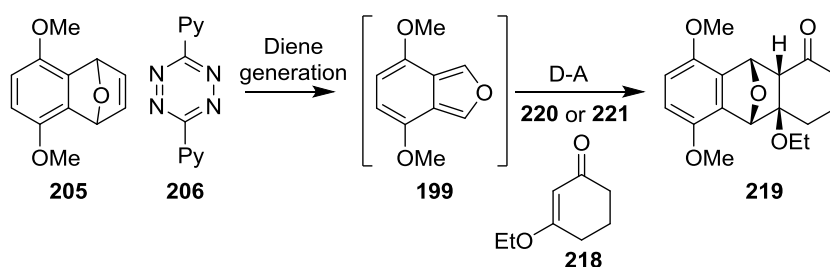
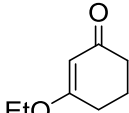


Figure 136: Structure of Schreiner's bistiourea catalyst **220** and proline **221**

5,8-Dimethoxy-1,4-dihydro-1,4-epoxynaphthalene **205** was reacted with 3,6-di-2-pyridyl-1,2,4,5-tetrazine **206** to generate 4,7-dimethoxyisobenzofuran **199**. When TLC indicated loss of starting material **205**, 3-ethoxycyclohex-2-en-1-one **218** and a chosen catalyst were added to the reaction mixture (Table 21).

Table 21: Diels-Alder reaction conditions examined using dienophile **218** in the presence of organocatalysts **220** or **221**



Entry	205 eq.	206 eq.	 218 eq.	Reaction conditions
1	1	1.1	1.1	220 (0.2 eq), DCM, rt, 18 h
2	1	1.0	1.0	221 (0.2 eq), MeOH, rt, 48 h

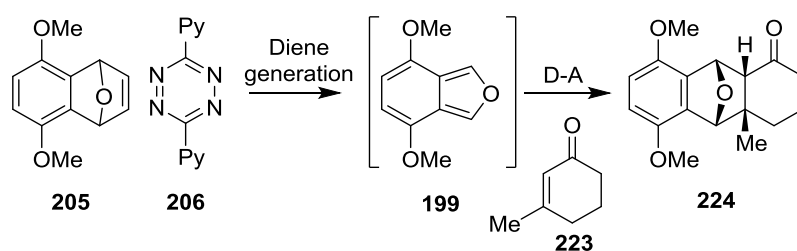
In both of the reactions we tested using organo-catalysts **220** and **221**, the ^1H NMR spectrum of the crude reaction material showed no signals corresponding to desired D-A cycloadduct **219**, and that diene **199** had decomposed. Consequently, we chose to examine an alternative dienophile in our D-A reactions.

4.3.2.2 Diels-Alder Reaction with 3-Methylcyclohex-2-en-1-one **223 as the Dienophile**

We postulated that the OEt group of 3-ethoxycyclohex-2-en-1-one **218** may have deactivated the alkene towards reaction with 4,7-dimethoxyisobenzofuran **199**. Therefore we decided to investigate an alternative dienophile, 3-methylcyclohex-2-en-1-one **223**, which is substituted with a less electron donating group.

4,7-Dimethoxyisobenzofuran **199** was synthesised as before from the reaction between 5,8-dimethoxy-1,4-dihydro-1,4-epoxynaphthalene **205** and 3,6-di-2-pyridyl-1,2,4,5-tetrazine **206**, with the reactions monitored by TLC for loss of epoxynaphthalene **205**. At this point, 3-methylcyclohex-2-en-1-one **223** was added to the reaction mixture (Table 22).

Table 22: Diels-Alder reaction conditions examined using 3-methylcyclohex-2-en-1-one **223**



Entry	205 eq.	206 eq.	 223 eq.	Reaction conditions
1	1	1.0	1.0	THF, 3 d, rt
2	1	1.1	1.0	DCM, rt 45 min, 50 °C 1 h ^[b]
3	1	1.0	9.0	DCM, rt, 18 h ^[a]
4	1	1.0	2.0	Toluene, reflux, 3 d
5	1	1.0	1.0	DMAC (0.5 eq.) THF -78 °C 3 h, -40 °C 18 h
6	1	1.1	1.1	220 (0.2 eq.), DCM, rt, 6 d
7	1	1.1	1.1	221 (0.2 eq.), MeOH, rt, 48 h

^[a]Dienophile **223** added at the beginning of the reaction

Once again, no D-A product **224** was observed through analysis of the ¹H NMR spectra of the crude material (Table 22, entries 1 – 4), even after a long reaction time at a high temperature

(Table 22, entry 4), or using a large excess of dienophile **223** (Table 22, entry 3). The addition of catalysts to increase the reactivity of dienophile **223**, namely a Lewis acid catalyst (Table 22, entry 5), H-bonding catalyst **220** (Table 22, entry 6), and proline **221** (Table 22, entry 7), also did not result in the formation of desired D-A cycloadduct **224**.

These observations prompted us to consider that 3-substituted cyclohexenones may be too sterically hindered to undergo the desired D-A reactions with diene **199**, and we proceeded to investigate alternative reagents.

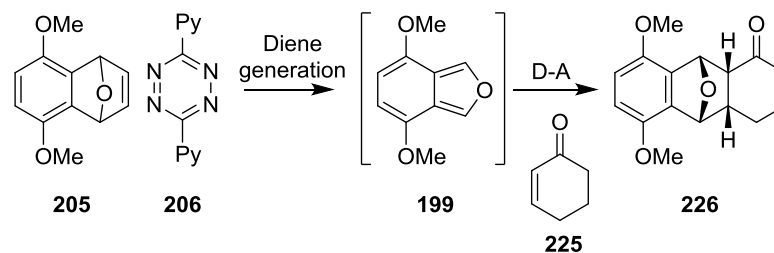
4.3.2.3 Diels-Alder Reaction with Cyclohexenone 225 as the Dienophile

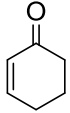
We anticipated that cyclohexenone **225** would be more reactive, both sterically and electronically, towards the D-A reaction with 4,7-dimethoxyisobenzofuran **199** than the 3-substituted cyclohexenones, **218** and **223** we had previously tested.

Epoxyaphthalene **205** and tetrazine **206** were reacted together to generate diene **199**. Cyclohexenone **225** was added to the reaction mixture following disappearance of epoxyaphthalene **205** by TLC (Table 23).

Chapter 4. Diels-Alder Synthesis of DEM30355/A

Table 23: Diels-Alder reaction conditions examined to synthesise cycloadduct **226**



Entry	205 eq.	206 eq.	 225 eq.	Reaction conditions
1	1	1.1	1.1	CDCl ₃ , rt, 48 h
2	1	1.1	1.1	DCM, 40 °C, 18 h
3	1	1.1	1.1	Toluene, 40 °C, 18 h
4	1	1.1	1.1	Toluene, 111 °C, 28 h
5	1	1.1	1.1	Toluene, 111 °C, 48 h
6	1	1.0	1.0	DMAC (0.5 eq), THF, -78 °C 3 h, -40 °C 18 h
7	1	1.1	1.1	220 (0.2 eq.), rt, CDCl ₃ , 48 h
8	1	1.1	1.1	220 (0.5 eq.), toluene, 40 °C, 18 h

In the D-A reactions we tested, no product **226** was observed in the reactions carried out at room temperature – 40 °C (Table 23, entries 1-3) and the use of Lewis acid and H-bonding catalyst **220** appeared to accelerate the degradation of diene **199** (Table 23, entries 6-8). However, signals corresponding to desired D-A cycloadduct **226** were observed in the ¹H NMR spectra of the crude material from the reactions conducted in refluxing toluene (Table 23, entries 4 and 5) and, following purification of the crude material by column chromatography, cycloadduct **226** was isolated in a modest yield of 40% (Table 23, entry 5).

With this positive result, we decided to examine alternative, more reactive dienophiles in our D-A reaction with 4,7-dimethoxyisobenzofuran **199**.

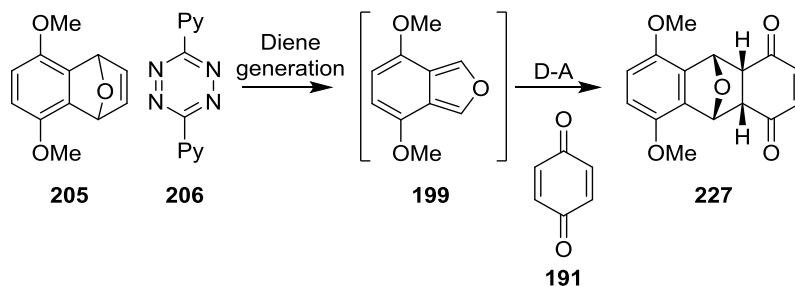
4.3.2.4 Diels-Alder Reaction with Benzoquinone **191** as the Dienophile

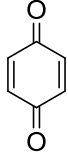
Next we investigated benzoquinone **191** as the dienophile. We expected the E_a barrier for these D-A reactions to be small, due to the additional electron withdrawing carbonyl group of

benzoquinone **191**, resulting in the compound having a much lower LUMO compared to cyclohexenone **225**.

Epoxy naphthalene **205** (1 eq.) and tetrazine **206** (1.1 eq.) were reacted in DCM for 1 hour to generate diene **199**, at which point the reaction mixture was cooled to 0 °C and benzoquinone **191** (1.1 eq.) was added (Table 24).

Table 24: Diels-Alder reaction conditions examined in the synthesis of cycloadduct **227**



Entry	205 eq.	206 eq.	 191 eq.	Reaction conditions	227 Isolated product yields ^[a]
1	1	1.1	1.1	DCM- <i>d</i> ₂ , 0 °C, 5 min	56%
2	1	1.1	1.1	DCM, rt, 5 min	59%
3	1	1.0	1.1	Toluene, 60 °C, 18 h	77% ^[b]

^[a]Isolated following column chromatography

^[b]Minor diastereomer **228** isolated in a 14% yield

The ¹H NMR spectrum of the reaction mixture after 5 minutes showed no peaks at 7.90 ppm (1H, s), 5.85 ppm (1H, s) and 3.77 ppm (3H, s) corresponding to diene **199**, suggesting the reaction had proceeded in 100% conversion. The ¹H NMR spectrum indicated a mixture of products, however following purification by column chromatography, only desired D-A adduct **227** was isolated in a 56% yield (Table 24, entry 1).

Increasing the temperature to room temperature (Table 24, entry 2) and increasing both the temperature and reaction time (Table 24, entry 3) did not result in a significant change in the product distribution, as shown by analysis of the ¹H NMR spectrum of the crude material. In the latter reaction, purification of the crude material by column chromatography yielded D-A adduct **227** in addition to a minor product **228** (Table 24, entry 3). The ¹H NMR spectrum of minor compound **228** was consistent with a diastereomer of major product **227** (Note: the lower isolated yields of product **227** (Table 24, entries 1 and 2) could be attributed to the small scale the reactions were conducted on).

Crystals of major product **227** were obtained through slow evaporation from chloroform and analysed by X-ray crystallography.

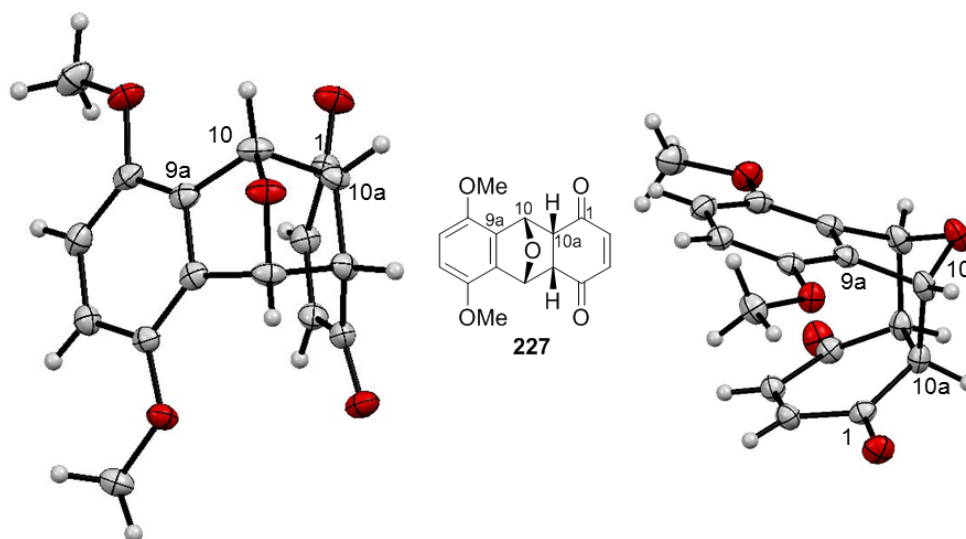
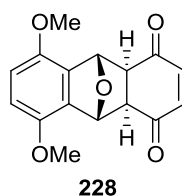


Figure 137: X-Ray crystal structure of Diels-Alder cycloadduct **227** from two different angles

Crystals of D-A cycloadduct **227** grow in the monoclinic space group, $P2_1/c$, with one molecule in the asymmetric unit (Figure 137). The X-ray crystal structure showed product **227** resulted from an *endo* D-A reaction, therefore we anticipated that the minor product was *exo* D-A cycloadduct **228**.



The success of the D-A reaction using benzoquinone **191** prompted us to examine alternative diketone dienophiles, to synthesise more varied D-A cycloadducts.

4.3.2.5 Diels-Alder Reaction with 2,6-Dimethylcyclohexa-2,5-diene-1,4-dione **231** as the Dienophile

We anticipated that substituted benzoquinones **229** may be sufficiently reactive to generate D-A cycloadduct **230**, which would contain a quaternary centre at C^{4a} as in DEM30355/A **94** (Figure 138).

Chapter 4. Diels-Alder Synthesis of DEM30355/A

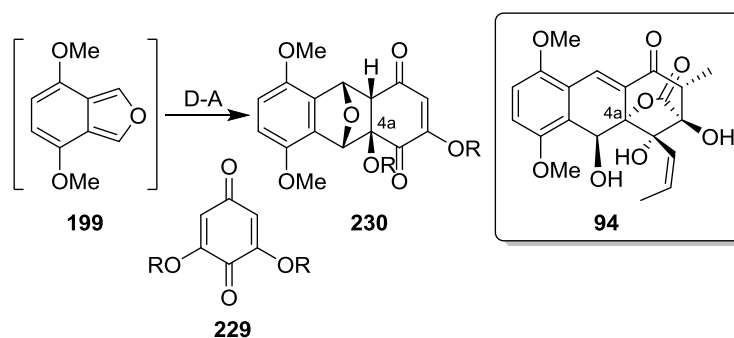


Figure 138: Planned synthesis of cycloadduct **230** with the oxygenated centre at C^{4a} in place

To test this theory, we examined 2,6-dimethylcyclohexa-2,5-diene-1,4-dione **231** as the dienophile (Figure 139). Diene **199** was generated following the reaction between epoxynaphthalene **205** (1 eq.) and tetrazine **206** (1.1 eq.). After a reaction time of 1 hour, the reaction mixture was cooled to 0 °C and 2,6-dimethylcyclohexa-2,5-diene-1,4-dione **231** was added (Table 25, entry 1).

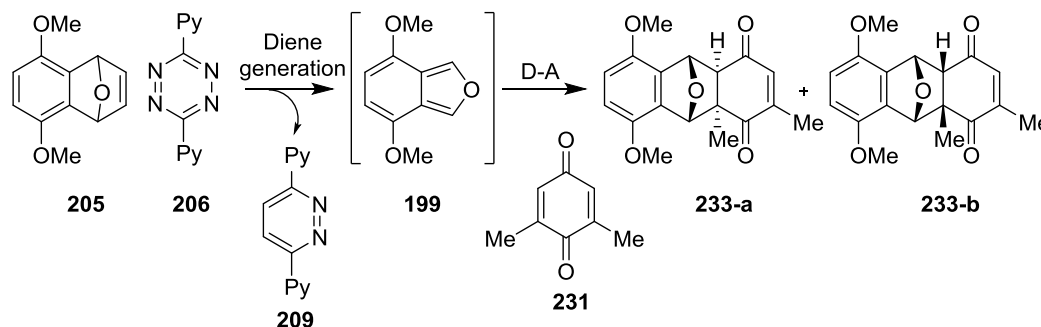
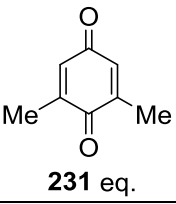


Figure 139: Synthesis of exo adduct **233-a** and endo adduct **233-b** from the Diels-Alder reaction between diene **199** and dienophile **231**

Table 25: Diels-Alder reaction conditions examined using 2,6-dimethylcyclohexa-2,5-diene-1,4-dione **231** as the dienophile

Entry	205 eq.	206 eq.	 231 eq.	Reaction conditions	Major 233-a : Minor 233-b product ratio ^[a]	Isolated yields Major 233-a Minor ^[b] 233-a 233-b
1	1	1.1	1.1	DCM, 0 °C, 15 min	1.0:0.9	- -
2	1	1.1	1.1	DCM, rt, 15 min	1.0:0.9	31% 27%
3	1	1.1	1.1	DCM, 1 h, rt	1.0:0.9	49% 27%
4	1	1.1	1.1	220 (0.2 eq.) DCM, rt, 18 h	1.0:0.9	41% 19%

^[a]Estimated from the ¹H NMR spectrum of the crude material

^[b]Isolated yields of the minor product were compromised due to difficulties in separating it from by-product **209**

The ^1H NMR spectrum of the reaction mixture indicated 100% conversion of diene **199** to D-A cycloadduct as a mixture of diastereomers (1.0: 0.9), after a reaction time of 15 minutes (Table 25, entry 1). We repeated the reaction at room temperature (Table 25, entry 2), using a longer reaction time (Table 25, entry 3) and using a H-bonding catalyst **220** (Table 25, entry 4). In each case, the ^1H NMR spectrum of the crude product showed 100% conversion of diene **199** to the same (1.0:0.9) diastereomeric ratio of products and, following purification of the crude material by column chromatography, D-A cycloadducts **233-a** and **233-b** were isolated in yields of 31-49% and 19-27% respectively.

A crystal structure of minor product **233-b** was obtained, which showed the compound resulted from an *endo* D-A reaction (). We anticipated that major product **233** arose from an *exo* D-A reaction, however we were unable to grow crystals of compound **233** to prove this.

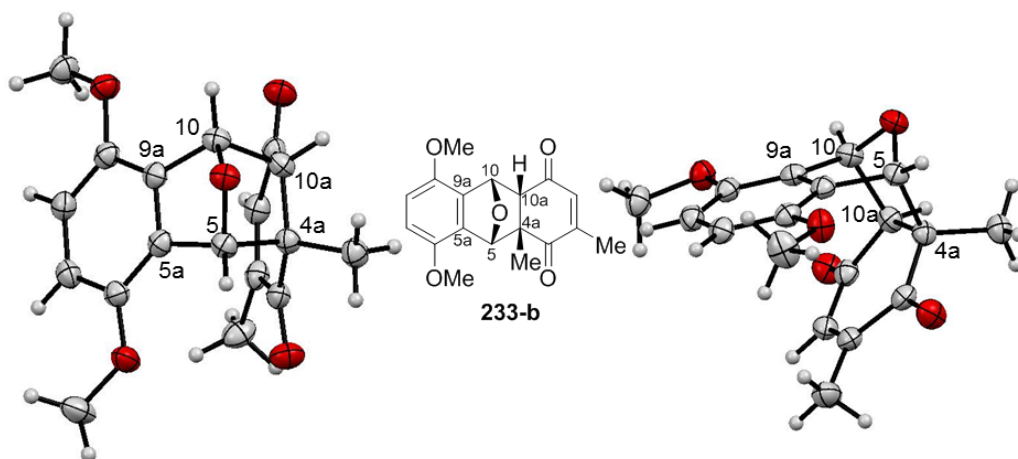


Figure 140: X-Ray crystal structure of Diels-Alder cycloadduct **233-b** from two different angles

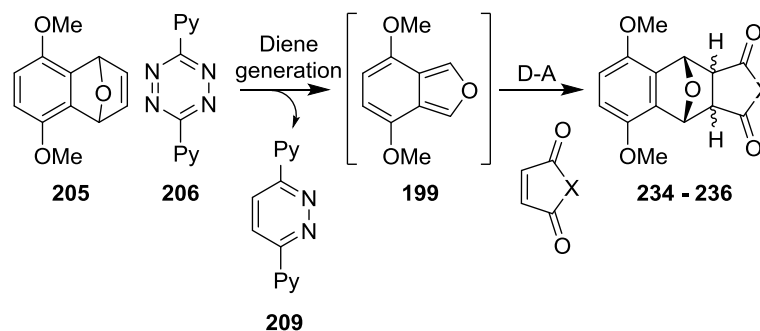
Crystals of *endo* cycloadduct **233-b** crystallise in the orthorhombic space group, *Fdd2*, with one molecule in the asymmetric unit.

With a working method to access D-A cycloadducts **233-a** and **233-b** developed, we then examined other dienophiles.

4.3.2.6 Diels-Alder Reactions with 5-Membered Ring Dienophiles

We applied our one-pot diene generation/ D-A reaction sequence to other, well studied, 5-membered ring dienophiles (Table 26).

Chapter 4. Diels-Alder Synthesis of DEM30355/A

 Table 26: Reaction conditions examined in the synthesis of cycloadducts **234** – **236**


Entry	205 eq.	206 eq.	Dienophile X	Eq.	Reaction conditions	Isolated product yield ^[a]	Product no.
1	1	1.1	NPh	1	DCM- <i>d</i> ₂ , 0 °C, 15 min	-	234
2	1	1.1	NH	1	DCM- <i>d</i> ₂ , 0 °C, 10 min	-	235
3	1	1.1	NH	1	DCM, 0 °C, 1 h	99% (2.0: 1.0 <i>dr</i>)	235
4	1	1.1	O	1	DCM- <i>d</i> ₂ , 0 °C, 5 min	-	236
5	1	1.1	O	1	DCM, 0 °C, 1 h	58% (1.0: 1.4 <i>dr</i>)	236
6	1	1.1	O	1	DCM, 0 °C, 1 h	68% (1.0: 1.4 <i>dr</i>)	236

^[a] Isolated following acid wash and solvent extraction

In each case, the D-A reaction proceeded with 100% conversion of the diene to the desired D-A cycloadduct as shown by TLC (Table 26, entries 3, 5 and 6) or by the ¹H NMR spectrum of the reaction mixture (Table 26, entries 1, 2 and 4). A reaction was also conducted in deuterated DCM, using 4-phenyl-1,2,4-triazoline-3,5-dione (PTAD) (1 eq.) as the dienophile. The ¹H NMR spectrum of the reaction mixture after 15 minutes at 0 °C indicated the desired D-A cycloadduct had been generated, in addition to compounds related to the degradation of diene **199**, therefore we did not pursue investigations into this dienophile further.

D-A cycloadducts **235** and **236** were isolated following an acid wash (to remove pyridazine by-product **209**) and solvent extraction of the reaction mixture, in good yields (Note: no isolated yields are reported for Table 26, entries 1, 2 and 4 as these were test scale reactions).

Once we had examined a range of diketone compounds in our D-A reactions with isobenzofuran **199**, we decided to investigate more functionalised dienophiles.

4.3.3 Diels-Alder Reaction with 4-Hydroxy-4-methylcyclohexa-2,5-dien-1-one **237** as the Dienophile

We had established that the D-A reactions proceeded well at 0 °C – room temperature using 1,4-diketone compounds as dienophiles, and the D-A reaction between isobenzofuran **199** and cyclohexanone **225** did proceed at high temperatures. Next we examined 4-hydroxy-4-methylcyclohexa-2,5-dien-1-one **237** as the dienophile, which we anticipated would be intermediate in reactivity in comparison to the 1,4-diketone compounds and cyclohexenone **225** previously tested (Figure 141). The resultant D-A cycloadduct **238** would be functionalised at the C⁴ position as in DEM30355/A **94**.

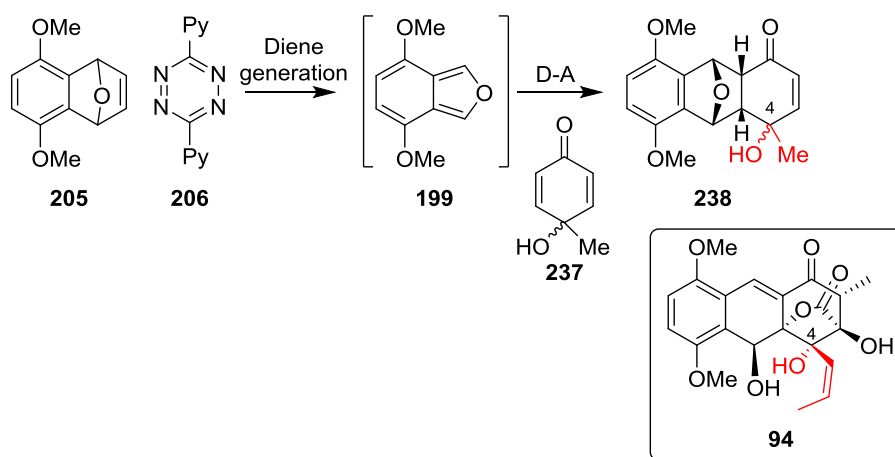


Figure 141: Synthesis of cycloadduct **238** via a D-A reaction between diene **199** and 4-hydroxy-4-methylcyclohexa-2,5-dien-1-one **237**

4.3.3.1 Synthesis of 4-Hydroxy-4-methylcyclohexa-2,5-dien-1-one **237**

The first step was to synthesise dienophile **237**. Benzoquinone **191** was reacted with methyl lithium to generate 4-hydroxy-4-methylcyclohexa-2,5-dien-1-one **237** (Figure 142).¹²⁷

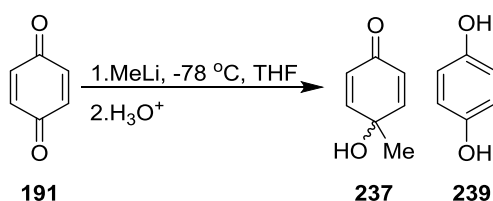


Figure 142: Synthesis of 4-hydroxy-4-methylcyclohexa-2,5-dien-1-one **237**

It is believed the reaction proceeds via a single electron transfer mechanism, with benzoquinone **191** as the electron acceptor (Figure 143).¹²⁷ The quantity of reduction product **239** compared to addition product **237** is dependent on the steric properties of the alkyl group of the organometallic.¹²⁷

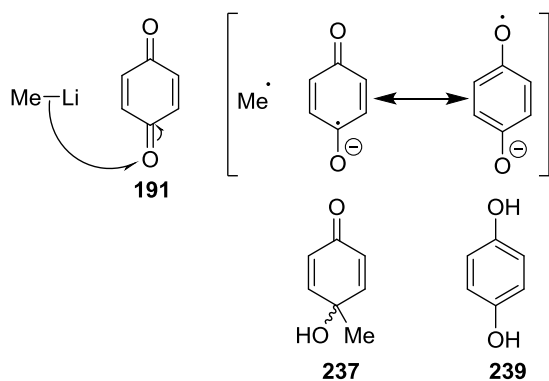


Figure 143: Proposed reaction mechanism to synthesise 4-hydroxy-4-methylcyclohexa-2,5-dien-1-one **237** and hydroquinone **239**¹²⁷

Following purification of the crude material by column chromatography, compound **237** was isolated in a 28% yield (Note: the ¹H NMR spectrum of the isolated product contained a small peak corresponding to by-product **239**).

Despite the low yield, a sufficient quantity of compound **237** was obtained to proceed to the next step.

4.3.3.2 Diels-Alder Reaction Between Isobenzofuran **199** and 4-Hydroxy-4-methylcyclohexa-2,5-dien-1-one **237**

Diene **199** was synthesised *in situ* from epoxynaphthalene **205** (1 eq.) and tetrazine (1 eq.). When TLC indicated starting material **205** had disappeared, 4-hydroxy-4-methylcyclohexa-2,5-dien-1-one **237** was added to the reaction mixture (Figure 144).

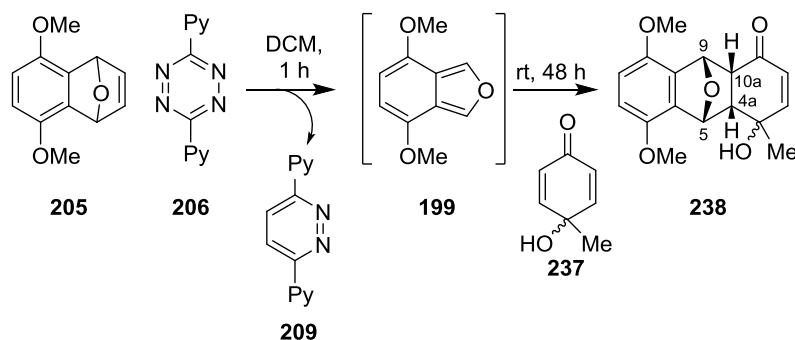


Figure 144: Diels-Alder synthesis of cycloadduct **238**

After a reaction time of 2 days, desired D-A cycloadduct **238** was isolated from the reaction mixture following an acid wash (to remove pyridazine by-product **209**) and solvent extraction, in an excellent yield of 92%, as a single diastereomer. The coupling constants $J_{H_{4a}-H_5} = 4.7$ Hz and $J_{H_{10a}-H_9} = 5.7$ Hz were comparable to the analogous coupling constant $J_{H_{10a}-H_9} = 5.4$ Hz in *endo* cycloadduct **233-b** previously synthesised, therefore we could deduce compound **238** also resulted from an *endo* D-A reaction.

After investigating a range of dienophiles to synthesise D-A cycloadducts, we could then proceed to the next stage in the synthetic procedure.

4.3.4 Examination of the Reaction of Diels-Alder Cycloadduct **233-b** with Base

The next step was to examine the base catalysed ring opening reactions of the D-A cycloadducts **211** synthesised.¹²⁸ We envisaged that deprotonation at C^{10a} would lead to enolate **240**, followed by an E1cB reaction to generate compound **212**, with a benzylic alcohol at C⁵ and an α - β unsaturated system as seen in DEM30355/A **94**.

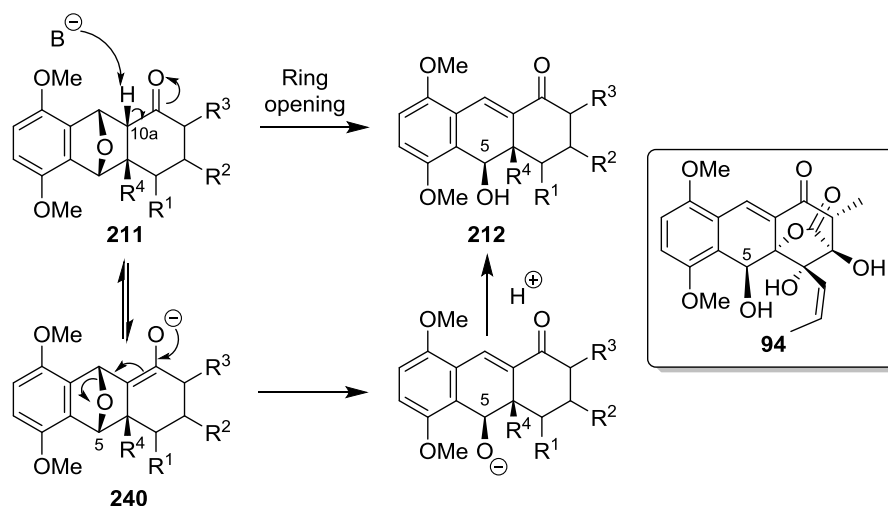


Figure 145: Planned synthesis of alcohol **212** via an E1cB reaction of Diels-Alder adduct **211**

We decided to first look at the base catalysed ring opening reaction using *endo* D-A cycloadduct **233-b**, which contained only one acidic proton at C^{10a}. D-A cycloadduct **233-b** was reacted with base and the reaction progress was monitored by TLC (Table 27).

Table 27: Basic reaction conditions examined to generate alcohol **241** from Diels-Alder adduct **233-b**

The reaction shows the conversion of Diels-Alder adduct **233-b** to alcohol **241** using a base. **233-b** has a bridgehead hydrogen at C^{10a} and a methyl group at C⁵. The reaction yields **241**, which has a benzylic alcohol group at C⁵ and a methyl group at C^{10a}.

Entry	233-b eq.	Base	Base eq.	Reaction conditions
1	1	NaH	1.5	THF, rt, 3 d
2	1	NaH	2.0	THF, rt, 3 d
3	1	NaOMe	1.5	MeOH, rt, 6 d
4	1	LDA	1.1	THF, -78 °C 75 min, 0 °C 105 min, rt 165 min

Our preliminary investigations have shown that NaH did not result in the desired E1cB reaction, possibly as a result of the poor organo-solubility of NaH, and starting material **233-b** was

recovered (Table 27, entries 1 and 2). Unreacted starting material **233-b** was also recovered from the reaction using NaOMe, which was likely due to the poor solubility of compound **233-b** in the reaction solvent (methanol) (Table 27, entry 3). In contrast, in the first reaction we have examined using LDA, TLC analysis showed disappearance of starting material **233-b** after 165 minutes at room temperature (Table 27, entry 4). The ^1H NMR spectrum of the sample following column chromatography showed signals which did not correspond to starting material **233-b**, including signals in the 6.79 - 6.56 region which suggested an AB spin system corresponding to a new product (Figure 146).

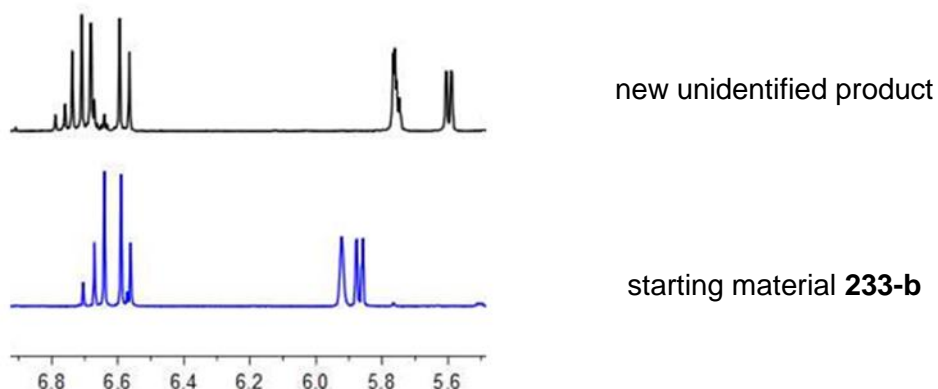


Figure 146: Expansion of the 6.8 - 5.6 ppm region of the ^1H NMR spectra of starting material **233-b** (bottom) and the new unidentified product from the reaction of **233-b** with LDA (top)

However, this reaction was carried out on a test scale and more investigation is required to determine whether the new product(s) correspond to desired alcohol **241**.

To coincide with our investigations into the D-A synthesis of analogues of DEM30355/A **94**, we have examined the synthesis of the A ring of DEM30355/A **94** as a dienophile, with the ultimate aim of generating DEM30355/A **94** as single enantiomer. Herein we will discuss our work towards this target.

4.3.5 Single Enantiomer Synthesis of DEM30355/A **94**

We imagined that DEM30355/A **94** could be synthesised as a single enantiomer following a D-A reaction from the enantiopure dienophile **214** (Figure 147). Through comparison of the specific rotation measurements of naturally occurring DEM30355/A **94** and synthesised DEM30355/A, the absolute stereochemistry of the molecule could be elucidated.

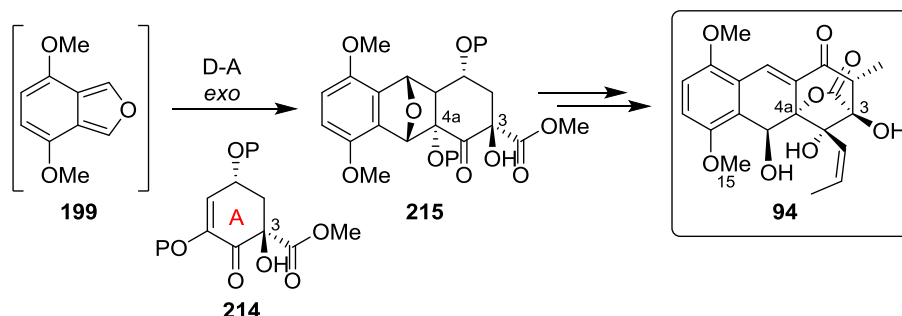


Figure 147: Proposed Diels-Alder synthesis of DEM30355/A **94** as a single enantiomer

The initial task was to synthesise dienophile **214**. We envisaged that dienophile **214** could be synthesised as a single enantiomer from commercially available shikimic acid **213** (Figure 148). We planned to protect the acid OH of shikimic acid **213** as the methyl ester **242**, followed by acetal protection of the *trans* vicinal diol, to generate acetal methyl shikimate **243**.¹²⁹ The construction of the stereogenic centre at C³ was fundamental to our synthetic plan. We would use the hydroxyl group at C^{4a} of acetal methyl shikimate **243** to hydrogen bond direct an epoxidation to the top face of the alkene, ultimately setting up the desired stereochemistry at the C³ position in product **244**.

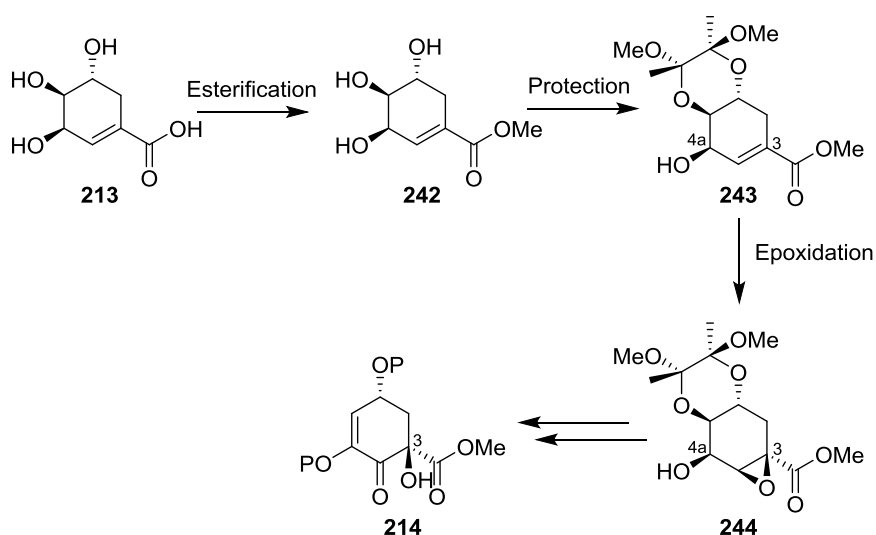


Figure 148: Proposed diastereoselective synthesis of dienophile **214**

The first stage was to develop a working synthetic method to gram quantities of acetal methyl shikimate **243**, via methyl shikimate **242**.

4.3.5.1 Synthesis of Methyl Shikimate **242**

Brønsted acid catalysed esterification of shikimic acid **213** was carried out in refluxing methanol.

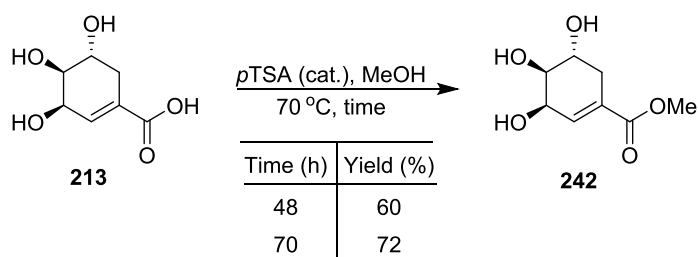


Figure 149: Synthesis of methyl shikimate **242** from shikimic acid **213**

After 48 hours, methyl shikimate **242** was isolated in a 60% yield, which could be improved to 72% by increasing the reaction time to 70 hours (Figure 149). We employed a recrystallisation as an efficient isolation approach to multi-gram quantities of methyl shikimate **242**, facilitating the examination of subsequent steps.

4.3.5.2 Synthesis of Acetal Methyl Shikimate **243**

The next stage was to selectively protect the *trans* vicinal diol of methyl shikimate **242** as the acetal.¹²⁹

Methyl shikimate **242**, trimethyl orthoformate and 2,3-butanedione were reacted together in refluxing methanol in the presence of a Brønsted acid catalyst (Figure 150).

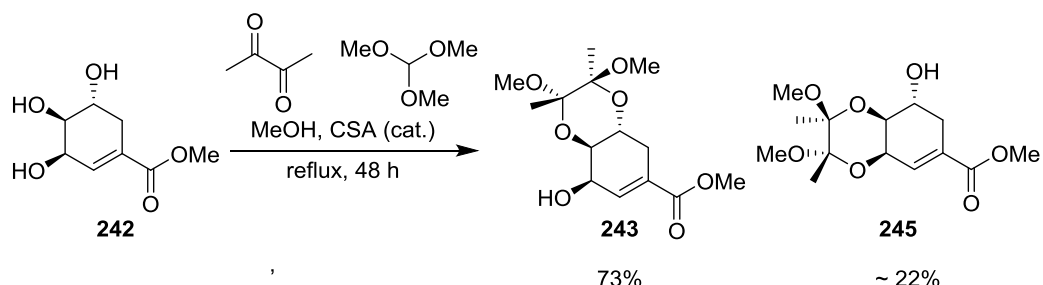


Figure 150: Synthesis of acetal methyl shikimate **243**

After 48 hours, two isomers were isolated in 73% and ~22% yields after column chromatography. The ¹H and ¹³C NMR data of the isomers were compared to literature values to determine the structures.¹²⁹ The major isomer **243** was shown to be the desired structure, with the minor isomer **245** arising from acetal protection of the *cis* vicinal diol.

With multi-gram quantities of acetal methyl shikimate **243** in hand, we then moved on to examine the epoxidation chemistry.

4.3.5.3 Investigations into the Epoxidation of Acetal Methyl Shikimate **243**

The next step was to examine the epoxidation of the alkene of acetal methyl shikimate **243**. We postulated that the allylic alcohol of compound **243** would direct epoxidation, via hydrogen

bonding, to the top face of the alkene to give epoxide **244** (Figure 151).¹³⁰ This would give the desired stereochemistry at C³. From here, an S_N2 reaction could be used to ring open the epoxide to give alcohol **246**.

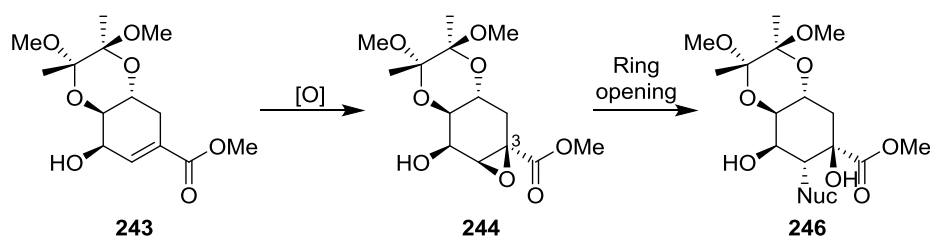
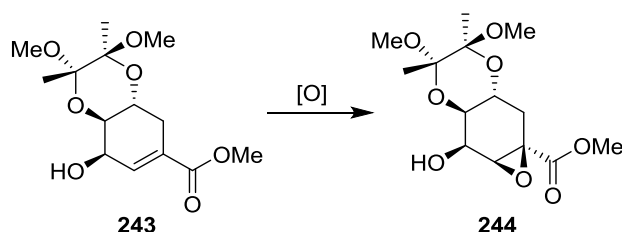


Figure 151: Proposed synthesis of alcohol **246** via hydrogen bond directed epoxidation of alkene **243** followed by nucleophilic ring opening

We screened acetal methyl shikimate **243** under a range of epoxidation conditions, using *m*CPBA and V(acac)₃/ BuOOH as oxidants (Table 28)

Table 28: Oxidation reaction conditions examined in the synthesis of epoxide **244**



Entry	243 eq.	Oxidant	Eq.	Reaction conditions	Reaction outcome ^[a] ratio of unreacted 243 : by-product 247
1	1	<i>m</i> CPBA	1.1	DCM, rt, 24 h	1.0: 0.0
2	1	<i>m</i> CPBA	1.1	DCM, 48 °C, 8 d	1.0: 1.5
3	1	<i>m</i> CPBA	1.4	CHCl ₃ , 48 °C, 8 d	1.0: 0.5
4	1	<i>m</i> CPBA	3.3	CHCl ₃ , 48 °C, 9 d	1.0: 0.6
5	1	<i>m</i> CPBA	1.5	NaHCO ₃ (2.3 eq.), DCM, 48 °C 2 d, rt 20 d	1.0: 0.2
6	1	<i>t</i> BuOOH	1.1	V(acac) ₃ (1 mol%), toluene, reflux, rt 19 d	1.0: 0.6

^[a] Estimated from ¹H NMR spectrum of the crude reaction material

In the first reaction we tested using *m*CPBA as the oxidant, we could not observe any signals corresponding to epoxide product **244** in the ¹H NMR spectrum of the crude material, only unreacted acetal **243** (Table 28, entry 1). Increasing the reaction temperature (Table 28, entries 2- 4) and increasing the equivalencies of a *m*CPBA (Table 28, entry 4) did not generate epoxide **244**, however signals corresponding to a new by-product **247** were observed in the ¹H NMR spectrum of the crude material. We postulated that by-product **247** may be the result

of an acid catalysed side reaction from the decomposition of *m*CPBA to *meta*-chlorobenzoic acid. Therefore a reaction using NaHCO₃ as a buffer was conducted and we also tested the alternative oxidant V(acac)₃/ ^tBuOOH. However, in both cases by-product **247** was still generated (Table 28, entries 5 and 6). We therefore decided to isolate by-product **247** and investigate its structure, to gain a better understanding of the reaction.

Following purification of the combined crude material from the *m*CPBA reactions (Table 28, entries 3 and 4), by-product **247** was isolated and investigated using NMR. Compared to the spectrum of starting material **243**, the ¹³C spectrum of by-product **247** contained an additional carbon signal at 194.5 ppm, characteristic of a ketone carbon atom. In addition, the ¹H NMR spectrum contained a signal at 6.80 ppm (1H, d, *J* = 3.1 Hz), characteristic of an alkene CH. Therefore we could deduce that the by-product was ketone **247**, the result of oxidation of the allylic alcohol in compound **243** (Figure 152).

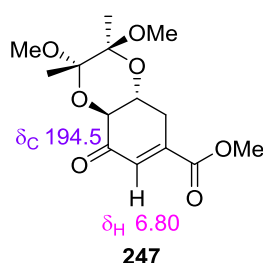


Figure 152: Structure of ketone **247**

As it was apparent from our experiments that the epoxidation of alkene **243** to epoxide **244** was not likely to be successful, we moved on to investigate an alternative synthetic method.

4.3.5.4 Dihydroxylation of Acetal Methyl Shikimate **243**

As an alternative method, we decided to examine the dihydroxylation of acetal methyl shikimate **243** to generate triol **248** (Figure 153). In an analogous way to the epoxide reactions, we anticipated that the alcohol group at C^{4a} of **243** would direct dihydroxylation to the top face of the alkene through hydrogen bonding, using OsO₄ in the presence of TMEDA.¹³¹ This would set up the desired stereochemistry at C³ as in our targeted enantiomer of DEM30355/A **94**.

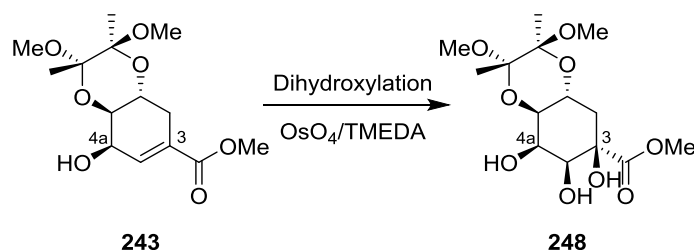


Figure 153: Planned synthesis of triol **248**

Firstly, as a test system, we reacted acetal methyl shikimate **243** with osmium tetroxide (5 mol%) and *N*-methylmorpholine *N*-oxide (NMO) (3 eq.) with the reaction progress monitored

by TLC (in the absence of TMEDA, we expected the dihydroxylation to occur on the opposite face to the allylic hydroxyl group of starting material **243**) (Figure 154).¹³²

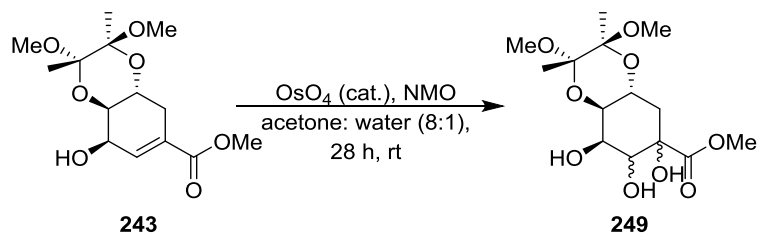


Figure 154: Dihydroxylation of alkene **243**

After 28 hours, TLC showed no starting material **243** remained in the reaction mixture and a new spot with a lower R_f value than **243** was apparent. We think it is likely that desired triol **249** was generated in the reaction, but could not be recovered following aqueous work-up, presumably as a result of its high water solubility. To circumvent this issue, we imagined protecting the OH of acetal methyl shikimate **243** with a hydrophobic group prior to the reaction with osmium tetroxide, so that the dihydroxylation product would be more organosoluble compared to our previous target **249**.

4.3.5.5 OH Protection of Acetal Methyl Shikimate **243**

We decided to protect the OH of acetal methyl shikimate **243** with TBDMS, to generate OH-protected compound **250**. TBDMS protected compound **250** would be used as a test system in the subsequent dihydroxylation step, as we anticipated the hydrophobic group would enable the recovery of dihydroxylation product **251** following an aqueous work-up (Figure 155).

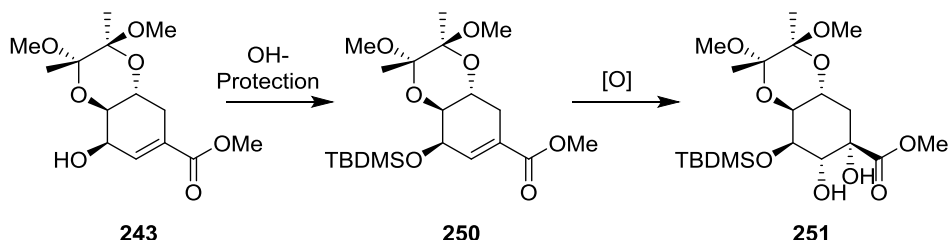


Figure 155: Planned synthesis of organo-soluble diol **251**

Consequently, acetal methyl shikimate **243** (1 eq.) was reacted TBDMSCl (1.6 eq) and imidazole (1.6 eq) in DCM.



Figure 156: OH protection of alkene **243**

After a reaction time of 4 days, OH-protected alcohol **250** was isolated in an 88% yield after purification by column chromatography.

With product **250** in hand, we could then examine the dihydroxylation reaction.

4.3.5.6 Dihydroxylation of TBDMS Alkene **250**

Using the same reaction conditions as before, TBDMS-compound **250** was reacted with osmium tetroxide at room temperature, in a sterically directed reaction (Figure 157). The reaction progress was monitored by TLC.

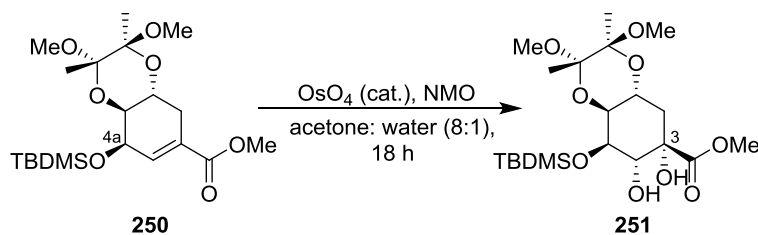


Figure 157: Dihydroxylation of TBDMS compound **250**

Following a reaction time of 18 hours, TLC showed no remaining starting material **243** and a new spot with a lower R_f was apparent. Following an aqueous work up, the ^1H NMR spectrum of the crude material showed the desired diol **251** had been generated, in 100% conversion of starting material **250**.

We expected that diol **251** would have the opposite stereochemistry at C^3 to our targeted enantiomer of DEM30355/A **94**, as a result of the bulky TBDMS group of starting material **250** sterically directing the reaction to the back face. To direct dihydroxylation to the top face of the molecule and hence construct the desired chiral centre at C^3 , we needed to invert the stereochemistry of the protected allylic alcohol at C^{4a} , so that the back face would be sterically blocked.

4.3.5.7 Mitsunobu Reactions of Acetal Methyl Shikimate **243**

We planned to use Mitsunobu chemistry to both invert the stereochemistry at C^{4a} of acetal methyl shikimate **243** and introduce an OH-protecting group, to give compound **252** (Figure 158). OH-Protected compound **252** would then be subjected to dihydroxylation conditions, whereby the protecting would sterically direct the formation of diol product **253**, with the desired stereochemistry at C^3 (Figure 158).

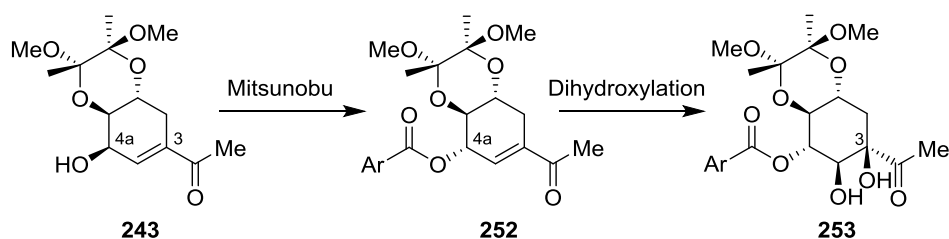
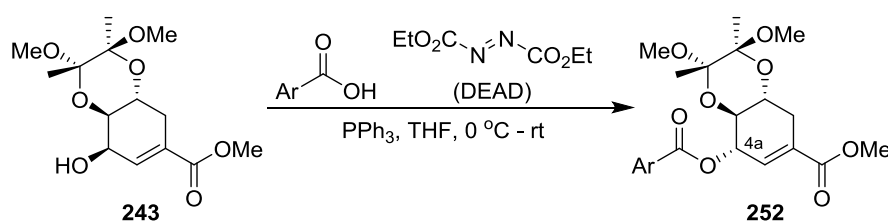


Figure 158: Planned synthesis of diol **253** with the correct stereochemistry at C^3

In all of our Mitsunobu experiments, acetal methyl shikimate **243** (1 eq.) was reacted with triphenylphosphine (1.5 eq.), a chosen aromatic carboxylic acid (1.5 eq) and diethyl azodicarboxylate (DEAD) (1.5 eq.) at room temperature, using THF as the solvent (Table 29).

We required X-ray crystallography data of Mitsunobu product **252** to monitor the stereochemistry at C^{4a}, therefore in the Mitsunobu reactions we used *para*-nitro benzoic acid, to encourage crystallisation of the product (Table 29, entry 5). We also examined the use of halogenated benzoic acids, as the presence of a heavy atom in the product would aid in the determination of the absolute stereochemistry of the molecule through X-ray analysis (Table 29, entries 2 - 4).

Table 29: Synthesis of Mitsunobu products **254** – **258** from acetal methyl shikimate **243**



Entry	Ar-COOH	Reaction time (h)	Isolated product yield (%)	Product number
1		3 h	85	254
2		18 h	76	255
3		18 h	58 ^[a]	256
4		18 h	77 ^[b]	257
5		18 h	78	258

^[a]Yield compromised by difficulty in separating product **256** and carboxylic acid due to similar R_f values

^[b]Product was contaminated with 4-iodobenzoic acid

In each experiment, analysis of the ^1H NMR spectrum of the crude material indicated the reactions proceeded with 100% conversion of starting material **243** to the desired product and, following purification by column chromatography, Mitsunobu products **254** - **258** were isolated in yields ranging from 58 – 85%. The low yield of product **256** was the result of poor separation obtained between the carboxylic acid starting material and product **256** (Table 29, entry 3) (Note: washing the solvated crude product with sodium bicarbonate aq. solution, failed to remove the excess aromatic acid).

To determine whether the Mitsunobu chemistry had successfully inverted the stereochemistry at C^{4a} , crystals of nitro Mitsunobu product **258** (Table 29, entry 5) were grown by slow evaporation from DCM/ toluene and analysed by X-ray crystallography.

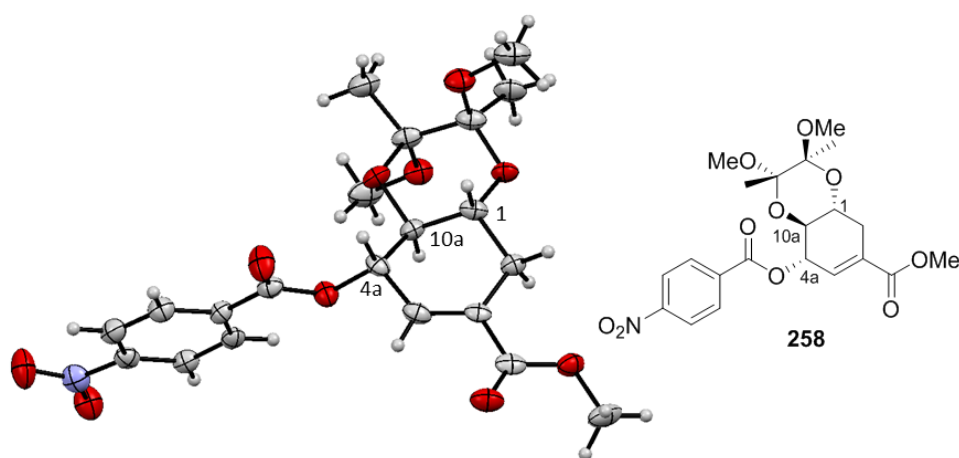


Figure 159: X-Ray crystal structure of Mitsunobu product **258**

Nitro compound **258** crystallises in the monoclinic space group P2_1 , with two molecules in the asymmetric unit. The crystal structure of nitro product **258** showed the compound had the desired stereochemistry at position C^{4a} , with the nitrobenzoyl moiety *syn* to the proton at C^{10a} (Figure 159).

With the stereochemistry of Mitsunobu product **258** ascertained, we could then examine the dihydroxylation chemistry.

4.3.5.8 Dihydroxylation Reaction of Benzoyl Mitsunobu Product **258**

The next step was to investigate the dihydroxylation chemistry of benzoyl compound **254**. Out of the Mitsunobu products **254** - **258** synthesised, benzoyl compound **254** was the most suitable in terms of electronic and steric properties for our planned *exo*, normal electron demand D-A reaction later in the synthetic route (Figure 160).

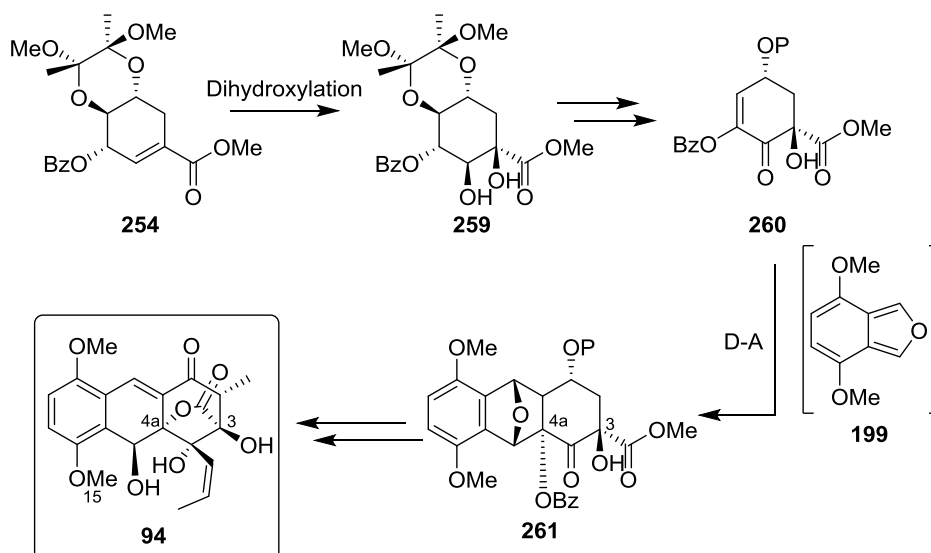


Figure 160: Planned synthesis of DEM30355/A **94** as a single enantiomer via an exo Diels-Alder reaction

Therefore benzoyl compound **254** was reacted with osmium tetroxide (5 mol%) and NMO (3 eq.), with the reaction progress monitored by TLC (Figure 161). We expected the benzoyl group to sterically direct the dihydroxylation reaction to the top face of the molecule, generating diol **259**, with the correct stereochemistry at C³.

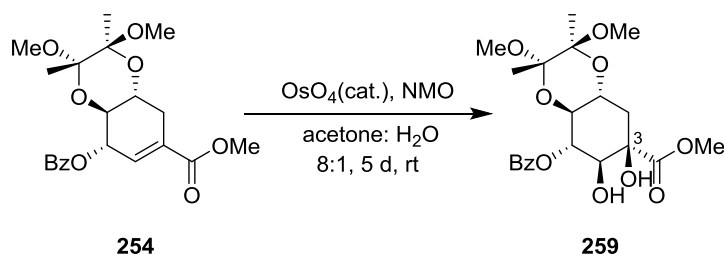


Figure 161: Synthesis of diol **259** via the sterically directed dihydroxylation of alkene **254**

After a reaction time of 5 days, the crude reaction material was purified by column chromatography and a new product was isolated. The ¹H NMR spectrum of the new product showed no signals corresponding to an alkene CH, and the IR spectrum showed peaks at 3468 and 3430 ν_{max} cm⁻¹ which were characteristic of OH groups. In combination with mass spectrometry data, we could deduce the new product was desired diol **259**, isolated in a good yield of 75%.

At this stage it was imperative to determine if the stereochemistry at C³ of diol **259** was the same as in our targeted enantiomer of DEM30355/A **94**, therefore crystals of diol **259** were grown by slow evaporation from diethyl ether/DCM/ toluene and analysed by X-ray crystallography (Figure 162).

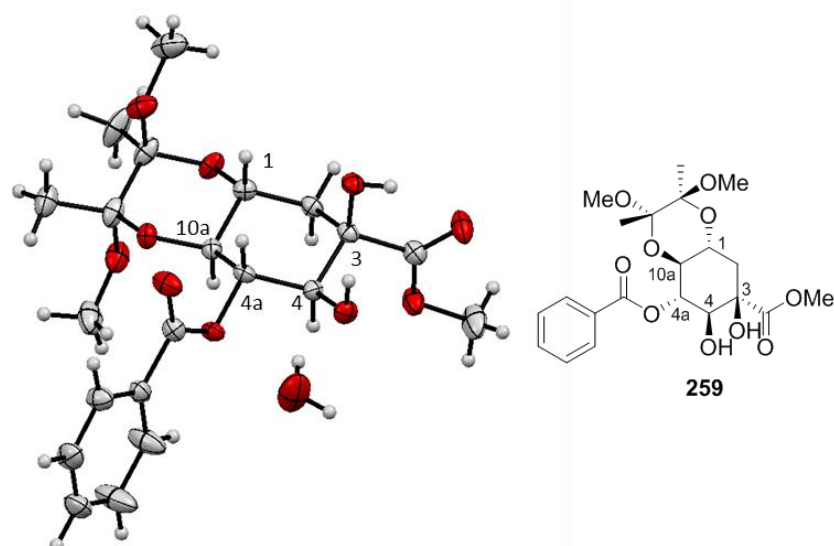


Figure 162: X-Ray crystal structure of diol **259**

Diol **259** crystallises in the orthorhombic space group $P2_12_12_1$. The asymmetric unit contains one molecule of **259** with a partial occupancy of water. The crystal structure showed the hydroxyl groups were positioned on the opposite face to the benzoyl moiety, with the desired stereochemistry at C^3 (Figure 162).

With a working synthetic route to diol **259** developed, we could progress to the next stage in the synthesis.

4.3.6 Synthesis of Ketone **262**

The next step was to oxidise the secondary alcohol of diol **259** to generate ketone **262**, followed sequentially by an E1cB reaction and selective OH protection to give dienophile **260** (Figure 163).

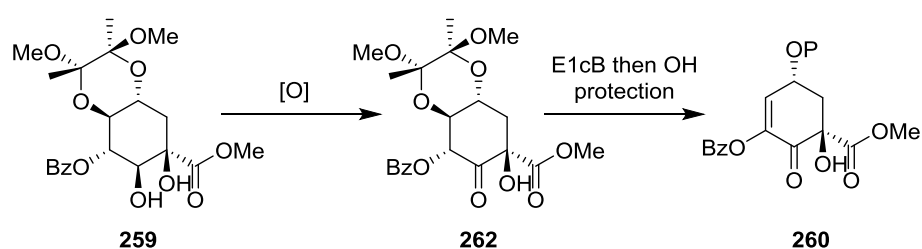


Figure 163: Planned synthesis of dienophile **260** from diol **259**

We investigated several oxidising conditions to oxidise the secondary alcohol of diol **259**, with the reaction progress monitored by TLC (Table 30).

Table 30: Reaction conditions examined to generate ketone **262**

Entry	259 eq.	Oxidant	Eq.	Reaction conditions	Reaction outcome ^[a]
1	1	DMP	1.1	rt, DCM 17 d, DMSO 5 d	unreacted 259 : 262 in 1.0:0.2 ratio
2	1	PCC	1.4	DCM, rt, 5 d	unreacted 259

^[a] Determined using ¹H NMR spectrum of the crude reaction material

TLC analysis of the reaction using DMP showed unreacted starting material **259** after a lengthy reaction time. We postulated that the insolubility of DMP in DCM may hinder the reaction, therefore DCM was replaced with DMSO. The ¹H NMR spectrum of the crude material showed lots of unreacted diol **259**, however signals corresponding to our desired ketone **262** were observed, with a starting material **259** to ketone product **262** ratio of 1.0: 0.2 (Table 30, entry 1). As the reaction with DMP was very slow, we decided to examine the alternative oxidant, pyridinium chlorochromate (PCC), however after a reaction time of 5 days, only unreacted diol **259** was recovered (Table 30, entry 2). We postulated that DMP and PCC were too bulky to efficiently oxidise the sterically hindered secondary alcohol of starting material **259**, therefore we decided to examine an alternative, less bulky oxidant.

4.3.6.1 Swern Oxidation of Diol **259**

Next we investigated the oxidation of diol **259** under Swern conditions. Diol **259** was reacted with oxalyl chloride and DMSO, with the reaction progress monitored by TLC (Figure 164).

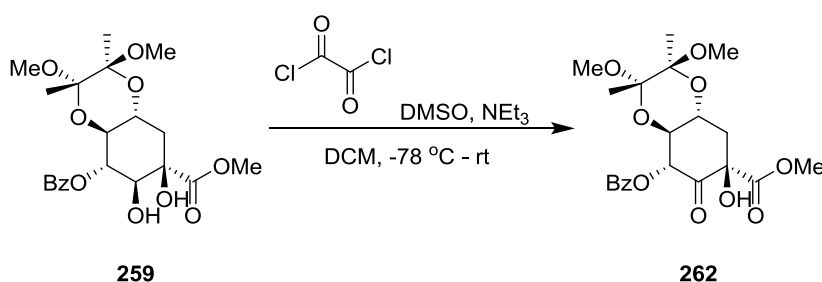


Figure 164: Swern oxidation of alcohol **259** to ketone **262**

Following a reaction time of 35 minutes at room temperature, the crude material was purified by column chromatography which resulted in the isolation of two new compounds. The ¹³C NMR spectrum of the more polar compound showed a new signal at 196.7 ppm, characteristic of a ketone carbon atom therefore, in addition to mass spectrometry data, we were able to conclude this compound was the target ketone **262**, isolated in a 25% yield.

The ¹H NMR spectrum of the less polar isolated compound **263** contained signals at 4.93 ppm (1H, d, *J* = 10.6 Hz) and 4.67 ppm (1H, d, *J* = 10.6 Hz), corresponding to two geminally coupled protons, in addition to a signal at 2.27 ppm (3H, s) suggesting a Me group. HMBC data showed

a correlation between the signal at 2.27 ppm, corresponding to the Me group, and a signal at 71.9 ppm, which corresponded to the carbon atom of the CH₂ group. Therefore we could deduce the CH₂ and Me groups were in close bonding proximity to one another. In addition, the ¹³C NMR spectrum showed a new carbonyl signal at 196.2 ppm, consistent with oxidation of the secondary alcohol in diol **259** to a ketone. Through analysis of the NMR spectra and in combination with HRMS data, we deduced this compound was thioacetal **263**, isolated in a 12% yield (Figure 165).

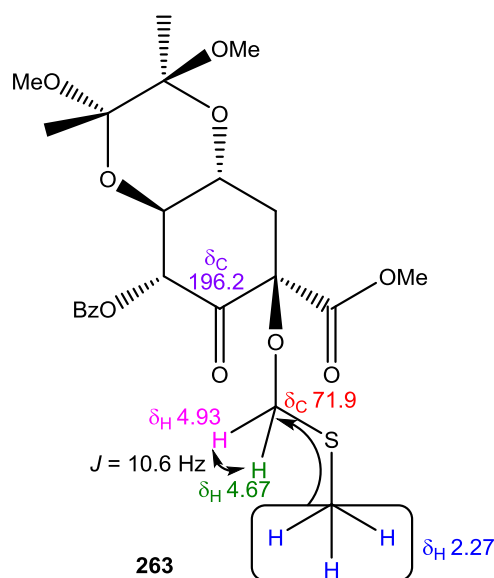


Figure 165: Structure of thioacetal **263**

The formation of thioacetal **263** can be explained by the reaction of the tertiary alcohol of ketone **262** with the sulfur ylide generated during the Swern reaction (Figure 166).

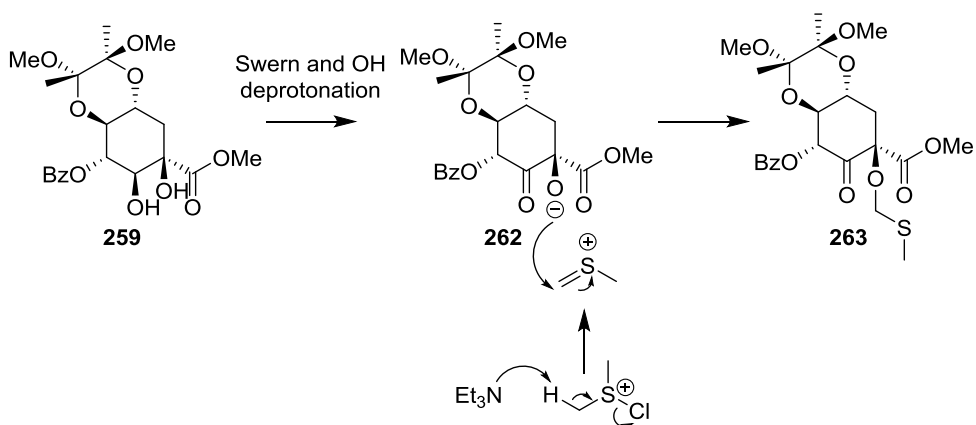
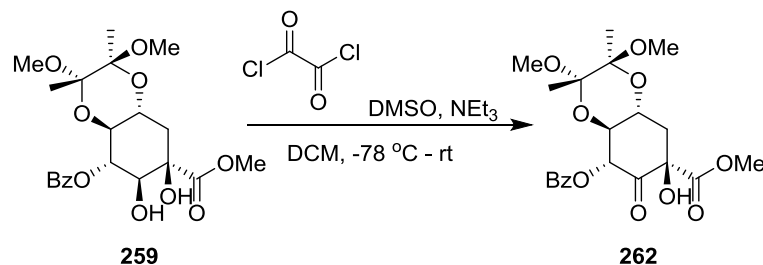


Figure 166: Mechanism of formation of thioacetal **263**

Although we anticipated that the thioacetal of compound **263** could readily be removed following hydrolysis, we decided to optimise the Swern reaction so that ketone **262** was the sole product, to simplify the purification step.

We hypothesised that the formation of thioacetal **263** may result from a large excess of base as used in the initial reaction (Table 31, entry 1), therefore we screened reaction conditions using fewer equivalencies of triethylamine (Table 31, entries 2-4).

Table 31: Swern reaction conditions examined to synthesise ketone **262**



Entry	259 eq.	Oxalyl chloride eq.	DMSO eq.	NEt ₃ eq.	Reaction conditions	Isolated yield
1	1	2.0	5	9	DCM, -78 °C 5 min, rt 35 min	262 (25%), 263 (12%)
2	1	1.5	5	1.5	DCM, -78 °C 1 h, rt 18 h	262 (20%) ^[a]
3	1	2.0	5	2.0	DCM, -78 °C 55 min, rt 5 min	262 (25%) ^[b]
4	1	2.0	5	5.0	DCM, -78 °C 2 h	262 (85%)

^[a]Estimated from the ¹H NMR spectrum of the crude reaction material, which showed unreacted **259** and product **262** in a 5:1 ratio

^[b]Estimated from the ¹H NMR spectrum of the crude reaction material, which showed unreacted **259** and product **262** in a 4:1 ratio

We found that the oxidation of diol **259** to ketone **262** did not go to completion when the equivalencies of base were reduced to 1.5 – 2.0, however no undesired thioacetal **263** was generated in the reactions (Table 31, entries 2 and 3). We anticipated that the equivalencies of base were too low, leading to only partial conversion of starting material **259** to ketone **262**. Hence the equivalencies of triethylamine were increased (5 eq.) which resulted in 100% conversion to desired ketone **262** as shown by the ¹H NMR spectrum of the crude material (Table 31, entry 4). Ketone **262** was subsequently isolated in an excellent yield of 85% following column chromatography

We were able to obtain a crystal structure of ketone **262**, following crystal growth using slow evaporation from petroleum ether/ diethyl ether (Figure 167).

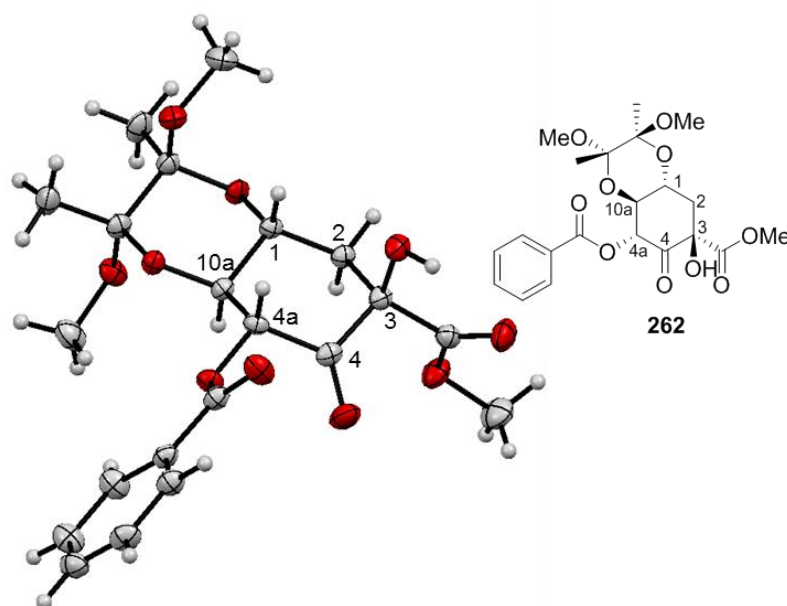


Figure 167: X-Ray crystal structure of ketone **262**

Ketone **262** crystallises in the monoclinic space group $P2_1$, with one molecule in the asymmetric unit (Figure 167). The crystal structure confirmed the stereochemistry of molecule **262** was consistent with our predictions.

Once we had developed a viable synthetic method to sufficient quantities of ketone **262**, we could proceed to the next step in the synthesis.

4.3.6.2 Reaction of Ketone **262** with Base

The next stage in our planned synthetic route to DEM30355/A **94** was to use an $E1cB$ reaction to synthesise diol **264** (Figure 168). Following OH protection, we would then use a D-A reaction with isobenzofuran **199** to generate adduct **261**, with the A, B, C ring core of DEM30355/A **94** in place.

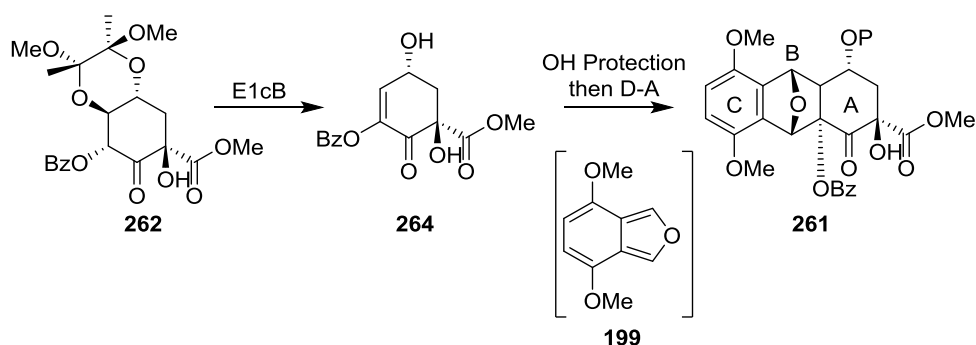
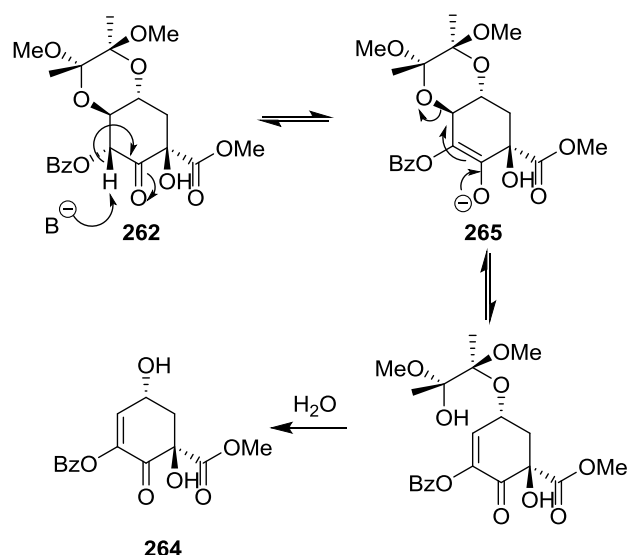


Figure 168: Planned synthesis of Diels-Alder adduct **261** from ketone **262**

We anticipated that, apart from the hydroxyl proton, the proton α to the ketone would be the most acidic in compound **262**. We envisaged that the reaction of ketone **262** with base would lead to the formation of enolate **265**, followed by ring opening of the acetal group via an $E1cB$ mechanism, leading to alkene **264** (Figure 169).

Figure 169: Proposed synthesis of alkene **264**

We screened a range of basic reaction conditions to generate alkene **264** from ketone **262** (Table 32).

Table 32: Reaction of ketone **262** under a range of basic reaction conditions

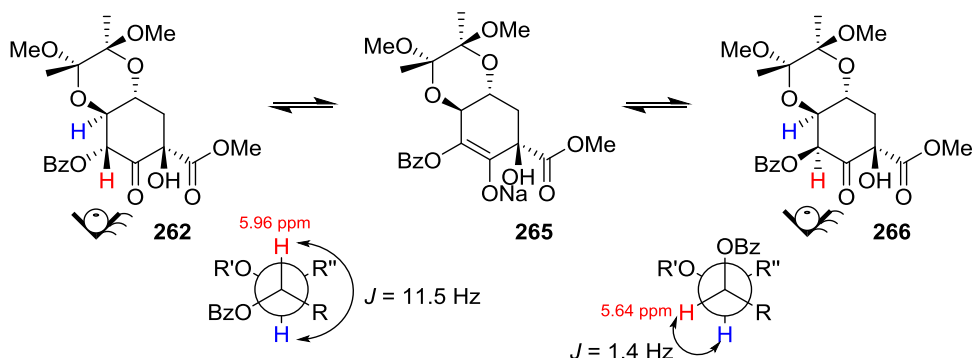
Entry	262 eq.	Base	Base eq.	Reaction conditions	Reaction outcome ^[a]
1	1	Pyridine	excess ^[b]	rt, 11 d	unreacted 262
2	1	NaH	2.0	THF, -78 °C 35 min, rt 7 d	diastereomer 266 and unreacted 262
3	1	NaHMDS	2.5	THF, -78 °C 90 min, rt 24 h	by-product 267
4	1	LDA	2.3	THF, -78 °C 35 min, rt 18 h	by-product 267
5	1	DBU	2.0	THF, rt, 2 d	by-product 267

^[a]Determined from analysis of the ¹H NMR spectrum of the crude reaction material

^[b]Pyridine was used as the solvent

In the first reaction we examined using pyridine as the base, only starting material **262** was recovered (Table 32, entry 1), therefore we opted to use a stronger base, namely NaH. Despite a long reaction time, the ¹H NMR spectrum of the crude material showed lots of unreacted ketone **262** remained, although new signals were observed. The spectrum contained a one proton doublet at 5.64 ppm ($J = 1.4$ Hz), suggesting a CH group bonded to an electron withdrawing moiety, vicinally coupled to a CH group. We believe this signal at 5.64 ppm corresponded to the C^{4a} proton of compound **266**, a diastereomer of starting material **262**,

which arises from the formation of enolate **265** followed by protonation from back face (Table 32, entry 2).



With this promising result we decided to examine the alternative, more organo-soluble bases, NaHMDS (Table 32, entry 3) and LDA (Table 32, entry 4), to try and generate desired alkene product **264**. In both cases, the ^1H NMR spectrum of the crude material showed signals corresponding to a new, aromatic by-product **267**, but no signals characteristic of desired alkene **264** were observed. We anticipated that the formation of this undesired by-product **267** may be avoided by using a less reactive base, therefore the reaction was repeated using 1,8-diazabicyclo[5.4.0]undec-7-ene (DBU), but once again by-product **267** was the sole product from the reaction (Table 32, entry 5). We therefore decided to isolate by-product **267** and investigate its structure, to gain a better understanding of the reaction.

The crude material from the reaction between ketone **262** and NaHMDS (Table 32, entry 3) was purified by column chromatography, which led to the isolation of by-product **267** as a 2:1 mixture of diastereomers as shown by the ^1H NMR spectrum (Figure 170). The NMR data discussed from herein refers to the major diastereomer of by-product **267**. The ^1H NMR spectrum showed signals at 7.34 ppm (1H, d, $J = 8.9$ Hz) and 6.42 ppm (1H, d, $J = 8.9$ Hz), characteristic of an AB spin system, corresponding to two adjacent aromatic CH groups. In addition, a signal at 3.84 ppm (3H, s), which showed a HMBC correlation to a carbon signal at 170.6 ppm, suggested a CO_2Me group. The proton signals at 3.22 ppm (3H, s), 1.67 ppm (3H, s) and 1.59 ppm (3H, s) belonged to the same spin system, which we deduced had originated from the acetal unit of ketone **262**. Furthermore, a peak at 10.99 ppm (1H, s) suggested the by-product **267** contained a hydrogen bonded hydroxyl group.

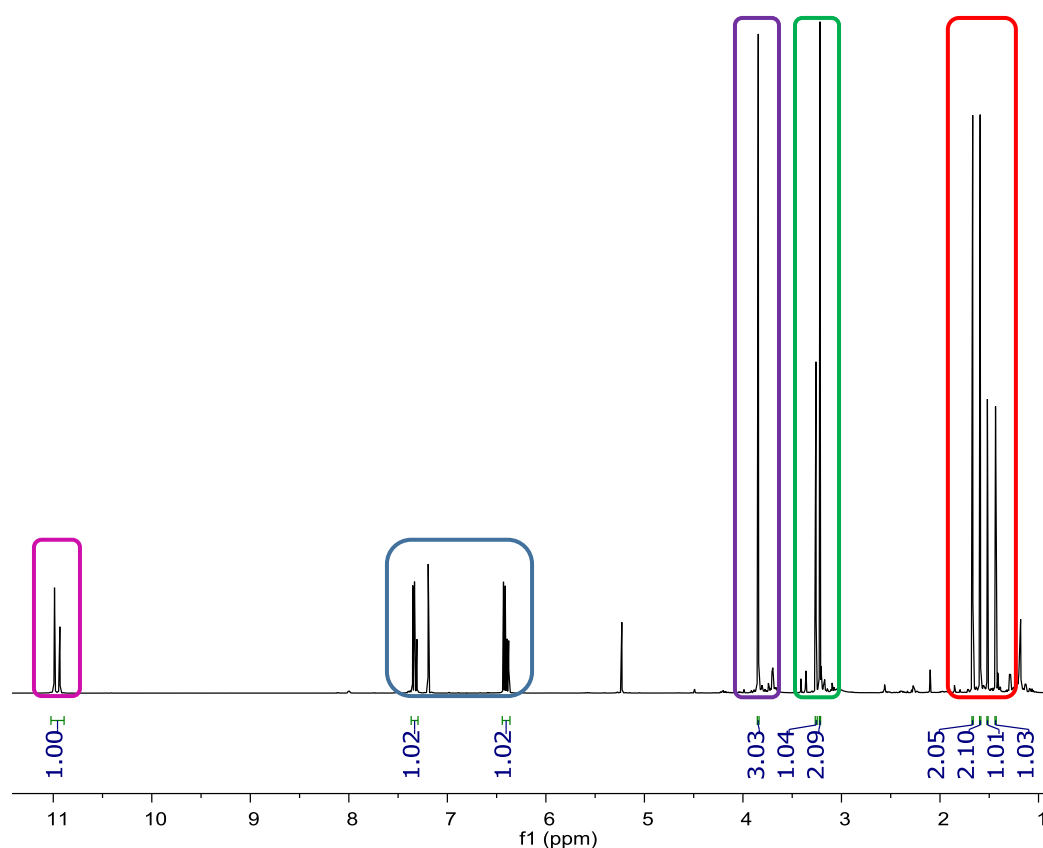


Figure 170: ^1H NMR spectrum of by-product **267**

Mass spectrometry analysis of the diastereomeric mixture of by-product **267** showed an m/z signal at 285.0970. Based on this NMR and HRMS data, we propose the structure of the by-product is aromatic compound **267** (Figure 171).

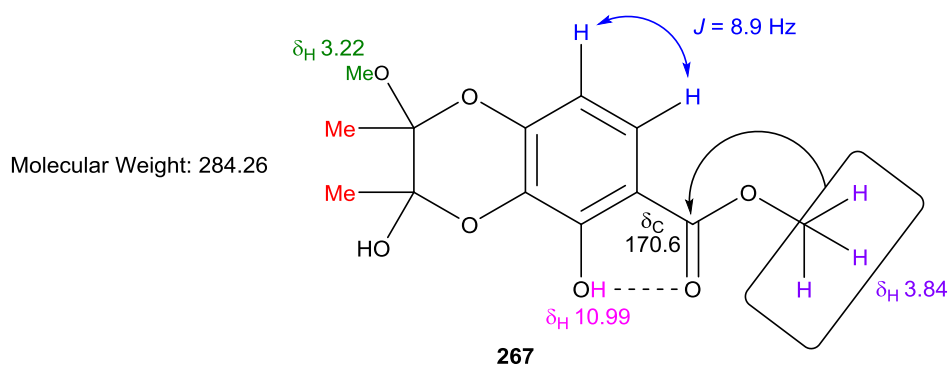


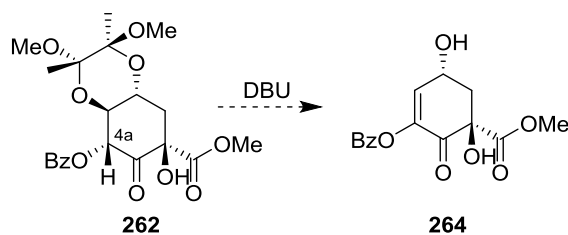
Figure 171: Proposed structure of by-product **267**

The formation of aromatic compound **267** suggested that the benzoyl OH protecting group at C^{4a} of the starting material, ketone **262**, was too unstable to the basic conditions tested, resulting in the removal of the benzoyl group followed by OH elimination at this position.

To determine whether it was possible to observe the formation of desired alkene **264** in our reactions between ketone **262** and base, we carried out a series of experiments in deuterated solvents using DBU as the base, with the reaction progress monitored by ^1H NMR (Table 33).

Chapter 4. Diels-Alder Synthesis of DEM30355/A

Table 33: NMR experiments using DBU as the base



Entry	262 eq.	DBU eq.	Reaction solvent	Reaction temperature	Observed product ^[a]
1	1	2.0	DCM- <i>d</i> ₂	rt	by-product 267
2	1	2.0	THF- <i>d</i> ₈	rt	by-product 267
3	1	2.0	DMSO- <i>d</i> ₆	rt	by-product 267

^[a]Determined from analysis of the ¹H NMR spectrum of the reaction mixture after 120 h

In all of the solvents we tested, the ¹H NMR spectra showed that the reactions proceeded with the formation of the same intermediates, with only slight variations in the time scale. Here we will discuss the ¹H NMR data for the reaction conducted in deuterated DCM (Figure 172).

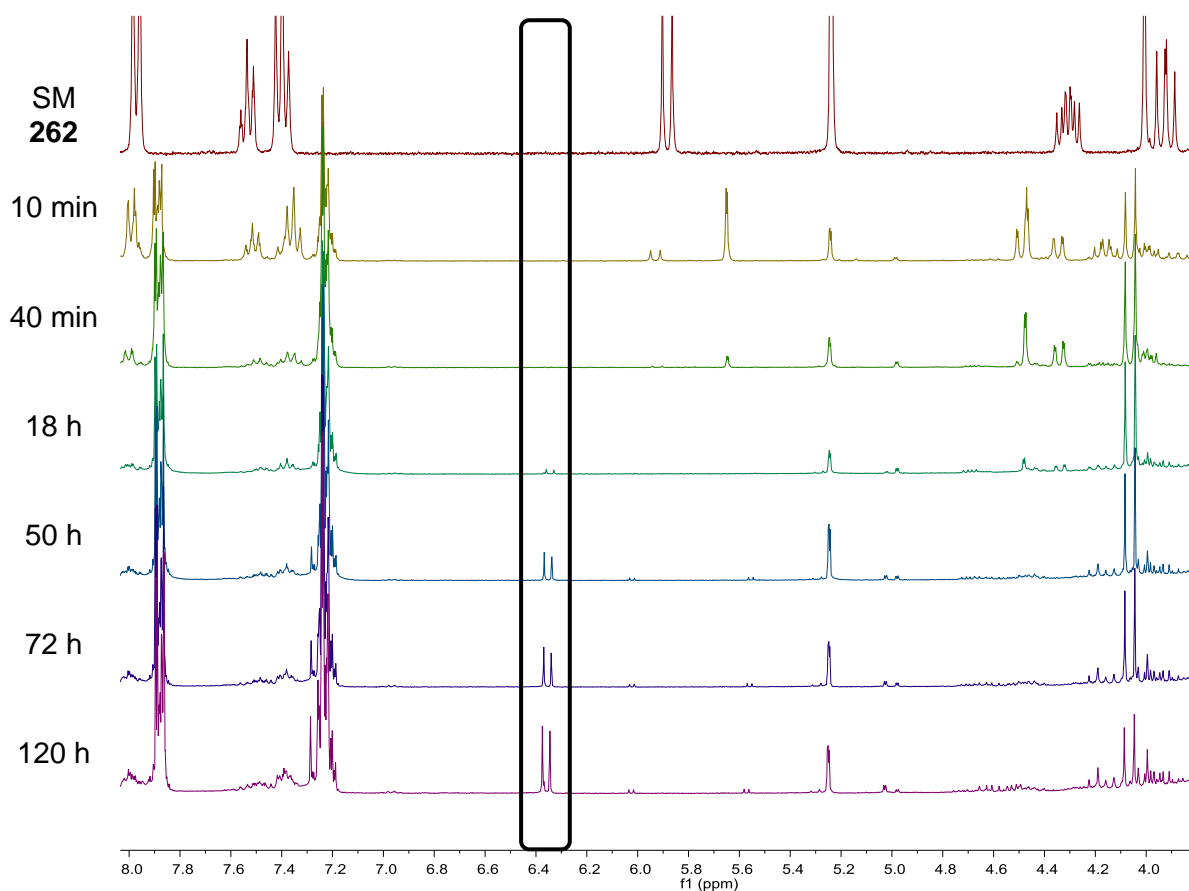


Figure 172: Expansion of the ¹H NMR spectra of the reaction of ketone **262** with DBU in DCM-*d*₂ at various time intervals

After a reaction time of 40 minutes, the spectrum showed loss of the peak at 5.88 ppm (1H, d, $J = 11.5$ Hz) corresponding to the C^{4a} proton of starting material **262**, which suggested the formation of enolate **265** (Figure 172). After 18 hours, the spectrum showed the emergence of a signal at 6.36 (1H, d, $J = 8.9$ Hz), corresponding to an aromatic proton of undesired by-product **267**. No signals corresponding to desired alkene **264** were observed throughout the reaction, suggesting the degradation of enolate **265** to aromatic compound **267** is a rapid process.

As the reaction between ketone **262** and DBU did not generate alkene **264** via an E1cB reaction mechanism, we decided to examine an alternative method.

4.3.6.3 Acetal Deprotection of Ketone **262**

We anticipated that removal of the acetal protecting group from ketone **262**, may make the hydroxyl group at C^{10a} of product **268** a better leaving group and hence encourage the desired E1cB reaction to occur (Figure 173).

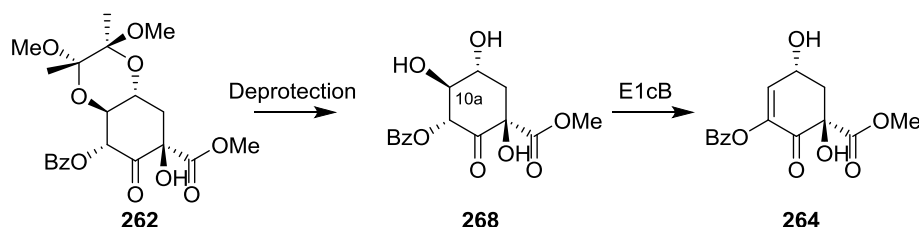


Figure 173: Proposed synthesis of alkene **264** via an E1cB reaction of triol **268**

Ketone **262** was reacted under standard acetal removal conditions, using trifluoroacetic acid (TFA): water (10:1 v/v) (Table 34).

Table 34: Diol deprotection reaction conditions examined

Entry	262 eq.	TFA eq.	Reaction conditions ^[a]	Reaction quenching	Reaction outcome ^[b]
1	1	10	DCM, rt, 24 h	aqueous work-up then solvent removed	product 268 lost in isolation
2	1	10	MeOD, rt, 24 h	-	starting material 262 recovered
3	1	10	DCM, rt, 24 h	solvent removed	product 268 recovered
4	1	10	DCM- <i>d</i> ₂ , rt, 24 h	solvent removed	product 268 recovered

^[a]H₂O was added to the reaction at 0.1 x the volume of TFA used

^[b]Determined from analysis of the ¹H NMR spectrum of the reaction mixture

In the first OH-deprotection reaction we examined, TLC showed loss of starting material **262** and a new spot with a lower R_f value was generated, however following aqueous work up, we were unable to recover any desired triol **268** from the aqueous extract, presumably due to the

high water solubility of product **268** (Table 34, entry 1). We repeated the reaction in deuterated methanol to allow the reaction progress to be monitored by ^1H NMR, however no reaction was observed and starting material **262** was recovered (Table 34, entry 2). We then repeated our original deprotection reaction in DCM and deuterated DCM, but omitted the aqueous work up step to avoid the loss of product **268**. In both cases, the ^1H NMR spectrum of the crude material showed no peaks corresponding to the acetal group, therefore we could deduce diol **268** had been generated (Table 34, entries 3 and 4). The crude triol **268** was used without purification in the subsequent synthetic step.

With triol **268** in hand, we moved on to examine the $\text{E}_{1\text{c}}\text{B}$ reaction to generate alkene **264**.

4.3.6.4 Reaction of Triol **268** with Base

Crude triol **268** from the deprotection reaction (1 eq.) was reacted with DBU (2 eq.) in deuterated methanol, with the reaction progress monitored by ^1H NMR (Figure 174).

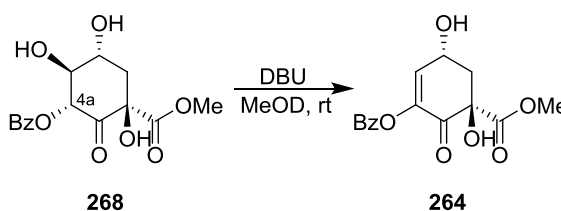


Figure 174: Proposed synthesis of alkene **264**

After a reaction time of 5 minutes, we observed the disappearance of the signal at 5.81 ppm (1H, d, $J = 10.3$ Hz), corresponding to the proton at $\text{C}^{4\text{a}}$. However, this was in concurrence with the appearance of new signals in the aromatic region at 7.88 – 7.80 (m) and 7.32 – 7.19 (m), suggesting that a similar aromatisation process had occurred as in the reaction of ketone **262** with DBU.

We believe that the aromatisation of OH-protected compound **262** and triol **268** occurs following base catalysed removal of the benzoyl group at $\text{C}^{4\text{a}}$, allowing elimination of the resultant deprotected alcohol group at this position. Therefore, in future we plan to replace the benzoyl group with a base stable protecting group, such as a benzyl, before continuing in our planned synthetic procedure.

4.4 Conclusions and Future Work

In this chapter we aimed to develop a synthetic route to DEM30355/A analogues **212**, in a two-step procedure consisting of a D-A reaction from isobenzofuran **199**, followed by base catalysed ring opening of the resultant D-A cycloadducts **211** (Figure 175). By developing this synthetic route we aimed to build the A, B, C ring core structure of DEM30355/A **94**, including the quaternary centre at C^{4a} and the benzylic alcohol and unsaturated bond in the central B ring.

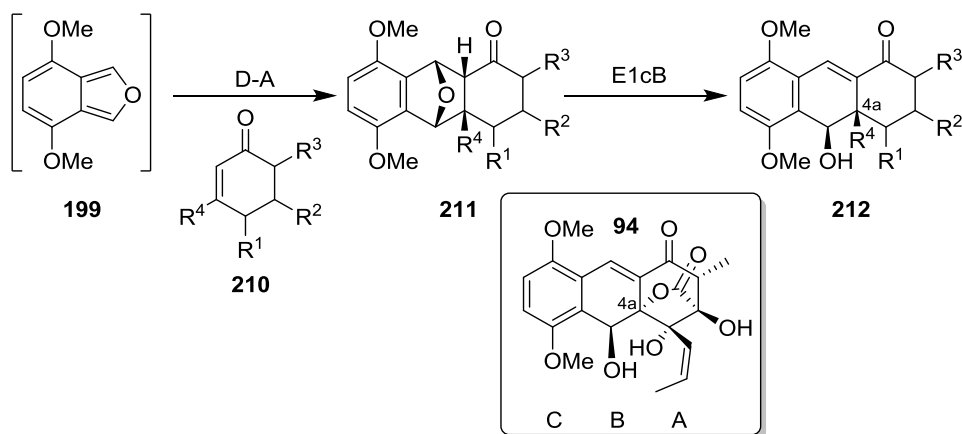


Figure 175: Planned synthetic route to DEM30355/A analogues **212**

The most successful D-A reaction to build the anthracene core and introduce the quaternary centre at C^{4a} used 2,6-dimethylcyclohexa-2,5-diene-1,4-dione **231** as the dienophile, which generated *exo* and *endo* cycloadducts **233-a** and **233-b** respectively (Figure 176).

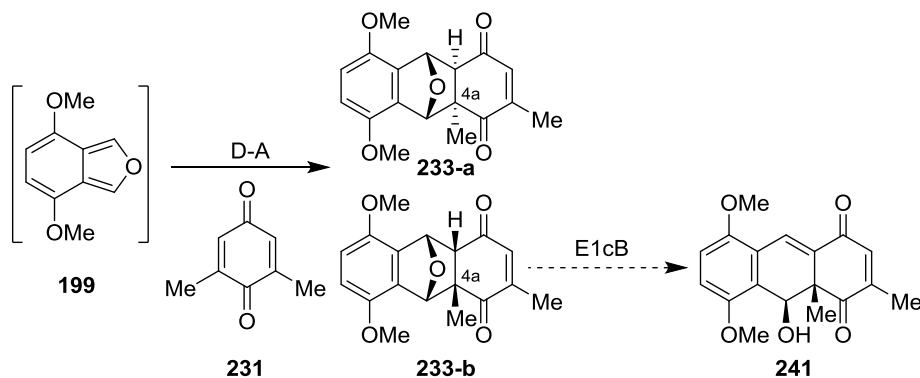


Figure 176: Diels-Alder synthesis of *exo* adduct **233-a** and *endo* adduct **233-b** and the proposed synthesis of alcohol **241**

We have learned that *endo* D-A cycloadduct **233-b** undergoes a reaction with LDA to generate a new product, however more investigation is required to determine whether the new product is alcohol **241** (Figure 176). To continue this route, we would scale up this reaction to aid in the isolation and structure elucidation of this new product, to determine if the E1cB reaction is successful.

The above investigations were prerequisite to our planned single enantiomer synthesis of DEM30355/A **94** using D-A chemistry, to ultimately determine the absolute stereochemistry of the molecule. We aimed to generate dienophile **260** as a single enantiomer from shikimic acid **213**, using diastereoselective synthesis to construct the stereocentre at C³.

The most successful synthetic route to build the stereogenic centre at C³ used a sterically directed dihydroxylation reaction of alkene **254** to give diol **259** (Figure 177). We learned the best method to oxidise diol **259** to ketone **262** used Swern conditions. We attempted to generate dienophile **260** via an E1cB reaction from ketone **262**, however the product of this reaction is not alkene **260**, rather aromatic compound **267** (Figure 177). We anticipate the formation of compound **267** may be avoided by replacement of the benzoyl protecting group with a base stable protecting group.

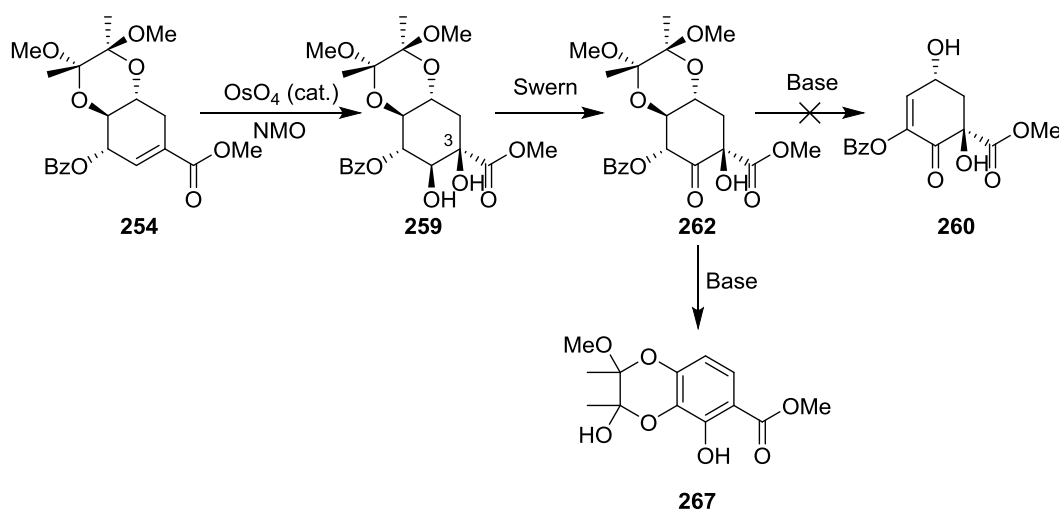


Figure 177: Reactions examined in the diastereoselective synthesis of ketone **262** and the subsequent base-catalysed formation of aromatic compound **267**

Therefore to continue this route to DEM30355/A **94**, we would investigate substitution of the benzoyl protecting group of ketone **262** with benzyl, followed by an E1cB reaction to generate alkene **270** (Figure 178). Subsequently, alkene **270** would be employed as a dienophile in an exo D-A reaction to generate cycloadduct **271**, with the quaternary oxygenated centre at C^{4a} of DEM30355/A **94** in place.

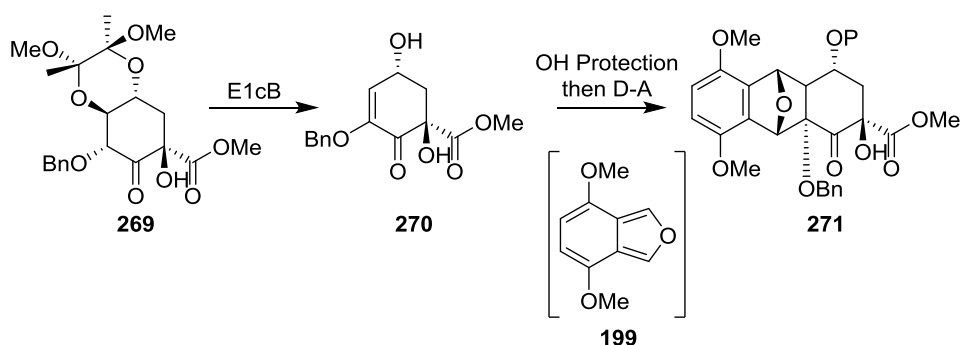


Figure 178: Proposed synthesis of dienophile **270**

As an alternative method, we would use a modified Danishefsky route to synthesise compound **272**, which would then be employed as a dienophile in a D-A reaction with isobenzofuran **199** (Figure 179).⁹⁹ Following the conversion of the resultant cycloadduct **273** to β -dicarbonyl **274**, we would use the reaction conditions developed by Miao and Sun to oxidise C^{4a} to generate the key oxygenated quaternary centre centre of DEM30355/A **94** (Figure 179).¹³³

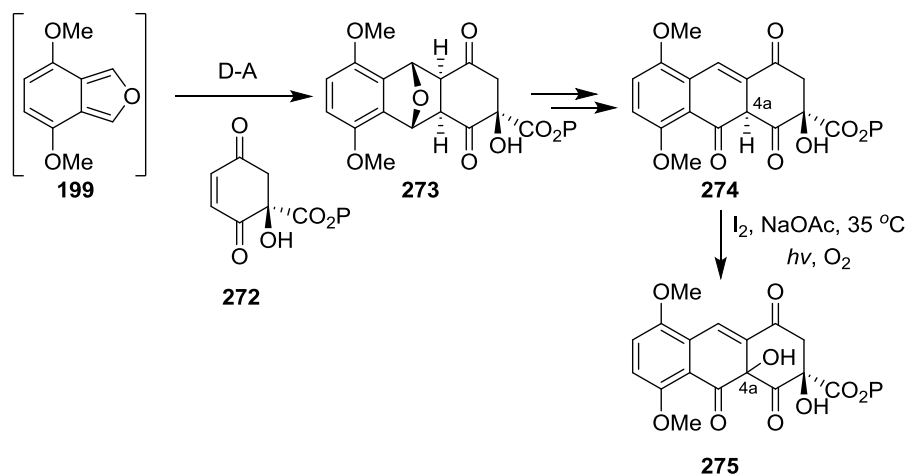


Figure 179: Proposed alternative synthetic route to construct the C^{4a} centre of DEM30355/A **94** through oxidation of β -dicarbonyl **274**

Chapter 5. Experimental

5.1 General Experimental Information

5.1.1 Analysis

Melting points were obtained using Stuart SMP3 melting point apparatus. Thin-layer chromatography (TLC) was conducted on silica gel 60 F₂₅₄ plates and visualised using ultraviolet light unless otherwise stated. ¹H and ¹³C{¹H} NMR spectra were recorded on a Bruker Avance III 300 MHz, JEOL ECS-400 MHz, Bruker Avance III HD 500 MHz or a Bruker Avance III HD 700 MHz spectrometer. Infrared (IR) spectra were recorded on a Varian 800 FTIR Scimitar Series spectrometer. High resolution mass spectra (HRMS) were obtained from the National Mass Spectrometry Facility (Swansea University). X-Ray diffraction data were obtained using an Oxford Diffraction Gemini Atlas instrument.

5.1.2 Procedures

Standard Schlenk techniques were used for all manipulations involving air-sensitive reagents, under an atmosphere of nitrogen. Solvents were distilled under an atmosphere of nitrogen and used directly; THF was distilled from sodium/benzophenone, toluene was distilled from sodium and DCM was distilled from calcium hydride. Manual flash column chromatography was conducted using Geduran silicagel 60 (40 – 63 µm). Automated flash column chromatography was performed using a Biotage Isolera One or a Biotage Isolera LS instrument using KP-Sil SNAP cartridges. Semi-preparative High Performance Liquid Chromatography (HPLC) was performed on an Agilent 1100 Series instrument using a 4.6 x 150 mm C18 (2.5 µm) column (gradient 100% water to 100% acetonitrile, buffered to 0.1% by v/v formic acid). Size exclusion chromatography was performed using Sephadex LH-20.

5.1.3 Isolation of DEM30355/B2 73

The crude isolate of a large scale fermentation of *Amycolatopsis DEM30355* was supplied by Dr B. Kepplinger. All solvents used in the silica gel chromatography steps were buffered with 0.1% (v/v) formic acid.

5.1.3.1 Protocol 1 (Full isolation)

The crude isolate of *A. DEM30355* (4.420 g) was dry loaded onto silica gel and subjected to normal phase flash column chromatography (Biotage Isolera One, SNAP 100 g cartridge, eluent = gradient 100% ethyl acetate to 100% MeOH). The active fractions were identified using TLC, combined and the solvent removed under reduced pressure, to afford 2.280 g of material. This was subsequently dry loaded onto silica gel and subjected to normal phase flash column chromatography (Biotage Isolera One, SNAP 100 g cartridge, eluent = gradient 100% diethyl ether to 100% ethyl acetate to 100% MeOH). The active fractions were combined based on TLC analysis into Fraction 1 and Fraction 2 and the solvent from each fraction was removed under reduced pressure. The ¹H NMR spectrum of Fraction 1 (0.563 g) indicated it contained DEM30355/A **94** and the fraction was stored under a nitrogen atmosphere in the freezer (- 20 °C). The ¹H NMR spectrum of Fraction 2 (0.558 g) showed it contained DEM30355/B2 **73**. Fraction 2 was dissolved in toluene (30 mL) and washed with acidic water (20 mL, acidified to pH 2 with 2 M HCl aq. solution). The organic extract was extracted with NaHCO₃ solution (3 x 30 mL, 5% w/v aqueous solution) and the aqueous extract was acidified to pH 2 with 2 M HCl aq. solution. The acidified aqueous extract was extracted with ethyl acetate (3 x 50 mL) and the organic extracts were combined, dried with sodium sulfate, filtered and the solvent removed under reduced pressure to afford DEM30355/B2 **73** (0.102 g, 2.3% yield based on the mass of the crude isolate) as a red/orange solid.

5.1.3.2 Protocol 2 (Partial Isolation)

Prior to the purification procedures described below, the crude isolate of *A. DEM30355* was subjected to normal phase column chromatography to isolate DEM30355/A **94** (Dr J. Cowell). The remaining fractions, which did not contain DEM30355/A **94** as shown by TLC, were combined and the solvent removed under reduced pressure (Dr J. Cowell) to afford the crude material (3.780 g).

The crude material (3.780 g) was dissolved in toluene (200 mL) and extracted with NaHCO₃ solution (3 x 150 mL, 7% w/v aqueous solution). The combined aqueous extracts were washed with toluene (3 x 300 mL) then acidified to pH 2 with 2 M HCl aq. solution. The acidified aqueous extract was extracted with ethyl acetate (3 x 300 mL) and the organic extracts were combined, washed with brine, dried with sodium sulfate, filtered and the solvent removed under reduced pressure to give 1.370 g of material. This was subsequently dry loaded onto silica gel and subjected to normal phase flash column chromatography (Biotage Isolera One, SNAP 100 g cartridge, eluent = gradient 100% ethyl acetate to 100% MeOH). The active fractions

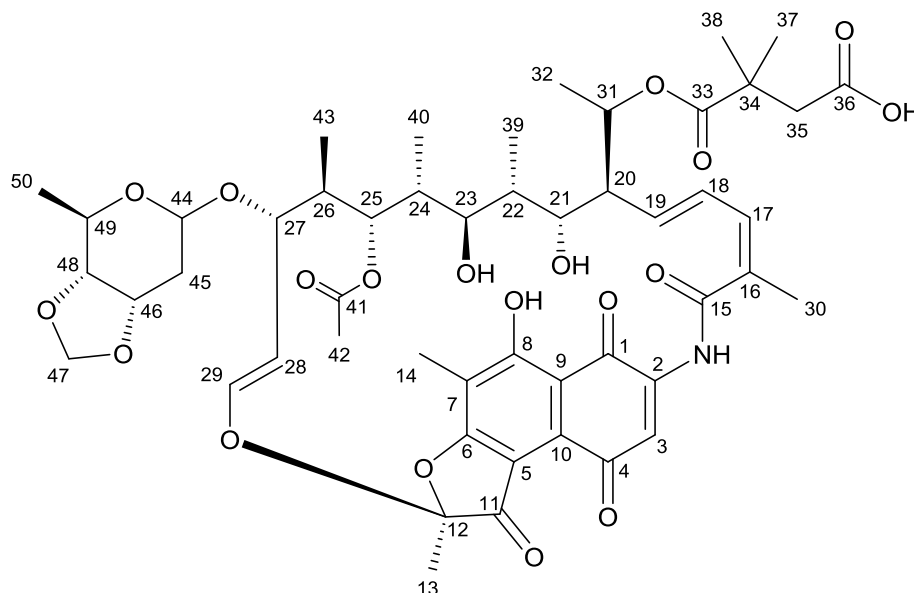
Chapter 5. Experimental

were identified using TLC, combined and the solvent removed under reduced pressure, to afford 1.164 g of material. This was dry loaded onto silica gel and subjected to normal phase flash column chromatography (Biotage Isolera One, SNAP 100 g cartridge, eluent = gradient 100% ethyl acetate to 100% MeOH). The active fractions were identified using TLC, combined and the solvent removed under reduced pressure, to afford 0.383 g of material. This was subsequently dissolved in toluene (100 mL) and extracted with NaHCO₃ solution (3 x 100 mL, 7% w/v aqueous solution). The combined aqueous extracts were washed sequentially with toluene (2 x 100 mL) and hexane (100 mL), then acidified to pH 2 with 2 M HCl aq. solution. The acidified aqueous extract was extracted with ethyl acetate (3 x 100 mL), washed with brine, dried with sodium sulfate, filtered and the solvent removed under reduced pressure to give 0.133 g of material. This was dissolved in MeOH (8 mL) and subjected to size exclusion column chromatography (LH-20, eluent = MeOH). The active fractions were identified using TLC, combined and the solvent removed under reduced pressure to give DEM30355/B2 **73** (0.043 g, 1.4% yield based on the mass of the crude material) as a red/orange solid.

$R_f = 0.35$ (100% ethyl acetate)

5.1.4 NMR Assignment of DEM30355/B2 73

All NMR data was collected on a sample of DEM30355/B2 **73** in methylene chloride- d_2 , on a Bruker Avance III HD 700 MHz spectrometer. ^1H NMR data were collected at 700 MHz. ^{13}C $\{^1\text{H}\}$ NMR data were collected at 176 MHz.

Table 35: Assignment of the ^1H and ^{13}C NMR data of DEM30355/B2 **73**

Atom no.	δ_c	^1H					$^{13}\text{C}-^1\text{H}$ (HMBC)
		δ_H	Number of protons	Multiplicity	J (Hz)	$^1\text{H}-^1\text{H}$ (COSY)	
35	43.1	2.54	1	d	16.8	2.66 (35)	1.18 (37), 1.23 (38)
		2.66	1	d	16.8	2.54 (35)	
36	172.0	-	-	-	-	-	2.54 (35), 2.66 (35)
34	40.4	-	-	-	-	-	2.54 (35), 2.66 (35), 1.18 (37), 1.23 (38)
38	24.6	1.23	3	s	-	-	2.54 (35), 2.66 (35)
37	25.7	1.18	3	s	-	-	2.54 (35), 2.66 (35)
33	176.0	-	-	-	-	-	2.54 (35), 2.66 (35), 1.18 (37), 1.23 (38), 5.07 (31)
31	67.7	5.07	1	"q"	6.4	1.09 (32)	3.70 (21), 1.09 (32), 5.83 (19)
32	19.3	1.09	3	d	6.4	5.07 (31)	5.07 (31), 2.17 (20)
20	52.4	2.17	1	"t"	9.7	5.83 (19), 3.70 (21)	5.97 (18), 5.83 (19), 5.07 (31), 3.70 (21), 3.52 (OH), 1.87 – 1.81 (22)
19	133.6	5.83	1	dd	15.6, 9.7	5.97 (18), 2.17 (20)	6.17 (17), 5.97 (18), 5.07 (31), 3.70 (21), 2.17 (20), 2.06 (30)

Chapter 5. Experimental

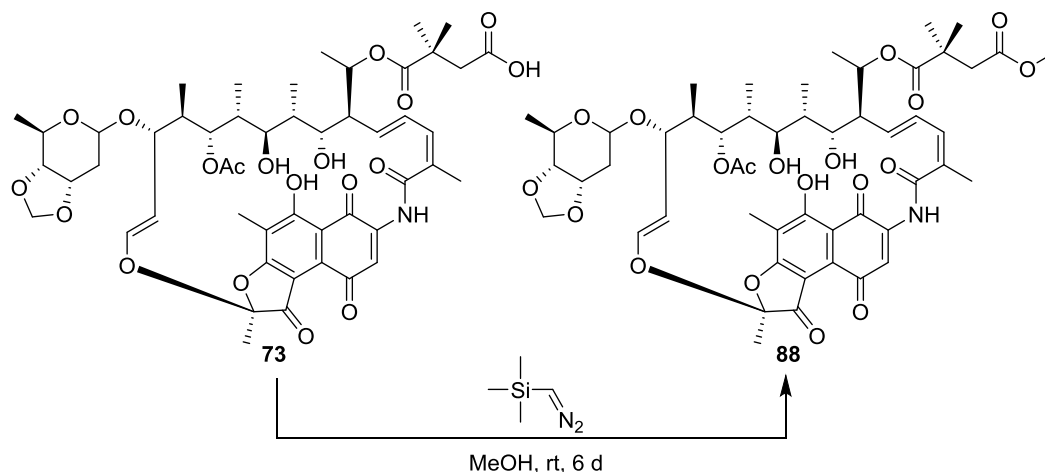
18	127.9	5.97	1	dd	15.9, 6.2	6.17 (17), 5.83 (19)	5.83 (19), 2.17 (20), 2.06 (30)
17	129.6	6.17	1	“dt”	6.2, 1.3	5.97 (18), 2.06 (30)	5.97 (18), 5.83 (19), 2.06 (30)
16	132.5	-	-	-	-	-	5.97 (18), 5.83 (19), 2.06 (30)
30	20.5	2.06	3	s	-	6.17 (17)	6.17 (17)
15	171.0	-	-	-	-	-	8.35 (NH), 6.17 (17), 2.06 (30)
21	68.5	3.70	1	d	10.1	2.17 (20)	5.83 (19), 5.07 (31), 3.52 (OH), 2.86 (23), 2.17 (20), 1.87 – 1.81 (22), 0.95 (39)
22	33.5	1.87 – 1.81 (overlaps with 45)	2 ^[a]	m	-	0.95 (39)	2.86 (23), 2.17 (20), 0.95 (39)
39	12.4	0.95	3	d	7.0	1.87 – 1.81 (22)	3.70 (21), 2.86 (23), 1.87 – 1.81 (22)
23	78.5	2.86	1	d	10.3	1.60 (24)	4.39 (25), 3.70 (21), 1.87 – 1.81 (22), 1.60 (24), 0.95 (39), 0.70 (40)
24	36.6	1.60	1	m	-	2.86 (23), 0.70 (40), 4.39 (25)	2.86 (23), 0.70 (40), 1.87 – 1.81 (22)
40	8.9	0.70	3	d	6.7	1.60 (24)	4.39 (25), 2.86 (23), 1.60 (24)
25	73.7	4.39	1	d	9.9	2.13-2.08 (26), 1.60 (24)	3.86 (27), 2.86 (23), 2.06 (30), 0.70 (40), 0.39 (43)
41	173.6	-	-	-	-	-	4.39 (25), 2.03 (42)
42	21.3	2.03	3	s	-	-	-
26	36.7	2.13-2.08	1	m	-	0.39 (43), 4.39 (25), 3.86 (27)	5.14 (28), 4.39 (25), 3.86 (27), 0.39 (43)
43	12.9	0.39	3	d	7.2	2.13-2.08 (26)	4.39 (25), 3.86 (27), 2.13-2.08 (26)
27	80.9	3.86	1	dd	9.1, 3.0	5.14 (28), 2.13-2.08 (26)	6.37 (29), 4.66 (44), 4.39 (25), 2.13-2.08 (26), 0.39 (43)
28	112.8	5.14 (overlaps with 47)	2	dd	12.8, 9.1	3.86 (27), 6.37 (29)	6.37 (29), 3.86 (27),), 2.13- 2.08 (26)
29	145.8	6.37	1	d	12.8	5.14 (28)	5.14 (28), 3.86 (27), 1.68 (13), 0.39 (43)
44	96.8	4.66	1	dd	8.9, 3.3	1.87 – 1.81 (45), 2.22 (45)	4.11 (46), 3.86 (27), 3.37 (49), 2.22 (45), 1.87 – 1.81 (45)

Chapter 5. Experimental

49	70.0	3.37	1	“dq”	9.0, 6.2	1.28 (50), 3.63 (48)	4.87 (47), 4.66 (44), 4.11 (46), 1.28 (50)
48	75.5	3.63	1	dd	9.0, 5.2	3.37 (49), 4.11 (46)	5.13 (47), 4.87 (47), 3.37 (49), 2.22 (45), 1.28 (50)
47	94.9	5.13 (overlaps with 28)	2	“s”	-	-	3.63 (48)
		4.87	1	“s”	-	-	
46	74.3	4.11	1	“td”	4.8, 2.8	1.87 – 1.81 (45), 2.22 (45), 3.63 (48)	5.13 (47), 4.87 (47), 4.66 (44), 3.63 (48), 2.22 (45)
45	33.0	2.22	1	“dt”	14.5, 2.4	1.87 – 1.81 (45), 4.11 (46), 4.66 (44)	4.66 (44)
		1.87 – 1.81 (overlaps with 22)	2 ^[a]	m	-	2.22 (45), 4.11 (46), 4.66 (44)	
50	18.3	1.28	3	d	6.2	3.37 (49)	3.63 (48), 3.37 (49)
13	23.1	1.68	3	s	-	-	-
12	109.3	-	-	-	-	-	6.37 (29), 1.68 (13)
11	193.5	-	-	-	-	-	1.68 (13)
6 ^[b]	171.4	-	-	-	-	-	2.34 (14)
14	7.3	2.34	3	s	-	-	-
7 ^[b]	116.4	-	-	-	-	-	2.34 (14)
5 ^[b]	111.3	-	-	-	-	-	2.34 (14)
8 ^[b]	166.9	-	-	-	-	-	2.34 (14)
9 ^[b]	110.9	-	-	-	-	-	2.34 (14)
10 ^[b]	131.5	-	-	-	-	-	7.80 (3), 2.34 (14)
1/4	185.3	-	-	-	-	-	8.35 (NH), 7.80 (3)
1/4	184.3	-	-	-	-	-	8.34 (NH)
2 ^[b]	140.4	-	-	-	-	-	7.80 (3)
3	116.7	7.80	1	s	-	-	8.35 (NH)
NH	-	8.35	1	-	-	-	-
Ar-OH	-	12.60	1	-	-	-	-
OH (21)	-	3.52	1	-	-	-	-

^[a]The integration of the signals in the 1.87 – 1.81 ppm region corresponded to 3 protons. 2 of these protons are assigned as C⁴⁵-H and C²²-H. It is possible that the remaining signal corresponds to an OH.

^[b]Assignments based on ‘best fit’ with ChemDraw model.

5.1.5 Synthesis of DEM30355/B2 Methyl Ester **88**

To a stirred solution of DEM30355/B2 **73** (2 mg, 2 μmol) in MeOH (500 μL) in a Schlenk flask under an atmosphere of nitrogen, was added trimethylsilyldiazomethane (4 μL , 8 μmol , 2 M solution in hexanes). The reaction mixture was stirred at rt for 48 h then trimethylsilyldiazomethane (4 μL , 0.008 mmol, 2 M solution in hexanes) was added and stirring was continued at rt for 4 d. The reaction mixture was quenched with 1: 1 MeOH: glacial acetic acid (v/v, 0.8 mL), stirred for 10 min and the solvent was removed with a stream of nitrogen. The residue was dissolved in DCM (15 mL), washed with saturated aq. NaHCO_3 solution (15 mL), dried with Na_2SO_4 , filtered and the solvent removed under reduced pressure. The crude material was purified by column chromatography (100% Et_2O to 100% ethyl acetate, then DCM: MeOH 9:1, column diameter = 0.5 cm, silica = 5.5 cm). An analytical HPLC run (100% water 5 min, gradient 100% water to 100% MeCN over 30 min, 100% MeCN 5 min, C18, column diameter = 4.6 mm, column length = 150 mm) of the sample showed a peak at 27.21 min (large), 27.41 min (small) and 28.00 min (medium). Mass spectrometric analysis of the same sample was consistent with methyl ester DEM30355/B2 **88** (0.9 mg, 0.9 μmol , 45%), isolated as a brown solid.

R_f = 0.9 (100% ethyl acetate); HRMS (pNSI) calcd for $\text{C}_{51}\text{H}_{65}\text{NO}_{19}\text{H}$ $[\text{M}+\text{H}]^+$:996.4224; observed: 996.4228; calcd for $\text{C}_{51}\text{H}_{65}\text{NO}_{19}\text{Na}$ $[\text{M}+\text{Na}]^+$:1018.4043; observed: 1018.4042;

^1H NMR Data of methyl-ester DEM30355/B2 **88** in methylene chloride- d_2 , were collected at 700 MHz data on a Bruker Avance III HD 700 MHz spectrometer. The ^1H NMR spectrum showed the sample contained a mixture of two derivatives in approximately a 1.0: 1.2 ratio (Figure 180).

Chapter 5. Experimental

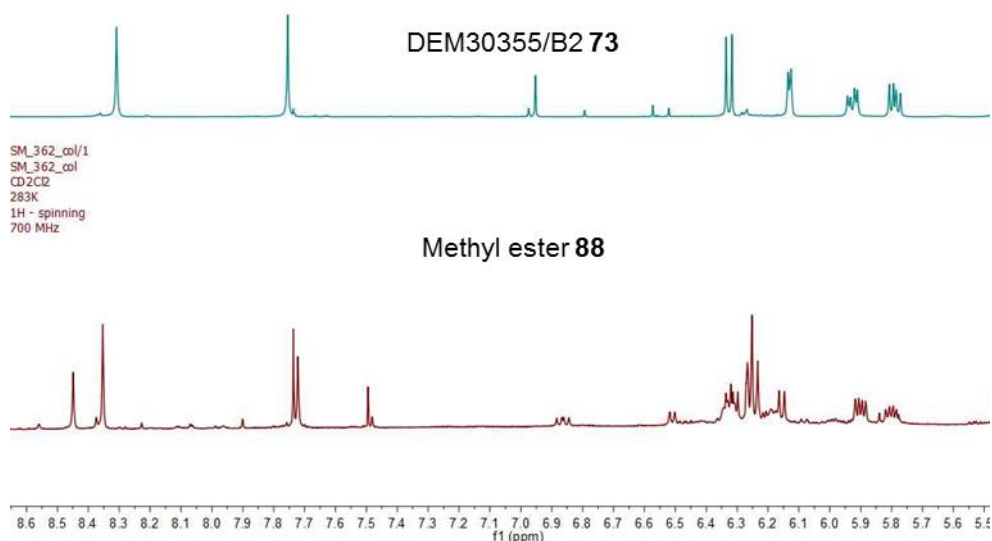


Figure 180: Comparison of the ¹H NMR spectra of DEM30355/B2 **73** (top) and methyl ester **88** (bottom) in the 8.60 - 5.60 ppm region

The ¹H NMR spectrum of methyl-ester DEM30355/B2 **88** showed new sharp singlet peaks in the 3.65 – 3.50 ppm region, consistent with ester O-CH₃ groups of major and minor products, further supporting our assignment (Figure 181).

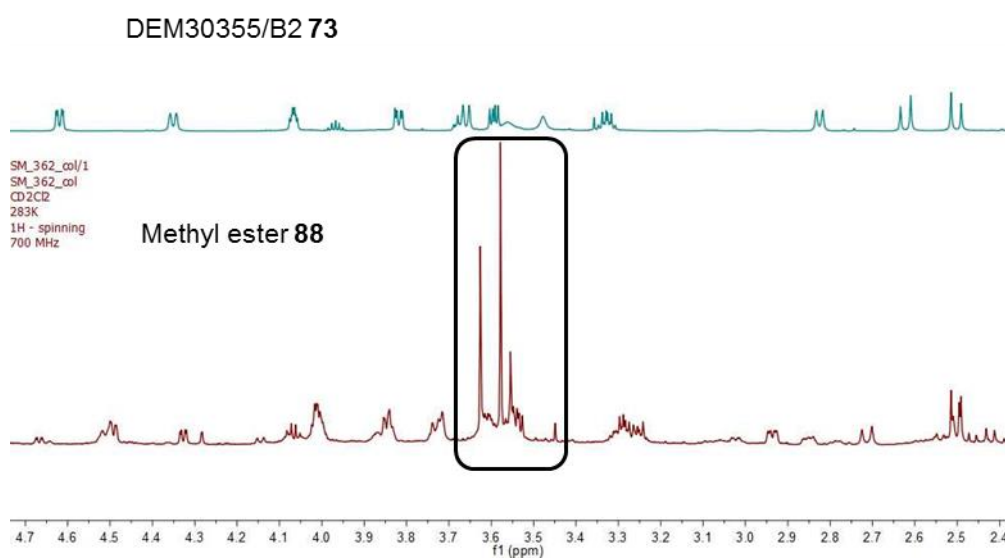
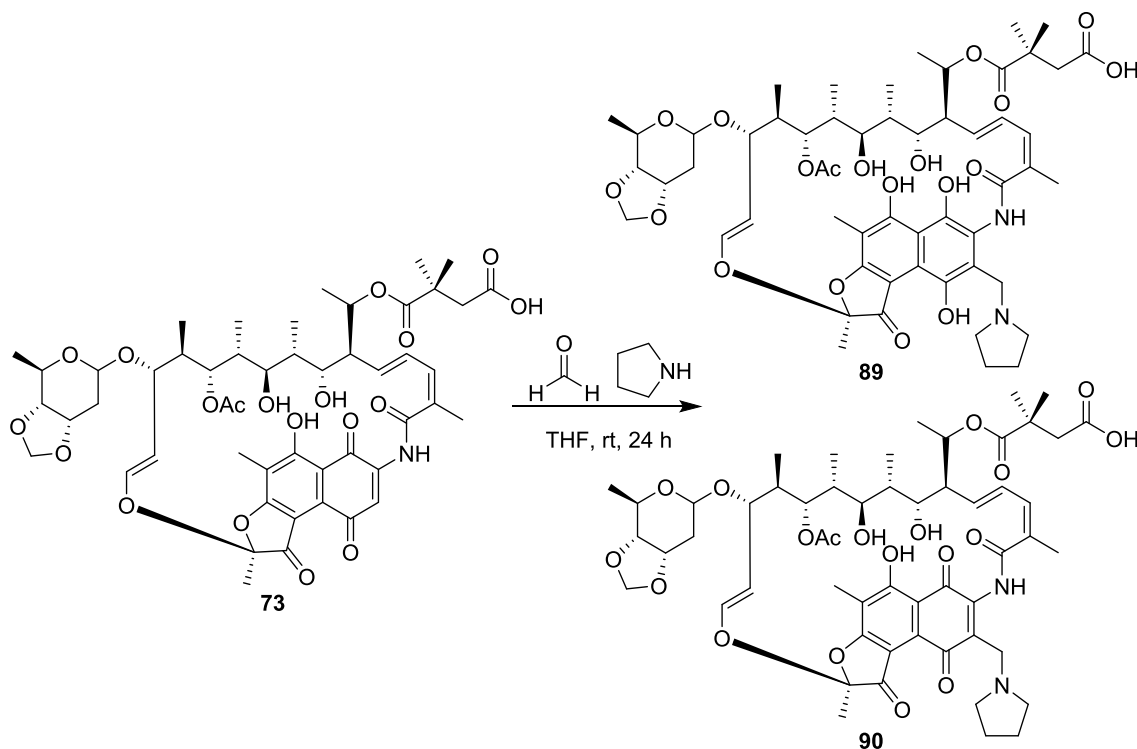


Figure 181: Comparison of the ¹H NMR spectra of DEM30355/B2 **73** (top) and methyl ester **88** (bottom) in the 4.70 - 2.40 ppm region. Signals corresponding to O-CH₃ groups of two methyl ester DEM30355/B2 derivatives are highlighted

5.1.6 Synthesis of Pyrrolidino DEM30355/B2 **89** and **90**

To a stirred solution of DEM30355/B2 **73** (15 mg, 15 μmol) in THF (1 mL) was added pyrrolidine (3 μL , 30 μmol) and formaldehyde (3 μL , 45 μmol , 37% w/v aq. solution). The solution was stirred at rt for 24 h then ascorbic acid aq. solution (1 mL, 10% w/v) was added and the temperature was maintained at 5 – 10 $^{\circ}\text{C}$. After stirring for 15 min, the reaction mixture was diluted with water (5 mL), extracted with ethyl acetate (3 x 20 mL), dried with sodium sulfate, filtered and the solvent removed under reduced pressure. The crude material was subjected to normal phase column chromatography (DCM: MeOH 9:1, column diameter = 2 cm, silica = 17 cm). Mass spectrometry analysis of the sample at this point indicated the sample was a mixture of hydroquinone pyrrolidino DEM30355/B2 **89** and unreacted DEM30355/B2 **73**, therefore the material was purified by size exclusion chromatography (MeOH, LH-20). An analytical HPLC run (100% water 5 min, gradient 100% water to 100% MeCN over 30 min, 100% MeCN 5 min, C18, column diameter = 4.6 mm, column length = 150 mm) of the resultant sample showed 3 peaks at 24.71 min (large), 26.64 min (small) and 27.00 min (medium). The sample was purified using semi-preparative HPLC (100% water 5 min, gradient 100% water to 100% MeCN over 30 min, 100% MeCN 5 min, C18, column diameter = 4.6 mm, column length = 150 mm). The compound corresponding to the peak at 24.71 min was collected in one fraction. The compound(s) corresponding to the peaks at 26.64 min and 27.00 min were collected as a mixed fraction. Mass spectroscopy analysis of the 24.71 min sample corresponded to hydroquinone pyrrolidino-DEM30355/B2 **89** (2.7 mg, 2.5 μmol , 17%), isolated as a yellow solid. Mass spectroscopy analysis of the mixed 26.64/ 27.00 min fraction

corresponded to a mixture of quinone pyrrolidino DEM30355/B2 **90** and hydroquinone pyrrolidino DEM30355/B2 **89** (2.0 mg).⁸²

Data for hydroquinone pyrrolidino DEM30355/B2 89

$R_f = 0.57$ (100% ethyl acetate); HRMS (pNSI) calcd $C_{55}H_{75}N_2O_{19}$ $[M+H]^+$: 1067.4964; observed: 1067.4965.

Data for hydroquinone pyrrolidino DEM30355/B2 89 and quinone pyrrolidino DEM30355/B2 90 mixture

HRMS (pNSI) calcd $C_{55}H_{73}N_2O_{19}$ $[M+H]^+$ (quinone pyrrolidino DEM30355/B2 **90**): 1065.4808; observed: 1065.4800; calcd $C_{55}H_{75}N_2O_{19}$ $[M+H]^+$ (hydroquinone pyrrolidino-DEM30355/B2 **89**): 1067.4964; observed: 1067.4914.

1H NMR data of hydroquinone pyrrolidino DEM30355/B2 **89** in methylene chloride- d_2 , were collected at 700 MHz data on a Bruker Avance III HD 700 MHz spectrometer. The 1H NMR spectrum of hydroquinone pyrrolidino-DEM30355/B2 **89** was compared with DEM30355/B2 **73**. The absence of an aromatic signal at 7.80 ppm corresponding to C^3 -H in DEM30355/B2 **73** suggests C^3 -H substitution, consistent with our assignment of hydroquinone pyrrolidino-DEM30355/B2 **89** (Figure 182).

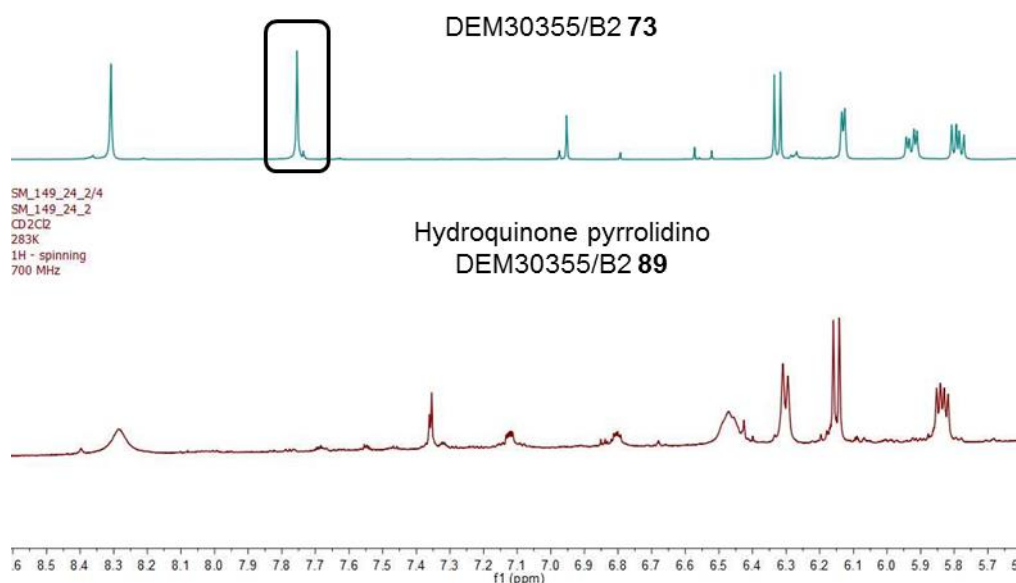


Figure 182: Comparison of the 1H NMR spectra of DEM30355/B2 **73** (top) and hydroquinone pyrrolidino DEM30355/B2 **89** (bottom) in the 8.50 - 5.70 ppm region. The signal corresponding to aromatic C^3 -H in DEM30355/B2 **73** is highlighted

The appearance of new signals at ~ 3.08 ppm and ~ 2.20 ppm in the spectrum of hydroquinone pyrrolidino-DEM30355/B2 **89** are consistent with pyrrolidine CH_2 groups, further supporting our assignment (Figure 183).

Chapter 5. Experimental

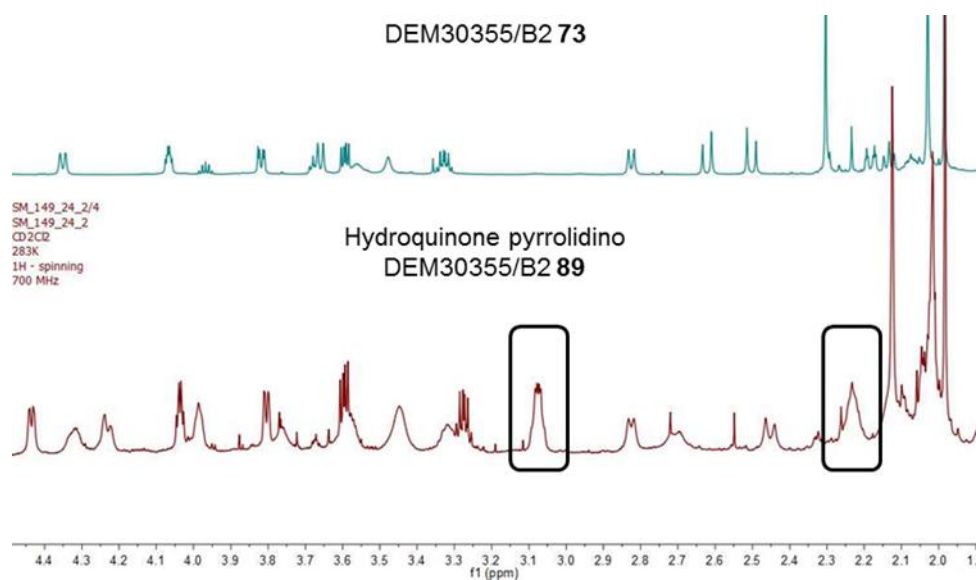


Figure 183: Comparison of the ¹H NMR spectra of DEM30355/B2 73 (top) and hydroquinone pyrrolidino DEM30355/B2 89 (bottom) in the 4.40 – 2.00 ppm region. Signals characteristic of pyrrolidino CH₂ groups are highlighted

5.1.7 Exemplar Procedures in the Semi-Synthesis of DEM30355/B2 73

5.1.7.1 EDCI Coupling Reaction of DEM30355/B2 73 with 4-Methylbenzylamine

To a stirred solution of DEM30355/B2 **73** (10.0 mg, 10 μ mol) in DCM (1 mL) was added 1-hydroxybenzotrazole (0.1 mg, 1 μ mol), *N*-(3-dimethylaminopropyl)-*N'*-ethylcarbodiimide hydrochloride (2.3 mg, 12 μ mol) and 4-methylbenzylamine (30 μ L of a 0.5 M solution in DCM, 15 μ mol) at rt. The solution was stirred for 25 h at room temperature, 4-methylbenzylamine (30 μ L of a 0.5 M solution in DCM, 15 μ mol) was added and stirring continued at rt for 22 h. The reaction mixture was poured into water (2 mL), the solution acidified with HCl aq. solution (1 mL, 1 M) and extracted with DCM (3 x 5 mL). The combined organic extracts were washed with brine (20 mL) and the solvent was removed under reduced pressure.

5.1.7.2 Attempted Synthesis of Rifalazil DEM30355/B2 Analogue 82

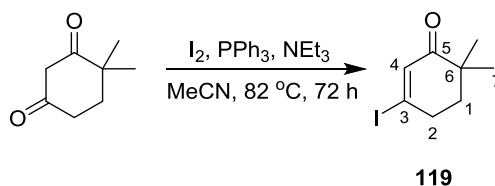
To a stirred solution of DEM30355/B2 **73** (2 mg, 2 μ mol) in THF 50%: toluene 50% (400 μ L) was added 2-aminorescorcinol (0.3 mg, 2 μ mol) at rt. The reaction mixture was stirred at rt for 12 d, the solvent was removed under reduced pressure and the residue was dissolved in ethyl acetate (5 mL). To the stirred solution was added potassium hexacyanoferrate (III) (1 mg, 3 μ mol) and stirring was continued at rt for 18 h. The reaction mixture was washed with PBS buffer (2 x 5 mL) then brine (5 mL) and the organic solvent was removed under reduced pressure.^{89,90}

5.1.7.3 Attempted Synthesis of Rifampicin DEM30355/B2 Analogue 81

To a stirred solution of DEM30355/B2 **73** (2 mg, 2 μ mol) in DMF (400 μ L) was added *tert*-butylamine (1 μ L, 5 μ mol), paraformaldehyde (~ 1 mg) and acetic acid (1 μ L, 17 μ mol). The solution was stirred at 50 °C for 3 h, 1-amino-4-methylpiperazine (1 μ L, 9 μ mol) was added and the solution was stirred at 50 °C for 1 h. The reaction mixture was cooled to rt and 2% acetic acid aq. solution (4 mL) was added. The reaction mixture was extracted with DCM (3 x 10 mL), washed with water (20 mL) then brine (2 x 20 mL) and the organic solvent was removed under reduced pressure.⁸⁶

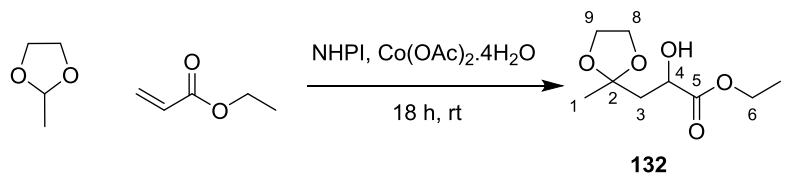
5.1.7.4 Reduction of Quinone DEM30355/B2 73 to hydroquinone DEM30355/B2 87

To a stirring solution of DEM30355/B2 **73** (2 mg, 2 μ mol) in THF (200 μ L) was added 10% ascorbic acid aq. solution (1 mL) and the reaction mixture was stirred vigorously at rt for 1.5 h. The reaction mixture was extracted with ethyl acetate (2 x 5 mL), washed with brine (10 mL) and the organic solvent was removed under reduced pressure.

5.1.8 3-Iodo-6,6-dimethylcyclohex-2-en-1-one **119**

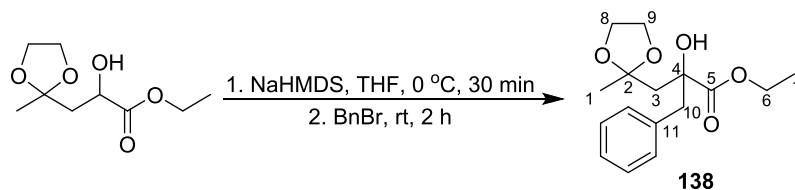
To a round bottomed flask was added iodine (1.198 g, 4.72 mmol) and MeCN (30 mL). To the resulting stirred suspension was added triphenylphosphine (1.238 g, 4.72 mmol), triethylamine (0.65 mL, 4.72 mmol) and 4,4-dimethylcyclohexane-1,3-dione (0.601 g, 4.29 mmol). The reaction mixture was heated at reflux for 72 h, concentrated *in vacuo*, and the crude product purified by column chromatography (petroleum ether: diethyl ether, 95: 5, column diameter = 3.5 cm, silica = 20 cm) to give 3-iodo-6,6-dimethylcyclohex-2-en-1-one **119** (0.925 g, 3.70 mmol, 86%) as a colourless oil.¹⁰³

$R_f = 0.33$ (petroleum ether: diethyl ether, 95:5); $^1\text{H NMR}$ (300 MHz, CDCl_3) δ_{H} 6.62 (1H, t, $J = 1.7$ Hz, H^4), 2.87 (2H, td, $J = 6.1, 1.7$ Hz, H^2), 1.77 (2H, t, $J = 6.1$ Hz, H^1), 1.05 (6H, s, H^7); $^{13}\text{C NMR}$ (101 MHz, CDCl_3) δ_{C} 200.4 (C^5), 139.1 (C^4), 124.8 (C^3), 40.8 (C^6), 38.6 ($\text{C}^{1/2}$), 37.9 ($\text{C}^{1/2}$), 23.96 (C^7); IR (neat): ν_{max} cm^{-1} 2965 – 2870 (CH), 1699 (C=O); HRMS (pAPCI): calcd for $\text{C}_8\text{H}_{12}\text{IO}$ $[\text{M}+\text{H}]^+$: 250.9927; observed: 250.9930.

5.1.9 Ethyl 2-hydroxy-3-(2-methyl-1,3-dioxolan-2-yl)propanoate **132**

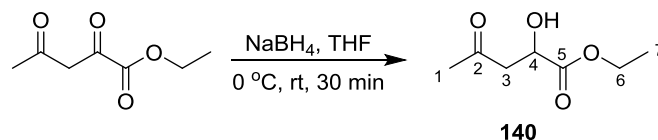
To a round bottomed flask was added 2-methyl-1,3-dioxolane (2.70 mL, 30.0 mmol), *N*-hydroxyphthalimide (49 mg, 0.3 mmol) and cobalt acetate tetrahydrate (0.7 mg, 3.0×10^{-3} mmol). To this was added ethyl acrylate (0.65 mL, 6.0 mmol), and the resulting solution was stirred at rt for 18 h. Excess 2-methyl-1,3-dioxolane was removed under reduced pressure and the crude product was purified through column chromatography (petroleum ether: ethyl acetate, 2:1, column diameter = 2 cm, silica = 20 cm) to give ethyl 2-hydroxy-3-(2-methyl-1,3-dioxolan-2-yl)propanoate **132** (157 mg, 0.8 mmol, 13%) as a colourless oil.¹⁰⁷

$R_f = 0.25$ (petroleum ether: ethyl acetate, 2:1, visualised with KMnO_4 aq. solution); $^1\text{H NMR}$ (300 MHz, CDCl_3) δ_{H} 4.38 – 4.30 (1H, m, H^4), 4.18 (2H, qd, $J = 7.1, 2.0$ Hz, H^6), 4.01 – 3.90 (4H, m, H^{8+9}), 3.66 (1H, d, $J = 5.2$ Hz, OH), 2.22 (1H, dd, $J = 14.8, 3.3$ Hz, H^3), 2.09 (1H, dd, $J = 14.8, 7.7$ Hz, H^3), 1.35 (3H, s, H^1), 1.26 (3H, t, $J = 7.2$ Hz, H^7); $^{13}\text{C NMR}$ (101 MHz, CDCl_3) δ_{C} 173.9 (C^5), 109.7 (C^2), 68.2 (C^4), 64.6 ($\text{C}^{8/9}$), 64.4 ($\text{C}^{8/9}$), 61.3 (C^6), 41.7 (C^3), 24.4 (C^1), 14.2 (C^7);); IR (neat): ν_{max} cm^{-1} 3470 (OH), 2984 – 2896 (CH), 1731 (C=O); HRMS (ASAP): calcd $\text{C}_9\text{H}_{17}\text{O}_5$ $[\text{M}+\text{H}]^+$: 205.1071; observed: 205.1069.

5.1.10 Ethyl 2-benzyl-2-hydroxy-3-(2-methyl-1,3-dioxolan-2-yl)propanoate **138**

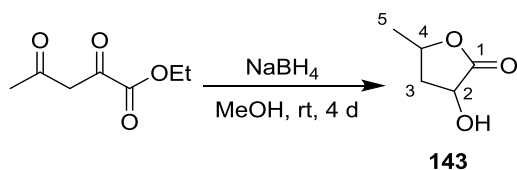
To a Schlenk flask was added ethyl 2-hydroxy-3-(2-methyl-1,3-dioxolan-2-yl)propanoate **132** (157 mg, 0.77 mmol) and THF (8 mL) under a nitrogen atmosphere. The solution was cooled to 0 °C, sodium bis(trimethylsilyl)amide (1.54 mL, 1.54 mmol, 1 M solution in THF) was added and the solution stirred for 30 min at 0 °C. Benzyl bromide (0.18 mL, 1.64 mmol) was added and the reaction mixture stirred at rt for 2 h then quenched with water (5 mL). The aqueous layer was extracted with ethyl acetate (3 x 15 mL) and the combined organic extracts were dried with sodium sulfate, filtered and the solvent removed under reduced pressure. The crude product was purified by column chromatography (petroleum ether: ethyl acetate, 2: 1, column diameter = 2 cm, silica = 18 cm) to give ethyl 2-benzyl-2-hydroxy-3-(2-methyl-1,3-dioxolan-2-yl)propanoate **138** (43 mg, 0.15 mmol, 19%) as a pale yellow oil.

$R_f = 0.48$ (petroleum ether: ethyl acetate 2: 1); $^1\text{H NMR}$ (300 MHz, CDCl_3) δ_{H} 7.32 – 7.01 (5H, m, Ar), 4.05 (2H, app td, $J = 7.2, 6.1$ Hz, H^6), 3.87 – 3.81 (4H, m, $\text{H}^{8/9}$), 2.95 (1H, d, $J = 13.3$ Hz, H^{10}), 2.84 (1H, d, $J = 13.3$ Hz, H^{10}), 2.41 (1H, d, $J = 14.8$ Hz, H^3), 2.07 (1H, d, $J = 14.8$ Hz, H^3), 1.26 (3H, s, H^1), 1.17 (3H, t, $J = 7.2$ Hz, H^7); $^{13}\text{C NMR}$ (101 MHz, CDCl_3) δ_{C} 175.1 (C^5), 135.7 (C^{11}), 130.6 (Ar), 128.1 (Ar), 126.9 (Ar), 109.8 (C^2), 76.2 (C^4), 64.3 ($\text{C}^{8/9}$), 64.2 ($\text{C}^{8/9}$), 61.3 (C^6), 46.6 (C^{10}), 46.0 (C^3), 25.3 (C^1), 14.3 (C^7); IR (neat): ν_{max} cm^{-1} 3533 (OH), 2982 – 2875 (CH), 1737 (C=O); HRMS (pNSI): calcd $\text{C}_{16}\text{H}_{22}\text{O}_5\text{Na}$ $[\text{M}+\text{Na}]^+$: 317.1359; observed: 317.1359.

5.1.11 Ethyl 2-hydroxy-4-oxopentanoate **140**

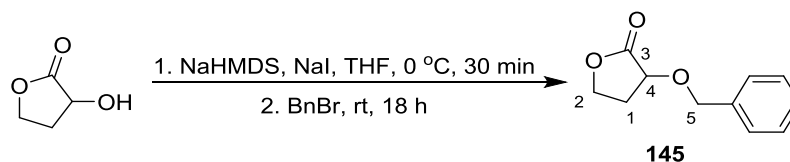
To a round bottomed flask was added ethyl acetopyruvate (0.27 mL, 1.90 mmol), THF (5 mL) and the resulting solution was cooled to 0 °C. Sodium borohydride (27 mg, 0.71 mmol) was added in small portions over 5 min. The reaction mixture stirred at 0 °C for 30 min, quenched with water (5 mL) and extracted with ethyl acetate (3 x 5 mL). The combined organic extracts were dried with sodium sulfate, filtered and the solvent removed under reduced pressure. The crude product was purified by column chromatography (petroleum ether: ethyl acetate, 2: 1, column diameter = 2 cm, silica = 17 cm) to give ethyl 2-hydroxy-4-oxopentanoate **140** (89 mg, 0.56 mmol, 29%) as a colourless oil.

$R_f = 0.15$ (petroleum ether: ethyl acetate, 2: 1, visualised with KMnO_4 aq. solution); $^1\text{H NMR}$ (300 MHz, CDCl_3) δ_{H} 4.44 (1H, dd, $J = 6.2, 4.1$ Hz, H^4), 4.20 (2H, q, $J = 7.1$ Hz, H^6), 3.23 (1H, br s, OH), 2.95 (1H, dd, $J = 17.4, 4.1$ Hz, H^3), 2.86 (1H, dd, $J = 17.4, 6.2$ Hz, H^3), 2.16 (3H, s, H^1), 1.25 (3H, t, $J = 7.1$ Hz, H^7); $^{13}\text{C NMR}$ (101 MHz, CDCl_3) δ_{C} 206.3 (C^2), 173.7 (C^5), 67.0 (C^4), 62.0 (C^6), 46.9 (C^3), 30.6 (C^1), 14.2 (C^7); IR (neat): ν_{max} cm^{-1} 3455 (OH), 2985 – 2919 (CH), 1713 (C=O); HRMS (pNSI): calcd $\text{C}_7\text{H}_{12}\text{O}_4\text{Na}$ $[\text{M}+\text{Na}]^+$: 183.0625; observed: 183.0628; calcd $(\text{C}_7\text{H}_{12}\text{O}_4)_2\text{Na}$ $[2\text{M} + \text{Na}]^+$: 341.1205; observed: 341.1207.

5.1.12 3-Hydroxy-5-methyldihydrofuran-2(3*H*)-one **143**

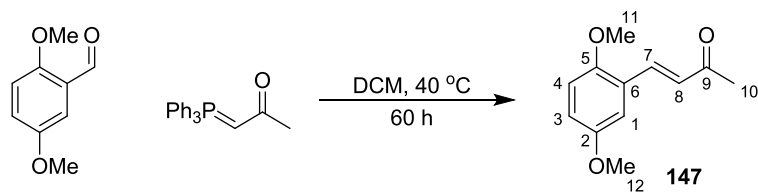
To a round bottomed flask was added ethyl acetoxyacetate (0.27 mL, 1.90 mmol) and MeOH (5 mL). The resultant solution was cooled to 0 °C and sodium borohydride (72 mg, 1.90 mmol) was added in portions over 5 min. The reaction mixture was stirred at rt for 4 d, quenched with water (10 mL) and extracted with ethyl acetate (3 x 20 mL). The combined organic extracts were washed with brine (50 mL), dried with sodium sulfate, filtered and the solvent removed under reduced pressure. The crude product was purified by column chromatography (petroleum ether: ethyl acetate, 1: 2, column diameter = 2 cm, silica = 20 cm) to give 3-hydroxy-5-methyldihydrofuran-2(3*H*)-one **143** (128 mg, 1.10 mmol, 58%) as a colourless oil.

$R_f = 0.34$ (petroleum ether: ethyl acetate, 1: 2, visualised with KMnO_4 aq. solution); $^1\text{H NMR}$ (300 MHz, CDCl_3) δ_{H} 4.64 – 4.45 (2H, m, H^{2+4}), 2.73 (1H, ddd, $J = 12.5, 8.3, 5.0$ Hz, H^3), 1.86 (1H, ddd, $J = 12.5, 11.2, 10.5$ Hz, H^3), 1.47 (3H, d, $J = 6.2$ Hz, H^5); $^{13}\text{C NMR}$ (75 MHz, CDCl_3) δ_{C} 177.3 (C^1), 73.6 ($\text{C}^{2/4}$), 69.0 ($\text{C}^{2/4}$), 38.8 (C^3), 20.9 (C^5); IR (neat): ν_{max} cm^{-1} 3408 (OH), 2984 – 2936 (CH), 1766 (C=O); HRMS (pNSI): calcd $\text{C}_5\text{H}_8\text{O}_3\text{Na}$ $[\text{M}+\text{Na}]^+$: 139.0366; observed: 139.0362.

5.1.13 3-(Benzyloxy)dihydrofuran-2(3H)-one **145**

To a Schlenk flask was added sodium iodide (150 mg, 1.00 mmol), α -hydroxy- γ -butyrolactone (0.39 mL, 5.00 mmol) and THF (25 mL) under a nitrogen atmosphere. The reaction mixture was cooled to 0 °C, sodium bis(trimethylsilyl)amide (5.00 mL, 5.00 mmol, 1 M solution in THF) was added and the reaction stirred for 30 min at 0 °C. Benzyl bromide (0.59 mL, 5.00 mmol) was added and the reaction mixture was stirred at rt for 18 h, quenched with water (30 mL) and extracted with ethyl acetate (3 x 30 mL). The combined organic extracts were dried with sodium sulfate, filtered and the solvent removed under reduced pressure. The crude product was purified by column chromatography (petroleum ether: ethyl acetate, 4:1, column diameter = 4 cm, silica = 18 cm) to give 3-(benzyloxy)dihydrofuran-2(3H)-one **145** (376 mg, 1.95 mmol, 39%) as a pale yellow solid.

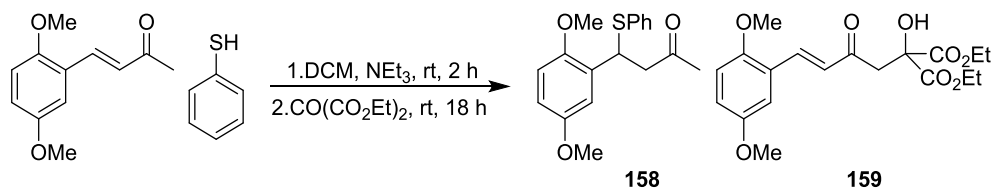
Mp = 29.1– 30.0 °C; R_f = 0.20 (petroleum ether: ethyl acetate, 4:1, visualised with KMnO_4 aq. solution); ^1H NMR (400 MHz, CDCl_3) δ_{H} 7.40 – 7.29 (5H, m, Ar), 4.91 (1H, d, J = 11.8 Hz, H^5), 4.71 (1H, d, J = 11.8 Hz, H^5), 4.45 – 4.31 (1H, m, H^4), 4.21 – 4.15 (2H, m, H^2), 2.49 – 2.39 (1H, m, H^1), 2.31 – 2.18 (1H, m, H^1); ^{13}C NMR (101 MHz, CDCl_3) δ_{C} 175.2 (C^3), 137.0 (Ar), 128.7 (Ar), 128.3 (Ar), 128.2 (Ar), 72.5 ($\text{C}^{2/4/5}$), 72.2 ($\text{C}^{2/4/5}$), 65.6 ($\text{C}^{2/4/5}$), 30.0 (C^1); IR (neat): ν_{max} cm^{-1} 3060 – 2880 (CH), 1768 (C=O); HRMS (pAPCI): calcd $\text{C}_{11}\text{H}_{13}\text{O}_3$ $[\text{M}+\text{H}]^+$: 193.0859; observed: 193.0857; calcd $\text{C}_{11}\text{H}_{12}\text{O}_3\text{NH}_4$ $[\text{M}+\text{NH}_4]^+$: 210.1125; observed: 210.1123.

5.1.14 (*E*)-4-(2,5-Dimethoxyphenyl)but-3-en-2-one **147**

To a Schlenk flask was added 2,5-dimethoxybenzaldehyde (1.66 g, 10.0 mmol), DCM (60 mL) and (acetylmethylene)triphenylphosphorane (3.18 g, 10.0 mmol) under a nitrogen atmosphere. The reaction mixture was heated at reflux for 60 h. The solvent was removed under reduced pressure and the crude product was purified by column chromatography (petroleum ether: diethyl ether, 7:3, column diameter = 4 cm, silica = 18 cm) to give (*E*)-4-(2,5-dimethoxyphenyl)but-3-en-2-one **147** (1.56 g, 7.6 mmol, 76%) as a yellow solid.

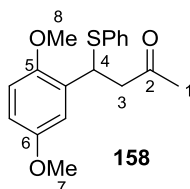
Mp = 49.3 – 51.5 °C (lit. Mp = 48.0 – 50.0 °C¹³⁴); R_f = 0.44 (petroleum ether: diethyl ether 7:3); $^1\text{H NMR}$ (300 MHz, CDCl_3) δ_{H} 7.84 (1H, d, J = 16.5 Hz, H^7), 7.05 (1H, d, J = 3.0 Hz, H^1), 6.91 (1H, dd, J = 9.0, 3.0 Hz, H^3), 6.83 (1H, d, J = 9.0 Hz, H^4), 6.69 (1H, d, J = 16.5 Hz, H^8), 3.83 (3H, s, $\text{H}^{11/12}$), 3.77 (3H, s, $\text{H}^{11/12}$), 2.37 (3H, s, H^{10}); $^{13}\text{C NMR}$ (101 MHz, CDCl_3) δ_{C} 199.3 (C^9), 153.7 ($\text{C}^{2/5}$), 152.9 ($\text{C}^{2/5}$), 138.6 (C^7), 128.0 (C^8), 124.0 (C^6), 117.8 (Ar), 112.6 (Ar), 112.5 (Ar), 56.2 ($\text{C}^{11/12}$), 55.9 ($\text{C}^{11/12}$), 27.2 (C^{10}); IR (neat): ν_{max} cm^{-1} 3002 – 2838 (CH), 1689 (C=O), 1646 (C=C), 1616 (C=C); HRMS (ASAP): calcd $\text{C}_{12}\text{H}_{15}\text{O}_3$ [$\text{M} + \text{H}$] $^+$: 207.1016; observed: 207.1016.

5.1.15 4-(2,5-Dimethoxyphenyl)-4-(phenylthio)butan-2-one **158** and Diethyl (*E*)-2-(4-(2,5-dimethoxyphenyl)-2-oxobut-3-en-1-yl)-2-hydroxymalonate **159**

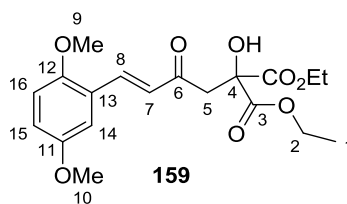


To a Schlenk flask was added (*E*)-4-(2,5-dimethoxyphenyl)but-3-en-2-one **147** (101 mg, 0.49 mmol) and DCM (5 mL) under a nitrogen atmosphere. The solution was cooled to 0 °C and thiophenol (50 μ L, 0.49 mmol) followed by triethylamine (100 μ L, 0.42 mmol) was added dropwise. The reaction was stirred at room temperature for 2 hours then diethyl ketomalonate (150 μ L, 0.98 mmol) was added. The reaction was stirred for a further 18 hours and quenched with 5% NaOH aq. solution (10 mL). The organic layer was separated and the aqueous layer extracted with DCM (3 x 15 mL). The combined organic extracts were washed with brine (50 mL), dried with sodium sulfate, filtered and the solvent removed under reduced pressure. The products were purified through column chromatography (petroleum ether: diethyl ether 1:1, column diameter = 2 cm, silica = 16 cm) to give 4-(2,5-dimethoxyphenyl)-4-(phenylthio)butan-2-one **158** (23 mg, 0.07 mmol, 15% yield) as a yellow solid and diethyl (*E*)-2-(4-(2,5-dimethoxyphenyl)-2-oxobut-3-en-1-yl)-2-hydroxymalonate **159** (28 mg, 0.07 mmol, 15% yield) as a yellow solid.

4-(2,5-Dimethoxyphenyl)-4-(phenylthio)butan-2-one **158**

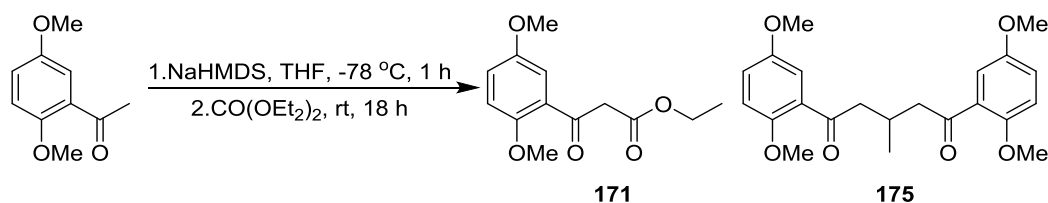


Mp = 72.2 – 72.7 °C; R_f = 0.48 (petroleum ether: diethyl ether, 1: 1); $^1\text{H NMR}$ (400 MHz, CDCl_3) δ_{H} 7.33 – 7.27 (2H, m, Ar), 7.24 – 7.17 (3H, m, Ar), 6.78 – 6.75 (2H, m, Ar), 6.73 – 6.68 (1H, m, Ar), 5.11 (1H, t, J = 7.4 Hz, H^4), 3.76 (3H, s, $\text{H}^{7/8}$), 3.70 (3H, s, $\text{H}^{7/8}$), 3.02 (2H, d, J = 7.4 Hz, H^3), 2.09 (3H, s, H^1); $^{13}\text{C NMR}$ (101 MHz, CDCl_3) δ_{C} 205.9 (C^2), 153.5 ($\text{C}^{5/6}$), 151.0 ($\text{C}^{5/6}$), 134.7 (Ar), 132.7 (Ar), 130.4 (Ar), 128.8 (Ar), 127.4 (Ar), 114.2 (Ar), 113.0 (Ar), 112.2 (Ar), 56.3 ($\text{C}^{7/8}$), 55.8 ($\text{C}^{7/8}$), 49.1 (C^3), 41.7 (C^4), 30.4 (C^1); IR (neat): ν_{max} cm^{-1} 3061 – 2837 (CH), 1713 (C=O); HRMS (pNSI): calcd for $\text{C}_{18}\text{H}_{21}\text{O}_3\text{S}$ [$\text{M}+\text{H}$] $^+$: 317.1206; observed: 317.1209.

Diethyl (E)-2-(4-(2,5-dimethoxyphenyl)-2-oxobut-3-en-1-yl)-2-hydroxymalonate 159

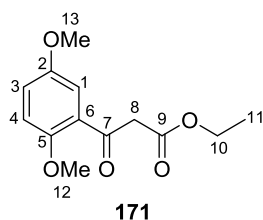
Mp = 73.9 – 74.3 °C; R_f = 0.18 (petroleum ether: diethyl ether, 1: 1); $^1\text{H NMR}$ (400 MHz, CDCl_3) δ_{H} 7.90 (1H, d, J = 16.4 Hz, H^8), 7.04 (1H, d, J = 3.0 Hz, H^{14}), 6.93 (1H, dd, J = 9.0, 3.0 Hz, H^{15}), 6.84 (1H, d, J = 9.0 Hz, H^{16}), 6.73 (1H, d, J = 16.4 Hz, H^7), 4.28 (4H, q, J = 7.1 Hz, H^2), 3.84 (3H, s, ($\text{H}^{9/10}$), 3.77 (3H, s, $\text{H}^{9/10}$), 3.55 (2H, s, H^5), 1.28 (6H, t, J = 7.1 Hz, H^1); $^{13}\text{C NMR}$ (101 MHz, CDCl_3) δ_{C} 197.0 (C^6), 169.7 (C^3), 153.6 ($\text{C}^{11/12}$), 153.2 ($\text{C}^{11/12}$), 139.5 (C^8), 126.6 (C^7), 123.6 (C^{13}), 118.2 (C^{15}), 112.9 (C^{14}), 112.5 (C^{16}), 77.3 (C^4), 62.8 (C^2), 56.1 ($\text{C}^{9/10}$), 55.9 ($\text{C}^{9/10}$), 44.7 (C^5), 14.1 (C^1); IR (neat): ν_{max} cm^{-1} 3475 (OH), 2982-2837 (CH), 1737 (C=O); HRMS (pNSI): calcd for $\text{C}_{19}\text{H}_{25}\text{O}_8$ $[\text{M}+\text{H}]^+$: 381.1544; observed: 381.1543.

5.1.16 Ethyl 3-(2,5-dimethoxyphenyl)-3-oxopropanoate **171** and 1,5-Bis(2,5-dimethoxyphenyl)-3-methylpentane-1,5-dione **175**

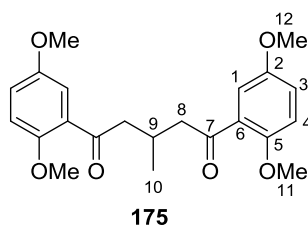


To a Schlenk flask was added (2,5-dimethoxy)acetophenone (0.16 mL, 1.00 mmol) and THF (5 mL) under a nitrogen atmosphere. The solution was cooled to $-78 \text{ }^\circ\text{C}$, sodium bis(trimethylsilyl)amide (1.5 mL, 1.50 mmol, 1 M solution in THF) was added and the reaction mixture stirred for 1 h. Diethyl carbonate (0.18 mL, 1.50 mmol) was added and the reaction mixture was warmed to rt and stirred for 20 h. The reaction mixture was quenched with water (5 mL), acidified with HCl aq. solution (2 M) and extracted with diethyl ether (2 x 10 mL). The combined organic extracts were washed with brine (30 mL), dried with sodium sulfate, filtered and the solvent removed under reduced pressure. The crude product was purified by column chromatography (petroleum ether: diethyl ether, 2: 1, column diameter = 2 cm, silica = 18 cm) to give ethyl 3-(2,5-dimethoxyphenyl)-3-oxopropanoate **171** (96 mg, 0.38 mmol, 38%) as a yellow oily solid and 1,5-bis(2,5-dimethoxyphenyl)-3-methylpentane-1,5-dione **175** (56 mg, 0.14 mmol, 14%) as a light brown solid.

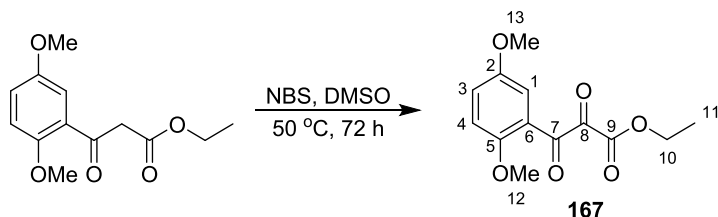
Ethyl 3-(2,5-dimethoxyphenyl)-3-oxopropanoate **171**



Mp = $37.2 - 38.5 \text{ }^\circ\text{C}$; $R_f = 0.28$ (petroleum ether: diethyl ether, 2: 1); $^1\text{H NMR}$ (300 MHz, CDCl_3) δ_{H} 7.39 (1H, d, $J = 3.2 \text{ Hz}$, H^1), 7.05 (1H, dd, $J = 9.1, 3.2 \text{ Hz}$, H^3), 6.88 (1H, d, $J = 9.1 \text{ Hz}$, H^4), 4.16 (2H, q, $J = 7.2 \text{ Hz}$, H^{10}), 3.94 (2H, s, H^8), 3.83 (3H, s, $\text{H}^{12/13}$), 3.77 (3H, s, $\text{H}^{12/13}$), 1.21 (3H, t, $J = 7.2 \text{ Hz}$, H^{11}); $^{13}\text{C NMR}$ (101 MHz, CDCl_3) δ_{C} 192.7 (C^7), 168.2 (C^9), 153.7 ($\text{C}^{2/5}$), 153.4 ($\text{C}^{2/5}$), 126.1 (C^6), 121.7 (C^3), 113.8 (C^1), 113.0 (C^4), 60.9 (C^{10}), 55.7 (C^{12+13}), 50.5 (C^8), 14.1 (C^{11}); IR (neat): $\nu_{\text{max}} \text{ cm}^{-1}$ 2981 – 2842 (CH), 1727 (C=O), 1665 (C=O); HRMS (pNSI): calcd $\text{C}_{13}\text{H}_{17}\text{O}_5$ [$\text{M} + \text{H}$] $^+$: 253.1071; observed: 253.1072.

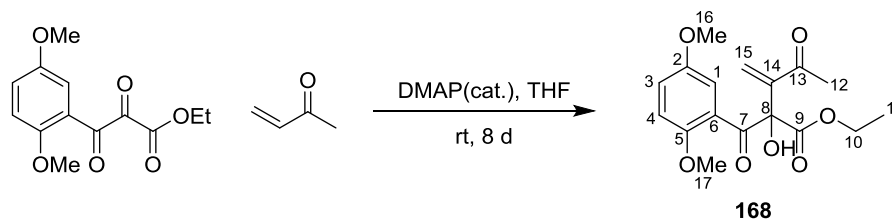
1,5-Bis(2,5-dimethoxyphenyl)-3-methylpentane-1,5-dione 175

Mp = 60.0 - 61.7 °C; R_f = 0.13 (petroleum ether: diethyl ether, 2: 1); ^1H NMR (400 MHz, CDCl_3) δ_{H} 7.19 (2H d, J = 3.2 Hz, H^1), 6.99 (2H, J = 9.0, 3.2 Hz, H^3), 6.87 (2H, d, J = 9.0 Hz, H^4), 3.82 (6H, s, $\text{H}^{11/12}$), 3.78 (6H, s, $\text{H}^{11/12}$), 3.06 (2H, dd, J = 16.1, 6.0 Hz, H^8), 2.89 (2H, dd, J = 16.1, 7.5 Hz, H^8), 2.80 – 2.65 (1H, app dt, J = 13.4, 6.6 Hz, H^9) 1.00 (3H, d, J = 6.6 Hz, H^{10}); ^{13}C NMR (101 MHz, CDCl_3) δ_{C} 201.9 (C^7), 153.5 ($\text{C}^{2/5}$), 152.9 ($\text{C}^{2/5}$), 129.1 (C^6), 119.6 (C^3), 114.1 (C^1), 113.2 (C^4), 56.1 ($\text{C}^{11/12}$), 55.9 ($\text{C}^{11/12}$), 50.6 (C^8), 26.6 (C^9), 20.6 (C^{10}); IR (neat): ν_{max} cm^{-1} 2956 – 2835 (CH), 1669 (C=O); HRMS (pNSI): calcd $\text{C}_{23}\text{H}_{26}\text{O}_6$ [$\text{M} + \text{H}$] $^+$: 387.1802; observed: 387.1795.

5.1.17 Ethyl 3-(2,5-dimethoxyphenyl)-2,3-dioxopropanoate **167**

To a round bottomed flask was added ethyl 3-(2,5-dimethoxyphenyl)-3-oxopropanoate **171** (482 mg, 1.9 mmol), *N*-bromosuccinimide (338 mg, 1.9 mmol) and DMSO (10 mL). The reaction mixture was heated at 50 °C for 72 h then poured into saturated aq. NaHCO₃ solution (10 mL) and extracted with DCM (3 x 20 mL). The combined organic extracts were washed with brine (50 mL), dried with sodium sulfate, filtered and the solvent removed under reduced pressure. The crude product was purified by column chromatography (petroleum ether: ethyl acetate, 2: 1, column diameter = 4 cm, silica = 18 cm) to give ethyl 3-(2,5-dimethoxyphenyl)-2,3-dioxopropanoate **167** (374 mg, 1.4 mmol, 74%) as a yellow oil.

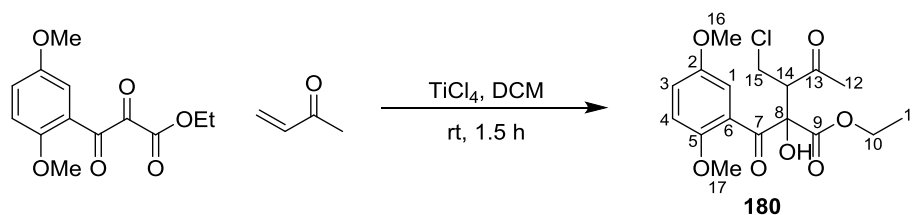
R_f = 0.32 (petroleum ether: ethyl acetate, 2: 1); ¹H NMR (400 MHz, CDCl₃) δ_H 7.42 (1H, d, J = 3.2 Hz, H¹), 7.19 (1H, dd, J = 9.1, 3.2 Hz, H³), 6.94 (1H, d, J = 9.1 Hz, H⁴), 4.36 (2H, q, J = 7.1 Hz, H¹⁰), 3.81 (3H, s, H^{12/13}), 3.75 (3H, s, H^{12/13}), 1.31 (3H, t, J = 7.1 Hz, H¹¹); ¹³C NMR (101 MHz, CDCl₃) δ_C 192.0 (C⁷), 183.5 (C⁸), 158.6 (C⁹), 155.4 (C^{2/5}), 154.7 (C^{2/5}), 125.3 (C³), 122.7 (C⁶), 114.2 (C⁴), 111.3 (C¹), 63.0 (C¹⁰), 56.7 (C^{12/13}), 56.0 (C^{12/13}), 14.1 (C¹¹); IR (neat): ν_{max} cm⁻¹ 3061 – 2840 (CH), 1760 (C=O), 1732 (C=O), 1666 (C=O); HRMS (pNSI): calcd C₁₃H₁₅O₆ [M + H]⁺: 267.0863; observed: 267.0864.

5.1.18 Ethyl 2-(2,5-dimethoxybenzoyl)-2-hydroxy-3-methylene-4-oxopentanoate **168**

To a Schlenk flask was added ethyl 3-(2,5-dimethoxyphenyl)-2,3-dioxopropanoate **167** (50 mg, 0.19 mmol), 4-dimethylaminopyridine (2 mg, 0.02 mmol) and THF (3 mL) under a nitrogen atmosphere. To the stirred solution was added methyl vinyl ketone (31 μ L, 0.38 mmol) and the reaction mixture was stirred at rt for 8 d. The solvent was removed under a stream of nitrogen and the crude product purified by column chromatography (petroleum ether: ethyl acetate, 2: 1, column diameter = 1 cm, silica = 15 cm) to give ethyl 2-(2,5-dimethoxybenzoyl)-2-hydroxy-3-methylene-4-oxopentanoate **168** (11 mg, 0.03 mmol, 17%) as a brown oil.

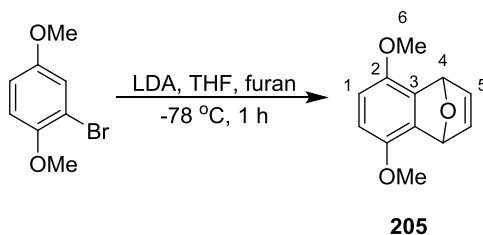
R_f = 0.13 (petroleum ether: ethyl acetate, 2: 1); ^1H NMR (300 MHz, CDCl_3) δ_{H} 7.16 (1H, d, J = 3.2 Hz, H^1), 7.01 (1H, dd, J = 9.0, 3.2 Hz, H^3), 6.85 (1H, d, J = 9.0 Hz, H^4), 6.28 (1H, d, J = 1.3 Hz, H^{15}), 6.02 (1H, d, J = 1.3 Hz, H^{15}), 4.35 (2H, qd, J = 7.1, 2.4 Hz, H^{10}), 3.81 (3H, s, $\text{H}^{16/17}$), 3.75 (3H, s, $\text{H}^{16/17}$), 2.38 (3H, s, H^{12}), 1.30 (3H, t, J = 7.1 Hz, H^{11}); ^{13}C NMR (101 MHz, CDCl_3) δ_{C} 199.0 ($\text{C}^{7/13}$), 198.8 ($\text{C}^{7/13}$), 169.1 (C^9), 154.2 ($\text{C}^{2/5}$), 151.6 ($\text{C}^{2/5}$), 148.4 (C^{14}), 127.6 (C^{15}), 127.2 (C^6), 120.1 (C^3), 115.1 (C^1), 112.7 (C^4), 84.9 (C^8), 62.8 (C^{10}), 56.0 ($\text{C}^{16/17}$), 55.8 ($\text{C}^{16/17}$), 26.5 (C^{12}), 14.2 (C^{11}); IR (neat): ν_{max} cm^{-1} 3483 (OH), 2923 – 2853 (CH), 1737 (C=O), 1708 (C=O), 1687 (C=O); HRMS (pNSI): calcd $\text{C}_{17}\text{H}_{22}\text{NO}_6$ $[\text{M}-\text{H}_2\text{O}+\text{NH}_4]^+$: 336.1447; observed: 336.1439.

5.1.19 Ethyl 3-(chloromethyl)-2-(2,5-dimethoxybenzoyl)-2-hydroxy-4-oxopentanoate **180**



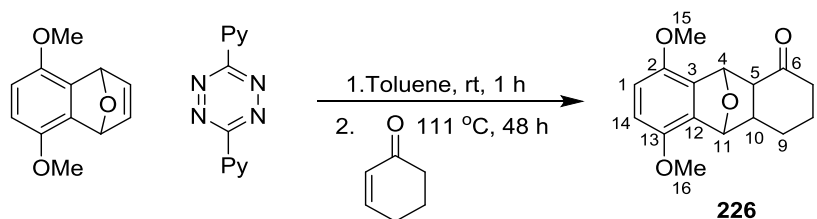
To a Schlenk flask was added ethyl 3-(2,5-dimethoxyphenyl)-2,3-dioxopropanoate **167** (32 mg, 0.12 mmol), DCM (1 mL) and methyl vinyl ketone (30 μ L, 0.36 mmol) under a nitrogen atmosphere at rt. To this was added titanium (IV) chloride (120 μ L, 0.12 mmol, 1 M solution in DCM) and the solution was stirred at rt for 1.5 h. The reaction was quenched with water (2 mL) and extracted with DCM (3 x 5 mL). The combined organic extracts were dried with sodium sulfate, filtered and the solvent removed under reduced pressure. The crude product was purified by column chromatography (petroleum ether: diethyl ether, 3: 2, column diameter = 1 cm, silica = 17cm) to give ethyl 3-(chloromethyl)-2-(2,5-dimethoxybenzoyl)-2-hydroxy-4-oxopentanoate **180** (14 mg, 0.04 mmol, 31%) as a brown oil.

R_f = 0.18 (petroleum ether: diethyl ether, 3: 2); $^1\text{H NMR}$ (300 MHz, CDCl_3) δ_{H} 7.11 – 6.99 (2H, m, Ar), 6.85 (1H, d, J = 8.8 Hz, Ar), 4.71 ppm (1H, br s, OH), 4.28 (2H, q, J = 7.2 Hz, H^{10}), 4.00 (1H, dd, J = 9.0, 4.4 Hz, H^{14}), 3.88 (1H, dd, J = 11.6, 4.4 Hz, H^{15}), 3.78 (3H, s, $\text{H}^{16/17}$), 3.77 (1H, dd, J = 11.6, 9.0 Hz, H^{15}), 3.75 (3H, s, $\text{H}^{16/17}$), 2.41 (3H, s, H^{12}), 1.27 (3H, t, J = 7.2 Hz, H^{11}); $^{13}\text{C NMR}$ (101 MHz, CDCl_3) δ_{C} 209.7 (C^{13}), 199.0 (C^7), 168.3 (C^9), 154.1 ($\text{C}^{2/5}$), 151.8 ($\text{C}^{2/5}$), 126.2 (Ar), 120.8 (Ar), 115.1 (Ar), 112.7 (Ar), 85.4 (C^8), 62.8 (C^{10}), 57.9 (C^{14}), 56.0 ($\text{C}^{16/17}$), 55.6 ($\text{C}^{16/17}$), 40.9 (C^{15}), 32.8 (C^{12}), 14.2 (C^{11}); IR (neat): ν_{max} cm^{-1} 3474 (OH), 2954 – 2838 (CH), 1716 (C=O); HRMS (pNSI): calcd $\text{C}_{17}\text{H}_{22}\text{ClO}_7$ [$\text{M}+\text{H}$] $^+$: 373.1049; observed: 373.1052; calcd $\text{C}_{17}\text{H}_{23}\text{ClO}_6\text{N}$ [$\text{M}-\text{H}_2\text{O}+\text{NH}_4$] $^+$: 373.1208; observed: 373.1213.

5.1.20 5,8-Dimethoxy-1,4-dihydro-1,4-epoxynaphthalene **205**

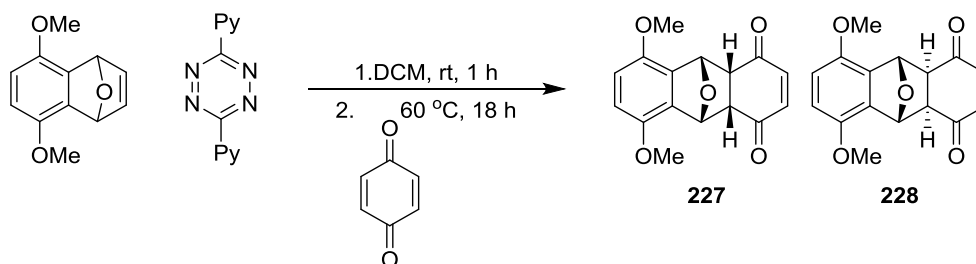
To a Schlenk flask was added THF (6 mL) and diisopropylamine (0.57 mL, 4.08 mmol) under a nitrogen atmosphere. The solution was cooled to $-78\text{ }^{\circ}\text{C}$, *n*-butyllithium (1.32 mL, 3.30 mmol, 2.5 M in hexanes) was added dropwise and the solution was stirred at $-78\text{ }^{\circ}\text{C}$ for 40 min. Furan (4.40 mL, 60.00 mmol) was added to the reaction vessel followed by a solution of 1-bromo-2,4-dimethoxybenzene (0.45 mL, 3.00 mmol) in THF (1.5 mL) dropwise. The reaction mixture was stirred at $-78\text{ }^{\circ}\text{C}$ for 1 h then quenched with water (20 mL), extracted with diethyl ether (3 x 40 mL), dried with sodium sulfate, filtered and the solvent removed under reduced pressure. The crude product was purified by column chromatography (petroleum ether: diethyl ether, 3:1, column diameter = 2 cm, silica = 18 cm) to give 5,8-dimethoxy-1,4-dihydro-1,4-epoxynaphthalene **205** (522 mg, 2.56 mmol, 85%) as a white solid.¹²³

Mp = $86.4 - 86.6\text{ }^{\circ}\text{C}$ (lit. Mp = $86.0 - 87.0\text{ }^{\circ}\text{C}$ ¹²³); $R_f = 0.22$ (petroleum ether: diethyl ether, 3:1); $^1\text{H NMR}$ (300 MHz, CDCl_3) δ_{H} 7.07 (2H, app t, $J = 1.0\text{ Hz}$, H^5), 6.54 (2H, s, H^1), 5.93 (2H, t, $J = 1.0\text{ Hz}$, H^4), 3.79 (6H, s, H^6); $^{13}\text{C NMR}$ (75 MHz, CDCl_3) δ_{C} 148.1 (C^2), 143.1 (C^3), 137.6 (C^5), 111.8 (C^1), 80.5 (C^4), 56.6 (C^6); IR (neat): $\nu_{\text{max}}\text{ cm}^{-1}$ 2959 – 2832 (CH); HRMS (pAPCI): calcd for $\text{C}_{12}\text{H}_{13}\text{O}_3$ $[\text{M}+\text{H}]^+$: 205.0859; observed: 205.0863.

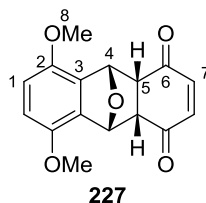
5.1.21 5,8-Dimethoxy-3,4,4a,9,9a,10-hexahydro-9,10-epoxyanthracen-1(2*H*)-one **226**

To a Schlenk flask was added 3,6-di-2-pyridyl-1,2,4,5-tetrazine (24 mg, 0.10 mmol) toluene (2 mL) and 5,8-dimethoxy-1,4-dihydro-1,4-epoxynaphthalene **205** (20 mg, 0.10 mmol) under a nitrogen atmosphere in the dark. The reaction mixture was stirred at rt for 1 h then cyclohex-2-en-1-one (10 μ L, 0.10 mmol) was added and the reaction mixture was stirred at reflux for 48 h. The solvent was removed under reduced pressure and the crude product was purified by column chromatography (petroleum ether: ethyl acetate, 1: 1, column diameter = 1 cm, silica = 15 cm) to give to give 5,8-dimethoxy-3,4,4a,9,9a,10-hexahydro-9,10-epoxyanthracen-1(2*H*)-one **226** (11 mg, 0.04 mmol, 40%) as a brown solid.

Mp = 144.5 – 144.8 °C (decomposed); R_f = 0.20 (petroleum ether: ethyl acetate, 5: 1); $^1\text{H NMR}$ (300 MHz, CDCl_3) δ_{H} 6.65 (1H, app s, $\text{H}^{1/14}$), 6.64 (1H, app s, $\text{H}^{1/14}$), 5.92 (1H, d, $J = 1.0$ Hz, $\text{H}^{4/11}$), 5.26 (1H, d, $J = 1.0$ Hz, $\text{H}^{4/11}$), 3.80 (3H, s, $\text{H}^{15/16}$), 3.79 (3H, s, $\text{H}^{15/16}$), 2.51 – 2.25 (4H, m, H^{5+10+7}), 2.25 – 2.15 (1H, m, $\text{H}^{8/9}$), 2.04 – 1.91 (1H, m, $\text{H}^{8/9}$), 1.79 – 1.64 (1H, m, $\text{H}^{8/9}$), 1.53 – 1.41 (1H, m, $\text{H}^{8/9}$); $^{13}\text{C NMR}$ (75 MHz, CDCl_3) δ_{C} 211.8 (C^6), 146.8 ($\text{C}^{2/13}$), 146.6 ($\text{C}^{2/13}$), 134.7 ($\text{C}^{3/12}$), 133.5 ($\text{C}^{3/12}$), 111.5 ($\text{C}^{1/14}$), 111.4 ($\text{C}^{1/14}$), 82.1 ($\text{C}^{4/11}$), 79.9 ($\text{C}^{4/11}$), 56.3 ($\text{C}^{15/16}$), 56.2 ($\text{C}^{15/16}$), 51.6 (C^5), 42.2 (C^{10}), 39.1 (C^7), 28.0 ($\text{C}^{8/9}$), 20.8 ($\text{C}^{8/9}$); IR (neat): ν_{max} cm^{-1} 2961 – 2835 (CH), 1699 (C=O); MS (pNSI): 257.1 (71%, $[\text{M}-\text{H}_2\text{O}+\text{H}]^+$), 275.1 (49%, $[\text{M}+\text{H}]^+$); HRMS (pNSI): calcd for $\text{C}_{16}\text{H}_{18}\text{O}_4\text{H}$ $[\text{M}+\text{H}]^+$; 275.1278; observed: 275.1279.

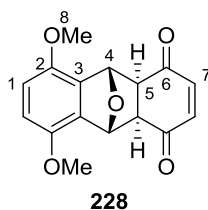
5.1.22 5,8-Dimethoxy-4a,9,9a,10-tetrahydro-9,10-epoxyanthracene-1,4-dione **227** and **228**

To a Schlenk flask was added 3,6-di-2-pyridyl-1,2,4,5-tetrazine (26 mg, 0.11 mmol), toluene (2 mL) and 5,8-dimethoxy-1,4-dihydro-1,4-epoxynaphthalene **205** (20 mg, 0.10 mmol) under a nitrogen atmosphere in the dark. The reaction mixture was stirred at rt for 1 h, *p*-benzoquinone (12 mg, 0.11 mmol) was added and the reaction mixture was stirred at 60 °C for 18 h. The solvent was removed under reduced pressure and the crude product purified by column chromatography (petroleum ether: ethyl acetate, 5: 1, column diameter = 2 cm, silica = 20 cm) to give two diastereomers of 5,8-dimethoxy-4a,9,9a,10-tetrahydro-9,10-epoxyanthracene-1,4-dione (major **227** - 22 mg, 0.08 mmol, 77%, minor **228** - 4 mg, 0.01 mmol, 14%) as yellow-brown solids.

Endo 5,8-dimethoxy-4a,9,9a,10-tetrahydro-9,10-epoxyanthracene-1,4-dione 227 (major diastereomer)

Mp = 133.2 – 134.1 °C; R_f = 0.23 (petroleum ether: ethyl acetate, 5: 1); ^1H NMR (300 MHz, CDCl_3) δ_{H} 6.64 (2H, s, H^1), 5.99 (2H, s, H^7), 5.93 (2H, dd, J = 3.5, 1.9 Hz, H^4), 3.75 (6H, s, H^8), 3.51 (2H, dd, J = 3.5, 1.9 Hz, H^5); ^{13}C NMR (75 MHz, CDCl_3) δ_{C} 195.0 (C^6), 147.5 (C^2), 138.7 (C^7), 131.2 (C^3), 112.8 (C^1), 80.7 (C^4), 56.4 (C^8), 49.0 (C^5); IR (neat): ν_{max} cm^{-1} 2962 – 2850 (CH), 1667 (C=O); MS (pNSI): 287.1 (100%, $[\text{M}+\text{H}]^+$), 309.1 (40%, $[\text{M}+\text{Na}]^+$), 325.0 (15%, $[\text{M}+\text{K}]^+$); HRMS (pNSI): calcd for $\text{C}_{16}\text{H}_{14}\text{O}_5\text{H}$ $[\text{M}+\text{H}]^+$: 287.0914; observed: 287.0916.

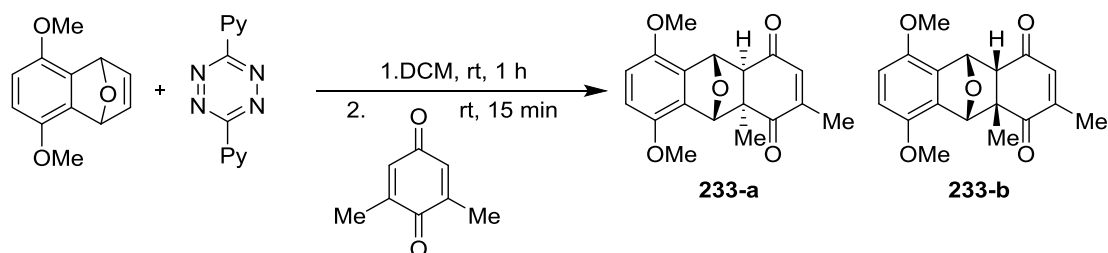
Note: The relative stereochemistry was determined through analysis of the X-ray crystal structure of the product.

Exo 5,8-dimethoxy-4a,9,9a,10-tetrahydro-9,10-epoxyanthracene-1,4-dione 228 (minor diastereomer)

Mp = 167.2 – 167.8 °C; R_f = 0.50 (petroleum ether: ethyl acetate, 5: 1); $^1\text{H NMR}$ (300 MHz, CDCl_3) δ_{H} 6.83 (2H, s, H^7), 6.70 (2H, s, H^1), 5.80 (2H, s, H^4), 3.83 (6H, s, H^8), 2.88 (2H, s, H^5); $^{13}\text{C NMR}$ (75 MHz, CDCl_3) δ_{C} 196.8 (C^6), 146.8 (C^2), 142.0 (C^7), 133.0 (C^3), 112.1 (C^1), 82.8 (C^4), 56.2 (C^8), 50.6 (C^5); IR (neat): ν_{max} cm^{-1} 2953 – 2852 (CH), 1668 (C=O); HRMS (pNSI): calcd for $\text{C}_{16}\text{H}_{14}\text{O}_5\text{H} [\text{M}+\text{H}]^+$: 287.0914; observed: 287.0917.

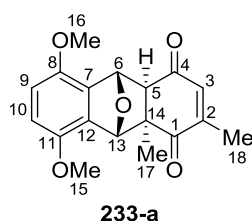
Note: Sample of **228** used for analysis was obtained in collaboration with L. Micheron.

5.1.23 5,8-Dimethoxy-2,9a-dimethyl-4a,9,9a,10-tetrahydro-9,10-epoxyanthracene-1,4-dione **233-a** and **233-b**

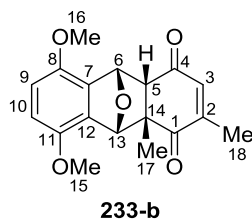


To a Schlenk flask was added 3,6-di-2-pyridyl-1,2,4,5-tetrazine (814 mg, 3.5 mmol) and DCM (40 mL) under a nitrogen atmosphere at rt. The solution was cooled to 0 °C and a solution of 5,8-dimethoxy-1,4-dihydro-1,4-epoxynaphthalene **205** (640 mg, 3.1 mmol) in DCM (10 mL) was added dropwise. The reaction mixture was stirred at rt for 1 h, 2,6-dimethylbenzoquinone (470 mg, 3.5 mmol) was added and stirring continued for 15 min. The reaction mixture was diluted with DCM (30 mL) and washed sequentially with HCl aq. solution (3 x 100 mL, 0.5 M), saturated aq. NaHCO₃ solution (100 mL) and brine (100 mL). The organic extract was dried with sodium sulfate, filtered and the solvent removed under reduced pressure. The ¹H NMR spectrum of the crude product showed a mixture of diastereomers in a 1.0: 0.9 ratio. The crude product was purified by column chromatography (petroleum ether: ethyl acetate 4: 1, column diameter = 4 cm, silica = 17 cm), to give two diastereomers of 5,8-dimethoxy-2,9a-dimethyl-4a,9,9a,10-tetrahydro-9,10-epoxyanthracene-1,4-dione (major **233-a** - 305 mg, 1.0 mmol, 31%, minor **233-b** - 266 mg, 0.8 mmol, 27%) as yellow solids.

Exo 5,8-dimethoxy-2,9a-dimethyl-4a,9,9a,10-tetrahydro-9,10-epoxyanthracene-1,4-dione **233-a (major diastereomer)**

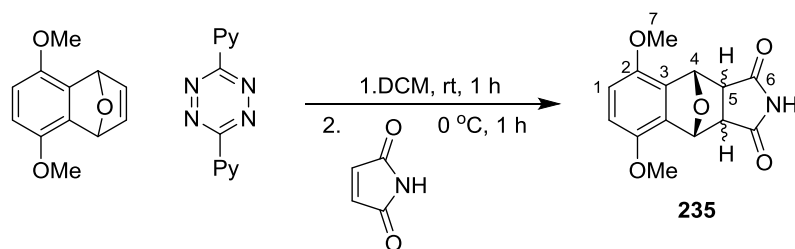


Mp = 109.4 – 110.1 °C; R_f = 0.32 (petroleum ether: ethyl acetate 3: 1); ¹H NMR (300 MHz, CDCl₃) δ_H 6.76 – 6.73 (1H, m, H³), 6.72 (2H, app s, H⁹⁺¹⁰), 5.68 (1H, d, J = 1.2 Hz, H^{6/13}), 5.63 (1H, d, J = 1.2 Hz, H^{6/13}), 3.83 (3H, s, H^{15/16}), 3.82 (3H, s, H^{15/16}), 2.42 (1H, s, H⁵), 2.09 (3H, d, J = 1.4 Hz, H¹⁸), 0.94 (3H, s, H¹⁷); ¹³C NMR (75 MHz, CDCl₃) δ_C 201.5 (C^{1/4}), 196.9 (C^{1/4}), 151.7 (C²), 148.9 (C^{8/11}), 146.4 (C^{8/11}), 139.2 (C³), 133.8 (C^{7/12}), 131.0 (C^{7/12}), 112.4 (C^{9/10}), 111.4 (C^{9/10}), 86.1 (C^{6/13}), 83.2 (C^{6/13}), 59.4 (C⁵), 56.2 (C^{15/16}), 56.1 (C^{15/16}), 53.8 (C¹⁴), 22.4 (C¹⁷), 17.3 (C¹⁸); IR (neat): ν_{max} cm⁻¹ 2962 – 2842 (CH), 1658 (C=O); HRMS (pNSI): calcd for C₁₈H₁₈O₅H [M+H]⁺: 315.1226; observed: 315.1227.

Endo 5,8-dimethoxy-2,9a-dimethyl-4a,9,9a,10-tetrahydro-9,10-epoxyanthracene-1,4-dione 233-b (minor diastereomer)

Mp = 181.0 - 181.1 °C; R_f = 0.19 (petroleum ether: ethyl acetate 3: 1); ^1H NMR (300 MHz, CDCl_3) δ_{H} 6.66 (1H, d, J = 8.8 Hz, $\text{H}^{9/10}$), 6.58 (1H, d, J = 8.8 Hz, $\text{H}^{9/10}$), 5.95 - 5.82 (1H, m, H^3), 5.87 (1H, dd, J = 5.4, 1.0 Hz, H^6), 5.35 (1H, br d, J = 1.0 Hz, H^{13}), 3.75 (3H, s, $\text{H}^{15/16}$), 3.74 (3H, s, $\text{H}^{15/16}$), 3.13 (1H, dd, J = 5.4, 0.8 Hz, H^5), 1.59 (3H, s, H^{17}), 1.55 (3H, d, J = 1.4 Hz); ^{13}C NMR (75 MHz, CDCl_3) δ_{C} 198.6 (C^1), 195.3 (C^4), 148.4 (C^2), 147.9 ($\text{C}^{8/11}$), 147.1 ($\text{C}^{8/11}$), 136.2 (C^3), 131.6 (C^7), 130.9 (C^{12}), 113.0 ($\text{C}^{9/10}$), 112.3 ($\text{C}^{9/10}$), 86.0 (C^{13}), 81.4 (C^6), 58.1 (C^5), 56.4 ($\text{C}^{15/16}$), 56.1 ($\text{C}^{15/16}$), 53.1 (C^{14}), 24.2 (C^{17}), 16.2 (C^{18}); IR (neat): ν_{max} cm^{-1} 2965 – 2843 (CH), 1656 (C=O); HRMS (pNSI): calcd for $\text{C}_{18}\text{H}_{18}\text{O}_5\text{H}^+ [M+\text{H}]^+$: 315.1231; observed: 315.1227.

Note: The relative stereochemistry of **233-b** was determined through analysis of the X-ray crystal structure of the product.

5.1.24 5,8-Dimethoxy-3a,4,9,9a-tetrahydro-1H-4,9-epoxybenzo[f]isoindole-1,3(2H)-dione **235**

To a Schlenk flask was added 3,6-di-2-pyridyl-1,2,4,5-tetrazine (26 mg, 0.11 mmol), DCM (2 mL) and 5,8-dimethoxy-1,4-dihydro-1,4-epoxynaphthalene **205** (20 mg, 0.11 mmol) under a nitrogen atmosphere in the dark. The reaction mixture was stirred at rt for 1 h, diluted with DCM (4 mL), cooled to 0 °C and maleimide (10 mg, 0.11 mmol) was added. The reaction mixture was stirred at 0 °C for 1 h and the solvent was removed under reduced pressure. The residue was dissolved in ethyl acetate (10 mL) and washed with HCl aq. solution (3 x 15 mL, 0.5 M). The organic layer was washed with saturated aq. NaHCO₃ solution (15 mL), dried with sodium sulfate, filtered and the solvent removed under reduced pressure to give 5,8-dimethoxy-3a,4,9,9a-tetrahydro-1H-4,9-epoxybenzo[f]isoindole-1,3(2H)-dione **235** (30 mg, 0.11 mmol, 99%) as a pale brown solid, as a 1: 2 mixture of diastereomers.

Mp = 184.1 - 186.0 °C; R_f = 0.30 (petroleum ether: ethyl acetate, 1: 1); IR (neat): ν_{\max} cm⁻¹ 3304 (NH), 3215 (NH), 2948 – 2838 (CH), 1706 (C=O); MS (pNSI) 293.1 (100%, [M+NH₄]⁺), 298.1 (89%, [M+Na]⁺); HRMS (pNSI): calcd for C₁₄H₁₃NO₅NH₄ [M+NH₄]⁺: 293.1132; observed: 293.1136.

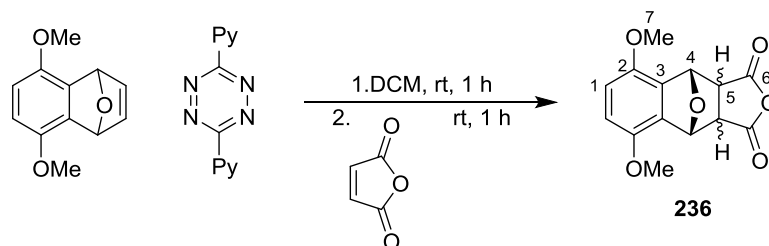
Major diastereomer

¹H NMR (300 MHz, CDCl₃) δ_H 8.51 (s, 1H, NH), 6.63 (2H, s, H¹), 5.78 (2H, s, H⁴), 3.74 (6H, s, H⁷), 2.95 (2H, s, H⁵); ¹³C NMR (75 MHz, CDCl₃) δ_C 175.9 (C⁶), 146.9 (C²), 132.5 (C³), 112.1 (C¹), 79.7 (C⁴), 56.0 (C⁷), 50.2 (C⁵).

Minor diastereomer

¹H NMR (300 MHz, CDCl₃) δ_H 7.37 (s, 1H, NH), 6.67 (2H, s, H¹), 5.82 (2H, dd, J = 3.9, 1.9 Hz, H⁴), 3.73 (6H, s, H⁷), 3.70 (2H, dd, J = 3.9, 1.9 Hz, H⁵); ¹³C NMR (75 MHz, CDCl₃) δ_C 173.5 (C⁶), 147.5 (C²), 130.0 (C³), 113.1 (C¹), 78.5 (C⁴), 56.3 (C⁷), 49.5 (C⁵).

5.1.25 5,8-dimethoxy-3a,4,9,9a-tetrahydro-4,9-epoxynaphtho[2,3-c]furan-1,3-dione



To a Schlenk flask was added 3,6-di-2-pyridyl-1,2,4,5-tetrazine (236 mg, 1.0 mmol) and DCM (4 mL) under a nitrogen atmosphere. The suspension was cooled to 0 °C and a solution of 5,8-dimethoxy-1,4-dihydro-1,4-epoxynaphthalene **205** (185 mg, 0.9 mmol) in DCM (2 mL) was added dropwise. The reaction mixture was stirred at room temperature for 1 h then maleic anhydride (98 mg, 1.0 mmol) was added in portions over 2 min. The reaction mixture was stirred at rt for 1 h, diluted with DCM (5 mL) and washed with HCl aq. solution (3 x 10 mL, 0.5 M). The organic layer was washed with saturated aq. NaHCO₃ solution (10 mL), dried with sodium sulfate, filtered and the solvent removed under reduced pressure to give 5,8-dimethoxy-3a,4,9,9a-tetrahydro-4,9-epoxynaphtho[2,3-c]furan-1,3-dione **236** (171 mg, 0.6 mmol, 68%) as an off-white solid, as a 1.0: 1.4 mixture of diastereomers.

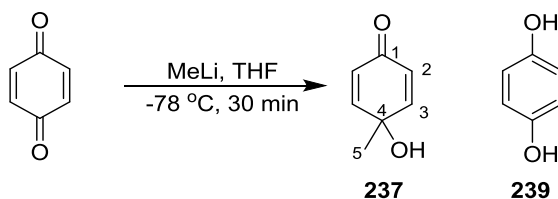
Mp = 144.8 – 145.1 °C; IR (neat): ν_{\max} cm⁻¹ 2963 – 2839 (CH), 1775 (C=O); HRMS (pAPCI): calcd for C₁₄H₁₃O₆ [M+H]⁺: 277.0707; observed: 277.0709; calcd for C₁₄H₁₆O₆N [M+NH₄]⁺: 294.0972; observed: 294.0975.

Major diastereomer

¹H NMR (400 MHz, CDCl₃) δ_{H} 6.72, (2H, s, H¹), 5.94 (2H, s, H⁴), 3.80 (6H, s, H⁷), 3.26 (2H, s, H⁵); ¹³C NMR (101 MHz, CDCl₃) δ_{C} 170.1 (C⁶), 147.0 (C²), 131.8 (C³), 112.4 (C¹), 80.8 (C⁴), 56.0 (C⁷), 50.1 (C⁵)

Minor diastereomer

¹H NMR (400 MHz, CDCl₃) δ_{H} 6.77 (2H, s, H¹), 5.95 – 5.94 (2H, m, H⁴), 3.99 (2H, dd, *J* = 3.7, 2.0 Hz H⁵), 3.79 (6H, s, H⁷); ¹³C NMR (101 MHz, CDCl₃) δ_{C} 167.4 (C⁶), 147.4 (C²), 129.5 (C³), 113.6 (C¹), 79.1 (C⁴), 56.3 (C⁷), 49.7 (C⁵).

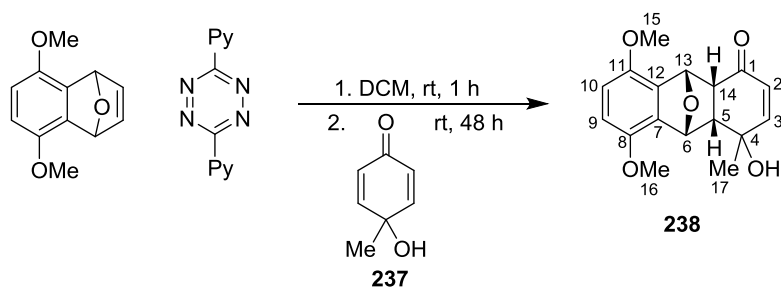
5.1.26 4-Hydroxy-4-methylcyclohexa-2,5-dien-1-one **237**

To a Schlenk flask was added *p*-benzoquinone (540 mg, 5.00 mmol) and THF (100 mL) under a nitrogen atmosphere. The solution was cooled to $-78\text{ }^\circ\text{C}$ and methyllithium (3.12 mL, 1.6 M solution in diethyl ether) was added dropwise. The reaction mixture was stirred at $-78\text{ }^\circ\text{C}$ for 30 min then quenched with saturated aq. ammonium chloride solution (150 mL) and extracted with DCM (3 x 200 mL). The combined organic extracts were washed with water (3 x 200 mL), dried with magnesium sulfate, filtered and the solvent removed under reduced pressure. The crude product was purified by column chromatography (petroleum ether: diethyl ether, 4: 1, 0.1% diethylamine, column diameter = 3 cm, silica = 20 cm) to give 4-hydroxy-4-methylcyclohexa-2,5-dien-1-one **237** (172 mg, 1.40 mmol, 28%) as a pale brown solid (Note: the isolated product contained ~ 6% hydroquinone **239** impurity as determined by analysis of the ^1H NMR spectrum of the sample).¹²⁷

Mp = $58.6 - 59.1\text{ }^\circ\text{C}$; $R_f = 0.05$ (petroleum ether: diethyl ether, 2: 1, 0.1% diethylamine); ^1H NMR (300 MHz, CDCl_3) δ_{H} 6.84 (2H, d, $J = 10.1\text{ Hz}$, H^3), 6.01 (2H, d, $J = 10.1\text{ Hz}$, H^2), 1.39 (3H, s, H^5); ^{13}C NMR (75 MHz, CDCl_3) δ_{C} 186.2 (C^1), 153.3 (C^3), 126.6 (C^2), 67.1 (C^4), 26.7 (C^5); IR (neat): $\nu_{\text{max}}\text{ cm}^{-1}$ 3425 (OH), 2979 - 2873 (CH), 1660 (C=O), 1616 (C=C); HRMS (pAPCI): calcd for $\text{C}_7\text{H}_7\text{O}_2$ $[\text{M}-\text{H}]^+$: 123.0441; observed: 123.0437; calcd for $\text{C}_7\text{H}_8\text{O}_2$ $[\text{M}]^+$: 124.0519; observed: 124.0515; calcd for $\text{C}_7\text{H}_8\text{O}_2\text{H}$ $[\text{M}+\text{H}]^+$: 125.0597; observed: 125.0593.

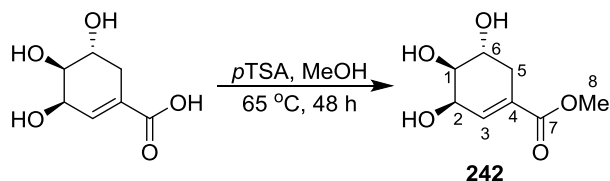
NMR data of hydroquinone 239 impurity

^1H NMR (300 MHz, CDCl_3) δ_{H} 6.61 (4H, s), ^{13}C NMR (75 MHz, CDCl_3) δ_{C} 149.5, 116.2.

5.1.27 4-Hydroxy-5,8-dimethoxy-4-methyl-4a,9,9a,10-tetrahydro-9,10-epoxyanthracen-1(4H)-one **238**

To a Schlenk flask was added 3,6-di-2-pyridyl-1,2,4,5-tetrazine (61 mg, 0.26 mmol) and DCM (1 mL) under a nitrogen atmosphere at rt. The stirred suspension was cooled to 0 °C and a solution of 5,8-dimethoxy-1,4-dihydro-1,4-epoxynaphthalene **205** (53 mg, 0.26 mmol) in DCM (1 mL) was added dropwise. The reaction mixture was stirred at rt for 1 h then a solution of 4-hydroxy-4-methylcyclohexa-2,5-dien-1-one (32 mg, 0.26 mmol) in DCM (1 mL) was added. The reaction mixture was stirred at rt for 48 h, diluted with DCM (3 mL) and washed with HCl aq. solution (3 x 5 mL, 0.5 M). The organic layer was washed with saturated aq. NaHCO₃ solution (5 mL), brine (5 mL) and dried with sodium sulfate, filtered and the solvent removed under reduced pressure to give 4-hydroxy-5,8-dimethoxy-4-methyl-4a,9,9a,10-tetrahydro-9,10-epoxyanthracen-1(4H)-one **238** (72 mg, 0.24 mmol, 92%) as a brown solid.

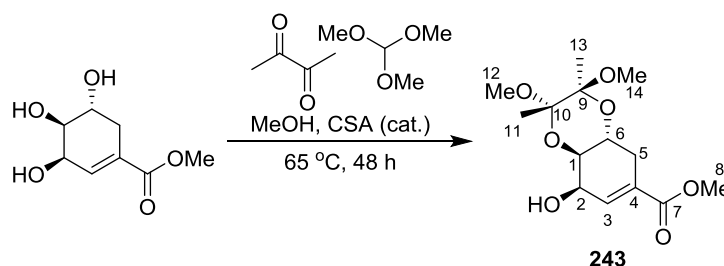
Mp = 171.7 – 173.0 °C; ¹H NMR (300 MHz, CDCl₃) δ_H 6.70 (1H, d, *J* = 8.9 Hz, H⁹), 6.65 (1H, d, *J* = 8.9 Hz, H¹⁰), 5.98 (1H, dd, *J* = 10.2, 1.7 Hz, H³), 5.80 (1H, d, *J* = 5.7 Hz, H¹³), 5.64 (1H, d, *J* = 4.7 Hz, H⁶), 5.00 (1H, d, *J* = 10.2 Hz, H²), 3.87 (3H, s, H¹⁵), 3.82 (1H, m, OH), 3.74 (3H, s, H¹⁶), 3.26 (1H, dd, *J* = 9.2, 5.7 Hz, H¹⁴), 3.11 (1H, ddd, *J* = 9.2, 4.7, 1.7 Hz, H⁵), 1.33 (3H, s, H¹⁷); ¹³C NMR (75 MHz, CDCl₃) δ_C 195.5 (C¹), 152.8 (C³), 148.2 (C⁸), 147.1 (C¹¹), 132.8 (C¹²), 131.4 (C⁷), 125.4 (C²), 112.7 (C¹⁰), 112.1 (C⁹), 81.3 (C¹³), 80.1 (C⁶), 69.2 (C⁴), 56.4 (C¹⁵), 50.2 (C⁵), 48.6 (C¹⁴), 33.2 (C¹⁷); IR (neat): ν_{max} cm⁻¹ 3461 (OH), 2925 – 2851 (CH), 1717 (C=O); HRMS (pNSI): calcd for C₁₇H₁₈O₅NH₄ [M+NH₄]⁺: 320.1492; observed: 320.1493.

5.1.28 Methyl (3*R*,4*S*,5*R*)-3,4,5-trihydroxycyclohex-1-ene-1-carboxylate **242**

To a round bottomed flask was added shikimic acid (5.00 g, 29.0 mmol), MeOH (100 mL) and *p*-toluenesulfonic acid monohydrate (0.55 g, 2.9 mmol). The resulting solution was heated at reflux for 48 h. The reaction mixture was cooled, filtered and the solvent removed under reduced pressure. The crude product was purified through hot recrystallization from ethyl acetate to afford methyl (3*R*,4*S*,5*R*)-3,4,5-trihydroxycyclohex-1-ene-1-carboxylate **242** (3.93 g, 21 mmol, 73%,) as an off-white solid.

Mp = 114.0 – 115.1 °C (lit. Mp = 112.0 – 113.0 °C¹²⁹); $[\alpha]_D^{20} = -126.8$ ($c = 1$, MeOH) (lit. $[\alpha]_D^{20} = -125.0$ ($c = 1.8$, EtOH)¹²⁹); ¹H NMR (300 MHz, MeOD-*d*₄) δ_H 6.80 (1H, app dtd, $J = 3.6, 1.9, 0.6$ Hz, H³), 4.46 – 4.32 (1H, m, H⁶), 4.01 (1H, dddd, $J = 7.2, 5.5, 4.9, 0.6$ Hz, H¹), 3.76 (3H, s, H⁸), 3.70 (1H, dd, $J = 7.2, 4.2$ Hz, H²), 2.82 – 2.63 (1H, m, H⁵), 2.22 (1H, app ddt, $J = 18.2, 5.4, 1.7$ Hz, H⁵); ¹³C NMR (75 MHz, MeOD-*d*₄) δ_C 168.6 (C⁷), 139.0 (C³), 130.2 (C⁴), 72.5 (C²), 68.3 (C¹), 67.2 (C⁶), 52.4 (C⁸), 31.5 (C⁵); IR (neat): ν_{max} cm⁻¹ 3308 (OH), 2956 (CH), 2901 (CH), 1716 (C=O); HRMS (pNSI): calcd for C₈H₁₂O₅Na (M+Na)⁺: 211.0575; observed: 211.0577.

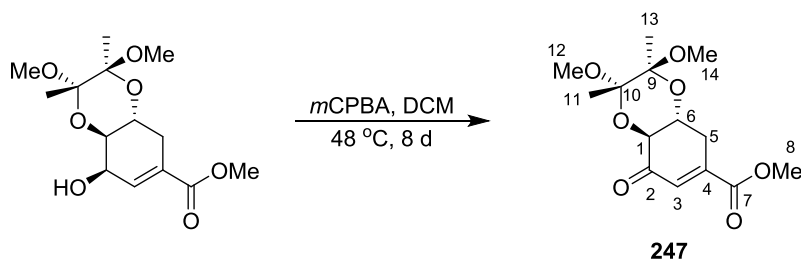
5.1.29 Methyl (2*S*,3*S*,4*aR*,8*R*,8*aR*)-8-hydroxy-2,3-dimethoxy-2,3-dimethyl-2,3,4*a*,5,8,8*a*-hexahydrobenzo[*b*][1,4]dioxine-6-carboxylate **243**



To a round bottomed flask was added methyl (3*R*,4*S*,5*R*)-3,4,5-trihydroxycyclohex-1-ene-1-carboxylate **242** (500 mg, 2.70 mmol), MeOH (10 mL), 2,3-butanedione (0.6 mL, 6.4 mmol) and camphorsulfonic acid (63 mg, 0.30 mmol). To the stirred solution was added trimethyl orthoformate (1.8 mL, 16.0 mmol) and the reaction mixture was stirred at reflux under a nitrogen atmosphere for 48 h. The reaction mixture was cooled to rt, NaHCO₃ (562 mg, 6.70 mmol) was added and the reaction mixture stirred for 10 min. The solvent was removed under reduced pressure and the crude product was purified by column chromatography (petroleum ether: acetone, 5: 1, column diameter = 3 cm, silica = 19 cm) to give methyl (2*S*,3*S*,4*aR*,8*R*,8*aR*)-8-hydroxy-2,3-dimethoxy-2,3-dimethyl-2,3,4*a*,5,8,8*a*-hexahydrobenzo[*b*][1,4]dioxine-6-carboxylate **243** (588 mg, 1.94 mmol, 73%) as an orange-brown oil.¹²⁹

$R_f = 0.20$ (petroleum ether: acetone, 5: 1, visualised with KMnO₄ aq. solution); $[\alpha]_D^{20} = +43.4$ ($c = 1$, MeOH) (lit. $[\alpha]_D^{20} = +23.1$ ($c = 0.89$, DCM)¹²⁹); ¹H NMR (300 MHz, CDCl₃) δ_H 6.92 – 6.85 (1H, m, H³), 4.40 – 4.34 (1H, m, H²), 4.09 (1H, td, $J = 10.7, 5.9$ Hz, H⁶), 3.73 (3H, s, H⁸), 3.61 (1H, dd, $J = 10.7, 4.3$ Hz, H¹), 3.26 (3H, s, H^{12/14}), 3.24 (3H, s, H^{12/14}), 2.82 (1H, dd, $J = 17.6, 5.9$ Hz, H⁵), 2.24 – 2.10 (1H, m, H⁵), 1.32 (s, 3H, H^{11/13}), 1.29 (s, 3H, H^{11/13}); ¹³C NMR (75 MHz, CDCl₃) δ_C 166.4 (C⁷), 135.2 (C³), 131.3 (C⁴), 99.8 (C^{9/10}), 99.1 (C^{9/10}), 70.6 (C¹), 64.8 (C²), 62.3 (C⁶), 51.9 (C⁸), 47.9 (C^{12/14}), 47.8 (C^{12/14}), 30.0 (C⁵), 17.7 (C^{11/13}), 17.5 (C^{11/13}); IR (neat): ν_{\max} cm⁻¹ 3468 (OH), 2993 – 2834 (CH), 1718 (C=O); MS (pNSI): 271.1 (38%, [M-OMe]⁺), 320.2 (100%, [M+NH₄]⁺), 627.3 (51%, [2M+Na]⁺); HRMS (pNSI): calcd for C₁₄H₂₂O₇NH₄ [M+NH₄]⁺: 320.1704; observed: 320.1702.

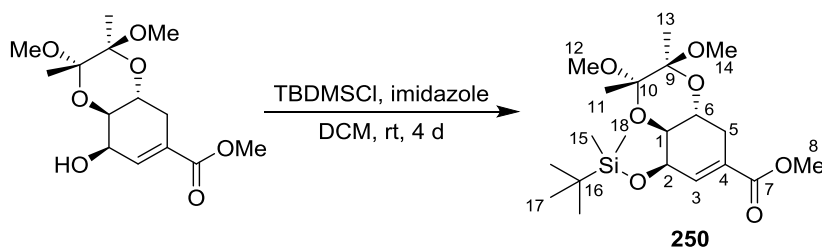
5.1.30 Methyl (2*S*,3*S*,4*aR*,8*aS*)-2,3-dimethoxy-2,3-dimethyl-8-oxo-2,3,4*a*,5,8,8*a*-hexahydrobenzo[*b*][1,4]dioxine-6-carboxylate **247**



To a Schlenk flask was added methyl (2*S*,3*S*,4*aR*,8*R*,8*aR*)-8-hydroxy-2,3-dimethoxy-2,3-dimethyl-2,3,4*a*,5,8,8*a*-hexahydrobenzo[*b*][1,4]dioxine-6-carboxylate **243** (95 mg, 0.31 mmol) and DCM (4 mL) and *meta*-chloroperoxybenzoic acid (60 mg, 0.35 mmol). The reaction mixture was stirred at 48 °C for 8 d, quenched with saturated aq. Na₂SO₃ solution (4 mL) and extracted with DCM (3 x 10 mL). The combined organic extracts were dried with sodium sulfate, filtered and the solvent removed under reduced pressure. The crude product was purified by column chromatography (petroleum ether: acetone, 4: 1, column diameter = 1 cm, silica = 18 cm) to give methyl (2*S*,3*S*,4*aR*,8*aS*)-2,3-dimethoxy-2,3-dimethyl-8-oxo-2,3,4*a*,5,8,8*a*-hexahydrobenzo[*b*][1,4]dioxine-6-carboxylate **247** (5 mg, 0.02 mmol, 6%) as a white solid.

Mp = 117.8 – 118.0 °C; *R*_f = 0.35 (petroleum ether: acetone, 4: 1, visualised with KMnO₄ aq. solution); [α]_D²⁰ = +86 (*c* = 0.1, DCM); ¹H NMR (300 MHz, CDCl₃) δ _H 6.80 (1H, d, *J* = 3.1 Hz, H³), 4.31 (1H, d, *J* = 11.6 Hz, H¹), 4.09 (1H, ddd, *J* = 11.6, 10.6, 5.3 Hz, H⁶), 3.84 (3H, s, H⁸), 3.30 (3H, s, H^{12/14}), 3.25 (3H, s, H^{12/14}), 3.07 (1H, dd, *J* = 18.4, 5.3 Hz, H⁵), 2.64 (1H, ddd, *J* = 18.4, 10.6, 3.1 Hz, H⁵), 1.41 (3H, s, H^{11/13}), 1.33 (3H, s, H^{11/13}); ¹³C NMR (75 MHz, CDCl₃) δ _C 194.5 (C²), 165.9 (C⁷), 144.7 (C⁴), 132.8 (C³), 100.4 (C^{9/10}), 99.4 (C^{9/10}), 75.2 (C¹), 67.1 (C⁶), 53.0 (C⁸), 48.5 (C^{12/14}), 48.2 (C^{12/14}), 30.6 (C⁵), 17.7 (C^{11/13}), 17.6 (C^{11/13}); IR (neat): ν _{max} cm⁻¹ 2957 – 2835 (CH), 1730 (C=O), 1700 (C=O); MS (pNSI): 269.1 (81%, [M-OMe]⁺), 318.2 (100%, [M+NH₄]⁺), 618.3 (71%, [2M+NH₄]⁺); HRMS (pNSI): calcd for C₁₄H₂₀O₇NH₄ [M+NH₄]⁺: 318.1547; observed: 318.1547.

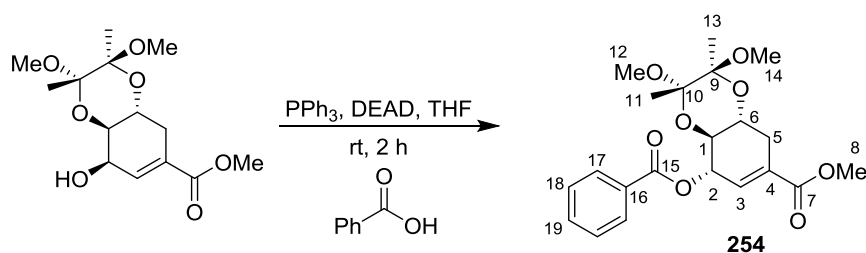
5.1.31 Methyl (2*S*,3*S*,4*aR*,8*R*,8*aS*)-8-((*tert*-butyldimethylsilyl)oxy)-2,3-dimethoxy-2,3-dimethyl-2,3,4*a*,5,8,8*a*-hexahydrobenzo[*b*][1,4]dioxine-6-carboxylate **250**



To a round bottomed flask was added methyl (2*S*,3*S*,4*aR*,8*R*,8*aR*)-8-hydroxy-2,3-dimethoxy-2,3-dimethyl-2,3,4*a*,5,8,8*a*-hexahydrobenzo[*b*][1,4]dioxine-6-carboxylate **243** (734 mg, 2.4 mmol), DCM (10 mL), *tert*-butyldimethylsilyl chloride (377 mg, 2.5 mmol) and imidazole (170 mg, 2.5 mmol) and the reaction mixture was stirred at rt for 18 h. DCM (20 mL), *tert*-butyldimethylsilyl chloride (180 mg, 1.2 mmol) and imidazole (81 mg, 1.20 mmol) were added to the reaction mixture and stirring was continued for 24 h. *Tert*-butyldimethylsilyl chloride (180 mg, 1.2 mmol) and imidazole (81 mg, 1.2 mmol) were added to the reaction mixture and stirring was continued for 54 h. The reaction mixture was poured into water (30 mL) and extracted with DCM (3 x 30 mL). The combined organic extracts were dried with sodium sulfate, filtered and the solvent removed under reduced pressure. The crude product was purified by column chromatography (petroleum ether: acetone, 9: 1, column diameter = 4 cm, silica = 15 cm) to give methyl (2*S*,3*S*,4*aR*,8*R*,8*aS*)-8-((*tert*-butyldimethylsilyl)oxy)-2,3-dimethoxy-2,3-dimethyl-2,3,4*a*,5,8,8*a*-hexahydrobenzo[*b*][1,4]dioxine-6-carboxylate **250** (880 mg, 2.1 mmol, 88%) as a white solid.

Mp = 73.7 – 74.1 °C; R_f = 0.23 (petroleum ether: acetone, 9: 1); $[\alpha]_D^{20}$ = -18.8 (c = 1, DCM); ^1H NMR (300 MHz, CDCl_3) δ_{H} 6.63 (1H, dd, J = 5.5, 2.5 Hz, H³), 4.19 (1H, dd, J = 5.5, 3.9 Hz, H²), 3.98 (1H, app td, J = 10.5, 6.0 Hz, H⁶), 3.6 (3H, s, H⁸), 3.35 (1H, dd, J = 10.8, 3.9 Hz, H¹), 3.11 (3H, s, H^{12/14}), 3.09 (3H, s, H^{12/14}), 2.66 (1H, dd, J = 17.6, 6.0 Hz, H⁵), 2.08 (1H, ddd, J = 17.6, 10.3, 2.5 Hz, H⁵), 1.16 (3H, s, H^{11/13}), 1.14 (3H, s, H^{11/13}), 0.76 (9H, s, H¹⁷), 0.00 (3H, s, H^{15/18}), -0.03 (3H, s, H^{15/18}); ^{13}C NMR (75 MHz, CDCl_3) δ_{C} 166.7 (C⁷), 136.5 (C³), 129.7 (C⁴), 99.4 (C^{9/10}), 98.6 (C^{9/10}), 70.8 (C¹), 65.9 (C²), 62.3 (C⁶), 51.8 (C⁸), 47.6 (C^{12/14}), 47.4 (C^{12/14}), 30.4 (C⁵), 25.7 (C¹⁷), 18.2 (C¹⁶), 17.7 (C^{11/13}), 17.6 (C^{11/13}), -4.8 (C^{15/18}), -4.9 (C^{15/18}); IR (neat): ν_{max} cm^{-1} 2994 – 2856 (CH), 1708 (C=O); MS (pNSI): 385.2 (82%, [M-OMe]⁺), 434.3 (100%, [M+NH₄]⁺); HRMS (pNSI): calcd for C₂₀H₃₆O₇SiNH₄ [M+NH₄]⁺: 434.2569; observed: 434.2561.

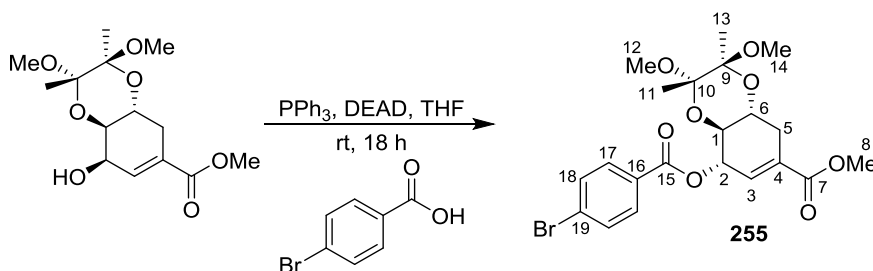
5.1.32 Methyl (2*S*,3*S*,4*aR*,8*S*,8*aS*)-8-(benzoyloxy)-2,3-dimethoxy-2,3-dimethyl-2,3,4*a*,5,8,8*a*-hexahydrobenzo[*b*][1,4]dioxine-6-carboxylate **254**



To a Schlenk flask was added methyl (2*S*,3*S*,4*aR*,8*R*,8*aR*)-8-hydroxy-2,3-dimethoxy-2,3-dimethyl-2,3,4*a*,5,8,8*a*-hexahydrobenzo[*b*][1,4]dioxine-6-carboxylate **243** (200 mg, 0.66 mmol), benzoic acid (121 mg, 0.99 mmol), triphenylphosphine (260 mg, 0.99 mmol) and THF (10 mL) under a nitrogen atmosphere. The solution was cooled to 0 °C and diethyl azodicarboxylate (155 μ L, 0.99 mmol) was added dropwise. The reaction mixture was stirred at room temperature for 2 h then poured into saturated aqueous NaHCO₃ solution (10 mL) and extracted with ethyl acetate (3 x 20 mL). The combined organic extracts were dried with sodium sulfate, filtered and solvent removed under reduced pressure. The crude product was purified by column chromatography (petroleum ether: acetone, 9:1, column diameter = 2 cm, silica = 17 cm) to give methyl (2*S*,3*S*,4*aR*,8*S*,8*aS*)-8-(benzoyloxy)-2,3-dimethoxy-2,3-dimethyl-2,3,4*a*,5,8,8*a*-hexahydrobenzo[*b*][1,4]dioxine-6-carboxylate **254** (91 mg, 0.22 mmol, 34%) as a white solid.

Mp = 65.3 – 66.0 °C; R_f = 0.19 (petroleum ether: acetone 9: 1, visualised with KMnO₄ aq. solution); $[\alpha]_D^{20}$ = +203.1 (c = 1, DCM); ¹H NMR (300 MHz, CDCl₃) δ_H 8.10 – 7.96 (2H, m, H¹⁷), 7.63 – 7.49 (1H, m, H¹⁹), 7.43 (2H, app t, J = 7.6 Hz, H¹⁸), 6.74 (1H, app t, J = 2.7 Hz, H³), 5.85 – 5.73 (1H, m, H²), 4.07 – 3.88 (2H, m, H¹⁺⁶), 3.72 (3H, s, H⁸), 3.28 (3H, s, H^{12/14}), 3.27 (3H, s, H^{12/14}), 2.86 – 2.75 (1H, m, H⁵), 2.45 – 2.30 (1H, m, H⁵), 1.31 (3H, s, H^{11/13}), 1.27 (3H, s, H^{11/13}); ¹³C NMR (75 MHz, CDCl₃) δ_C 166.1 (C^{7/15}), 165.9 (C^{7/15}), 134.9 (C³), 133.3 (C¹⁹), 130.4 (C⁴), 129.9 (C¹⁶), 129.7 (C¹⁷), 128.5 (C¹⁸), 99.4 (C^{9/10}), 99.3 (C^{9/10}), 72.2 (C²), 70.9 (C⁶), 65.6 (C¹), 52.2 (C⁸), 48.1 (C^{12/14}), 47.9 (C^{12/14}), 29.4 (C⁵), 17.7 (C^{11/13}), 17.7 (C^{11/13}); IR (neat): ν_{max} cm⁻¹ 2995 – 2833 (CH), 1720 (C=O); MS (pNSI): 375.1 (100%, [M-OMe]⁺), 424.2 (23% [M+NH₄]⁺), 830.4 (68% [2M+NH₄]⁺); HRMS (pNSI): calcd for C₂₁H₂₆O₈NH₄ [M+NH₄]⁺: 424.1966; observed: 424.1956.

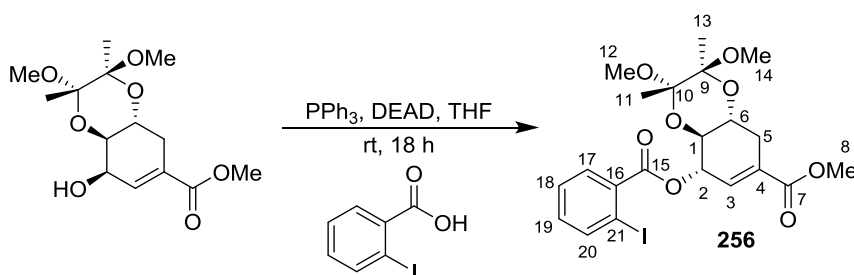
5.1.33 Methyl (2*S*,3*S*,4*aR*,8*S*,8*aS*)-8-((4-bromobenzoyl)oxy)-2,3-dimethoxy-2,3-dimethyl-2,3,4*a*,5,8,8*a*-hexahydrobenzo[*b*][1,4]dioxine-6-carboxylate **255**



To a Schlenk flask was added methyl (2*S*,3*S*,4*aR*,8*R*,8*aR*)-8-hydroxy-2,3-dimethoxy-2,3-dimethyl-2,3,4*a*,5,8,8*a*-hexahydrobenzo[*b*][1,4]dioxine-6-carboxylate **243** (212 mg, 0.70 mmol), 4-bromobenzoic acid (211 mg, 1.05 mmol), triphenylphosphine (275 mg, 1.05 mmol) and THF (10 mL) under a nitrogen atmosphere. The solution was cooled to 0 °C and diethyl azodicarboxylate (165 μ L, 1.05 mmol) was added dropwise. The reaction mixture was stirred at rt for 18 h then poured into saturated aq. NaHCO₃ solution (10 mL) and extracted with ethyl acetate (3 x 20 mL). The combined organic extracts were dried with sodium sulfate, filtered and the solvent removed under reduced pressure. The crude product was purified by column chromatography (petroleum ether: acetone, 4: 1, column diameter = 3 cm, silica = 18 cm) to give methyl (methyl (2*S*,3*S*,4*aR*,8*S*,8*aS*)-8-((4-bromobenzoyl)oxy)-2,3-dimethoxy-2,3-dimethyl-2,3,4*a*,5,8,8*a*-hexahydrobenzo[*b*][1,4]dioxine-6-carboxylate **255** (257 mg, 0.53 mmol, 76%) as a white solid.

Mp = 145.0 – 145.7 °C; R_f = 0.4 (petroleum ether: acetone, 4:1); $[\alpha]_D^{20}$ = +141.8 (c = 1, MeOH); ¹H NMR (300 MHz, CDCl₃) δ_H 7.86 (2H, d, J = 8.5 Hz, H^{17/18}), 7.55 (2H, d, J = 8.5 Hz, H^{17/18}), 6.71 (1H, app t, J = 2.6 Hz, H³), 5.82 – 5.71 (1H, m, H²), 4.05 – 3.86 (2H, m, H¹⁺⁶), 3.71 (3H, s, H⁸), 3.25 (3H, s, H^{12/14}), 3.24 (3H, s, H^{12/14}), 2.80 (1H, dd, J = 17.4, 5.6 Hz, H⁵), 2.44 – 2.29 (1H, m, H⁵), 1.29 (3H, s, H^{11/13}), 1.25 (3H, s, H^{11/13}); ¹³C NMR (75 MHz, CDCl₃) δ_C 166.0 (C^{7/15}), 165.1 (C^{7/15}), 134.5 (C³), 131.9 (C^{17/18}), 131.2 (C^{17/18}), 130.6 (C⁴), 128.8 (C^{16/19}), 128.4 (C^{16/19}), 99.4 (C^{9/10}), 99.2 (C^{9/10}), 72.5 (C²), 70.9 (C^{1/6}), 65.5 (C^{1/6}), 52.2 (C⁸), 48.1 (C^{12/14}), 47.8 (C^{12/14}), 29.4 (C⁵), 17.7 (C^{11/13}), 17.7 (C^{11/13}); IR (neat): ν_{max} cm⁻¹ 2950 – 2832 (CH), 1717 (C=O); MS (pNSI): 453.1 (100%, [M-OMe]⁺), 507.1 (43% [M+Na]⁺), 988.2 (26% [2M+NH₄]⁺); HRMS (pNSI): calcd for C₂₁H₂₅BrO₈Na [M+Na]⁺: 507.0625, 509.0605; observed : 507.0612, 509.0591.

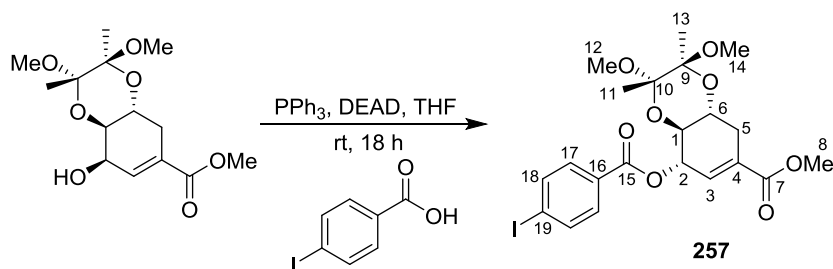
5.1.34 Methyl (2*S*,3*S*,4*aR*,8*S*,8*aS*)-8-((2-iodobenzoyl)oxy)-2,3-dimethoxy-2,3-dimethyl-2,3,4*a*,5,8,8*a*-hexahydrobenzo[*b*][1,4]dioxine-6-carboxylate **256**



To a Schlenk flask was added methyl (2*S*,3*S*,4*aR*,8*R*,8*aR*)-8-hydroxy-2,3-dimethoxy-2,3-dimethyl-2,3,4*a*,5,8,8*a*-hexahydrobenzo[*b*][1,4]dioxine-6-carboxylate **243** (610 mg, 2.0 mmol), 2-iodobenzoic acid (744 mg, 3.0 mmol), triphenylphosphine (787 mg, 3.0 mmol) and THF (20 mL) under a nitrogen atmosphere. The solution was cooled to 0 °C and diethyl azodicarboxylate (472 μ L, 3.0 mmol) was added dropwise. The reaction mixture was stirred at rt for 18 h then poured into saturated aq. NaHCO₃ solution (20 mL) and extracted with ethyl acetate (3 x 40 mL). The combined organic extracts were dried with sodium sulfate, filtered and the solvent removed under reduced pressure. The crude product was purified by column chromatography (petroleum ether: acetone, 3: 1, column diameter = 4 cm, silica = 17 cm) to give methyl (2*S*,3*S*,4*aR*,8*S*,8*aS*)-8-((2-iodobenzoyl)oxy)-2,3-dimethoxy-2,3-dimethyl-2,3,4*a*,5,8,8*a*-hexahydrobenzo[*b*][1,4]dioxine-6-carboxylate **256** (622 mg, 1.2 mmol, 58%) as a colourless crystalline solid.

Mp = 108.5 - 109.9 °C; R_f = 0.38 (petroleum ether: acetone, 3: 1, visualised with KMnO₄ aq. solution); $[\alpha]_D^{20}$ = +99 (c = 1, DCM); ¹H NMR (300 MHz, CDCl₃) δ_H 7.97 (1H, dd, J = 8.0, 1.1 Hz, H²⁰), 7.78 (1H, dd, J = 7.7, 1.7 Hz, H¹⁷), 7.37 (1H, td, J = 7.7, 1.2 Hz, H¹⁸), 7.13 (1H, td, J = 7.6, 1.7 Hz, H¹⁹), 6.78 (1H, app t, J = 2.6 Hz, H³), 5.82 - 5.72 (1H, m, H²), 4.06 - 3.83 (2H, m, H¹⁺⁶), 3.72 (3H, s, H⁸), 3.26 (3H, s, H^{12/14}), 3.25 (3H, s, H^{12/14}), 2.80 (1H, ddd, J = 17.4, 5.3, 1.5 Hz, H⁵), 2.43 - 2.29 (1H, m, H⁵), 1.29 (3H, s, H^{11/13}), 1.28 (3H, s, H^{11/13}); ¹³C NMR (75 MHz, CDCl₃) δ_C 166.0 (C⁷), 165.6 (C¹⁵), 141.5 (C²⁰), 134.5 (C²), 134.5 (C¹⁶), 132.9 (C¹⁹), 130.9 (C¹⁷), 130.5 (C⁴), 128.0 (C¹⁸), 99.4 (C^{9/10}), 99.2 (C^{9/10}), 94.3 (C²¹), 72.9 (C²), 70.8 (C^{1/6}), 65.5 (C^{1/6}), 52.3 (C⁸), 48.1 (C^{12/14}), 48.1 (C^{12/14}), 29.4 (C⁵), 17.7 (C^{11/13}), 17.7 (C^{11/13}); IR (neat): ν_{max} cm⁻¹ 2953 - 2831 (CH), 1722 (C=O); HRMS (pNSI): calcd for C₂₁H₂₅I O₈Na [M+Na]⁺: 555.0486; observed: 507.0471.

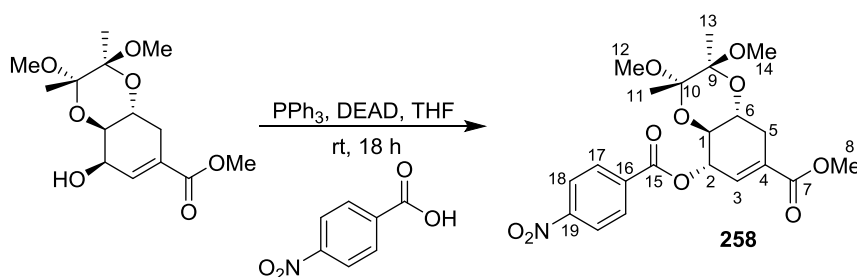
5.1.35 Methyl (2*S*,3*S*,4*aR*,8*S*,8*aS*)-8-((4-iodobenzoyl)oxy)-2,3-dimethoxy-2,3-dimethyl-2,3,4*a*,5,8,8*a*-hexahydrobenzo[*b*][1,4]dioxine-6-carboxylate **257**



To a Schlenk flask was added methyl (2*S*,3*S*,4*aR*,8*R*,8*aR*)-8-hydroxy-2,3-dimethoxy-2,3-dimethyl-2,3,4*a*,5,8,8*a*-hexahydrobenzo[*b*][1,4]dioxine-6-carboxylate **243** (500 mg, 1.7 mmol), 4-iodobenzoic acid (615 mg, 2.5 mmol), triphenylphosphine (650 mg, 2.5 mmol) and THF (15 mL) under a nitrogen atmosphere. The solution was cooled to 0 °C and diethyl azodicarboxylate (390 μ L, 2.5 mmol) was added dropwise. The reaction mixture was stirred at rt for 18 h then poured into saturated aq. NaHCO₃ solution (20 mL) and extracted with ethyl acetate (3 x 40 mL). The combined organic extracts were dried with sodium sulfate, filtered and the solvent removed under reduced pressure. The crude product was purified by column chromatography (petroleum ether: acetone, 4: 1, column diameter = 3 cm, silica = 22 cm) to give methyl (2*S*,3*S*,4*aR*,8*S*,8*aS*)-8-((4-iodobenzoyl)oxy)-2,3-dimethoxy-2,3-dimethyl-2,3,4*a*,5,8,8*a*-hexahydrobenzo[*b*][1,4]dioxine-6-carboxylate **257** (680 mg, 1.3 mmol, 77%) as an off-white solid (Note: the isolated sample was contaminated with ~13% 4-iodobenzoic acid as estimated by analysis of the ¹H NMR spectrum).

Mp = 100.1 – 100.8 °C; R_f = 0.54 (petroleum ether: acetone, 4: 1); $[\alpha]_D^{20}$ = +137.4 (c = 1, DCM); ¹H NMR (300 MHz, CDCl₃) δ_H 7.71 (2H, d, J = 8.3 Hz, H¹⁸), 7.65 (2H, d, J = 8.3 Hz, H¹⁷), 6.65 (1H, app t, J = 2.6 Hz, H³), 5.74 – 5.67 (1H, m, H²), 3.98 – 3.81 (2H, m, H¹⁺⁶), 3.65 (3H, s, H⁸), 3.19 (3H, s, H^{12/14}), 3.19 (3H, s, H^{12/14}), 2.75 (1H, dd, J = 17.1, 5.3 Hz, H⁵), 2.30 (1H, m, H⁵), 1.23 (3H, s, H^{11/13}), 1.19 (3H, s, H^{11/13}); ¹³C NMR (75 MHz, CDCl₃) δ_C 165.9 (C⁷), 165.2 (C¹⁵), 137.8 (C¹⁸), 134.5 (C³), 131.0 (C¹⁷), 130.5 (C⁴), 129.3 (C¹⁶), 101.1 (C¹⁹), 99.2 (C^{9/10}), 99.2 (C^{9/10}), 72.4 (C²), 70.8 (C^{1/6}), 65.4 (C^{1/6}), 52.2 (C⁸), 48.0 (C^{12/14}), 47.8 (C^{12/14}), 29.3 (C⁵), 17.7 (C^{11/13}), 17.6 (C^{11/13}); IR (neat): ν_{max} cm⁻¹ 2955 – 2835 (CH), 1714 (C=O); HRMS (pNSI): calcd for C₂₁H₂₅I₂O₈NH₄ [M+NH₄]⁺: 550.0932; observed: 550.0917.

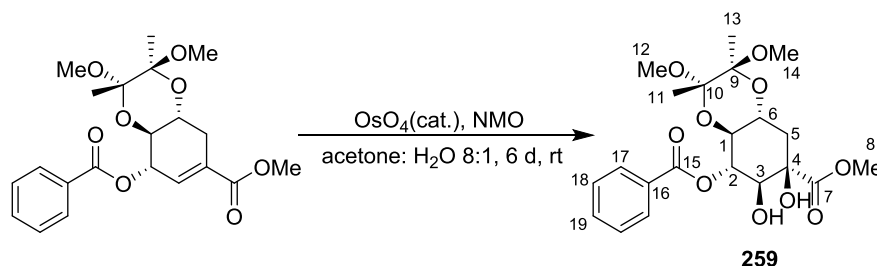
5.1.36 Methyl (2*S*,3*S*,4*aR*,8*S*,8*aS*)-2,3-dimethoxy-2,3-dimethyl-8-((4-nitrobenzoyl)oxy)-2,3,4*a*,5,8,8*a*-hexahydrobenzo[*b*][1,4]dioxine-6-carboxylate **258**



To a Schlenk flask was added methyl (2*S*,3*S*,4*aR*,8*R*,8*aR*)-8-hydroxy-2,3-dimethoxy-2,3-dimethyl-2,3,4*a*,5,8,8*a*-hexahydrobenzo[*b*][1,4]dioxine-6-carboxylate **243** (500 mg, 1.7 mmol), 4-nitrobenzoic acid (414 mg, 2.5 mmol), triphenylphosphine (650 mg, 2.5 mmol) and THF (15 mL) under a nitrogen atmosphere. The solution was cooled to 0 °C and diethyl azodicarboxylate (390 μ L, 2.5 mmol) was added dropwise. The reaction mixture was stirred at rt for 18 h then poured into saturated aq. NaHCO₃ solution (20 mL) and extracted with ethyl acetate (3 x 40 mL). The combined organic extracts were dried with sodium sulfate, filtered and the solvent removed under reduced pressure. The crude product was purified by column chromatography (petroleum ether: acetone, 6: 1, column diameter = 4 cm, silica = 22 cm) to give methyl (2*S*,3*S*,4*aR*,8*S*,8*aS*)-2,3-dimethoxy-2,3-dimethyl-8-((4-nitrobenzoyl)oxy)-2,3,4*a*,5,8,8*a*-hexahydrobenzo[*b*][1,4]dioxine-6-carboxylate **258** (578 mg, 1.3 mmol, 78%) as a white solid.

Mp = 190.1 – 190.4 °C; R_f = 0.33 (petroleum ether: acetone, 6: 1); $[\alpha]_D^{20}$ = +220.4 (c = 1, DCM); ¹H NMR (300 MHz, CDCl₃) δ_H 8.28 (2H, d, J = 8.9 Hz, H¹⁸), 8.19 (2H, d, J = 8.9 Hz, H¹⁷), 6.72 (1H, app t, J = 2.5 Hz, H³), 5.87 - 5.76 (1H, m, H²), 4.11 - 3.87 (2H, m, H¹⁺⁶), 3.73 (3H, s, H⁸), 3.27 (3H, s, H^{12/14}), 3.26 (3H, s, H^{12/14}), 2.82 (1H, dd, J = 17.2, 5.2 Hz, H⁵), 2.46 - 2.30 (1H, m, H⁵), 1.31 (3H, s, H^{11/13}), 1.26 (3H, s, H^{11/13}); ¹³C NMR (75 MHz, CDCl₃) δ_C 166.0 (C¹⁵), 164.1 (C⁷), 150.8 (C¹⁹), 135.3 (C¹⁶), 134.0 (C³), 131.1 (C⁴), 130.9 (H¹⁷), 123.7 (C¹⁸), 99.5 (C^{9/10}), 99.3 (C^{9/10}), 73.3 (C²), 70.9 (C^{1/6}), 65.5 (C^{1/6}), 52.3 (C⁸), 48.2 (C^{12/14}), 47.9 (C^{12/14}), 29.4 (C⁵), 17.8 (C^{11/13}), 17.7 (C^{11/13}); IR (neat): ν_{max} cm⁻¹ 2958 – 2838 (CH), 1720 (C=O); MS (pNSI): 474.1 (100%, [M+Na]⁺), 420.1 (53%, [M-MeO]⁺); HRMS (pNSI): calcd for C₂₁H₂₅NO₁₀Na [M+Na]⁺: 474.1371; observed: 474.1363.

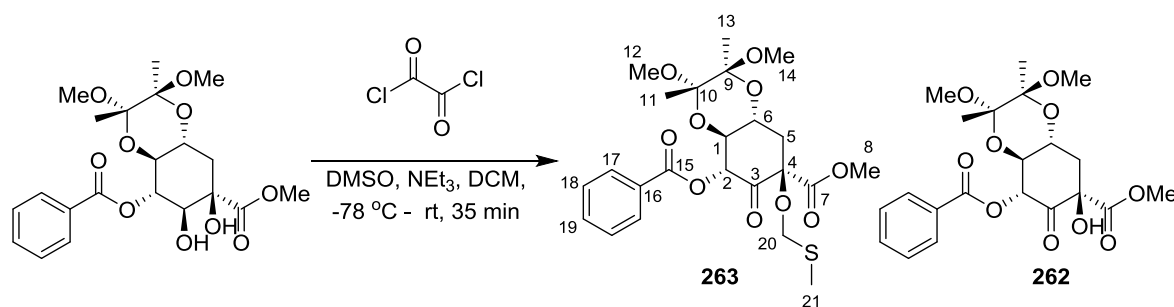
5.1.37 Methyl (2*S*,3*S*,4*aR*,6*R*,7*S*,8*S*,8*aS*)-8-(benzoyloxy)-6,7-dihydroxy-2,3-dimethoxy-2,3-dimethyloctahydrobenzo[*b*][1,4]dioxine-6-carboxylate **259**



To a round bottomed flask was added methyl (2*S*,3*S*,4*aR*,8*S*,8*aS*)-8-(benzoyloxy)-2,3-dimethoxy-2,3-dimethyl-2,3,4*a*,5,8,8*a*-hexahydrobenzo[*b*][1,4]dioxine-6-carboxylate **254** (1.11 g, 2.74 mmol) and acetone: water (8:1 v/v, 14 mL). To the resultant stirred solution was added 4-methylmorpholine-*N*-oxide (1.11 g, 8.22 mmol) followed by osmium tetroxide (0.9 mL 4% aqueous solution, 0.14 mmol) at rt. The reaction mixture was stirred at rt for 6 d then quenched with saturated aq. Na₂SO₃ solution (30 mL), diluted with water (80 mL) and extracted with DCM (3 x 50 mL). The combined organic extracts were washed with brine (50 mL), dried with sodium sulfate, filtered and the solvent removed under reduced pressure. The crude product was purified by column chromatography (petroleum ether: acetone, 2: 1, column diameter = 3 cm, silica = 20 cm) to give methyl (2*S*,3*S*,4*aR*,6*R*,7*S*,8*S*,8*aS*)-8-(benzoyloxy)-6,7-dihydroxy-2,3-dimethoxy-2,3-dimethyloctahydrobenzo[*b*][1,4]dioxine-6-carboxylate **259** (0.924 g, 2.08 mmol, 76%) as a colourless crystalline solid.

Mp = 221.2 - 222.2 °C; R_f = 0.35 (petroleum ether: acetone, 2: 1); $[\alpha]_D^{20}$ = +52 (c = 0.1, DCM); ¹H NMR (300 MHz, CDCl₃) δ_H 8.11 – 8.03 (2H, m, H¹⁷), 7.64 – 7.54 (1H, m, H¹⁹), 7.51 – 7.41 (2H, m, H¹⁸), 5.43 (1H, app t, J = 9.8 Hz, H²), 4.17 (1H, dt, J = 9.6, 8.5 Hz, H⁶), 4.05 (1H, d, J = 9.5 Hz, H³), 3.95 – 3.87 (1H, m, H¹), 3.85 (3H, s, H⁸), 3.31 (3H, s, H^{12/14}), 3.28 (3H, s, H^{12/14}), 2.01 (2H, app d, J = 8.5 Hz, H⁵), 1.32 (3H, s, H^{11/13}), 1.27 (3H, s, H^{11/13}); ¹³C NMR (75 MHz, CDCl₃) δ_C 174.0 (C⁷), 167.2 (C¹⁵), 133.2 (C¹⁹), 129.8 (C¹⁶), 129.8 (C¹⁷), 128.4 (C¹⁸), 99.6 (C^{9/10}), 99.5 (C^{9/10}), 76.4 (C⁴), 75.2 (C³), 74.0 (C²), 70.9 (C¹), 64.9 (C⁶), 53.5 (C⁸), 48.0 (C^{12/14}), 47.8 (C^{12/14}), 35.3 (C⁵), 17.7 (C^{11/13}), 17.6 (C^{11/13}); IR (neat): ν_{max} cm⁻¹ 3468 (OH), 3430 (OH), 2945 – 2894 (CH), 1749 (C=O), 1724 (C=O); MS (pNSI): 409.1 (100%, [M-OMe]⁺), 458.2 (86%, [M+NH₄]⁺); HRMS (pNSI): calcd for C₂₁H₃₂O₁₀N [M+NH₄]⁺: 458.2021; observed: 458.2014.

5.1.38 Methyl (2*S*,3*S*,4*aR*,6*R*,8*R*,8*aS*)-8-(benzoyloxy)-2,3-dimethoxy-2,3-dimethyl-6-((methylthio)methoxy)-7-oxooctahydrobenzo[*b*][1,4]dioxine-6-carboxylate **263**



To a Schlenk flask was added DCM (0.5 mL) and oxalyl chloride (40 μ L, 0.47 mmol). The resultant solution was cooled to -78 $^{\circ}$ C and DMSO (80 μ L, 1.15 mmol) was added dropwise. The solution was stirred for 10 min and a solution of (2*S*,3*S*,4*aR*,6*R*,7*S*,8*S*,8*aS*)-8-(benzoyloxy)-6,7-dihydroxy-2,3-dimethoxy-2,3-dimethyloctahydrobenzo[*b*][1,4]dioxine-6-carboxylate **259** (100 mg, 0.23 mmol) in DCM (1.0 mL) was added dropwise. The reaction mixture was stirred for 5 min at -78 $^{\circ}$ C then triethylamine (0.29 mL, 2.07 mmol) was added. The reaction mixture was stirred for 10 min at -78 $^{\circ}$ C, then at rt for 35 min. The reaction mixture was quenched with water (20 mL) and extracted with DCM (3 x 20 mL). The combined organic extracts were washed with water (40 mL) and brine (40 mL) then dried with sodium sulfate, filtered and the solvent removed under reduced pressure. The crude compound was purified by column chromatography (petroleum ether: diethyl ether, 1: 1, column diameter = 1.5 cm, silica = 20 cm) to give methyl (2*S*,3*S*,4*aR*,6*R*,8*R*,8*aS*)-8-(benzoyloxy)-2,3-dimethoxy-2,3-dimethyl-6-((methylthio)methoxy)-7-oxooctahydrobenzo[*b*][1,4]dioxine-6-carboxylate **263** (14 mg, 0.03 mmol, 12%) as a colourless solid and methyl (2*S*,3*S*,4*aR*,6*R*,8*R*,8*aS*)-8-(benzoyloxy)-6-hydroxy-2,3-dimethoxy-2,3-dimethyl-7-oxooctahydrobenzo[*b*][1,4]dioxine-6-carboxylate **262** (25 mg, 0.06 mmol, 25%) as a white crystalline solid.

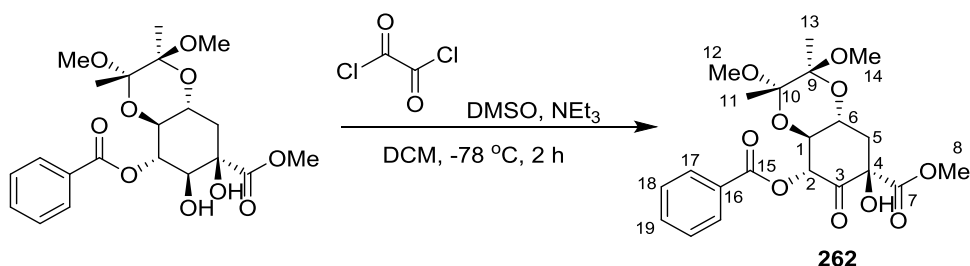
Methyl (2*S*,3*S*,4*aR*,6*R*,8*R*,8*aS*)-8-(benzoyloxy)-2,3-dimethoxy-2,3-dimethyl-6-((methylthio)methoxy)-7-oxooctahydrobenzo[*b*][1,4]dioxine-6-carboxylate **263**

Mp = 143.0 – 144.3 $^{\circ}$ C (decomposed); R_f = 0.43 (petroleum ether: diethyl ether, 1: 1); $[\alpha]_D^{20}$ = +48 (c = 0.1, DCM); $^1\text{H NMR}$ (300 MHz, CDCl_3) δ_{H} 8.02 – 7.94 (2H, m, H¹⁷), 7.56 – 7.47 (1H, m, H¹⁹), 7.39 (2H, app t, J = 7.6 Hz, H¹⁸), 5.81 (1H, d, J = 11.6 Hz, H²), 4.93 (1H, d, J = 10.6 Hz, H²⁰), 4.67 (1H, d, J = 10.6 Hz, H²⁰), 4.39 (1H, ddd, J = 12.0, 9.7, 4.9 Hz, H⁶), 3.97 (1H, dd, J = 11.6, 9.7 Hz, H¹), 3.71 (3H, s, H⁸), 3.26 (6H, app s, H¹²⁺¹⁴), 2.39 (1H, dd, J = 14.3, 4.9 Hz, H⁵), 2.29 – 2.20 (1H, m, H⁵), 2.27 (3H, s, H²¹), 1.27 (3H, s, H^{11/13}), 1.25 (3H, s, H^{11/13}); $^{13}\text{C NMR}$ (75 MHz, CDCl_3) δ_{C} 196.2 (C³), 168.3 (C⁷), 165.3 (C¹⁵), 133.4 (C¹⁹), 129.9 (C¹⁷), 129.2 (C¹⁶), 128.5 (C¹⁸), 99.8 (C^{9/10}), 99.6 (C^{9/10}), 85.0 (C⁴), 75.8 (C²), 71.9 (C²⁰), 71.0 (C¹), 64.1 (C⁶), 52.7 (C⁸), 48.3 (C^{12/14}), 48.0 (C^{12/14}), 35.0 (C⁵), 17.6 (C^{11/13}), 17.5 (C^{11/13}), 15.2 (C²¹); IR (neat): ν_{max}

Chapter 5. Experimental

cm⁻¹ 2989 – 2831 (CH), 1759 (C=O), 1740 (C=O), 1716 (C=O); HRMS (pNSI): calcd for C₂₃H₃₀O₁₀SNH₄ [M+NH₄]⁺: 516.1898; observed: 516.1888.

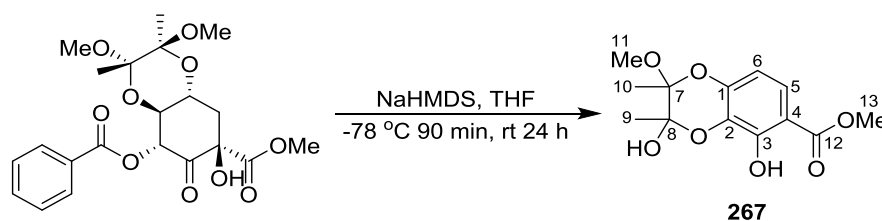
5.1.39 Methyl (2*S*,3*S*,4*aR*,6*R*,8*R*,8*aS*)-8-(benzoyloxy)-6-hydroxy-2,3-dimethoxy-2,3-dimethyl-7-oxooctahydrobenzo[*b*][1,4]dioxine-6-carboxylate **262**



To a Schlenk flask was added DCM (2 mL) and oxalyl chloride (0.12 mL, 1.43 mmol). The resultant solution was cooled to -78 °C and DMSO (0.26 mL, 3.60 mmol) was added dropwise. After 10 min at -78 °C, a solution of (2*S*,3*S*,4*aR*,6*R*,7*S*,8*S*,8*aS*)-8-(benzoyloxy)-6,7-dihydroxy-2,3-dimethoxy-2,3-dimethyloctahydrobenzo[*b*][1,4]dioxine-6-carboxylate **259** (315 mg, 0.72 mmol) in DCM (8 mL) was added to the reaction mixture and stirring was continued for 10 min. Triethylamine (0.50 mL, 3.6 mmol) was added. The reaction mixture was stirred at -78 °C for 2 h, quenched with water (10 mL) and extracted with DCM (3 x 15 mL). The combined organic extracts were washed with water (50 mL) and brine (50 mL), then dried with sodium sulfate, filtered and the solvent removed under reduced pressure. The crude product was purified by column chromatography (petroleum ether: acetone, 4: 1, column diameter = 2 cm, silica = 18 cm) to give methyl (2*S*,3*S*,4*aR*,6*R*,8*R*,8*aS*)-8-(benzoyloxy)-6-hydroxy-2,3-dimethoxy-2,3-dimethyl-7-oxooctahydrobenzo[*b*][1,4]dioxine-6-carboxylate **262** (269 mg, 0.61 mmol, 85%) as a colourless crystalline solid.

Mp = 235.7 – 237.1 °C; R_f = 0.3 (petroleum ether: diethyl ether, 1: 1); $[\alpha]_D^{20}$ = +133.8 (c = 1, DCM); $^1\text{H NMR}$ (300 MHz, CDCl_3) δ_{H} 8.02 – 7.94 (2H, m, H^{17}), 7.55 – 7.45 (1H, m, H^{19}), 7.40 – 7.35 (2H, m, H^{18}), 5.96 (1H, d, J = 11.5 Hz, H^2), 4.38 (1H, ddd, J = 11.7, 9.7, 5.2 Hz, H^6), 4.11 (1H, s, OH), 3.96 (1H, dd, J = 11.5, 9.7 Hz, H^1), 3.77 (3H, s, H^8), 3.25 (6H, app s, H^{12+14}), 2.25 – 2.12 (2H, m, H^5), 1.26 (3H, s, $\text{H}^{11/13}$), 1.24 (3H, s, $\text{H}^{11/13}$); $^{13}\text{C NMR}$ (75 MHz, CDCl_3) δ_{C} 196.7 (C^3), 170.7 (C^7), 165.1 (C^{15}), 133.3 (C^{19}), 129.9 (C^{17}), 129.3 (C^{16}), 128.4 (C^{18}), 99.7 ($\text{C}^{9/10}$), 99.5 ($\text{C}^{9/10}$), 79.1 (C^4), 74.5 (C^2), 71.1 (C^1), 64.3 (C^6), 53.7 (C^8), 48.2 ($\text{C}^{12/14}$), 47.9 ($\text{C}^{12/14}$), 34.8 (C^5), 17.6 ($\text{C}^{11/13}$), 17.5 ($\text{C}^{11/13}$); IR (neat): ν_{max} cm^{-1} 3412 (OH), 3003 – 2831 (CH), 1762 (C=O), 1744 (C=O), 1725 (C=O); HRMS (pAPCI): calcd for $\text{C}_{21}\text{H}_{27}\text{O}_{10}$ $[\text{M}+\text{H}]^+$: 439.1599; observed: 439.1595; calcd for $\text{C}_{21}\text{H}_{26}\text{O}_{10}\text{NH}_4$ $[\text{M}+\text{NH}_4]^+$: 456.1864; observed: 456.1861.

5.1.40 Methyl 3,5-dihydroxy-2-methoxy-2,3-dimethyl-2,3-dihydrobenzo[*b*][1,4]dioxine-6-carboxylate **267**



To a Schlenk flask was added methyl (2*S*,3*S*,4*aR*,6*R*,8*R*,8*aS*)-8-(benzoyloxy)-6-hydroxy-2,3-dimethoxy-2,3-dimethyl-7-oxooctahydrobenzo[*b*][1,4]dioxine-6-carboxylate **262** (51 mg, 0.12 mmol) and THF (2.5 mL) and the resultant solution was cooled to -78 °C. To this was added sodium bis(trimethylsilyl)amide (0.3 mL, 0.30 mmol, 1 M solution in THF) and the reaction mixture was stirred at -78 °C for 90 min, then at rt for 24 h. The reaction mixture was quenched with saturated aq. ammonium chloride solution (10 mL), extracted with DCM (3 x 10 mL), dried with sodium sulfate, filtered and the solvent removed under reduced pressure. The crude product was purified by column chromatography (petroleum ether: acetone, 4: 1, column diameter = 1 cm, silica = 15 cm) to give methyl 3,5-dihydroxy-2-methoxy-2,3-dimethyl-2,3-dihydrobenzo[*b*][1,4]dioxine-6-carboxylate **267** (24 mg, 0.08 mmol, 70%) as a white solid, as an inseparable 1: 2 mixture of diastereomers.

Mp = 163.8 – 165.2 °C; R_f = 0.25 (petroleum ether: acetone, 4: 1); IR (neat): ν_{\max} cm⁻¹ 3453 (OH), 3000 – 2850 (CH), 1670 (C=O); HRMS (pNSI): calcd for C₁₃H₁₇O₇ [M+H]⁺: 285.0969; observed: 285.0970.

Major diastereomer

¹H NMR (500 MHz, CDCl₃) δ_H 10.99 (1H, s, OH), 7.34 (1H, d, J = 8.9 Hz, H⁵), 6.42 (1H, d, J = 8.9 Hz, H⁶), 3.84 (3H, s, H¹³), 3.22 (3H, s, H¹¹), 1.67 (3H, s, H^{9/10}), 1.59 (3H, s, H^{9/10}); ¹³C NMR (126 MHz, CDCl₃) δ_C 170.6 (C¹²), 152.0 (C³), 145.6 (C¹), 129.8 (C²), 122.3 (C⁵), 108.4 (C⁶), 107.0 (C⁴), 99.1 (C^{7/8}), 96.0 (C^{7/8}), 52.1 (C¹³), 49.5 (C¹¹), 22.7 (C^{9/10}), 17.3 (C^{9/10}).

Minor diastereomer

¹H NMR (500 MHz, CDCl₃) δ_H 10.93 (1H, s, OH), 7.32 (1H, d, J = 8.9 Hz, H^{5/6}), 6.39 (1H, d, J = 8.9 Hz, H^{5/6}), 3.85 (3H, s, H¹³), 3.26 (3H, s, H¹¹), 1.52 (3H, s, H^{9/10}), 1.44 (3H, s, H^{9/10}); ¹³C NMR (126 MHz, CDCl₃) δ_C 170.5 (C¹²), 151.8 (C³), 144.4 (C¹), 131.0 (C²), 122.0 (C⁵), 108.0 (C⁶), 107.1 (C⁴), 98.7 (C^{7/8}), 97.2 (C^{7/8}), 52.2 (C¹³), 49.5 (C¹¹), 20.3 (C^{9/10}), 16.7 (C^{9/10}).

References

1. A. Gurib-Fakim, *Mol. Aspects. Med.*, 2006, **27**, 1 – 93
2. D. J. Newman, G. M. Cragg, K. M. Snader, *Nat. Prod. Rep.*, 2000, **17**, 215 – 234
3. A. Fleming, *Brit. J. Exp. Path.*, 1929, **10**, 226 - 236
4. P. J. Rutledge, G. L. Challis, *Nature Rev. Microbiol.*, 2015, **13**, 509-523
5. D. J. Newman, G. M. Cragg, *J. Nat. Prod.*, 2012, **75**, 311 - 335
6. N. P. Shah, C. Tran, F. Y. Lee, P. Chen, D. Norris, C. L. Sawyers, *Science*, 2004, **305**, 399 – 401
7. E. De Clercq, *Nat. Rev. Drug Discov.*, 2002, **1**, 13 – 25
8. A. Uruno, N. Noguchi, K. Matsuda, K. Nata, T. Yoshikawu, Y. Chikamatsu, H. Kagechika, H. Harigae, S. Ito, H. Okamoto, A. Sugawara, *J. Leukoc. Biol.*, 2011, **90**, 235 – 247
9. S. Punjabi, L. J. Cook, P. Kersey, R. Marks, R. Cerio, *Int. J. Dermatol*, 2008, **47**, 78 – 82
10. J. F. Chantot, A. Bryskier, J. C. Gasc, *J. Antibiot.*, 1986, **36**, 660 – 668
11. A. Ganesan, *Curr. Opin. Chem. Biol.*, 2008, **12**, 306 – 317
12. a) M. C. Wani, H. L. Taylor, M. E. Wall, P. Coggon, A. T. McPhail, *J. Am. Chem. Soc.*, 1971, **93**, 2325 – 2327 b) K. V. Rao, *J. Heterocyclic Chem.*, 1997, **34**, 675 - 680
13. G. M. Cragg, S. A. Schepartz, M. Suffness, M. R. Grever, *J. Nat. Prod.*, 1993, **56**, 1657 – 1668
14. T. K. Yeung, C. Germond, X. Chen, Z. Wang, *Biochem. Biophys. Res. Commun.*, 1999, **263**, 398 – 404
15. M. D'Incalci, C. M. Galmarini, *Mol. Cancer Ther.*, 2010, **9**, 2157 - 2163
16. A. Cuevas, A. Francesch, *Nat. Prod. Rep.*, 2009, **26**, 322 - 337
17. S. Malik, R. M. Cusidó, M. H. Mirjalili, E. Moyano, J. Palazón, M. Bonfill, *Process Biochem.*, 2011, **46**, 23 - 34
18. C. Cuevas, M. Pérez, M. J. Martin, J. L. Chicharro, C. Fernández-Rivas, M. Flores, A. Francesch, P. Gallego, M. Zarzuelo, F. Calle, J. Garcia, C. Polanco, I. Rodríguez, I. Manzanares, *Org. Lett.*, 2000, **2**, 2545 – 2548
19. C. Fletcher, *Brit. Med. J.*, 1984, **289**, 1721 – 1723
20. J. Houbraken, J. C. Frisvad, R. A. Samson, *IMA Fungus*, 2011, **2**, 97 – 95
21. D. L. Waxman, J. L. Strominger, *Annu. Rev. Biochem.*, 1983, **52**, 825 – 869
22. F. P. Tally, M. F. DeBruin, *J. Antimicrob. Chemother.*, 2000, **46**, 523 – 526
23. J. A. Silverman, L. I. Mortin, A. D. G. VanPraagh, T. Li, J. Alder, *J. Infect. Dis.*, 2005, **191**, 2149 – 2152
24. A. Raja, J. LaBonte, J. Lebbos, P. Kirkpatrick, *Nat. Rev. Drug Discov.*, 2003, **2**, 943 – 944

Appendix

25. S. K. Straus, R. E. W. Hancock, *Biochim. Biophys. Acta*, 2006, **1758**, 1215 - 1223
26. R. Garcia-Carbonero, J. G. Supko, *Clin. Cancer Res.*, 2002, **8**, 641 – 661
27. J. F. Pizzolato, L. B. Saltz, *Lancet*, 2003, **361**, 2235 – 2242
28. W. Du, *Tetrahedron*, 2003, **59**, 8649 – 8687
29. S. M. Catnach, P. D. Fairclough, *Gut*, 1992, **33**, 397 – 401
30. T. Mazzei, E. Mini, A. Novelli, P. Periti, *J. Antimicrob. Chemother.*, 1993, **31**, 1 – 9
31. H. A. Kirst, G. D. Sides, *Antimicrob. Agents Chemother.*, 1989, **33**, 1413 – 1418
32. J. C. Gasc, S. G. D'Ambrieres, A. Lutz, J. F. Chantot, *J. Antibiot.*, 1991, **44**, 313 – 330
33. R. J. M. Goss, S. Shankar, A. A. Fayad, *Nat. Prod. Rep.*, 2012, **29**, 870 - 889
34. M. A. Peñalva, R. T. Rowlands, G. Turner, *Trends Biotechnol.*, 1998, **16**, 483 – 489
35. L. P. Pickens, Y. Tang, Y. Chooi, *Annu. Rev. Chem. Biomol. Eng.*, 2011, **2**, 211 – 236
36. H. Tabata, *Adv. Biochem. Eng. Biotechnol.*, 2004, **7**, 1 – 23
37. J. J. Zhong, *J. Biosci. Bioeng.*, 2002, **94**, 591 – 599
38. Y. Yukimune, H. Tabata, Y. Higashi, Y. Hara, *Nature Biotechnol.*, 1996, **14**, 1129 – 1132
39. G. M. Cragg, D. J. Newman, *Pharm. Biol.*, 2001, **39**, 8 – 17
40. B. A. Pfeifer, S. J. Admiraal, H. Gramajo, D. E. Cane, C. Khosla, *Science*, 2001, **291**, 1790 – 1792
41. S. P. Gunasekera, M. Gunasekera, R. E. Longley, G. K. Schulte, *J. Org. Chem.*, 1990, **55**, 4912 – 4915
42. C. E. Salomon, N. A. Magarvey, D. H. Sherman, *Nat. Prod. Rep.*, 2004, **21**, 105 - 121
43. a) S. J. Mickel, G. H. Sedelmeier, D. Niederer, R. Daeffler, A. Osmani, K. Schreiner, M. Seeger-Weibel, B. Béro, K. Schaer, R. Gamboni, S. Chen, W. Chen, C. T. Jagoe, F. R. Kinder, M. Loo, K. Prasod, O. Repič, W. Shieh, R. Wang, L. Waykole, D. Xu, S. Xue, *Org. Process. Res. Dev.*, 2004, **8**, 92 – 100 b) S. J. Mickel, G. H. Sedelmeier, D. Niederer, F. Schuerch, D. Grimler, G. Koch, R. Daeffler, A. Osmani, A. Hirni, K. Schaer, R. Gamboni, A. Bach, A. Chaudhary, S. Chen, W. Chen, B. Hu, C. T. Jagoe, H. Kim, F. R. Kinder, Y. Liu, Y. Lu, J. McKenna, M. Prashad, T. M. Ramsey, O. Repič, L. Rogers, W. Shieh, R. Wang, L. Waykole, *Org. Process. Res. Dev.*, 2004, **8**, 101 – 106 c) S. J. Mickel, G. H. Sedelmeier, D. Niederer, F. Schuerch, G. Koch, E. Kuesters, R. Daeffler, A. Osmani, M. Seeger-Weibel, A. Hirni, K. Schaer, R. Gamboni, A. Bach, S. Chen, W. Chen, P. Geng, C. T. Jagoe, F. R. Kinder, G. T. Lee, J. McKenna, T. M. Ramsey, O. Repič, L. Rogers, W. Shieh, R. Wang, L. Waykole, *Org. Process. Res. Dev.*, 2004, **8**, 107 – 112 d) S. J. Mickel, G. H. Sedelmeier, D. Niederer, F. Schuerch, M. Seger, K. Schreiner, R. Daeffler, A. Osmani, D. Bixel, O. Loiseleur, J. Cercus, H. Stettler, K. Schaer, R. Gamboni, A. Bach, G. Chen, W. Chen, P. Geng, G. T. Lee, E. Loeser, J. McKenna, F. R. Kinder, K. Konigsberger, K. Pasad, T. M. Ramsey, N. Reel, O. Repič, L. Rogers, W. Shieh, R. Wang, L. Waykole, S. Xue,

Appendix

- G. Florence, I. Paterson, *Org. Process. Res. Dev.*, 2004, **8**, 113 – 121 e) S. J. Mickel, D. Niederer, R. Daeffler, A. Osmani, E. Kuesters, E. Schmid, K. Schaer, R. Gamboni, W. Chen, E. Loeser, F. R. Kinder, K. Konigsberger, K. Pasad, T. M. Ramsey, N. Reel, O. Repič, R. Wang, G. Florence, I. Lyothier, I. Paterson, *Org. Process. Res. Dev.*, 2004, **8**, 122 – 130
44. J. Kennedy, *Nat. Prod. Rep.*, 2008, **25**, 25 – 34
45. C. Cui, H. Kakeya, H. Osada, *Tetrahedron*, 1996, **52**, 12651 – 12666
46. S. D. Edmondson, S. J. Danishefsky, *Angew. Chem. Int. Ed.*, 1998, **37**, 1138 – 1140
47. S. Edmondson, S. J. Danishefsky, L. Sepp-Lorenzino, N. Rosen, *J. Am. Chem. Soc.*, 1999, **121**, 2147 - 2155
48. A. Di Paolo, R. Danesi, D. Nardini, G. Bocci, F. Innocenti, S. Fogli, S. Barachini, A. Marchetti, G. Bevilacqua, M. Del. Tacca, *Br. J. Cancer*, 2000, **82**, 905 – 912
49. R. Thiericke, H. Langer, A. Zeeck, *J. Chem. Soc. Perkin Trans. 1*, 1989, 851 – 855
50. R. Thiericke, J. Rohr, *Nat. Prod. Rep.*, 1993, **10**, 265 – 289
51. L. Toscano, G. Fioriello, R. Spagnoli, L. Cappellitti, G. Zanuso, *J. Antibiot.*, 1983, **36**, 1439 – 1450
52. S. Gaisser, J. Reather, G. Wirtz, L. Kellenberger, J. Staunton, P. F. Leadlay, *Mol. Microbiol.*, 2000, **36**, 391 – 401
53. K. J. Weissman, P. F. Leadlay, *Nat. Rev. Microbiol.*, 2005, **3**, 925 – 936
54. K. Scherlach, C. Hertweck, *Org. Biomol. Chem.*, 2006, **4**, 3517 – 3520
55. W. K. W. Chou, I. Fanizza, T. Uchiyama, M. Komatsu, H. Ikeda, D. E. Cane, *J. Am. Chem. Soc.*, 2010, **132**, 8850 – 8851
56. G. L. Challis, *J. Med. Chem.*, 2008, **51**, 2618 - 2628
57. A. A. Stierle, D. B. Stierle, K. Kelly, *J. Org. Chem.*, 2006, **71**, 5357 – 5360
58. L. L. Ling, T. Schneider, A. J. Peoples, A. L. Spoering, I. Engels, B. P. Conlon, A. Mueller, T. F. Schäberle, D. E. Hughes, S. Epstein, M. Jones, L. Lazarides, V. A. Steadman, D. R. Cohen, C. R. Felix, K. A. Fetterman, W. P. Millet, A. G. Nitti, . M. Zuello, C. Chen, K. Lewis, *Nature*, 2015, **517**, 455 – 473
59. B. Kepplinger, PhD Thesis, Newcastle University, 2016
60. The World Health Organisation Tuberculosis Fact Sheet, <http://www.who.int/mediacentre/factsheets/fs104/en/>, (accessed January 2016)
61. M. Gengenbacher, S. H. E. Kaufmann, *FEMS Microbiol. Rev.*, 2012, **36**, 514 – 532
62. J. M. Tufariello, J. Chan, J. L. Flynn, *Lancet Infect. Dis.*, 2003, **3**, 578 – 590
63. N. M. Parrish, J. D. Dick, W. R. Blshal, *Trends Microbiol.*, 1998, **6**, 107 - 112
64. Y. Zhang, *Annu. Rev. Pharmacol. Toxicol.*, 2005, **45**, 529 – 564
65. A. Somoskovi, L. M. Parsons, M. Salfinger, *Respir. Res.*, 2001, **2**, 164 – 168

Appendix

66. a) K. Takayama, H. K. Schnoes, E. L. Armstrong, R. W. Boyle, *J. Lip. Res.*, 1975, **16**, 308 – 317 b) R. Yendapally, R. E. Lee, *Bioorg. Med. Chem. Lett.*, 2008, **18**, 1607 – 1611
67. A. Jain, R. Mondal, S. Srivastava, R. Prasad, K. Singh, R. C. Ahuja, *Indian J. Med. Res.*, 2008, **128**, 634 – 639
68. J. Schneeweiss, G. W. Poole, *Brit. Med. J.*, 1960, **2**, 830 – 832
69. Y. Zhang, M. M. Wade, A. Scorpio, H. Zhang, Z. Sun, *J. Antimicrob. Chemother.*, 2003, **52**, 790 – 795
70. P. Sensi, *Rev. Infect. Dis.*, 1983, **5**, S402 – S406
71. S. Bala, R. Khanna, M. Dadhwal, S. R. Prabakaran, S. Shivaji, J. Cullum, R. Lal, *Int. J. Syst. Evol. Microbiol.*, 2004, **54**, 1145 – 1149
72. P. A. Aristoff, G. A. Garcia, P. D. Kirchhoff, H. D. H. Showalter, *Tuberculosis*, 2010, **90**, 94 – 118
73. N. Wang, Y. Fu, G. Yan, G. Bao, C. Xu, C. He, *J. Antibiot.*, 1988, **41**, 264 – 267
74. E. A. Campbell, N. Korzeheva, A. Mustaev, K. Murakami, S. Nair, A. Goldfarb, S. A. Darst, *Cell*, 2001, **104**, 901 – 912
75. H. G. Floss, T. Yu, *Chem. Rev.*, 2005, **105**, 621 – 632
76. M. X. Ho, B. P. Hudson, K. Das, E. Arnold, R. H. Ebricht, *Curr. Opin. Struct. Biol.*, 2009, **19**, 715 – 723
77. W. Wehrli, M. Staehelin, *Biochim. Biophys. Acta*, 1969, **182**, 24 – 29
78. M. Brufani, S. Cerrini, W. Fedeli, A. Vactago, *J. Mol. Biol.*, 1974, **87**, 409 – 435
79. S. Ramaswamy, J. M. Musser, *Tuber. Lung Dis.*, 1998, **79**, 3 – 29
80. G. Lancini, G. Satori, *J. Antibiot.*, 1976, **29**, 466 – 468
81. P. Sensi, N. Maggi, R. Ballota, S. Fürész, R. Pallanza, V. Arioli, *J. Med. Chem.*, 1964, **7**, 596 – 602
82. N. Maggi, V. Arioli, P. Sensi, *J. Med. Chem.*, 1965, **8**, 790 – 793
83. US Pat. US3342810, 1967
84. US Pat., US3963705, 1976
85. M.F. Dampier, C. Chen, H. W. Whitlock, *J. Am. Chem. Soc.*, 1976, **98**, 7064 – 7069
86. US Pat., US4174320, 1979
87. R. Dietze, L. Teixeira, L. Márcia, C. Rocha, M. Palaci, J. J. Johnson, C. Wells, L. Rose, K. Eisenach, J. J. Ellner, *Antimicrob. Agents Chemother.*, 2001, **45**, 1972 – 1976
88. Z. Saribaş, T. Kocagöz, A. Alp, A. Günalp, *J. Clin. Microbiol.*, 2003, **41**, 816 – 818
89. J. Li, Z. Ma, K. Chapo, D. Yan, A. S. Lynch, C. Z. Dhing, *Bioorg. Med. Chem. Lett.*, 2007, **17**, 5510 – 5513

Appendix

90. Y. Yamane, T. Hashizume, K. Yamashita, E. Konishi, K. Hosoe, T. Hidaka, K. Watanabe, H. Kawaharada, T. Yamamoto, F. Kuze, *Chem. Pharm. Bull.*, 1993, **41**, 148 – 155
91. K. C. Nicolaou, D. Vourloumis, N. Winssinger, P. S. Baran, *Angew. Chem. Int. Ed.*, 2000, **39**, 44 – 122
92. K. C. Nicolaou, S. A. Snyder, *Proc. Natl. Acad. Sci.*, 2004, **101**, 11929 – 11936
93. R. Hoffmann, R. B. Woodward, *J. Am. Chem. Soc.*, 1965, **87**, 2946 – 2048
94. D. H. Barton, J. M. Beaton, *J. Am. Chem. Soc.*, 1960, **82**, 2640 – 2641
95. D. T. Hung, J. B. Nerenberg, S. L. Schreiber, *Chem. Biol.*, 1994, **1**, 67 - 71
96. H. Iwaki, Y. Nakayama, M. Takahashi, S. Uetsuki, M. Kido, Y. Fukuyama, *J. Antibiot.*, 1984, **37**, 1091 – 1093
97. D. Komagata, R. Sawa, N. Kinoshita, C. Imada, T. Sawa, H. Naganawa, M. Hamada, Y. Okami, T. Takeuchi, *J. Antibiot.*, 1992, **45**, 1681 – 1683
98. D. M. Townsend, K. D. Tew, *Oncogene*, 2003, **22**, 7369 – 7375
99. K. Yamamoto, M. F. Hentemann, J. G. Allen, S. J. Danishefsky, *Chem., Eur. J.*, 2003, **22**, 7369 – 7375
100. L. H. Mejorado, T. R. R. Pettus, *J. Am. Chem. Soc.*, 2006, **128**, 15625 – 15631
101. D. Magdziak, S. J. Meek, T. R. R. Pettus, *Chem. Rev.*, 2004, **104**, 1383 – 1429
102. J. Augé, N. Lubin – Germain, J. Uziel, *Synthesis*, 2007, **12**, 1739 – 1764
103. K. S. Feldman, D. K. Hester, C. S. López, O. N. Faza, *Org. Lett.*, 2008, **10**, 1665-1668
104. Y. Chen, P. Knochel, *Angew. Chem. Int. Ed.*, 2008, **47**, 7648 – 7651
105. A. A. Frimer, P. Gilinsky-Sharon, G. Aljadeff, H. E. Gottlieb, J. Hameiri-Buch, V. Marks, R. Philosofof, Z. Rosental, *J. Org. Chem.*, 1989, **54**, 4853 – 4866
106. R. L. Y. Bao, R. Zhao, L. Shi, *Chem. Commun.*, 2015, **51**, 6884 – 6900
107. K. Hirano, T. Iwahama, S. Sakaguchi, Y. Ishii, *Chem. Commun.*, 2000, 2457 – 2458
108. Y. F. Chen, Y. C. Lin, P. K. Huang, H. C. Chan, S. C. Kuo, K. H. Lee, L. J. Huang, *Biorg. Med. Chem.*, 2013, **21**, 5064 – 5075
109. T. Dei, K. Morino, A. Sudo, T. Endo, *J. Polym. Sci. A Polym. Chem.*, 2011, **49**, 2245 - 2251
110. D. Basavaiah, A. J. Rao, T. Satyanarayana, *Chem. Rev.*, 2003, **103**, 811 - 891
111. M. Shi, J. K. Jiang, Y. S. Feng, *Org. Lett.*, 2000, **2**, 2397 – 2400
112. a) E. J. Enholm, J. P. Schulte, *J. Org. Chem.*, 1999, **64**, 2610 – 2611 b) D. A. Evans, K. T. Chapman, E. M. Carreira, *J. Am. Chem. Soc.*, 1988, **110**, 3560 – 3578
113. K. Takai, R. Morita, H. Matsushita, C. Toratsu, *Chirality*, 2003, **15**, 17 - 23
114. K. C. Nicolaou, S. A. Snyder, T. Montagnon, G. Vassilikogiannakis, *Angew. Chem. Int. Ed.*, 2002, **41**, 1668 – 1698
115. Y. Kobuke, T. Fueno, J. Furukawa, *J. Am. Chem. Soc.*, 1970, **92**, 6548 – 6553

Appendix

116. R. B. Woodward, F. E. Bader, H. Bickel, A. J. Frey, R. W. Kierstead, *Tetrahedron*, 1958, **2**, 1 – 57
117. a) D. S. Fabricant, N. R. Farnsworth, *Environ. Health. Perspect.*, 2001, **109**, 69 – 75
b) V. S. Bhatara, J. N. Sharma, S. Gupta, Y. K. Gupta, *Am. J. Psychiat.*, 1997, **154**, 894
118. R. B. Woodward, F. E. Bader, H. Bickel, A. J. Frey, R. W. Kierstead, *J. Am. Chem. Soc.*, 1956, **78**, 2023 – 2025
119. D. M. Roll, P. J. Scheuer, G. K. Matsumoto, J. Clardy, *J. Am. Chem. Soc.*, 1983, **105**, 6177 – 6178
120. H. S. Sutherland, F. E. S. Souza, R. G. A. Rodrigo, *J. Org. Chem.*, 2001, **66**, 3639 – 3641
121. M. Konishi, H. Ohkuma, K. Matsumoto, T. Tsuno, H. Kamei, T. Miyaki, T. Oki, H. Kawaguchi, G. D. VanDuyne, J. Clardy, *J. Antibiot.*, 1989, **42**, 1449 – 1452
122. P. Magnus, S. A. Eisenbeis, N. A. Magnus, *J. Chem. Soc. Chem. Commun.*, 1994, 1545 – 1546
123. M. Lautens, K. Fagnou, D. Yang, *J. Am. Chem. Soc.*, 2003, **125**, 14884 – 14892
124. V. M. Lynch, R. A. Fairhurst, P. Magnus, B. E. Davis, *Acta Cryst.*, 1995, **C51**, 780 – 782
125. P. R. Schreiner, *Chem. Soc. Rev.*, 2003, **32**, 289 – 296
126. W. Notz, F. Tanaka, C. F. Barbas, *Acc. Chem. Rev.*, 2004, **37**, 580 – 591
127. J. McKinley, A. Aponick, J. C. Raber, C. Fritz, D. Montgomery, C. T. Wigal, *J. Org. Chem.*, 1997, **62**, 4874 - 4876
128. a) K. H. Chung, H. G. Lee, I. Y. Choi, J. R. Choi, *J. Org. Chem.*, 2001, **66**, 5937 – 5939 b) D. B. Berkowitz, S. Choi, J. H. Maeng, *J. Org. Chem.*, 2000, **65**, 847 – 860
129. A. Liu, Z. Z. Liu, Z. M. Zou, S. Z. Chen, L. Z. Xu, S. L. Yang, *Tetrahedron*, 2004, **60**, 3689 – 3694
130. H. B. Henbest, R. A. L. Wilson, *J. Chem. Soc.*, 1957, 1958 – 1965
131. T. J. Donohoe, K. Blades, P. R. Moore, M. J. Waring, J. J. C. Winter, M. Helliwell, N. J. Newcombe, G. Stemp, *J. Org. Chem.*, 2002, **67**, 7946 – 7956
132. a) J. K. Cha, W. J. Christ, Y. Kishi, *Tetrahedron Lett.*, 1983, **24**, 3943 – 3946 b) G. Stork, M. Kahn, *Tetrahedron Lett.*, 1983, **24**, 3951 - 3954
133. C. B. Miao, Y. H. Wang, M. L. Xing, X. W. Lu, X. Q. Sun, H. T. Yang, *J. Org. Chem.*, 2013, **78**, 11584 – 11589
134. A. Rosowsky, C. E. Mota, J. E. Wright, J. H. Freisheim, J. J. Heusner, J. J. McCormack, S. F. Queener, *J. Med. Chem.*, 1993, **36**, 3103 – 3112

Appendix

4-(2,5-Dimethoxyphenyl)-4-(phenylthio)butan-2-one 158

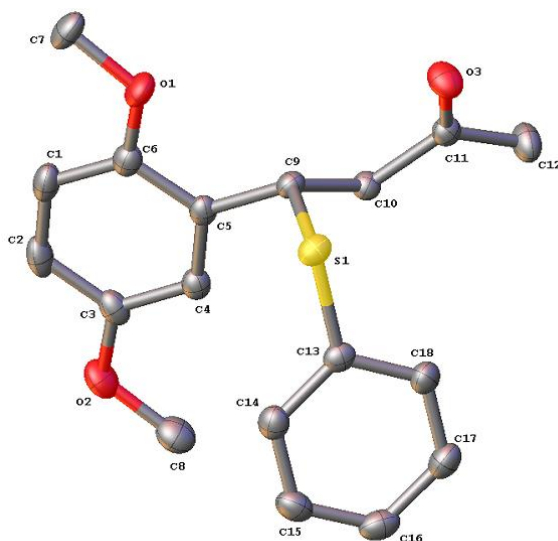


Table 1 Crystal data and structure refinement for mjh150005_fa.

Identification code	mjh150005_fa
Empirical formula	C ₁₈ H ₂₀ O ₃ S
Formula weight	316.40
Temperature/K	150.0(2)
Crystal system	monoclinic
Space group	P2 ₁ /c
a/Å	16.69736(17)
b/Å	5.57877(4)
c/Å	18.13732(17)
α/°	90
β/°	110.3522(11)
γ/°	90
Volume/Å ³	1584.03(3)
Z	4

Appendix

$\rho_{\text{calc}}/\text{cm}^3$	1.327
μ/mm^{-1}	1.897
F(000)	672.0
Crystal size/ mm^3	0.26 × 0.16 × 0.1
Radiation	CuK α ($\lambda = 1.54184$)
2 Θ range for data collection/ $^\circ$	5.646 to 133.86
Index ranges	-19 ≤ h ≤ 19, -6 ≤ k ≤ 6, -21 ≤ l ≤ 21
Reflections collected	40835
Independent reflections	2820 [$R_{\text{int}} = 0.0304$, $R_{\text{sigma}} = 0.0101$]
Data/restraints/parameters	2820/0/202
Goodness-of-fit on F^2	1.033
Final R indexes [$I \geq 2\sigma(I)$]	$R_1 = 0.0275$, $wR_2 = 0.0683$
Final R indexes [all data]	$R_1 = 0.0303$, $wR_2 = 0.0701$
Largest diff. peak/hole / e \AA^{-3}	0.23/-0.20

Appendix

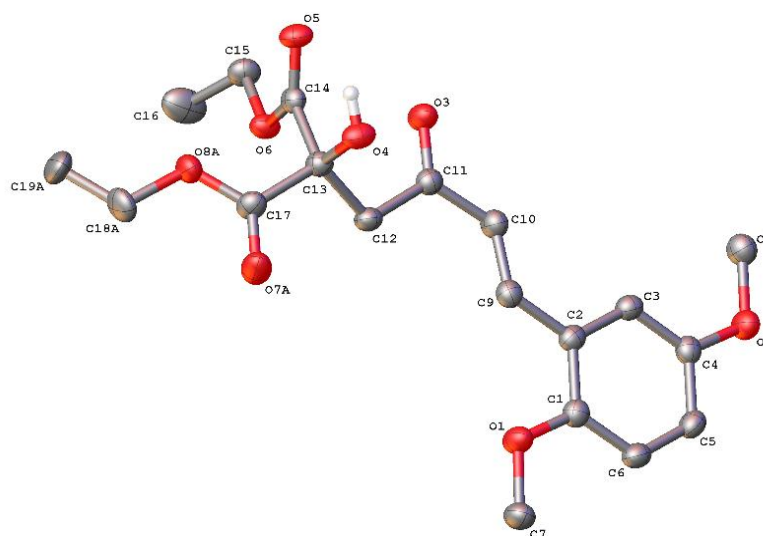
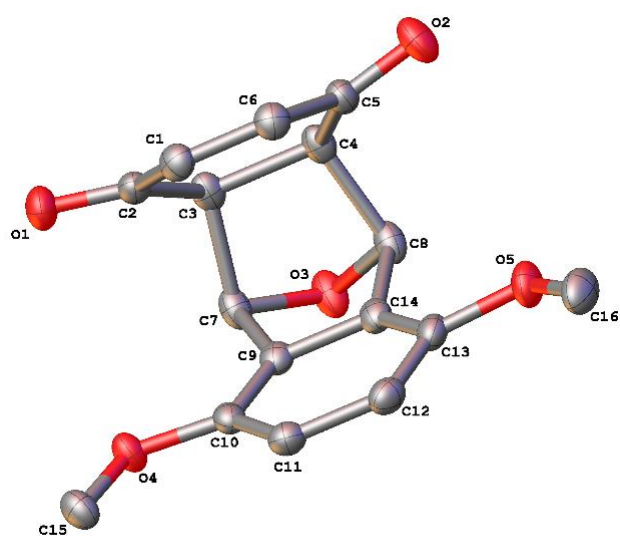
Diethyl (*E*)-2-(4-(2,5-dimethoxyphenyl)-2-oxobut-3-en-1-yl)-2-hydroxymalonate 159

Table 1 Crystal data and structure refinement for mjh150020.

Identification code	mjh150020
Empirical formula	C ₁₉ H ₂₄ O ₈
Formula weight	380.38
Temperature/K	150.0(2)
Crystal system	monoclinic
Space group	C2/c
a/Å	29.9185(15)
b/Å	9.2785(4)
c/Å	13.9811(8)
α/°	90
β/°	103.344(6)
γ/°	90
Volume/Å ³	3776.3(3)
Z	8

Appendix

$\rho_{\text{calc}}/\text{g}/\text{cm}^3$	1.338
μ/mm^{-1}	0.880
F(000)	1616.0
Crystal size/ mm^3	$0.44 \times 0.23 \times 0.2$
Radiation	CuK α ($\lambda = 1.54184$)
2Θ range for data collection/ $^\circ$	6.072 to 133.658
Index ranges	$-34 \leq h \leq 35, -11 \leq k \leq 8, -16 \leq l \leq 15$
Reflections collected	13592
Independent reflections	3332 [$R_{\text{int}} = 0.0302, R_{\text{sigma}} = 0.0230$]
Data/restraints/parameters	3332/5/264
Goodness-of-fit on F^2	1.048
Final R indexes [$I \geq 2\sigma(I)$]	$R_1 = 0.0404, wR_2 = 0.0975$
Final R indexes [all data]	$R_1 = 0.0526, wR_2 = 0.1074$
Largest diff. peak/hole / $e \text{ \AA}^{-3}$	0.20/-0.34

5,8-Dimethoxy-4a,9,9a,10-tetrahydro-9,10-epoxyanthracene-1,4-dione 227**Table 1 Crystal data and structure refinement for mjh150019.**

Identification code	mjh150019
Empirical formula	C ₁₆ H ₁₄ O ₅
Formula weight	286.27
Temperature/K	150.0(2)
Crystal system	monoclinic
Space group	P2 ₁ /c
a/Å	7.27400(10)
b/Å	25.1661(3)
c/Å	7.79454(11)
α/°	90
β/°	110.0773(16)
γ/°	90
Volume/Å ³	1340.14(3)
Z	4

Appendix

$\rho_{\text{calc}}/\text{g}/\text{cm}^3$	1.419
μ/mm^{-1}	0.886
F(000)	600.0
Crystal size/ mm^3	$0.47 \times 0.3 \times 0.23$
Radiation	CuK α ($\lambda = 1.54184$)
2Θ range for data collection/ $^\circ$	7.026 to 134.012
Index ranges	$-8 \leq h \leq 8, -29 \leq k \leq 29, -9 \leq l \leq 7$
Reflections collected	9593
Independent reflections	2383 [$R_{\text{int}} = 0.0203, R_{\text{sigma}} = 0.0143$]
Data/restraints/parameters	2383/0/192
Goodness-of-fit on F^2	1.080
Final R indexes [$I \geq 2\sigma(I)$]	$R_1 = 0.0372, wR_2 = 0.0981$
Final R indexes [all data]	$R_1 = 0.0401, wR_2 = 0.1008$
Largest diff. peak/hole / $e \text{ \AA}^{-3}$	0.42/-0.25

5,8-Dimethoxy-2,9a-dimethyl-4a,9,9a,10-tetrahydro-9,10-epoxyanthracene-1,4-dione
233-b

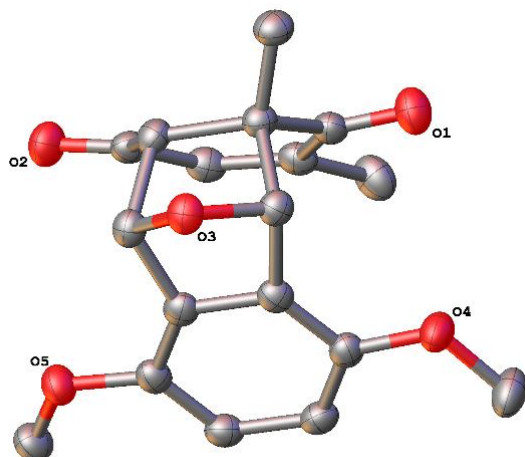


Table 1 Crystal data and structure refinement for mjh150017_off_2.

Identification code	mjh150017_off_2
Empirical formula	C ₁₈ H ₁₈ O ₅
Formula weight	314.32
Temperature/K	150.0(2)
Crystal system	orthorhombic
Space group	Fdd2
a/Å	52.964(16)
b/Å	14.9766(17)
c/Å	7.5116(7)
α/°	90
β/°	90
γ/°	90
Volume/Å ³	5958(2)
Z	16
ρ _{calc} /cm ³	1.402

Appendix

μ/mm^{-1}	0.846
F(000)	2656.0
Crystal size/ mm^3	0.24 × 0.16 × 0.15
Radiation	CuK α ($\lambda = 1.54184$)
2 Θ range for data collection/ $^\circ$	6.676 to 134.356
Index ranges	-62 ≤ h ≤ 61, -15 ≤ k ≤ 17, -8 ≤ l ≤ 8
Reflections collected	20456
Independent reflections	2624 [$R_{\text{int}} = 0.0322$, $R_{\text{sigma}} = 0.0141$]
Data/restraints/parameters	2624/1/212
Goodness-of-fit on F^2	1.048
Final R indexes [$I \geq 2\sigma(I)$]	$R_1 = 0.0274$, $wR_2 = 0.0673$
Final R indexes [all data]	$R_1 = 0.0282$, $wR_2 = 0.0680$
Largest diff. peak/hole / $e \text{ \AA}^{-3}$	0.10/-0.16
Flack parameter	-0.05(7)

Methyl (2*S*,3*S*,4*aR*,8*S*,8*aS*)-2,3-dimethoxy-2,3-dimethyl-8-((4-nitrobenzoyl)oxy)-2,3,4*a*,5,8,8*a*-hexahydrobenzo[*b*][1,4]dioxine-6-carboxylate 258

MJH150021

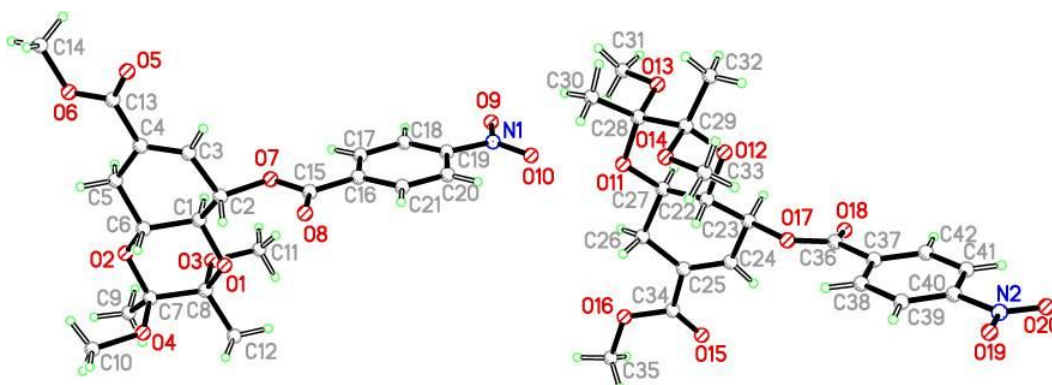
355

Data collected at Diamond Light Source, July 2015

Bill Clegg, Mike Probert and Paul Waddell

There are two molecules in the asymmetric unit, with the same relative and absolute configuration; the absolute configuration cannot be reliably established from the diffraction experiment and has been assumed from the synthesis information provided.

The crystal was found to be a non-merohedral twin with approximately equal components.



The two molecules in the asymmetric unit

Table 1. Crystal data and structure refinement for mjh150021.

Identification code	mjh150021
Chemical formula (moiety)	C ₂₁ H ₂₅ NO ₁₀
Chemical formula (total)	C ₂₁ H ₂₅ NO ₁₀
Formula weight	451.42

Appendix

Temperature	100(2) K
Radiation, wavelength	synchrotron, 0.6889 Å
Crystal system, space group	monoclinic, P2 ₁
Unit cell parameters	a = 14.912(4) Å α = 90° b = 7.466(2) Å β = 104.150(3)° c = 21.319(6) Å γ = 90°
Cell volume	2301.5(11) Å ³
Z	4
Calculated density	1.303 g/cm ³
Absorption coefficient μ	0.098 mm ⁻¹
F(000)	952
Crystal colour and size	colourless, 0.100 × 0.040 × 0.010 mm ³
Reflections for cell refinement	4185 (θ range 2.6 to 20.2°)
Data collection method	Rigaku Saturn 724+ on kappa diffractometer wide-frame ω scans
θ range for data collection	1.4 to 24.2°
Index ranges	h -17 to 17, k -8 to 8, l -25 to 25
Completeness to θ = 24.2°	99.9 %
Reflections collected	25692
Independent reflections	7519 (R _{int} = 0.0921)
Reflections with F ² >2σ	4672
Absorption correction	none
Structure solution	direct methods
Refinement method	Full-matrix least-squares on F ²
Weighting parameters a, b	0.0591,
Data / restraints / parameters	25692 / 1 / 589

Appendix

Final R indices [$F^2 > 2\sigma$]	R1 = 0.0572, wR2 = 0.1152
R indices (all data)	R1 = 0.1151, wR2 = 0.1365
Goodness-of-fit on F^2	0.938
Absolute structure parameter	-0.7(6)
Extinction coefficient	0.013(2)
Largest and mean shift/su	0.000 and 0.000
Largest diff. peak and hole	0.24 and -0.25 e \AA^{-3}

Appendix

Methyl (2*S*,3*S*,4*aR*,6*R*,7*S*,8*S*,8*aS*)-8-(benzoyloxy)-6,7-dihydroxy-2,3-dimethoxy-2,3-dimethyloctahydrobenzo[*b*][1,4]dioxine-6-carboxylate 259

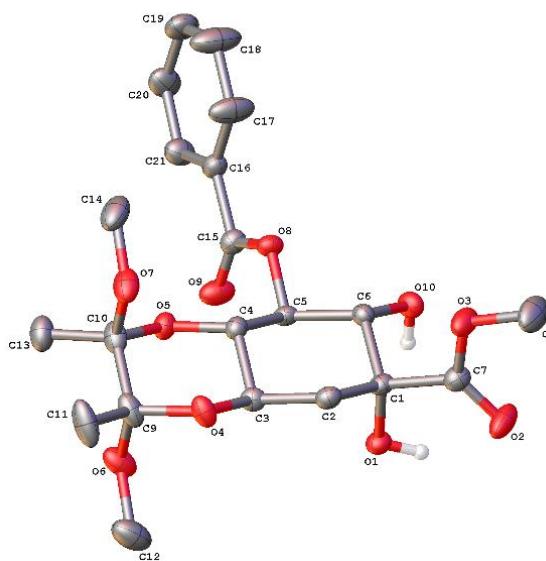


Table 1 : Crystal data and structure refinement for mjh150029_fa.

Identification code	mjh150029_fa
Empirical formula	C ₂₁ H _{28.4} O _{10.2}
Formula weight	444.04
Temperature/K	150.0(2)
Crystal system	orthorhombic
Space group	P2 ₁ 2 ₁ 2 ₁
a/Å	10.98455(7)
b/Å	12.06305(9)
c/Å	16.99567(11)
α/°	90
β/°	90
γ/°	90
Volume/Å ³	2252.05(3)
Z	4

Appendix

$\rho_{\text{calc}}/\text{g}/\text{cm}^3$	1.310
μ/mm^{-1}	0.889
F(000)	944.0
Crystal size/ mm^3	$0.23 \times 0.21 \times 0.11$
Radiation	CuK α ($\lambda = 1.54184$)
2Θ range for data collection/ $^\circ$	8.99 to 134.022
Index ranges	$-13 \leq h \leq 13, -14 \leq k \leq 14, -20 \leq l \leq 20$
Reflections collected	62461
Independent reflections	4009 [$R_{\text{int}} = 0.0471, R_{\text{sigma}} = 0.0147$]
Data/restraints/parameters	4009/0/297
Goodness-of-fit on F^2	1.061
Final R indexes [$I \geq 2\sigma(I)$]	$R_1 = 0.0292, wR_2 = 0.0707$
Final R indexes [all data]	$R_1 = 0.0314, wR_2 = 0.0722$
Largest diff. peak/hole / $e \text{ \AA}^{-3}$	0.16/-0.20
Flack parameter	0.01(4)

Appendix

Methyl (2*S*,3*S*,4*aR*,6*R*,8*R*,8*aS*)-8-(benzoyloxy)-6-hydroxy-2,3-dimethoxy-2,3-dimethyl-7-oxooctahydrobenzo[*b*][1,4]dioxine-6-carboxylate 262

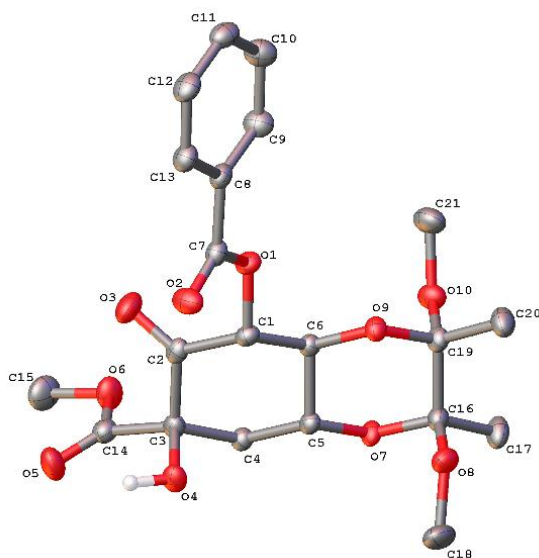


Table 1 : Crystal data and structure refinement for mjh150032.

Identification code	mjh150032
Empirical formula	C ₂₁ H ₂₆ O ₁₀
Formula weight	438.42
Temperature/K	150.0(2)
Crystal system	monoclinic
Space group	P2 ₁
a/Å	9.83490(11)
b/Å	10.70993(10)
c/Å	10.79595(14)
α/°	90
β/°	111.7181(14)
γ/°	90
Volume/Å ³	1056.43(2)
Z	2

Appendix

$\rho_{\text{calc}}/\text{g}/\text{cm}^3$	1.378
μ/mm^{-1}	0.936
F(000)	464.0
Crystal size/ mm^3	$0.52 \times 0.12 \times 0.08$
Radiation	CuK α ($\lambda = 1.54184$)
2 Θ range for data collection/ $^\circ$ 8.816 to 133.936	
Index ranges	$-11 \leq h \leq 11, -12 \leq k \leq 12, -12 \leq l \leq 12$
Reflections collected	36511
Independent reflections	3744 [$R_{\text{int}} = 0.0461, R_{\text{sigma}} = 0.0183$]
Data/restraints/parameters	3744/1/288
Goodness-of-fit on F^2	1.080
Final R indexes [$I \geq 2\sigma(I)$]	$R_1 = 0.0283, wR_2 = 0.0716$
Final R indexes [all data]	$R_1 = 0.0301, wR_2 = 0.0730$
Largest diff. peak/hole / $e \text{ \AA}^{-3}$	0.22/-0.19
Flack parameter	-0.04(5)

Cite this: *RSC Adv.*, 2015, 5, 16125

Diastereoselective synthesis of functionalised carbazoles *via* a sequential Diels–Alder/ene reaction strategy†

Joseph Cowell, Matokah Abualnaja, Stephanie Morton,‡ Ruth Linder, Faye Buckingham, Paul G. Waddell, Michael R. Probert and Michael J. Hall*

An operationally simple one-pot, three-component, diastereoselective synthesis of saturated carbazoles and related pyridazino[3,4-*b*]indoles, based on two sequential intermolecular pericyclic reactions, is described. The reaction sequence involves an intermolecular Diels–Alder (D–A) reaction of a 3-vinyl-1*H*-indole, containing an electron withdrawing N-protecting group, with a suitable dienophile. Due to the electron withdrawing nature of the N-protecting group the resultant D–A cycloadducts are sufficiently stabilised to allow for a subsequent *in situ* diastereospecific intermolecular ene reaction to take place with an added enophile, generating functionalised carbazoles with relative stereocontrol of up to four stereocentres.

Received 9th January 2015
Accepted 19th January 2015

DOI: 10.1039/c5ra00499c

www.rsc.org/advances

Introduction

Carbazole scaffolds are common in many bioactive compounds (*e.g.* staurosporine)^{1,2} with the indolocarbazole scaffold in particular being found in a number of molecules with potential therapeutic application, several of which have entered clinical trials for the treatment of cancer (midostaurin (PKC412), lestaurtinib (CEP-701), CEP-751, CEP-1347, edotecarin and becatarin).^{3,4} Therefore there is a growing interest in the development of new synthetic routes to functionalised carbazoles.^{5–9} Herein we describe our progress in the development of a diastereoselective one-pot, three-component approach for the synthesis of functionalised, partially saturated carbazoles and pyridazino[3,4-*b*]indoles.

Results and discussion

The vinyl-indole synthesis of carbazoles, originally developed by Nolan, Pindur, Porter and others, involves the D–A cycloaddition of a 2- or 3-vinyl-1*H*-indole (typically either unprotected or containing an electron donating N-protecting group) with a dienophile.^{10–22} The resulting D–A cycloadducts are often

unstable and are therefore typically oxidised or undergo an *in situ* 1,3-H shift to rearomatise the indole. We postulated that if the intermediate D–A cycloadduct could instead be intercepted *via* an alternative intermolecular reaction this would provide a new multi-component route to functionalised carbazoles. Following on from our recent work on the D–A reactions of vinyl-imidazoles,^{23,24} we decided to investigate if the D–A cycloadducts of 3-vinyl-1*H*-indoles could be reacted *in situ* with enophiles to give a new stereoselective three-component, intermolecular D–A/intermolecular ene approach to the carbazole or pyridazino[3,4-*b*]indole scaffold (Fig. 1).^{25–29}

We decided to focus our investigation on the D–A reactions of 3-vinyl-1*H*-indoles containing an electron withdrawing

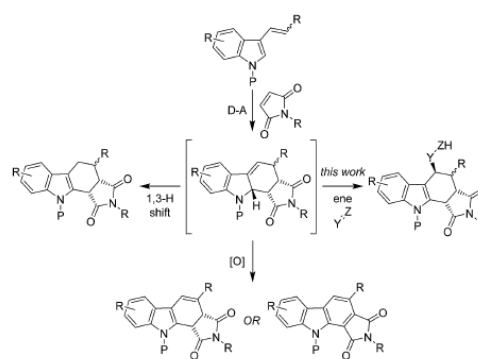
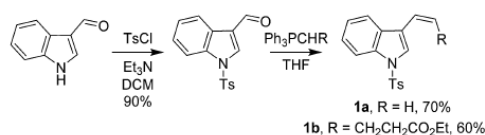


Fig. 1 Typical products of the D–A reaction between 3-vinyl-1*H*-indoles and maleimides versus our proposed trapping of the D–A cycloadduct *via* an intermolecular ene reaction.

School of Chemistry, Newcastle University, Newcastle upon Tyne, NE1 7RU, UK.
E-mail: michael.hall@newcastle.ac.uk

† Electronic supplementary information (ESI) available: ¹H and ¹³C spectra for all new compounds, crystal data and structure refinement tables for compounds 2a, 2b, 2d, 3l, 3r, 3u and 3v. The crystallographic coordinates of 2a, 2b, 2d, 3l, 3r, 3u and 3v have been deposited with the Cambridge Crystallographic Data Centre, deposition nos. CCDC 952356, 1040305, 1040306, 952229, 1040307, 1040308 and 952357. For ESI and crystallographic data in CIF or other electronic format see DOI: 10.1039/c5ra00499c

‡ Authors contributed equally.

Scheme 1 Synthesis of *N*-tosyl-3-alkenyl-1*H*-indoles **1a** and **b**.

N-protecting group as we postulated that this would stabilise the desired D–A cycloadducts sufficiently to allow either isolation or further *in situ* chemistry.^{19,20} Despite the extensive body of work that has been published on the vinyl-indole synthesis of carbazoles,^{11–18} the incorporation of electron withdrawing *N*-protecting groups has been less well studied with the phenylsulfonyl group being the most common.^{25,30–33} We therefore decide to focus our initial investigation on tosyl protected systems and embarked on the synthesis of two *N*-tosyl protected 3-alkenyl-indoles through reaction of 1*H*-indole-3-carbaldehyde with tosyl chloride, followed by a Wittig reaction with methylenetriphenyl- λ^5 -phosphane or ethyl 4-(triphenyl- λ^5 -phosphanylidene)butanoate to give **1a** and **1b** respectively (Scheme 1).

When we reacted 1-tosyl-3-vinyl-1*H*-indole **1a** with 1-methyl-1*H*-pyrrole-2,5-dione in DCM at reflux for 48 hours, we were pleased to isolate, in a 74% yield, the *N*-tosyl protected *endo*-cycloadduct **2a**, which showed little propensity towards spontaneous rearomatisation or oxidation. Whilst 4-phenyl-1,2,4-triazole-3,5-dione (PTAD) reacted rapidly with **1a** at -78°C in DCM to give the stable D–A cycloadduct **2b** in 88% yield (Table 1).

Attempts to react the more sterically demanding ethyl (*Z*)-5-(1-tosyl-1*H*-indol-3-yl)pent-4-enoate **1b** with 1*H*-pyrrole-2,5-diones under thermal conditions proved unsuccessful with no D–A reaction being observed after prolonged heating in toluene,

DCM or iso-propanol. The addition of 20 mol% of 1,3-bis(3,5-bis(trifluoromethyl)phenyl)thiourea³⁴ also showed no improvement in the D–A reaction, whilst the addition of one equivalent of TiCl_4 at -78°C for 10 minutes resulted in an efficient D–A reaction but was accompanied by the unwanted rearomatisation of the indole. Addition of one equivalent of AlCl_3 or Me_2AlCl in DCM at r.t., followed by heating to reflux gave low yields of the desired product **2c** along with recovered starting material. Further optimisation resulted in a final protocol whereby 2 equivalents of Me_2AlCl were added to a DCM solution of **1b** and the requisite 1*H*-pyrrole-2,5-dione at -78°C , followed by warming to reflux in DCM for 48 hours to give *N*-tosyl protected D–A cycloadducts **2(c–e)** in good yields (Table 2). The structures of **2(a)**, **2(b)** and **2(d)** were confirmed by single crystal X-ray analysis and are consistent with an *endo*-selective D–A reaction (see ESI†).

Next we examined the reactivity of *N*-tosyl protected *endo*-cycloadducts **2(a–e)** towards enophiles. Reaction of **2a** with nitrosobenzene proceeded well at r.t. in 18 hours to give the ene adduct **3a** in 68% isolated yield. We therefore reacted D–A adducts **2(a–e)** with nitrosobenzene and 1-methyl-2-nitrosobenzene at r.t. in DCM, giving high yields of the corresponding ene adducts **3(a, b and e–h)**. The ene reactions of **2(a–c)** also proceeded smoothly with PTAD at 0°C to give **3(c, i and j)**. The reaction of **2a** with 2,3,4,5,6-pentafluorobenzaldehyde under thermal conditions was unsuccessful. However addition of one equivalent of Me_2AlCl at -78°C to a mixture of **2a** and 2,3,4,5,6-pentafluorobenzaldehyde resulted in formation of the ene cycloadduct **3d** as a 6 : 1 mixture of diastereomers, epimeric at the *exo*-cyclic hydroxyl position³⁵ (Table 3).

Since both the D–A and ene reactions are performed in DCM we then decided to examine the potential for reaction telescoping by attempting a D–A/ene reaction sequence under “domino” conditions.³⁶ 1-Tosyl-3-vinyl-1*H*-indole **1a**, 1-methyl-

Table 1 D–A reactions of *N*-tosyl protected 1-tosyl-3-vinyl-1*H*-indole **1a**

	Starting material	Dienophile	Reaction Conditions	R'	X	Yield ^a	Product
1	1a		40 °C, 48 h	Me	CH	76%	2a ^b
2	1a		-78°C , 3.5 h	Ph	N	88%	2b ^b

^a Isolated yields. ^b Structure confirmed by single crystal X-ray analysis.

Table 2 D–A reactions of ethyl (Z)-5-(1-tosyl-1H-indol-3-yl)pent-4-enoate **1b**

1b + $\text{O}=\text{N}(\text{R}')\text{X}=\text{X}$ → **2(c-e)**

	Starting material	Dienophile	Reaction conditions	R'	X	Yield ^a	Product
1	1b		2 eq. Me ₂ AlCl, –78 °C 30 min, then 40 °C 48 h	Me	CH	85%	2c
2	1b		2 eq. Me ₂ AlCl, –78 °C 30 min, then 40 °C 48 h	H	CH	64%	2d^b
3	1b		2 eq. Me ₂ AlCl, –78 °C 30 min, then 40 °C 48 h	Ph	CH	71%	2e

^a Isolated yields. ^b Structure confirmed by single crystal X-ray analysis.

1H-pyrrole-2,5-dione and nitrosobenzene were stirred together for 5 days at r.t. in DCM, until **1a** had been consumed by TLC. Examination of the crude reaction mixture showed the formation of a number of by-products (including a rearomatised isomer of D–A cycloadduct **2a**) but the desired domino D–A/ene product **3a** could be isolated as a single diastereomer in a 40% yield.

To improve both the yield and reaction flexibility whilst maintaining operational simplicity we next examined a one-pot, sequential addition approach. 1-Tosyl-3-vinyl-1H-indole **1a** and 5-methoxy-1-tosyl-3-vinyl-1H-indole **1c** (synthesised as previously *via* tosyl protection of 5-methoxy-1H-indole-3-carbaldehyde followed by a Wittig reaction with methylenetriphenyl-λ⁵-phosphane) were reacted with 1-methyl-1H-pyrrole-2,5-dione or 1H-pyrrole-2,5-dione in refluxing DCM for 48 hours to give the corresponding D–A cycloadducts. Nitrosobenzene, 1-methyl-2-nitrosobenzene, 2,3,4,5,6-pentafluorobenzaldehyde with one equivalent of Me₂AlCl, or PTAD, were then added directly to the reaction vessels containing the D–A cycloadducts and the ene reactions conducted were under the previously optimised conditions, depending on the enophile. This one-pot three-component approach gave the corresponding D–A/ene products **3(a–d and k–q)** in excellent (70–89%) yields with no purification or work-up of the intermediate D–A cycloadducts required (Table 4).

We therefore continued with this approach, reacting **1a** and **1c** with PTAD as the dienophile followed by *in situ* addition of enophiles (nitrosobenzene, 1-methyl-2-nitrosobenzene, or PTAD) again giving the D–A/ene products **3(e, f, r and s)** cleanly and in good yields (Table 4).

We then decided to examine the range of electron withdrawing N-protecting groups tolerated in our one-pot D–A/ene reaction sequence with a view towards flexibility in the

deprotection of the products. Boc protection of 1H-indole-3-carbaldehyde proceeded in high yield (triethylamine, Boc anhydride, DCM, 18 h, r.t.), however attempts to synthesise *tert*-butyl 3-vinyl-1H-indole-1-carboxylate, by reaction of *tert*-butyl 3-formyl-1H-indole-1-carboxylate with methylenetriphenyl-λ⁵-phosphane, gave only a 13% yield of the desired product with the major products arising from loss of the Boc group. We therefore focused our efforts on use of the DMAS (dimethylaminosulfonyl) and Cbz protecting groups, and synthesised *N,N*-dimethyl-3-vinyl-1H-indole-1-sulfonamide **1d** (DMAS), benzyl-3-vinyl-1H-indole-1-carboxylate **1e** and benzyl-5-methoxy-3-vinyl-1H-indole-1-carboxylate **1f** (Cbz) *via* appropriate protection of 1H-indole-3-carbaldehyde followed by reaction with methylenetriphenyl-λ⁵-phosphane as previously.

N,N-Dimethyl-3-vinyl-1H-indole-1-sulfonamide **1d** was reacted in DCM with 1H-pyrrole-2,5-dione, 1-methyl-1H-pyrrole-2,5-dione, 1-phenyl-1H-pyrrole-2,5-dione and PTAD. After 48 hours at 40 °C for the maleimides, or 1 hour at –78 °C for PTAD, the D–A reactions were complete and *in situ* ene reactions with nitrosobenzene, 1-methyl-2-nitrosobenzene, 1,3-dibromo-2-nitrosobenzene²³ or 2,3,4,5,6-pentafluorobenzaldehyde (catalysed by one equivalent of Me₂AlCl) were carried out to give 69–77% isolated yields of the desired three-component D–A/ene products **3(t–x)** (Table 4). Cbz protected 3-vinyl-1H-indoles **1(e and f)** also underwent D–A reactions with 1H-pyrrole-2,5-dione, 1-methyl-1H-pyrrole-2,5-dione or PTAD followed by *in situ* ene reactions with nitrosobenzene, 1-methyl-2-nitrosobenzene or PTAD to give 54–82% yields of **3(y–ll)** (Table 4). The Cbz protected products **3(y–ll)** were isolable by silica gel chromatography but proved less stable than their DMAS or Tos protected counterparts. NMR investigations of these compounds showed evidence of decomposition in solution at r.t., however they could be stored as solids under an

Table 3 Ene reactions of *N*-tosyl protected cycloadducts 2(a–e)

Reaction scheme: **2(a-e)** + enophile $\xrightarrow{\text{DCM}}$ **3(a-j)**

	Starting material	R	R'	X	Enophile	Reaction conditions	R''	Yield ^a	Product
1	2a	H	Me	CH		r.t., 18 h	N(Ph)OH	68%	3a
2	2a	H	Me	CH		r.t., 18 h	N(o-Tol)OH	72%	3b
3	2a	H	Me	CH		0 °C, 2.5 h		73%	3c
4	2a	H	Me	CH		1 eq. Me ₂ AlCl, -78 °C, 15 min r.t., 18 h	CH(C ₆ F ₅)OH	82%	3d ^b
5	2b	H	Ph	N		r.t., 18 h	N(Ph)OH	74%	3e
6	2b	H	Ph	N		r.t., 18 h	N(o-Tol)OH	72%	3f
7	2c	(CH ₂) ₂ CO ₂ Et	Me	CH		r.t., 24 h	N(o-Tol)OH	59%	3g
8	2e	(CH ₂) ₂ CO ₂ Et	Ph	CH		r.t., 24 h	N(o-Tol)OH	58%	3h
9	2c	(CH ₂) ₂ CO ₂ Et	Me	CH		0 °C, 6 h		56%	3i
10	2d	(CH ₂) ₂ CO ₂ Et	H	CH		0 °C, 6 h		56%	3j

^a Isolated yields. ^b Isolated as a 6 : 1 mixture of diastereomers.

atmosphere of nitrogen at -20 °C for months at a time. Interestingly the ene reactions of 2,3,4,5,6-pentafluorobenzaldehyde with D-A cycloadducts 3(d, m, p and v) gave a mixture of diastereomers at the *exo*-cyclic hydroxyl group, with ratios from 5 : 1 to >25 : 1. The relative stereochemistry of 3v was confirmed through the solution of a single crystal X-ray structure (see ESI†) and is consistent with an *endo*-selective ene reaction, providing some support for an ene mechanism in this reaction rather than a nucleophilic attack of the D-A cycloadducts to the carbonyl carbon of the aldehyde in the manner of a vinylogous enamine.³⁷

Finally we investigated the deprotection of our D-A/ene reaction products. Tosyl and DMAS protected compounds 3(a-x) proved intransient to a range of basic (NaOH, KOH or KOEt in EtOH, MeOH or H₂O with Bu₄NBr) and reducing (Mg, Mg/Hg or Na/Hg) deprotection conditions. We therefore focused on the deprotection of Cbz protected compounds 3(y-II). Initial attempts at Cbz removal with H₂ and Pd/C proved unsuccessful. Atmospheric pressure hydrogenation with Adam's catalyst in either MeOH and EtOH resulted in the removal of the Cbz group from 3z, however unexpected

Table 4 One-pot D–A/ene reactions of N-protected 3-vinyl-1*H*-indoles

	Starting Material	P	R'''	R'	X	Enophile	R'	Reaction conditions	Product	Yield ^d
1	1a	Tos	H	Me	CH		–N(Ph)OH	(i) 40 °C, 48 h, (ii) r.t., 18 h	3a	71%
2	1a	Tos	H	Me	CH		–N(o-Tol)OH	(i) 40 °C, 48 h, (ii) r.t., 18 h	3b	71%
3	1a	Tos	H	Me	CH			(i) 40 °C, 48 h, (ii) 0 °C, 4 h	3c	76%
4	1a	Tos	H	Me	CH		–CH(C ₆ F ₅)OH	(i) 40 °C, 48 h, (ii) Me ₂ AlCl, –78 °C to r.t., 18 h	3d	72% ^b
5	1a	Tos	H	Ph	N		–N(Ph)OH	(i) –78 °C, 4 h, (ii) r.t., 24 h	3e	66%
6	1a	Tos	H	Ph	N		–N(o-Tol)OH	(i) –78 °C, 4 h, (ii) r.t., 24 h	3f	66%
7	1a	Tos	H	H	CH		–N(Ph)OH	(i) 40 °C, 48 h, (ii) r.t., 4 h	3k	89%
8	1a	Tos	H	H	CH		–N(o-Tol)OH	(i) 40 °C, 48 h, (ii) r.t., 4 h	3l	82% ^c
9	1a	Tos	H	H	CH		–CH(C ₆ F ₅)OH	(i) 40 °C, 48 h, (ii) Me ₂ AlCl, 0 °C to r.t., 18 h	3m	71% ^d
10	1a	Tos	H	H	CH			(i) 40 °C, 48 h, (ii) 0 °C, 4 h	3n	75%
11	1c	Tos	OMe	H	CH		–N(o-Tol)OH	(i) 40 °C, 48 h, (ii) r.t., 24 h	3o	76%
12	1c	Tos	OMe	Me	CH		–CH(C ₆ F ₅)OH	(i) 40 °C, 48 h, (ii) Me ₂ AlCl, –78 °C, 15 min then r.t., 18 h	3p	70% ^e
13	1c	Tos	OMe	H	CH			(i) 40 °C, 48 h, (ii) 0 °C, 4 h	3q	72%

Table 4 (Contd.)

Starting Material	P	R'''	R'	X	Enophile	R''	Reaction conditions	Product	Yield ^d
14	1a	Tos	H	Ph	N		(i) -78 °C, 4 h, (ii) 0 °C, 4 h	3r	65% ^c
15	1c	Tos	OMe	Ph	N		(i) -78 °C then r.t., 23 h, (ii) r.t., 23 h	3s	72%
16	1d	DMAS	H	Me	CH		(i) 40 °C, 48 h, (ii) r.t., 3 h	3t	74%
17	1d	DMAS	H	Ph	CH		(i) 40 °C, 48 h, (ii) r.t., 18 h	3u	69% ^c
18	1d	DMAS	H	Me	CH		(i) 40 °C, 48 h, (ii) Me ₂ AlCl, -78 °C, 1 h	3v	77% ^{c,f}
19	1d	DMAS	H	Ph	N		(i) -78 °C, 1 h, (ii) r.t., 4 h	3w	76%
20	1d	DMAS	H	H	CH		(i) 40 °C, 48 h, (ii) r.t., 3 h	3x	77%
21	1e	Cbz	H	Me	CH		(i) 40 °C, 24 h, (ii) r.t., 18 h	3y	74%
22	1e	Cbz	H	Me	CH		(i) 40 °C, 24 h, (ii) r.t., 18 h	3z	78%
23	1e	Cbz	H	Me	CH		(i) 40 °C, 24 h, (ii) 0 °C, 1 h then r.t., 18 h	3aa	54%
24	1e	Cbz	H	H	CH		(i) 40 °C, 24 h, (ii) r.t., 18 h	3bb	70%
25	1e	Cbz	H	H	CH		(i) 40 °C, 24 h, (ii) r.t., 4 h	3cc	83%
26	1e	Cbz	H	H	CH		(i) 40 °C, 24 h, (ii) 0 °C, 1 h	3dd	58%

Table 4 (Contd.)

Starting Material	P	R'''	R'	X	Enophile	R''	Reaction conditions	Product	Yield ^d
27	1e	Cbz	H	Ph	N		(i) -78 °C, 5 h, (ii) r.t., 3 h	3ee	72%
28	1e	Cbz	H	Ph	N		(i) -78 °C, 5 h, (ii) r.t., 18 h	3ff	68%
29	1f	Cbz	OMe	Me	CH		(i) 40 °C, 18 h, (ii) r.t., 1.5 h	3gg	73%
30	1f	Cbz	OMe	Me	CH		(i) 40 °C, 18 h, (ii) r.t., 3 h	3hh	74%
31	1f	Cbz	OMe	H	CH		(i) 40 °C, 18 h, (ii) r.t., 2.5 h	3ii	79%
32	1f	Cbz	OMe	H	CH		(i) 40 °C, 18 h, (ii) r.t., 3.5 h	3jj	76%
33	1f	Cbz	OMe	Ph	N		(i) -78 °C, 1.5 h, (ii) r.t., 20 h	3kk	78%
34	1f	Cbz	OMe	Ph	N		(i) -78 °C, 1.5 h, (ii) r.t., 24 h	3ll	82%

^a Isolated yields. ^b 5 : 1 *endo* : *exo*. ^c Structure confirmed by single crystal X-ray analysis. ^d 25 : 1 *endo* : *exo*. ^e 10 : 1 *endo* : *exo*. ^f Only one diastereomer observed.

nucleophilic substitutions of the hydroxy(aryl)amino group by MeOH or EtOH also occurred to give 4a and 4b respectively. This gave the first indication that the removal of the electronically stabilising N-protecting group perhaps unsurprisingly lowers the activation energy barrier towards substitution chemistry at the indolylic position.³⁸⁻⁴⁰ Replacement of the alcoholic solvent with THF resulted in a cleaner deprotection of Cbz protected indoles 3(y-II) to give 4(c-p) in 38-91% yields. However the products 4(c-p) showed some evidence of decomposition in CDCl₃ after a few hours at r.t., with the appearance of new peaks in the ¹H NMR spectra. Therefore NMR analysis of 4(c-p) was carried out in either d₂-DCM or d₆-DMSO (depending on solubility) in which decomposition was slowed, although the appearance of minor peaks in the ¹H

NMR could still be observed over time. The deprotection of indoles 3(y-II) with H₂ and Adam's catalyst in THF has allowed us to successfully demonstrate a one-pot, three-component approach to our target library of deprotected partially saturated carbazoles and pyridazino[3,4-*b*]indoles, which will be the focus of future investigations (Table 5).

Conclusions

In conclusion, we have developed a practically simple three-component approach to Tos, DMAS and Cbz protected partially saturated carbazoles and pyridazino[3,4-*b*]indoles, based on a one-pot D-A/ene reaction, including the examination of a deprotection strategy of the Cbz

Table 5 Deprotection of 3(y, z, bb and cc)

	Starting material	R'	X	R''	R'''	Solvent	Product	Yield ^a
1	3z	Me	CH	-N(<i>o</i> -Tol)OH	H	MeOH	4a	60%
2	3z	Me	CH	-N(<i>o</i> -Tol)OH	H	EtOH	4b	24%
3	3y	Me	CH	-N(Ph)OH	H	THF	4c	75%
4	3z	Me	CH	-N(<i>o</i> -Tol)OH	H	THF	4d	87%
5	3aa	Me	CH		H	THF	4e	91%
6	3bb	H	CH	-N(Ph)OH	H	THF	4f	41%
7	3cc	H	CH	-N(<i>o</i> -Tol)OH	H	THF	4g	70%
8	3dd	H	CH		H	THF	4h	64%
9	3ee	Ph	N	-N(Ph)OH	H	THF	4i	65%
10	3ff	Ph	N	-N(<i>o</i> -Tol)OH	H	THF	4j	44%
11	3gg	Me	CH	-N(Ph)OH	OMe	THF	4k	70%
12	3hh	Me	CH	-N(<i>o</i> -Tol)OH	OMe	THF	4l	70%
13	3ii	H	CH	-N(Ph)OH	OMe	THF	4m	60%
14	3jj	H	CH	-N(<i>o</i> -Tol)OH	OMe	THF	4n	85%
15	3kk	Ph	N	-N(Ph)OH	OMe	THF	4o	38%
16	3ll	Ph	N	-N(<i>o</i> -Tol)OH	OMe	THF	4p	61%

^a Isolated yields.

group. Current work is looking into controlling the reactivity and biological activity of the final products as well as investigating enantioselective D-A/ene approaches for molecules of this type.

Experimental

3-Vinyl-1*H*-indole

In a Schlenk flask, methyltriphenylphosphonium iodide (2.14 g, 5.3 mmol) was dissolved in dry THF (13 mL). The solution was cooled to $-78\text{ }^{\circ}\text{C}$ and ⁿbutyllithium (2.9 mL, 4.6 mmol) was added over 10 minutes. The yellow solution was warmed to $0\text{ }^{\circ}\text{C}$ and was left to stir for 1 hour before being cooled to $-78\text{ }^{\circ}\text{C}$. In a separate Schlenk flask, 1*H*-indole-3-carboxylate (0.67 g, 4.6 mmol) was dissolved in THF (7 mL) and to the solution sodium bis(trimethylsilyl)amide (2.3 mL, 4.6 mmol) was added. This solution was transferred into the first Schlenk flask and the red solution was allowed to stir at room temperature for 1 hour. The reaction was poured into water (30 mL) and extracted with ethyl acetate ($2 \times 20\text{ mL}$). The combined organic layers were dried over MgSO_4 , filtered and the solvent removed under pressure to leave the crude product as yellow oil. The product was purified using column chromatography (petrol (40/60)-diethyl

ether 7 : 3, column diameter = 4 cm, silica = 20 cm) to give 3-vinyl-1*H*-indole (0.636 g, 4.4 mmol, 95%) as a yellow powder.

Mp: $78.4\text{--}80.7\text{ }^{\circ}\text{C}$; R_f : 0.76 (Pet(40/60)-EA, 1 : 1); ¹H NMR (300 MHz, CDCl_3): δ_{H} 8.02 (1H, br s), 7.85–7.80 (1H, m), 7.32–7.28 (1H, m), 7.18 (1H, s), 7.18–7.09 (2H, m), 6.83 (1H, ddd, $J = 17.7, 11.2, 0.5\text{ Hz}$), 5.65 (1H, dd, $J = 17.7, 1.5\text{ Hz}$), 5.11 (1H, dd, $J = 11.2, 1.5\text{ Hz}$); ¹³C NMR (101 MHz, CDCl_3): δ 136.8, 129.5, 125.7, 123.6, 122.6, 120.4, 120.2, 115.9, 111.4, 110.9; IR (neat): $\nu_{\text{max}}/\text{cm}^{-1}$ 3660, 2981.

1a - 1-tosyl-3-vinyl-1*H*-indole

In a Schlenk flask, was placed 1*H*-indole-3-carbaldehyde (5.0 g, 34.5 mmol) and DCM (100 mL). The resulting stirred solution was cooled to $0\text{ }^{\circ}\text{C}$ before triethylamine (12 mL, 86.2 mmol) was added dropwise *via* syringe. To the stirred solution, *p*-toluenesulfonyl chloride (7.23 g, 37.9 mmol) in DCM was added dropwise over a period of 20 minutes. The solution was stirred at $0\text{ }^{\circ}\text{C}$ for a further one hour before warming to room temperature over 18 hours. The solution was washed into a separating funnel with DCM (20 mL) and washed with water ($2 \times 100\text{ mL}$) and brine (100 mL). The organic extracts were dried over MgSO_4 , filtered and the solvent removed under reduced pressure to give the crude product as a pale orange oil.

The product was purified by recrystallisation from hot ethyl acetate (150 mL) to give 1-tosyl-1*H*-indole-3-carbaldehyde (8.38 g, 28 mmol, 82%) as orange crystals.

Mp: 145.3–148.8 °C; R_f : 0.83 (Pet(40/60)-EA 1 : 4); $^1\text{H NMR}$ (300 MHz, CDCl_3): δ_{H} 10.11 (1H, s), 8.29–8.26 (1H, m), 8.19–8.16 (1H, m), 8.16 (1H, s), 7.89–7.85 (1H, m), 7.78 (2H, d, $J = 8.4$ Hz), 7.36–7.25 (2H, m), 7.22 (2H, d, $J = 8.4$ Hz), 2.29 (3H, s); $^{13}\text{C NMR}$ (101 MHz, CDCl_3): δ_{C} 185.3, 146.1, 136.2, 135.4, 134.1, 130.3, 130.2, 127.2, 127.1, 126.2, 124.9, 122.5, 122.2, 113.1, 21.5; IR (neat): $\nu_{\text{max}}/\text{cm}^{-1}$ 3140, 1663; anal. calcd for $\text{C}_{16}\text{H}_{13}\text{NO}_3\text{S}$: C, 64.20; H, 4.38; N, 4.68. Found: C, 63.97; H, 4.52; N, 4.72.

A Schlenk flask was charged with methyltriphenylphosphonium iodide (1.29 g, 3.2 mmol) dissolved in dry THF (25 mL) under a nitrogen atmosphere. The solution was cooled to -78 °C and n -butyllithium (1.81 mL, 2.97 mmol) was added dropwise *via* syringe over 10 minutes. The solution was warmed to 0 °C and left to stir for 2 hours. In a separate Schlenk flask, 1-tosylindoline-3-carbaldehyde (0.8 g, 2.7 mmol) was dissolved in THF (5 mL). The indole solution was transferred *via* cannula to the Schlenk flask containing the solution of methyltriphenylphosphonium iodide and the solution was stirred for 18 hours. The reaction poured into water (50 mL) and extracted with ether (3×40 mL). The organic layers were washed with brine (20 mL), dried over MgSO_4 , filtered and the solvent was removed under reduced pressure to leave the crude product as an orange oil. The crude product was purified by column chromatography (petrol (40/60)-ethyl acetate; 10 : 1, 2 cm diameter column) to give 1-tosyl-3-vinyl-1*H*-indole (0.56 g, 3.9 mmol, 70%) as a pale yellow powder.

Mp: 90.3–94.6 °C; R_f : 0.86 (Pet(40/60)-EA, 1 : 1); $^1\text{H NMR}$ (300 MHz, CDCl_3): δ_{H} 7.93–7.90 (1H, m), 7.69 (2H, d, $J = 8.4$ Hz), 7.70–7.65 (1H, m), 7.53 (1H, s), 7.29–7.19 (2H, m), 7.29–7.17 (2H, m), 7.15 (2H, d, $J = 8.4$ Hz), 6.70 (1H, app ddd, $J = 17.9, 11.3, 0.7$ Hz), 5.72 (dd, 1H, $J = 17.9, 1.2$ Hz), 5.28 (1H, dd, $J = 11.3, 1.2$ Hz), 2.26 (3H, s); $^{13}\text{C NMR}$ (101 MHz, CDCl_3): δ_{C} 145.1, 135.6, 135.2, 130.0, 129.1, 127.6, 126.9, 125.0, 124.2, 123.6, 121.0, 120.5, 115.4, 113.8, 21.7; IR (neat): $\nu_{\text{max}}/\text{cm}^{-1}$ 3119, 3072; anal. calcd for $\text{C}_{17}\text{H}_{15}\text{NO}_2\text{S}$: C, 68.66; H, 5.08; N, 4.71. Found: C, 68.70; H, 5.21; N, 4.61.

1b – ethyl (*Z*)-5-(1-tosyl-1*H*-indol-3-yl)pent-4-enoate

In a Schlenk flask, (4-ethoxy-4-oxobutyl) triphenylphosphonium bromide (3.32 g, 7.26 mmol) was dissolved in dry THF (20 mL). The solution was cooled to -78 °C and sodium bis(trimethylsilyl) amide (1.00 M in THF, 8.58 mL, 8.58 mmol) was added dropwise over 10 min. The mixture was warmed to 0 °C and left to stir. After 2 hours, 1-(toluene-4-sulfonyl)-1*H*-indol-3-carboxaldehyde (2.00 g, 6.60 mmol) was dissolved in dry THF (10 mL) in a separate round bottomed flask, and transferred *via* cannula into the reaction solution. The reaction mixture was stirred at room temperature and for 48 hours, quenched with saturated $\text{NH}_4\text{Cl}_{(\text{aq})}$ (30 mL), extracted with EtOAc (2×200 mL), and the combined organic layers washed with brine, dried over MgSO_4 and filtered. The solvent was removed under reduced pressure to give a crude product as orange oil. The product was purified by column chromatography (petrol (40/60)-ethyl

acetate 10 : 1) to give two fractions the first containing ethyl (*Z*)-5-(1-tosyl-1*H*-indol-3-yl)pent-4-enoate (1.568 g, 3.94 mmol, 60%) as a colourless oil, and a second fraction containing a 20 : 1 mixture of (*Z*) and (*E*) ethyl-5-(1-tosyl-1*H*-indol-3-yl)pent-4-enoate (0.294 g, 0.739 mmol, 11%) also as a colourless oil.

R_f : 0.70 (Pet(40/60)-EA 7 : 3); $^1\text{H NMR}$ (400 MHz, CDCl_3): δ_{H} 7.97 (1H, d, $J = 7.9$ Hz, 1H), 7.77 (2H, d, $J = 7.8$ Hz), 7.57 (1H, s), 7.49 (1H, d, $J = 7.9$ Hz), 7.32 (1H, t, $J = 7.9$ Hz), 7.25 (1H, t, $J = 7.9$ Hz), 7.20 (2H, d, $J = 7.8$ Hz), 6.44 (1H, d, $J = 11.2$ Hz), 5.78 (1H, dt, $J = 11.2, 7.5$ Hz), 4.14 (2H, q, $J = 6.5$ Hz), 2.67–2.62 (2H, m), 2.48 (2H, t, $J = 6.9$ Hz), 2.30 (3H, s), 1.24 (3H, t, $J = 6.5$ Hz); $^{13}\text{C NMR}$ (100 MHz, CDCl_3): δ_{C} 172.8, 145.1, 135.1, 134.6, 132.1, 130.8, 129.9, 126.8, 124.9, 123.6, 123.4, 119.5, 118.96, 113.6, 60.5, 34.1, 25.2, 21.6, 14.3; IR (neat): $\nu_{\text{max}}/\text{cm}^{-1}$: 1727, 1597. MS (pNSI): 415.2 (100%, $[\text{M} + \text{NH}_4]^+$), 398.1 (20%, $[\text{M} + \text{H}]^+$), 420.1 (10%, $[\text{M} + \text{Na}]^+$); HRMS (pNSI): calcd $\text{C}_{22}\text{H}_{24}\text{NO}_4\text{S}$ $[\text{M} + \text{H}]^+$: 398.14120; observed: 398.14120.

1c – 5-methoxy-1-tosyl-3-vinyl-1*H*-indole

To a stirred round bottomed flask was added 5-methoxy-1*H*-indole-3-carbaldehyde (0.70 g, 4.00 mmol) and DCM (20 mL) and the solution was cooled to 0 °C. To the stirred solution was added triethylamine (1.40 mL, 10.0 mmol) and the resulting solution was stirred at 0 °C for 1 hour. To the stirred solution was added *p*-toluenesulfonyl chloride (0.84 g, 4.40 mmol) in DCM (10 mL) and the solution was stirred at room temperature for 18 hours. The reaction was poured into water (50 mL) and extracted with DCM (3×20 mL). The combined organic extracts were dried over MgSO_4 , filtered and the solvent was removed under reduced pressure to leave the crude product as a pale orange solid. The product was purified using column chromatography (petrol (40/60)-ether-DCM 2 : 1 : 1, column diameter = 2 cm, silica = 15 cm) to give 5-methoxy-1-tosyl-1*H*-indole-3-carbaldehyde (1.14 g, 3.48 mmol, 87%) as a pale brown powder.

Mp: 126.1–128.4 °C; R_f : 0.71 (Pet(40/60)-Et₂O-DCM 2 : 1 : 1); $^1\text{H NMR}$ (300 MHz, CDCl_3): δ_{H} 10.07 (1H, s), 8.19 (1H, s), 7.86–7.83 (1H, m), 7.84 (2H, d, $J = 8.5$ Hz), 7.72 (1H, d, $J = 2.6$ Hz), 7.29 (2H, d, $J = 8.5$ Hz), 7.02 (1H, dd, $J = 9.1, 2.6$ Hz), 3.86 (3H, s), 2.38 (3H, s); $^{13}\text{C NMR}$ (101 MHz, CDCl_3): δ_{C} 185.6, 157.8, 146.2, 136.8, 134.4, 130.4, 129.8, 127.4, 127.2, 122.3, 116.2, 114.2, 104.1, 55.8, 21.8; IR (neat): $\nu_{\text{max}}/\text{cm}^{-1}$ 3128, 2832, 1671; anal. calcd for $\text{C}_{17}\text{H}_{15}\text{NO}_4\text{S}$: C, 61.99; H, 4.59; N, 4.25. Found: C, 61.77; H, 4.70; N, 4.29.

In a Schlenk flask, methyltriphenylphosphonium iodide (1.35 g, 3.34 mmol) was dissolved in dry THF (30 mL). The solution was cooled to -78 °C and n -BuLi (1.2 mL, 3.03 mmol) was added over 5 minutes. The yellow solution was warmed to 0 °C and was allowed to stir for 1 hour before being cooled to -78 °C. To the stirred solution, 5-methoxy-1-tosyl-1*H*-indole-3-carbaldehyde (1.00 g, 3.03 mmol) in DCM (10 mL) was added and the solution was stirred at room temperature for 3 hours. The reaction was poured into water (40 mL) and extracted with ethyl acetate (3×20 mL). The combined organic layers were dried over MgSO_4 , filtered and the solvent removed under pressure to leave the crude product as orange oil. The product was purified using column chromatography (petrol (40/60)-

ethyl acetate 2 : 1, column diameter = 2 cm, silica = 16 cm) to give 5-methoxy-1-tosyl-3-vinyl-1*H*-indole (0.79 g, 2.42 mmol, 80%) as a brown powder.

Mp: 101.4–103.9 °C; R_f : 0.66 (Pet(40/60)–EA 2 : 1); ^1H NMR (300 MHz, CDCl_3): δ_{H} 7.87 (1H, d, $J = 9.0$ Hz), 7.73 (2H, d, $J = 8.4$ Hz), 7.55 (1H, s), 7.19 (2H, d, $J = 8.3$ Hz), 7.14 (1H, d, $J = 2.5$ Hz), 6.93 (1H, dd, $J = 9.0, 2.5$ Hz), 6.72 (1H, dd, $J = 17.9, 11.3$ Hz), 5.73 (1H, dd, $J = 17.9, 1.1$ Hz), 5.32 (1H, dd, $J = 11.3, 1.1$ Hz), 3.82 (3H, s), 2.31 (3H, s); ^{13}C NMR (101 MHz, CDCl_3): δ_{C} 156.7, 145.0, 135.1, 130.3, 130.1, 130.0, 127.6, 126.9, 124.9, 121.1, 115.2, 114.7, 113.7, 103.2, 55.8, 21.7; IR (neat): $\nu_{\text{max}}/\text{cm}^{-1}$ 3128, 2832, 1671; MS (pNSI): 328.1 (100%, (M + H) $^+$), 350.1 (15%, (M + Na) $^+$), 672.2 (2M + NH $_4^+$); HRMS (pNSI): calcd for $\text{C}_{18}\text{H}_{18}\text{NO}_3\text{S}$ [M + H] $^+$: 328.1002; observed: 328.1007.

1d – *N,N*-dimethyl-3-vinyl-1*H*-indole-1-sulfonamide

To a stirred round bottomed flask was added 1*H*-indole-3-carbaldehyde (3.0 g, 20.7 mmol) and THF (70 mL) and the solution was cooled to 0 °C. To the stirred solution was added sodium hydride (1.7 g, 41.4 mmol) in THF (30 mL) and the resulting solution was stirred at 0 °C for 1 hour. To the stirred solution was added dimethylsulfamoyl chloride (2.4 mL, 20.7 mmol) and the solution was stirred at room temperature for 18 hours. The reaction was poured into water (100 mL) and extracted with DCM (3 × 60 mL). The combined organic extracts were dried over MgSO_4 , filtered and the solvent was removed under reduced pressure to leave the crude product as a pale red pink solid. The product was purified by recrystallization from ethyl acetate to give 3-formyl-*N,N*-dimethyl-1*H*-indole-1-sulfonamide (97%, 5.07 g, 20.1 mmol) as a pink powder.

Mp: 149.0–150.9 °C; R_f : 0.63 (Pet(40/60)–EA, 1 : 1); ^1H NMR (300 MHz, CDCl_3): δ_{H} 10.08 (1H, s), 8.31 (1H, app dd, $J = 7.2, 1.4$ Hz), 8.09 (1H, s), 7.94–7.88 (1H, m), 7.40 (2H, app ddd, $J = 5.9, 3.3, 1.6$ Hz), 2.91 (6H, s); ^{13}C NMR (101 MHz, CDCl_3): δ_{C} 185.5, 137.3, 136.0, 126.1, 125.9, 124.9, 122.6, 120.8, 113.6, 38.6; IR (neat): $\nu_{\text{max}}/\text{cm}^{-1}$ 3124, 2945, 1662; anal. calcd for $\text{C}_{11}\text{H}_{12}\text{N}_2\text{O}_3\text{S}$: C, 52.37; H, 4.79; N, 11.10. Found: C, 52.23; H, 4.91; N, 10.92.

In a Schlenk flask, methyltriphenylphosphonium iodide (7.00 g, 17.4 mmol) was dissolved in dry THF (75 mL). The solution was cooled to –78 °C and $^n\text{BuLi}$ (6.4 mL, 15.9 mmol) was added over 10 minutes. The yellow solution was warmed to 0 °C and was left to stir for 1 hour before being cooled to –78 °C. To the stirred solution, 3-formyl-*N,N*-dimethyl-1*H*-indole-1-sulfonamide (4.00 g, 15.9 mmol) was added and the solution was stirred at room temperature for 3 hours. The reaction was poured into water (70 mL) and extracted with ethyl acetate (3 × 50 mL). The combined organic layers were dried over MgSO_4 , filtered and the solvent removed under pressure to leave the crude product as yellow oil. The product was purified using column chromatography (petrol (40/60)–diethyl ether 4 : 1, column diameter = 3 cm, silica = 14 cm) to give *N,N*-dimethyl-3-vinyl-1*H*-indole-1-sulfonamide (3.11 g, 12.4 mmol, 78%) as a pale orange powder.

Mp: 68.7–67.8 °C; R_f : 0.63 (Pet(40/60)–EA 2 : 1); ^1H NMR (300 MHz, CDCl_3): δ_{H} 7.98 (1H, dd, $J = 8.0, 1.4$ Hz), 7.85 (1H, dd, $J = 7.7, 1.5$ Hz), 7.35 (2H, app ddd, $J = 7.0, 5.3, 1.6$ Hz), 6.83 (1H,

dd, $J = 17.8, 11.2$ Hz), 5.84 (1H, dd, $J = 17.8, 1.2$ Hz), 5.38 (1H, dd, $J = 11.3, 1.2$ Hz), 2.86 (6H, s); ^{13}C NMR (101 MHz, CDCl_3): δ_{C} 136.1, 128.2, 127.8, 125.2, 124.7, 123.1, 120.4, 118.8, 114.9, 114.0, 38.6; IR (neat): $\nu_{\text{max}}/\text{cm}^{-1}$ 3123, 2945; anal. calcd for $\text{C}_{12}\text{H}_{14}\text{N}_2\text{O}_2\text{S}$: C, 57.58; H, 5.64; N, 11.19. Found: C, 57.68; H, 5.75; N, 11.05.

1e – benzyl-3-vinyl-1*H*-indole-1-carboxylate

To a solution of 1*H*-indole-3-carbaldehyde (1.0 g, 6.9 mmol) in DCM (20 mL) at 0 °C was added triethylamine (1.8 mL, 17.3 mmol) dropwise. The solution was stirred at room temperature for 1 hour before benzyl chloroformate (1.4 mL, 8.3 mmol) was added. The solution was stirred for 18 hours after which it was poured into water and extracted with DCM (3 × 20 mL). The organic fractions were combined, dried with MgSO_4 , filtered and the solvent was removed under reduced pressure to give the crude product as an orange powder. The crude product was purified by column chromatography (column diameter = 2.5 cm, eluent = petrol (40/60)–ethyl acetate 2 : 1) to give benzyl-3-formyl-1*H*-indole-1-carboxylate (1.74 g, 6.35 mmol, 92%) as a pale orange powder.

Mp: 91–92 °C; R_f : 0.68 (Pet–EA, 2 : 1); ^1H NMR (300 MHz, CDCl_3): δ_{H} 10.06 (1H, s), 8.30–8.25 (1H, m), 8.23 (1H, s), 8.17 (1H, d, $J = 8.0$ Hz), 7.50 (2H, app dd, $J = 7.7, 1.8$ Hz), 7.42 (3H, app ddd, $J = 6.6, 5.1, 1.5$ Hz), 7.38 (1H, app t, $J = 1.6$ Hz), 7.37–7.34 (1H, m), 5.49 (2H, s); ^{13}C NMR (101 MHz, CDCl_3): δ_{C} 185.8, 150.2, 136.1, 136.1, 134.3, 129.3, 129.0, 128.9, 126.5, 126.1, 125.0, 122.3, 122.3, 115.2, 69.9; IR (neat): $\nu_{\text{max}}/\text{cm}^{-1}$ 3127, 3008, 1733; MS (pNSI): 280.1 (100%, (M + H) $^+$), 302.1 (96%, (M + Na) $^+$), 581.2 (25%, (2M + Na) $^+$); HRMS (pNSI): calcd for $\text{C}_{17}\text{H}_{14}\text{NO}_3$ [M + H] $^+$: 280.0968; observed: 280.0970.

To a stirred Schlenk flask, methylenetriphenylphosphorane (2.38 g, 5.90 mmol) was dissolved in dry THF (30 mL). The solution was cooled to –78 °C and $^n\text{BuLi}$ (2.15 mL, 5.35 mmol) was added over 10 minutes. The yellow solution was warmed to 0 °C and was left to stir for 1 hour before being cooled to –78 °C. To the stirred solution, benzyl 3-formyl-1*H*-indole-1-carboxylate (1.50 g, 5.35 mmol) was added and the solution was stirred at room temperature for 3 hours. The reaction was poured into water (50 mL) and extracted with ethyl acetate (3 × 40 mL). The combined organic layers were dried with MgSO_4 , filtered and the solvent removed under pressure to leave the crude product as yellow oil. The product was purified using column chromatography (petrol (40/60)–ethyl acetate 2 : 1, column diameter = 2 cm, silica = 15 cm) to give benzyl-3-vinyl-1*H*-indole-1-carboxylate (1.14 g, 4.07 mmol, 76%) as a yellow powder.

Mp: 43–45 °C; R_f : 0.73 (Pet(40/60)–EA, 2 : 1); ^1H NMR (300 MHz, CDCl_3): δ_{H} 8.33 (1H, d, $J = 7.1$ Hz), 7.91–7.86 (1H, m), 7.74 (1H, s), 7.58–7.55 (2H, m), 7.52–7.44 (4H, m), 7.43–7.36 (1H, m), 6.87 (1H, dd, $J = 17.8, 11.3$ Hz), 5.96–5.87 (1H, d, $J = 17.8$ Hz), 5.51 (2H, s), 5.44 (1H, d, $J = 11.3$ Hz); ^{13}C NMR (101 MHz, CDCl_3): δ_{C} 150.8, 135.1, 128.9, 128.9, 128.8, 128.6, 128.4, 128.0, 125.1, 123.6, 123.4, 120.2, 120.2, 115.5, 115.0, 68.9; IR (neat): $\nu_{\text{max}}/\text{cm}^{-1}$ 3153, 2962, 1729; MS (pAPCI): 181.1 (50%), 260.1 (100%), 278.1 (25%, (M + H) $^+$);

HRMS (pAPCI): calcd for $C_{18}H_{16}NO_2$ $[M + H]^+$: 278.1176; observed: 278.1173.

1f – benzyl-5-methoxy-3-vinyl-1*H*-indole-1-carboxylate

To a stirred Schlenk flask, methylenetriphenylphosphorane (3.54 g, 8.70 mmol) was dissolved in dry THF (34 mL). The solution was cooled to -78 °C and n BuLi (3.1 mL, 7.87 mmol) was added over 10 minutes. The yellow solution was warmed to 0 °C and was left to stir for 1 hour before being cooled to -78 °C. In a separate Schlenk flask, 5-methoxy-1*H*-indole-3-carbaldehyde (1.38 g, 7.87 mmol) was dissolved in THF (10 mL) and to the solution sodium bis(trimethylsilyl)amide (7.87 mL, 7.87 mmol) was added. This solution was transferred into the first Schlenk flask and the red solution was allowed to stir at room temperature for 1 hour. The reaction was poured into water (50 mL) and extracted with ethyl acetate (2×30 mL). The combined organic layers were dried with $MgSO_4$, filtered and the solvent removed under pressure to leave the crude product as yellow oil. The product was purified using column chromatography (petrol (40/60)-diethyl ether 2 : 1, column diameter = 2.5 cm, silica = 16 cm) to give 5-methoxy-3-vinyl-1*H*-indole (1.38 g, 7.6 mmol, 97%) as a yellow powder.

Mp: 190–193 °C; R_f : 0.49 (Pet-Et₂O, 2 : 1); 1H NMR (300 MHz, $CDCl_3$): δ_H 8.28 (1H, s), 7.66 (1H, d, $J = 2.4$ Hz), 7.29 (1H, d, $J = 8.8$ Hz), 7.24 (1H, d, $J = 2.7$ Hz), 7.20–7.10 (2H, m), 7.18 (1H, d, $J = 2.5$ Hz), 7.15 (2H, dd, $J = 4.5, 2.1$ Hz), 7.10 (1H, s), 5.95 (1H, dd, $J = 17.8, 1.5$ Hz), 5.46 (1H, dd, $J = 11.2, 1.5$ Hz), 4.07 (3H, s); ^{13}C NMR (101 MHz, $CDCl_3$): δ_C 154.4, 132.5, 130.8, 126.4, 126.1, 114.2, 113.0, 112.0, 109.1, 102.0, 55.9; IR (neat): ν_{max}/cm^{-1} 3410, 2925, 2836; MS (pNSI): 174.1 (100%, $(M + H)^+$), 520.3 (100%, $(3M + H)^+$); HRMS (pNSI): calcd for $C_{11}H_{12}NO$ $[M + H]^+$: 174.0913; observed: 174.0912.

To a stirred Schlenk flask, 5-methoxy-3-vinyl-1*H*-indole (1.15 g, 6.61 mmol) was dissolved in THF (30 mL) and the solution was cooled to 0 °C. To the stirred solution, sodium bis(trimethylsilyl)amide (7.27 mL, 7.27 mmol) was added and the solution was stirred for 30 minutes before benzyl chloroformate (0.90 mL, 6.61 mmol) was added. The solution was stirred for 30 minutes at room temperature before being added to water (50 mL) and extracted with ethyl acetate (3×30 mL). The combined organic washings were dried with $MgSO_4$, filtered and the solvent was removed under reduced pressure to give the crude product as an orange oil. The product was purified using column chromatography (petrol (40/60)-ethyl acetate 5 : 1, column diameter = 2.0 cm, silica = 15 cm) to give benzyl-5-methoxy-3-vinyl-1*H*-indole-1-carboxylate (1.78 g, 4.7 mmol, 71%) as a pale yellow oil.

R_f : 0.82 (Pet(40/60)-EA, 5 : 1); 1H NMR (400 MHz), δ_H 8.09 (1H, s), 7.66 (1H, s), 7.50 (2H, d, $J = 7.2$ Hz), 7.45–4.37 (1H, m), 7.25 (1H, d, $J = 2.5$ Hz), 6.96 (1H, dd, $J = 9.0, 2.2$ Hz), 6.79 (1H, dd, $J = 17.8, 11.4$ Hz), 5.80 (1H, d, $J = 17.8$ Hz), 5.42 (2H, s), 5.34 (1H, d, $J = 11.4$ Hz), 3.85 (3H, s); ^{13}C NMR (101 MHz, $CDCl_3$): δ_C 156.4, 135.2, 129.7, 128.9, 128.9, 128.7, 128.6, 128.0, 124.1, 124.1, 120.0, 116.1, 114.8, 113.3, 103.3, 68.8, 55.8; IR (neat): ν_{max}/cm^{-1} 2955, 2834, 1726; MS (pAPCI):

181.1 (32%), 260.1 (100%), 308.1 (28%, $(M + H)^+$); HRMS (pAPCI): calcd for $C_{19}H_{18}NO_3$ $[M + H]^+$: 308.1281; observed: 308.1277.

2a – (3a*S**,10b*S**)-2-methyl-10-tosyl-4,10,10a,10b-tetrahydropyrrolo[3,4-*a*]carbazole-1,3(2*H*,3a*H*)-dione

Into a round bottomed flask, 1-tosyl-3-vinyl-1*H*-indole (2.0 g, 6.7 mmol) and DCM (10 mL) was added. To the stirred solution, *N*-methylmaleimide (0.75 g, 6.7 mmol) was added and the solution was stirred at 40 °C for 48 hours. The solvent was removed under reduced pressure to leave the crude product as orange oil. The product was purified by column chromatography (petrol (40/60)-ethyl acetate, 4 : 1, column diameter = 4 cm, silica = 15 cm) to give (3a*S**,10b*S**)-2-methyl-10-tosyl-4,10,10a,10b-tetrahydropyrrolo[3,4-*a*]carbazole-1,3(2*H*,3a*H*)-dione (2.01 g, 5.0 mmol, 76%) as a white powder.

Mp: 204.2–208.0 °C; R_f : 0.09 (Pet(40/60)-EA, 1 : 1); 1H NMR (300 MHz, $CDCl_3$): δ_H 7.72 (2H, d, $J = 8.0$ Hz), 7.61 (1H, d, $J = 8.5$ Hz), 7.21–7.19 (2H, d, $J = 8.0$), 7.21–7.16 (1H, m), 6.92 (1H, app t, $J = 7.5$ Hz), 6.01–5.96 (1H, m), 4.47 (1H, dd, $J = 7.0, 3.3$ Hz), 3.99 (1H, app t, $J = 8.1$ Hz), 3.12 (1H, app t, $J = 8.1$ Hz), 2.99–2.92 (1H, m), 2.76 (3H, s), 2.30 (3H, s), 2.11 (1H, ddd, $J = 18.0, 6.4, 2.4$ Hz); ^{13}C NMR (101 MHz, $CDCl_3$): δ_C 178.9, 174.2, 144.7, 144.6, 137.4, 134.3, 130.4, 129.9, 127.5, 126.4, 123.9, 121.0, 115.4, 112.9, 61.6, 43.3, 37.2, 25.3, 25.1, 21.7; IR (neat): ν_{max}/cm^{-1} 2981, 2889, 1694; MS (pNSI): 409.2 (61%, $(M + H)^+$), 426.1 (100%, $(M + (NH_4))^+$), 834.3 (52%, $(2M + (NH_4))^+$); HRMS (pNSI): calcd $C_{22}H_{21}N_2O_4S$ $[M + H]^+$: 409.1217; observed: 409.1218.

2b – 2-phenyl-11-tosyl-11,11a-dihydro-1*H*,5*H*-[1,2,4]triazolo[1',2':1,2]pyridazino[3,4-*b*]indole-1,3(2*H*)-dione

To a stirred round bottomed flask was added 1-tosyl-3-vinyl-1*H*-indole (100 mg, 0.34 mmol) and DCM (7 mL) and the solution was cooled to -78 °C. To the stirred solution was added 4-phenyl-3*H*-1,2,4-triazole-3,5(4*H*)-dione (60 mg, 0.34 mmol) and the resulting solution was stirred at -78 °C for 3.5 hours before the solvent was removed under reduced pressure to leave the crude product as a pale red solid. The product was purified by column chromatography (petrol (40/60)-ether-DCM 2 : 1 : 1, column diameter = 1 cm, silica = 20 cm) to give 2-phenyl-11-tosyl-11,11a-dihydro-1*H*,5*H*-[1,2,4]triazolo[1',2':1,2]pyridazino[3,4-*b*]indole-1,3(2*H*)-dione (88%, 140 mg, 0.30 mmol) as a pale red powder.

Mp: 160.1–162.8 °C; R_f : 0.14 (Pet(40/60)-Et₂O-DCM 2 : 1 : 1); 1H NMR (300 MHz, $CDCl_3$): δ_H 7.86 (2H, d, $J = 8.4$ Hz), 7.63–7.55 (2H, m), 7.51–7.46 (2H, m), 7.46–7.42 (1H, m), 7.42–7.39 (1H, m), 7.38–7.34 (2H, m), 7.26–7.22 (2H, m), 7.09 (1H, app td, $J = 7.5, 1.0$ Hz), 6.26 (1H, td, $J = 2.6, 1.8$ Hz), 6.18 (1H, app dt, $J = 5.3, 2.7$ Hz), 4.56–4.46 (1H, app td, $J = 17.6, 2.8$ Hz), 4.39 (1H, ddd, $J = 17.6, 5.2, 1.9$ Hz), 2.37 (3H, s); ^{13}C NMR (75 MHz, $CDCl_3$): δ_C 152.7, 150.8, 144.7, 143.7, 135.6, 134.8, 131.5, 130.4, 129.6, 128.9, 128.5, 128.1, 126.8, 125.7, 125.2, 120.9, 117.4, 113.8, 74.8, 44.6, 21.4; IR (neat): ν_{max}/cm^{-1} 3070, 2926, 1719; MS (pNSI): 473.1 (100%, $(M + H)^+$),

522.2 (30%); HRMS (pNSI): calcd for $C_{25}H_{21}N_4O_4S [M + H]^+$: 473.1278; observed: 473.1277.

2c - ethyl-3-((3aS*,4R*,10bS*)-2-methyl-1,3-dioxo-10-tosyl-1,2,3,3a,4,10,10a,10b-octahydropyrrolo[3,4-a]carbazol-4-yl)propanoate

Dimethylaluminum chloride (1.0 M in hexane, 9.38 mL, 9.38 mmol) was added dropwise to a solution of *N*-methylmaleimide (0.521 g, 4.69 mmol) in dry DCM (15 mL) at -78°C . The mixture left to stir for 30 min. A solution of ethyl-(*Z*)-5-(1-tosyl-1*H*-indol-3-yl) pent-4-enoate (4.69 mmol, 1.863 g) in dry DCM (15 mL) was added dropwise at -78°C . The reaction mixture was then warmed to reflux for 48 hours and quenched with saturated $\text{NaHCO}_3(\text{aq.})$ (20 mL) and extracted with DCM (2×100 mL). The combined organic layers were washed with brine, dried over MgSO_4 and filtered. The solvent was removed under reduced pressure to give the crude yellow solid. The product was purified by column chromatography (petrol (40/60)-ethyl acetate 2 : 1) to yield ethyl 3-((3aS*,4R*,10bS*)-2-methyl-1,3-dioxo-10-tosyl-1,2,3,3a,4,10,10a,10b-octahydropyrrolo[3,4-a]carbazol-4-yl)propanoate in (2.038 g, 4.01 mmol, 85%) a bright yellow solid.

Mp: $187-188^\circ\text{C}$; R_f : 0.3 (Pet(40/60)-EA 2 : 1); ^1H NMR (400 MHz, CDCl_3): δ_{H} 7.79 (2H, d, $J = 7.3$ Hz), 7.62 (1H, d, $J = 7.0$ Hz), 7.25-7.21 (4H, m), 6.95 (1H, t, $J = 7.0$ Hz), 6.09 (1H, dd, $J = 3.7, 6.7$ Hz), 4.85 (1H, dd, $J = 3.7, 6.9$ Hz), 4.15 (1H, t, $J = 6.9$ Hz), 4.07 (2H, m), 3.15-3.12 (1H, m), 3.05-3.02 (1H, m), 2.83 (3H, s), 2.43-2.36 (2H, m), 2.35 (3H, s), 1.91-1.75 (2H, m), 1.19 (3H, t, $J = 7.3$ Hz); ^{13}C NMR (101 MHz, CDCl_3): δ_{C} 178.6, 174.0, 172.79, 144.6, 144.0, 136.6, 134.0, 130.5, 130.0, 127.5, 126.6, 123.9, 121.0, 116.3, 115.4, 60.6, 59.9, 44.22, 42.98, 37.2, 33.1, 28.3, 25.3, 21.70, 14.3; IR (neat): $\nu_{\text{max}}/\text{cm}^{-1}$: 1776, 1698; HRMS (pNSI): calcd $C_{27}H_{29}N_2O_6S [M + H]^+$: 509.1741; observed: 509.1731.

2d - ethyl-3-((3aS*,4R*,10bS*)-1,3-dioxo-10-tosyl-1,2,3,3a,4,10,10a,10b-octahydropyrrolo[3,4-a]carbazol-4-yl)propanoate

Dimethyl aluminum chloride (1.0 M in hexane, 2.86 mL, 2.86 mmol) was added dropwise to a solution of *N*-maleimide (0.14 g, 1.43 mmol) in dry DCM (5 mL) at -78°C . The mixture left to stir for 30 min. A solution of ethyl-(*Z*)-5-(1-tosyl-1*H*-indol-3-yl)pent-4-enoate (0.57 g, 1.43 mmol) in dry DCM (10 mL) was added. The reaction mixture was slowly heated to reflux for 48 h, quenched with saturated $\text{NaHCO}_3(\text{aq.})$ (5 mL). The organic layer was extracted with DCM (1×100 mL), washed with brine, dried over MgSO_4 and filtered. The solvent was removed under reduced pressure to give the crude yellow solid product which was purified by column chromatography (petrol (40/60)-ethyl acetate 2 : 1 gradient to 1 : 1 petrol-ethyl acetate) to yield ethyl 3-((3aS*,4R*,10bS*)-1,3-dioxo-10-tosyl-1,2,3,3a,4,10,10a,10b-octahydropyrrolo[3,4-a]carbazol-4-yl)propanoate in (0.452 g, 0.91 mmol, 64%) as a white solid.

Mp: $218-220^\circ\text{C}$; R_f : 0.14 (Pet(40/60)-EA 1 : 1); ^1H NMR (400 MHz, CDCl_3): δ_{H} 7.78 (2H, d, $J = 6.9$ Hz), 7.64 (1H, d, $J = 6.8$ Hz), 7.27-7.22 (4H, m), 6.98 (1H, t, $J = 7.8$ Hz), 6.16 (1H, dd,

$J = 3.6, 7.1$ Hz), 4.84 (1H, dd, $J = 3.6, 7.3$ Hz), 4.18 (1H, t, $J = 7.3$ Hz), 4.12-4.05 (2H, m), 3.16-1.12 (1H, m), 3.10 (1H, t, $J = 7.3$ Hz), 2.40 (2H, t, $J = 7.3$ Hz), 2.35 (3H, s), 1.89-1.76 (2H, m), 1.20 (3H, t, $J = 7.5$ Hz). ^{13}C NMR (101 MHz, CDCl_3): δ_{C} 178.3, 173.6, 172.7, 144.5, 144.1, 136.6, 133.8, 130.5, 129.8, 127.5, 126.6, 123.8, 120.0, 116.4, 115.5, 60.8, 59.6, 45.2, 44.0, 36.9, 33.0, 27.8, 21.5, 14.1; IR (neat): $\nu_{\text{max}}/\text{cm}^{-1}$: 3657, 2981, 1776, 1703; MS (pNSI): 512.18 (100%, $[M + \text{NH}_4]^+$), 495.15 (55%, $[M + H]^+$), 340.14 (31%, $[M - \text{Ts}]$); HRMS (pNSI): calcd $C_{26}H_{27}N_2O_6S [M + H]^+$: 495.1584; observed: 495.1585.

2e - ethyl 3-((3aS*,4R*,10bS*)-1,3-dioxo-2-phenyl-10-tosyl-1,2,3,3a,4,10,10a,10b-octahydropyrrolo[3,4-a]carbazol-4-yl)propanoate

Dimethyl aluminum chloride (1.0 M in THF, 2.39 mL, 2.39 mmol) was added dropwise to a solution of *N*-phenylmaleimide (0.207 g, 1.19 mmol) in dry DCM (5 mL) at -78°C . The mixture left to stir for 30 min. A solution of ethyl (*Z*)-5-(1-tosyl-1*H*-indol-3-yl) pent-4-enoate (0.475 g, 1.19 mmol) in dry DCM (10 mL) was added. The reaction mixture was heated to reflux for 48 h, quenched with saturated $\text{NaHCO}_3(\text{aq.})$ (10 mL) and extracted with DCM (100 mL). The organic layer was washed with brine, dried over MgSO_4 and filtered. The solvent was removed under reduced pressure to give the crude yellow solid product which was purified by column chromatography (petrol (40/60)-ethyl acetate 2 : 1) to yield ethyl 3-((3aS*,4R*,10bS*)-1,3-dioxo-2-phenyl-10-tosyl-1,2,3,3a,4,10,10a,10b-octahydropyrrolo[3,4-a]carbazol-4-yl)propanoate in (0.5095 g, 0.84 mmol, 71%) as a white solid.

Mp: $201-203^\circ\text{C}$; R_f : 0.2 (Pet(40/60)-EA 2 : 1); ^1H NMR (400 MHz, CDCl_3): δ_{H} 7.81 (2H, d, $J = 7.3$ Hz), 7.60 (1H, d, $J = 7.3$ Hz), 7.34-7.21 (7H, m), 7.06 (2H, d, $J = 7.3$ Hz), 6.97 (1H, t, $J = 7.3$ Hz), 6.20 (1H, dd, $J = 3.4, 7.1$ Hz), 4.59 (1H, dd, $J = 3.4, 7.1$ Hz), 4.18 (1H, t, $J = 7.3$ Hz), 4.13-4.05 (2H, m), 3.26-3.20 (2H, m), 2.45-2.40 (2H, m), 2.35 (3H, s), 1.89-1.85 (2H, m), 1.20 (3H, t, $J = 6.9$ Hz); ^{13}C NMR (101 MHz, CDCl_3): δ_{C} 177.5, 172.9, 172.7, 144.6, 144.3, 137.0, 134.1, 131.7, 130.7, 130.0, 129.0, 128.5, 127.6, 126.7, 126.3, 124.0, 120.9, 116.2, 115.5, 60.8, 60.0, 44.3, 43.1, 37.7, 33.2, 28.3, 21.6, 14.2; IR (neat): $\nu_{\text{max}}/\text{cm}^{-1}$: 1776, 1703; MS (pNSI): 588.21 (100%, $[M + \text{NH}_4]^+$), 1158.39 (33%, $[2M + \text{NH}_4]^+$); HRMS (pNSI): calcd $C_{32}H_{31}N_2O_6S [M + H]^+$: 571.18; observed: 571.1891.

3a - (3aS*,5S*,10bS*)-5-(hydroxy(phenyl)amino)-2-methyl-10-tosyl-4,5,10,10b-tetrahydropyrrolo[3,4-a]carbazole-1,3(2*H*,3*aH*)-dione

To a stirred round bottomed flask was added 1-tosyl-3-vinyl-1*H*-indole (100 mg, 0.34 mmol), DCM (5 mL) and 1-methyl-1*H*-pyrrole-2,5-dione (38 mg, 0.34 mmol). The resulting solution was heated at reflux for 48 hours. The reaction was allowed to cool to room temperature, nitrosobenzene (40 mg, 0.34 mmol) was added, and the solution was stirred at room temperature for 18 hours. The solvent was removed under reduced pressure to leave the crude product as a pale yellow solid which was purified by column chromatography (petrol (40/60)-ethyl acetate 4 : 1, column diameter = 1 cm, silica = 16 cm) to give (3aS*,5S*,10bS*)-5-(hydroxy(phenyl)amino)-2-methyl-10-tosyl-

4,5,10,10b-tetrahydropyrrolo[3,4-*a*]carbazole-1,3(2*H*,3*aH*)-dione as a yellow powder (71%, 128 mg, 0.24 mmol).

Mp: 196.8–199.5 °C; *R*_f: 0.64 (Pet(40/60)-EA, 1 : 1); ¹H NMR (500 MHz, CD₂Cl₂): δ_H 7.94 (1H, d, *J* = 8.4 Hz), 7.69 (2H, d, *J* = 8.2 Hz), 7.60 (1H, d, *J* = 7.9 Hz), 7.32–7.25 (3H, m), 7.23 (2H, d, *J* = 8.0 Hz), 7.18–7.13 (3H, m), 7.02 (1H, t, *J* = 7.3 Hz), 5.06 (1H, d, *J* = 8.0 Hz), 4.75 (1H, app. t, *J* = 5.9 Hz), 4.72 (1H, s), 3.64 (1H, app q, *J* = 7.2 Hz), 2.95 (3H, s), 2.43 (1H, app dt, *J* = 13.6, 6.4 Hz), 2.35 (3H, s), 2.06 (1H, ddd, *J* = 13.6, 7.2, 4.9); ¹³C NMR (101 MHz, CD₂Cl₂): δ_C 178.1, 173.6, 150.7, 145.3, 137.5, 134.9, 131.4, 129.7, 128.9, 128.9, 126.8, 125.2, 124.2, 122.6, 121.7, 120.2, 117.2, 115.4, 58.0, 40.5, 39.5, 25.0, 23.3, 21.4; IR (neat): ν_{max}/cm⁻¹ 3661, 2990, 2886, 1690; MS (pNSI): 407.1 (66%, (M - (C₆H₅NOH))⁺), 516.2 (49%, (M + H)⁺), 533.2 (100%, (M + NH₄)⁺), 1031.3 (57%, (2M + H)⁺), 1053.3 (13%, (2M + Na)⁺); HRMS (pNSI): calcd for C₂₈H₂₆N₃O₅S [M + H]⁺: 516.1588; observed: 516.1584.

Note: ¹H NMR run at 35 °C, broad signals observed at room temperature.

3b - (3*aS,5*S**,10*bS**)-5-(hydroxy(*o*-tolyl)amino)-2-methyl-10-tosyl-4,5,10,10b-tetrahydropyrrolo[3,4-*a*]carbazole-1,3(2*H*,3*aH*)-dione**

To a stirred round bottomed flask was added 1-tosyl-3-vinyl-1*H*-indole (100 mg, 0.34 mmol), DCM (5 mL) and 1-methyl-1*H*-pyrrole-2,5-dione (38 mg, 0.34 mmol). The resulting solution was heated at reflux for 48 hours. The reaction was allowed to cool to room temperature, 1-methyl-2-nitrosobenzene (42 mg, 0.17 mmol) was added and the solution was stirred at room temperature for 18 hours. The solvent was removed under reduced pressure to leave the crude product as a pale yellow solid. The product was purified by column chromatography (petrol (40/60)-ethyl acetate 4 : 1, column diameter = 1 cm, silica = 14 cm) to give (3*aS**,5*S**,10*bS**)-5-(hydroxy(*o*-tolyl)amino)-2-methyl-10-tosyl-4,5,10,10b-tetrahydropyrrolo[3,4-*a*]carbazole-1,3(2*H*,3*aH*)-dione (71%, 128 mg, 0.24 mmol) as a yellow powder.

Mp: 193.0–196.7 °C; *R*_f: 0.59 (Pet(40/60)-EA 1 : 1); ¹H NMR (400 MHz, CD₂Cl₂): δ_H 7.89 (1H, d, *J* = 8.3 Hz), 7.65 (2H, d, *J* = 8.4 Hz), 7.40 (1H, d, *J* = 7.9 Hz), 7.28 (1H, d, *J* = 7.7 Hz), 7.21–7.18 (3H, m), 7.13–6.99 (4H, m), 5.04 (1H, d, *J* = 8.1 Hz), 4.87 (1H, s), 4.27 (1H, app t, *J* = 5.4 Hz), 3.73 (1H, app td, *J* = 8.0, 6.1 Hz), 2.91 (3H, s), 2.58 (1H, app dt, *J* = 12.9, 6.2 Hz), 2.32 (3H, s), 2.25 (3H, s), 1.95 (1H, ddd, *J* = 12.9, 7.8, 4.5 Hz); ¹³C NMR (101 MHz, CD₂Cl₂): δ_C 178.2, 173.6, 149.3, 145.3, 137.3, 134.9, 131.6, 130.9, 129.7, 129.7, 129.2, 126.8, 126.2, 125.0, 124.9, 124.1, 121.4, 120.5, 115.3, 57.3, 40.6, 39.4, 25.0, 24.6, 21.4, 18.3; IR (neat): ν_{max}/cm⁻¹ 3662, 2990, 2886, 1701; MS (pNSI): 407.1 (98%, (M - ((*o*-CH₃) - C₆H₄NOH))⁺), 530.2 (52%, (M + H)⁺), 547.2 (65%, (M + NH₄)⁺), 1059.3 (100%, (2M + H)⁺); HRMS (pNSI): calcd for C₂₉H₂₈N₃O₅S [M + H]⁺: 530.1744; observed: 530.1743.

3c - (3*aS,5*S**,10*bS**)-5-(3,5-dioxo-4-phenyl-1,2,4-triazolidin-1-yl)-2-methyl-10-tosyl-4,5,10,10b-tetrahydropyrrolo[3,4-*a*]carbazole-1,3(2*H*,3*aH*)-dione**

To a stirred round bottomed flask was added 1-tosyl-3-vinyl-1*H*-indole (100 mg, 0.34 mmol), DCM (5 mL) and 1-methyl-1*H*-

pyrrole-2,5-dione (38 mg, 0.34 mmol) and the resulting solution was heated at reflux for 48 hours. The reaction was cooled to 0 °C before PTAD (60 mg, 0.34 mmol) was added. The reaction was stirred at 0 °C for 4 hours. The solvent was removed under reduced pressure to leave the crude product as a pale red powder. The product was purified by column chromatography (petrol (40/60)-ethyl acetate 4 : 1, column diameter = 1 cm, silica = 14 cm) to give (3*aS**,5*S**,10*bS**)-5-(3,5-dioxo-4-phenyl-1,2,4-triazolidin-1-yl)-2-methyl-10-tosyl-4,5,10,10b-tetrahydropyrrolo[3,4-*a*]carbazole-1,3(2*H*,3*aH*)-dione (76%, 150 mg, 0.26 mmol) as a white powder.

Mp: 183.4–187.7 °C; *R*_f: 0.05 (Pet(40/60)-EA 1 : 1); ¹H NMR (400 MHz, CDCl₃): δ_H 7.84 (2H, d, *J* = 8.4 Hz), 7.67 (1H, d, *J* = 8.2 Hz), 7.52 (1H, d, *J* = 7.6 Hz), 7.46–7.31 (5H, m), 7.29–7.19 (2H, m), 7.17 (2H, d, *J* = 8.3 Hz), 5.55 (1H, app t, *J* = 4.7 Hz), 5.08 (1H, d, *J* = 7.7 Hz), 3.66 (1H, ddd, *J* = 10.5, 7.7, 5.8 Hz), 2.96 (3H, s), 2.49 (1H, app dt, *J* = 14.8, 5.3 Hz), 2.28 (3H, s), 2.14 (1H, ddd, *J* = 14.8, 10.5, 5.5 Hz); ¹³C NMR (101 MHz, CDCl₃): δ_C 177.4, 173.4, 153.6, 152.8, 145.5, 137.0, 135.3, 132.3, 130.8, 130.0, 129.3, 128.5, 127.5, 126.9, 125.7, 125.6, 124.3, 119.4, 115.4, 114.9, 47.8, 40.3, 39.0, 28.4, 25.4, 21.7; IR (neat): ν_{max}/cm⁻¹ 3665, 2984, 2884, 1699; MS (pNSI): 601.2 (100%, (M + NH₄)⁺), 1184.3 (13%, (2M + NH₄)⁺); HRMS (pNSI): calcd for C₃₀H₂₉N₆O₆S [M + NH₄]⁺: 601.1864; observed: 601.1861.

3d - (3*aS,5*S**,10*bS**)-5-((*S**)-hydroxy(perfluorophenyl)methyl)-2-methyl-10-tosyl-4,5,10,10b-tetrahydropyrrolo[3,4-*a*]carbazole-1,3(2*H*,3*aH*)-dione**

To a stirred round bottomed flask was added 1-tosyl-3-vinyl-1*H*-indole (100 mg, 0.34 mmol) DCM (5 mL) and 1-methyl-1*H*-pyrrole-2,5-dione (38 mg, 0.34 mmol) and the resulting solution was heated at reflux for 48 hours. The reaction was cooled to -78 °C and 2,3,4,5,6-pentafluorobenzaldehyde (0.04 mL, 0.34 mmol) was added followed by DMAC (1 M in hexane, 0.34 mL, 0.34 mmol). The reaction was stirred at -78 °C for 15 minutes before being allowed to warm to room temperature. The reaction was stirred at room temperature for 18 hours. The reaction was poured into saturated sodium bicarbonate solution (10 mL) and extracted with DCM (2 × 10 mL). The combined organic layers were dried with MgSO₄, filtered and the solvent was removed under reduced pressure to give the crude product as a pale brown solid. The product was purified by column chromatography (petrol (40/60)-ethyl acetate 3 : 1, column diameter = 2 cm, silica = 15 cm) to give a separable 5 : 1 mixture of (3*aS**,5*S**,10*bS**)-5-((*S**)-hydroxy(perfluorophenyl)methyl)-2-methyl-10-tosyl-4,5,10,10b-tetrahydropyrrolo[3,4-*a*]carbazole-1,3(2*H*,3*aH*)-dione and (3*aS**,5*S**,10*bS**)-5-((*R**)-hydroxy(perfluorophenyl)methyl)-2-methyl-10-tosyl-4,5,10,10b-tetrahydropyrrolo[3,4-*a*]carbazole-1,3(2*H*,3*aH*)-dione (72%, 149 mg, 0.25 mmol).

Major diastereomer: Mp: 120.4–121.7 °C; *R*_f: 0.24 (Pet(40/60)-EA 3 : 1); ¹H NMR (300 MHz, CDCl₃): δ_H 7.85 (3H, app d, *J* = 8.4 Hz), 7.31–7.22 (4H, m), 7.22–7.14 (1H, m), 5.13 (1H, d, *J* = 8.1 Hz), 4.99 (1H, d, *J* = 7.5 Hz), 3.71–3.52 (2H, m), 3.01 (3H, s), 2.38 (3H, s), 2.20–2.10 (1H, m), 1.67 (1H, app td, *J* = 13.8, 5.3 Hz); ¹³C NMR (101 MHz, CDCl₃): δ_C 177.7, 173.3, 145.3, 137.4, 135.4, 129.8,

129.7, 129.6, 127.2, 125.3, 123.9, 120.1, 119.9, 115.2, 70.2, 41.5, 39.1, 36.9, 28.7, 25.2, 21.7; IR (neat): $\nu_{\text{max}}/\text{cm}^{-1}$ 3371, 2981, 2889, 1690; MS (pNSI): 605.1 (40%, (M + H)⁺), 622.1 (88%, (M + NH₄)⁺), 627.1 (100%, (M + Na)⁺), 643.1 (17%), 709.1 (15%); HRMS (pNSI): calcd for C₂₉H₂₁F₅N₂NaO₅S [M + Na]⁺: 627.0984; observed: 627.0968. Note: ¹³C NMR missing peaks due to C–F coupling.

3c – 6-(hydroxy(phenyl)amino)-2-phenyl-11-tosyl-5,6-dihydro-[1,2,4]triazolo[1',2':1,2]pyridazino[3,4-*b*]indole-1,3(2*H*,11*H*)-dione

To a stirred round bottomed flask was added 1-tosyl-3-vinyl-1*H*-indole (100 mg, 0.34 mmol) and DCM (5 mL) and the solution was cooled to –78 °C. To this solution PTAD (70 mg, 0.34 mmol) was added and the reaction was stirred at –78 °C for 3.5 hours. The reaction was warmed to room temperature, nitrosobenzene (44 mg, 0.34 mmol) was added and the reaction was stirred for 18 hours. The solvent was removed under reduced pressure to leave the crude product as a pale yellow oil. The product was purified by column chromatography (column diameter = 1 cm, silica = 16 cm, eluent = petrol (40/60)-ether-DCM 2 : 1 : 1) to give 6-(hydroxy(phenyl)amino)-2-phenyl-11-tosyl-5,6-dihydro-[1,2,4]triazolo[1',2':1,2]pyridazino[3,4-*b*]indole-1,3(2*H*,11*H*)-dione (72%, 54 mg, 0.09 mmol) as a white powder.

Mp: 176.1–180.0 °C; *R*_f: 0.48 (Pet(40/60)-Et₂O 2 : 1); ¹H NMR (400 MHz, CDCl₃): δ_{H} 8.03 (1H, d, *J* = 8.3 Hz), 7.62 (2H, d, *J* = 8.1 Hz), 7.56 (2H, d, *J* = 7.6 Hz), 7.46 (2H, app t, *J* = 7.7 Hz), 7.42–7.36 (1H, m), 7.23–7.07 (7H, m), 7.05–6.99 (2H, m), 6.59 (1H, d, *J* = 7.4 Hz), 5.81 (1H, br s), 5.18 (1H, d, *J* = 13.5 Hz), 4.59 (1H, s), 3.23 (1H, d, *J* = 13.5 Hz), 2.30 (3H, s); ¹³C NMR (101 MHz, DMSO-*d*₆): δ_{C} 152.7, 152.2, 150.5, 146.0, 134.9, 132.9, 132.5, 131.8, 130.4, 129.8, 129.3, 129.2, 128.5, 127.3, 127.3, 125.5, 125.4, 122.5, 119.8, 117.6, 116.6, 108.6, 55.9, 44.6, 21.6; IR (neat): $\nu_{\text{max}}/\text{cm}^{-1}$ 2981, 2884, 1714; MS (pAPCI): 138.1 (100%), 157.0 (95%), 213.1 (50%), 248.1 (86%), 279.1 (62%), 317.1 (33%), 333.1 (29%), 471.1 (31%), 564.2 (11%), 580.2 (10%, (M + H)⁺); HRMS (pAPCI): calcd for C₃₁H₂₆N₅O₅S [M + H]⁺: 580.1649; observed: 580.1640.

3f – 6-(hydroxy(*o*-tolyl)amino)-2-phenyl-11-tosyl-5,6-dihydro-[1,2,4]triazolo[1',2':1,2]pyridazino[3,4-*b*]indole-1,3(2*H*,11*H*)-dione

To a stirred round bottomed flask was added 1-tosyl-3-vinyl-1*H*-indole (100 mg, 0.34 mmol) and DCM (5 mL) and the solution cooled to –78 °C. To this solution PTAD (70 mg, 0.34 mmol) was added and the reaction was stirred at –78 °C for 3.5 hours. The reaction was warmed to room temperature and 1-methyl-2-nitrosobenzene (42 mg, 0.34 mmol) was added and the reaction was stirred for 18 hours. The solvent was removed under reduced pressure to leave the crude product as a pale yellow oil. The product was purified by column chromatography (column diameter = 1 cm, silica = 14 cm, eluent = petrol (40/60)-ether-DCM 2 : 1 : 1) to give 6-(hydroxy(*o*-tolyl)amino)-2-phenyl-11-tosyl-5,6-dihydro-[1,2,4]triazolo[1',2':1,2]pyridazino[3,4-*b*]indole-1,3(2*H*,11*H*)-dione as a white powder (78%, 60 mg, 0.10 mmol).

Mp: 149.7–153.1 °C; *R*_f: 0.32 (Pet(40/60)-Et₂O-DCM 2 : 1 : 1); ¹H NMR (300 MHz, CDCl₃): δ_{H} 7.99 (1H, d, *J* = 8.3 Hz), 7.61–7.58

(5H, m), 7.43–7.40 (1H, m), 7.47 (2H, app t, *J* = 7.7 Hz), 7.40–7.37 (1H, m), 7.18 (2H, app t, *J* = 7.8 Hz), 7.11 (2H, d, *J* = 8.2 Hz), 6.97 (2H, app q, *J* = 7.2 Hz), 6.85 (1H, d, *J* = 7.5 Hz), 6.50 (1H, d, *J* = 7.8 Hz), 5.93 (1H, s), 5.24 (1H, d, *J* = 13.5 Hz), 4.44 (1H, s), 3.11 (1H, d, *J* = 13.5 Hz), 2.29 (3H, s), 1.91 (3H, s); ¹³C NMR (101 MHz, CDCl₃): δ_{C} 153.3, 150.3, 148.7, 145.4, 135.1, 133.7, 132.0, 131.7, 131.3, 130.6, 129.6, 129.3, 128.7, 127.9, 127.2, 127.0, 126.8, 125.9, 124.9, 124.8, 122.6, 118.0, 116.8, 107.0, 59.1, 44.5, 21.7, 17.8; IR (neat): $\nu_{\text{max}}/\text{cm}^{-1}$ 3068, 2981, 1713; MS (pAPCI): 138.1 (100%), 157.0 (82%), 262.1 (55%), 279.1 (76%), 317.1 (50%), 391.3 (37%), 471.1 (21%), 594.2 (10%, (M + H)⁺); HRMS (pAPCI): calcd for C₃₂H₂₈N₅O₅S [M + H]⁺: 594.1806; observed: 594.1801.

3g – ethyl 3-((3*aS**,4*S**,5*S**,10*bS**)-5-(hydroxy(*o*-tolyl)amino)-2-methyl-1,3-dioxo-10-tosyl-1,2,3,3*a*,4,5,10,10*b*-octahydropyrrolo[3,4-*a*]carbazol-4-yl)propanoate

A solution of 2-nitrosotoluene (0.035 g, 0.29 mmol) and ethyl 3-((3*aS**,4*R**,10*bS**)-2-methyl-1,3-dioxo-10-tosyl-1,2,3,3*a*,4,10,10*a*,10*b*-octahydropyrrolo[3,4-*a*]carbazol-4-yl)propanoate (0.150 g, 0.29 mmol) in dry DCM (10 mL) was stirred at room temperature for 24 hours. The solvent was removed under reduced pressure to give the crude green solid product which was purified by column chromatography (petrol (40/60)-ethyl acetate 2 : 1) to give ethyl 3-((3*aS**,4*S**,5*S**,10*bS**)-5-(hydroxy(*o*-tolyl)amino)-2-methyl-1,3-dioxo-10-tosyl-1,2,3,3*a*,4,5,10,10*b*-octahydropyrrolo[3,4-*a*]carbazol-4-yl)propanoate (0.109 g, 0.17 mmol, 59%) as a bright yellow solid.

Mp: 190–192 °C; *R*_f: 0.26 (Pet(40/60)-EA 2 : 1); ¹H NMR (400 MHz, CDCl₃): δ_{H} 7.95 (1H, d, *J* = 7.2 Hz), 7.61 (2H, d, *J* = 7.2 Hz), 7.18 (2H, d, *J* = 7.2 Hz), 7.10 (1H, d, *J* = 7.2 Hz), 7.05 (1H, t, *J* = 7.2 Hz), 6.81 (1H, t, *J* = 7.2 Hz), 6.65 (1H, t, *J* = 7.5 Hz), 6.19 (1H, t, *J* = 7.5 Hz), 5.88 (1H, d, *J* = 7.2 Hz), 5.46 (1H, d, *J* = 7.2 Hz), 4.99 (1H, br s), 4.95 (1H, d, *J* = 7.2 Hz), 4.30 (1H, d, *J* = 4.6 Hz), 4.11 (2H, q, *J* = 7.0 Hz), 3.80–3.75 (1H, m), 3.01 (3H, s), 2.70–2.54 (4H, m), 2.41 (3H, s), 2.33 (3H, s), 1.92–1.85 (1H, m), 1.24 (3H, t, *J* = 7.0 Hz). ¹³C NMR (101 MHz, CDCl₃): δ_{C} 178.2, 173.3, 149.9, 144.6, 139.9, 137.1, 134.1, 131.9, 130.6, 130.3, 129.4, 128.7, 127.0, 125.7, 124.8, 124.4, 123.6, 122.1, 118.9, 118.0, 115.7, 60.6, 57.8, 45.1, 42.4, 40.0, 32.5, 25.2, 23.3, 21.6, 18.5, 14.3; IR (neat): $\nu_{\text{max}}/\text{cm}^{-1}$: 3655, 2980, 1702; MS (pNSI): 507.15 (100%, [M – (Tol-N-OH)]), 652.20 (55%, [M + Na]⁺); HRMS (pNSI): calcd C₃₄H₃₅N₅O₇S [M + Na]⁺: 652.2088; observed: 652.2082.

3h – ethyl 3-((3*aS**,4*S**,5*S**,10*bS**)-5-(hydroxy(*o*-tolyl)amino)-1,3-dioxo-2-phenyl-10-tosyl-1,2,3,3*a*,4,5,10,10*b*-octahydropyrrolo[3,4-*a*]carbazol-4-yl)propanoate

A solution of 2-nitrosotoluene (0.016 g, 0.13 mmol) and ethyl 3-((3*aS**,4*R**,10*bS**)-1,3-dioxo-2-phenyl-10-tosyl-1,2,3,3*a*,4,10,10*a*,10*b*-octahydropyrrolo[3,4-*a*]carbazol-4-yl)propanoate (0.08 g, 0.13 mmol) in dry DCM (10 mL) was stirred at room temperature for 24 hours. The solvent was removed under reduced pressure to give the crude yellow product which was purified by column chromatography (petrol (40/60)-ethyl acetate 2 : 1) to give ethyl 3-((3*aS**,4*S**,5*S**,10*bS**)-5-(hydroxy(*o*-tolyl)amino)-1,3-dioxo-2-

phenyl-10-tosyl-1,2,3,3a,4,5,10,10b-octahydropyrrolo[3,4-*a*]carbazol-4-yl]propanoate in (0.415 g, 0.059 mmol, 58%) as a bright yellow solid.

Mp: 182–184 °C; *R*_f: 0.34 (Pet(40/60)-EA 2 : 1); ¹H NMR (400 MHz, CDCl₃): δ_H 7.94 (1H, d, *J* = 6.7 Hz), 7.64 (2H, d, *J* = 6.7 Hz), 7.45–7.37 (5H, m), 7.20–7.00 (4H, m), 6.84 (1H, t, *J* = 6.9 Hz), 6.66 (1H, t, *J* = 6.9 Hz), 6.24 (1H, t, *J* = 6.2 Hz), 5.95 (1H, d, *J* = 6.9 Hz), 5.66 (1H, d, *J* = 6.4 Hz), 5.20 (1H, d, *J* = 7.4 Hz), 4.99 (1H, br s), 4.39 (1H, d, *J* = 4.0 Hz), 4.08 (2H, q, *J* = 7.2 Hz), 4.03–3.98 (1H, m), 2.72–2.61 (4H, m), 2.42 (3H, s), 2.33 (3H, s), 2.14–2.08 (1H, m). 1.20 (3H, t, *J* = 7.2 Hz); ¹³C NMR (101 MHz, CDCl₃): δ_C 177.0, 173.3, 172.2, 150.1, 144.6, 137.1, 134.2, 131.0, 131.8, 130.5, 130.3, 129.4, 129.0, 128.6, 128.5, 127.0, 126.5, 125.8, 124.8, 124.5123.5, 122.2, 119.1, 118.1, 115.6, 60.0, 57.7, 45.3, 42.6, 40.0, 32.4, 23.1, 21.6, 18.5, 14.5; IR (neat): ν_{max}/cm⁻¹: 3858, 3826, 1709, 1595; MS (pNSI): 569.17 (100%, [M – N(OH)(*o*-Tol)]), 692.24 (30%, [M + H]⁺); HRMS (pNSI): calcd C₃₉H₃₆N₃O₅S [M – H]⁺: 690.2268; observed: 690.2266.

3i – ethyl 3-((3aS*,4S*,5S*,10bS*)-5-(3,5-dioxo-4-phenyl-1,2,4-triazolidin-1-yl)-2-methyl-1,3-dioxo-10-tosyl-1,2,3,3a,4,5,10,10b-octahydropyrrolo[3,4-*a*]carbazol-4-yl)propanoate

A solution of 4-phenyl-3*H*-1,2,4-triazole-3,5(4*H*)-dione (0.052 g, 0.29 mmol) and ethyl 3-((3aS*,4*R**,10bS*)-2-methyl-1,3-dioxo-10-tosyl-1,2,3,3a,4,10,10a,10b-octahydropyrrolo[3,4-*a*]carbazol-4-yl)propanoate (0.150 g, 0.29 mmol) in dry DCM (10 mL) was stirred at 0 °C for 6 hours. The solvent was removed under reduced pressure to give the crude product which was purified by column chromatography (petrol (40/60)-ethyl acetate 1 : 1) to give ethyl 3-((3aS*,4S*,5S*,10bS*)-5-(3,5-dioxo-4-phenyl-1,2,4-triazolidin-1-yl)-2-methyl-1,3-dioxo-10-tosyl-1,2,3,3a,4,5,10,10b-octahydropyrrolo[3,4-*a*]carbazol-4-yl)propanoate in (56%, 0.110 g, 0.161 mmol) as a white solid.

Mp: 264–265 °C; *R*_f: 0.30 (Pet(40/60)-EA 1 : 1); ¹H NMR (400 MHz, CDCl₃): δ_H 8.86 (1H, br s), 7.78 (2H, d, *J* = 7.0 Hz), 7.71 (1H, d, *J* = 7.9 Hz), 7.47 (1H, d, *J* = 7.9 Hz), 7.44–7.40 (1H, m), 7.36–7.30 (3H, m), 7.23–7.17 (2H, m), 7.02 (2H, d, *J* = 7.0 Hz), 5.66 (1H, d, *J* = 6.2 Hz), 5.04 (1H, d, *J* = 6.5 Hz), 4.08 (2H, q, *J* = 6.2 Hz), 3.44 (1H, dd, *J* = 6.5, 11.9 Hz), 3.02 (3H, s), 2.68–2.51 (3H, m), 2.15 (3H, s), 2.14–2.09 (1H, m), 1.90–1.82 (1H, m), 1.20 (3H, t, *J* = 6.2 Hz); ¹³C NMR (101 MHz, CDCl₃): δ_C 176.6, 173.4, 173.2, 153.6, 152.6, 145.2, 136.8, 135.5, 132.1, 130.7, 129.7, 129.3, 128.6, 127.2, 126.8, 125.6, 124.2, 119.0, 114.8, 114.4, 60.8, 44.3, 42.0, 39.3, 30.9, 25.4, 23.0, 21.5, 14.2; IR (neat): ν_{max}/cm⁻¹: 3659, 1775, 1691; MS (pNSI): 701.23 (100%, [M + NH₄]⁺), 1384.44 (17%, [2M + NH₄]⁺); HRMS (pNSI): calcd C₃₅H₃₄N₅O₈S [M + H]⁺: 684.2123; observed: 684.2115.

3j – ethyl 3-((3aS*,4S*,5S*,10bS*)-5-(3,5-dioxo-4-phenyl-1,2,4-triazolidin-1-yl)-1,3-dioxo-10-tosyl-1,2,3,3a,4,5,10,10b-octahydropyrrolo[3,4-*a*]carbazol-4-yl)propanoate

A solution of 4-phenyl-3*H*-1,2,4-triazole-3,5(4*H*)-dione (0.037 g, 0.21 mmol) and ethyl 3-((3aS*,4*R**,10bS*)-1,3-dioxo-10-tosyl-1,2,3,3a,4,10,10a,10b-octahydropyrrolo[3,4-*a*]carbazol-4-yl)-

propanoate (0.105 g, 0.21 mmol) in dry DCM (10 mL) was stirred at 0 °C for 6 h. The solvent was removed to give the crude white solid product which was purified by trituration from DCM to yield ethyl 3-((3aS*,4S*,5S*,10bS*)-5-(3,5-dioxo-4-phenyl-1,2,4-triazolidin-1-yl)-1,3-dioxo-10-tosyl-1,2,3,3a,4,5,10,10b-octahydropyrrolo[3,4-*a*]carbazol-4-yl)propanoate in (57%, 0.08 g, 0.119 mmol) as a white solid.

Mp: 269–271 °C; ¹H NMR (300 MHz, d₆-DMSO): δ_H 11.44 (1H, br s), 10.68 (1H, br s), 7.87–7.76 (3H, m), 7.51–7.39 (4H, m), 7.29–7.25 (6H, m), 5.69 (1H, d, *J* = 6.1 Hz), 5.28 (1H, d, *J* = 6.8 Hz), 4.05 (2H, q, *J* = 6.8 Hz), 3.45 (1H, dd, *J* = 6.8, 11.3 Hz), 3.58–3.52 (1H, m), 2.67–2.65 (1H, m), 2.25 (3H, s), 2.49–2.44 (2H, m), 1.80–1.70 (1H, m), 1.18 (3H, t, *J* = 6.8 Hz); ¹³C NMR (101 MHz, d₆-DMSO): 178.6, 175.0, 172.99, 154.4, 153.1, 145.5, 136.6, 134.9, 133.1, 131.7, 130.4, 129.4, 128.6, 127.6, 127.1, 126.3, 125.6, 124.5, 119.3, 115.9, 114.9, 60.3, 45.2, 43.0, 38.0, 30.7, 23.6, 21.4, 14.5; IR (neat): ν_{max}/cm⁻¹: 3659, 1775, 1692; MS (pNSI): 687.22 (100%, [M + NH₄]⁺), 1356.41 (27%, [2M + NH₄]⁺), 692.17 (12%, [M + Na]⁺); HRMS (pNSI): calcd C₃₄H₃₅N₆O₈S [M + H]⁺: 687.2232; observed: 687.2229.

3k – (3aS*,5S*,10bS*)-5-(hydroxy(phenyl)amino)-10-tosyl-4,5,10,10b-tetrahydropyrrolo[3,4-*a*]carbazole-1,3(2*H*,3*aH*)-dione

To a stirred round bottomed flask was added 1-tosyl-3-vinyl-1*H*-indole (100 mg, 0.34 mmol), DCM (5 mL) and 1*H*-pyrrole-2,5-dione (33 mg, 0.34 mmol) and the resulting solution was heated at reflux for 48 hours. The reaction was cooled to room temperature and nitrosobenzene (36 mg, 0.34 mmol) was added. The reaction was stirred at room temperature for 4 hours before the solvent was removed under reduced pressure to leave the crude product as a white solid. The product was purified by trituration from DCM to give (3aS*,5S*,10bS*)-5-(hydroxy(phenyl)amino)-10-tosyl-4,5,10,10b-tetrahydropyrrolo[3,4-*a*]carbazole-1,3(2*H*,3*aH*)-dione (89%, 151 mg, 0.30 mmol) as a white powder.

Mp: 203.7–206.9 °C; *R*_f: 0.15 (Pet(40/60)-EA 2 : 1); ¹H NMR (300 MHz, DMSO-*d*₆): δ_H 11.26 (1H, s), 8.45 (1H, s), 7.88 (1H, d, *J* = 8.3 Hz), 7.76 (2H, d, *J* = 8.2 Hz), 7.42 (1H, d, *J* = 7.8 Hz), 7.33 (2H, d, *J* = 8.2 Hz), 7.29–7.04 (5H, m), 6.89 (1H, t, *J* = 7.2 Hz), 5.17 (1H, d, *J* = 7.8 Hz), 4.88 (1H, app t, *J* = 4.4 Hz), 3.65 (1H, app td, *J* = 8.8, 5.9 Hz), 2.32 (3H, s), 2.36–2.27 (1H, m), 1.81 (1H, ddd, *J* = 14.0, 9.4, 5.0 Hz); ¹³C NMR (101 MHz, DMSO-*d*₆): δ_C 179.4, 174.7, 152.0, 144.7, 136.4, 135.0, 131.5, 129.8, 128.9, 128.4, 126.6, 124.4, 123.4, 121.2, 120.7, 120.6, 117.0, 114.4, 56.8, 41.5, 40.6, 25.2, 20.9; IR (neat): ν_{max}/cm⁻¹: 3452, 2981, 1715; MS (pNSI): 393.1 (100%, [M – (C₆H₅NOH)]⁺), 502.1 (14%, [M + H]⁺), 519.2 (96%, [M + NH₄]⁺), 524.1 (17%, [M + Na]⁺), 1003.3 (40%, [2M + H]⁺), 1025.3 (15%, [2M + Na]⁺); HRMS (pNSI): calcd for C₂₇H₂₄N₃O₅S [M + H]⁺: 502.1431; observed: 502.1428.

3l – (3aS*,5S*,10bS*)-5-(hydroxy(*o*-tolyl)amino)-10-tosyl-4,5,10,10b-tetrahydropyrrolo[3,4-*a*]carbazole-1,3(2*H*,3*aH*)-dione

To a stirred round bottomed flask was added 1-tosyl-3-vinyl-1*H*-indole (100 mg, 0.34 mmol), DCM (5 mL) and 1*H*-pyrrole-2,5-dione (33 mg, 0.34 mmol) was added and the resulting

solution was heated at reflux for 48 hours. The reaction was cooled to room temperature and 1-methyl-2-nitrosobenzene (41 mg, 0.34 mmol) was added. The reaction was stirred at room temperature for 4 hours before the solvent was removed under reduced pressure to leave the crude product as a pale yellow solid. The product was purified by column chromatography (petrol (40/60)-ether-DCM 2 : 1 : 1, column diameter = 2 cm, silica = 14 cm) to give (3aS*,5S*,10bS*)-5-(hydroxy(*o*-tolyl)amino)-10-tosyl-4,5,10,10b-tetrahydropyrrolo[3,4-*a*]carbazole-1,3(2*H*,3*aH*)-dione (82%, 143 mg, 0.28 mmol) as a yellow powder.

Mp: 171.1–174.0 °C; R_f : 0.13 (Pet(40/60)-EA 2 : 1); ^1H NMR (400 MHz, CDCl_3): δ 7.90 (1H, d, J = 8.4 Hz), 7.73 (2H, d, J = 8.2 Hz), 7.77 (1H, s), 7.35 (2H, dd, J = 15.7, 7.9 Hz), 7.20 (3H, app d, J = 8.2 Hz), 7.09 (2H, d, J = 7.5 Hz), 7.07–7.00 (2H, m), 5.17 (1H, d, J = 8.1 Hz), 4.75 (1H, s), 4.39 (1H, app t, J = 5.1 Hz), 3.80 (1H, app q, J = 8.3, 5.7 Hz), 2.64 (1H, app dt, J = 13.1, 5.5 Hz), 2.34 (3H, s), 2.26 (3H, s), 1.96 (1H, ddd, J = 15.9, 7.9, 3.7 Hz); ^{13}C NMR (75 MHz, CDCl_3): δ_c 178.3, 173.4, 149.3, 144.7, 137.4, 135.8, 131.3, 130.9, 129.8, 129.6, 129.5, 129.0, 127.0, 126.3, 125.1, 124.7, 123.7, 121.5, 120.1, 115.3, 57.3, 42.0, 40.8, 26.0, 21.4, 18.3; IR (neat): $\nu_{\text{max}}/\text{cm}^{-1}$ 3294, 2981, 1713; MS (pAPCI): 293.1 (16%), 332.1 (13%), 342.1 (16%), 393.1 (100%, (M – (*o*-Tol)N(OH)) $^+$), 489.1 (54%, (M – H $_2$ O) $^+$), 516.2 (26%, (M + H) $^+$); HRMS (pAPCI): calcd for $\text{C}_{28}\text{H}_{26}\text{N}_3\text{O}_5\text{S}$ [M + H] $^+$: 516.1588; observed: 516.1576.

3m – (3aS*,5S*,10bS*)-5-((S*)-hydroxy(perfluorophenyl)methyl)-10-tosyl-4,5,10,10b-tetrahydropyrrolo[3,4-*a*]carbazole-1,3(2*H*,3*aH*)-dione

To a stirred round bottomed flask was added 1-tosyl-3-vinyl-1*H*-indole (100 mg, 0.34 mmol), DCM (5 mL) and 1*H*-pyrrole-2,5-dione (33 mg, 0.34 mmol). The resulting solution was heated at reflux for 48 hours. The reaction was cooled to 0 °C and pentafluorobenzaldehyde (67 mg, 0.34 mmol) and DMAC (1 M in hexane, 0.34 mL, 0.34 mmol) were added. The solution was stirred at 0 °C for 1 hour and then warmed to room temperature for 18 hours. The reaction was poured into sodium bicarbonate (15 mL) and extracted with DCM. The combined organic layers were dried with MgSO_4 , filtered and the solvent was removed under reduced pressure to give the crude product as an off white solid. The product was purified by column chromatography (diameter = 1.5 cm, silica = 15 cm, eluent = petrol (40/60)-EA 2 : 1) to give (3aS*,5S*,10bS*)-5-((S*)-hydroxy(perfluorophenyl)methyl)-10-tosyl-4,5,10,10b-tetrahydropyrrolo[3,4-*a*]carbazole-1,3(2*H*,3*aH*)-dione (71%, 0.1427 g, 0.24 mmol) as an off white solid.

Mp: 181.3–185.1 °C; R_f : 0.22 (Pet(40/60)-EA 2 : 1); ^1H NMR (400 MHz, CDCl_3): δ_{H} 8.03 (1H, br s), 7.81 (3H, app d, J = 7.9 Hz), 7.28 (1H, d, J = 8.0 Hz), 7.25–7.22 (3H, m), 7.16 (1H, app t, J = 7.6 Hz), 5.08 (1H, d, J = 8.3 Hz), 5.05 (1H, d, J = 7.4 Hz), 3.61–3.66 (1H, m), 3.49–3.57 (1H, m), 2.34 (3H, s), 2.09 (1H, dd, J = 14.0, 4.5 Hz), 1.74 (1H, app td, J = 13.9, 5.3 Hz); ^{13}C NMR (101 MHz, CDCl_3): δ_c 177.4, 173.0, 145.3, 137.4, 135.5, 129.8, 129.7, 129.1, 127.1, 125.5, 123.9, 120.2, 120.0, 115.3, 70.2, 42.5, 40.3, 36.8, 28.5, 21.7; IR (neat): $\nu_{\text{max}}/\text{cm}^{-1}$ 3240, 2981, 1717; MS

(pAPCI): 157.0 (79%), 221.1 (61%), 393.1 (15%, (M – ($\text{C}_6\text{F}_5\text{COH}$) $^+$), 443.1 (51%), 573.1 (8%, (M – H $_2$ O) $^+$), 591.1 (100%, (M + H) $^+$); HRMS (pAPCI): calcd for $\text{C}_{28}\text{H}_{20}\text{F}_5\text{N}_2\text{O}_5\text{S}$ [M + H] $^+$: 591.1008; observed: 591.1001. Note: ^{13}C NMR missing peaks due to C–F coupling.

3n – (3aS*,5S*,10bS*)-5-(3,5-dioxo-4-phenyl-1,2,4-triazolidin-1-yl)-10-tosyl-4,5,10,10b-tetrahydropyrrolo[3,4-*a*]carbazole-1,3(2*H*,3*aH*)-dione

To a stirred round bottomed flask was added 1-tosyl-3-vinyl-1*H*-indole (100 mg, 0.34 mmol), DCM (5 mL) and 1*H*-pyrrole-2,5-dione (33 mg, 0.34 mmol). The resulting solution was heated at reflux for 48 hours. The reaction was cooled to 0 °C and PTAD was added. The solution was stirred at 0 °C for 4 hours and the solvent was removed under reduced pressure to give the crude product as pale red. The product was purified by column chromatography (diameter = 1.5 cm, silica = 17 cm, eluent = petrol (40/60)-EA 1 : 1) to give (3aS*,5S*,10bS*)-5-(3,5-dioxo-4-phenyl-1,2,4-triazolidin-1-yl)-10-tosyl-4,5,10,10b-tetrahydropyrrolo[3,4-*a*]carbazole-1,3(2*H*,3*aH*)-dione (23%, 0.044 g, 0.08 mmol) as an off white solid.

Mp: 206.4–209.7 °C; R_f : 0.10 (Pet(40/60)-EA 2 : 1); ^1H NMR (400 MHz, DMSO-d_6): δ_c 11.37 (1H, s), 10.77 (1H, s), 7.82 (2H, d, J = 8.3 Hz), 7.72 (1H, d, J = 7.9 Hz), 7.48–7.43 (2H, m), 7.42–7.35 (4H, m), 7.28 (2H, d, J = 8.5 Hz), 7.25–7.18 (2H, m), 5.46 (1H, app t, J = 4.9 Hz), 5.19 (1H, d, J = 7.7 Hz), 3.77–3.65 (1H, m), 2.41 (1H, app dt, J = 9.8, 5.1 Hz), 2.26 (3H, s), 2.24–2.16 (1H, m); ^{13}C NMR (101 MHz, CDCl_3): δ_{H} 178.8, 173.6, 153.6, 152.4, 145.4, 136.9, 135.3, 132.2, 130.9, 129.9, 129.2, 128.4, 127.5, 126.9, 125.7, 125.6, 124.2, 119.3, 115.1, 114.8, 47.3, 41.5, 40.2, 28.8, 21.7; IR (neat): $\nu_{\text{max}}/\text{cm}^{-1}$ 3194, 2981, 2980, 1699; MS (pNSI): 587.2 (100% (M + NH $_4$) $^+$), 592.1 (30% (M + Na) $^+$); HRMS (pNSI): calcd for $\text{C}_{29}\text{H}_{27}\text{N}_6\text{O}_6\text{S}$ [M + NH $_4$] $^+$: 587.1707; observed: 587.1706.

3o – (3aS*,5S*,10bS*)-5-(hydroxy(*o*-tolyl)amino)-7-methoxy-10-tosyl-4,5,10,10b-tetrahydropyrrolo[3,4-*a*]carbazole-1,3(2*H*,3*aH*)-dione

To a stirred round bottomed flask was added 6-methoxy-1-tosyl-3-vinyl-1*H*-indole (111 mg, 0.34 mmol), DCM (5 mL) and 1*H*-pyrrole-2,5-dione (33 mg, 0.34 mmol). The resulting solution was heated at reflux for 48 hours. The reaction was cooled to room temperature and 1-methyl-2-nitrosobenzene (41 mg, 0.34 mmol) was added. The reaction was stirred at room temperature for 24 hours before the solvent was removed under reduced pressure to leave the crude product as a pale yellow solid. The product was purified by column chromatography (petrol (40/60)-ethyl acetate 2 : 1) to give (3aS*,5S*,10bS*)-5-(hydroxy(*o*-tolyl)amino)-7-methoxy-10-tosyl-4,5,10,10b-tetrahydropyrrolo[3,4-*a*]carbazole-1,3(2*H*,3*aH*)-dione (76%, 141 mg, 0.26 mmol) as a light brown solid.

Mp: 185 °C decomposed; R_f : 0.26 (Pet(40/60)-EA 4 : 3); ^1H NMR (400 MHz, DMSO-d_6): δ_{H} 11.19 (1H, s), 8.34 (1H, s), 7.69 (1H, d, J = 9.1 Hz), 7.61 (2H, d, J = 8.2 Hz), 7.27 (2H, d, J = 8.2 Hz), 7.08–6.97 (2H, m), 6.95–6.85 (2H, m), 6.72 (1H, dd, J = 9.1, 2.4 Hz), 6.40 (1H, s), 5.07 (1H, d, J = 7.9 Hz), 4.20 (1H, app t, J = 4.4 Hz), 3.76 (1H, app q, J = 8.4 Hz), 3.47 (3H, s), 2.53–2.47 (1H,

Paper

m), 2.28 (s, 3H), 2.08 (s, 3H), 1.75 (1H, ddd, $J = 13.6, 9.8, 4.4$ Hz); ^{13}C NMR (101 MHz, DMSO- d_6): δ_{C} 180.5, 175.4, 156.3, 151.7, 145.3, 134.7, 133.1, 131.1, 131.0, 130.8, 130.3, 129.7, 127.1, 126.4, 124.6, 122.1, 121.2, 115.9, 113.8, 103.3, 57.1, 55.3, 42.2, 26.9, 21.5, 21.3, 18.5; IR (neat): $\nu_{\text{max}}/\text{cm}^{-1}$ 3388, 3071, 2552, 1727; MS (pNSI): 355.1 (50%), 371.1 (100%), 423.1 (57%), 445.1 (30%), 546.2 (5%, $(\text{M} + \text{H})^+$), 568.2 (16%, $(\text{M} + \text{Na})^+$), 584.1 (21%); HRMS (pNSI): calcd for $\text{C}_{29}\text{H}_{28}\text{N}_5\text{O}_6\text{S}_1$ $[\text{M} + \text{H}]^+$: 546.1693; observed: 546.1690.

3p – (3aS*,5S*,10bS*)-5-((S*)-hydroxy(perfluorophenyl)methyl)-7-methoxy-2-methyl-10-tosyl-4,5,10,10b-tetrahydropyrrolo[3,4-*a*]carbazole-1,3(2*H*,3*aH*)-dione

To a stirred round bottomed flask was added 5-methoxy-1-tosyl-3-vinyl-1*H*-indole (112 mg, 0.34 mmol), DCM (5 mL) and 1-methyl-1*H*-pyrrole-2,5-dione (38 mg, 0.34 mmol). The reaction was heated at reflux for 48 hours. The reaction was cooled to -78°C and pentafluorobenzaldehyde (0.04 mL, 0.34 mmol) and DMAC (1 M in hexane, 0.34 mL, 0.34 mmol) were added. The solution was stirred at -78°C for 15 minutes and then at room temperature for 18 hours. The solvent was removed under reduced pressure to give the crude product as an off white solid. The product was purified by column chromatography (column diameter = 2 cm, silica = 15 cm, eluent = petrol (40/60)-EA 3 : 1) to give a 8 : 1 mixture of (3aS*,5S*,10bS*)-5-((S*)-hydroxy(perfluorophenyl)methyl)-7-methoxy-2-methyl-10-tosyl-4,5,10,10b-tetrahydropyrrolo[3,4-*a*]carbazole-1,3(2*H*,3*aH*)-dione and (3aS*,5S*,10bS*)-5-((R*)-hydroxy(perfluorophenyl)methyl)-7-methoxy-2-methyl-10-tosyl-4,5,10,10b-tetrahydropyrrolo[3,4-*a*]carbazole-1,3(2*H*,3*aH*)-dione (70%, 0.151 mg, 0.24 mmol) as a white powder.

Major diastereomer: Mp: 136.7–139.0 $^\circ\text{C}$; R_f : 0.40 (Pet(40/60)-EA 2 : 1); ^1H NMR (400 MHz, CDCl_3): δ_{H} 7.76 (2H, d, $J = 8.3$ Hz), 7.69 (1H, d, $J = 9.1$ Hz), 7.22 (2H, d, $J = 8.3$ Hz), 6.83 (1H, dd, $J = 9.1, 2.5$ Hz), 6.72 (1H, d, $J = 2.5$ Hz), 5.08 (1H, d, $J = 8.3$ Hz), 4.87 (1H, d, $J = 7.4$ Hz), 3.71 (3H, s), 3.58–3.47 (2H, m), 2.94 (3H, s), 2.34 (3H, s), 2.11–2.04 (1H, m), 1.60 (1H, td, $J = 13.9, 5.3$ Hz); ^{13}C NMR (101 MHz, CDCl_3): δ_{C} 177.7, 173.2, 156.8, 145.2, 135.2, 132.0, 130.9, 130.3, 129.8, 127.0, 120.6, 116.2, 114.0, 102.6, 70.2, 55.6, 41.5, 39.0, 36.9, 28.6, 25.3, 21.7; IR (neat): $\nu_{\text{max}}/\text{cm}^{-1}$ 2981, 2884, 1709; MS (pAPCI): 157.0 (80%), 221.1 (92%), 281.1 (49%) 475.1 (94%), 635.1 (100%, $(\text{M} + \text{H})^+$); HRMS (pAPCI): calcd for $\text{C}_{30}\text{H}_{24}\text{F}_3\text{N}_2\text{O}_6\text{S}$ $[\text{M} + \text{H}]^+$: 635.1270; observed: 635.1266. Note: ^{13}C NMR missing peaks due to C-F coupling.

3q – (3aS*,5S*,10bS*)-5-(3,5-dioxo-4-phenyl-1,2,4-triazolidin-1-yl)-7-methoxy-10-tosyl-4,5,10,10b-tetrahydropyrrolo[3,4-*a*]carbazole-1,3(2*H*,3*aH*)-dione

To a stirred round bottomed flask was added 5-methoxy-1-tosyl-3-vinyl-1*H*-indole (112 mg, 0.34 mmol), DCM (5 mL) and 1*H*-pyrrole-2,5-dione (33 mg, 0.34 mmol). The reaction was heated at reflux for 48 hours. The reaction was cooled to 0°C and PTAD (60 mg, 0.34 mmol) was added. The reaction was stirred at 0°C for 4 hours before the solvent was removed under reduced pressure to give the crude product as a pale red solid. The product was purified by column chromatography (column

diameter = 2 cm, silica = 16 cm, eluent = petrol (40/60)-EA 1 : 1) to give (3aS*,5S*,10bS*)-5-(3,5-dioxo-4-phenyl-1,2,4-triazolidin-1-yl)-7-methoxy-10-tosyl-4,5,10,10b-tetrahydropyrrolo[3,4-*a*]carbazole-1,3(2*H*,3*aH*)-dione (75%, 0.152 mg, 0.25 mmol) as a pale yellow powder.

Mp: 189.9–193.3 $^\circ\text{C}$; R_f : 0.07 (Pet(40/60)-EA 1 : 1); ^1H NMR (400 MHz, CDCl_3): δ_{H} 9.31 (1H, br), 7.67 (2H, d, $J = 7.5$ Hz), 7.55 (1H, d, $J = 8.8$ Hz), 7.38–7.23 (5H, m), 7.00 (2H, d, $J = 7.8$ Hz), 6.90 (1H, s), 6.80 (1H, d, $J = 8.9$ Hz), 5.53 (1H, br s), 5.18 (1H, d, $J = 6.7$ Hz), 3.74–3.69 (1H, m), 3.64 (3H, s), 2.48–2.55 (1H, m), 2.17 (3H, s), 2.12–2.02 (2H, m); ^{13}C NMR (101 MHz, CDCl_3): δ_{C} 179.0, 173.9, 156.9, 153.7, 152.7, 145.2, 135.1, 132.7, 131.5, 131.0, 129.8, 129.2, 128.4, 128.0, 127.2, 125.6, 115.9, 115.5, 114.3, 101.9, 55.7, 47.6, 41.6, 40.1, 28.8, 21.6; IR (neat): $\nu_{\text{max}}/\text{cm}^{-1}$ 2972, 2885, 1781, 1709; MS (pNSI): 617.2 (69%, $(\text{M} + \text{NH}_4)^+$), 622.1 (100%, $(\text{M} + \text{Na})^+$), 644.1 (48%); HRMS (pNSI): calcd for $\text{C}_{30}\text{H}_{29}\text{N}_6\text{O}_7\text{S}$ $[\text{M} + \text{NH}_4]^+$: 617.1813; observed: 617.1817.

3r – 6-(3,5-dioxo-4-phenyl-1,2,4-triazolidin-1-yl)-2-phenyl-11-tosyl-5,6-dihydro-[1,2,4]triazolo[1',2':1,2]pyridazino[3,4-*b*]indole-1,3(2*H*,11*H*)-dione

To a stirred round bottomed flask was added 1-tosyl-3-vinyl-1*H*-indole (100 mg, 0.34 mmol) and DCM (5 mL). The resulting solution was cooled to -78°C and then PTAD (70 mg, 0.34 mmol) was added. The reaction was stirred at -78°C for 3.5 hours. The reaction was warmed to 0°C and a further equivalent of PTAD (60 mg, 0.34 mmol) was added. The reaction was stirred 0°C for 4 hours, resulting in the formation of a white precipitate. The reaction mixture was filtered and 6-(3,5-dioxo-4-phenyl-1,2,4-triazolidin-1-yl)-2-phenyl-11-tosyl-5,6-dihydro-[1,2,4]triazolo[1',2':1,2]pyridazino[3,4-*b*]indole-1,3(2*H*,11*H*)-dione (65%, 134 mg, 0.207 mmol) was recovered as a white powder.

Mp: 227.8–230.6 $^\circ\text{C}$; ^1H NMR (400 MHz, DMSO- d_6): δ_{H} 10.76 (1H, s, NH), 7.91 (1H, d, $J = 7.8$ Hz), 7.61 (2H, d, $J = 8.3$ Hz), 7.48–7.24 (15H, m), 5.52 (1H, s), 4.76 (1H, d, $J = 13.8$ Hz), 3.86 (1H, d, $J = 13.8$ Hz), 2.24 (3H, s); ^{13}C NMR (101 MHz, DMSO- d_6): δ_{C} 154.3, 153.5, 150.6, 149.5, 146.0, 135.1, 133.3, 133.0, 131.7, 131.5, 130.4, 129.6, 129.5, 129.4, 128.8, 128.1, 127.6, 127.5, 126.9, 125.9, 125.4, 119.3, 116.8, 104.1, 48.8, 43.3, 21.6; IR (neat): $\nu_{\text{max}}/\text{cm}^{-1}$ 2971, 2883, 1714; MS (pNSI): 263.0 (36%), 345.0 (51%), 371.1 (42%), 665.2 (89%, $(\text{M} + \text{NH}_4)^+$), 670.1 (100%, $(\text{M} + \text{Na})^+$); HRMS (pNSI): calcd for $\text{C}_{33}\text{H}_{25}\text{N}_7\text{NaO}_6\text{S}$ $[\text{M} + \text{Na}]^+$: 670.1479; observed: 670.1475.

3s – 6-(hydroxy(phenyl)amino)-2-phenyl-11-tosyl-5,6-dihydro-[1,2,4]triazolo[1',2':1,2]pyridazino[3,4-*b*]indole-1,3(2*H*,11*H*)-dione

To a stirred round bottomed flask was added 1-tosyl-3-vinyl-1*H*-indole (100 mg, 0.34 mmol) and DCM (5 mL) and the solution was cooled to -78°C . To this solution PTAD (70 mg, 0.34 mmol) was added and the reaction was stirred at -78°C for 3.5 hours. The reaction was warmed to room temperature nitrosobenzene (44 mg, 0.34 mmol) was added and the reaction was stirred for 18 hours. The solvent was removed under reduced pressure to leave the crude product as a pale

yellow oil. The product was purified by column chromatography (column diameter = 1 cm, silica = 16 cm, eluent = petrol (40/60)-ether-DCM 2 : 1 : 1) to give 6-(hydroxy(phenyl)amino)-2-phenyl-11-tosyl-5,6-dihydro-[1,2,4]triazolo[1',2':1,2]pyridazino[3,4-*b*]indole-1,3-(2*H*,11*H*)-dione (72%, 141 mg, 0.24 mmol) as a white powder.

Mp: 176.1–180.0 °C; *R*_f: 0.48 (Pet(40/60)-Et₂O 2 : 1); ¹H NMR (400 MHz, CDCl₃): δ_H 8.03 (1H, d, *J* = 8.3 Hz), 7.62 (2H, d, *J* = 8.1 Hz), 7.56 (2H, d, *J* = 7.6 Hz), 7.46 (2H, app t, *J* = 7.7 Hz), 7.42–7.36 (1H, m), 7.23–7.07 (7H, m), 7.05–6.99 (2H, m), 6.59 (1H, d, *J* = 7.4 Hz), 5.81 (1H, br s), 5.18 (1H, d, *J* = 13.5 Hz), 4.59 (1H, s), 3.23 (1H, d, *J* = 13.5 Hz), 2.30 (3H, s); ¹³C NMR (101 MHz, DMSO-*d*₆): δ_C 152.7, 152.2, 150.5, 146.0, 134.9, 132.9, 132.5, 131.8, 130.4, 129.8, 129.3, 129.2, 128.5, 127.3, 127.3, 125.5, 125.4, 122.5, 119.8, 117.6, 116.6, 108.6, 55.9, 44.6, 21.6; IR (neat): ν_{max}/cm⁻¹ 2981, 2884, 1714; MS (pAPCI): 138.1 (100%), 157.0 (95%), 213.1 (50%), 248.1 (86%), 279.1 (62%), 317.1 (33%), 333.1 (29%), 471.1 (31%), 564.2 (11%), 580.2 (10%, (M + H)⁺); HRMS (pAPCI): calcd for C₃₁H₂₆N₅O₅S [M + H]⁺: 580.1649; observed: 580.1640.

3t – (3a*S*^{*},5*S*^{*},10*bS*^{*})-5-(hydroxy(*o*-tolyl)amino)-*N,N,N*,2-trimethyl-1,3-dioxo-1,3,3a,4,5,10*b*-hexahydropyrrolo[3,4-*a*]carbazole-10(2*H*)-sulfonamide

To a stirred bottomed flask was added *N,N*-dimethyl-3-vinyl-1*H*-indole-1-sulfonamide (85 mg, 0.34 mmol), DCM (5 mL) and 1-methyl-1*H*-pyrrole-2,5-dione (38 mg, 0.34 mmol). The solution was heated at reflux for 48 hours. The reaction was cooled to room temperature and 1-methyl-2-nitrosobenzene (41 mg, 0.34 mmol) was added. The reaction was stirred for 3 hours at room temperature before the solvent was removed under reduced pressure to give the crude product. The crude product was purified by column chromatography (column diameter = 2 cm, silica = 16 cm, eluent = petrol (40/60)-ethyl acetate 2 : 1) to give (3a*S*^{*},5*S*^{*},10*bS*^{*})-5-(hydroxy(*o*-tolyl)amino)-*N,N,N*,2-trimethyl-1,3-dioxo-1,3,3a,4,5,10*b*-hexahydropyrrolo[3,4-*a*]carbazole-10(2*H*)-sulfonamide (74%, 0.122 g, 0.25 mmol) as an off white solid.

Mp: 169.3–171.9 °C; *R*_f: 0.32 (Pet(40/60)-EA 2 : 1); ¹H NMR (400 MHz, CDCl₃): δ_H 7.84 (1H, d, *J* = 8.4 Hz), 7.60 (1H, d, *J* = 7.9 Hz), 7.50 (1H, d, *J* = 8.0 Hz), 7.28 (1H, app t, *J* = 7.8 Hz), 7.21–7.16 (2H, m), 7.13 (1H, d, *J* = 8.1 Hz), 7.07–7.03 (1H, m), 4.98–4.96 (2H, m), 4.35–4.31 (1H, m), 3.69 (1H, app t, *J* = 7.7 Hz), 2.93 (9H, s), 2.60 (1H, app dt, *J* = 13.1, 6.2 Hz), 2.33 (3H, s), 1.97 (1H, ddd, *J* = 13.1, 7.7, 4.6 Hz); ¹³C NMR (101 MHz, CDCl₃): δ_C 178.4, 173.8, 149.2, 137.4, 131.9, 131.1, 129.6, 128.4, 126.6, 125.3, 124.7, 123.7, 121.5, 120.4, 118.8, 115.0, 57.5, 40.5, 39.4, 38.4, 25.2, 24.7, 18.7; IR (neat): ν_{max}/cm⁻¹ 3426, 2981, 1712; MS (pAPCI): 221.1 (9%), 251.1 (13%), 360.1 (100%, (M – (*o*-Tol)N(OH))⁺), 465.2 (15%, (M – H₂O)⁺), 483.2 (15%, (M + H)⁺); HRMS (pAPCI): calcd for C₂₄H₂₇N₄O₅S₁ [M + H]⁺: 483.1697; observed: 483.1685.

3u – (3a*S*^{*},5*S*^{*},10*bS*^{*})-5-((2,6-dibromophenyl) (hydroxy)amino)-*N,N,N*-dimethyl-1,3-dioxo-2-phenyl-1,3,3a,4,5,10*b*-hexahydropyrrolo[3,4-*a*]carbazole-10(2*H*)-sulfonamide

To a stirred round bottomed flask was added *N,N*-dimethyl-3-vinyl-1*H*-indole-1-sulfonamide (85 mg, 0.34 mmol), DCM (5 mL) and 1-phenyl-1*H*-pyrrole-2,5-dione (59 mg, 0.34 mmol) and the

resulting solution was heated at reflux for 48 hours. The reaction was cooled to room temperature and 2,6-dibromonitrosobenzene (90 mg, 0.34 mmol) was added. The reaction was stirred at room temperature for 18 hours and the solvent was removed under reduced pressure to give the crude product as a pale yellow solid. The product was purified by column chromatography (petrol (40/60)-ethyl acetate 3 : 1, column diameter = 2 cm, silica = 17 cm) to give (3a*S*^{*},5*S*^{*},10*bS*^{*})-5-((2,6-dibromophenyl) (hydroxy)amino)-*N,N*-dimethyl-1,3-dioxo-2-phenyl-2,3,3a,4,5,10*b*-hexahydropyrrolo[3,4-*a*]carbazole-10(1*H*)-sulfonamide (69%, 162 mg, 0.23 mmol) as a pale orange powder.

Mp: 241–242 °C; *R*_f: 0.43 (Pet(40/60)-Et₂O 4 : 1); ¹H NMR (400 MHz, CDCl₃): δ 7.53 (2H, d, *J* = 7.8 Hz), 7.46–7.30 (7H, m), 7.15 (1H, app t, *J* = 7.4 Hz), 7.02 (1H, app t, *J* = 7.5 Hz), 6.71 (1H, app td, *J* = 8.0, 2.1 Hz), 6.05 (1H, s), 5.49–5.47 (1H, m), 5.17–5.12 (1H, m), 4.35–4.27 (1H, m), 3.18–3.11 (1H, m), 2.92 (6H, s), 1.80 (1H, app t, *J* = 13.1 Hz); ¹³C NMR (101 MHz, CD₂Cl₂): δ_C 177.9, 172.5, 144.6, 136.1, 134.3, 132.7, 132.1, 132.0, 129.5, 129.1, 128.6, 128.2, 126.6, 124.0, 122.8, 119.2, 115.1, 113.6, 77.6, 54.7, 42.7, 39.0, 38.0, 30.0; IR (neat): ν_{max}/cm⁻¹ 3431, 2927, 1780, 1715; MS (pNSI): 422.1 (25%, (M – N(OH)C₆H₃Br₂)⁺), 689.0 (76% (M + H)⁺), 711.0 (54%, (M + Na)⁺), HRMS (pNSI): calcd C₂₈H₂₅Br₂N₄O₅S [M + H]⁺: 688.9888; observed: 688.9886.

3v – (3a*S*^{*},5*S*^{*},10*bS*^{*})-5-((*S*^{*})-hydroxy(perfluorophenyl)methyl)-*N,N*-dimethyl-1,3-dioxo-1,3,3a,4,5,10*b*-hexahydropyrrolo[3,4-*a*]carbazole-10(2*H*)-sulfonamide

To a stirred round bottomed flask was added *N,N*-dimethyl-3-vinyl-1*H*-indole-1-sulfonamide (85 mg, 0.34 mmol), DCM (5 mL) and 1-methyl-1*H*-pyrrole-2,5-dione (38 mg, 0.34 mmol). The reaction was heated at reflux for 48 hours. The reaction was cooled to –78 °C and pentafluorobenzaldehyde (66 mg, 0.34 mmol) and DMAC (1 M in hexane, 0.34 mL, 0.34 mmol) were added and the reaction was stirred for 1 hour. The reaction was poured into a solution of sodium bicarbonate (10 mL) and extracted with DCM (3 × 10 mL). The combined organic extracts were dried with MgSO₄, filtered and the solvent was removed under reduced pressure to leave the crude product as a pale pink solid. The product was purified by column chromatography (diameter = 2 cm, silica = 17 cm, eluent = petrol (40/60)-EA 2 : 1) to give (3a*S*^{*},5*S*^{*},10*bS*^{*})-5-((*S*^{*})-hydroxy(perfluorophenyl)methyl)-*N,N*-dimethyl-1,3-dioxo-1,3,3a,4,5,10*b*-hexahydropyrrolo[3,4-*a*]carbazole-10(2*H*)-sulfonamide (77%, 0.145 g, 0.26 mmol) as a pale pink solid.

Mp: 255.8–257.2 °C; *R*_f: 0.30 (Pet(40/60)-EA 2 : 1); ¹H NMR (400 MHz, CDCl₃): δ_H 7.77 (1H, d, *J* = 8.3 Hz), 7.39 (1H, d, *J* = 7.8 Hz), 7.33–7.28 (1H, m), 7.21 (1H, app t, *J* = 7.8 Hz), 5.14 (1H, d, *J* = 8.0 Hz), 4.80 (1H, d, *J* = 7.3 Hz), 3.67–3.62 (1H, m), 3.48 (1H, ddd, *J* = 12.8, 7.2, 5.0 Hz), 2.98 (6H, s), 2.93 (3H, s), 2.49 (1H, br s), 2.06 (1H, app dd, *J* = 14.9, 4.1 Hz), 1.59 (1H, app dt, *J* = 13.8, 6.9 Hz); ¹³C NMR (101 MHz, CDCl₃): δ_C 177.8, 173.4, 137.2, 130.0, 129.3, 125.0, 123.5, 120.0, 118.2, 114.6, 70.3, 41.5, 39.2, 38.2, 36.7, 28.6, 25.2; IR (neat): ν_{max}/cm⁻¹ 3415, 2972, 2884, 1713; MS (pNSI): 371.1 (22%), 558.1 (81% (M + H)⁺), 580.1 (100%, (M + Na)⁺), HRMS (pNSI): calcd C₂₄H₂₀F₅N₄O₅S [M + H]⁺: 558.1117; observed: 558.1118.

Note: ^{13}C NMR missing peaks due to C-F coupling.

3w – 6-(hydroxy(*o*-tolyl)amino)-*N,N*-dimethyl-1,3-dioxo-2-phenyl-2,3,5,6-tetrahydro-[1,2,4]triazolo[1',2':1,2]pyridazino[3,4-*b*]indole-11(*1H*)-sulfonamide

To a stirred round bottomed flask was added *N,N*-dimethyl-3-vinyl-1*H*-indole-1-sulfonamide (85 mg, 0.34 mmol), DCM (5 mL) and cooled to $-78\text{ }^\circ\text{C}$. To this solution PTAD (60 mg, 0.34 mmol) was added and the reaction stirred at $-78\text{ }^\circ\text{C}$ for 1 hour. 1-Methyl-2-nitrosobenzene (41 mg, 0.34 mmol) was added and the reaction was stirred 4 hours before the solvent was removed under reduced pressure to give the crude product. The crude product was purified by column chromatography (column diameter = 2 cm, silica = 16 cm, eluent = petrol (40/60)-ethyl acetate 2 : 1) to give 6-(hydroxy(*o*-tolyl)amino)-*N,N*-dimethyl-1,3-dioxo-2-phenyl-2,3,5,6-tetrahydro-[1,2,4]triazolo[1',2':1,2]pyridazino[3,4-*b*]indole-11(*1H*)-sulfonamide (76%, 0.141 g) as an off white solid.

Mp: 168.5–172.8 $^\circ\text{C}$; R_f : 0.25 (Pet(40/60)-EA 2 : 1); ^1H NMR (300 MHz, CDCl_3): δ_{H} 7.87 (1H, d, J = 8.3 Hz), 7.73 (1H, d, J = 8.1 Hz), 7.60 (2H, d, J = 7.4 Hz), 7.51 (2H, t, J = 7.6 Hz), 7.46–7.38 (1H, m), 7.30–7.18 (2H, m), 7.04 (2H, t, J = 7.5 Hz), 6.90 (1H, d, J = 7.6 Hz), 6.71 (1H, d, J = 7.8 Hz), 5.76 (1H, s), 5.37 (1H, d, J = 14.1 Hz), 4.66 (1H, s), 3.46 (1H, d, J = 14.1 Hz), 2.90 (6H, s), 1.94 (3H, s); ^{13}C NMR (101 MHz, CDCl_3): δ_{C} 153.5, 150.5, 148.7, 135.1, 132.1, 131.9, 131.2, 130.6, 129.4, 128.7, 127.1, 126.9, 126.8, 125.9, 124.4, 124.2, 122.7, 118.1, 115.9, 104.7, 59.4, 44.7, 38.7, 17.9; IR (neat): $\nu_{\text{max}}/\text{cm}^{-1}$ 3322, 2971, 1707; MS (pNSI): 339.1 (33%), 424.1 (94%, (M – $\text{MeC}_6\text{H}_4\text{NOH}$) $^+$), 547.2 (72%, (M + H) $^+$), 569.2 (100%, (M + Na) $^+$); HRMS (pNSI): calcd $\text{C}_{27}\text{H}_{27}\text{N}_6\text{O}_5\text{S}$ [M + H] $^+$: 547.1758; observed: 547.1761.

3x – (3aS*,5S*,10bS*)-5-(hydroxy(*o*-tolyl)amino)-*N,N*-dimethyl-1,3-dioxo-1,3,3a,4,5,10b-hexahydropyrrolo[3,4-*a*]carbazole-10(2*H*)-sulfonamide

To a round bottomed flask was added *N,N*-dimethyl-3-vinyl-1*H*-indole-1-sulfonamide (85 mg, 0.34 mmol), DCM (5 mL) and 1*H*-pyrrole-2,5-dione (33 mg, 0.34 mmol). The reaction was heated at reflux for 48 hours and then cooled to room temperature. 1-Methyl-2-nitrosobenzene (41 mg, 0.34 mmol) was added and the reaction is stirred for 4.5 hours. The solvent was removed to give the crude product as pale yellow solid. The crude product was purified by titration from DCM to give (3aS*,5S*,10bS*)-5-(hydroxy(*o*-tolyl)amino)-*N,N*-dimethyl-1,3-dioxo-1,3,3a,4,5,10b-hexahydropyrrolo[3,4-*a*]carbazole-10(2*H*)-sulfonamide (77%, 123 mg, 0.26 mmol) as a white solid.

Mp: 199.9–201.0 $^\circ\text{C}$; R_f : 0.64 (Pet(40/60)-EA 3 : 1); ^1H NMR (300 MHz, $\text{DMSO}-d_6$): δ_{H} 11.15 (1H, s), 8.38 (1H, s), 7.88 (1H, d, J = 8.4 Hz), 7.36 (1H, d, J = 7.9 Hz), 7.31–7.20 (2H, m), 7.13 (3H, app dt, J = 14.3, 7.3 Hz), 7.01 (1H, d, J = 7.3 Hz), 4.98 (1H, d, J = 7.8 Hz), 4.38 (1H, app t, J = 4.8 Hz), 3.73 (1H, app q, J = 7.8 Hz), 2.70 (6H, s), 2.45–2.37 (1H, m), 2.36 (3H, s), 1.77–1.65, 1.77 (1H, m); ^{13}C NMR (101 MHz, $\text{DMSO}-d_6$): δ_{C} 180.4, 175.5, 151.6, 137.2, 133.2, 131.1, 129.3, 129.1, 126.6, 124.4, 124.3, 123.4, 121.8, 121.1, 118.6, 115.3, 56.5, 42.2, 41.1, 38.7, 26.6, 18.9; IR (neat): $\nu_{\text{max}}/\text{cm}^{-1}$ 3426, 2981, 1712; MS (pAPCI): 237.1 (60%), 346.1 (100%, (M – $\text{MeC}_6\text{H}_4\text{NOH}$) $^+$), 451.1 (25%, (M – H_2O) $^+$), 469.2

(22%, (M + H) $^+$); HRMS (pAPCI): calcd $\text{C}_{23}\text{H}_{25}\text{N}_4\text{O}_5\text{S}$ [M + H] $^+$: 469.1540; observed: 469.1537.

3y – benzyl (3aS*,5S*,10bS*)-5-(hydroxy(phenyl)amino)-2-methyl-1,3-dioxo-2,3,3a,4,5,10b-hexahydropyrrolo[3,4-*a*]carbazole-10(1*H*)-carboxylate

To a stirred Schlenk flask was added benzyl 3-vinyl-1*H*-indole-1-carboxylate (94 mg, 0.34 mmol), DCM (5 mL) and 1-methyl-1*H*-pyrrole-2,5-dione (33 mg, 0.34 mmol). The resulting solution was heated at reflux for 24 hours. The reaction was allowed to cool to room temperature and to the stirred solution nitrosobenzene (36 mg, 0.34 mmol) was added and the solution was stirred for 18 hours. The solvent was removed under reduced pressure to leave the crude product as a pale yellow solid. The product was purified by column chromatography (petrol (40/60)-ethyl acetate 3 : 1, column diameter = 2 cm, silica = 14 cm) to give benzyl (3aS*,5S*,10bS*)-5-(hydroxy(phenyl)amino)-2-methyl-1,3-dioxo-2,3,3a,4,5,10b-hexahydropyrrolo[3,4-*a*]carbazole-10(1*H*)-carboxylate (74%, 124 mg, 0.25 mmol) as a yellow powder.

Mp: 105.7–109.2 $^\circ\text{C}$; R_f : 0.34 (Pet(40/60)-EA 2 : 1); ^1H NMR (400 MHz, CD_2Cl_2): δ_{H} 8.10 (1H, br d, J = 8.1 Hz), 7.70 (1H, br d, J = 7.3 Hz), 7.49 (2H, br d, J = 6.6 Hz), 7.39 (3H, br app q, J = 6.9, 6.4 Hz), 7.35–7.25 (3H, br m), 7.22–7.13 (3H, br m), 7.01 (1H, br app t, J = 6.7 Hz), 5.55 (1H, d, J = 11.8 Hz), 5.41 (1H, d, J = 11.8 Hz), 4.88 (1H, br d, J = 6.8 Hz), 4.87 (1H, br s), 4.80–4.77 (1H, br m), 3.54–3.41 (1H, br m), 2.85 (3H, s), 2.40–2.25 (1H, br m), 2.08–1.93 (1H, br m); ^{13}C NMR (101 MHz, CD_2Cl_2): δ_{C} 178.4, 174.6, 151.6, 151.0, 137.0, 135.0, 130.0, 129.0, 128.9, 128.8, 128.8, 127.6, 125.0, 123.3, 122.3, 120.0, 118.3, 117.1, 115.1, 69.5, 57.7, 40.2, 39.2, 24.9, 22.6; IR (neat): $\nu_{\text{max}}/\text{cm}^{-1}$ 3433, 2953, 1699; MS (pNSI): 387.1 (97%, (M – $\text{N}(\text{OH})\text{Ph}$) $^+$), 494.2 (100%, (M – H) $^+$), 518.2 (30%, (M + Na) $^+$), 991.4 (15%, (2M + H) $^+$), 1013.3 (10%, (2M + Na) $^+$); HRMS (pNSI): calcd $\text{C}_{29}\text{H}_{25}\text{N}_3\text{O}_5\text{Na}$ [M + Na] $^+$: 518.1686; observed: 518.1676.

3z – benzyl (3aS*,5S*,10bS*)-5-(hydroxy(*o*-tolyl)amino)-2-methyl-1,3-dioxo-2,3,3a,4,5,10b-hexahydropyrrolo[3,4-*a*]carbazole-10(1*H*)-carboxylate

To a stirred Schlenk flask was added benzyl 3-vinyl-1*H*-indole-1-carboxylate (94 mg, 0.34 mmol), DCM (5 mL) and 1-methyl-1*H*-pyrrole-2,5-dione (33 mg, 0.34 mmol). The resulting solution was heated at reflux for 24 hours. The reaction was allowed to cool to room temperature and to the stirred solution 1-methyl-2-nitrosobenzene (41 mg, 0.34 mmol) was added and the solution was stirred for 18 hours. The solvent was removed under reduced pressure to leave the crude product as a pale yellow solid. The product was purified by column chromatography (petrol (40/60)-ethyl acetate 3 : 1, column diameter = 2 cm, silica = 16 cm) to give benzyl (3aS*,5S*,10bS*)-5-(hydroxy(*o*-tolyl)amino)-2-methyl-1,3-dioxo-2,3,3a,4,5,10b-hexahydropyrrolo[3,4-*a*]carbazole-10(1*H*)-carboxylate (78%, 135 mg, 0.26 mmol) as a yellow powder.

Mp: 128.4–131.5 $^\circ\text{C}$; R_f : 0.45 (Pet(40/60)-EA 3 : 1); ^1H NMR (400 MHz, CDCl_3): δ_{H} 8.11 (1H, d, J = 8.3 Hz), 7.59 (1H, d, J = 7.8 Hz), 7.55 (1H, d, J = 8.1 Hz), 7.50–7.48 (2H, m), 7.45–7.38

(3H, m), 7.29–7.23 (1H, m), 7.20 (1H, app t, $J = 7.6$ Hz), 7.14 (1H, d, $J = 7.6$ Hz), 7.10 (1H, d, $J = 7.8$ Hz), 7.05 (1H, d, $J = 7.3$ Hz), 5.56 (1H, d, $J = 11.8$ Hz), 5.46 (1H, d, $J = 11.8$ Hz), 5.02 (1H, s), 4.93 (1H, d, $J = 7.6$ Hz), 4.38 (1H, t, $J = 5.2$ Hz), 3.63 (1H, app q, $J = 6.9$ Hz), 2.91 (3H, s), 2.59 (1H, app dt, $J = 12.3, 6.0$ Hz), 2.29 (3H, s), 1.92 (1H, ddd, $J = 12.5, 7.5, 4.6$ Hz); ^{13}C NMR (101 MHz, CDCl_3): δ_{C} 178.5, 174.6, 151.7, 149.2, 136.8, 134.8, 131.1, 129.9, 129.0, 129.0, 128.9, 128.9, 127.7, 126.6, 125.3, 125.0, 123.3, 121.5, 120.1, 118.1, 115.3, 69.6, 57.4, 40.4, 39.1, 25.2, 24.1, 18.6; IR (neat): $\nu_{\text{max}}/\text{cm}^{-1}$ 3450, 2954, 1699; MS (pNSI): 343.1 (40%), 387.1 (82%, $(\text{M} - (\text{N}(\text{OH})(\text{o-Tol})))^+$), 508.2 (100%, $(\text{M} - (\text{H}_2) + \text{H})^+$), 532.2 (59%, $(\text{M} + \text{Na})^+$); HRMS (pNSI): calcd $\text{C}_{30}\text{H}_{27}\text{N}_3\text{O}_5\text{Na} [\text{M} + \text{Na}]^+$: 532.1843; observed: 532.1834.

3aa – (3aS*,5S*,10bS*)-5-(3,5-dioxo-4-phenyl-1,2,4-triazolidin-1-yl)-2-methyl-1,3-dioxo-2,3,3a,4,5,10b-hexahydropyrrolo[3,4-*a*]carbazole-10(1H)-carboxylate

To a stirred Schlenk flask was added benzyl 3-vinyl-1H-indole-1-carboxylate (189 mg, 0.68 mmol), 1-methyl-1H-pyrrole-2,5-dione (76 mg, 0.68 mmol) and DCM (10 mL). The reaction mixture was heated at reflux for 24 hours. The reaction was cooled to 0 °C and then 4-phenyl-1,2,4-triazolidine-3,5-dione (120 mg, 0.68 mmol) was added. The reaction was stirred at 0 °C for 1 hour then at room temperature for 18 hours. The solvent was removed under reduced pressure to leave the crude product as an orange powder. The product was purified by column chromatography (petrol (40/60)-ethyl acetate 1 : 1, column diameter = 2 cm, silica = 20 cm) to give (3aS*,5S*,10bS*)-5-(3,5-dioxo-4-phenyl-1,2,4-triazolidin-1-yl)-2-methyl-1,3-dioxo-2,3,3a,4,5,10b-hexahydropyrrolo[3,4-*a*]carbazole-10(1H)-carboxylate (54%, 207 mg, 0.37 mmol) as an off-white powder and (3aS*,5S*,10bS*)-5-(3,5-dioxo-4-phenyl-1,2,4-triazolidin-1-yl)-2-methyl-1,3-dioxo-2,3,3a,4,5,10b-hexahydropyrrolo[3,4-*a*]carbazole-10(1H)-carboxylate (27%, 76 mg, 0.19 mmol) as a white powder.

Mp: 202.3–203.9 °C; R_f : 0.15 (Pet(40/60)-EA 1 : 1); ^1H NMR (400 MHz, CDCl_3): δ_{H} 8.38 (1H, s), 8.07 (1H, d, $J = 8.4$ Hz), 7.51 (1H, app dt, $J = 7.6, 0.9$ Hz), 7.49–7.37 (4H, m), 7.39–7.33 (6H, m), 7.30 (1H, ddd, $J = 8.6, 7.3, 1.3$ Hz), 7.21 (1H, app td, $J = 7.5, 1.0$ Hz), 5.53 (1H, app t, $J = 5.2$ Hz), 5.44 (1H, d, $J = 11.8$ Hz), 5.38 (1H, d, $J = 11.8$ Hz), 4.89 (1H, d, $J = 8.0$ Hz), 3.50 (1H, ddd, $J = 9.6, 8.0, 5.5$ Hz), 2.87 (3H, s), 2.41 (1H, app dt, $J = 14.2, 5.5$ Hz), 2.14 (1H, ddd, $J = 14.2, 9.5, 5.5$ Hz); ^{13}C NMR (101 MHz, CDCl_3): δ_{C} 177.4, 173.6, 153.6, 152.2, 151.3, 136.9, 134.5, 130.9, 130.8, 129.3, 129.1, 128.9, 128.9, 128.4, 126.1, 125.8, 125.3, 123.8, 118.8, 115.7, 113.8, 69.8, 47.5, 40.0, 38.4, 27.5, 25.2; IR (neat): $\nu_{\text{max}}/\text{cm}^{-1}$ 3462, 2969, 1699; MS (pNSI): 199.2 (16%), 387.1 (19%, $(\text{M} - \text{PTAD})^+$), 564.2 (59%, $(\text{M} + \text{H})^+$), 581.2 (100%, $(\text{M} + \text{NH}_4)^+$), 643.2 (15%), 1144.4 (39%, $(2\text{M} + \text{NH}_4)^+$); HRMS (pNSI): calcd $\text{C}_{31}\text{H}_{26}\text{N}_5\text{O}_6 [\text{M} + \text{H}]^+$: 564.1878; observed: 564.1873.

3bb – benzyl (3aS*,5S*,10bS*)-5-(hydroxy(phenyl)amino)-1,3-dioxo-2,3,3a,4,5,10b-hexahydropyrrolo[3,4-*a*]carbazole-10(1H)-carboxylate

To a stirred Schlenk flask was added benzyl 3-vinyl-1H-indole-1-carboxylate (189 mg, 0.68 mmol), 1H-pyrrole-2,5-dione (66 mg,

0.68 mmol) and DCM (10 mL). The resulting solution was heated at reflux for 24 hours. The reaction was allowed to cool to room temperature and to the stirred solution nitrosobenzene (73 mg, 0.68 mmol) was added and the solution was stirred for 18 hours. The solvent was removed under reduced pressure to leave the crude product as a yellow powder. The product was purified by column chromatography (petrol (40/60)-ethyl acetate 2 : 1, column diameter = 2 cm, silica = 20 cm) to give benzyl(3aS*,5S*,10bS*)-5-(hydroxy(phenyl)amino)-1,3-dioxo-2,3,3a,4,5,10b-hexahydropyrrolo[3,4-*a*]carbazole-10(1H)-carboxylate (70%, 230 mg, 0.48 mmol) as a yellow powder.

Mp: 177.1–177.8 °C; R_f : 0.38 (Pet(40/60)-EA 2 : 1); ^1H NMR (500 MHz, CD_2Cl_2): δ_{H} 8.20 (1H, s), 8.11 (1H, d, $J = 8.3$ Hz), 7.66 (1H, d, $J = 7.8$ Hz), 7.50 (2H, dd, $J = 7.9, 1.6$ Hz), 7.43–7.36 (3H, m), 7.33 (2H, app t, $J = 7.8$ Hz), 7.28 (1H, app t, $J = 7.8$ Hz), 7.22 (2H, d, $J = 8.0$ Hz), 7.16 (1H, app t, $J = 7.5$ Hz), 7.02 (1H, app t, $J = 7.3$ Hz), 5.55 (1H, d, $J = 11.9$ Hz), 5.40 (1H, d, $J = 11.9$ Hz), 5.19 (1H, s), 4.96 (1H, br d, $J = 8.1$ Hz), 4.82 (1H, app t, $J = 5.7$ Hz), 3.56 (1H, br app q, $J = 7.4$ Hz), 2.35 (1H, br app dd, $J = 13.4, 6.7$ Hz), 2.00–1.92 (1H, br m); ^{13}C NMR (101 MHz, CD_2Cl_2): δ_{C} 178.5, 174.5, 151.6, 150.7, 136.9, 134.9, 129.7, 129.0, 128.9, 128.9, 128.8, 127.6, 125.1, 123.3, 122.6, 119.8, 118.0, 117.3, 115.2, 69.5, 57.7, 41.4, 40.6, 23.0; IR (neat): $\nu_{\text{max}}/\text{cm}^{-1}$ 3418, 3329, 2970, 1705; MS (pNSI): 199.2 (87%), 373.1 (68%, $(\text{M} - (\text{N}(\text{OH})\text{Ph}))^+$), 480.2 (100%, $(\text{M} - (\text{H}_2) + \text{H})^+$); HRMS (pNSI): calcd $\text{C}_{28}\text{H}_{23}\text{N}_3\text{O}_5\text{Na} [\text{M} + \text{Na}]^+$: 504.1530; observed: 504.1522.

3cc – benzyl (3aS*,5S*,10bS*)-5-(hydroxy(*o*-tolyl)amino)-1,3-dioxo-2,3,3a,4,5,10b-hexahydropyrrolo[3,4-*a*]carbazole-10(1H)-carboxylate

To a stirred Schlenk flask was added benzyl 3-vinyl-1H-indole-1-carboxylate (94 mg, 0.34 mmol), DCM (5 mL) and 1H-pyrrole-2,5-dione (33 mg, 0.34 mmol). The resulting solution was heated at reflux for 24 hours. The reaction was allowed to cool to room temperature and to the stirred solution 1-methyl-2-nitrosobenzene (41 mg, 0.34 mmol) was added and the solution was stirred for 4 hours. The solvent was removed under reduced pressure to leave the crude product as a pale yellow solid. The product was purified by column chromatography (petrol (40/60)-ethyl acetate 3 : 2, column diameter = 2 cm, silica = 16 cm) to give benzyl-(3aS*,5S*,10bS*)-5-(hydroxy(*o*-tolyl)amino)-1,3-dioxo-2,3,3a,4,5,10b-hexahydropyrrolo[3,4-*a*]carbazole-10(1H)-carboxylate (83%, 140 mg, 0.28 mmol) as a yellow powder.

Mp: 181.4–183.9 °C; R_f : 0.48 (Pet(40/60)-EA 3 : 2); ^1H NMR (400 MHz, $\text{DMSO}-d_6$): δ_{H} 11.26 (1H, s), 8.41 (1H, s), 7.93 (1H, d, $J = 8.3$ Hz), 7.51 (2H, d, $J = 7.0$ Hz), 7.45–7.33 (4H, m), 7.18–7.08 (3H, m), 7.03–6.91 (3H, m), 5.56 (1H, d, $J = 12.1$ Hz), 5.32 (1H, d, $J = 12.1$ Hz), 4.96 (1H, d, $J = 8.0$ Hz), 4.34 (1H, app t, $J = 3.7$ Hz), 3.73 (1H, app q, $J = 8.7$ Hz), 2.50–2.44 (1H, m), 2.17 (3H, s), 1.74–1.64 (1H, m); ^{13}C NMR (101 MHz, $\text{DMSO}-d_6$): δ_{C} 180.6, 176.5, 151.6, 136.2, 135.7, 131.1, 130.8, 130.0, 129.2, 129.1, 129.1, 128.2, 126.6, 124.7, 124.5, 122.9, 122.2, 120.6, 117.5, 114.4, 69.2, 57.1, 41.8, 40.2, 26.7, 18.6; IR (neat): $\nu_{\text{max}}/\text{cm}^{-1}$ 3495, 3325, 2953, 1711; MS (pNSI): 373.1 (51%, $(\text{M} - (\text{N}(\text{OH})(\text{o-Tol})))^+$), 494.2

(16%, (M - (H₂) + H)⁺), 518.2 (21%, (M + Na)⁺); HRMS (pNSI): calcd C₂₉H₂₅N₃O₅Na [M + Na]⁺: 518.1686; observed: 518.1681.

3dd – benzyl (3aS*,5S*,10bS*)-5-(3,5-dioxo-4-phenyl-1,2,4-triazolidin-1-yl)-1,3-dioxo-2,3,3a,4,5,10b-hexahydropyrrolo[3,4-a]carbazole-10(1H)-carboxylate

To a stirred Schlenk flask was added benzyl 3-vinyl-1H-indole-1-carboxylate (189 mg, 0.68 mmol), DCM (10 mL) and 1H-pyrrole-2,5-dione (66 mg, 0.68 mmol). The resulting solution was heated at reflux for 24 hours. The reaction was cooled to 0 °C and 4-phenyl-1,2,4-triazolidine-3,5-dione (120 mg, 0.68 mmol) was added. The solution was stirred at 0 °C for 1 hour. The solvent was removed under reduced pressure to leave the crude product as an off white solid. The product was purified by column chromatography (petrol (40/60)-ethyl acetate 1 : 1, column diameter = 2 cm, silica = 13 cm) to give benzyl (3aS*,5S*,10bS*)-5-(3,5-dioxo-4-phenyl-1,2,4-triazolidin-1-yl)-1,3-dioxo-2,3,3a,4,5,10b-hexahydropyrrolo[3,4-a]carbazole-10(1H)-carboxylate (58%, 216 mg, 0.39 mmol) as a pale pink powder.

Mp: 174.6–177.1 °C; R_f: 0.06 (Pet(40/60)-EA 1 : 1); ¹H NMR (400 MHz, CD₂Cl₂): δ_H 8.78 (1H, s), 8.05 (1H, d, J = 8.3 Hz), 7.54 (1H, d, J = 7.7 Hz), 7.44–7.38 (6H, m), 7.38–7.30 (4H, m), 7.30–7.24 (1H, m), 7.20 (1H, app t, J = 7.5 Hz), 5.51 (1H, app t, J = 5.3 Hz), 5.45 (1H, d, J = 11.9 Hz), 5.31 (1H, d, J = 11.9 Hz), 4.98 (1H, d, J = 7.9 Hz), 3.46 (1H, app q, J = 8.1 Hz), 2.36–2.30 (1H, m), 2.18 (1H, ddd, J = 13.9, 8.6, 5.3 Hz); ¹³C NMR (101 MHz, CD₂Cl₂): δ_C 178.1, 173.8, 153.7, 152.4, 151.4, 136.8, 134.7, 131.1, 130.6, 129.1, 128.9, 128.8, 128.8, 128.4, 126.2, 125.7, 125.6, 123.7, 119.0, 115.5, 114.2, 69.7, 47.7, 41.0, 39.5, 26.8; IR (neat): ν_{max}/cm⁻¹ = 3169, 2975, 1699; MS (pNSI): 279.1 (38%), 373.1 (13%, (M - PTAD)⁺), 550.2 (21%, (M + H)⁺), 567.2 (100% (M + NH₄)⁺), 1116.4 (39%, (2M + NH₄)⁺), 1666.5 (6%, (3M + NH₄)⁺); HRMS (pNSI): calcd C₃₀H₂₄N₅O₆ [M + H]⁺: 550.1721; observed: 550.1719.

3ce – benzyl (R*)-6-(hydroxy(phenyl)amino)-1,3-dioxo-2-phenyl-2,3,5,6-tetrahydro-1H,11H-[1,2,4]triazolo[1',2':1,2]pyridazino[3,4-b]indole-11-carboxylate

To a stirred Schlenk flask was added benzyl 3-vinyl-1H-indole-1-carboxylate (189 mg, 0.68 mmol) and DCM (10 mL). The solution was cooled to -78 °C and 4-phenyl-1,2,4-triazolidine-3,5-dione (120 mg, 0.68 mmol) was added. The reaction was stirred at -78 °C for 5 hours. The reaction was warmed to room temperature, nitrosobenzene (73 mg, 0.68 mmol) was added and the reaction was stirred for 3 hours. The solvent was removed under reduced pressure to leave the crude product as a pale yellow oil. The product was purified by column chromatography (petrol (40/60)-ethyl acetate 2 : 1, column diameter = 1 cm, silica = 16 cm) to give benzyl (R*)-6-(hydroxy(phenyl)amino)-1,3-dioxo-2-phenyl-2,3,5,6-tetrahydro-1H,11H-[1,2,4]triazolo[1',2':1,2]pyridazino[3,4-b]indole-11-carboxylate (72%, 274 mg, 0.49 mmol) as a white powder.

Mp: 101.2–103.1 °C; R_f: 0.53 (Pet(40/60)-EA 2 : 1); ¹H NMR (400 MHz, CD₂Cl₂): δ_H 8.09 (1H, d, J = 8.2 Hz), 7.51–7.38 (8H, m), 7.38–7.24 (5H, m), 7.23–7.07 (4H, m), 6.87 (1H, d, J = 7.9 Hz), 6.36 (1H, s), 5.52 (1H, d, J = 12.1 Hz), 5.39 (1H, d, J = 12.1

Hz), 5.22 (1H, dd, J = 14.0, 1.7 Hz), 4.97–4.89 (1H, m), 3.66 (1H, dd, J = 14.0, 3.4 Hz); ¹³C NMR (101 MHz, CD₂Cl₂): δ_C 147.2, 147.0, 146.6, 145.6, 131.0, 130.1, 127.3, 126.2, 125.4, 125.2, 124.9, 124.9, 124.9, 124.8, 124.8, 122.4, 122.3, 120.7, 120.5119.7, 115.8, 114.5, 110.5, 97.2, 66.2, 55.1, 39.6; IR (neat): ν_{max}/cm⁻¹ = 3337, 3063, 1716; MS (pAPCI): 395.1 (100%), 451.1 (59%, (M - (N(OH)Ph))⁺), 542.2 (5%, (M - (H₂O) + H)⁺), 558.2 (1%, (M - H)⁺), 560.2 (1%, (M + H)⁺); HRMS (pAPCI): calcd C₃₂H₂₆N₅O₅ [M + H]⁺: 560.1928; observed: 560.1913.

3ff – benzyl (R*)-6-(hydroxy(o-tolyl)amino)-1,3-dioxo-2-phenyl-2,3,5,6-tetrahydro-1H,11H-[1,2,4]triazolo[1',2':1,2]pyridazino[3,4-b]indole-11-carboxylate

To a stirred Schlenk flask was added benzyl 3-vinyl-1H-indole-1-carboxylate (94 mg, 0.34 mmol) and DCM (10 mL). The reaction mixture was cooled to -78 °C and 4-phenyl-1,2,4-triazolidine-3,5-dione (60 mg, 0.34 mmol) was added. The reaction mixture was stirred at -78 °C for 5 hours, 1-methyl-2-nitrosobenzene was added (41 mg, 0.34 mmol) and the reaction stirred at room temperature for 18 hours. The solvent was removed under reduced pressure to leave the crude product as a yellow powder. The product was purified by column chromatography (petrol (40/60)-ethyl acetate 3 : 1, column diameter = 2 cm, silica = 20 cm) to give benzyl (R*)-6-(hydroxy(o-tolyl)amino)-1,3-dioxo-2-phenyl-2,3,5,6-tetrahydro-1H,11H-[1,2,4]triazolo[1',2':1,2]pyridazino[3,4-b]indole-11-carboxylate (68%, 132 mg, 0.23 mmol) as an off white powder.

Mp: 163.8–165.1 °C; R_f: 0.49 (Pet(40/60)-EA 3 : 1); ¹H NMR (400 MHz, CD₂Cl₂): δ_H 8.01 (1H, d, J = 8.3 Hz), 7.65 (1H, dd, J = 8.1, 1.3 Hz), 7.54–7.38 (7H, m), 7.35 (3H, dd, J = 5.0, 2.1 Hz), 7.19 (2H, app tdd, J = 8.5, 7.2, 6.7, 1.4 Hz), 6.99 (2H, app tdd, J = 7.5, 3.4, 1.2 Hz), 6.90 (1H, dd, J = 7.7, 1.4 Hz), 6.75 (1H, d, J = 7.8 Hz), 5.87 (1H, s, OH), 5.48 (1H, d, J = 11.9 Hz), 5.34 (1H, d, J = 11.9 Hz), 5.19 (1H, dd, J = 14.1, 2.3 Hz), 4.63 (1H, app t, J = 2.3 Hz), 3.52 (1H, dd, J = 14.1, 2.3 Hz), 1.94 (3H, s); ¹³C NMR (101 MHz, CDCl₃): δ_C 151.9, 150.3, 150.0, 148.8, 134.6, 133.6, 131.6, 131.1, 130.6, 130.0, 129.4, 128.9, 128.9, 128.8, 128.8, 127.0, 126.6, 126.0, 125.7, 124.4, 123.6, 122.7, 117.9, 114.6, 101.7, 70.1, 58.6, 43.5, 17.7; IR (neat): ν_{max}/cm⁻¹ = 3291, 2981, 1782, 1737, 1699; MS (pNSI): 199.2 (100%), 407.2 (79%), 451.1 (81%, (M - (N(OH)(o-Tol)))⁺), 572.2 (25%, (M - H)⁺), 596.2 (65%, (M + Na)⁺); HRMS (pNSI): calcd C₃₃H₂₇N₅O₅Na [M + Na]⁺: 596.1904; observed: 596.1898.

3gg – benzyl (3aS*,5S*,10bS*)-5-(hydroxy(phenyl)amino)-7-methoxy-2-methyl-1,3-dioxo-2,3,3a,4,5,10b-hexahydropyrrolo[3,4-a]carbazole-10(1H)-carboxylate

To a stirred Schlenk flask was added benzyl 5-methoxy-3-vinyl-1H-indole-1-carboxylate (209 mg, 0.68 mmol), DCM (10 mL) and 1-methyl-1H-pyrrole-2,5-dione (76 mg, 0.68 mmol). The resulting solution was heated at reflux for 18 hours. The reaction was cooled to room temperature and nitrosobenzene (72 mg, 0.68 mmol) was added and the reaction was stirred for 1.5 hours. The solvent was removed under reduced pressure to leave the crude product as a pale orange oil. The product was purified by column chromatography (petrol (40/60)-ethyl acetate 2 : 1,

column diameter = 1 cm, silica = 16 cm) to give benzyl (3aS*,5S*,10bS*)-5-(hydroxy(phenyl)amino)-7-methoxy-2-methyl-1,3-dioxo-2,3,3a,4,5,10b-hexahydropyrrolo[3,4-a]carbazole-10(1H)-carboxylate (73%, 218 mg, 0.44 mmol) as an orange powder.

Mp: 106.8–110.2 °C; R_f : 0.65 (Pet(40/60)-EA 2 : 1); $^1\text{H NMR}$ (400 MHz, CD_2Cl_2): δ_{H} 7.97 (1H, br d, $J = 8.3$ Hz), 7.49–7.47 (2H, m), 7.41–7.37 (3H, m), 7.33–7.30 (2H, m), 7.21–7.19 (2H, m), 7.05–7.00 (2H, m), 6.85 (1H, br d, $J = 8.4$ Hz), 5.53 (1H, d, $J = 11.9$ Hz), 5.39 (1H, d, $J = 11.9$ Hz), 5.02 (1H, br s), 4.91–4.87 (1H, m), 4.75 (1H, br s), 3.68 (3H, s), 3.50 (1H, br s), 2.86 (3H, s), 2.36 (1H, br s), 2.01 (1H, br s); $^{13}\text{C NMR}$ (101 MHz, CD_2Cl_2): δ_{C} 178.3, 174.5, 156.3, 151.5, 151.1, 135.0, 131.5, 130.7, 129.0, 128.9, 128.8, 128.8, 128.4, 122.4, 117.7, 117.2, 115.9, 113.4, 102.4, 69.4, 57.9, 55.6, 40.3, 39.2, 24.9, 23.4; IR (neat): $\nu_{\text{max}}/\text{cm}^{-1} = 3408, 2969, 2890, 1699$; MS (pNSI): 417.1 (100%, $(\text{M} - (\text{N}(\text{OH})\text{Ph}))^+$), 524.2 (68%, $(\text{M} - (\text{H}_2) + \text{H})^+$), 548.2 (16%, $(\text{M} + \text{Na})^+$), 1073.4 (4%, $(2\text{M} + \text{Na})^+$); HRMS (pNSI): calcd $\text{C}_{30}\text{H}_{27}\text{N}_3\text{O}_6\text{Na} [\text{M} + \text{Na}]^+$: 548.1792; observed: 548.1785.

3hh – benzyl (3aS*,5S*,10bS*)-5-(hydroxy(*o*-tolyl)amino)-7-methoxy-2-methyl-1,3-dioxo-2,3,3a,4,5,10b-hexahydropyrrolo[3,4-a]carbazole-10(1H)-carboxylate

To a stirred Schlenk flask was added benzyl 5-methoxy-3-vinyl-1H-indole-1-carboxylate (209 mg, 0.68 mmol), DCM (10 mL) and 1-methyl-1H-pyrrole-2,5-dione (76 mg, 0.68 mmol). The resulting solution was heated at reflux for 18 hours. The reaction was cooled to room temperature and 1-methyl-2-nitrosobenzene (82 mg, 0.68 mmol) was added. The solution was stirred at room temperature for 3 hours. The solvent was removed under reduced pressure to leave the crude product as a pale yellow solid. The product was purified by column chromatography (petrol (40/60)-ethyl acetate 2 : 1, column diameter = 2 cm, silica = 15 cm) to give benzyl (3aS*,5S*,10bS*)-5-(hydroxy(*o*-tolyl)amino)-7-methoxy-2-methyl-1,3-dioxo-2,3,3a,4,5,10b-hexahydropyrrolo[3,4-a]carbazole-10(1H)-carboxylate (74%, 279 mg, 0.50 mmol) as a pale yellow powder.

Mp: 107.6–110.1 °C; R_f : 0.29 (Pet(40/60)-EA 2 : 1); $^1\text{H NMR}$ (400 MHz, CD_2Cl_2): δ_{H} 7.93 (1H, d, $J = 9.1$ Hz), 7.54 (1H, dd, $J = 8.1, 1.3$ Hz), 7.49–7.45 (2H, m), 7.43–7.35 (3H, m), 7.19 (1H, ddd, $J = 7.6, 6.9, 1.9$ Hz), 7.10–7.01 (2H, m), 6.88 (1H, d, $J = 2.6$ Hz), 6.80 (1H, dd, $J = 9.1, 2.6$ Hz), 5.52 (1H, d, $J = 11.9$ Hz), 5.37 (1H, d, $J = 11.9$ Hz), 5.18 (1H, s), 4.87 (1H, d, $J = 8.1$ Hz), 4.33–4.29 (1H, m), 3.65 (3H, s), 3.67–3.61 (1H, m), 2.86 (3H, s), 2.61 (1H, app dt, $J = 13.4, 5.9$ Hz), 2.22 (3H, s), 1.86 (1H, ddd, $J = 13.4, 8.5, 4.3$ Hz); $^{13}\text{C NMR}$ (101 MHz, CD_2Cl_2): δ_{C} 178.4, 174.4, 156.1, 151.6, 149.8, 135.0, 134.9, 131.2, 130.8, 130.6, 130.4, 128.8, 128.8, 128.5, 126.4, 125.3, 121.7, 117.5, 115.7, 113.6, 102.0, 69.3, 57.8, 55.4, 40.5, 38.9, 25.0, 24.9, 18.2; IR (neat): $\nu_{\text{max}}/\text{cm}^{-1} = 3370, 2965, 2887, 1699$; MS (pNSI): 207.1 (39%), 417.1 (34%, $(\text{M} - (\text{N}(\text{OH})(\text{o-Tol}))^+$), 438.2 (100%, $(\text{M} - (\text{H}_2) + \text{H})^+$), 1075.4 (15%, $(2\text{M} - (\text{H}_2) + \text{H})^+$); HRMS (pNSI): calcd $\text{C}_{31}\text{H}_{28}\text{N}_3\text{O}_6 [\text{M} - (\text{H}_2) + \text{H}]^+$: 538.1976; observed: 538.1973.

3ii – benzyl (3aS*,5S*,10bS*)-5-(hydroxy(phenyl)amino)-7-methoxy-1,3-dioxo-2,3,3a,4,5,10b-hexahydropyrrolo[3,4-a]carbazole-10(1H)-carboxylate

To a stirred Schlenk flask was added benzyl 5-methoxy-3-vinyl-1H-indole-1-carboxylate (209 mg, 0.68 mmol), DCM (10 mL) and

1H-pyrrole-2,5-dione (66 mg, 0.68 mmol). The resulting solution was heated at reflux for 18 hours. The reaction was cooled to room temperature and nitrosobenzene (72 mg, 0.68 mmol) was added and the reaction was stirred for 2.5 hours. The solvent was removed under reduced pressure to leave the crude product as a pale orange oil. The product was purified by column chromatography (petrol (40/60)-ethyl acetate 2 : 1, column diameter = 1 cm, silica = 16 cm) to give benzyl (3aS*,5S*,10bS*)-5-(hydroxy(phenyl)amino)-7-methoxy-1,3-dioxo-2,3,3a,4,5,10b-hexahydropyrrolo[3,4-a]carbazole-10(1H)-carboxylate (79%, 317 mg, 0.54 mmol) as a pale orange powder.

Mp: 134.2–136.9 °C; R_f : 0.34 (Pet(40/60)-EA 3 : 2); $^1\text{H NMR}$ (400 MHz, CD_2Cl_2): δ_{H} 8.42 (1H, br s), 7.94 (1H, d, $J = 9.0$ Hz), 7.47–7.44 (2H, m), 7.40–7.34 (3H, m), 7.30–7.27 (2H, m), 7.19–7.17 (2H, m), 7.01–6.98 (1H, m), 6.93 (1H, br s), 6.81 (1H, d, $J = 9.0$ Hz), 5.49 (1H, d, $J = 11.9$ Hz), 5.39 (1H, br s), 5.34 (1H, d, $J = 11.9$ Hz), 4.92 (1H, br d, $J = 6.2$ Hz), 4.74 (1H, br s), 3.64 (3H, s), 3.57–3.51 (1H, br m), 2.39–2.35 (1H, br m), 1.91–1.89 (1H, br m); $^{13}\text{C NMR}$ (101 MHz, CD_2Cl_2): δ_{C} 178.6, 174.4, 156.2, 151.5, 151.0, 135.0, 131.4, 130.3, 129.0, 128.9, 128.8, 128.8, 128.4, 122.6, 117.5, 117.4, 116.0, 113.5, 102.3, 69.4, 57.9, 55.6, 41.5, 40.5, 24.0; IR (neat): $\nu_{\text{max}}/\text{cm}^{-1} = 3233, 2952, 1708$; MS (pNSI): 403.1 (37%, $(\text{M} - (\text{N}(\text{OH})\text{Ph}))^+$), 510.2 (100%, $(\text{M} - (\text{H}_2) + \text{H})^+$), 532.1 (26%, $(\text{M} - (\text{H}_2) + \text{Na})^+$); HRMS (pNSI): calcd $\text{C}_{29}\text{H}_{24}\text{N}_3\text{O}_6 [\text{M} - (\text{H}_2) + \text{H}]^+$: 510.1654; observed: 510.1660.

3jj – benzyl (3aS*,5S*,10bS*)-5-(hydroxy(*o*-tolyl)amino)-7-methoxy-1,3-dioxo-2,3,3a,4,5,10b-hexahydropyrrolo[3,4-a]carbazole-10(1H)-carboxylate

To a stirred Schlenk flask was added benzyl 5-methoxy-3-vinyl-1H-indole-1-carboxylate (209 mg, 0.68 mmol), DCM (10 mL) and 1H-pyrrole-2,5-dione (66 mg, 0.68 mmol). The resulting solution was heated at reflux for 18 hours. The reaction was cooled to room temperature and 1-methyl-2-nitrosobenzene (82 mg, 0.68 mmol) was added. The solution was stirred at room temperature for 3.5 hours. The solvent was removed under reduced pressure to leave the crude product as a pale yellow solid. The product was purified by column chromatography (petrol (40/60)-ethyl acetate 2 : 1, column diameter = 2 cm, silica = 14 cm) to give benzyl (3aS*,5S*,10bS*)-5-(hydroxy(*o*-tolyl)amino)-7-methoxy-1,3-dioxo-2,3,3a,4,5,10b-hexahydropyrrolo[3,4-a]carbazole-10(1H)-carboxylate (76%, 255 mg, 0.52 mmol) as a pale yellow powder.

Mp: 193.0–195.6 °C; R_f : 0.20 (Pet(40/60)-EA 2 : 1); $^1\text{H NMR}$ (400 MHz, CD_2Cl_2): δ_{H} 7.92 (1H, d, $J = 9.7$ Hz), 7.81 (1H, s), 7.53 (1H, d, $J = 7.8$ Hz), 7.46 (2H, dd, $J = 7.8, 1.6$ Hz), 7.42–7.33 (3H, m), 7.21–7.15 (1H, m), 7.09–7.00 (2H, m), 6.84–6.75 (2H, m), 5.50 (1H, d, $J = 11.9$ Hz), 5.35 (1H, d, $J = 11.9$ Hz), 5.16 (1H, s), 4.96 (1H, d, $J = 7.6$ Hz), 4.37 (1H, app t, $J = 4.9$ Hz), 3.71 (1H, app td, $J = 8.7, 5.6$ Hz), 3.64 (3H, s), 2.64 (1H, app dt, $J = 13.6, 5.6$ Hz), 2.21 (3H, s), 1.88 (1H, ddd, $J = 13.6, 9.3, 4.3$ Hz); $^{13}\text{C NMR}$ (101 MHz, $\text{DMSO}-d_6$): δ_{C} 180.6, 176.4, 155.6, 151.8, 151.7, 135.8, 131.6, 130.8, 130.7, 130.2, 129.1, 129.1, 129.0, 126.7, 124.8, 122.3, 117.2, 115.2, 113.5, 102.7, 69.1, 57.3, 55.5, 41.9, 40.3, 27.2, 18.5; IR (neat): $\nu_{\text{max}}/\text{cm}^{-1} = 3457, 3367, 2981, 2886, 1712$; MS (pNSI): 403.1 (100%, $(\text{M} - (\text{N}(\text{OH})(\text{o-Tol}))^+$), 524.1 (75%, $(\text{M} - (\text{H}_2) + \text{H})^+$), 548.2 (16%, $(\text{M} + \text{Na})^+$),

1073.4 (5%, (2M + Na)⁺); HRMS (pNSI): calcd C₃₀H₂₇N₅O₆Na [M + Na]⁺: 548.1792; observed: 548.1785.

3kk – benzyl (*R*^{*})-6-(hydroxy(phenyl)amino)-8-methoxy-1,3-dioxo-2-phenyl-2,3,5,6-tetrahydro-1*H*,11*H*-[1,2,4]triazolo[1',2':1,2]pyridazino[3,4-*b*]indole-11-carboxylate

To a stirred Schlenk flask was added benzyl 5-methoxy-3-vinyl-1*H*-indole-1-carboxylate (209 mg, 0.68 mmol) and DCM (10 mL). The solution was cooled to –78 °C and 4-phenyl-1,2,4-triazolidine-3,5-dione (120 mg, 0.68 mmol) was added. The reaction was stirred at –78 °C for 1.5 hours. The reaction was warmed to room temperature, nitrosobenzene (73 mg, 0.68 mmol) was added and the reaction was stirred for 20 hours. The solvent was removed under reduced pressure to leave the crude product as a pale yellow oil. The product was purified by column chromatography (petrol (40/60)–ethyl acetate 2 : 1, column diameter = 1 cm, silica = 16 cm) to give benzyl (*R*^{*})-6-(hydroxy(phenyl)amino)-8-methoxy-1,3-dioxo-2-phenyl-2,3,5,6-tetrahydro-1*H*,11*H*-[1,2,4]triazolo[1',2':1,2]pyridazino[3,4-*b*]indole-11-carboxylate (78%, 312 mg, 0.53 mmol) as a white powder.

Mp: 110.4–113.2 °C; *R*_f: 0.20 (Pet(40/60)–EA 2 : 1); ¹H NMR (400 MHz, CD₂Cl₂): δ_H 7.88 (1H, d, *J* = 9.1 Hz), 7.42–7.38 (5H, m), 7.36–7.32 (3H, m), 7.29–7.26 (2H, m), 7.24–7.20 (2H, m), 7.13 (2H, d, *J* = 8.1 Hz), 7.05 (1H, app t, *J* = 7.3 Hz), 6.76 (1H, dd, *J* = 9.1, 2.6 Hz), 6.24 (1H, s), 6.10 (1H, d, *J* = 2.5 Hz), 5.43 (1H, d, *J* = 12.0 Hz), 5.32–5.29 (1H, m), 5.25–5.18 (1H, m), 4.84–4.80 (1H, m), 3.64 (1H, dd, *J* = 14.0, 3.3 Hz), 3.55 (3H, s); ¹³C NMR (101 MHz, CD₂Cl₂): δ_C 156.5, 151.1, 150.3, 149.4, 134.8, 131.2, 130.3, 129.2, 129.0, 129.0, 128.70, 128.7, 128.7, 128.6, 128.2, 126.9, 126.2, 124.6, 119.7, 115.3, 113.2, 101.0, 100.5, 69.9, 59.1, 55.5, 44.0; IR (neat): ν_{max}/cm^{–1} = 3336, 2935, 1716; MS (pNSI): 481.1 (17%, (M – (N(OH)Ph))⁺), 588.2 (100%, (M – (H₂) + H)⁺), 612.2 (15%, (M + Na)⁺); HRMS (pNSI): calcd C₃₃H₂₇N₅O₆Na [M + Na]⁺: 612.1854; observed: 612.1838.

3ll – benzyl (*R*^{*})-6-(hydroxy(*o*-tolyl)amino)-8-methoxy-1,3-dioxo-2-phenyl-2,3,5,6-tetrahydro-1*H*,11*H*-[1,2,4]triazolo[1',2':1,2]pyridazino[3,4-*b*]indole-11-carboxylate

To a stirred Schlenk flask was added benzyl 5-methoxy-3-vinyl-1*H*-indole-1-carboxylate (209 mg, 0.68 mmol) and DCM (10 mL). The solution was cooled to –78 °C and 4-phenyl-1,2,4-triazolidine-3,5-dione (120 mg, 0.68 mmol) was added. The reaction was stirred at –78 °C for 1.5 hours. The reaction was warmed to room temperature, 1-methyl-2-nitrosobenzene (73 mg, 0.68 mmol) was added and the reaction was stirred for 24 hours. The solvent was removed under reduced pressure to leave the crude product as a pale orange oil. The product was purified by column chromatography (petrol (40/60)–ethyl acetate 2 : 1, column diameter = 2 cm, silica = 17 cm) to give benzyl (*R*^{*})-6-(hydroxy(*o*-tolyl)amino)-8-methoxy-1,3-dioxo-2-phenyl-2,3,5,6-tetrahydro-1*H*,11*H*-[1,2,4]triazolo[1',2':1,2]pyridazino[3,4-*b*]indole-11-carboxylate (82%, 338 mg, 0.56 mmol) as an off white powder.

Mp: 181.1–183.0 °C; *R*_f: 0.55 (Pet(40/60)–EA 2 : 1); ¹H NMR (400 MHz, DMSO-*d*₆): δ_H 8.70 (1H, s), 7.84 (1H, d, *J* = 9.0 Hz),

7.55–7.48 (2H, m), 7.46–7.41 (3H, m), 7.41–7.33 (4H, m), 7.33–7.29 (2H, m), 7.13–7.03 (2H, m), 6.97 (1H, app td, *J* = 7.4, 1.3 Hz), 6.83 (1H, dd, *J* = 9.1, 2.6 Hz), 6.38 (1H, s), 5.43 (1H, d, *J* = 12.1 Hz), 5.33 (1H, d, *J* = 12.1 Hz), 4.80 (1H, dd, *J* = 13.7, 1.8 Hz), 4.71 (1H, dd, *J* = 3.3, 1.8 Hz), 3.68–3.61 (1H, dd, *J* = 13.7, 3.3 Hz), 3.58 (s, 3H), 2.30 (s, 3H); ¹³C NMR (101 MHz, CD₂Cl₂): δ_C 156.3, 151.6, 150.8, 150.3, 149.8, 135.3, 131.6, 130.9, 130.3, 130.0, 129.7, 129.2, 129.1, 129.1, 128.9, 128.0, 127.4, 127.1, 126.8, 125.2, 121.8, 115.3, 113.2, 103.1, 101.9, 69.9, 55.9, 55.6, 43.9, 18.2; IR (neat): ν_{max}/cm^{–1} = 3212, 2939, 1720; MS (pNSI): 481.2 (100%, (M – N(OH)(*o*-Tol))⁺), 602.2 (34%, (M – (H₂) + H)⁺), 626.2 (100%, (M + Na)⁺); HRMS (pNSI): calcd C₃₄H₂₉N₅O₆Na [M + Na]⁺: 626.2010; observed: 626.2006.

4a – (3*aS*^{*},5*S*^{*},10*bS*^{*})-5-methoxy-2-methyl-4,5,10,10b-tetrahydropyrrolo[3,4-*a*]carbazole-1,3(2*H*,3*aH*)-dione

To a stirred Schlenk flask was added benzyl (3*aS*^{*},5*S*^{*},10*bS*^{*})-5-(hydroxy(*o*-tolyl)amino)-2-methyl-1,3-dioxo-2,3,3*a*,4,5,10*b*-hexahydropyrrolo[3,4-*a*]carbazole-10(1*H*)-carboxylate (120 mg, 0.24 mmol), platinum(IV) oxide (53 mg, 0.24 mmol) and methanol (5 mL). The resulting suspension was placed under an atmosphere of H₂ and stirred at room temperature for 18 hours. The suspension was filtered through celite and the solvent was removed under reduced pressure to leave the crude product as an orange solid. The crude product was purified by column chromatography (petrol (40/60)–ethyl acetate 1 : 1, column diameter = 2 cm, silica = 13 cm) to give (3*aS*^{*},5*S*^{*},10*bS*^{*})-5-methoxy-2-methyl-4,5,10,10b-tetrahydropyrrolo[3,4-*a*]carbazole-1,3(2*H*,3*aH*)-dione (60%, 41 mg, 0.14 mmol) as a pale yellow powder.

Mp: 139.4–142.7 °C; *R*_f: 0.25 (Pet(40/60)–EA 1 : 1); ¹H NMR (400 MHz, CD₂Cl₂): δ_H 8.91 (1H, s), 7.56 (1H, d, *J* = 7.8 Hz), 7.34 (1H, d, *J* = 7.7 Hz), 7.14 (1H, app t, *J* = 7.5 Hz), 7.09 (1H, app t, *J* = 7.4 Hz), 4.73 (1H, app t, *J* = 2.7 Hz), 4.14 (1H, d, *J* = 8.8 Hz), 3.31–3.25 (1H, m), 3.22 (3H, s), 2.94 (1H, app t, *J* = 2.4 Hz), 2.90 (3H, s), 1.88 (1H, ddd, *J* = 14.2, 6.9, 2.2 Hz); ¹³C NMR (101 MHz, CD₂Cl₂): δ_C 178.9, 176.1, 136.4, 128.8, 126.6, 122.3, 120.1, 118.2, 111.9, 111.3, 69.4, 56.1, 39.5, 37.3, 27.4, 25.1; IR (neat): ν_{max}/cm^{–1} 3398, 2931, 2870, 1689; MS (pNSI): 285.0 (29%), 355.1 (100%), 371.1 (57%), 560.0 (21%); HRMS (pNSI): calcd C₁₅H₁₃N₂O₂ [M – OMe]⁺: 253.0972; observed: 253.0974.

4b – (3*aS*^{*},5*S*^{*},10*bS*^{*})-5-ethoxy-2-methyl-4,5,10,10b-tetrahydropyrrolo[3,4-*a*]carbazole-1,3(2*H*,3*aH*)-dione

To a stirred Schlenk flask was added benzyl (3*aS*^{*},5*S*^{*},10*bS*^{*})-5-(hydroxy(*o*-tolyl)amino)-2-methyl-1,3-dioxo-2,3,3*a*,4,5,10*b*-hexahydropyrrolo[3,4-*a*]carbazole-10(1*H*)-carboxylate (100 mg, 0.20 mmol), platinum(IV) oxide (45 mg, 0.20 mmol) and ethanol (5 mL). The resulting suspension was placed under an atmosphere of H₂ and stirred at room temperature for 18 hours. The suspension was filtered through celite and the solvent was removed under reduced pressure to leave the crude product as a yellow solid. The crude product was purified by column chromatography (petrol (40/60)–ethyl acetate 2 : 1, column diameter = 2 cm, silica = 15 cm) to give (3*aS*^{*},5*S*^{*},10*bS*^{*})-5-

ethoxy-2-methyl-4,5,10,10b-tetrahydropyrrolo[3,4-*a*]carbazole-1,3(2*H*,3*aH*)-dione (24%, 20 mg, 0.04 mmol) as a brown powder.

Mp: 100.6–102.8 °C; R_f : 0.16 (Pet(40/60)–EA 2 : 1); ^1H NMR (400 MHz, CD_2Cl_2): δ_{H} 8.78 (1H, s), 7.54 (1H, d, $J = 7.7$ Hz), 7.35 (1H, d, $J = 7.7$ Hz), 7.17–7.12 (1H, m), 7.09 (1H, app t, $J = 7.0$ Hz), 4.83 (1H, app t, $J = 2.8$ Hz), 4.16 (1H, d, $J = 8.8$ Hz), 3.55 (1H, app td, $J = 6.9, 1.8$ Hz), 3.32–3.26 (2H, m), 2.93–2.91 (1H, m), 2.90 (3H, s), 1.88 (1H, ddd, $J = 14.3, 7.1, 2.7$ Hz), 0.97 (1H, t, $J = 7.0$ Hz); ^{13}C NMR (101 MHz, CD_2Cl_2): δ_{C} 178.9, 176.0, 136.3, 128.8, 126.5, 122.3, 120.1, 118.1, 112.5, 111.3, 67.4, 63.5, 39.5, 37.3, 27.9, 25.0, 15.2; IR (neat): $\nu_{\text{max}}/\text{cm}^{-1}$ 3300, 2969, 1690; MS (pAPCI): 108.1 (24%), 298.1 (6%, (M) $^+$), 299.1 (5%, (M + H) $^+$); HRMS (pAPCI): calcd $\text{C}_{17}\text{H}_{19}\text{N}_2\text{O}_3$ [M + H] $^+$: 299.1390; observed: 299.1387.

4c – (3*aS**,5*S**,10*bS**)-5-(hydroxy(phenyl)amino)-2-methyl-4,5,10,10b-tetrahydropyrrolo[3,4-*a*]carbazole-1,3(2*H*,3*aH*)-dione

To a stirred Schlenk flask was added benzyl (3*aS**,5*S**,10*bS**)-5-(hydroxy(phenyl)amino)-2-methyl-1,3-dioxo-2,3,3*a*,4,5,10*b*-hexahydropyrrolo[3,4-*a*]carbazole-10(1*H*)-carboxylate (120 mg, 0.25 mmol), platinum(IV) oxide (57 mg, 0.25 mmol) and THF (5 mL). The resulting suspension was placed under an atmosphere of H_2 and stirred at room temperature for 5 hours. The suspension was filtered through celite and the solvent was removed under reduced pressure to leave the crude product as a yellow solid. The crude product was purified by trituration from DCM to give (3*aS**,5*S**,10*bS**)-5-(hydroxy(phenyl)amino)-2-methyl-4,5,10,10b-tetrahydropyrrolo[3,4-*a*]carbazole-1,3(2*H*,3*aH*)-dione (75%, 68 mg, 0.19 mmol) as a pale yellow powder.

Mp: 157.2–161.9 °C; R_f : 0.17 (Pet(40/60)–EA 1 : 1); ^1H NMR (400 MHz, $\text{DMSO}-d_6$): δ_{H} 11.06 (1H, s), 8.20 (1H, s), 7.35 (1H, d, $J = 8.0$ Hz), 7.26 (1H, d, $J = 8.0$ Hz), 7.24–7.19 (2H, m), 7.17–7.08 (2H, m), 6.98 (1H, app ddd, $J = 8.2, 7.0, 1.2$ Hz), 6.91–6.81 (1H, m), 6.81 (1H, app ddd, $J = 8.0, 6.9, 1.0$ Hz), 4.88 (1H, app t, $J = 4.9$ Hz), 4.27 (1H, d, $J = 8.8$ Hz), 3.64 (1H, app td, $J = 8.8, 6.1$ Hz), 2.81 (3H, s), 2.33 (1H, app dt, $J = 13.7, 6.1$ Hz), 1.84 (1H, ddd, $J = 13.7, 8.8, 4.9$ Hz); ^{13}C NMR (101 MHz, $\text{DMSO}-d_6$): δ_{C} 179.8, 176.3, 153.3, 137.0, 130.0, 129.0, 126.3, 121.5, 121.2, 119.9, 119.0, 117.2, 111.7, 110.0, 57.4, 39.6, 39.3, 25.8, 25.1; IR (neat): $\nu_{\text{max}}/\text{cm}^{-1}$ 3374, 3306, 2919, 1683; MS (pAPCI): 108.0 (28%), 251.1 (100%), 253.1 (68%, (M – (N(OH)Ph) + H) $^+$), 344.1 (13%, (M – (OH) + H) $^+$), 361.1 (3%, (M + H) $^+$); HRMS (pAPCI): calcd $\text{C}_{21}\text{H}_{20}\text{N}_3\text{O}_3$ [M + H] $^+$: 362.1499; observed: 362.1501.

Note: ^1H NMR ran at 40 °C.

4d – (3*aS**,5*S**,10*bS**)-5-(hydroxy(*o*-tolyl)amino)-2-methyl-4,5,10,10b-tetrahydropyrrolo[3,4-*a*]carbazole-1,3(2*H*,3*aH*)-dione

To a stirred Schlenk flask was added benzyl (3*aS**,5*S**,10*bS**)-5-(hydroxy(*o*-tolyl)amino)-2-methyl-1,3-dioxo-2,3,3*a*,4,5,10*b*-hexahydropyrrolo[3,4-*a*]carbazole-10(1*H*)-carboxylate (100 mg, 0.20 mmol), platinum(IV) oxide (45 mg, 0.20 mmol) and THF (5 mL). The resulting suspension was placed under an atmosphere of H_2 and stirred at room temperature for 7 hours. The suspension

was filtered through celite and the solvent was removed under reduced pressure to leave the crude product as a yellow solid. The crude product was purified by column chromatography (petrol (40/60)–ethyl acetate 1 : 1, column diameter = 2 cm, silica = 16 cm) to give (3*aS**,5*S**,10*bS**)-5-(hydroxy(*o*-tolyl)amino)-2-methyl-4,5,10,10b-tetrahydropyrrolo[3,4-*a*]carbazole-1,3(2*H*,3*aH*)-dione (87%, 65 mg, 0.17 mmol) as a pale orange powder.

Mp: 179.3–181.0 °C; R_f : 0.60 (Pet(40/60)–EA 1 : 1); ^1H NMR (400 MHz, $\text{DMSO}-d_6$): δ_{H} 11.08 (1H, s), 8.28 (1H, s), 7.50 (1H, d, $J = 8.0$ Hz), 7.29 (1H, d, $J = 8.1$ Hz), 7.14–7.10 (1H, m), 6.91–6.87 (4H, m), 6.67 (1H, app t, $J = 7.4$ Hz), 4.29 (1H, d, $J = 8.2$ Hz), 4.27 (1H, app t, $J = 3.9$ Hz), 3.83–3.74 (1H, m), 2.81 (3H, s), 2.65–2.56 (1H, m), 1.98 (3H, s), 1.67 (1H, ddd, $J = 13.6, 10.5, 3.9$ Hz); ^{13}C NMR (101 MHz, $\text{DMSO}-d_6$): δ_{C} 180.0, 176.3, 152.2, 136.7, 130.7, 130.5, 130.3, 126.5, 126.5, 124.5, 122.4, 121.2, 119.3, 118.9, 111.7, 109.7, 58.3, 40.0, 38.6, 27.3, 25.1, 18.3; IR (neat): $\nu_{\text{max}}/\text{cm}^{-1}$ 3379, 2955, 2873, 1691; MS (pAPCI): 108.1 (98%), 251.1 (100%), 253.1 (61%, (M – (N(OH)(*o*-Tol)) + H) $^+$), 271.1 (6%, (M – (N(OH)(*o*-Tol)) + OH) $^+$), 358.2 (13%, (M – OH) $^+$); HRMS (pAPCI): calcd $\text{C}_{22}\text{H}_{22}\text{N}_3\text{O}_3$ [M + H] $^+$: 376.1656; observed: 376.1658.

4e – (3*aS**,5*S**,10*bS**)-5-(3,5-dioxo-4-phenyl-1,2,4-triazolidin-1-yl)-2-methyl-4,5,10,10b-tetrahydropyrrolo[3,4-*a*]carbazole-1,3(2*H*,3*aH*)-dione

To a stirred Schlenk flask was added benzyl (3*aS**,5*S**,10*bS**)-5-(3,5-dioxo-4-phenyl-1,2,4-triazolidin-1-yl)-2-methyl-1,3-dioxo-2,3,3*a*,4,5,10*b*-hexahydropyrrolo[3,4-*a*]carbazole-10(1*H*)-carboxylate (110 mg, 0.20 mmol), platinum(IV) oxide (46 mg, 0.20 mmol) and THF (5 mL). The resulting suspension was placed under an atmosphere of H_2 and stirred at room temperature for 5 hours. The suspension was filtered through celite and the solvent was removed under reduced pressure to leave the crude product as a yellow solid. The product was purified by trituration from DCM to give (3*aS**,5*S**,10*bS**)-5-(3,5-dioxo-4-phenyl-1,2,4-triazolidin-1-yl)-2-methyl-4,5,10,10b-tetrahydropyrrolo[3,4-*a*]carbazole-1,3(2*H*,3*aH*)-dione (91%, 79 mg, 0.18 mmol) as an off-white solid.

Mp: 262.4–264.0 °C; ^1H NMR (400 MHz, $\text{DMSO}-d_6$): δ_{H} 11.43 (1H, s), 10.67 (1H, br s), 7.52–7.42 (4H, m), 7.39–7.37 (2H, m), 7.21 (1H, d, $J = 7.9$ Hz), 7.06 (1H, app t, $J = 7.6$ Hz), 6.94 (1H, app t, $J = 7.5$ Hz), 5.39 (1H, app t, $J = 6.1$ Hz), 4.33 (1H, d, $J = 8.0$ Hz), 3.72 (1H, app q, $J = 6.8$ Hz), 2.81 (3H, s), 2.35–2.31 (2H, m); ^{13}C NMR (101 MHz, $\text{DMSO}-d_6$): δ_{C} 178.9, 175.8, 152.7, 152.7, 137.2, 132.3, 130.7, 129.5, 128.5, 126.7, 125.3, 122.2, 119.9, 118.4, 112.3, 107.3, 48.1, 39.5, 38.3, 27.7, 25.3; IR (neat): $\nu_{\text{max}}/\text{cm}^{-1}$ 3229, 1693; MS (pAPCI): 178.1 (35%), 253.1 (100%, (M – (PTAD) + H) $^+$); HRMS (ASAP) calcd $\text{C}_{15}\text{H}_{13}\text{N}_3\text{O}_2$ [M – (PTAD) + H] $^+$: 253.0972; observed: 253.0969.

4f – (3*aS**,5*S**,10*bS**)-5-(hydroxy(phenyl)amino)-4,5,10,10b-tetrahydropyrrolo[3,4-*a*]carbazole-1,3(2*H*,3*aH*)-dione

To a stirred Schlenk flask was added benzyl (3*aS**,5*S**,10*bS**)-5-(hydroxy(phenyl)amino)-1,3-dioxo-2,3,3*a*,4,5,10*b*-hexahydropyrrolo[3,4-*a*]carbazole-10(1*H*)-carboxylate (90 mg, 0.18 mmol), platinum(IV) oxide (41 mg, 0.18 mmol) and THF (5 mL). The

resulting suspension was placed under an atmosphere of H₂ and stirred at room temperature for 10 hours. The suspension was filtered through celite and the solvent was removed under reduced pressure to leave the crude product as a yellow solid. The crude product was purified by column chromatography (petrol (40/60)–ethyl acetate 1 : 1, column diameter = 2 cm, silica = 14 cm) to give (3aS*,5S*,10bS*)-5-(hydroxy(phenyl)amino)-4,5,10,10b-tetrahydropyrrolo[3,4-*a*]carbazole-1,3(2*H*,3*aH*)-dione (41%, 26 mg, 0.07 mmol) as a yellow powder.

Mp: 150.0–153.1 °C; *R*_f: 0.33 (Pet(40/60)–EA 1 : 1); ¹H NMR (400 MHz, DMSO-*d*₆): δ_H 11.22 (1H, s), 11.09 (1H, s), 8.24 (1H, s), 7.33 (1H, d, *J* = 8.1 Hz), 7.27–7.23 (1H, m), 7.20 (2H, app d, *J* = 7.3 Hz), 7.12 (2H, d, *J* = 7.7 Hz), 7.00–6.95 (1H, m), 6.85 (1H, app t, *J* = 7.2 Hz), 6.80 (1H app t, *J* = 7.3 Hz), 4.89 (1H, app t, *J* = 4.9 Hz), 4.25 (1H, d, *J* = 8.1 Hz), 3.63–3.52 (1H, m), 2.27 (1H, app dt, *J* = 13.6, 5.6 Hz), 1.80 (1H, ddd, *J* = 13.6, 9.2, 4.8 Hz); ¹³C NMR (101 MHz, DMSO-*d*₆): δ_C 181.2, 177.6, 153.3, 137.0, 130.3, 129.0, 126.3, 121.4, 121.1, 119.9, 118.9, 117.2, 111.7, 109.9, 57.4, 40.9, 40.6, 25.7; IR (neat): ν_{max}/cm⁻¹ 3302, 2924, 1706; MS (pAPCI): 108.1 (18%), 237.1 (100), 239.1 (46%, (M – (N(OH)Ph) + H)⁺); HRMS (pAPCI): calcd C₁₄H₁₁N₂O₂ [M – (N(OH)Ph) + H]⁺: 239.0815; observed: 239.0810.

4g – (3aS*,5S*,10bS*)-5-(hydroxy(*o*-tolyl)amino)-4,5,10,10b-tetrahydropyrrolo[3,4-*a*]carbazole-1,3(2*H*,3*aH*)-dione

To a stirred Schlenk flask was added benzyl (3aS*,5S*,10bS*)-5-(hydroxy(*o*-tolyl)amino)-1,3-dioxo-2,3,3a,4,5,10b-hexahydropyrrolo[3,4-*a*]carbazole-10(1*H*)-carboxylate (120 mg, 0.24 mmol), platinum(IV) oxide (54 mg, 0.24 mmol) and THF (5 mL). The resulting suspension was placed under an atmosphere of H₂ and stirred at room temperature for 6 hours. The suspension was filtered through celite and the solvent was removed under reduced pressure to leave the crude product as a yellow solid. The crude product was purified by column chromatography (petrol (40/60)–ethyl acetate 2 : 3, column diameter = 2 cm, silica = 17 cm) to give (3aS*,5S*,10bS*)-5-(hydroxy(*o*-tolyl)amino)-4,5,10,10b-tetrahydropyrrolo[3,4-*a*]carbazole-1,3(2*H*,3*aH*)-dione (70%, 61 mg, 0.17 mmol) as an off white solid.

Mp: 149.9–153.2 °C; *R*_f: 0.52 (Pet(40/60)–EA 2 : 3); ¹H NMR (400 MHz, CD₂Cl₂): δ_H 8.81 (1H, s), 8.21 (1H, s), 7.56 (1H, d, *J* = 8.0 Hz), 7.30 (1H, d, *J* = 7.9 Hz), 7.18 (2H, d, *J* = 6.9 Hz), 7.06 (1H, app t, *J* = 7.6 Hz), 7.03–6.99 (2H, m), 6.91–6.85 (1H, m), 5.36 (1H, s), 4.51 (1H, app t, *J* = 4.5 Hz), 4.19 (1H, d, *J* = 8.6 Hz), 3.80 (1H, app td, *J* = 9.3, 6.4 Hz), 2.74 (1H, app dt, *J* = 13.6, 5.5 Hz), 2.15 (3H, s), 1.83 (1H, ddd, *J* = 13.6, 10.1, 4.1 Hz); ¹³C NMR (101 MHz, DMSO-*d*₆): δ_C 181.5, 177.6, 152.2, 136.7, 130.6, 130.5, 130.5, 126.5, 126.5, 124.5, 122.4, 121.1, 119.3, 118.9, 111.6, 109.5, 58.3, 55.5, 40.9, 27.3, 18.3; IR (neat): ν_{max}/cm⁻¹ 3372, 3298, 1683; MS (nNSI) = 186.0 (100%), 237.1 (97%, (M – (N(OH)(*o*-Tol)) – H)⁻), 358.1 (35%, (M – H₂)⁻), 394.1 (23%); HRMS (nNSI): calcd C₂₁H₁₈N₃O₃ [M – H]⁻: 360.1354; observed: 360.1348.

4h – (3aS*,5S*,10bS*)-5-(3,5-dioxo-4-phenyl-1,2,4-triazolidin-1-yl)-4,5,10,10b-tetrahydropyrrolo[3,4-*a*]carbazole-1,3(2*H*,3*aH*)-dione

To a stirred Schlenk flask was added benzyl (3aS*,5S*,10bS*)-5-(3,5-dioxo-4-phenyl-1,2,4-triazolidin-1-yl)-1,3-dioxo-2,3,3a,4,5,

10b-hexahydropyrrolo[3,4-*a*]carbazole-10(1*H*)-carboxylate (110 mg, 0.20 mmol), platinum(IV) oxide (46 mg, 0.20 mmol) and THF (5 mL). The resulting suspension was placed under an atmosphere of H₂ and stirred at room temperature for 5 hours. The suspension was filtered through celite and the solvent was removed under reduced pressure to leave the crude product as a white solid. The crude product was purified by trituration from DCM to give (3aS*,5S*,10bS*)-5-(3,5-dioxo-4-phenyl-1,2,4-triazolidin-1-yl)-4,5,10,10b-tetrahydropyrrolo[3,4-*a*]carbazole-1,3(2*H*,3*aH*)-dione (64%, 53 mg, 0.13 mmol) as a white powder.

Mp: 212.6–213.9 °C; ¹H NMR (400 MHz, DMSO-*d*₆): δ_H 11.39 (1H, s), 11.36 (1H, s), 10.66 (1H, s), 7.51–7.44 (4H, m), 7.41–7.37 (2H, m), 7.23 (1H, d, *J* = 7.8 Hz), 7.07 (1H, app t, *J* = 7.5 Hz), 6.96 (1H, app t, *J* = 7.5 Hz), 5.42 (1H, app t, *J* = 6.0 Hz), 4.29 (1H, d, *J* = 8.0 Hz), 3.69 (1H, app q, *J* = 6.8 Hz), 2.37–2.21 (2H, m); ¹³C NMR (101 MHz, DMSO-*d*₆): δ_C 180.3, 177.1, 152.7, 152.6, 137.2, 132.3, 131.0, 129.5, 128.5, 126.7, 125.3, 122.2, 119.9, 118.4, 112.3, 107.1, 55.5, 48.1, 40.9, 27.5; IR (neat): ν_{max}/cm⁻¹ = 3310, 3155, 3077, 1719, 1674; MS (pAPCI): 239.1 (100%), (M – (PTAD) + H)⁺, 414.1 (2%, (M – H)⁺); HRMS (pAPCI): calcd C₂₂H₁₆N₅O₄ [M – H]⁺: 414.1197; observed: 414.1185.

4i – (R*)-6-(hydroxy(phenyl)amino)-2-phenyl-6,11-dihydro-1*H*,5*H*-[1,2,4]triazolo[1',2':1,2]pyridazino[3,4-*b*]indole-1,3(2*H*)-dione

To a stirred Schlenk flask was added benzyl (R*)-6-(hydroxy(phenyl)amino)-1,3-dioxo-2-phenyl-2,3,5,6-tetrahydro-1*H*,11*H*-[1,2,4]triazolo[1',2':1,2]pyridazino[3,4-*b*]indole-11-carboxylate (110 mg, 0.20 mmol), platinum(IV) oxide (46 mg, 0.20 mmol) and THF (5 mL). The resulting suspension was placed under an atmosphere of H₂ and stirred at room temperature for 5 hours. The suspension was filtered through celite and the solvent was removed under reduced pressure to leave the crude product as a yellow solid. The product was purified by trituration from DCM to give (R*)-6-(hydroxy(phenyl)amino)-2-phenyl-6,11-dihydro-1*H*,5*H*-[1,2,4]triazolo[1',2':1,2]pyridazino[3,4-*b*]indole-1,3(2*H*)-dione (65%, 55 mg, 0.13 mmol) as an off-white solid.

Mp: 174.3–175.2 °C; ¹H NMR (400 MHz, DMSO-*d*₆): δ_H 11.63 (1H, s), 8.61 (1H, s), 7.54–7.38 (6H, m), 7.18 (2H, app t, *J* = 7.8 Hz), 7.10 (2H, app d, *J* = 7.8 Hz), 7.00–6.96 (2H, m), 6.91–6.83 (2H, m), 5.18–5.15 (1H, m), 4.48 (1H, dd, *J* = 13.0, 2.0 Hz), 3.77 (1H, dd, *J* = 13.0, 4.2 Hz); ¹³C NMR (101 MHz, DMSO-*d*₆): δ_C 152.6, 149.6, 146.6, 134.2, 131.7, 129.8, 129.6, 128.9, 128.9, 127.0, 125.8, 122.3, 121.1, 120.2, 118.5, 118.3, 112.3, 92.4, 57.4, 43.4; IR (neat): ν_{max}/cm⁻¹ 3431, 3054, 1698; MS (pAPCI): 317.1 (100%), (M – (N(OH)Ph) + H)⁺, 407.1 (5%, (M – H₂O)⁺); HRMS (pAPCI) calcd C₂₄H₁₉N₅O₃ [M – H]⁺: 424.1404; observed: 424.1398.

4j – (R*)-6-(hydroxy(*o*-tolyl)amino)-2-phenyl-6,11-dihydro-1*H*,5*H*-[1,2,4]triazolo[1',2':1,2]pyridazino[3,4-*b*]indole-1,3(2*H*)-dione

To a stirred Schlenk flask was added benzyl (R*)-6-(hydroxy(*o*-tolyl)amino)-1,3-dioxo-2-phenyl-2,3,5,6-tetrahydro-1*H*,11*H*-[1,2,4]triazolo[1',2':1,2]pyridazino[3,4-*b*]indole-11-carboxylate (140 mg, 0.24 mmol), platinum(IV) oxide (55 mg, 0.24 mmol) and THF (5 mL). The resulting suspension was placed under an

atmosphere of H₂ and stirred at room temperature for 5 hours. The suspension was filtered through celite and the solvent was removed under reduced pressure to leave the crude product as a white solid. The crude product was purified by trituration from DCM to give (R*)-6-(hydroxy(*o*-tolyl)amino)-2-phenyl-6,11-dihydro-1*H*,5*H*-[1,2,4]triazolo[1',2':1,2]pyridazino[3,4-*b*]indole-1,3(2*H*)-dione (44%, 46 mg, 0.11 mmol) as a white powder.

Mp: 188.1–189.6 °C; ¹H NMR (400 MHz, DMSO-*d*₆): δ_H 11.65 (1H, s), 8.58 (1H, s), 7.59–7.51 (5H, m), 7.47–7.42 (1H, m), 7.36 (1H, d, *J* = 8.0 Hz), 7.17–7.13 (1H, m), 6.96–6.91 (3H, m), 6.79–6.69 (2H, m), 4.69 (1H, d, *J* = 12.8 Hz), 4.58 (1H, br s), 3.62 (1H, dd, *J* = 12.8, 3.3 Hz), 2.06 (3H, s); ¹³C NMR (101 MHz, DMSO-*d*₆): δ_C 151.4, 150.4, 146.8, 134.0, 131.8, 131.2, 130.6, 129.8, 129.7, 128.9, 127.0, 126.7, 126.0, 125.1, 122.6, 121.0, 120.1, 118.1, 112.2, 92.3, 57.8, 43.5, 18.2; IR (neat): ν_{max}/cm⁻¹ = 3426, 3380, 2950, 1712; MS (pAPCI): 108.1 (100%), 317.1 (37%), (M – (N(OH)(*o*-Tol) + H)⁺), 422.2 (4%, (M – (H₂O) + H)⁺), 438.2 (6%, (M – H)⁺); HRMS (pAPCI): calcd C₂₅H₂₀N₅O₃ [M – H]⁺: 438.1561; observed: 438.1553.

4k – (3*aS,5*S**,10*bS**)-5-(hydroxy(phenyl)amino)-7-methoxy-2-methyl-4,5,10,10*b*-tetrahydropyrrolo[3,4-*a*]carbazole-1,3(2*H*,3*aH*)-dione**

To a stirred Schlenk flask was added benzyl (3*aS**,5*S**,10*bS**)-5-(hydroxy(phenyl)amino)-7-methoxy-2-methyl-1,3-dioxo-2,3,3*a*,4,5,10*b*-hexahydropyrrolo[3,4-*a*]carbazole-10(1*H*)-carboxylate (130 mg, 0.25 mmol), platinum(IV) oxide (57 mg, 0.25 mmol) and THF (5 mL). The resulting suspension was placed under an atmosphere of H₂ and stirred at room temperature for 5 hours. The suspension was filtered through celite and the solvent was removed under reduced pressure to leave the crude product as an orange solid. The crude product was purified by column chromatography (petrol (40/60)-ethyl acetate 3 : 2, column diameter = 2 cm, silica = 14 cm) to give (3*aS**,5*S**,10*bS**)-5-(hydroxy(phenyl)amino)-7-methoxy-2-methyl-4,5,10,10*b*-tetrahydropyrrolo[3,4-*a*]carbazole-1,3(2*H*,3*aH*)-dione (70%, 69 mg, 0.18 mmol) as a pale yellow powder.

Mp: 149.1–151.2 °C; R_f: 0.19 (Pet(40/60)-EA 3 : 2); ¹H NMR (400 MHz, DMSO-*d*₆): δ_H 10.95 (1H, s), 8.29 (1H, s), 7.23–7.19 (2H, m), 7.18 (1H, d, *J* = 2.8 Hz), 7.14–7.10 (2H, m), 6.87–6.83 (1H, m), 6.57 (1H, dd, *J* = 8.7, 2.5 Hz), 6.51 (1H, d, *J* = 2.5 Hz), 4.83 (1H, app t, *J* = 4.8 Hz), 4.24 (1H, d, *J* = 8.2 Hz), 3.64 (1H, app td, *J* = 9.1, 6.1 Hz), 3.48 (3H, s), 2.80 (3H, s), 2.35 (1H, ddd, *J* = 13.7, 6.1, 4.8 Hz), 1.83 (1H, ddd, *J* = 13.7, 9.1, 4.8 Hz); ¹³C NMR (101 MHz, DMSO-*d*₆): δ_C 179.9, 176.3, 153.6, 153.4, 132.0, 130.6, 129.0, 126.6, 121.2, 117.4, 112.3, 111.5, 109.5, 101.7, 57.7, 55.5, 39.5, 39.1, 27.1, 25.1; IR (neat): ν_{max}/cm⁻¹ = 3394, 2937, 2833, 1690; MS (pAPCI): 283.1 (100%), (M – (N(OH)Ph + H)⁺), 374.1 (18%, (M – (H₂O) + H)⁺), 390.1 (2%, (M – H)⁺), 392.2 (1%, (M + H)⁺); HRMS (pAPCI): calcd C₂₂H₂₂N₃O₄ [M + H]⁺: 392.1605; observed: 392.1597.

4l – (3*aS,5*S**,10*bS**)-5-(hydroxy(*o*-tolyl)amino)-7-methoxy-2-methyl-4,5,10,10*b*-tetrahydropyrrolo[3,4-*a*]carbazole-1,3(2*H*,3*aH*)-dione**

To a stirred Schlenk flask was added benzyl (3*aS**,5*S**,10*bS**)-5-(hydroxy(*o*-tolyl)amino)-7-methoxy-2-methyl-1,3-dioxo-2,3,3*a*,

4,5,10*b*-hexahydropyrrolo[3,4-*a*]carbazole-10(1*H*)-carboxylate (108 mg, 0.20 mmol), platinum(IV) oxide (46 mg, 0.20 mmol) and THF (5 mL). The resulting suspension was placed under an atmosphere of H₂ and stirred at room temperature for 5 hours. The suspension was filtered through celite and the solvent was removed under reduced pressure to leave the crude product as a white solid. The crude product was purified by column chromatography (petrol (40/60)-ethyl acetate 1 : 1, column diameter = 2 cm, silica = 15 cm) to give (3*aS**,5*S**,10*bS**)-5-(hydroxy(*o*-tolyl)amino)-7-methoxy-2-methyl-4,5,10,10*b*-tetrahydropyrrolo[3,4-*a*]carbazole-1,3(2*H*,3*aH*)-dione (70%, 57 mg, 0.14 mmol) as an off white powder.

Mp: 139.7–142.5 °C; R_f: 0.36 (Pet(40/60)-EA 1 : 1); ¹H NMR (400 MHz, DMSO-*d*₆): δ_H 10.89 (1H, s), 8.36 (1H, s), 7.52 (1H, d, *J* = 8.0 Hz), 7.15–7.11 (2H, d, *J* = 8.7 Hz), 6.93–6.85 (2H, m), 6.49 (1H, dd, *J* = 8.7, 2.4 Hz), 6.23–6.17 (1H, m), 4.28 (1H, d, *J* = 8.2 Hz), 4.22 (1H, app t, *J* = 3.8 Hz), 3.78 (1H, ddd, *J* = 10.8, 8.2, 6.1 Hz), 3.45 (3H, s), 2.81 (3H, s), 2.70–2.63 (1H, m), 1.89 (3H, s), 1.66 (1H, ddd, *J* = 14.1, 10.8, 3.8 Hz); ¹³C NMR (101 MHz, DMSO-*d*₆): δ_C 180.1, 176.3, 153.2, 152.5, 131.6, 131.1, 130.7, 130.4, 126.8, 126.5, 124.7, 122.7, 112.2, 111.4, 109.2, 100.6, 58.8, 55.3, 39.6, 38.4, 28.3, 25.1, 18.1; IR (neat): ν_{max}/cm⁻¹ = 3384, 2954, 2866, 1693; MS (pAPCI): 283.1 (100%), (M – (N(OH)(*o*-Tol) + H)⁺), 388.2 (34%, (M – (H₂O) + H)⁺), 404.2 (13%, (M – H)⁺), 406.2 (11%, (M + H)⁺); HRMS (pAPCI): calcd C₂₃H₂₄N₃O₄ [M + H]⁺: 406.1761; observed: 406.1750.

4m – (3*aS,5*S**,10*bS**)-5-(hydroxy(phenyl)amino)-4,5,10,10*b*-tetrahydropyrrolo[3,4-*a*]carbazole-1,3(2*H*,3*aH*)-dione**

To a stirred Schlenk flask was added benzyl (3*aS**,5*S**,10*bS**)-5-(hydroxy(phenyl)amino)-1,3-dioxo-2,3,3*a*,4,5,10*b*-hexahydropyrrolo[3,4-*a*]carbazole-10(1*H*)-carboxylate (90 mg, 0.18 mmol), platinum(IV) oxide (41 mg, 0.18 mmol) and THF (5 mL). The resulting suspension was placed under an atmosphere of H₂ and stirred at room temperature for 10 hours. The suspension was filtered through celite and the solvent was removed under reduced pressure to leave the crude product as a yellow solid. The crude product was purified by column chromatography (petrol (40/60)-ethyl acetate 1 : 1, column diameter = 2 cm, silica = 14 cm) to give (3*aS**,5*S**,10*bS**)-5-(hydroxy(phenyl)amino)-4,5,10,10*b*-tetrahydropyrrolo[3,4-*a*]carbazole-1,3(2*H*,3*aH*)-dione (41%, 26 mg, 0.07 mmol) as a yellow powder.

Mp: 150.0–153.1 °C; R_f: 0.33 (Pet(40/60)-EA 1 : 1); ¹H NMR (400 MHz, DMSO-*d*₆): δ_H 11.22 (1H, s), 11.09 (1H, s), 8.24 (1H, s), 7.33 (1H, d, *J* = 8.1 Hz), 7.27–7.23 (1H, m), 7.20 (2H, app d, *J* = 7.3 Hz), 7.12 (2H, d, *J* = 7.7 Hz), 7.00–6.95 (1H, m), 6.85 (1H, app t, *J* = 7.2 Hz), 6.80 (1H app t, *J* = 7.3 Hz), 4.89 (1H, app t, *J* = 4.9 Hz), 4.25 (1H, d, *J* = 8.1 Hz), 3.63–3.52 (1H, m), 2.27 (1H, app dt, *J* = 13.6, 5.6 Hz), 1.80 (1H, ddd, *J* = 13.6, 9.2, 4.8 Hz); ¹³C NMR (101 MHz, DMSO-*d*₆): δ_C 181.2, 177.6, 153.3, 137.0, 130.3, 129.0, 126.3, 121.4, 121.1, 119.9, 118.9, 117.2, 111.7, 109.9, 57.4, 40.9, 40.6, 25.7; IR (neat): ν_{max}/cm⁻¹ 3302, 2924, 1706; MS (pAPCI): 108.1 (18%), 237.1 (100), 239.1 (46%, (M – (N(OH)Ph + H)⁺); HRMS (pAPCI): calcd C₁₄H₁₁N₂O₂ [M – (N(OH)Ph) + H]⁺: 239.0815; observed: 239.0810.

4n – (3aS*,5S*,10bS*)-5-(hydroxy(*o*-tolyl)amino)-4,5,10,10b-tetrahydropyrrolo[3,4-*a*]carbazole-1,3(2*H*,3*aH*)-dione

To a stirred Schlenk flask was added benzyl (3aS*,5S*,10bS*)-5-(hydroxy(*o*-tolyl)amino)-1,3-dioxo-2,3,3a,4,5,10b-hexahydropyrrolo[3,4-*a*]carbazole-10(1*H*)-carboxylate (120 mg, 0.24 mmol), platinum(IV) oxide (54 mg, 0.24 mmol) and THF (5 mL). The resulting suspension was placed under an atmosphere of H₂ and stirred at room temperature for 6 hours. The suspension was filtered through celite and the solvent was removed under reduced pressure to leave the crude product as a yellow solid. The crude product was purified by column chromatography (petrol (40/60)–ethyl acetate 2 : 3, column diameter = 2 cm, silica = 17 cm) to give (3aS*,5S*,10bS*)-5-(hydroxy(*o*-tolyl)amino)-4,5,10,10b-tetrahydropyrrolo[3,4-*a*]carbazole-1,3(2*H*,3*aH*)-dione (70%, 61 mg, 0.17 mmol) as an off white solid.

Mp: 149.9–153.2 °C; *R*_F: 0.52 (Pet(40/60)–EA 2 : 3); ¹H NMR (400 MHz, CD₂Cl₂): δ_H 8.81 (1H, s), 8.21 (1H, s), 7.56 (1H, d, *J* = 8.0 Hz), 7.30 (1H, d, *J* = 7.9 Hz), 7.18 (2H, d, *J* = 6.9 Hz), 7.06 (1H, app t, *J* = 7.6 Hz), 7.03–6.99 (2H, m), 6.91–6.85 (1H, m), 5.36 (1H, s), 4.51 (1H, app t, *J* = 4.5 Hz), 4.19 (1H, d, *J* = 8.6 Hz), 3.80 (1H, app td, *J* = 9.3, 6.4 Hz), 2.74 (1H, app dt, *J* = 13.6, 5.5 Hz), 2.15 (3H, s), 1.83 (1H, ddd, *J* = 13.6, 10.1, 4.1 Hz); ¹³C NMR (101 MHz, DMSO-*d*₆): δ_C 181.5, 177.6, 152.2, 136.7, 130.6, 130.5, 130.5, 126.5, 126.5, 124.5, 122.4, 121.1, 119.3, 118.9, 111.6, 109.5, 58.3, 55.5, 40.9, 27.3, 18.3; IR (neat): ν_{max}/cm⁻¹ 3372, 3298, 1683; MS (nESI) = 186.0 (100%), 237.1 (97%), (M – (N(OH)(*o*-Tol) – H)⁺), 358.1 (35%), (M – H₂)⁺, 394.1 (23%); HRMS (nESI): calcd C₂₁H₁₈N₃O₃ [M – H]⁺: 360.1354; observed: 360.1348.

4o – (R*)-6-(hydroxy(phenyl)amino)-8-methoxy-2-phenyl-6,11-dihydro-1*H*,5*H*-[1,2,4]triazolo[1',2':1,2]pyridazino[3,4-*b*]indole-1,3(2*H*)-dione

To a stirred Schlenk flask was added benzyl (R*)-6-(hydroxy(phenyl)amino)-8-methoxy-1,3-dioxo-2-phenyl-2,3,5,6-tetrahydro-1*H*,11*H*-[1,2,4]triazolo[1',2':1,2]pyridazino[3,4-*b*]indole-11-carboxylate (118 mg, 0.20 mmol), platinum(IV) oxide (46 mg, 0.20 mmol) and THF (5 mL). The resulting suspension was placed under an atmosphere of H₂ and stirred at room temperature for 5 hours. The suspension was filtered through celite and the solvent was removed under reduced pressure to leave the crude product as a yellow solid. The product was purified by trituration from DCM to give (R*)-6-(hydroxy(phenyl)amino)-8-methoxy-2-phenyl-6,11-dihydro-1*H*,5*H*-[1,2,4]triazolo[1',2':1,2]pyridazino[3,4-*b*]indole-1,3(2*H*)-dione (38%, 35 mg, 0.08 mmol) as an off-white solid.

Mp: 173.7–176.4 °C; *R*_F: 0.18 (Pet–EA 3 : 1); ¹H NMR (400 MHz, DMSO-*d*₆): δ_H 11.44 (1H, s), 8.62 (1H, s), 7.54–7.47 (4H, m), 7.44–7.41 (1H, m), 7.25–7.18 (3H, m), 7.12 (2H, d, *J* = 7.7 Hz), 6.90 (1H, app t, *J* = 6.8 Hz), 6.56 (1H, d, *J* = 8.7 Hz), 6.26 (1H, s), 5.12 (1H, br s), 4.51 (1H, d, *J* = 13.0 Hz), 3.81 (1H, dd, *J* = 13.0, 3.3 Hz), 3.49 (3H, s); ¹³C NMR (101 MHz, DMSO-*d*₆): δ_C 154.3, 152.9, 149.7, 146.4, 131.8, 130.1, 129.6, 129.6, 128.9, 128.9, 127.0, 126.3, 122.3, 118.4, 112.9, 110.7, 100.8, 92.3, 57.7, 55.5, 44.3; IR (neat): ν_{max}/cm⁻¹ 3362, 3000, 1758, 1700; MS (pAPCI): 213.1 (70%), 347.1

(100%, (M – (N(OH)Ph) + H)⁺); HRMS (pAPCI): calcd C₂₅H₂₀N₅O₄ [M – H]⁺: 454.1510; observed: 454.1502.

4p – (R*)-6-(hydroxy(*o*-tolyl)amino)-8-methoxy-2-phenyl-6,11-dihydro-1*H*,5*H*-[1,2,4]triazolo[1',2':1,2]pyridazino[3,4-*b*]indole-1,3(2*H*)-dione

To a stirred Schlenk flask was added benzyl (R*)-6-(hydroxy(*o*-tolyl)amino)-8-methoxy-1,3-dioxo-2-phenyl-2,3,5,6-tetrahydro-1*H*,11*H*-[1,2,4]triazolo[1',2':1,2]pyridazino[3,4-*b*]indole-11-carboxylate (120 mg, 0.20 mmol), platinum(IV) oxide (46 mg, 0.20 mmol) and THF (5 mL). The resulting suspension was placed under an atmosphere of H₂ and stirred at room temperature for 5 hours. The suspension was filtered through celite and the solvent was removed under reduced pressure to leave the crude product as a white solid. The crude product was purified by trituration from DCM to (R*)-6-(hydroxy(*o*-tolyl)amino)-8-methoxy-2-phenyl-6,11-dihydro-1*H*,5*H*-[1,2,4]triazolo[1',2':1,2]pyridazino[3,4-*b*]indole-1,3(2*H*)-dione (64%, 53 mg, 0.13 mmol) as a white powder.

Mp: 171.9–173.8 °C; ¹H NMR (400 MHz, DMSO-*d*₆): δ_H 11.44 (1H, s), 8.64 (1H, s), 7.59 (1H, d, *J* = 8.1 Hz), 7.54–7.50 (4H, m), 7.46–7.43 (1H, m), 7.19 (1H, d, *J* = 8.5 Hz), 7.15 (1H, d, *J* = 7.5 Hz), 6.97–6.91 (2H, m), 6.50 (1H, dd, *J* = 8.7, 2.2 Hz), 6.01 (1H, s), 4.73 (1H, d, *J* = 12.8 Hz), 4.52 (1H, s), 3.67–3.61 (1H, m), 3.47 (3H, s), 1.96 (3H, s); ¹³C NMR (101 MHz, DMSO-*d*₆): δ_C 154.1, 151.8, 150.5, 146.4, 131.8, 131.6, 130.6, 130.0, 129.7, 128.9, 128.7, 127.0, 126.7, 126.5, 125.3, 122.8, 112.7, 110.7, 100.0, 91.8, 58.3, 55.4, 44.3, 18.0; IR (neat): ν_{max}/cm⁻¹ = 3442, 3394, 2939, 1699; MS (pAPCI): 347.1 (68%), (M – (N(OH)(*o*-Tol) + H)⁺), 391.1 (100%), 452.2 (4%), (M – (H₂O) + H)⁺, 468.2 (2%), (M – H)⁺; HRMS (pAPCI): calcd C₂₆H₂₂N₅O₄ [M – H]⁺: 468.1666; observed: 468.1658.

Acknowledgements

The authors thank Newcastle University and EPSRC (EP/I033959/1) for funding, MA thanks the Ministry of Higher Education of Saudi Arabia for a PhD scholarship, EPSRC for X-ray crystallography facilities at Newcastle (EP/F03637X/1), Prof. W. McFarlane and Dr C. Wills (Newcastle) for NMR support, L. Watson and S. Thompson (Newcastle) for preliminary studies. Mass spectrometry data was acquired at the EPSRC UK National Mass Spectrometry Facility at Swansea University.

References

- 1 S. Omura, Y. Iwai, A. Hirano, A. Nakagawa, J. Awaya, H. Tsuchiya, Y. Takahashi and R. Asuma, *J. Antibiot.*, 1977, 30, 275–282.
- 2 N. Funato, H. Takayanagi, Y. Konda, Y. Toda, Y. Harigaya, Y. Iwai and S. Omura, *Tetrahedron Lett.*, 1994, 35, 1251–1254.
- 3 O. A. B. S. M. Gani and R. A. Engh, *Nat. Prod. Rep.*, 2010, 27, 489–498.
- 4 M. S. Lopez, J. W. Choy, U. Peters, M. L. Sos, D. O. Morgan and K. M. Shokat, *J. Am. Chem. Soc.*, 2013, 135, 18153–18159.
- 5 E. Conchon, F. Anizon, R. M. Golsteyn, S. Léonce, B. Pfeiffer and M. Prudhomme, *Tetrahedron*, 2006, 62, 11136–11144.

- 6 A. Voldoire, M. Sancelme, M. Prudhomme, P. Colson, C. Houssier, C. Bailly, S. Léonce and S. Lambel, *Bioorg. Med. Chem.*, 2001, 9, 357–365.
- 7 N. Ty, G. Dupeyre, G. G. Chabot, J. Seguin, L. Quentin, A. Chiaroni, F. Tillequin, D. Scherman, S. Michel and X. Cachet, *Eur. J. Med. Chem.*, 2010, 45, 3726–3739.
- 8 E. Conchon, F. Anizon, B. Aboab, R. M. Golsteyn, S. Léonce, B. Pfeiffer and M. Prudhomme, *Eur. J. Med. Chem.*, 2008, 43, 282–292.
- 9 E. Pereira, A. Youssef, M. El-Ghozzi, D. Avignant, J. Bain, M. Prudhomme, F. Anizon and P. Moreau, *Tetrahedron Lett.*, 2014, 55, 834–837.
- 10 M. Eitel and U. Pindur, *J. Org. Chem.*, 1990, 55, 5368–5374.
- 11 W. E. Noland, W. C. Kuryla and R. F. Lange, *J. Am. Chem. Soc.*, 1959, 81, 6010–6017.
- 12 W. E. Noland and S. R. Wann, *J. Org. Chem.*, 1979, 44, 4402–4410.
- 13 M. Bleile, T. Wagner and H.-H. Otto, *Helv. Chim. Acta*, 2005, 88, 2879–2891.
- 14 U. Pindur and M.-H. Kim, *Tetrahedron Lett.*, 1988, 29, 3927–3928.
- 15 M. Medion-Simon and U. Pindur, *Helv. Chim. Acta*, 1991, 74, 430–437.
- 16 U. Pindur and C. Otto, *Tetrahedron*, 1992, 48, 3515–3526.
- 17 R. Bergamasco, Q. N. Porter and C. Yap, *Aust. J. Chem.*, 1977, 30, 1531–1544.
- 18 J. D. Lambert and Q. N. Porter, *Aust. J. Chem.*, 1981, 34, 1483–1490.
- 19 C. Gioia, A. Hauville, L. Bernardi, F. Fini and A. Ricci, *Angew. Chem., Int. Ed.*, 2008, 47, 9236–9239.
- 20 C. Gioia, L. Bernardi and A. Ricci, *Synthesis*, 2010, 2010, 161–170.
- 21 B. Tan, G. Hernández-Torres and C. F. Barbas, *J. Am. Chem. Soc.*, 2011, 133, 12354–12357.
- 22 U. Pindur, M. H. Kim, M. Rogge, W. Massa and M. Molinier, *J. Org. Chem.*, 1992, 57, 910–915.
- 23 L. J. Watson, R. W. Harrington, W. Clegg and M. J. Hall, *Org. Biomol. Chem.*, 2012, 10, 6649–6655.
- 24 L. J. Cotterill, R. W. Harrington, W. Clegg and M. J. Hall, *J. Org. Chem.*, 2010, 75, 4604–4607.
- 25 L. Pfeuffer and U. Pindur, *Helv. Chim. Acta*, 1988, 71, 467–471.
- 26 K. Suzuki, K. Inomata and Y. Endo, *Org. Lett.*, 2004, 6, 409–411.
- 27 G. A. Kraus and J. Kim, *Org. Lett.*, 2004, 6, 3115–3117.
- 28 R. B. Ruggeri, M. M. Hansen and C. H. Heathcock, *J. Am. Chem. Soc.*, 1988, 110, 8734–8736.
- 29 D. Li, Y. Cao, A. Shi and Z. Xi, *Chem.-Asian J.*, 2011, 6, 392–395.
- 30 D. G. Hingane, S. K. Goswami, V. Puranik and R. S. Kusurkar, *Synth. Commun.*, 2011, 42, 1786–1795.
- 31 B. t. Joseph, M. Facompré, H. Da Costa, S. Routier, J.-Y. Mérour, P. Colson, C. Houssier and C. Bailly, *Bioorg. Med. Chem.*, 2001, 9, 1533–1541.
- 32 B. Saroja and P. C. Srinivasan, *Synthesis*, 1986, 1986, 748–749.
- 33 X. Zhang, S. I. Khan and C. S. Foote, *J. Org. Chem.*, 1993, 58, 7839–7847.
- 34 P. R. Schreiner, *Chem. Soc. Rev.*, 2003, 32, 289–296.
- 35 J. Robertson, M. J. Hall, P. M. Stafford and S. P. Green, *Org. Biomol. Chem.*, 2003, 1, 3758–3767.
- 36 L. F. Tietze, *Chem. Rev.*, 1996, 96, 115–136.
- 37 C. J. Lovely, H. Du, Y. He and H. V. Rasika Dias, *Org. Lett.*, 2004, 6, 735–738.
- 38 N. Uludag and S. Patir, *J. Heterocycl. Chem.*, 2007, 44, 1317–1322.
- 39 P. Magnus, N. L. Sear, C. S. Kim and N. Vicker, *J. Org. Chem.*, 1992, 57, 70–78.
- 40 R. Yang and F. G. Qiu, *Angew. Chem., Int. Ed.*, 2013, 52, 6015–6018.